

# 26th Annual Precise Time and Time Interval (PTTI) Applications and Planning Meeting



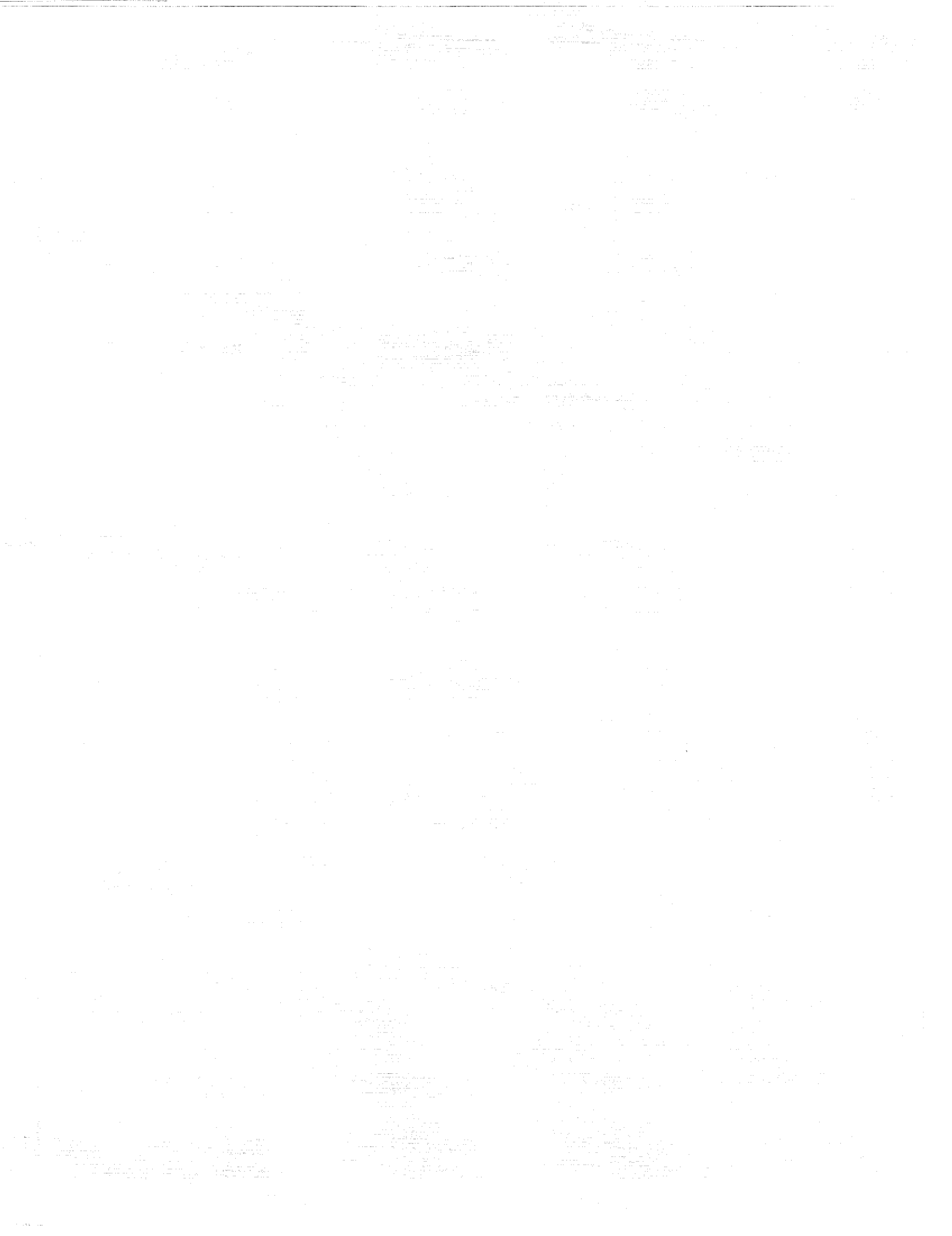
*Proceedings of a meeting held at  
the Hyatt Regency Hotel  
Reston, Virginia  
December 6-December 8, 1994*

(NASA-CR-3302) THE 26TH ANNUAL  
PRECISE TIME AND TIME INTERVAL  
(PTTI) APPLICATIONS AND PLANNING  
MEETING (NASA, Goddard Space  
Flight Center) 473 p

N95-32319  
--THRU--  
N95-32349  
Unclass

H1/70 0052276





*NASA Conference Publication 3302*

# **26th Annual Precise Time and Time Interval (PTTI) Applications and Planning Meeting**

*Editorial Committee Chairman*  
Richard L. Sydnor  
*Jet Propulsion Laboratory*  
*California Institute of Technology*

Proceedings of a meeting sponsored by the  
U.S. Naval Observatory, the NASA Goddard  
Space Flight Center, the NASA Jet Propulsion  
Laboratory, the Space and Naval Warfare  
Systems Command, the Naval Research Laboratory,  
the U.S. Army Research Laboratory, and  
the Air Force Office of Scientific Research  
and held at the  
Hyatt Regency Hotel  
Reston, Virginia  
December 6- December 8, 1994



National Aeronautics  
and Space Administration

**Goddard Space Flight Center**  
Greenbelt, Maryland 20771

**1995**

This publication is available from the NASA Center for Aerospace Information,  
800 Elkridge Landing Road, Linthicum Heights, MD 21090-2934, (301) 621-0390.

**PRECISE TIME AND TIME INTERVAL (PTTI)  
APPLICATIONS AND PLANNING MEETING**

**ORDER FORM FOR THE PROCEEDINGS**

	<u>Year</u>	<u>Cost</u>	<u>Available</u>	<u>Unavailable</u>
1	1969			X
2	1970			X
3	1971			X
4	1972			X
5	1973			X
6	1974	\$25.00	X	
7	1975	\$25.00	X	
8	1976			X
9	1977			X
10	1978	\$25.00	X	
11	1979	\$25.00	X	
12	1980	\$25.00	X	
13	1981	\$25.00	X	
14	1982			X
15	1983			X
16	1984	\$25.00	X	
17	1985	\$25.00	X	
18	1986	\$20.00	X	
19	1987	\$25.00	X	
20	1988	\$35.00	X	
21	1989	\$65.00	X	
22	1990	\$70.00	X	
23	1991	\$85.00	X	
24	1992	\$85.00	X	
25	1993	\$85.00	X	
26	1994	\$95.00	X	

Please circle copy(ies) requested and make the check payable to "Treasurer, PTTI". **Please do not add personal names or addresses to the pay line on the check. We cannot accept invoices.** Please return the check and the Order Form to:

**Mrs. Sheila Faulkner  
Chairman, PTTI Executive Committee  
U. S. Naval Observatory  
Directorate of Time (DTS)  
3450 Massachusetts Avenue, N.W.  
Washington, DC 20392-5420  
(202) 653-1460 FAX: 202/653-0909**

When you register for the PTTI Meeting or order the Proceedings, your name is added to the PTTI Mailing list to automatically receive future meeting information.



## **EXECUTIVE COMMITTEE**

**Mrs. Sheila C. Faulkner**, Chairman  
U.S. Naval Observatory

**Mr. Ronald L. Beard**  
U.S. Naval Research Laboratory

**Mr. Raymond L. Granata**  
NASA/Goddard Space Flight Center

**Dr. Helmut Hellwig**  
U.S. Air Force Office of Scientific Research

**Dr. William J. Klepczynski**  
U.S. Naval Observatory

**Mr. Paul F. Kuhnle**  
NASA Jet Propulsion Laboratory

**Commander David G. Markham**  
Space and Naval Warfare Systems Command

**Mr. John J. Rush**  
NASA Headquarters

**Dr. Richard L. Sydnor**  
NASA Jet Propulsion Laboratory

**Dr. John R. Vig**  
U.S. Army Research Laboratory

**Dr. Joseph D. White**  
U.S. Naval Research Laboratory

**Dr. Gernot M. R. Winkler**  
U.S. Naval Observatory

**Ms. Nicolette Jardine**  
U.S. Naval Observatory

# **OFFICERS**

## **GENERAL CHAIRMAN**

**DR. RICHARD L. SYDNOR**

Jet Propulsion Laboratory  
California Institute of Technology

## **TECHNICAL PROGRAM COMMITTEE CHAIRMAN**

**MR. RONALD L. BEARD**

U.S. Naval Research Laboratory

## **ASSISTANT CHAIRMEN**

**DR. LEONARD S. CUTLER**

Hewlett-Packard Laboratories

**DR. HENRY F. FLIEGEL**

The Aerospace Corporation

**MR. PAUL F. KUHNLE**

Jet Propulsion Laboratory

**DR. RICHARD L. SYDNOR**

Jet Propulsion Laboratory

**MR. S. CLARK WARDRIP**

AlliedSignal Technical Services Corporation

**EDITORIAL COMMITTEE CHAIRMAN**

**DR. RICHARD L. SYDNOR**

Jet Propulsion Laboratory  
California Institute of Technology

**EDITORIAL COMMITTEE ASSISTANT CHAIRMAN**

**MR. PAUL F. KUHNLE**

Jet Propulsion Laboratory  
California Institute of Technology

**EDITORIAL COMMITTEE MEMBERS**

**MR. DAVID W. ALLAN**

Allan's Time

**MRS. MATTIE GREEN**

Jet Propulsion Laboratory  
California Institute of Technology

**DR. G. JOHN DICK**

Jet Propulsion Laboratory  
California Institute of Technology

**MR. THOMAS K. TUCKER**

Jet Propulsion Laboratory  
California Institute of Technology

**PUBLICITY AND EXHIBITS CHAIRMAN**

**MR. DON MITCHELL**

TrueTime

**TECHNICAL ASSISTANCE**

**MR. JEFFREY S. INGOLD**

AlliedSignal Technical Services Corporation

**MRS. BEA BELOVARICH**

AlliedSignal Technical Services Corporation

# **SESSION CHAIRMEN**

## **SESSION I**

**CDR David G. Markham**

Space and Naval Warfare Systems Command

## **SESSION II**

**Dr. Raymond L. Filler**

U.S. Army Research Laboratory

## **SESSION III**

**Ms. Francine M. Vannicola**

U.S. Naval Observatory

## **SESSION IV**

**Professor Sigfrido M. Leschiutta**

Istituto Elettrotecnico Nazionale

## **SESSION VA**

**Dr. John Luck**

Orroral Geodetic Observatory

## **SESSION VB**

**Mr. Paul F. Kuhnle**

Jet Propulsion Laboratory

## **TUTORIAL**

**Dr. Fred L. Walls**

National Institute of Standards and Technology

## **SESSION VI**

**Mr. Edward D. Powers, Jr.**

U.S. Naval Research Laboratory

## **SESSION VII**

**Dr. Henry F. Fliegel**

The Aerospace Corporation

## **SESSION VIII**

**Dr. Judah Levine**

National Institute of Standards and Technology

# ARRANGEMENTS

Sheila C. Faulkner  
Paul F. Kuhnle  
Dr. Richard L. Sydnor

## FINANCE COMMITTEE

Dr. William J. Klepczynski  
Sheila C. Faulkner

## RECEPTIONISTS

The receptionists at the 26th Annual PTTI meeting were:

Mrs. Bea Belovarich, AlliedSignal Technical Services Corporation  
Ms. Brenda Hicks, U.S. Naval Observatory  
Ms. Nicolette Jardine, U.S. Naval Observatory  
Mrs. Aline Kuhnle, Jet Propulsion Laboratory  
Mrs. Betty Wardrip, AlliedSignal Technical Services Corporation

# **1994 ADVISORY BOARD MEMBERS**

**Mr. S. Clark Wardrip, Chairman**

**AlliedSignal Technical Services Corporation**

Mr. David W. Allan  
Allan's Time

Professor Carroll O. Alley  
University of Maryland

Dr. James A. Barnes  
Austron, Incorporated

Mr. Martin B. Bloch  
Frequency Electronics, Incorporated

Mrs. Mary Chiu  
Applied Physics Laboratory

Dr. Leonard S. Cutler  
Hewlett-Packard Company

Dr. Henry F. Fliegel  
The Aerospace Corporation

Mr. Jeffrey S. Ingold  
AlliedSignal Technical  
Services Corporation

Mr. Robert H. Kern  
Kernco, Incorporated

Mr. Pete R. Lopez  
TRAK Microwave

Mr. Donald H. Mitchell  
TrueTime, Incorporated

Mr. Jerry R. Norton  
Applied Physics Laboratory

Mr. Allen W. Osborne III  
Allen Osborne Associates

Mr. Terry N. Osterdock  
Stellar GPS Corporation

Dr. Bradford W. Parkinson  
Stanford University

Mr. Harry E. Peters  
Sigma Tau Standards Corporation

Dr. Victor S. Reinhardt  
Hughes Aircraft

Mr. William J. Riley  
EG&G, Incorporated

Dr. Harry Robinson  
Duke University

Mr. Ronald C. Roloff  
FTS/Austron  
Datum Companies

Dr. Samuel R. Stein  
Timing Solutions Corporation

Mr. Michael R. Tope  
TrueTime, Incorporated

Mr. James L. Wright  
Computer Science Raytheon

# TABLE OF CONTENTS

## PTTI DISTINGUISHED SERVICE AWARD

Presented by  
Captain Richard E. Blumberg  
Superintendent  
United States Naval Observatory

to

Dr. Gernot M. R. Winkler  
Director of Time  
U.S. Naval Observatory

## KEYNOTE ADDRESS GLOBAL POSITIONING SYSTEM (GPS) STATUS AND FUTURE PLANS

Jules G. McNeff  
Navigation and Air Control Systems  
Office of the Assistant Secretary of Defense (C31)  
Pentagon, Washington, DC

### SESSION I

#### PTTI Status Report

Chairman: CDR David G. Markham  
Space and Naval Warfare Systems Command

<b>DoD PTTI Report</b> .....	<b>11</b>
Captain Richard E. Blumberg, Superintendent, United States Naval Observatory	
<b>Precise Timing Applications at the Defense Mapping Agency</b> .....	<b>17</b>
Stephen Malys, Defense Mapping Agency	
<b>Navy PTTI Report</b> .....	<b>25</b>
CDR Jim Burton, United States Navy	
<b>Status of PTTI in the U.S. Air Force</b> .....	<b>27</b>
Howard A. Hopkins and Robert E. Blair, Jr., Directorate of Metrology, Newark Air Force Base	

## SESSION II

### WORKSHOPS

#### Three Simultaneous In-Depth Moderator and Audience Discussions:

**Chairman: Raymond L. Filler**  
**U.S. Army Research Laboratory**

#### WORKSHOP 1

**Real World User Requirements** ..... 33  
**Moderator:** Richard L. Sydnor, Jet Propulsion Laboratory

#### WORKSHOP 2

**User Environmental Effects** ..... 35  
**Moderator:** Helmut Hellwig, Air Force Office of Scientific Research

#### WORKSHOP 3

**Real Time Automated Systems** ..... 36  
**Moderator:** Joseph D. White, U.S. Naval Research Laboratory

## SESSION III

### Operational PTTI Dissemination/Distribution

**Chairman: Francine M. Vannicola**  
**U.S. Naval Observatory**

- The 1994 International Transatlantic Two-Way Satellite Time and Frequency Transfer Experiment: Preliminary Results** ..... 39 ✓  
J. A. DeYoung, W. J. Klepczynski, A. D. McKinley, W. Powell, and P. Mai, U.S. Naval Observatory; P. Hetzel and A. Bauch, Physikalisch-Technische Bundesanstalt; J. A. Davis and P. R. Pearce, National Physical Laboratory; F. Baumont, P. Claudon, and P. Grudler, Observatoire de la Côte d'Azur; G. de Jong, NMI, Van Swinden Laboratorium; D. Kirchner, Technische Universität Graz; H. Ressler, Space Research Institute; A. Söring, Forschungs- und Technologiezentrum; C. Hackman, National Institute of Standards and Technology; and L. Veenstra, Communications Satellite Corporation
- High Accuracy Time Transfer Synchronization** ..... 51 ✓  
Paul Wheeler, Paul Koppang, David Chalmers, Angela Davis, Anthony Kubik, and William Powell, U.S. Naval Observatory
- Fine Tuning GPS Clock Estimation in the MCS** ..... 63 ✓  
Captain Steven T. Hutsell, United States Air Force
- Implementation of a Standard Format for GPS Common View Data** .... 75 ✓  
Marc A. Weiss, National Institute of Standards and Technology and Claudine Thomas, Bureau International des Poids et Mesures

<b>Some Preliminary Results of the Fast Calibration Trip During the INTELSAT Field Trials</b> .....	<b>89</b>
W. J. Klepczynski, U.S. Naval Observatory; J. A. Davis, National Physical Laboratory; D. Kirchner, Technical University of Graz; H. Ressler, Space Research Institute; G. De Jong, NMI, Van Swinden Laboratories; F. Baumont, Observatoire de la Côte d'Azur; P. Hetzel, Physikalisch-Technische Bundesanstalt; A. Söring, Forschungs-und Technologiezentrum; Ch. Hackman, National Institute of Standards and Technology, M. Granveaud, Observatoire de Paris; W. Lewandowski, Bureau International des Poids et Mesures	

## PANEL DISCUSSION

**Moderator:** Raymond L. Filler, U.S. Army Research Laboratory

## PANEL DISCUSSION ON WORKSHOPS: 1, 2, AND 3

### SESSION IV

#### International Activities/Coordination

**Chairman: Sigfrido M. Leschiutta**  
Istituto Elettrotecnico Nazionale

<b>European Plans for New Clocks in Space</b> .....	<b>101</b> ✓
Sigfrido M. Leschiutta, Istituto Elettrotecnico Nazionale and Politecnico di Torino, Elettronica and Patrizia Tavella, Istituto Elettrotecnico Nazionale	
<b>Time Activities at the BIPM</b> .....	<b>111</b> ✓
Claudine Thomas, Bureau International des Poids et Mesures	
<b>Anticipated Uncertainty Budgets of Praretime and T2L2 Techniques as Applied to ExTRAS</b> .....	<b>127</b> ✓
C. Thomas, Bureau International des Poids et Mesures; P. Wolf, Bureau International des Poids et Mesures and Queen Mary and Westfield College; P. Uhrich, Laboratoire Primaire du Temps et des Fréquences; W. Schäfer, Institut für Navigation; H. Nau, Deutsche Forschungsanstalt für Luft und Raumfahrt e.V.; and C. Veillet, Observatoire de la Côte d'Azur	

### SESSION VA

#### Time Transfer

**Chairman: John Luck**  
Orroral Geodetic Observatory

<b>PTTI Applications at the Limits of GPS</b> .....	<b>141</b> ✓
R.J. Douglas, National Research Council of Canada and J. Popelar, Department of Natural Resources	
<b>Time Aspects of the European Complement to GPS: Continental and Transatlantic Experimental Phases</b> .....	<b>153</b> ✓
P Uhrich, B. Juompan, and R. Tourde, Observatoire de Paris; M. Brunet and J-F. Dutrey, Centre National d'études spatiales	

<b>LASSO Experiment Intercalibration Trip for the Two LASSO Ranging Stations</b> .....	167
J. Gaignebet and J.L. Hatat, Lunar Laser Ranging Team; P. Grudler, Observatoire de la Côte d'Azur; W.J. Klepczynski and L. McCubbin, U.S. Naval Observatory; J. Wiant and R. Ricklefs, McDonald Observatory	

## SESSION VB

### Poster Session

**Chairman: Paul F. Kuhnle**  
**Jet Propulsion Laboratory**

<b>Network Time Synchronization Servers at the U.S. Naval Observatory</b> .....	175 ✓
R.E. Schmidt, U.S. Naval Observatory	
<b>Custom Turnkey Time and Frequency Systems A Structured, Expandable Approach</b> .....	185 ✓
David F. Wright, Radiocode Clocks Ltd.	
<b>High Resolution Time Interval Counter</b> .....	191 ✓
Victor S. Zhang, Dick D. Davis, and Michael A. Lombardi, National Institute of Standards and Technology	
<b>Investigation into the Effects of VHF and UHF Band Radiation on Hewlett-Packard (HP) Cesium Beam Frequency Standards</b> .....	201 ✓
Andrew Dickens, United States Naval Observatory and University of Virginia	
<b>Relativistic Timescale Analysis Suggests Lunar Theory Revision</b> .....	209 ✓
Steven D. Deines, Collins Avionics and Communications Division and Carol A. Williams, University of South Florida	
<b>The Deep Space Network Stability Analyzer</b> .....	221 ✓
Julian C. Breidenthal, Charles A. Greenhall, Robert L. Hamell, and Paul F. Kuhnle, Jet Propulsion Laboratory	
<b>A Globally Efficient Means of Distributing UTC Time and Frequency Through GPS</b> .....	235 ✓
John A. Kusters, Robin P. Giffard, and Leonard S. Cutler, Hewlett-Packard Company; David W. Allan, Allan's TIME; Mihran Miranian, U.S. Naval Observatory	

## TUTORIAL

### PTTI Measurement Technology

**Chairman: Fred L. Walls**  
**National Institute of Standards and Technology**

<b>Fundamental Concepts and Definitions in PM and AM Noise Metrology</b> .....	255
Eva Pikal, National Institute of Standards and Technology and University of Colorado	

<b>Discussion of Error Models for PM and AM Noise Measurements</b> .....	<b>269</b>
Fred L. Walls, National Institute of Standards and Technology	
<b>State-of-the-Art Measurement Techniques for PM and AM Noise</b> .....	<b>280</b>
Craig W. Nelson, SpectraDynamics, Incorporated	

## SESSION VI

### PTTI Technology

**Chairman: Edward D. Powers, Jr.**  
**U.S. Naval Research Laboratory**

### PANEL DISCUSSION

**Joint Defense Laboratories (JDL) Timing Research Status**

**Moderator: Edward D. Powers, Jr., U.S. Naval Research Laboratory**

### PANEL MEMBERS

**John R. Vig**

**U.S. Army Research Laboratory**

**Ronald L. Beard**

**and**

**Frederick E. Betz**

**U.S. Naval Research Laboratory**

<b>Monte Carlo Simulations of Precise Timekeeping in the Milstar Communication Satellite System</b> .....	<b>291</b> ✓
J.C. Camparo and R.P. Frueholz, The Aerospace Corporation	
<b>Automated Delay Measurement System for an Earth Station for Two-Way Satellite Time and Frequency Transfer</b> .....	<b>305</b> ✓
Gerrit de Jong and Michel C. Polderman, NMI Van Swinden Laboratorium	
<b>Study of Tropospheric Correction for Intercontinental GPS Common-View Time Transfer</b> .....	<b>319</b> ✓
W. Lewandowski, Bureau International des Poids et Mesures; W.J. Klepczynski and M. Miranian, United States Naval Observatory; P. Grüdler and F. Baumont, Observatoire de la Côte d'Azur; M. Imae, Communications Research Laboratory	
<b>Prospects for High Accuracy Time Dissemination and Synchronization Using Coded Radar Pulses From a Low-Earth Orbiting Spacecraft</b> .....	<b>333</b> ✓
E. Detoma, Fiat CIEI Division SEPA and C. Dionisio, Alenia Spazio	

## SESSION VII

### Time Scale Technology

Chairman: Henry F. Fliegel  
The Aerospace Corporation

<b>Metafitting: Weight Optimization for Least-Squares Fitting of PTTI Data</b> .....	347 ✓
R.J. Douglas and J.-S. Boulanger, National Research Council of Canada	
<b>Methodologies for Steering Clocks</b> .....	361 ✓
H. Chadsey, U.S. Naval Observatory	
<b>The Effects of Clock Errors on Timescale Stability</b> .....	369 ✓
Lee A. Breakiron, U.S. Naval Observatory	
<b>Relativistic Theory for Syntonization of Clocks in the Vicinity of the Earth</b> .....	381 ✓
G. Petit, Bureau International des Poids et Mesures and P. Wolf, Bureau International des Poids et Mesures and Queen Mary and Westfield College	
<b>Allan Deviation Computations of a Linear Frequency Synthesizer System Using Frequency Domain Techniques</b> .....	393 ✓
Andy Wu, The Aerospace Corporation	

## SESSION VIII

### PTTI Applications

Chairman: Judah Levine  
National Institute of Standards and Technology

<b>SVN 9 End-of-Life Testing</b> .....	405 ✓
1Lt Gregory E. Hattan, Falcon Air Force Base	
<b>Fiber Optic Reference Frequency Distribution to Remote Beam Waveguide Antennas</b> .....	415 ✓
Malcolm Calhoun, Paul Kuhnle, and Julius Law, Jet Propulsion Laboratory	
<b>Laser Retroreflector Experiment on NAVSTAR 35 and 36</b> .....	427 ✓
E.C. Pavlis, University of Maryland; Ronald L. Beard, U.S. Naval Research Laboratory	
<b>T2L2 Time Transfer by Laser Link</b> .....	443 ✓
Christian Veillet and Patricia Fridelance, Observatoire de la Côte d'Azur	
<b>Satellite Test of the Isotropy of the One-Way Speed of Light Using ExTRAS</b> .....	455 ✓
Peter Wolf, Bureau International des Poids et Mesures and Queen Mary and Westfield College	

ORIGINAL PAGE  
BLACK AND WHITE PHOTOGRAPH



Gernot M. R. Winkler

# PTTI DISTINGUISHED SERVICE AWARD

Presented by  
Captain Richard E. Blumberg  
Superintendent  
United States Naval Observatory  
Washington, DC 20392-5420

to

Dr. Gernot M.R. Winkler  
Director of Time  
U.S. Naval Observatory

Distinguished visitors, fellow scientists, ladies and gentlemen.

Today, it is my pleasure to preside over the inaugural PTTI Distinguished Service Award Ceremony and I am pleased to present the award to someone whose life's work has earned him an international reputation in the field of precise time.

The criteria for the award are that the award shall recognize an individual for any of the following contributions to the field of PTTI:

- a. provided exceptional leadership and demonstrated ability and ingenuity in the development or application of PTTI over a number of years;
- b. designed or developed a significant PTTI system.

It is my personal pleasure to present this first PTTI Distinguished Services Award to Dr. Gernot M.R. Winkler, Director of Time, U.S. Naval Observatory.

Dr. Winkler is renowned worldwide for his knowledge of precise time and his accomplishments in establishing and maintaining, at the U.S. Naval Observatory, the most accurate time standard in the world.

Early in his career, Dr. Winkler recognized the requirements for and importance of worldwide time synchronization. He pioneered the development of the "flying clock" in conjunction with Very Low Frequency (VLF) monitoring projects studying propagation path delays. His work laid the foundation for the use of VLF for timing and navigation (e.g., using Navy VLF Communications Stations to supplement the Omega Navigation System). His most important

achievement has been the development of the most stable and universally accessible atomic timescale in the world. This timescale has become the primary vehicle for the formulation of International Atomic Time. The statistical basis of this timescale, the development of the algorithm for its implementation, and its practical utilization were performed with his guidance and participation every step of the way.

Throughout his career, Dr. Winkler has cooperated not only with other Federal agencies, but also with private industry, to improve the accuracy and timeliness of the dissemination of precise time. One of his most outstanding contributions to both government and the private sector was his establishing the annual Precise Time and Time Interval Applications and Planning Meeting. These meetings have increased knowledge and cooperation and have reduced markedly the duplication of effort among various national and international agencies and organizations, both public and private. He persuaded the Coast Guard to synchronize its Loran-C Navigation System and was also successful in bringing about the synchronization of the OMEGA Navigation System. He has worked with the Global Positioning System (GPS) Program Office in coordinating the timing of the NAVSTAR GPS. Synchronization of these systems improved significantly, the long-range navigation precision for strategic and tactical weapon systems. Dr. Winkler has also worked closely with a number of organizations – the Naval Astronautics Group in timing the worldwide Navy Navigation Satellite System (TRANSIT); with the Applied Physics Laboratory, Johns Hopkins University, on LORAN-C timing; with the National Security Agency on special experiments; with the National Aeronautics and Space Administration in timing its worldwide tracking network, and with the National Institute of Standards and Technology and Hewlett-Packard in solving timing problems of mutual concern to ensure the nation has a single time standard.

Through his efforts, Dr. Winkler has brought international recognition to the U.S. Naval Observatory by providing timely and accurate publication and distribution of time-related data and information. Each year, ten different Time Service announcements, comprising more than 150,000 pages, are composed, printed and distributed to more than 1200 users worldwide. As the need for “real time” access to USNO timing data has grown, Dr. Winkler has developed a system for distributing timing data on a computer-to-computer basis.

Dr. Winkler is widely recognized as the preeminent world leader in precise time, time interval, timescales and time distribution. He has established the United States Navy, through the Naval Observatory, as the largest single contributor (currently at 38%) to the international time standard, Universal Time Coordinated. He thus ensures that satellite, navigation, command, control, and communications systems are all operating on precise, accurate time standards; absolutely vital for data synchronization in the information age. His leadership as Chairman of the Subcommittee on International Atomic Time (TAI) of the International Consulting Committee for the definition of the second for atomic time and active coordination with other national Time Services have ensured that international standards for time and frequency measurements are strictly adhered to, thus guaranteeing the stability of time for DoD, the United States, and the world.

Dr. Winkler has played a critical role in a new initiative to improve the accuracy of the Global Positioning System (GPS). Air Force Space Command specifically requested Dr. Winkler's technical expertise and willing assistance in designing, and planning an upgrade to the timing

systems at the GPS Monitor Stations, The project, a joint venture with the Naval Research Laboratory and U.S. Air Force, is proceeding, with software development almost complete, hardware on order and installation scheduled to begin shortly. His thorough knowledge of this national asset illustrates the global breadth of Dr. Winkler's interests and willingness to pursue a vital project. Not only will the project improve GPS timing signals to better than 10 nanoseconds, but we anticipate improved position accuracy as well.

Visionary and tireless, with unsurpassed expertise, Dr. Winkler is a world leader, and national asset. A renowned scientist he deals routinely, on a global scale, coordinating national and international efforts in support of the DoD. His diplomatic skills, ability to work cooperatively with other national time service organizations and to make continuous improvements in precise time and time interval even in the face of declining resources are a tribute to his skill, leadership, and scientific excellence. He deserves the highest recognition that the PTTI community can bestow.

# KEYNOTE ADDRESS GLOBAL POSITIONING SYSTEM (GPS) STATUS AND FUTURE PLANS\*

Jules G. McNeff  
Navigation and Air Control Systems  
Office of the Assistant Secretary of Defense (C3I)  
Pentagon, Washington, DC

## Abstract

*This presentation will update the status of GPS policy development within the Department of Defense and between the Departments of Defense and Transportation. Subjects discussed will be several studies currently underway on aspects of GPS management, financing, operations, security, contributions to national competitiveness, the broad acceptance of GPS as a global military force enhancement system, and the implications of that acceptance for operational planning. Also included are highlights of important near-term issues which will contribute to continued successful implementation of GPS by the DoD.*

Before I get into any prepared remarks I had, I would like to be among the first to publicly congratulate Dr. Winkler on being the recipient of the award. I think if there's anybody in the world you can pick for an introductory award such as this, Dr. Winkler is certainly the right choice. So congratulations, Doctor.

I would like to start by first of all welcoming all of you to Washington. For those of you who came from out of town, I hope you understand that what you are seeing here is just a typical December day, sunny and in the 70s. We do this all the time here.

I would like to personally thank you for inviting me to kick off your PTTI planning meeting. It's a great honor for me to be able to begin the festivities and the round of discussions that will continue. As Ron said, I work in the Office of the Assistant Secretary of Defense for Command Control Communications and Intelligence. As such, I am really just kind of a minor cog in the great machine that's the Department of Defense (DoD) of the United States. I am very proud of the fact that the great machine has been the producer of a number of tremendous systems like LORAN and TRANSIT and GPS. In fact, GPS is what I will talk about a little later here today.

Really, in comparison to all of the assembled scientists in this august body, I'm just a layman when it comes to the timing business. As I thought about what kind of things I could say in

---

\*This is an editorial transcript of the Keynote Address given by Mr. McNeff

a keynote address for this conference, I was really perplexed as to what sorts of things I as a layman could offer to a group such as this. I really think that's one of the reasons we are here today in this meeting, is to bring what is really a very esoteric technology, in some cases a difficult to understand technology, down to layman's terms.

So to start with, I would like to offer a few of my observations about time that I've picked up here as I've worked through GPS and dealing with a number of you folks. To you, though, many of these observations may sound patently obvious and pedestrian. However, to the person who views time as most people do, kind of akin to air and sunlight which are free and always available, they may not be so obvious. People tend to expect time to be a resource that's always there in abundance and to be used whenever they feel like it. As you all know, that's not necessarily the case.

I do have another agenda. It is one that I've pushed several times before to many of you; and that is we all need to make time and timing familiar to the program management people, to the system designers who produce systems that depend on time and time interval, so they can understand how PTTI can both contribute to the systems, but also limit the ability of their systems to do everything that they want to do. In addition, the knowledge of PTTI needs to be accounted for in all stages of system design and operation. In fact, we're finding that out as we enter the operational stage of GPS in its day-to-day operations. I'll talk a little more about that when I get to the GPS part.

First of all, my basic perspective says that time is the ultimate, nonrenewable resource. We try to save it; we try to make it; and we certainly spend it. In fact, we really can't save time because it moves inexorably onward, and once it passes, it's gone. Anyone who has ever faced a deadline knows that once that time is up, it's up; and you don't get it back again. We can't make more of it, much as we'd like to, so we try to shave it into its smallest possible components, and then do everything faster, on the theory that ultimately this will make more time available to us.

With regards to time and that kind of technology, my observation is that in the last year, in my office, I've had a simple word processor replaced with two extremely powerful computers — one, so I can deal with classified and the other so I can deal with unclassified, both of which I used to deal with in my word processor. My telephone with human answering support has been replaced with voice mail, on the presumption that all of this high-speed, high-powered technology and electronics will give me more time to be efficient. Frankly, I don't necessarily find that to be the case. What I do find is that some of these timesaving devices enable us to put more volume into less space at a faster rate; but at some point we need to step back and take a look at the utility of what we're doing in all this flurry of activity and make sure that when it comes down to the end user, it really is useful to him/her. Again, I expect that is why we need conferences like this — not only to show each other how we're pressing the limits of technology in a particular area of PTTI, but also so the decision-makers and the laymen in the business (if you will) can see the human-useful results in ways that we can grasp and then apply.

So now I get to using time, or "spending it," more properly said. We need to think about that as if we're spending it out of our own pockets. Because, as I said before, it is our most

valuable resource: it's nonrenewable and it's a resource for which even the best technology today cannot create a substitute. That is why I continue to be concerned with time and time's contribution to GPS and all its facets — in fact, concerned to the extent that right now my watch says it's 9:26; and if any of you are hooked up to GPS time, you know that's about five minutes or so fast. The reason is that I don't want to be late to things and waste my time or the time of others; but it's also a measure of the way we think about these kinds of things that makes me concerned when I look at my watch and I wonder if it's "just" five minutes fast; it could maybe be four minutes and 50 seconds fast, or five minutes and 10 seconds fast. So even trying to measure with a micrometer and cut with an ax, we still tend to think in terms of micromanaging time. So, enough of that general pedestrian observation.

Let me move now to a discussion of current applications of time and, specifically, time in the way it applies to GPS, and of a GPS status update in general. I put this slide (Figure 1) up to give you all an indication of the way we do GPS today. GPS isn't just a DoD program; it's not just a military program; although it's called the "Positioning System," it's not just a positioning or navigation system. It is, in fact, a commodity resource. It's a dual-use system for use by civil, commercial, scientific enterprises as well as by military users in the U. S. and abroad.

What I would like to run through today in this part of the discussion is a general program status, and draw some particular references to PTTI in a GPS context. I put this slide (Figure 2) up not to show you how GPS works — because most all of you know how GPS works — but to highlight the key component of GPS, and that's time. A lot of people who think about GPS in the Washington area, at a policy level or just generically, don't really think of time; they think of location, position. They don't understand that, fundamentally, GPS is a timing system; that timing is absolutely key to GPS, the way it works, what makes it successful, and ultimately the range of benefits that will be obtained from GPS.

I would just like to quickly run through our current policies so that everyone knows where we're coming from policy-wise. This really isn't a policy discussion per se, though. I'll talk a little bit about our extensive involvement with the civil community; and then some current updates on a number of studies that are in progress looking at the GPS. How is long-term use affected by initiatives in a civil community anxious to use GPS? A quick military perspective on how GPS plays in a tactical environment; and finally, some conclusions.

Policy statements that deal with GPS you've seen many times before. I just put them up here to remind you of what they are. We have two different services in GPS: a Precise Positioning Service (PPS) available to U. S. and allied military, which is defined as a positioning accuracy of 16 meters, 50 percent spherical error probability; and we also have a widely — available, generally — available Standard Positioning Service (SPS), defined at a positioning error of 100 meters, 95 percent probability, which was established based on civil aviation requirements for non-precision approach; but today we see many, many civil requirements that are far in excess of 100 meters, and, in fact, far in excess of the 16 meters that we provide or that the system expects to provide to military users; and so, drives a number of civil initiatives in the GPS area. We do continue to put protection on the GPS signals, both selective availability and anti-spoofing, which are implemented continuously on all the operational satellites. The PPS, as I said, is available to U. S. and allied military, and, with memoranda of agreement with our office, to a variety of other users. We have a number of agreements in place with foreign

militaries, and also with federal civil agencies in the United States. Of course, the Standard Positioning Service is available to everyone.

Our work with the civil community has been long-term. (Figure 3) We've been involved with the Department of Transportation (DOT) in production of federal radionavigation plans for over 10 years. The latest iteration, the 1994 edition of the Federal Radionavigation Plan, is in the final stages of staffing, prior to signature by the Department's secretary. We have agreements in place with the DOT on civil use of GPS, and we've got provisions for civil DOT representatives to take positions at both Air Force Space Command (AFSPACECOM) and at the Joint Program Office. In fact, the AFSPACECOM slot has just been filled, Mr. Hank Skalski from the DOT has been designated to take that position out in Colorado Springs. Hank, would you stand up? Hank will be the senior DOT representative in the DoD GPS community. He'll represent civil interests at AFSPACECOM, at the Operations Center, in the requirements development process which leads to satisfying future civil requirements and future versions of GPS development. So Hank will be a very important contributor and representative of the civil community within the GPS business. In fact, he will be holding a meeting tomorrow on civil GPS requirements.

Also with the DOT, as most of you probably know, we had a rather extensive task force that reported out last year in a variety areas on management financing and operation of GPS. The DOT has put several of those management recommendations into practice already. The Federal Aviation Administration (FAA) is actively pushing a wide-area technique for integrity and availability improvement, and also looking at ways to improve GPS accuracy for precision approach and other applications. I will talk a little bit more about that in just a minute.

Those are the parts of the civil augmentation initiatives that are growing like mushrooms out there. Every time you turn around, there's a new initiative underway to improve on the performance of GPS or to use GPS in some new way. There is a tremendously broad civil user community, both in the government and out in the private sector. You only have to read GPS World Magazine or just turn on your television and see the rental car advertisements. I just got a copy of an off-road magazine from Japan, and the center section had to do with after-market GPS navigation equipment that you can put in your off-road vehicle over there. There were probably 10 or 15 different manufacturers marketing little video screens and GPS receivers, along with CD ROMs with all the pertinent games and navigation data. There was even one company that had one called "Karaoke Navigator." You spend a lot of time in your cars in Japan, I guess, and so you need something to divert yourself besides finding your way around. It is a tremendous market and growing all the time.

Even though we in the DoD and DoT sort of thought we had all the answers last year, there were others that thought that it would be a better idea if other agencies took an independent look at the answers we came up with and saw whether they were truly the right answers; or whether there were other things that needed to be looked at in terms of how GPS will contribute to U. S. competitive advantage and to the quality of life for all of us here for the next 20 or 30 years or more. So there were a number of other studies that were undertaken, and some of them are starting to show results.

First of all, (Figure 4) there was a study run by the Institute of Telecommunication Sciences (ITS)

on GPS augmentations, looking at how the Federal Government can best provide augmented GPS services. This was really an outgrowth of our task force of last year. This particular study started early in '94 and is now in sort of the final stages of reporting out; the Secretary of the DOT reviewed the report in November; it's being briefed right now, and I expect it will be released shortly by the DOT. It was performed by ITS, which is part of the NIST under the Department of Commerce; but the contract was awarded by DOT and we participated in that work. It did look toward the differential services that are being provided to augment GPS by the Coast Guard, by the FAA, Planned Applications by Highways and other federal agencies.

At the same time, on the military side of things, the Defense Science Board last spring started to look at GPS, particularly as GPS was going to be used in Precision-Guided Munitions. Some folks in the PGM world were surprised, I guess, to learn that the GPS has some vulnerabilities in the jamming area. When you really think about it, a radionavigation system, a radiopositioning system that depends on electromagnetics is going to be susceptible to jamming. Once you get past that basic idea that GPS does have some jamming susceptibility, then you can start looking at what does it take to make it as robust as we need to have it in a tactical environment. Frankly, until GPS began to become operational and be considered for some of these tactical applications, people hadn't really started thinking about it in a total tactical environment; but we are now. I will cover more about that in a little bit.

One of the aspects of GPS robustness that the Defense Science Board is looking at is the contribution of timing for that tactical robustness. How can we use time, which is again the fundamental driver of GPS, to make the system more robust, to enable us to operate longer at Y-code, to enable us to re-acquire Y-code or to acquire Y-code faster in competitive situations and those kinds of things? So timing has a direct tie-in to some of the work that the Defense Science Board and some of the recommendations coming out of the Defense Science Board in looking at improvements to GPS.

We also have the National Academy of Public Administration and National Academy of Science in a Congressionally-directed joint study, looking at the totality of GPS. The National Academy of Public Administration is looking at management and financing of the system, governance, international aspects; the National Academy of Science is looking at some of the technical issues associated with the operation of GPS, and also, by the way, with the features of selective availability and anti-spoofing. That report is due out in April.

At the same time, also based on some congressional language, the Office of Science and Technology Policy, a White House office, has initiated a separate study of GPS through Rand Critical Technologies Institute to look at GPS competitive advantages and vulnerability. These include military advantages and vulnerabilities, but they also include some of the more macro-issues of GPS contributions to United States economic competitiveness, technical competitiveness in the world market, and those kinds of things. Also, by the way, looking at GPS as a specific contributor to the national information infrastructure (NII) in where (at least in some people's minds) the less well-known timing aspects become very critical. When you are talking about moving millions of bytes of data at very high data rates, your ability to time those transfers and to synchronize your computers, and all that, becomes key. So here GPS again is shaving time to nanoseconds and is a very significant contributor of that kind of technology.

What the results of those studies will be I can't forecast at this point. We don't in the DoD, even though we've paid for most of them (other than the Defense Science Board), we don't have the inside story on what the National Academy of Public Administration (NAPA), the National Academy of Sciences and Rand ultimately will come out with in terms of recommendations. That, frankly, is part of the business we're in. If we need to learn how to best operate a system like this for the national good, we need to be able to stand the scrutiny of independent groups and deal with the recommendations that come out of those groups. So we're looking forward with great anticipation to the completion of the NAPA, NAS, as well as the Rand studies next spring.

At the same time the studies are going on, GPS, for all intents and purposes, is in fact operational. We have a number of other civil initiatives that are going on and have been for some time. (Figure 5) The Coast Guard, for several years now, has been working on radio beacon-based differential; and, in fact, putting in place differential stations around the coastline of the United States; and now working with the Army Corps of Engineers to put differential stations in the Mississippi and Missouri watersheds. So through the Coast Guard and the Corps of Engineers, virtually the entire coastal area, plus a good bit of inland U. S., will be covered with radio beacon-based differential signals in the very near future.

Civil aviation is pursuing several different initiatives. First of all, there is an international construct called a "global navigation satellite system" (GNSS), which uses signals from GPS and its augmentations, plus other signals as may be available at some point in the future, to take care of global international civil aviation. At the same time, they're looking at augmentations to that to improve accuracy to precision approach levels and also to improve the integrity and availability of the GPS signals at the levels where civil aviation can operate safely with them, even on the most precise stages of flight. They're also looking at local area differential and pseudolites to aid in the most critical Cat II and III precision landings, and also for airport surface control.

At the same time, highway systems are looking at using GPS; transit systems — not the Transit Satellite System, but Metrobus and other transit systems — are looking at GPS for fleet management and control. GPS is being used in farming to control applications of fertilizers and pesticides. And also in construction, in quite a variety of high precision applications. So again, the market is mushrooming.

I will now move back to the military perspective. Whenever I talk to the operational guys in the services, this is a slide (Figure 6) I intend to use. I have used it out in the Operational Users Conference in Colorado Springs, and I will continue to use it time and time again as we talk about GPS and the tactical environment, because it's something that we need to think thoroughly through as we apply GPS for our military purposes.

We need to consider a whole range of users of GPS out there. Of course, the U.S. and Allied Military Forces were the intended recipients of GPS improvements, and so will be using them for a tremendously wide variety of missions. We will use Precise Positioning Service equipment with Selective Availability and Anti-Spoofing capabilities in virtually all combat and combat-support missions. So GPS will in a tremendously wide use in the military services of the U.S. and our allies. At the same time, we know that commercial equipment will be present

in whatever theater we're engaged in; and, frankly, to the extent it is, it will probably be a hazard to users and a problem for planners because the same commercial equipment that our guys will have access to, our adversary will quite likely have access to as well. And so for that reason, we're working very hard to equip all of our forces with PPS equipment and to get away from the commercial SPS equipment.

Because, when we get down to the next bullet, we recognize right now that our adversaries and other forces around the world are also devising ways to use GPS. We see evidence of it every day. You only have to pick up the latest international defense review, or any other sort of arms market publication, or general avionics military kind of publication and you will see that GPS is coming into wide use in militaries around the world. There will be militarized commercial SPS receivers in use in any theater you can pick; there will likely be SPS guided weapons in use, not today, but in the very near future; and those will be augmented by differential GPS wherever it's available. That's a reality that our own tactical planners will have to account for as they think about tactics and contingencies down the road.

At the same time, we have to take into account civil use and adjacent non-combatants. The fact that what is a military SPS advantage to an adversary is also in use right next to the theater for a wide variety of peaceful transportation and commerce. It will also be in use with available DGPS. So there's a distinction that we'll need to make between adversaries and non-related neighbors when we deal with GPS in hostile situations. Frankly, as I said before, that message hadn't really been internalized too much among much the planners until just recently, that we are starting to work within the Joint Staff, and where the operations plans are done, to take some of these global kinds of issues into consideration in the future.

For conclusion, I put up a couple of what I call "Obvious Statements of the Week." (Figure 7) As I said in the beginning, GPS isn't just any one thing, a positioning or navigation system or whatever; it's an information resource. I borrow that term, that characterization from Charlie Trimble, who runs Trimble Navigation, and some of the presentations he's made to the National Academy of Sciences and other panels. A lot of the manufacturers feel the same way; GPS is a resource to be used; it provides a whole variety of information, position, velocities, time, a number of things that can be used for a whole variety of purposes other than just knowing exactly where you are.

At the bottom, PTTI is fundamental to the effectiveness of GPS. If we don't continue to take account of time and time interval in GPS and its applications, then we limit the benefits that we're going to get out of it. In the operational environment, timing is critical to satellite operations and control. We've got a number of initiatives underway to look at managing time, and managing time better, and the contributions of time within the control segment functions. We're looking, as I said during the DSB discussion, at the contribution of time to improving the tactical robustness of user equipment and the responsiveness with which it deals with the Y-code. Of course in science and National Information Infrastructure (NII) and commerce, time is equally important along with the other positioning and velocity solutions that you get from GPS. Also, looking at the strategic environment, this is a truly dual-use resource. It's in use globally. We need to recognize that. We need to do the best we can to balance the competing objectives of science and commerce against security.

With that, I'll close my introductory remarks. I hope that the Planning Conference is a great success. I appreciate all of you devoting your attention to me this morning.

## GLOBAL POSITIONING SYSTEM

### A NATIONAL / INTERNATIONAL

### DUAL-USE COMMODITY

PROGRAM STATUS & THE PTTI CONNECTION

- PRESENTATION BY
  - JULES McNEFF
  - OASD(C3I)

FIGURE 1

### GPS DUAL USE DISCUSSION OUTLINE

- CURRENT POLICIES
- CIVIL INVOLVEMENT IN GPS
  - MANAGEMENT
  - USE
- GPS STUDIES IN PROCESS
- CIVIL USE INITIATIVES
- GPS TACTICAL ENVIRONMENT
- CONCLUSION - IMPLICATIONS FOR PTTI

FIGURE 2

## GPS SECURITY POLICY POLICY STATEMENTS

- DIRECT ACCESS SERVICES
  - PRECISE POSITIONING SERVICE (PPS) - 16 M (C/A, P, Y CODES)
    - FORCE ENHANCEMENT REQUIREMENTS - MILITARY
  - STANDARD POSITIONING SERVICE (SPS) 100 M (C/A ONLY)
    - CIVIL AVIATION REQUIREMENTS
- IMPLEMENTATION OF PROTECTION
  - SELECTIVE AVAILABILITY AND ANTI-SPOOFING ON
    - CONTINUOUS - ALL OPERATIONAL SATELLITES
- ACCESS
  - PPS - AVAILABLE TO U.S./ALLIED MILITARY
    - FOREIGN / CIVIL USE REQUIRES MOA WITH ASD(C3I)
  - SPS - AVAILABLE WORLDWIDE FOR CIVIL USE

FIGURE 3

## GLOBAL POSITIONING SYSTEM CURRENT CIVIL INVOLVEMENT

- 1992 FEDERAL RADIONAVIGATION PLAN (DOD / DOT)
  - 1994 EDITION NEARLY COMPLETE
- DOD / DOT MOA ON CIVIL USE OF GPS (JAN 93)
  - CIVIL REPRESENTATIVES AT AFSPACOM & GPS JPO
  - AFSPACOM SLOT FILLED - MR. HANK SKALSKI
- DOD/DOT TASK FORCE REPORT - DEC 93
  - MANAGEMENT
  - FUNDING
  - STANDARD POSITIONING SERVICE ACCURACY
  - INTEGRITY AND AVAILABILITY
  - REGULATION OF AUGMENTATIONS
  - INTERNATIONAL ACCEPTANCE
  - SPOOFING AND JAMMING
- CIVIL GPS AUGMENTATION INITIATIVES
- BROAD CIVIL USER COMMUNITY (GOV'T / PRIVATE)

FIGURE 4

## GLOBAL POSITIONING SYSTEM (GPS) STUDIES – DECEMBER 1994

- INSTITUTE OF TELECOMM SCIENCES (NOV / DEC 94)
  - \* GPS AUGMENTATION
  - \* CONTRACTED BY DOT (DOD PARTICIPATING)
- DEFENSE SCIENCE BOARD (JAN 95)
  - \* GPS USE IN PGMS
  - \* ROBUSTNESS IN TACTICAL ENVIRONMENT
  - \* CONTRIBUTION OF TIMING TO ROBUSTNESS
- NATIONAL ACADEMY OF PUBLIC ADMINISTRATION / NATIONAL ACADEMY OF SCIENCE (APR 95)
  - \* CONGRESSIONALLY DIRECTED
  - \* STUDY ON THE FUTURE OF GPS
- OFC OF SCIENCE & TECHNOLOGY POLICY (JUN 95)
  - \* RAND CTI
  - \* GPS COMPETITIVE ADVANTAGES & VULNERABILITIES
  - \* GPS IN THE NH

FIGURE 5

## GLOBAL POSITIONING SYSTEM (GPS) CIVIL INITIATIVES (TRANSPORTATION)

- US COAST GUARD DIFFERENTIAL (COASTAL BEACONS)
- USCG / ARMY COE DIFFERENTIAL (INLAND RIVERS)
- CIVIL AVIATION
  - GLOBAL NAVIGATION SATELLITE SYSTEM (GNSS) - ICAO
    - \* GPS + GLONASS + AUGMENTATIONS TO EITHER
  - WIDE-AREA AUGMENTATION SYSTEM (WAAS) - FAA
    - \* NEAR CATEGORY I PRECISION APPROACH
    - \* INTEGRITY, AVAILABILITY (+ DIFFERENTIAL GPS)
  - LOCAL AREA DIFFERENTIAL GPS / PSEUDOLITES
    - \* CATEGORY II / III PRECISION APPROACH, LANDING
    - \* AIRPORT SURFACE CONTROL
- INTELLIGENT VEHICLE HIGHWAY SYSTEMS, TRANSIT, FARMING
  - USE AVAILABLE DIFFERENTIAL GPS SERVICE(S)

FIGURE 7

## GPS DUAL USE TACTICAL ENVIRONMENT

- U.S. / ALLIED MILITARY FORCES
  - PPS EQUIPMENT IN GENERAL USE
    - \* SA AND A-S CAPABILITIES (L1 AND L2)
    - \* ALL COMBAT / COMBAT SUPPORT MISSIONS
  - COMMERCIAL SPS EQUIPMENT PRESENT
    - \* HAZARD TO USERS / PROBLEM FOR PLANNERS
- ADVERSARIES / OTHER FORCES
  - MILITARIZED COMMERCIAL SPS RECEIVERS IN USE
  - SPS GUIDED WEAPONS LIKELY
  - AUGMENTED BY DGPS WHERE AVAILABLE
- CIVILIANS / ADJACENT NON-COMBATANTS
  - SPS WITH AVAILABLE DGPS IN WIDESPREAD USE
  - PEACEFUL TRANSPORTATION AND COMMERCE

## GPS DUAL USE CONCLUSION IMPLICATIONS FOR PTII PLANNERS

- OBVIOUS STATEMENTS OF THE WEEK
  - GPS IS AN INFORMATION RESOURCE
  - PTII IS FUNDAMENTAL TO THE EFFECTIVENESS OF GPS
- GPS OPERATIONAL ENVIRONMENT
  - SATELLITE OPERATIONS / CONTROL
  - USER EQUIPMENT TACTICAL ROBUSTNESS
  - ROLE IN SCIENCE / NATIONAL INFORMATION INFRASTRUCTURE / COMMERCE
- GPS STRATEGIC ENVIRONMENT
  - GLOBAL, DUAL USE RESOURCE
  - SCIENCE, COMMERCE AND SECURITY MUST BE BALANCED

FIGURE 8

## QUESTIONS AND ANSWERS:

**JIM WRIGHT (CSR):** Is there a published doctrine, or will there soon be a published doctrine, that suggests that DoD activities used in GPS will have to have Y-code receivers?

**JULES McNEFF:** Within the DoD there is already published guidance that says that we expect the services to use Y-code equipment and not commercial equipment. Unfortunately, that is contained in some otherwise classified documents so I don't that it's published. It's in our security policy document, which is a classified document for other reasons. It's in some other correspondence.

It is in an unclassified letter we sent to the services back on the 30th of April, '92. This sort of fundamentally lays out a whole range of user equipment procurement guidance that applies to GPS equipment, such as that the services will use PPS equipment for all of combat and combat-related missions; and only consider SPS for missions that don't involve combat, such as training, some developmental work, and things like that where the platforms won't stand a chance of being involved in combat and a bunch of other things.

So it has been published. That memo's been pretty widely distributed throughout the DoD. But not publicly per se.

**JIM WRIGHT:** How can one get a copy of that memo?

**JULES McNEFF:** Give me a call.

**JOHN VIG (ARL):** A great deal of money has been spent on developing GPS and the PTTI aspects of GPS. But most of that money was spent on the satellite clocks. Do any of those studies that you mentioned address the role of PTTI in the user segment? And are there any plans for using better clocks in the user equipment to acquire the Y-code, for example, and things like that?

**JULES McNEFF:** The study that would look at that is, I would say, is the Defense Science Board Study where they are looking at ways to improve the individual performance of user equipment in a face of jamming or other loss of signal. But what recommendations they're going to come out with in terms of upgrading the user equipment with different on-board timing sources, I don't know. That's the one study that would likely address that aspect of it.

**JOHN VIG:** Do you know who the technical experts are in that study? Is there any way of getting to them to let them know what might be do-able?

**JULES McNEFF:** I'll tell you who they are. We can do that off line. In fact, Dr. Winkler briefed the DSB group here a couple of months ago, I guess, on some aspects of time, related to the issues that they were looking at.

# DoD PTTI Report

CAPTAIN RICHARD E. BLUMBERG  
Superintendent  
United States Naval Observatory  
Washington, DC

## Abstract

*The widespread application of Precise Time and Time Interval (PTTI) in modern electronic systems has been rapidly expanding. This growth reflects the importance of PTTI to many advanced systems. Precise time is closely related to precise distance measurements, the coordination of remote actions over extended periods of time, and the better utilization of the frequency spectrum. DoD Instruction 5000.2 emphasizes the need for a common time reference (The USNO Master Clock) for these systems of vital interest to our security. This report will present the results of the Annual PTTI Summary which describes the utilization of PTTI among the different components of the Department of Defense and highlight areas of primary interest and concerns.*

It's a pleasure to once again address you this morning. I'm still tickled over the award presentation earlier this morning. It's well deserved and always nice to get recognition from your peers. And I'm honored to have had the opportunity to present the award in their behalf.

What I would like to do is talk a little bit about major PTTI accomplishments in '94 (Figure 1), where we're headed, and where you can help us in terms of PTTI. Validation of requirements was a significant effort last year, particularly in this day and age of downsizing of resources. Everything is tied back to a requirement; and it's absolutely vital that every one of those requirements be stated and documented in order to go on from there. I'll talk a little bit about improvements to the Master Clock and then to two-way satellite time transfer. With regard to requirements (Figure 2), we took the 1990 survey as a baseline, and essentially re-validated that. In the re-validation process, we determined what the requirements really were for precise time and time interval and who our customers are out there – who uses it and of those who use it who don't recognize that they use it (which is a big problem in precise time). As Mr. McNeff stated, it's free, it's available anytime you want it; you just don't appreciate what's behind that timing signal. Our requirements have been validated by the Oceanographer of the Navy and have been submitted to the Office of the Secretary of Defense. So the requirements are, in fact, entered into the official DoD requirements process, covering not only Navy, but also the Air Force and Army requirements as well.

Improvements to the Master Clock (Figure 3): We are continuously improving the Master Clock. The big improvements for the previous year, a plus year, were replacing a number of the older 5061s with the newer HP 5071 cesium beam clocks. There are 10 hydrogen masers which have been incorporated into the time scale. The biggest comment I could say

on the Master Clock is that the effects of the improvements to the Master Clock can be seen by the contribution of the U.S. Naval Observatory (USNO) to the Bureau International des Poids et Mesures (BIPM), changing to 38 percent from last year's 20 percent. This significant improvement, is largely due to the better stability and, I should say, maybe the better reliability, of these clocks. We retain many of the 5061s, as they're still providing accurate, precise time, and we will continue to keep these clocks in the time scale as long as they continue to perform.

Keeping time is one thing, getting it out to the people who need it is another issue altogether. It doesn't do us any good to have the best time in Washington, D.C., if we can't disseminate it. We have made some significant improvements in the two-way satellite time transfer (Figure 4) this year. The technology transfer from the Naval Research Laboratory (NRL) of their modem to the commercial market was a big accomplishment. These modems are, in fact, operating much better than previously expected. Certainly the production models are really doing the job that they were designed to do.

We've been using the Defense Satellite Communication System (DSCS) for time transfer. It has been working exceptionally well. We have also been doing some experiments with commercial satellites as well. You will hear early in the program discussions of two of the calibration trips, one to Europe, between some of the laboratories in Europe, as well as a trip to the West Coast, using satellite two-way time transfer and an ensemble of clocks from the USNO.

Now, with regard to some of the newer issues in '94 (Figure 5), we are trying to tell our story to the people who need it. We did strengthen the master navigation plan. The reference for the wide-area augmentation system (WAAS) of the FAA will be UTC(USNO), the same reference that is used for the GPS system. So we will have again a single timing reference for both the FAA wide-area augmentation system and the GPS system, itself.

With regard to the GPS monitor station upgrade: By creating an independent clock ensemble at each of the GPS monitoring stations, we will allow the GPS operational community to detect immediately if they have a problem, because they will have the capability of an independent timing signal with which to compare the satellite performance with the monitor station timing signal. This program is underway. You will hear a little bit more about that later on, as well. Development of ultra-high precision timing reference stations at a number of special sites is also continuing worldwide.

Continuing on with accomplishments for '94 (Figure 6): The NATO standard agreement, STANAG 4430, on precise time and frequency interface for NATO was signed. It uses UTC(USNO), tied to the BIPM, as the standard for NATO operations. In support of DISA and the DSCS, as LORAN is shifting from U.S. control to European and Japanese control, USNO is helping to coordinate the timing signals for those systems at the local levels. Our role, particularly in the European area, is to provide some atomic clocks during that transition period, to ensure that timing — again, particularly in Europe — is maintained without interruption until alternate sources are provided. Some cesium clocks have been loaned to the Defense Satellite Communication System so that their timing could be maintained to a standard time. USNO has also transferred clocks to the Autodyn system for the same sort of function — to provide a standard to compare their time to ours.

One of the other items that I wish to stress is the fact that what has been accomplished has been done in the face of DoD downsizing. Our resources are really getting smaller. One of the keys to being able to accomplish those things that I showed for '94 have been the people who have been involved in the programs, and their efforts to get the job done, and to do it on a shoestring, so to speak. Keep in mind, as we will talk a little bit about these things later on in the conference, that we are facing downsizing reduction in the funds that not only buy hardware and improve the software, but also in the number of people who are able to perform these functions. And it's really vital that the folks in this room carry the message of PTTI.

Some of the functions and objectives of the PTTI manager are shown in Figures 7 and 8, respectively. This is a slide from last year, but I wanted to bring it back this year because it still applies. We need to ensure the uniformity of PTTI. We're doing that and working continuously to tell the story that all the communication and navigation systems need to be tied into one standard for time. I can't imagine a more chaotic situation than to have two timing standards and have them off by even a few nanoseconds. It would just create a nightmare. And again, most of you in here appreciate that. But we really need to get that message to the program managers and project managers, both in the commercial market as well as in the DoD, and ensure that they pay attention to the timing signals within their systems.

The requirements process which we went through last year did a good scrub on the requirements. But I'll guarantee you that there are many that have emerged since then that we are not aware of and have not begun to even look at in terms of their impact. The most stringent requirement that came out of that, potentially a future requirement at the 100 picosecond ("ps") level. If we're going to push to that level, certainly the Observatory needs to have a tenfold better capability, in-house, so that we can transfer time to that 100 ps level to those customers. We aren't there yet. We need to get there.

And that leads into the necessity for research. Such things as the mercury ion device — we have three of those that we are using and will add them into the time scale in the near future. It is still an R&D effort. We are still not certain exactly whether the mercury ion device is the device of the future or will allow us to approach that 100 ps level. But again, industry is looking in that direction, and I think we will push that technology edge here in the near future.

Adequate infrastructure support is really a problem in the downsizing world. As I alluded a little earlier, our dollars that were there two or three or four years ago are not there now. We continue to decrease and lose funding. We aren't seeing the impacts yet; the 5071s are brand new clocks, and there is very little maintenance required for them. But in the out years, I have concerns on the funding levels. Will we be able to maintain the infrastructure and the number of pieces necessary to keep the Master Clock ensemble accurate as well as reliable?

Concerning the utilization of PTTI resources: We work very closely with the GPS in two ways, operations and development. We need to continue similar cooperative efforts for PTTI resources in other areas such as fleet support and planning conferences. There is also a particular problem in the training area. The training in precise time and the ability to maintain equipment on site at the various stations is a concern. In all of our training courses, particularly in the DoD, the emphasis is to minimize the training pipeline and get people through as quickly as you can. Timing is certainly one of those things that is frequently overlooked. It's an

issue with which we continually do battle. We will continue to try to strengthen the training opportunities in PTTI.

That's a quick and dirty overview of the highlights for '94. The challenges for '95 are even more severe in terms of our resources. I'm happy to report that right now we're able to protect our people, who are our most valuable resource. Conversely, our people will then be challenged to continue to do more with less. We've heard it for years; it is a reality today. It certainly is a reality at the Observatory.

## QUESTIONS AND ANSWERS

**MR. KEATING:** This is not so much a question as a comment. I just want to reiterate Capt. Blumberg's comment about training, because I have actually listened to some conversations over a telephone to remote locations such as Hawaii and the Far East. And when you tell a person to move his clock ahead by two microseconds, 50 percent of the time the person on the other end causes actions which moves the clock in the exact opposite direction. And while that could be considered funny, when you're trying to maintain timing synchronization, that's a disaster. So I just want to emphasize that if you're a manager, don't downplay the need for training of your people.

**RAYMOND CLAFFIN (CLAFFIN ASSOCIATES):** Do you see in the new Congress any chance that this type of scientific military endeavor is going to receive any additional funding? Because, your needs really aren't as big as that of some of the other programs.

**CAPT. BLUMBERG:** That's one of our biggest problems, we are not as big as other programs and don't get the visibility that a lot of other programs do get. But I am a little optimistic that we will see the DoD budget grow in the future. How long it will take and at what point it does really benefit us is a real question mark. I mean, we have some serious problems across the board within DoD in terms of funding capabilities of getting our ships to sea, getting them properly manned, getting the personnel trained. And unfortunately, as I mentioned earlier, the timing is lost a lot of times in the hustle and bustle in trying to get things done. And so, again, it's our role in here as program managers, certainly my role, to promote timing with my resource sponsor and get him to promote within the Navy and the DoD to try to get the additional funding we need to get on with it.

So in answer to your question, I don't know specifically whether I can be optimistic or not. But I at least feel that we have an opportunity now to fight for a small share anyway.



# Precise Timing Applications at the Defense Mapping Agency

Stephen Malys  
Defense Mapping Agency

## Abstract

*The mission of the Defense Mapping Agency (DMA) focuses on satisfying the Mapping, Charting and Geodesy (MC&G) requirements of the U.S. Department of Defense (DoD). DMA satisfies these requirements by supplying a broad spectrum of products and services to its DoD customers. In many cases, DMA's products and services are also available to civilian and international organizations. Within this myriad of products and services, two DMA processes employ atomic frequency standards. Both of these operational processes fall in the discipline of geodesy.*

*DMA's geodetic exploitation of the Navstar Global Positioning System (GPS) is one area which requires precise timing. Since 1989, DMA has generated precise ephemerides and clock state estimates for the GPS satellites. This process depends on the performance of atomic oscillators in place at five DMA and five Air Force GPS monitor stations. This geodetic application also requires routine knowledge of the difference between Coordinated Universal Time (UTC) and the Earth's rotation rate (UT1). Another DMA process which relies on precise timing falls under the discipline of gravimetric geodesy. In addition to the routine collection of conventional (relative) gravity observations, DMA also collects measurements of absolute gravity at discrete points on the Earth's land surface. These absolute gravity observations are collected with a specialized instrument (an absolute gravity meter) which measures the speed of a falling object. This instrument employs an integrated rubidium frequency standard which is used in the measurement process. These DMA applications of precise timing are reviewed and discussed.*

## INTRODUCTION

Beginning in the 1970s, before the dawn of the Navstar Global Positioning System (GPS), DMA employed precise timing devices at a globally-distributed network of Doppler tracking stations. This network, when terminated in September 1993, consisted of approximately 40 stations. These tracking stations used either the MX 1502 DS receiver or the TRANET II receiver. In this network application, both receiver types employed rubidium frequency standards as a precise timing source. The satellites tracked by these stations emitted the well-known 150/400 MHz 'Beacon' signals. The Navy's TRANSIT and GEOSAT satellites are probably the most widely-known examples of DoD missions which relied on the DMA Doppler tracking network. Perhaps one of the largest collections of atomic oscillators managed by one organization, the frequency standards associated with the DMA Doppler network have now been dispersed to other applications within the DoD. Some of these frequency standards now serve as backup units to the DMA GPS monitor stations.

Currently, DMA uses precise timing devices in the geodetic exploitation of GPS and in a gravimetric geodesy application. These applications are discussed below.

## PRECISE GPS ORBIT DETERMINATION

As most GPS users know, the entire GPS concept is based on our ability to precisely measure time and time interval. A common phrase used to describe the GPS concept to new users of this technology is 'clocks in space'. While these on-board cesium and rubidium frequency standards have been studied and described elsewhere, the clocks on the ground at the DoD GPS monitor stations are also an important component of the GPS constellation and will be discussed in some detail here. The global distribution of Air Force and DMA tracking stations is shown in Figure 1. The 'smoothed' pseudorange data collected by these stations are used in the DMA orbit process to estimate orbit, clock, and other parameters on a routine basis. Unlike the estimation process used at the GPS Operational Control Segment (GPSOCS), the DMA orbit/clock estimation process requires the designation of a 'master clock'. The offset and drift (phase and frequency) of this master with respect to 'GPS time' is held fixed during the estimation process. Because the designated master clock is not synchronized and syntonized with GPS time, all clock estimates generated in the DMA process are subsequently adjusted into coincidence with respect to GPS time through an empirical procedure which computes and applies the mean difference between DMA satellite clock estimates and the GPSOCS satellite clock estimates which are referenced to the GPS 'composite clock'. A detailed description of the GPS composite clock is given in Brown [1991].

To provide additional geographic coverage and to eliminate the complication of choosing a master clock for each weekly processing span, a sixth DMA station is being installed at the US Naval Observatory (USNO), located in Washington D.C. This DMA/USNO station will consist of hardware which is identical to other DMA stations (Figure 2) with one important exception. In place of the usual single cesium frequency standard, this station will employ the USNO atomic clock ensemble which supplies our national time standard: UTC (USNO). Beginning in mid-1995, the continuous stream of GPS tracking data collected by this station will be used in the DMA orbit/clock estimation process. Because of its extremely high reliability, the USNO clock ensemble will serve as the permanent master clock in the DMA process. The empirical adjustment procedure described above will remain in use because GPS time is not completely synchronized with UTC(USNO). If the adjustment procedure is not performed, the DMA satellite clock estimates would be expressed with respect to an extrapolation of UTC(USNO) based on a particular epoch, rather than GPS time. Of course, the magnitude of these adjustments is commensurate with the level of coincidence between UTC (USNO) and GPS time, currently on the order of 10 nanoseconds [NRL, 1995].

## UT1-UTC

Any precise orbit determination process requires the application of a transformation from an Earth-Centered, Earth-Fixed (ECEF) reference frame (WGS 84 in DoD applications) to an Earth-Centered Inertial (ECI) Reference Frame (such as J2000). This transformation

incorporates knowledge of the variations in the Earth's rotation rate and polar motion. The difference between UTC and the time scale based on the Earth's rotation (UT1) enters directly into the ECEF to ECI transformation. To satisfy this need for several DoD satellite applications, DMA generates weekly predictions of UT1-UTC and polar motion which are collectively referred to as Earth Orientation Prediction Parameters (EOPP). These DMA predictions are generated in conformance with an Interface Control Document (ICD-GPS-211) and are based on weekly 'Bulletin A' International Earth Rotation Service (IERS) rapid service information supplied by the USNO Earth Orientation Division.

While significant advancements in atomic frequency standards have occurred over the last few decades and GPS-time was designed to allow most users to avoid the complication of leap seconds, GPS and other practical orbit determination applications continue to employ these advancements in concert with precise knowledge of the Earth's rotation rate. The predictability of the UT1-UTC parameter will continue to play a key role in these practical DoD applications. Inevitably, all satellite tracking measurements must be tied to stations which reside on the rotating Earth.

## **ABSOLUTE GRAVITY MEASUREMENTS**

The structure of Earth's gravitational field has been studied through the use of several technologies including traditional relative gravity meters, analysis of orbit perturbations observed through satellite tracking data, satellite altimetry data and the recently-developed transportable absolute gravity meter. The absolute gravity meters developed in the US measure the speed of a falling corner-cube reflector in an evacuated 'dropping chamber'. A detailed description of this instrument can be found in Carter et al, 1994. To obtain a gravity observation accuracy of a few microgals (1 microgal =  $1 \times 10^{-8} \text{ m.s}^{-2}$ ) an accurate length standard and an accurate time standard are needed. The length standard is established by an iodine stabilized laser while the time standard is established by a rubidium frequency standard. To obtain the microgal-level gravity observations, the stability of the frequency standard used in this process needs to be on the order of 5 parts in  $10^{10}$  (over a range of intervals) and the length standard needs to be accurate at a level of 1 part in 1010 (Niebauer, 1994). While the requirements on the frequency standard are not particularly demanding, practical considerations such as the size of the instrument and the amount of time needed to 'warm-up' limit the widespread use of these absolute gravity meters. Technological advancements which would reduce the size and warm-up time of atomic frequency standards would help to promote further miniaturization and portability of these devices.

## **SUMMARY**

Two areas of DMA's geodetic mission require the application of atomic frequency standards. The first area revolves around precise GPS orbit and clock estimation. To assist this process, a sixth DMA GPS monitor station will be installed at the USNO in Washington D.C. in mid-1995. The USNO clock ensemble will serve as the time standard for this DMA 'master station'. Additionally, the USNO's Earth Orientation Division will continue to supply the basic

observational data on the variation of the Earth's rotation and its polar motion.

The second area of DMA's mission which requires atomic frequency standards is the measurement of absolute gravity on the Earth's surface. The transportable absolute gravity meters developed in the U.S. require a frequency stability of 5 parts in  $10^{10}$  over a range of intervals. This requirement is now met by an off-the-shelf rubidium standard. Advancements in the development of future, smaller, easily portable absolute gravity meters require that the frequency standard also becomes smaller and more portable. For this reason, further miniaturization of atomic frequency standards would directly benefit the development of smaller absolute gravity meters.

## REFERENCES

- Brown, K.R., "The Theory of the GPS Composite Clock", Proceedings of the ION Satellite Division's 4th International Technical Meeting, ION GPS-91, Oct 91
- Carter, W.E., Peter, G., Sasagawa, S., Klopping, F.J., Berstis, K.A., Hilt, R.L., Nelson, P., Christy, G.L., Niebauer, T.M., Hollander, W., Seeger, H., Richter, B., Wilmes, H., and Lothammer, A., "New Gravity Meter Improves Measurements", Eos, Transactions, American Geophysical Union, Vol 75, No. 08, Feb 22, 1994, Pages 90-92.
- Naval Research Lab, GPS Performance Improvement Options Meeting, GPSJPO, 17 Jan 95.
- Niebauer, T.M., Personal Communication, Nov 1994.



# DoD GPS Tracking Network

- Air Force Tracking Station
- DMA Tracking Station

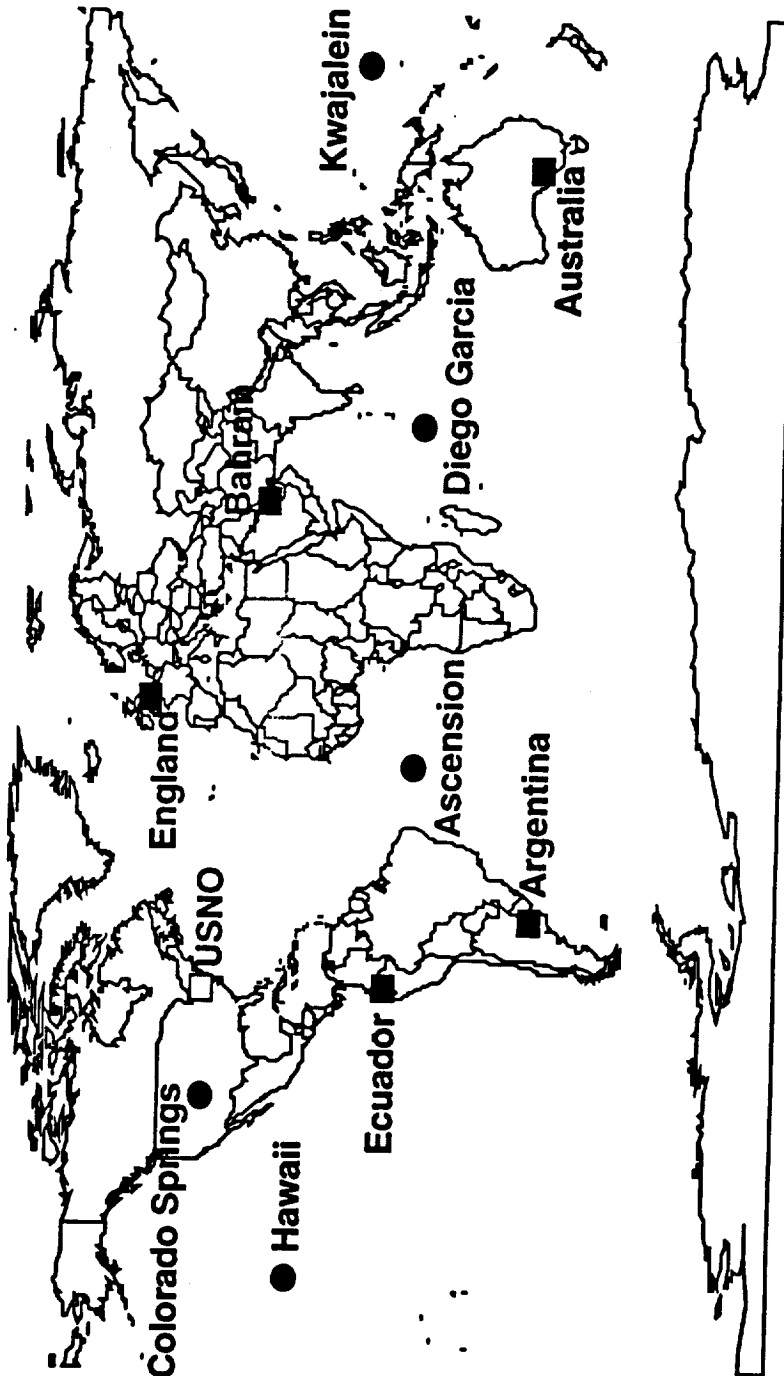


Figure 1

# DMA GPS Monitor Station

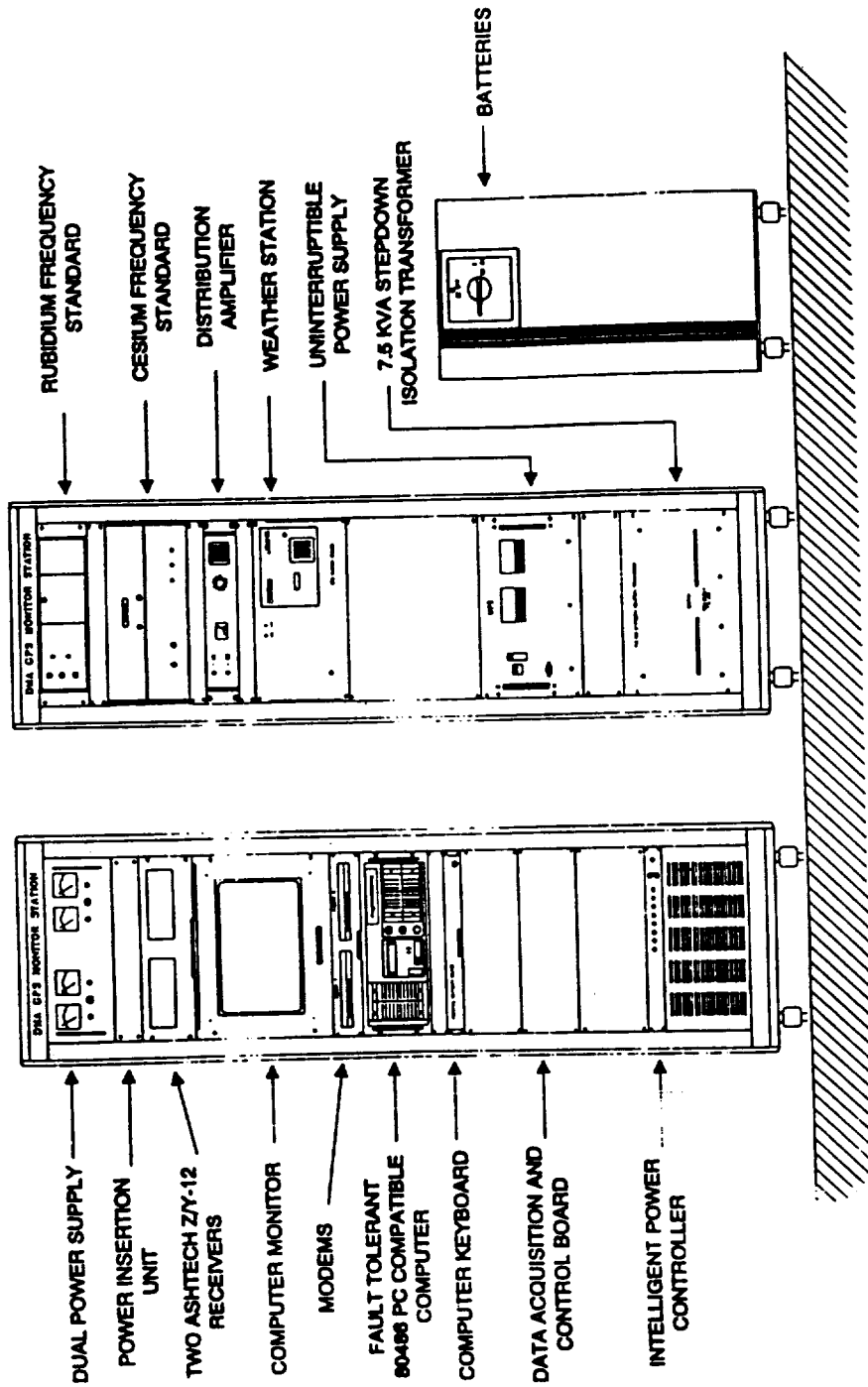


Figure 2

## QUESTIONS AND ANSWERS

**PETER WOLFF (BIPM):** I have two questions. First, can you give an order of magnitude on your orbit accuracies and clock offset accuracies?

**STEPHEN MALYS (DEFENSE MAPPING AGENCY):** Yes. Together, if you think about the orbit accuracy in terms of range error when you use the DMA ephemeris and clock together, we get range errors on the order of a half a meter. That would be considered an RMS over a day or the general performance level.

If you're asking for a more specific breakdown of orbit error versus clock error, it's somewhat higher than half a meter. We see each component to run about one meter, but it varies by component.

**PETER WOLF (BIPM):** Okay. And secondly, the order that you use for your orbit determination, is it in the form of differences of data between two stations? Are you differencing the ranges or is it just the direct range measurements that you get by each station?

**STEPHEN MALYS:** It is the direct range measurement. We refer to it as a smooth pseudo-range. It's the same observable that's used in the master control station's orbit determination process, but it is strictly a range measurement.

**PETER WOLF:** And that's affected by SA in new data?

**STEPHEN MALYS:** Well we remove SA; we have a facility to remove it.

**JUDAH LEVINE (NIST):** The absolute gravity measurements have a first order correction to the barometric pressure of both local and regional. Could you say a little bit about how you do those kind of corrections?

**STEPHEN MALYS:** I didn't come prepared to answer that particular question. I know that the clock stability and, of course, the link standard are two of the primary things you have control over when you make the measurement. We certainly do take barometric pressure into consideration when we take those gravity observations.

When you're looking for the best possible precision, there are many things that you have to take account of, even things such as the amount of ground water that's present at the time that you take the observation. So it's get rather complicated when you're trying to squeeze out every single milligal.



# Navy PTTI Report

CDR. JIM BURTON  
United States Navy

## Abstract

*The U.S. Naval Observatory is charged under Department of Defense (DoD) instruction 5000.2 with the responsibility for maintaining the timing standard in support of all DoD operations. Accomplishment of this task involves generating a time reference and then disseminating the Precise Time and Time Interval (PTTI) information to users within, as well as outside, DoD. A major effort has been undertaken by Navy scientists in recent years to upgrade and improve these services. Understanding the characteristics of atomic clocks, such as hydrogen masers, cesium beam frequency standards, and stored ion devices, is a prerequisite for modelling their performance and developing the most stable time reference possible. Algorithms for optimum clock ensembling and precision clock steering must be developed to ensure the stability of the time reference. Implementing new methods for time transfer, such as two-way satellite time transfer and laser ranging, will lead to improved accuracies to less than one nanosecond. In addition, the determination of astronomical time based on the Earth's rotation and definition of parameters for the position of the poles, enable the correction of the dynamical reference frame of Earth-orbiting satellites to an inertial reference frame, which is needed to improve the precision of satellite orbits. Current and planned initiatives in PTTI within the Navy, such as those listed above, are described.*

It is a great pleasure to address you this morning. I'm Jim Burton. I'm the GPS Action Officer for N6 and I am the U.S. representative to a NATO subcommittee on navigation. Ron Beard is also a member of this NATO subgroup. Today, I will talk very briefly about Navy-funded initiatives concerning work in PTTI (Figure 1).

There are three major achievements which I will address today:

- a) the GPS monitor station upgrade;
- b) the technology transfer of the modem that NRL developed; and
- c) the USNO Time Service Substation being rebuilt in Florida.

First, the GPS monitor station upgrades (Figure 2). When the upgrades are completed, each monitor station will be an ensemble of three cesium clocks, one of which will be a standard that's connected to the USNO through a two-way time transfer. As we collect the data from this ensemble and compare it to the existing operations, it will enable us to better model the clock rate errors and separate the clock and ephemeris errors a little bit better than is being done right now. This is all part of Navy initiatives to improve the accuracy of GPS and the integrity as well.

With the third clock that we'll be installing in each of the monitor stations, we'll have the capability to work independently of the two clocks that are currently operating within the monitor station. But even if it's operating independently, it will enable us to gather the data and do the diagnostics to better model the system for accuracy improvements in the future.

Secondly, NRL developed a pseudorandom noise time transfer modem (Figure 3) for the basic requirement of providing a communications capability besides just passing time pulses back and forth through the modem. It also gets a U.S. vendor into the market, so we are not relying on vendors from Germany; now we have Allen Osborne and Associates as the American vendor.

Finally, concerning the restoration of the USNO Time Service Substation (Figure 4) which was destroyed in Hurricane Andrew, a couple of years back, it is basically restored. It is going through the final stages of testing before it's back on line as a fully certified backup.

Since I'm here to replace Dave Markham, who was not supposed to be here, I will be happy to answer any questions – or at least point them in the right direction.

**DAVE MARKHAM:** Let me elaborate on Cdr. Burton's last comment. Those of you who didn't hear the story yet, I was supposed to be in Bahrain today. But unfortunately through a "snafu," as we say in the Navy, my orders and tickets were withdrawn and I'm here instead. He was gracious enough to stand in for me and give the presentation that I was supposed to give. So I thank him and I appreciate your support, Jim.

# STATUS OF PTTI IN THE U.S. AIR FORCE

Howard A. Hopkins and Robert E. Blair, Jr.  
Directorate of Metrology  
Newark Air Force Base, Ohio

## Abstract

*Throughout the world, Air Force activities rely on timing equipment calibrated and maintained by a network of Precision Measurement Equipment Laboratories (PMELs). These PMELs operate within guidelines established at Newark Air Force Base under the Air Force Metrology and Calibration Program. What will happen to the Program when the Newark base closes in October, 1996, a victim of government downsizing? This paper looks at the plan to privatize in place, i.e. to bring a contractor on site to perform the same workloads that are presently done by Federal workers. It discusses the reasons for privatization and looks at some of the changes expected to occur. Most importantly, it considers the problems involved and the potential impact of privatization on timing support throughout the Air Force.*

## INTRODUCTION

Many Air Force activities need precision timing systems for a variety of applications. These include tracking satellites in space, operating command and control communications networks, test ranges, radar warning systems, and other electronic surveillance programs. For precise time support, these activities rely on timing equipment calibrated and maintained by their local base Precision Measurement Equipment Laboratory (PMEL). Under the Air Force Metrology and Calibration (AFMETCAL) Program, PMELs located throughout the Air Force have a responsibility to provide precise time and frequency (PTTI) support to their area customers.

## NEWARK AIR FORCE BASE FUNCTIONS

The Directorate of Metrology (ML), located at the Aerospace Guidance and Metrology Center (AGMC) at Newark Air Force Base, Ohio, provides the capability for PTTI support at twenty-seven PMELs selected to meet that responsibility around the world. As managers of the AFMETCAL Program, ML provides those PMELs with the measurement standards and equipment, calibration procedures, and management data that they need. Equally important, ML analyzes new calibration requirements and provides an integrated planning function to assure that PMEL support for PTTI is in place when needed. Finally, ML provides technical assistance to all PMELs through its staff of engineers, technicians, and logisticians.

Another important function of the Directorate of Metrology is the operation and maintenance of its computer controlled Precise Time Reference Station (PTRS). Using the common-view

technique, the station interfaces via modem to the United States Naval Observatory (USNO). ML receives timing data continuously from Global Positioning System (GPS) satellites and the LORAN-C system and compares it with signals from ML's master cesium beam frequency standard. Each day, the USNO extracts data from ML's PTRS and adjusts the master standard to maintain a reference with an uncertainty no greater than twenty nanoseconds. ML owns two additional cesium standards which it tracks against the master standard. Having this redundancy is useful in identifying the cause of any systematic problems which may occur in the PTRS.

ML has provided a Precise Time and Frequency Console (PTFC) to each PMEL with responsibility for timing support. The PTFC includes a cesium standard, GPS receiver, LORAN-C receiver, and the associated equipment required to maintain a time reference without additional support from ML. What then is the purpose for ML to maintain its PTRS? First, the PTRS provides what is officially recognized as the Air Force Standard for Time and Frequency. Using portable cesium standards, this reference can be transferred quickly to any PMEL or remote site to restore service lost to equipment failure or damage caused by man made or natural disasters. Secondly, the PTRS serves as an in-house reference for several activities at Newark Air Force Base which require a precise frequency reference. One of these is the Technical Repair Center for precision frequency standards, otherwise known as the Clock Shop. This activity, located in the Directorate of Maintenance, provides repair services for cesium, rubidium, and other types of precision frequency standards located throughout the Air Force. A third use of the PTRS is to provide ML the capability to test new time and frequency equipment prior to acceptance.

## BASE CLOSURE

Over the past two years, the draw down in Defense spending has had a major impact on Newark Air Force Base. In June, 1993, the Base Realignment and Closure Commission (BRACC) added Newark to the list of recommended base closures. By September, the closure was signed by President Clinton and approved by Congress. The closing date established as an Air Force goal is 1 October, 1996.

While many DOD installations have closed or are scheduled to close, Newark is different in one respect. The workload being performed at Newark is recognized as work that must continue to be performed there. Even though it is scheduled to close as an Air Force base, there is still a requirement to keep the facility open and operating to accomplish the same workload. To accomplish this, the Air Force has come up with the concept of privatization in place. Essentially, this means a contractor will take over the same facility and equipment used by the Government and continue to perform the same workload as the Government does now. This all becomes complicated by questions such as: a. Is the contractor expected to buy the facility and/or the equipment? b. What wage rates will the contractor pay? c. Will the contractor be able to retain the expertise of the present government work force? d. Who will ensure the contractor provides adequate support to the field? These issues and many more are being addressed now as a statement of work and request for bids are being prepared.

The Directorate of Metrology presents an especially sticky problem to the planners for base closure. After months of study, cost analysis and discussion, officials were able to convince first, the Air Force Materiel Command and later, the Base Closure Executive Group in Washington

D.C. that specific functions of the AFMETCAL Program must remain as government functions. These functions are calibration procedure management, laboratory certification, and equipment budgeting and acquisition. The remaining functions, including preparation of calibration procedures and all elements of the Air Force Measurement Standards Laboratories, will be privatized in place. This latter category includes the laboratory group responsible for the Precise Time Reference Station.

What will happen to the PTRS and what effect will privatization have on PTTI support for the Air Force PMELs? At this point, it is impossible to say with any certainty. Even major decisions are subject to change at any time. We know for sure the PTRS will be upgraded this fiscal year with three new cesium standards, a new GPS receiver, time interval counter, 486 computer, and other associated equipment. At this time, the plan is to turn the new system over to the privatization contractor as government furnished equipment when the base closes.

What will happen then depends upon the level of expertise brought in by the contractor and the interaction of the contractor with the remaining government personnel. We assume the contractor will want to retain the present Federal workers as much as possible. This may be possible in some cases and not in others because of each individual's situation. For example, how close to retirement is the person? How many social security credits does he have? Does he want to stay in the local area? The DOD's Priority Placement Program is working too well in providing employees other job opportunities in Government. By the time the base closes, there may be no expertise left for the contractor to use. There is supposed to be a one-year transition period, beginning 1 October 1995, during which Government personnel will be expected to train the contractors to take over their jobs. This experience should provide some interesting insights to human behavior.

Since the PMELs have a Precise Time and Frequency Console providing their time reference, they require little from Newark on a daily basis. If the contractor lacks expertise in this area, the impact on PMELs may be limited to the problem of technical assistance not being available. The impact at home may be much worse if accurate frequencies cannot be provided to local customers and new equipment cannot be tested with any validity.

"What will happen to Newark's Clock Shop?" is another question frequently asked by those customers who rely on the Clock Shop to repair their frequency standards. At this moment, it looks like the Clock Shop will remain an Air Force function and transfer to one of the large Air Force depots. If that happens, it would lose access to Newark's PTRS, but could still function well with the reference available through GPS. Again, the level of expertise in the Clock Shop could become a problem if that activity is relocated.

## **OTHER ISSUES**

Outside of base closure, another issue affecting the status of PTTI is the formal training provided by the Air Force. With the closure of Lowry Air Force Base in Colorado, the PMEL School located there was moved to Keesler Air Force Base in Mississippi. As far as we know, the PTTI Course is still being taught at the new location.

A final issue being addressed now is the loss of the overseas LORAN-C chains as the U.S. Coast

Guard turns over control of them to the host countries at the end of this year. Many overseas bases, beyond those having the PTFC, have depended on LORAN-C for a frequency reference. Anticipating there may be a problem with reliability under the host country arrangement, Newark has purchased cesium frequency standards for each of those bases, thereby eliminating their requirement for LORAN-C.

## **SUMMARY**

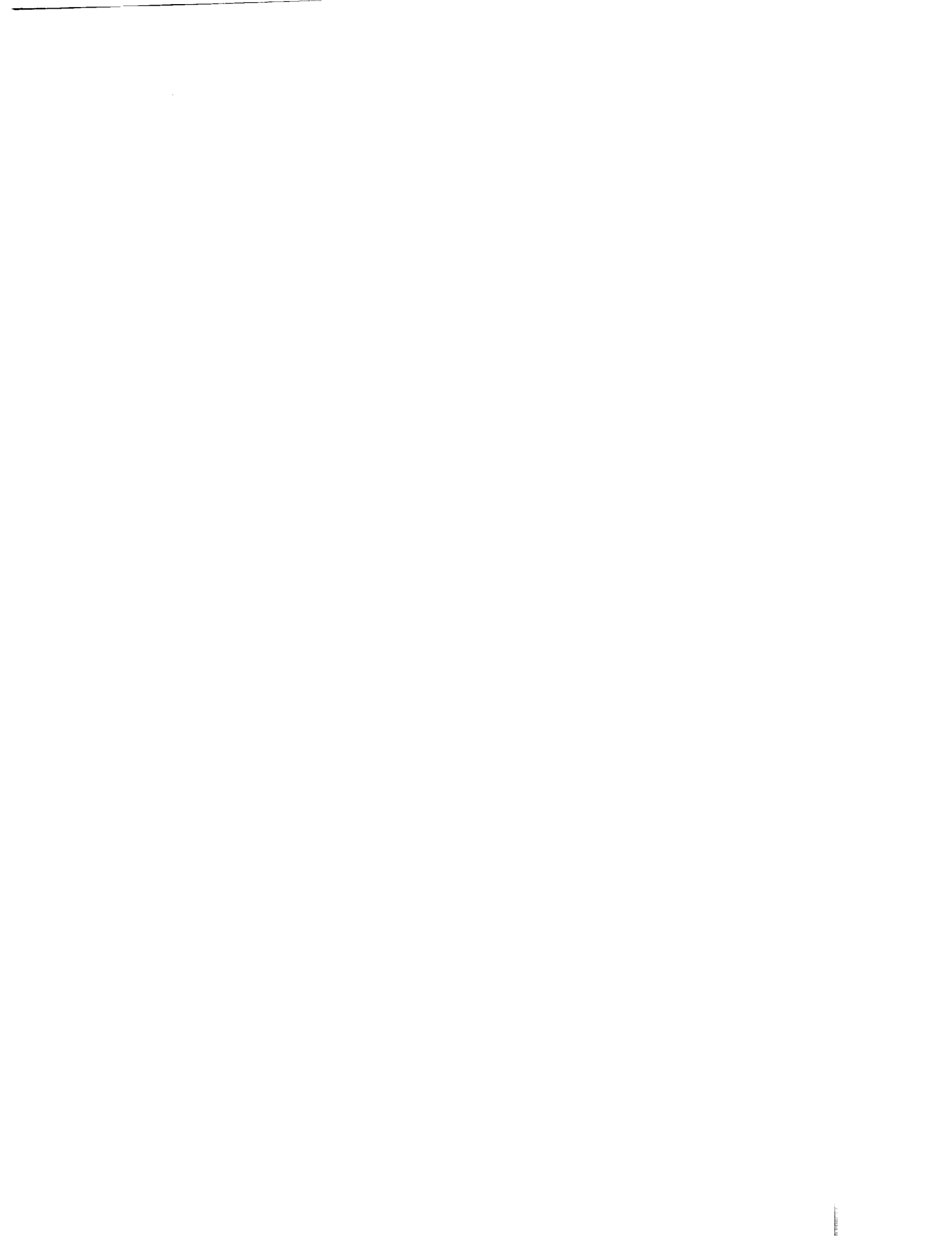
Stepping back for a broad look at the issues affecting PTTI in the Air Force, we see the closure of Newark Air Force Base as the number one potential problem. Uncertainty surrounds the whole concept of privatization in place and how it will be implemented at Newark. Planners are working hard to achieve a stable transition to a contractor environment but, at the same time, a steady stream of employees with decades of experience are leaving for new jobs.

## QUESTIONS AND ANSWERS

**WILLIAM WOODEN (DEFENSE MAPPING AGENCY):** Is the intent that the contractor will go and do all of these calibrations of all the sites that you have for the testing? Is that part of the plan?

**ROBERT BLAIR (USAF):** I'm not certain of that. That's to be determined. Right now that could create a sticky situation having one contractor verify that another contractor is living up to his obligation. That's part of the unknowns at the moment. Nothing will be firm probably until October of this year. At the level I'm at, I am the precise time technician, I'm not a manager. So I don't know if I would ever know the answer to that.

But I would certainly hope that there needs to be something in there to guarantee that the Air Force is going to continue getting what it's paying for.



# WORKSHOP 1; REAL WORLD USER REQUIREMENTS

Some of the problem areas discussed were:

- Incomplete specifications from users.

User either doesn't know enough about the subject to give complete specifications or is not capable of generating the necessary specifications for his application. The supplier can't get complete specifications as a result.

- Incomplete specifications from suppliers.

The suppliers/manufacturers usually supply the basic generic information on the units, expecting the user to be able to ask the specific questions pertaining to the particular application. Many users are unaware that other (non-standard and usually not tested) specifications may be available at an increased cost that will make the unit under question fit his application. The problem here is a lack of communication between the supplier and user. Often the supplier could eliminate some of the possible trouble later on by careful questioning of the user as to the exact application.

As a result of the above problems, these actions should be taken:

1. Suppliers should **question** the user supplied specifications and assist the user in generating the correct ones.
2. User misunderstanding of specifications and applications should be educated, either by studying the literature or by efforts of the supplier. Typical sources for this information are the MIL SPECS, PTTI Proceedings, FCS Proceedings, etc.
3. A clear understanding of such environmental problems as vibration is often missing. Since this data is usually missing from data sheets, the user forgets about it, especially since his application is in a "non-vibrating environment". Suggestion is for the supplier to give some indication in the data sheets about the vibration sensitivity of the unit and vibration levels for typical environments.

Another problem that was brought out was the supplying of precise time to various users within an installation with long cable runs. It was pointed out that a number of papers have been given on this problem and the use of fiber optics to remedy the stability of the time as delivered and the availability of special units which have the capability of compensating for (fixed) cable delays. Again, the information is available in the literature. This appears to be another case of the user not availing himself of the literature in the solution of a problem.

I was suggested that the suppliers remain in the procurement loop during the entire procurement in order to ensure adequate performance specifications for the user. Legal problems aside, this appears to be a worth-while suggestion.

## WORKSHOP 2; USER ENVIRONMENTAL EFFECTS

- IEEE Standard 1193-1994 "Guide for Measurement of Environmental Sensitivities of Standard Frequency Generators" is in print and should be available to the general public early 1995.
- Future focus on guidelines for the time and frequency community should be "dynamic (time-dependent) effects/environmental changes." This may include recommendations for studies and research needed.
- User environmental effects are particularly difficult to characterize because of the problems encountered in mapping manufacturers' specifications (sensitivity coefficients for the individual environmental sensitivities) into the overlapping/interacting actual environments. Resolution often requires expensive simulation of an actual environment.
- The following suggestions were made:
  - Users to characterize both (and independently) the systems' environment for the T&F components (e.g. cables, voltages and fluctuations, internal temperatures, etc.) and the environment of the system itself.
  - Manufacturers to ask, in a guiding and systematic way (develop a "questionnaire"), the user about the environment(s): What temperatures? What cables? Use in vacuum? When needed after turn-on? Will there be high humidity? .... Based on returned data, the manufacturer can apply his *total* knowledge about interactive environmental effects and customize environmental prediction (at little cost) and recommend environmental acceptance tests only where no knowledge exists (minimizing costly testing).
- Failure predictions and warranties have more business/risk factor content than technical value; also, failure definitions depend on a convoluted interpretation of actual performance versus "usually observed" performance versus specified performance. E.g. current GPS on-board failure rates for cesium were stated as one per three years but could be much smaller using a different failure criterion.
- In GPS, temperature sensitivity is used to determine clock health: Eclipse triggers the temperature change; clock health relates to frequency-temperature behavior as compared to prior eclipse data from the same clock. This type of environmental; monitoring may be useful, in general, as a predictor for latent T&F hardware failures.

# Workshop 3: Real Time Automated Systems

## Definition

Provides time/frequency to user specification in real time

- May have historical calibration

Do not require frequent operator action

- No full time operator
- May be fully unattended or remotely controlled

Typical applications include

- National time scales
- Remote time stations
- Imbedded part in Military systems and Telecommunications systems

## Performance

- Time Accuracy – typically 100 nsec or better
- Frequency accuracy –  $10^{-11}$  or better
- Frequency Stability – as good as  $10^{-13}$  at 1 second to  $10^{-13}$  at 1 day
- Usually require synchronization to national standard via GPS or 2 Way

## Measurements

- Accurate time tagging of measurements very important
  - Use telephone or network time sync for control computer time
- Measurement system must produce quiet, unambiguous measurements
  - RF (5 MHz) measurements preferred over tick measurements
  - 1PPS measurements problems are rise time, triggering, cable length

## Distribution Systems

- Environmental effects, temperature & humidity
- Use of high quality cable and connectors
- Greater than 100 db isolation between ports including output to input
- Widely distributed systems such as communication networks have special problems

## Robustness

- Small errors should only cause small problems
  - e.g. loss of 1 device shouldn't kill the system
- Computer needs stable operating system and user software
- There is a trade-off between single point failures and problems caused trying to avoid single point failures.
- User equipment driven from real time systems should be tolerant of small output glitches
- Robustness is difficult to specify
  - Depends on user environment
  - Hard to think of everything

## Maintenance and testing

- Box level field maintenance
  - Hardware is too complex to fix in the field
- Built-in test
- Remote diagnostic capability



P. 11

# The 1994 International Transatlantic Two-Way Satellite Time and Frequency Transfer Experiment: Preliminary Results

J. A. DeYoung, W. J. Klepczynski,  
A. D. McKinley, W. Powell & P. Mai  
U.S. Naval Observatory,  
Time Service Department  
Washington, DC, USA

P. Hetzel & A. Bauch,  
Physikalisch-Technische Bundesanstalt  
Braunschweig, Germany

J. A. Davis & P. R. Pearce  
National Physical Laboratory,  
Queens Road, Teddington  
Middlesex, United Kingdom

F. Baumont, P. Claudon & P. Grudler  
Observatoire de la Côte d'Azur  
Grasse, France

G. de Jong  
NMI, Van Swinden Laboratorium  
Delft, The Netherlands

D. Kirchner  
Technische Universität Graz  
Graz, Austria

H. Ressler  
Space Research Institute  
Graz, Austria

A. Söring  
Forschungs-und Technologiezentrum,  
DBP Telekom  
Darmstadt, Germany

C. Hackman  
National Institute of  
Standards and Technology  
Boulder, CO, USA

and

L. Veenstra  
Communications Satellite Corporation  
Washington, DC, USA

## Abstract

*The international transatlantic time and frequency transfer experiment was designed by participating laboratories and has been implemented during 1994 to test the international communications path involving a large number of transmitting stations. This paper will present empirically determined clock and time scale differences, time and frequency domain instabilities, and a representative power spectral density analysis. The experiments by the method of co-location which will allow absolute calibration of the participating laboratories have been performed. Absolute time differences and accuracy levels of this experiment will be assessed in the near future.*

## INTRODUCTION

The 1994 European/U.S. transatlantic two-way satellite time and frequency transfer (TWSTFT) experiment was designed to test the international communication path, the transfer of time and frequency between a large number of timing laboratories, the calibration accuracies, the non-reciprocal satellite delays, the estimates of time and frequency instabilities, and the exchange and

processing of the data. The geostationary satellite INTELSAT-VA(F-13), located at longitude 307 degrees East, has been used for the communication link. The eight timing laboratories who participated in this experiment are: FTZ (Darmstadt, Germany), NIST (Boulder CO, USA), NPL (Teddington, United Kingdom), OCA (Grasse, France), PTB (Braunschweig, Germany), TUG (Graz, Austria), USNO (Washington DC, USA) and VSL (Delft, Netherlands). The first experiments were conducted on 1994 February 4 (MJD 49387.5).

Many papers exist in the literature covering the development of the formulae and methods currently used in producing time differences over the wide-band communication links used on commercial geostationary communication satellites and readers are referred to a selection of the many papers in the literature for specifics of how and why TWSTFT works<sup>[1,2,3,4,5,6]</sup>. At the 25th Annual PTTI meeting Gerrit de Jong of NMI Van Swinden Laboratorium gave an overview paper discussing recent developments, engineering aspects, data formats, and related details of the individual TWSTFT experiments specifically related to this international communication link<sup>[7]</sup>.

Since PTTI is an "applications and planning meeting" an additional focus of this paper will be to present an example case where the empirically calibrated data are being used as an information source for management of real-time time and frequency resources.

## INSTABILITIES AND NOISE PROCESSES

Figure 1 shows an example of raw uncalibrated time differences of the USNO(MC2)-VSL(HP5071A) time transfer of 1994 October 12 (MJD 49637). USNO(MC2) is the real-time realization of UTC(USNO) by the Sigma Tau hydrogen maser clock N3 which is steered by small daily frequency changes in its synthesizer. In general a white noise behavior is noticed. There is structure in the data so that even over 300 seconds (5 minutes) the TWSTFT process is not purely white. Depending on the experiment analyzed the structure is sometimes sinusoidal and other times possibly a step. This type of subtle structure manifests itself as flicker phase noise in the time domain instability estimates that will be shown later. The physical source generating this structure is not known but may originate from environmentally caused drift in the electronics, for example. The identification and physical understanding of the flicker phase noise sources and then the reduction or removal of the effects will improve the TWSTFT phase flicker floor instability and is an area where future effort should be placed.

The formulation used to generate the uncalibrated time differences is

$$\begin{aligned}
 UTC(USNO(MC2)) - UTC(LAB) = & 1/2[T_i(USNO) - T_i(LAB)] & (1) \\
 & - [T_x(LAB) - T_x(USNO)] \\
 & - [\delta 1pps(LAB) - \delta 1pps(USNO)] \\
 & - [i_c(USNO) - i_c(LAB)] \\
 & - Sagnac \\
 & - RF
 \end{aligned}$$

The first term is the value of one half the of the sum of the differences of the recorded time interval counter readings recorded at each site. The second term is the transmit-to-receive delay differences of the MITREX modems also measured at each site. The third term is the delays from on time of the 1-pulse-per-second references as

measured at each site. The fourth term allows for any time difference introduced by intermediate clocks and allows adjustment to the true UTC(Lab) reference clock. The fifth term is the computed relativistic time delay, Sagnac delay, due to a rotating reference frame system. The sixth and final term is an unknown term for an uncalibrated timing link and is commonly called the "RF term." The RF term contains the sum of the unknown delays contributed from waveguides, RF

filters, and non-reciprocal satellite delays to name a few. This is the term that was adjusted empirically to put the time differences "on time" for this paper. Using an independent timing source, usually GPS or BIPM Circular T, we may then determine an empirical constant correction which is the sum of the unknown delays which may then applied to put the daily mean values computed from equation 1 "on time." The empirical calibrations then are only as good as the timing link used as the empirical reference plus any systematic deviations introduced by the TWSTFT method. Evidence from closure tests<sup>[8]</sup> indicate that TWSTFT will contribute less than 10 nanoseconds worth of error to the error budget where the error may is contributed from environmentally caused drift of electronics, nonidentical hardware at each laboratory, hardware problems, and hardware failures among others.

Figure 2 shows the empirically calibrated USNO(MC2)-FTZ(HP5070A) which was referenced to time differences published in the BIPM Circular T by the method given above. A clock change occurred at FTZ on MJD 49429.375 and the operational transition was smooth.

Time deviation (TDEV) instability estimates were generated from a C language program developed from pseudocode<sup>[9]</sup>. The TDEV instability estimate is ideal for visualizing time-domain noise processes, because the instability estimate resolves the two phase noise processes and the slopes are easily distinguished in a TDEV plot. The three main frequency-domain noise processes are also isolated when using TDEV, but the slope changes are a bit harder to distinguish because of the large slopes. Another pleasing aspect of using TDEV is that no preparation of the data is required or recommended other than making sure the data are equally spaced. Any data modification, such as first-differencing, acts as a digital filter removing some of the interesting signals in the data and is undesirable<sup>[10]</sup>. The two-Allan Deviation (ADEV) was used in monitoring the FM noise processes at tau greater than one day.

Figure 3 shows a log sigma x (nanoseconds) versus log tau (seconds) plot of the time deviation (TDEV) instability estimate for USNO(MC2)-TUG(HP5071A). This plot contains instability estimates from 78 daily runs each made up of 300 seconds worth of 1-pulse-per-second comparisons. In addition, the plot contains the daily means which have been interpolated to daily values from unequally spaced data. White phase modulation noise, probably originating in the electronic equipment (MITREX modems) used to perform the experiments, dominates during tau (averaging time) 1 to 50 seconds and appears as a slope of  $\tau^{-frac{1}{2}}$ . After an inflection near  $\tau^{1.7}$  (50 seconds) a slope of  $\tau^0$  is seen which is the

characteristic slope of flicker phase modulation noise (the "structure" seen in Figure. 1). The physical source related to the flicker phase noise is not known with certainty. The average phase flicker floor as determined by the TDEV statistic is near 200 picoseconds which is close to but not exactly at the classical variance of the mean of a typical 300 second time transfer experiment, which is where the location of the inflection point should be if the noise were strictly white PM[9], which it is not. Near  $\tau^5$  seconds ( $\approx 1$  day) the slope is  $\tau^1$  which indicates flicker frequency modulation noise and is contributed by the TUG commercial cesium clock. The ADEV statistic at a sampling time of  $\tau^{6.1}$  seconds (15 days) gives an estimated instability level of 8 parts in  $10^{15}$  as the flicker frequency floor. These results are similar to the results presented at the 25th Annual PTTI meeting in a paper on the calibrated TWSTFT link between the U.S. Naval Observatory in Washington, DC (USNO(MC2)) and the U.S. Naval Observatory Time Service Substation in Richmond, FL (NOTSS(HP5071A))[11]. The flicker phase floor determined from the TDEV instability statistic for TWSTFT, compared at an averaging time of 100 seconds, is more than an order of magnitude improved over that recently estimated from a new low-cost generation of GPS timing receivers[12].

Figure 4 shows a log sigma x (nanoseconds) versus log tau (seconds) plot of the time deviation (TDEV) instability for USNO(MC2)-NPL(H-maser). This plot contains instability estimates from 63 daily runs each made up of 300 seconds worth of 1-pulse-per-second comparisons with one run being of 1500 seconds duration. In addition, the plot contains the daily means which have been interpolated to daily values from the unequally spaced data. As expected there is little difference in the phase noise compared to that shown for TUG in Figure 3 so the phase instabilities are similar. The frequency performance of the maser-to-maser timing link shows improved FM instability estimates when compared to the Figure 3 maser-to-cesium comparison. The ADEV statistic at an sampling time  $\tau^{6.1}$  seconds (15-days) gives a value of 4 parts in  $10^{15}$  as the flicker frequency floor.

## CLOCK AND TIME SCALE MONITORING USING TWSTFT

Figure 5 shows time differences of commercial cesium clocks from FTZ, TUG and NOTSS against PTB(CS2) which is a laboratory cesium frequency standard operated as a clock. The USNO(MC2)-NOTSS(HP5071A) timing data are obtained by an independent and calibrated, by the method of co-located antennas, TWSTFT link using SBS-6[11].

Figure 6 shows USNO hydrogen maser clocks N4 and N5 and the USNO(A.1MEAN) time scale compared, by empirically calibrated TWSTFT, again against PTB(CS2). Individual linear rates have also been removed from each clock difference by the method of linear least squares. From inspection of Figure 5 and Figure 6 shows that the clocks stay together very well in time. The cesium clocks shown in figure 5 indicates a slightly higher amplitude of variation over the hydrogen maser clocks in this comparison. There is perhaps some common structure seen in both in Figure 5 and Figure 6 and best indicated by the "dip" near MJD 49565. This simple analysis using TWSTFT time comparison data might be useful because it will allow for detection, characterization, and isolation of correlated local environmental effects on clocks that might not otherwise be detected, and it can be done in near real time.

An extremely useful and elegant algorithm, given with pseudocode, has been recently reported

that generates power spectral density (PSD) estimates, "a digital spectrum analyzer (DSA)." The DSA makes use of digital filters and by application of one or two stages of filtering to form an estimate of the PSD of the input data<sup>[13]</sup>. The DSA method, when added to Fourier, phase dispersion minimization and other methods of periodic signal detection, is a nice independent way to detect periodic signals in time and frequency data, since no single method is "best" for analysis of periodic signals in all data. Figure 7 shows a PSD estimate generated using the DSA method on TWSTFT frequency data where the original unequally spaced timing data was interpolated to daily intervals and then converted to frequencies in parts in  $10^{6.1}$ . The total data interval reflected in the PSD is 281 days. The low significance peaks at frequencies greater than 0.1 are related to the original unequally spaced sampling rates. The peak at 1 month is probably related to monthly steering of USNO(MC2) towards UTC(BIPM).

## CONCLUSION

These preliminary results shown in this paper point out that much more work needs to be done in all areas of TWSTFT. Completion of the calibration data analysis, continued monitoring of the performance of TWSTFT over longer and longer averaging times, and the continued comparison and improvement of the performance of remote clocks and/or time scales are important. The new knowledge and information that TWSTFT supplies to decision makers is extremely useful. New hardware, especially the new generation modems, hopefully, will make TWSTFT more automated and make data analysis much easier and more automated. Data formats such as the newly proposed international format are improving and allow much more information to be passed about technical and environmental conditions related to the TWSTFT and can only improve accuracy and stability estimates.

## ACKNOWLEDGEMENTS

J. DeYoung thanks Gernot M. R. Winkler (USNO) for coding up the C program that computes the TDEV instability estimates and for useful discussions.

## REFERENCES

- [1] D. A. Howe, 1987, "*Ku-Band Satellite Two-way Timing Using a Very Small Aperture Terminal (VSAT)*", Proceedings of the 41st Annual Symposium on Frequency Control, 27-29 May 1987, Philadelphia, Pennsylvania, pp. 149-159.
- [2] D. A. Howe, 1988 "*High Accuracy Time Transfer via Geostationary Satellites: Preliminary Results*", IEEE Transactions on Instrumentation and Measurement, Vol. 37, pp. 418-423.
- [3] D. W. Hanson, 1989, "*Fundamentals of Two[insert 4]Way Time Transfers by Satellite*", Proceedings of the 43rd Annual Symposium on Frequency Control, 31 May -2 June 1989, Denver, Colorado, pp. 174-178.

- [4] D. Kirchner, 1991, "Two-Way Time Transfer via Communications Satellites", IEEE Proceedings, Vol 79, pp. 983-990.
- [5] D. Kirchner, U. Thyr, H. Ressler, R. Robnik, P. Grudler, F. Baumont, Ch. Veillet, W. Lewandowski, W. Hanson, A. Clements, J. Jespersen, D. Howe, M. Lombardi, W. Klepczynski, P. Wheeler, W. Powell, A. Davis, P. Uhrich, R. Tourde, and M. Granveaud, 1992, "Comparison of Two-Way Satellite Time Transfer and GPS-Common-View Time Transfer Between OCA and TUG", 23rd Annual Precise Time and Time Interval (PTTI) Applications and Planning Meeting, 3-5 December 1991, Pasadena, California, pp. 71-86.
- [6] D. Kirchner, H. Resler, R. Robnik, W. Klepczynski, P. Wheeler, W. Powell, and A. Davis, 1993, "Two-Way Satellite Time Transfer Between USNO and TUG Using the INTELSAT Satellite at 307 degrees East", Proceedings of the 7th European Frequency and Time Forum, 16-18 March 1993, Neuchatel, France, pp. 1-5.
- [7] G. de Jong, 1994, "Two-way Satellite Time Transfers: Overview and Recent Developments", Proceedings of the 25th Annual Precise Time and Time Interval (PTTI) Applications and Planning meeting, 29 November-3 December, 1993, Marina Del Ray, California, pp. 101-117.
- [8] J. A. Davis, P. R. Pearce, D. Kirchner, H. Ressler, P. Hetzel, A. Söring, G. de Jong, P. Grudler, F. Baumont, L. Veenstra, 1995, "European Two-Way Satellite Time Transfer Experiments Using the Intelsat Satellite at 307 Degrees E", Accepted for publication in a special issue of Proc. IEEE Trans. Instrm. and Meas.
- [9] M. A. Weiss and D. Zirkle, 1994, "Efficient Algorithms for Computing Time Variance (TVAR) and Time Deviation (TDEV) with the Zampetti Time Interval Error (ZTIE)", in Preparation.
- [10] D. W. Allan, M. A. Weiss, and J. L. Jespersen, 1991, "A Frequency-Domain View of Time-Domain Characterization of Clock and Time and Frequency Distribution Systems", Proceedings of the 45th Annual Symposium on Frequency Control, 29-31 May 1991, Los Angeles, California, pp. 667-678.
- [11] J. A. DeYoung and R. J. Andrukitis, 1994, "Remote Clocks Linked By A Fully Calibrated Two-Way Timing Link", Proceedings of the 25th Annual Precise Time and Time Interval (PTTI) Applications and Planning meeting, 29 November-3 December, 1993, Marina Del Rey, California, pp. 285-291.
- [12] M. King, D. Busch, and M. Miranian, 1994, "Test results and Analysis of a Low Cost Core GPS Receiver for Time Transfer Application", Proceedings of the Institute of Navigation National Technical Meeting: Navigating the Earth and Beyond, San Diego, California, pp. 99-102.
- [13] J. A. Barnes, 1993, "A Digital Equivalent of an Analog Spectrum Analyzer", Proceedings of the 1993 IEEE International Frequency Control Symposium (47th Annual), 2-4 June 1993, Salt Lake City, Utah, pp. 270-281.

# (USNO(MC2) - VSL) / 2) Time Differences

1994 October 12 (UT)

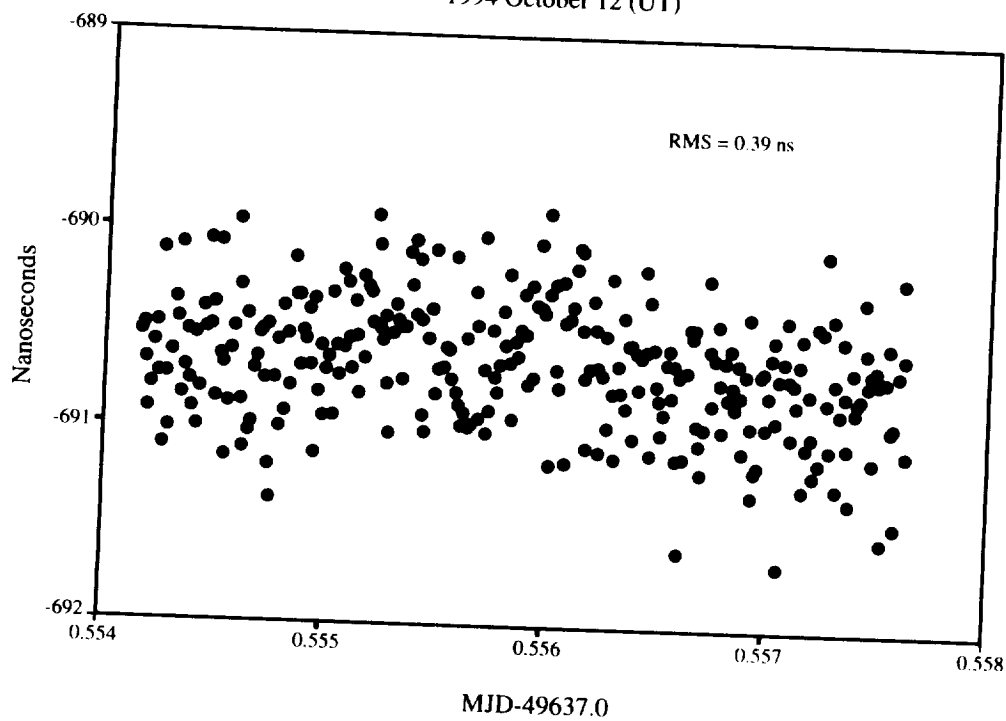


Figure 1

# USNO(MC2) - FTZ Empirically Calibrated to BIPM Circ. T

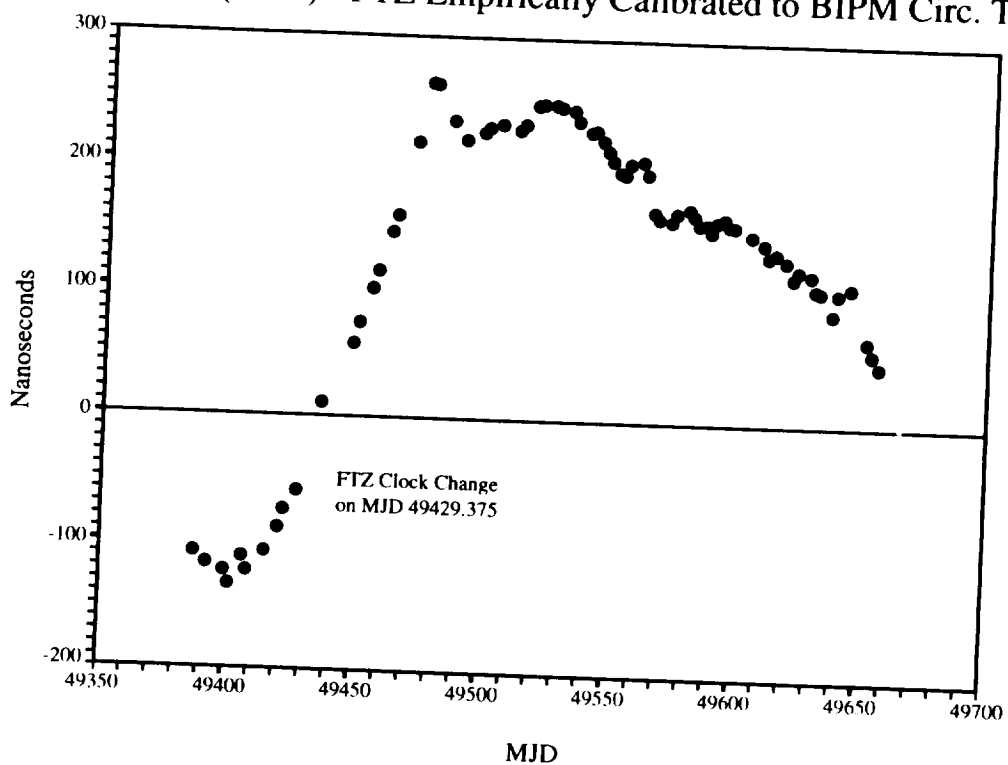


Figure 2

TDEV Instability Plot of USNO(MC2) - TUG(HP5071A) via TWSTFT  
 Combined Plot of 78-Days Worth of 1-PPS and Daily Time Differences

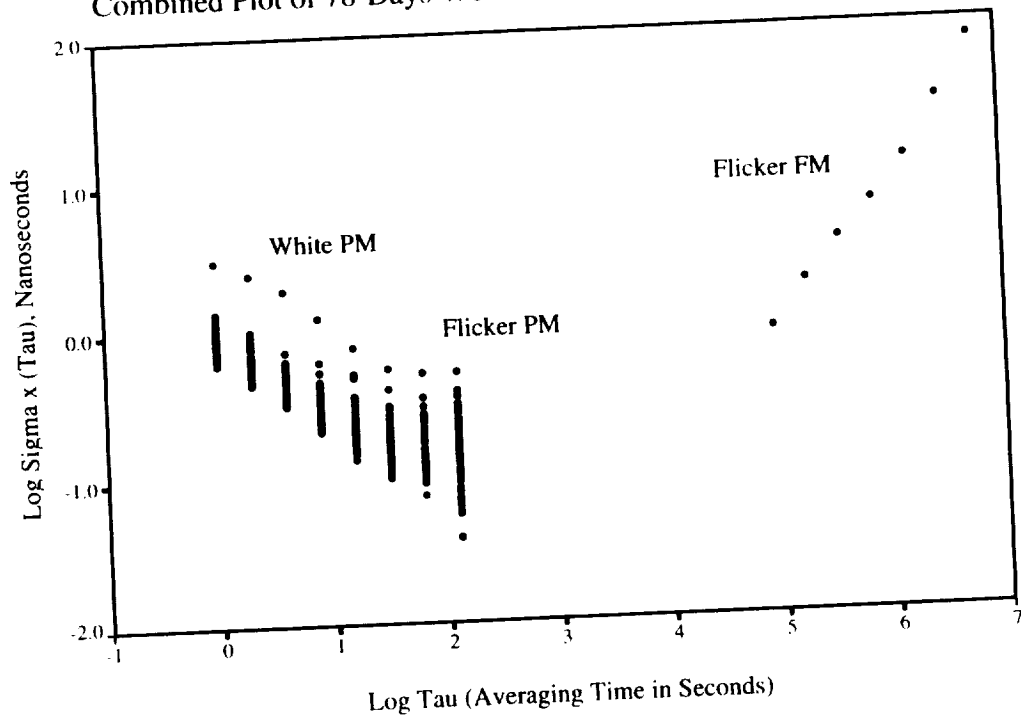


Figure 3

TDEV Instability Plot of USNO(MC2) - NPL(H-maser) TWSTFT  
 Combined Plot of 63-Days Worth of 1-PPS and Daily Time Differences

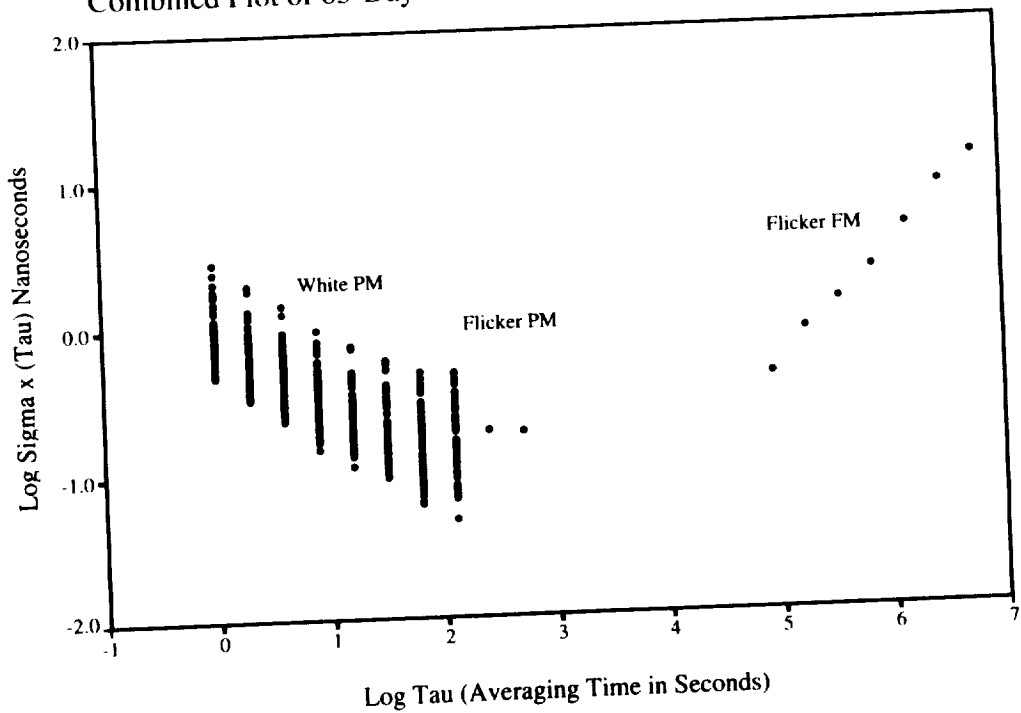


Figure 4

# TWSTFT Cesium Clock comparisons against PTB(CS2)

Known Steps and Linear Rates Removed

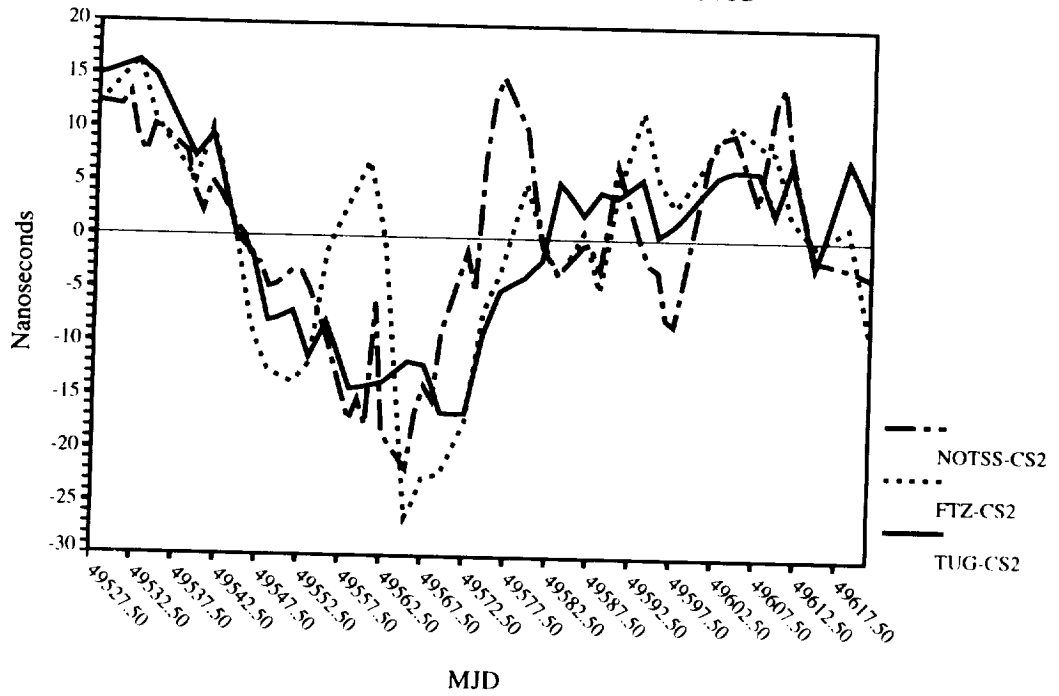


Figure 5

# TWSTFT H-Maser and Time Scale comparisons against PTB(CS2)

Two Unsteered Hydrogen masers and USNO(A1Mean)

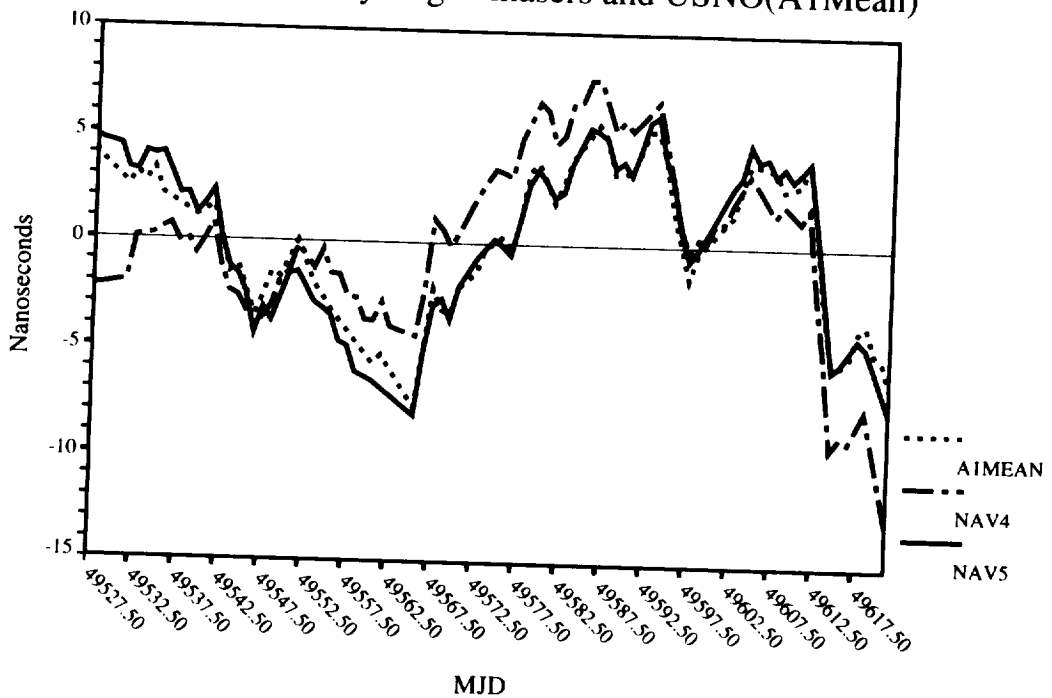


Figure 6

# Two-Stage Power Spectral Density

TWSTFT USNO(MC2)-PTB(CS2) Frequency (parts in e15)

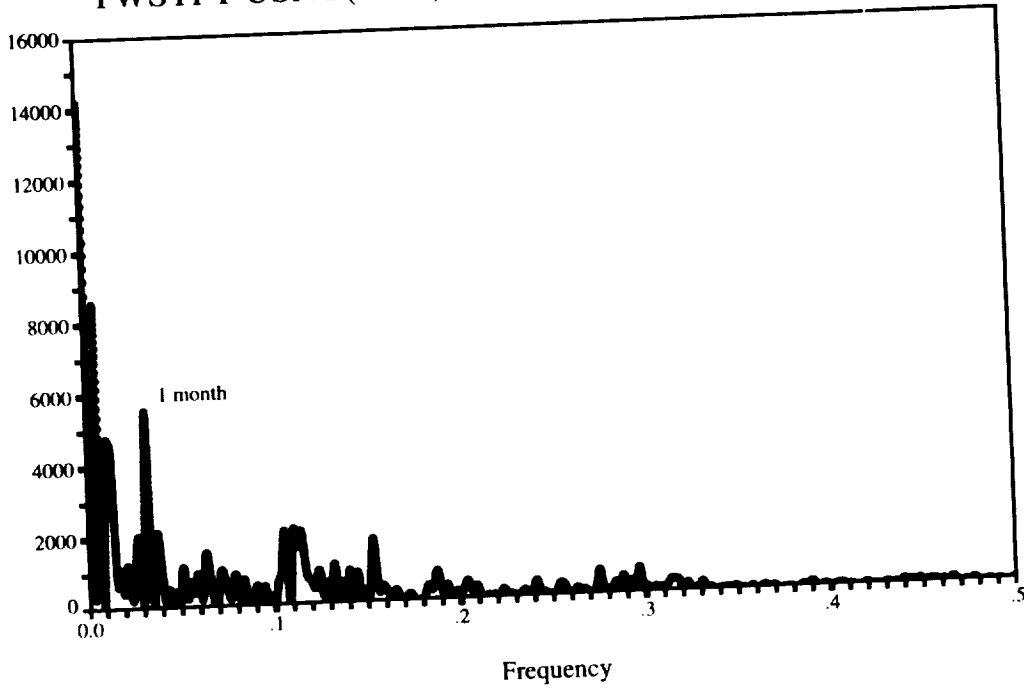


Figure 7

## QUESTIONS AND ANSWERS

**MARC A. WEISS (NIST):** For the one-day estimate of TDEV, you said the data were not evenly spaced. I'm wondering how you got a one-day estimate.

**J.A. DeYOUNG (USNO):** Right. What I did was, the data is taken three times a week; so we have Monday, Wednesday and Friday. I simply interpolated linearly interpolated values to fill in in-between the actual measured values. I mean, that's the best we can do.

Well, I see a few heads shaking out there. There are lots of ways we can do something like that. I mean, you just have to pick one, and that's the one I picked to do. There was another one somewhere up here I believe.

**FRED WALLS (NIST, BOULDER):** The seven-day, 14-day, and 31-day peaks are what you would expect from environmental things in laboratories where people come and go. I'm pleased actually to see it show up in your data, because I think it means that if you would make your sampling coincident with a one-week period, that a lot of those fluctuations would be diminished.

**J.A. DeYOUNG (USNO):** Yes, that's quite possible. PSDs are very inherently difficult to interpret as to the source of where those peaks are coming from. That's one possibility that it's coming from that source. I just assumed it was coming from my interpolating the data that was at two-day intervals. Because if you look at all the combinations of the sampling, from Monday, Wednesday to Friday, that's two-day gaps. Then over the weekend, you have a three-day gap; and then over the week you have the five-day sampling Monday to Friday; and then you have the week again. Almost all of those peaks are almost exactly right where you expect those to be from that. It's possible it's from the source that you're mentioning.

**TOM PARKER (NIST):** By doing a linear interpolation on data with typically Monday-Wednesday-Friday-type analysis, you're going to underestimate TDEV at one day by about a factor of somewhere between two and three. So the data is overly optimistic at one day.

**J.A. DeYOUNG (USNO):** Do you have a suggestion as to how to -- I mean, if we're dealing with unequally-spaced data, what's the better way then? Do have a suggestion for that?

**TOM PARKER (NIST):** Well, I'll tell you what I did. I took some comparable GPS data that I had on one-day intervals and edited out all the points that didn't correspond to the two-way. So with the GPS data, I could get both ways with the two-way density and with the full one-day density and just made a comparison. That's where the two-to-three comes from.



52273  
1 11

# HIGH ACCURACY TIME TRANSFER SYNCHRONIZATION

Paul Wheeler, Paul Koppang, David Chalmers,  
Angela Davis, Anthony Kubik and William Powell  
U.S. Naval Observatory  
Washington, DC 20392

## Abstract

*In July 1994, the US Naval Observatory (USNO) Time Service System Engineering Division conducted a field test to establish a baseline accuracy for two-way satellite time transfer synchronization. Three Hewlett-Packard model 5071 high performance cesium frequency standards were transported from the USNO in Washington, DC to Los Angeles, California in the USNO's mobile earth station. Two-Way Satellite Time Transfer links between the mobile earth station and the USNO were conducted each day of the trip, using the Naval Research Laboratory(NRL) designed spread spectrum modem, built by Allen Osborne Associates(AOA). A Motorola six channel GPS receiver was used to track the location and altitude of the mobile earth station and to provide coordinates for calculating Sagnac corrections for the two-way measurements, and relativistic corrections for the cesium clocks.*

*This paper will discuss the trip, the measurement systems used and the results from the data collected. We will show the accuracy of using two-way satellite time transfer for synchronization and the performance of the three HP 5071 cesium clocks in an operational environment.*

## INTRODUCTION

The purpose of this experiment was to demonstrate our ability to accurately calibrate remote precise time laboratories and Department of Defense (DOD) installations using two-way satellite time transfer techniques [1]. Although the USNO has participated in two-way experiments for years, little work has been done in performing absolute calibrations of remote sites using this technique. When the need for high accuracy calibrations to remote DOD sites arose, the two-way satellite time transfer technique was selected because of its greater accuracy ( $\pm 1$  ns) than the Global Positioning System (GPS). This accuracy of two-way has been demonstrated at the USNO and other laboratories, but two-way accuracy had not been demonstrated in the field, in particular in the east-west direction where Sagnac effects are significant.

## CLOCK TRIP

For this experiment a two-member team drove the USNO's mobile earth station from the USNO in Washington, DC to Los Angeles, California and a second two-member team drove

it back to the USNO (see Figure 1). Two-way measurements were made each day to provide a precise time link between the three cesium clocks in the van and the USNO. The trip was started on July 11th, 1994 and completed on July 22nd.

The USNO's mobile earth station is a Ford Econoline 350 van with a folding Ku-band 1.8 meter dish antenna on the roof, a generator, air conditioning and three equipment racks of electronics to support the antenna and two-way operations. For this trip three Hewlett-Packard 5071A high performance cesium frequency standards, a PC-based data acquisition system, and a Motorola six channel GPS receiver were added.

The data acquisition system consisted of an industrial grade PC manufactured by Texas Microsystems Inc. controlling a Stanford Research SR650 time interval counter, a Hewlett-Packard 3488 VHF switch and the GPS receiver. The GPS receiver was mounted inside the PC and connected to one of the PC serial ports. The clocks and the GPS receiver 1 pps (1 pulse per second) were intercompared every minute with the time interval counter. The GPS position information was logged every 10 minutes. While the mobile earth station was at the USNO, a 1 pps from the Master Clock was also connected to the VHF switch so that the clocks were compared against UTC USNO. This was done before and after the trip to establish the performance of the clocks while they were in the van.

In order to calibrate the two-way system, repetitive two-way measurements between our 4.5 meter base station and the mobile earth station were taken. A calibrated 1 pps and a 5 MHz reference signal, both from the USNO Master Clock, were connected to the modem in each earth station. With this setup the resulting measurement, one clock measured against itself, should be zero, if the transmit and receive delays are identical through the modem, the earth station, the satellite and back, and the cable delays from the reference clock are the same. In reality this is not the case and the resulting measurement will be the calibration factor that is applied to the measurements throughout the experiment. The calibration factor measured to be 243.3 nanoseconds. After returning from the trip this calibration procedure was repeated to verify that the delays through the two-way system had not changed.

The trip was started after a final calibration run. After arriving at a destination in the evening, the van was fueled and parked in the hotel parking lot so that there was good satellite visibility. The clocks and measurement equipment were transferred from inverter power to generator which kept the equipment and air conditioner operating throughout the night. The satellite was located and the equipment was set up in preparation for the time transfer measurement in the morning. For this experiment and most of our domestic two-way operations we use Satellite Business Systems satellite SBS-6.

In the morning the satellite was re-acquired and then, typically, three two-way measurements were obtained. Each result consisted of 300 averaged 1 pps measurements. The AOA modems used for this experiment operate in a source/target configuration. The modem in the van was operated as the source and the target was at the USNO. This gave the travelers control of the satellite link and the two-way measurements. The two-way measurement data from the target modem was transmitted back over the satellite link to the source modem, allowing the results of the measurement set to be calculated. This allowed the field members to evaluate the measurements and to look for anomalies in the data being collected.

The two-way data collected each morning were used to measure the time of the three cesium clocks in the van. The GPS receiver position data were used to calculate Sagnac corrections for the two-way measurements and to calculate relativity corrections for the clock data. The 1 pps from the GPS receiver was used as a coarse rule to compare the clocks.

## RELATIVISTIC EFFECTS

The data collected throughout this experiment needed to be corrected for relativistic effects. There are many excellent references [1-5] on the derivation and theory behind these effects; therefore, they will only be touched upon briefly in this paper. Due to the rotation of the earth and the satellite, the path lengths (from one earth station to the satellite to the other earth station and back) during a satellite two-way time transfer are not symmetrical. This phenomenon is referred to as the Sagnac effect. The time difference caused by this effect is given by  $2\omega A/c^2$ , where  $c$  is the velocity of light,  $\omega$  is the Earth's rotation rate, and  $A$  is the area defined by the projection onto the equatorial plane by the segments connecting the satellite and the Earth's center to the two earth stations [1]. Figure 2 is a plot of the Sagnac corrections needed for the two-way data taken during the trip.

There are three main components of relativistic corrections that need to be addressed for the clock trip elapsed time. These corrections are due to height (red shift), velocity (Doppler shift), and east-west motion. The equation used to calculate these corrections is:

$$\Delta t = \int_{path} ds \left[ 1 - g(\phi)h/c^2 + \frac{1}{2}(v/c)^2 + \frac{\omega}{c^2}av_E \cos \phi \right] \quad (1)$$

where  $g(\phi)$  is the acceleration of gravity,  $v_E$  is the ground velocity of the clock having an eastward component,  $h$  is the altitude above the geoid,  $\omega$  is the angular velocity of rotation of the Earth,  $a$  is the Earth's equatorial radius, and  $\phi$  is the geographical latitude [3].

The GPS receiver provided most of the information needed to solve the above equation. Every 10 minutes the position of the van (height, latitude, and longitude) and the time were gathered from the GPS receiver and stored on the PC.

The height correction:

$$g(\phi)h/c^2 \quad (2)$$

of 82.57 ns turns out to be the dominant clock trip relativistic correction term in this experiment due to the trip length of 11 days and the vast height differences encountered along the trip, for instance Washington, DC is at 55 meters while part of Colorado is over 3000 meters (see Figure 3). Since this term does not depend on velocity, but on height, it is continuing to have an effect as long as there is a height differential. Therefore, the clocks were realizing a relativistic change of rate even when the van was parked for the night at a location with a different elevation than that of Washington, DC.

The east-west correction:

$$\frac{\omega}{c^2} a v_E \cos \phi \quad (3)$$

ends up being an integration of east(west) velocity over time, which is then just the distance traveled east(west). Since this term turns out to be proportional to the distance traveled and independent of velocity, it would be the same whether a van or, for instance, an airplane was used for the clock trip. For a round trip (east–west, west–east) this term cancels out at the conclusion of the trip, but gives a necessary correction to the data during the trip.

The Doppler term is:

$$\frac{1}{2}(v/c)^2 \quad (4)$$

Even though the van traveled very slowly compared to the speed of light, the 11 day trip was long enough to give the Doppler term a non-negligible correction of 1.24 ns. Figure 4 shows the three different contributions along with the total relativistic correction for the trip.

It is interesting to compare these clock trip data to what we would have seen on a airplane trip from Washington, DC to Los Angeles and back. We will assume an average air speed of 550 miles per hour and an average altitude of 25,000 feet. The height correction for the round trip calculates to be -28.2 ns, while the velocity correction would be 11.4 ns. Therefore the total correction to the clock data would be -16.8 ns as compared to the -82.6 ns of the van trip.

## DATA

The two-way time transfer method was used to compare cesium clock serial #254 vs. the Master Clock at 12 different sites during the round trip. The phase data being logged between clocks #254, #416, and #227 locally in the van (see Fig. 5) along with the two-way data was used to calculate the differences between the Master Clock and the clocks #416 and #227 during the trip. The relativistic corrections due to the clock trip were then made to the cesium clock – Master Clock data after Sagnac effect corrections to the two-way data had been taken into account. Figures 6–8 show the raw data and the data corrected for both the two-way Sagnac and relativistic clock trip effects. In Figures 6–8 the data that are bunched together at the beginning and the end of the plots were taken at USNO with the Master Clock directly connected to the measurement system, while the individual points were obtained via the two-way time transfer method.

The cesium clocks performed very well considering the less than ideal environmental conditions inside the van during the trip. The clocks experienced approximately 40 degree temperature swings and considerable vibration. The Allan deviations of the cesium clocks as measured in the van during the trip were:

hr	#227-#416	#254-#227	#254-#416	#points
1	1.14e-13	1.18e-13	1.18e-13	415
2	8.21e-14	8.06e-14	8.44e-14	207
4	5.93e-14	5.85e-14	6.38e-14	103
8	4.52e-14	3.81e-14	4.47e-14	51
16	3.18e-14	2.80e-14	3.59e-14	25
32	2.32e-14	2.46e-14	3.24e-14	12
64	1.83e-14	1.39e-14	2.38e-14	6
128	1.50e-14	7.38e-15	1.82e-14	3

Clock pairs 227–416 and 254–227 had stabilities that were below the specifications given by the manufacturer for clocks under environmental control(see Figure 9).

## CONCLUSION

This experiment has shown that the two-way time transfer method can be used to accurately calibrate remote precise time laboratories and DOD installations using the necessary Sagnac corrections to the data. Also, it is necessary to take into account the effects of relativity when using a portable clock to do remote synchronization no matter what the mode of transportation of the clock. The three HP 5071 clocks performed very well in less than ideal conditions.

## REFERENCES

- [1] D.W. Hanson, "*Fundamentals of two-way time transfers by satellite*", Proceedings of the 43rd Annual Symposium on Frequency and Control, 31 May – 3 June 1989, Denver, Colorado, pp. 174-178.
- [2] G.M.R. Winkler, "*Synchronization and Relativity*", Proceedings of the IEEE, Vol. 79, No. 6, June 1991. (This paper gives references to many excellent papers on relativity.)
- [3] N. Ashby and D.W. Allan, "*Practical implications of relativity for a global coordinate time scale*", Radio Science, Vol. 14, 1979, pp. 649–669.
- [4] J.C. Hafele and R.E. Keating, "*Around the world atomic clocks*", Science, Vol. 177, pp. 166–170, July 1972.
- [5] N. Ashby, "*RELATIVITY and GPS*", GPS World, Nov. 1993. pp. 42–47.

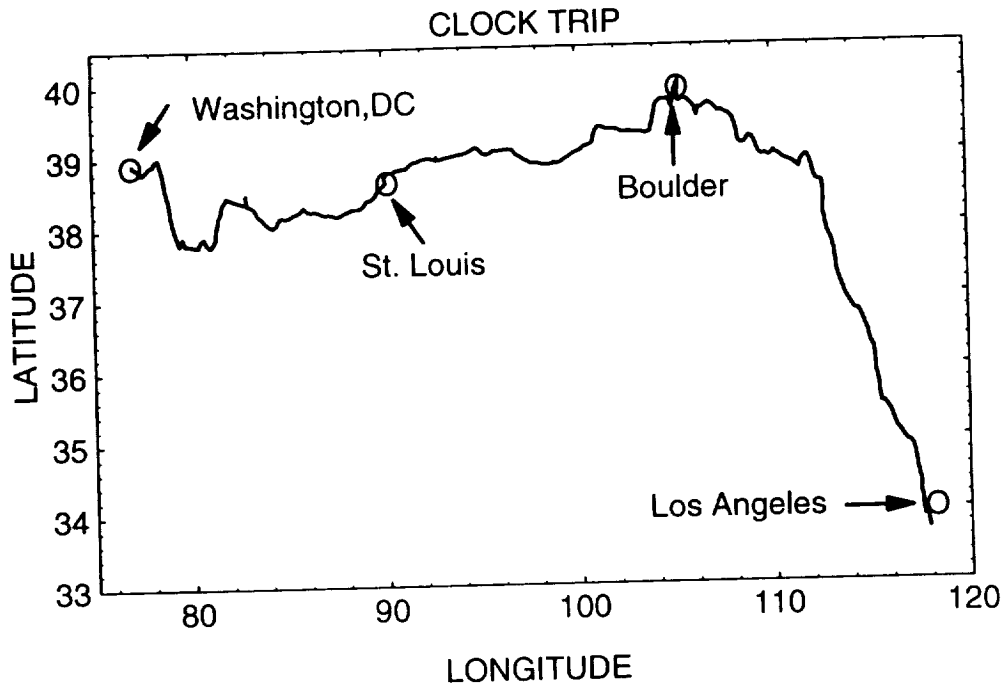


Figure 1. Clock trip as measured by the GPS receiver.

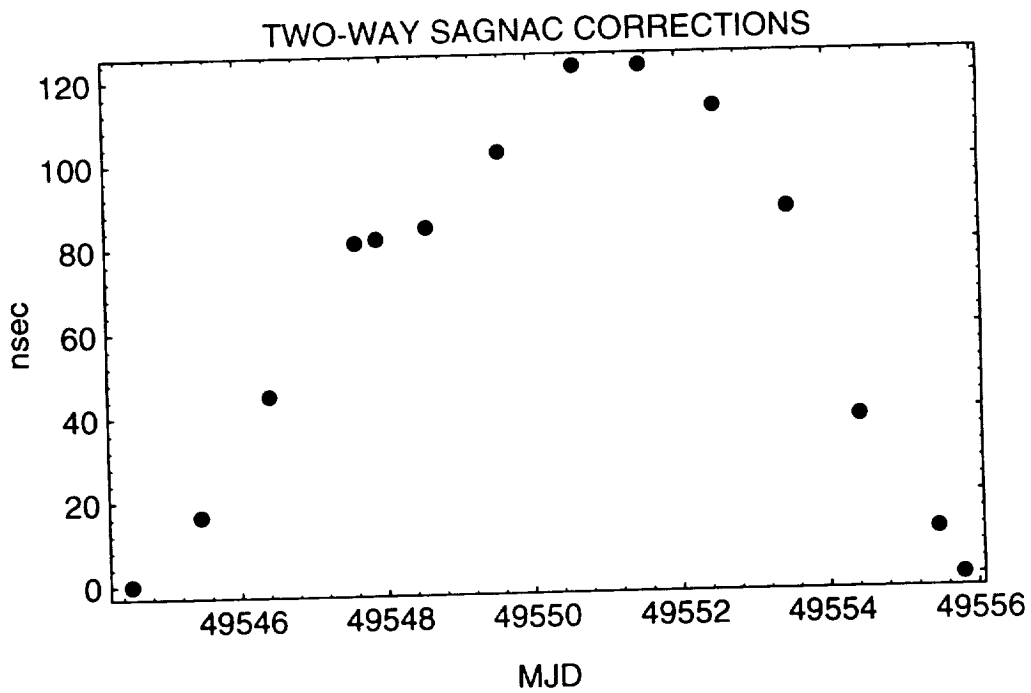


Figure 2. Sagnac corrections calculated for the two-way data.

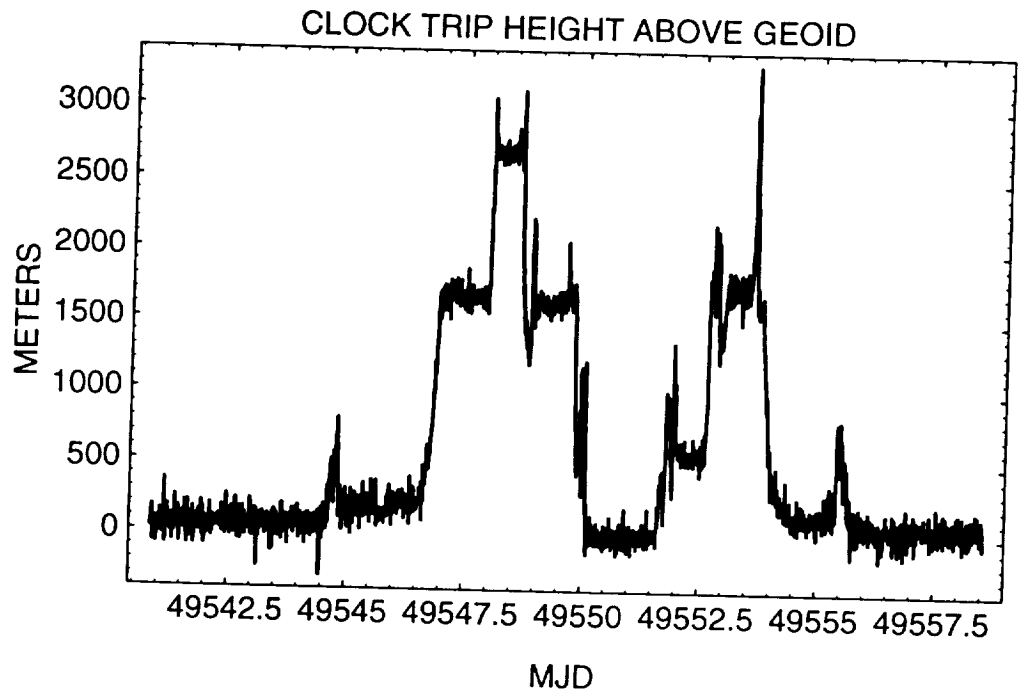


Figure 3. The height of the van above the geoid during the trip as measured by the GPS receiver.

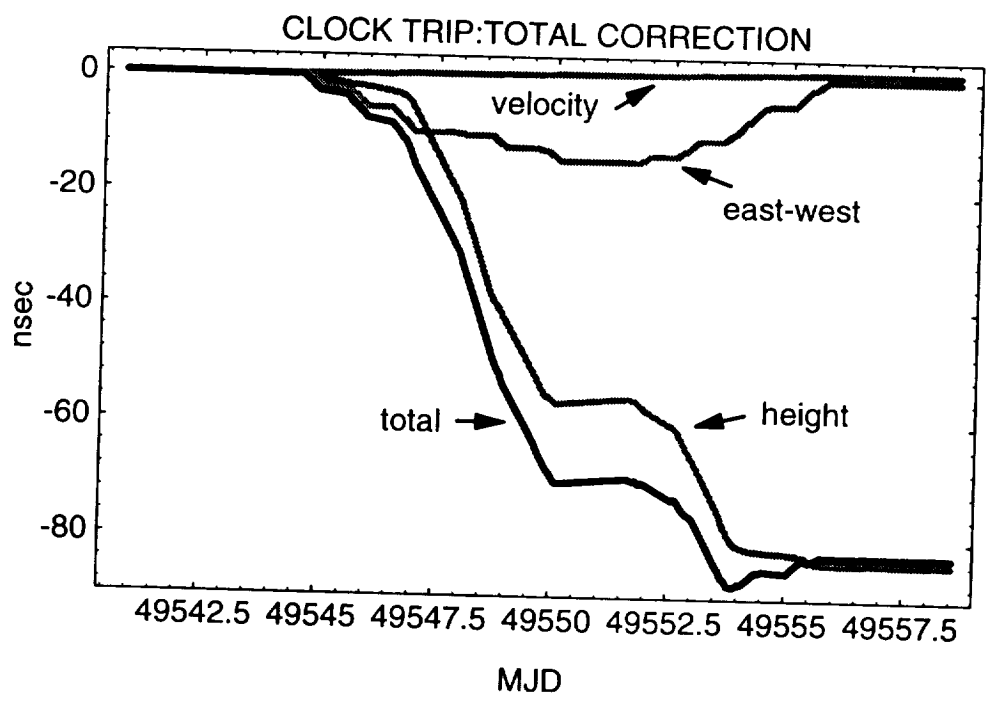


Figure 4. The total relativistic clock trip corrections along with the individual components.

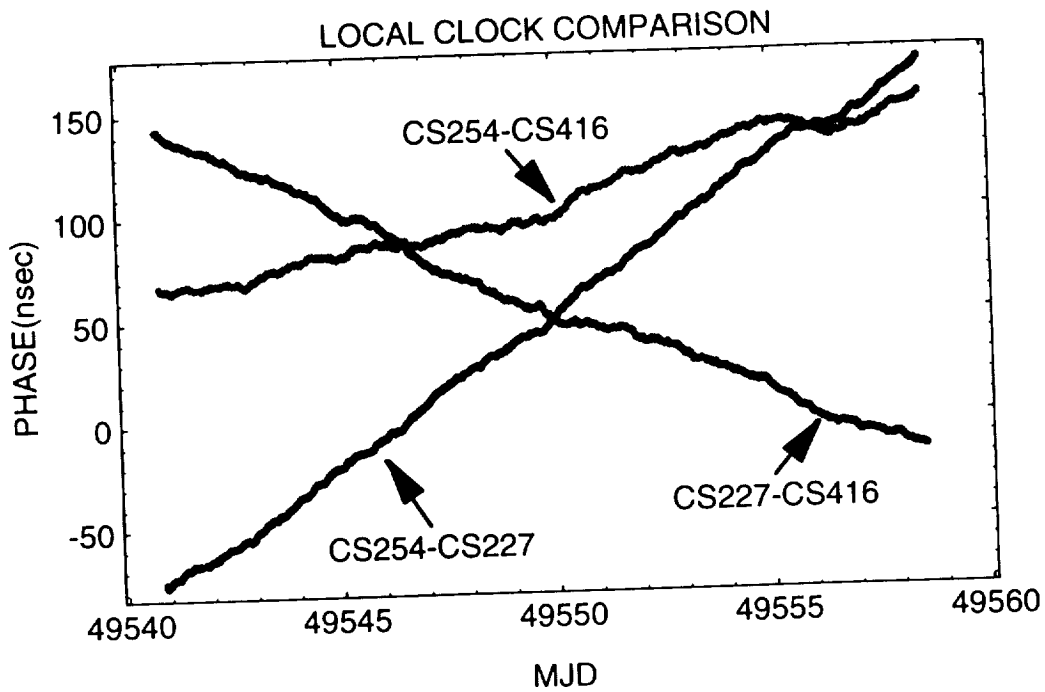


Figure 5. The cesium clocks inter-compared as measured locally in the van.

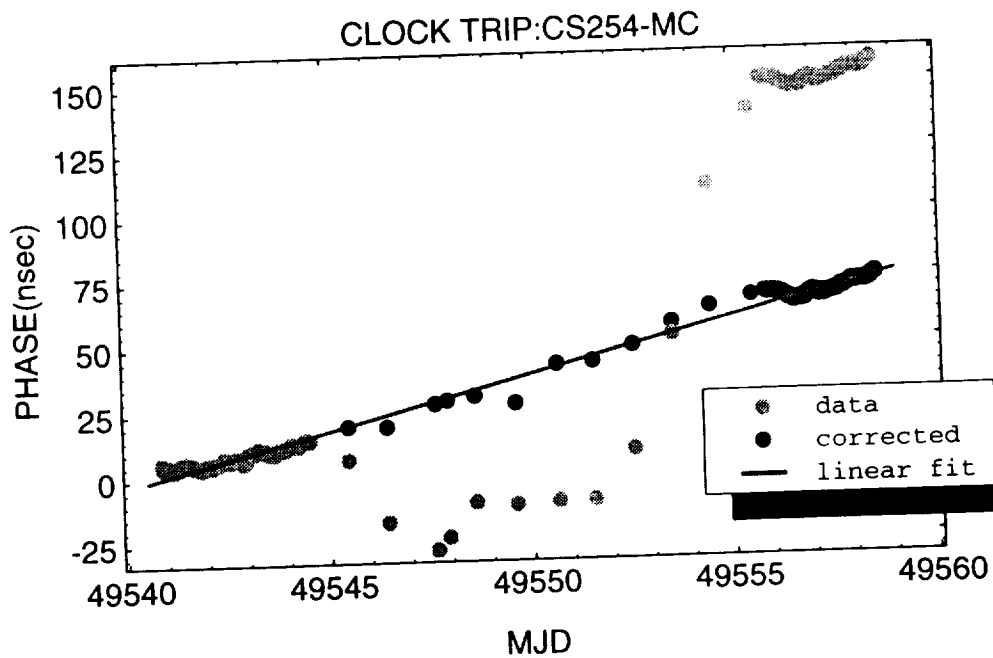


Figure 6. Shows the original cesium #254-Master Clock data along with the data corrected for two-way Sagnac and the clock trip relativistic effects.

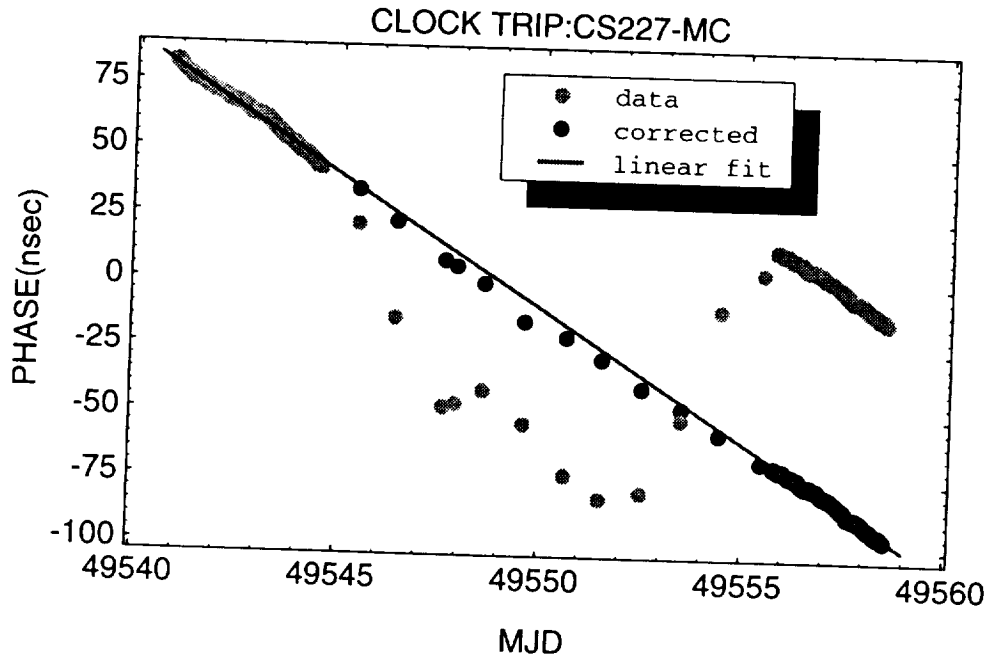


Figure 7. Shows the original cesium #227-Master Clock data along with the data corrected for two-way Sagnac and the clock trip relativistic effects.

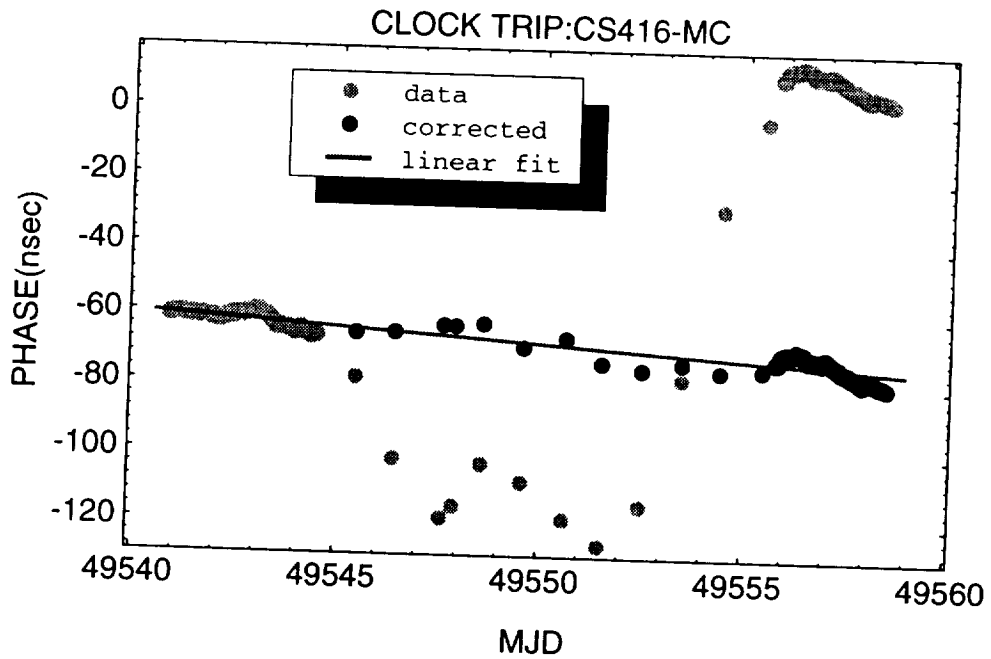


Figure 8. Shows the original cesium #416-Master Clock data along with the data corrected for two-way Sagnac and the clock trip relativistic effects.

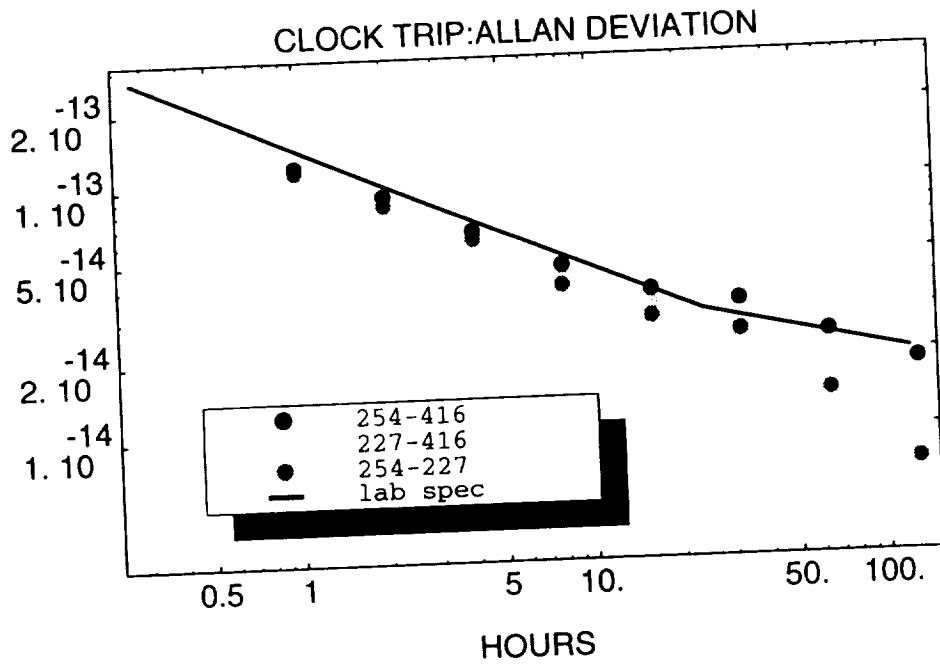


Figure 9. Stability of the cesium clocks as measured in the van during the trip.

## QUESTIONS AND ANSWERS

**DAVID ALLAN (ALLAN'S TIME):** A question regarding the regression that you did to determine the frequency during the trip from the data. As near as I can tell, it looks like you did a linear regression to all of the phase points. Is that correct?

**PAUL WHEELER (USNO):** Yes.

**DAVID ALLAN (ALLAN'S TIME):** Given your sigma tau plot that the noise is white noise frequency modulation, which is random walk of phase, the optimum interpolater for the frequency while you were on the trip would be the end-point from the beginning and the beginning point of the end, to give you a better estimate of frequency than the linear regression. Thank you.

**SIGFRIDO M. LESCHIUTTA (IEN):** Could you please elaborate to me concerning the two calibration processes? One was done before and after the trip. What was done really?

The second, have you made any calibration before and after each session, calibration of the orbital treatment?

**PAUL WHEELER (USNO):** The calibration -- we do it a couple different ways. For this experiment, since the clocks in the van, we wanted to measure the clocks that were taken with us the same way at the Observatory as we did in the field. So we did two-way time transfer between the two stations right there at USNO, our base station being measured against the USNO Master Clock. The mobile air station being measured against one of the clocks in the van. Right after that session, we then measured that clock with a cable, to our acquisition system, against the Master Clock and determined the difference between the two ways.

The second question, the answer is no. It was strictly before we left and when we returned, and nothing in-between.



6-12-94  
P. 12

# FINE TUNING GPS CLOCK ESTIMATION IN THE MCS

Capt Steven T. Hutsell, USAF  
2d Space Operations Squadron  
300 O'Malley Avenue Suite 41  
Falcon AFB CO 80912-3041

## Abstract

*With the completion of a 24 operational satellite constellation, GPS is fast approaching the critical milestone, Full Operational Capability (FOC). Although GPS is well capable of providing the timing accuracy and stability figures required by system specifications, the GPS community will continue to strive for further improvements in performance.*

*The GPS Master Control Station (MCS) recently demonstrated that timing improvements are always composite Clock, and hence, Kalman Filter state estimation, providing a small improvement to user accuracy.*

## INTRODUCTION

Though well capable of meeting and/or exceeding customer expectations, the GPS Master Control Station (MCS) will continuously search for safe and efficient methods for improving GPS timing accuracy and stability performance. The most recent improvements have focused on fine tuning the Continuous Time Update Process Noises (a.k.a.  $qs$ ) for all GPS satellite frequency standards.

Process noises are nothing new to the timing community. Many time scale algorithms update these parameters dynamically for their respective systems. As in many Kalman Filters, the Defense Mapping Agency (DMA) periodically reviews their  $q$  values for their OMNIS computation program. OMNIS, like the MCS Kalman filter, estimates the ephemeris, solar, and clock states for 25 GPS satellites<sup>[3]</sup>. However, up until 6 Oct 94, the timing community had never undertaken the task of re- $q$ ing an entire operational GPS constellation in the MCS Kalman Filter.

Thanks to the generous input from several outside agencies, we now employ process noise values that are unique to the individual characteristics of the 25 operating frequency standards on orbit. Perhaps more importantly, we now also have the precise data, know-how, tools, and procedures to safely and efficiently review and update our  $q$  values on a periodic basis.

## RUBIDIUM CLOCK ESTIMATION

Each GPS satellite uses one of two different types of atomic clocks to provide a stable output frequency, to, in turn, generate accurate navigation signals. The majority of Block II/IIA GPS satellites currently use one of two available Cesium (Cs) frequency standards. Orbiting Cs clocks demonstrate reliable performance, with one-day stabilities ranging between  $0.8 \times 10^{-13}$  to  $2.0 \times 10^{-13}$  [13,14,15]. The drift rate term for a Cs frequency standard is typically on the order of  $1 \times 10^{-20}$  s/s<sup>2</sup> or less. Such a small drift rate term, an order of magnitude smaller than our time steering magnitude, has negligible effects on GPS timing (hundredths of a nanosecond over one day). Because of its relatively insignificant effect on frequency estimation, the MCS currently fixes the drift rate estimate to zero for all Cs frequency standards (on-orbit and ground based).

Two Rubidium (Rb) clocks also reside on each Block II/IIA satellite. Rb clocks do exhibit a significant aging characteristic, typically on the order of  $1 \times 10^{-18}$  s/s<sup>2</sup>. However, if a filter properly corrects for drift rate, the typical one-day frequency stability of a Rb clock *state* is significantly better than that of a Cs ( $0.6 \times 10^{-13}$  versus  $1.0 \times 10^{-13}$ ) [13,14,15]. Unfortunately, in the past, our Kalman Filter had difficulty estimating drift rate. As a result, Rb clock estimates have had somewhat large variances, causing, in turn, increased difficulty in estimating frequency. Although a Rb clock itself is usually more stable than a Cs at one day, the stabilities of the MCS's Kalman filter Rb clock *states* have, in the past, been *worse* than those for Cs clocks.

This filter instability has impeded the MCS from incorporating their inherently better stability into GPS time calculations. Consequently, the timing community has been uneasy about using Rb clocks in GPS. Of the first 24 operational satellites, we initialized only *three* with Rubidium clocks.

Despite this reluctant attitude towards using Rubidium clocks, many have realized that as Cesium clocks reach their respective ends of operational life, we will have *no choice* but to use more Rubidium clocks. In any case, it seemed counterintuitive that GPS was not making the most use of our most stable clocks. In early 1994, the 2 SOPS Navigation Analysis Section began tackling this long-standing concern. Because the problem resided in estimation, as opposed to physical clock performance, the Kalman Filter really only needed a fine tuning.

### Deriving New Rubidium Clock $qs$

The MCS Kalman filter performs recursive time and measurement updates of the state residuals and covariances. In pure prediction, the clock state covariances are functions of the system  $qs$  [18]:

$$P = \begin{bmatrix} q_1 t + q_2 t^2 + q_3 t^5 / 20 & q_2 t^2 / 2 + q_3 t^4 / 8 & q_3 t^3 / 6 \\ q_2 t^2 / 2 + q_3 t^4 / 8 & q_2 t + q_3 t^3 / 3 & q_3 t^2 / 2 \\ q_3 t^3 / 6 & q_3 t^2 / 2 & q_3 t \end{bmatrix} \quad (1)$$

The Naval Research Laboratory (NRL) produced a report for 2 SOPS (ALL-5, 27 Jan 94), on SVN25. The report included a series of drift rate plots for the Rb clock that was active from

Mar 1992 until Dec 1993. NRL plotted 5, 10, 20, and 30-day averaged values for drift rate[11]. In analyzing the 30-day average plot, we noticed that the drift rate changed significantly more during the first 90 days than during the remaining operational time [Figure 1].

From the above P matrix, in pure filter prediction, the system variance for drift rate is the scalar time product of  $q_3$ :

$$C_3 = q_3(\tau)(2) \tag{2}$$

Using the above equation, along with the NRL data, we derived new  $q$  values, both from the 90-day initialization period, and from the remaining period, and we compared these to the old system  $q$  values:

q value	OLD	INITIAL	NEW NORMAL
Drift Rate ( $q_3$ )	$9.00 \times 10^{-42} s^2/s^4$	$1.35 \times 10^{-43} s^2/s^5$	$6.66 \times 10^{-45} s^2/s^5$

We also looked at calculating a new drift (frequency)  $q$  value. The old Rb  $q$  value for drift,  $4.44 \times 10^{-32} s^2/s^3$ , was the same as that for Cs. We chose  $q_2 = 2.22 \times 10^{-32} s^2/s^3$ [4]. Again, to be conservative, and to allow the filter to handle any possible instability resulting from clock “warm-up”, we set the initialization  $q_2$  value to  $3.33 \times 10^{-32} s^2/s^3$ . We kept the phase (bias)  $q$  unchanged. Below is a comparison of the old set and the two new sets of process noise values for Rubidiums:

q Value	OLD	INITIAL	NEW NORMAL
Bias ( $q_1$ )	$1.11 \times 10^{-22} s^2/s$	$1.11 \times 10^{-22} s^2/s$	$1.11 \times 10^{-22} s^2/s$
Drift ( $q_2$ )	$4.44 \times 10^{-32} s^2/s^3$	$3.33 \times 10^{-32} s^2/s^3$	$2.22 \times 10^{-32} s^2/s^3$
Drift Rate ( $q_3$ )	$9.00 \times 10^{-42} s^2/s^5$	$1.35 \times 10^{-43} s^2/s^5$	$6.66 \times 10^{-45} s^2/s^5$

Of course, one might question using 30-day averaged drift rate values for deriving  $q_3$ —could the drift rate change by an unacceptable amount during those 30 days, thus undermining the premise of these calculations? Well, in the past, NRL has been able to apply as much as a 150 day flat-average aging correction to their Allan Deviation plots—plots showing one-day stability figures similar to SVN25’s[10]. The implication is, if the Filter has a good drift rate term, that value can essentially be fixed for, in some cases, up to 150 days, without significantly degrading the one-day accuracy of the other clock states. Certainly, assuming drift rate consistency over 30 days, let alone 150, was safe for deriving the above  $q$  values for the MCS Kalman filter.

### SVN9 End Of Life Testing

50th Space Wing approved a 1 SOPS and 2 SOPS joint effort to conduct End Of Life testing on SVN9 during March and April 1994 [19]. As part of the plan, Rockwell suggested dedicating

7–8 days for testing Rubidium clock drift rate estimation. We used the “New Normal”  $q$  values, and monitored the resulting system performance.

The test, which lasted 8.7 days, produced very encouraging results<sup>[19]</sup>. At the end of the test, with tighter process noise values, the Kalman Filter converged on a drift rate value of  $-2.38 \times 10^{-18} \text{s/s}^2$ , with an associated standard deviation of  $1.99 \times 10^{-19} \text{s/s}^2$  (compared to a typical standard deviation of  $1.0 \times 10^{-18} \text{s/s}^2$ , using the old  $q$  values). Using an off-line tool, Rockwell derived post-processed values for comparison. Using a simple slope of their  $A_1$  (frequency) estimates over 7 days, Rockwell’s drift rate estimate was  $-2.44 \times 10^{-18} \text{s/s}^2$ , well within one sigma of the filter’s estimate. The National Institute of Standards and Technology (NIST) Report on SVN9 End of Life Testing pointed to a value of  $-2.32 \times 10^{-18} \text{s/s}^2$ <sup>[8]</sup>, also well within one sigma of the Filter estimate. These comparisons indicated that the Filter had performed as designed—to converge on a more accurate drift rate estimate, with a correspondingly representative error estimate (standard deviation) [Figure 2].

By, in effect, “clamping” on the filter estimate, one must question whether this covariance tightening is too restrictive, limiting the filter’s capability to respond to normal clock movement. We used two MCS parameters to test this capability.

- a. The first parameter was the Measurement Residual Statistical Consistency Test (MRSCCT). Essentially, the MRSCCT decides whether or not to accept Pseudorange (PRs). Over 8.7 days, the Filter accepted each and every smoothed PR for SVN9. The average PR residual (PRR) was no higher than that of a typical healthy, operational vehicle, or SVN9’s prior to the test.
- b. The second parameter was the Estimated Range Deviation (ERD). The ERD gives a good indication of the range error a user is experiencing, based on the current navigation upload residing in the vehicle. Over the 8.7 days, we uploaded SVN9 only once per day, and the ERD RMS never once exceeded 3.1 meters—well within our ERD criteria of 10 meters. Correspondingly, the one-day User Range Accuracy (URA) dropped from 5.0 to 3.8 meters, and the four-day URA dropped from 33.0 to 13.0 meters. In hindsight, we could have even set SVN9 healthy during the test, and netted a small improvement to global coverage and accuracy [Figure 2].

In short, results from the SVN9 drift rate test indicated that Filter estimation worked quite better with the reduced process noise ( $q$ ) values.

### Real World Implementation Of The New Rubidium $q$ s

On 18 Mar 94, we began applying these results towards real-world SVN10 and SVN24 clock estimation. Since, at that time, SVN24’s Rb was less than three months old, and since SVN10 is a Block I, always susceptible to the effects of eclipse seasons, we selected the “Initialization”  $q$ s instead of the “New Normal”  $q$ s.

For SVN10, during the three months prior to the test, ERDs exceeded 5.0 meters on 19 separate days. During the three months after the new  $q$ s were installed, SVN10 ERDs didn’t once

exceed 4.8 meters. In addition, our Smoothed Measurement Residual (SMRES) tool showed that SVN10 residuals from the DMA monitor stations, since 18 Mar 94, have been consistent with those prior to 18 Mar 94, as well as those for our other satellites. Similarly, between these two time periods, SVN10's time transfer error dropped from 14.6 to 9.9 nanoseconds (RMS), according to United States Naval Observatory (USNO) data<sup>[5]</sup>. These data points, from independent agencies, further show a significant improvement in satellite accuracy.

Similar to SVN10's, the ERDs for SVN24 decreased after 18 Mar 94. Additionally, after installing the "New Normal"  $qs$  on 24 Apr 94, from that time to the present, the Filter has easily and consistently accepted SVN24 PRs. Likewise, SVN24 residuals from DMA, since 24 Apr 94, have been as good or better than those prior to 24 Apr 94, and better than those of the other 23 operational satellites. In terms of upload accuracy, SVN24's ERDs routinely exceeded 4.0 meters prior to 24 Apr 94. Since 24 Apr 94, SVN24's ERDs have rarely exceeded 3.5 meters, and have typically stayed under 2.5 meters. SVN24, now, is one of our two most accurate satellites. To complete the usefulness of this improvement, on 28 Apr 94, we included SVN24 into the GPS composite clock, allowing it to better stabilize GPS time.

For the time being, after the 2 SOPS has initialized a Rubidium clock for 7-14 days, we'll probably install the "Initialization"  $qs$  for 90 days. At the three month point, assuming nominal clock performance, we'll likely install the "New Normal"  $qs$ . Also, at three months, we will aggressively consider including that satellite into the GPS composite clock—a Block II/IIA Rubidium clock estimate, now properly corrected for drift rate, now has a better one-day frequency stability than those of each of the on-orbit Cesiums. The GPS community, as a whole, can now at least tame a long existing ambivalence we've had about using Rubidium clocks in operational satellites. A Rubidium clock, now properly tuned in the Kalman Filter, significantly improves GPS timing and positioning accuracies. Currently, five GPS satellites use Rubidium clocks. One, in particular, SVN36, is arguably now our most accurate satellite.

## CESIUM CLOCK ESTIMATION

Having resolved perhaps the most significant recent problem with GPS clock estimation through improved Rubidium  $qs$ , we decided to expand this opportunity for improvement to the remainder of all on-orbit GPS frequency standards: Cesium (Cs) clocks. As demonstrated earlier, deriving clock  $qs$  involves two main steps: 1) obtaining data that can accurately describe the behavior of the clocks involved, and 2) mathematically translating this behavior into the  $qs$  themselves.

DMA has already been doing exactly this. A snapshot of some recently-derived DMA  $qs$  shows values that are, for the most part, unique to the individual clocks<sup>[3]</sup>. DMA's  $qs$  vary significantly between satellites. In contrast, prior to 6 Oct 94, the MCS  $qs$  were equal for most GPS Cs clocks. Also noteworthy is that the MCS's  $q_1$  value was less than each of DMA's equivalent  $q_1$  values<sup>[3]</sup>:

	MCS $q$ Values	DMA $q$ Values	
		Smallest	Largest
Bias ( $q_1$ )	$1.11 \times 10^{-22} \text{s}^2/\text{s}$	$4.25 \times 10^{-22} \text{s}^2/\text{s}$	$4.35 \times 10^{-21} \text{s}^2/\text{s}$
Drift ( $q_2$ )	$4.44 \times 10^{-32} \text{s}^2/\text{s}^3$	$7.35 \times 10^{-33} \text{s}^2/\text{s}^3$	$5.16 \times 10^{-32} \text{s}^2/\text{s}^3$

This comparison raised two questions: 1) Would uniquely tuning the  $qs$  provide a significant improvement to GPS performance? 2) Does a legitimate reason exist for deliberately having lower  $q_1$  terms in the MCS Kalman Filter? The remainder of this paper answers the first question. The second question, however, is more philosophical.

MCS software experts will argue that a fundamental difference in purpose between the respective Kalman Filters at the MCS and at DMA constitutes a legitimate reason for using different  $q_1$  terms. Since the MCS Kalman Filter is designed, in part, to provide accurate 24 hour predictions for navigation uploads, one could argue that we might want to deliberately keep our  $q_1$  low to reduce the gain, and hence, prevent a situation whereby a noisy Kalman update could skew a 24-hour navigation upload prediction. Timing experts, however, will argue that tinkering with this parameter can be dangerous, since doing so can impose a configuration inconsistent with the basic intended design of a Kalman Filter. Both sides have very legitimate arguments.

### Deriving New Cesium Clock $qs$

Analysts at NRL provide timely, accurate, and understandable reports on GPS clock performance. In particular, we now greatly utilize their Allan Deviation [ $\sigma^2(\tau)$ ] plots, created from DMA precise ephemeris data. The following equation relates the Allan Variance [ $\sigma^2(\tau)$ ] to Kalman Filter  $qs$ . This equation assumes independence between each sample frequency pair<sup>[2]</sup>.

$$\sigma^2(\tau) = q_1(\tau^{-1}) + q_2(\tau)/3 + q_3(\tau^3)/20 \quad (3)$$

In order to relate current clock performance (via the Allan Deviation) to the system  $qs$ , we try not to use data more than 90 days old. Unfortunately, by only using 90 days of data, we experience the tradeoff of degraded confidence intervals for  $\tau > 20$  days. For Cesium clocks, this is a non-concern, since we currently fix the drift rate and  $q_3$  values to zero. For Rubidium clocks, however, the degraded confidence intervals, combined with the difficulty of correcting for drift rate without violating the sample frequency pair independence assumption, makes calculating the last term dangerous. As demonstrated earlier in this paper, we now have very suitable  $q_3$  values for Rubidium clocks. Thus, for  $\tau < 20$  days, we can substitute these into the Allan Variance equation, and simply solve for  $q_1$  and  $q_2$ . Then, we can compare our theoretical values to empirical values, using NRL Allan Deviation plots (with flat aging corrections applied for Rubidium clocks)<sup>[12]</sup>.

One other concern relates to measurement noise. The data from NRL, and hence from DMA, has a fairly certain amount of measurement noise. The MCS's parameter for measurement

noise, which we'll call  $q_0$ , accounts for some of the GPS monitor station (MS) receiver noise, some of the satellite clock's white and flicker phase noise, MS location errors, and general modeling errors. DMA has a similar parameter designed to account for measurement noise, currently set to  $(45 \text{ cm})^2 \cong 0.20 \text{ m}^2$ . For years, the MCS set this parameter at  $1.0 \text{ m}^2$ . Thanks to recently refined MS location coordinates from DMA[6], the MCS was recently able to reduce  $q_0$  to  $(0.86 \text{ m})^2 \cong 0.74 \text{ m}^2$ . We derived this value using 500 Pseudorange Residual values from a widely distributed assortment of times and satellite-MS combinations. Our new value of  $0.74 \text{ m}^2$ , not surprisingly, is not a dramatic reduction from  $1.0 \text{ m}^2$ , but nonetheless is consistent with our expectation of improvement from the new coordinates:

$$\sqrt{(1.00^2 - 0.86^2)} = .51(\text{meters}) \quad (4)$$

One might suggest using DMA's lower value. However, since our parameter accounts for more than just pure white measurement "noise", our parameter is higher for a legitimate reason. Although not purely white phase noise in nature, noise associated with measurements can tend to misrepresent the stability of the estimated clock states. We can roughly express the instability resulting from this representation error as[1]:

$$\sigma_r^2(\tau) = 3q_0(\tau^{-2}) \quad (5)$$

By assuming independence between this representation error and the other noise processes on a given clock, the equation for the Allan Variance of the measured clock adds an additional term[7]:

$$\sigma_m^2(\tau) = 3q_0(\tau^{-2}) + q_1(\tau^{-1})/3 + q_3(\tau^3)/20 \quad (6)$$

We created a Basic program to plot the theoretical  $\sigma(\tau)$  values, using the above equation, for  $\tau = 0.1$  to 100 days. Using recent precise ephemeris  $\sigma(\tau)$  plots from NRL[12], along with the Basic program, we derived new  $q$  values for all satellites [Figure 3]. Note that the Rubidium  $qs$  remained unchanged. The Rb  $qs$  we derived earlier this year are, and have been, consistent with true clock performance. Nonetheless, Figure 4 shows how the theoretical Allan Deviation does change significantly for, in particular, SVN21 and SVN23, by using the newer  $qs$ .

The current MS bias and drift  $qs$ ,  $1.11 \times 10^{-22} \text{ s}^2/\text{s}$  and  $4.44 \times 10^{-32} \text{ s}^2/\text{s}^3$ , respectively, are not representative of true MS clock performance. However, the MCS uses three separate mini-Kalman Filters, a.k.a. "partitions" to individually estimate MS clock states. Since a partition reconciliation algorithm keeps these states fairly consistent[4,4], over time, the MCS estimation structure effectively triples the weighting of the long term effects of MS clocks. With this current  $q_2$  value for MSs, this "triple weighting" produces, in a roundabout fashion, the effect of using a  $q_2$  roughly the same as the smallest satellite  $q_2$ . We may tweak this parameter in the future, but, for the time being, this effect produces a fairly accurate result[16].

We also began using a newer set of  $q_s$  during Cesium clock initialization. Below is a comparison of the old  $q_s$ , and new initialization  $q_s$  we've derived:

Old q1	Old q2	Old q3	New q1	New q2	New q3
$10^{-22} \text{s}^2/\text{s}$	$10^{-32} \text{s}^2/\text{s}^3$	$10^{-45} \text{s}^2/\text{s}^5$	$10^{-22} \text{s}^2/\text{s}$	$10^{-32} \text{s}^2/\text{s}^3$	$10^{-45} \text{s}^2/\text{s}^5$
1.11	4.44	0	4.44	3.33	0

## Testing The New Cesium $q$ Values

We safely tested the validity of these changes on 3 Oct 94, using a Test & Training simulator in the MCS. The results were impressive.

- a As expected, the state covariances converged to steady state values more truly representative of the unique short- and long-term variances of the individual clocks. Also as expected, none of these new steady state covariances differed drastically from the typical older values. The implication of these small, but significant changes is that the Filter safely re-weighted clock state estimation based on true frequency standard performance, as opposed to assumed performance equality (equal  $q_s$ ):

Value	OLD VARIANCES	NEW VARIANCES	
	(All Cs)	(Minimum)	(Maximum)
Bias	$1.25 \times 10^{-17} \text{s}^2$	$1.07 \times 10^{-17} \text{s}^2$	$1.83 \times 10^{-17} \text{s}^2$
Drift	$3.20 \times 10^{-27} \text{s}^2/\text{s}^2$	$1.38 \times 10^{-27} \text{s}^2/\text{s}^2$	$4.38 \times 10^{-27} \text{s}^2/\text{s}^2$

- b As expected, the current state residuals experienced small (not trivial, not severe) changes, indicating that the Filter more responsibly distributed error to the appropriate states.
- c The MCS Pseudorange Residuals (PRRs) dropped from 1.61 m (RMS) to 0.87 m (RMS), after the Filter reprocessed the same raw data with the new set of  $q_s$ . This more dramatically indicates that the Filter more responsibly distributed error to the appropriate states, so well that Filter predictions can now have less systematic error, and hence, less error when compared to smoothed measurements.
- d The consistency of MS clock states across the Kalman Filter partitions experienced a small, but not trivial improvement (A 3.8% reduction in Bias divergence error, and 21.6% reduction in Drift divergence error). Again, by more responsibly appropriating error to the respective clock states, short-term MS clock state instability across the partitions dropped.

## Real-World Implementation Of The New Cesium $q_s$

By installing these new  $q_s$  on 6 Oct 94, we safely improved a) Kalman Filter clock estimation, b) navigation error representation, and c) the stability of the GPS composite clock.

The stability of GPS time, defined by the GPS composite clock, intuitively, should have improved simply as a result of the improved weighting, again, by uniquely tuning the  $q_s$  based on true clock performance. When we used equal  $q_s$ , the Allan Variance,  $\sigma_{\Delta}^2(\tau)$ , of the implicit ensemble of  $N$  equally weighted clocks (for  $\tau = 1$  day) was approximately<sup>[4]</sup>:

$$\sigma_{\Delta}^2(\tau) \cong 1/(N^2) \sum_{i=1}^N \sigma_{y_i}^2(\tau) \quad (7)$$

Using the one-day Allan Deviation figures from NRL Quarterly Report 94-3<sup>[5]</sup>, the one-day stability of this implicit ensemble was approximately  $1.55 \times 10^{-14}$ .

By using clock-unique  $q_s$ , the Allan Deviation of the now finely tuned implicit ensemble (for  $\tau = 1$  day) is approximately<sup>[1,4]</sup>:

$$\sigma_{\Delta}^2(\tau) \cong \left[ \sum_{i=1}^N (\sigma_{y_i}^2(\tau))^{-1} \right]^{-1} \quad (8)$$

Incorporating the same one-day NRL Allan Deviation figures into the above equation, the one-day stability of the implicit ensemble dropped to approximately  $1.22 \times 10^{-14}$ . Similarly, the *observed* Allan Deviation of GPS time, derived from USNO-smoothed measurements<sup>[5,9]</sup>, also dropped, not only for  $\tau = 1$  day, but for  $1 \leq \tau \leq 10$  days [Figure 5].

Important to note is a large improvement in extended (14 day) navigation performance. By utilizing more representative (lower)  $q_2$  values, the 14-day URA predictions have dropped to lower, more representative values for most satellites. Figure 6 shows a comparison of the typical 14-day URA values before and after 6 Oct 94, for all Block IIA satellites in estimating partitions. Though not an absolute indication of extended navigation accuracy, by uniquely tuning the  $q_s$ , these URA values now, at least, have more validity than before. The 14-day URA values for all healthy GPS satellites, since 6 Oct 94, have been well below the NAVSTAR GPS System Operational Requirements Document (SOR) User Range Error (URE) specification of 200 meters<sup>[17]</sup>.

## CONCLUSION

This fine tuning reinforces how deriving and installing clock-unique MCS Kalman Filter process noise values can safely and significantly improve GPS timing performance. We will continue to update these parameters on a regular basis. In the near future, we plan to review these values every three months, and as needed (after a clock swap or a dramatic change in clock performance).

Loral Federal Systems Division received a tasking to more comprehensively review these and other data base parameters in 1995. We expect the results from their analysis to be more precise than the above results, due to the extensive background of the team of experts that will tackle this project.

Nonetheless, this successful attempt at fine tuning the MCS qs helps pave a path for future MCS data base analyses, and hence for future refinements to GPS timing performance.

## ACKNOWLEDGMENTS

The author wishes to thank the following people and agencies for their generous assistance with both our timing improvements and this paper:

Ronald Beard, NRL  
Don Brown, Major, USAF Reserve  
Ken Brown, Loral Federal Systems Division  
Jim Buisson, SFA  
James W. Chaffee, Associate Member, IEEE  
M. K. Chien, Loral Federal Systems Division  
Bruce Hermann, Naval Surface Warfare Center  
Steve Holm, Retired, Defense Mapping Agency  
Judah Levine, NIST  
Steve Malys, Defense Mapping Agency  
Sam R. Stein, Timing Solutions Corporation  
Everett R. Swift, Naval Surface Warfare Center  
John V. Taylor IV, formerly of Rockwell International, now with Martin Marietta  
The people of the 2 SOPS  
Francine Vannicola, USNO  
Marc A. Weiss, NIST

## REFERENCES

- [1] Brown, Kenneth R., "*The Theory of the GPS Composite Clock*", Proceedings of ION GPS-91, 11-13 Sept. 91
- [2] Chaffee, James W., "*Relating the Allan Variance to the Diffusion Coefficients of a Linear Stochastic Differential Equation Model for Precision Oscillators*", from the IEEE Transactions on Ultrasonics, Ferroelectrics, and Frequency Control, Vol. UFFC-34, No. 6, November 1987
- [3] Hermann, Bruce R., : "*Allan Variance Model Parameters Determined From OMNIS Satellite Clock Files*", 23 Mar 94
- [4] Hutsell, Steven T., Capt, USAF, "*Recent MCS Improvements to GPS Timing*", Proceedings of ION GPS-94, 20-23 Sep 94
- [5] ICD-GPS-202, 21 Nov 84

- [6] Malys, Stephen, and Slater, James, "*Defense Mapping Agency, Maintenance and Enhancement of the World Geodetic System 1984*", Proceedings of PAWG '94, 3-4 Aug 94
- [7] Maybeck, Peter S., "*Stochastic Models, Estimation and Control*", Volume 1, 1979
- [8] NIST Report on End of Life Testing, 25 Apr 94
- [9] NIST Technical Note 1337, Mar 90
- [10] NRL Analysis Update, SVN25, 15 Oct 92
- [11] NRL Analysis Update, 25-6, 17 May 94
- [12] NRL Analysis Update All-9, 17 Aug 94
- [13] NRL Quarterly Report No. 94-1, 15 Jan 94
- [14] NRL Quarterly Report No. 94-2, 15 Apr 94
- [15] NRL Quarterly Report No. 94-3, 15 Jul 94
- [16] NRL Technical Update No. 1, 5 Oct 94
- [17] NAVSTAR GPS System Operational Requirements Document (SORD), 22 Jan 90
- [18] Taylor, John V., IV, Rockwell International, "*Estimation of Clock Drift Rate States on GPS SVs Using Rb Frequency Standards MFR*", 31 Jan 94
- [19] 1 SOPS/2 SOPS/Rockwell SVN9 End of Life Test Results, Mar-Apr 94

## QUESTIONS AND ANSWERS

**GERNOT M. WINKLER (USNO):** Do you apply, or do you know whether anyone has every applied, any modeling for the ground stations, the same as you model your 12-hour satellite frequency change, which you observe? Has there been any modeling of the ground station?

**STEVEN HUTSELL (USAF):** Ground station 12-hour periodics?

**GERNOT M. WINKLER (USNO):** Whatever.

**STEVEN HUTSELL (USAF):** Not that I'm aware of. I'm sure that there are seasonal and other effects. We try to model some of our tropospheric values. Right now, we have default values for those. LORAL Federal Systems Division has been working on that. The biggest problem we've had is getting environmental sensors that we're comfortable with. Granted, we haven't tested it as much as we could, and that's probably something we could look into more. But for the time being, we are using database values.

92-302  
P. 17

# IMPLEMENTATION OF A STANDARD FORMAT FOR GPS COMMON VIEW DATA\*

Marc A. Weiss  
Time and Frequency Division  
National Institute of Standards  
and Technology  
325 Broadway  
Boulder, CO 80303 USA

Claudine Thomas  
Time Section  
Bureau International des Poids  
et Mesures  
Pavillon de Breteuil  
92312 SÈVRES FRANCE

## Abstract

*A new format for standardizing common view time transfer data, recommended by the Consultative Committee for the Definition of the Second, is being implemented in receivers commonly used for contributing data for the generation of International Atomic Time. We discuss three aspects of this new format that potentially improve GPS common-view time transfer: (1) the standard specifies the method for treating short term data, (2) it presents data in consistent formats including needed terms not previously available, and (3) the standard includes a header of parameters important for the GPS common-view process. In coordination with the release of firmware conforming to this new format the Bureau International des Poids et Mesures will release future international track schedules consistent with the new standard.*

## INTRODUCTION

A new format for standardizing common view time transfer data, recommended by the Consultative Committee for the Definition of the Second (CCDS), is being implemented in receivers commonly used for contributing data for the generation of International Atomic Time (TAI). The primary means of remote clock comparison for generating TAI is common-view GPS time transfer<sup>[1]</sup>. The global accuracy for this type of time transfer is currently less than 10 ns<sup>[2]</sup>. Understanding the sources of inaccuracy, the BIPM initiated an effort to standardize data-taking methods used in receivers and data transfer methods used for reporting to the BIPM. By combining this effort with the use of good coordinates, precise GPS satellite ephemerides, and measured local ionospheric delays, we hope to increase the accuracy for common-view time transfer<sup>[3]</sup>.

One of the major motivations for standardization is the implementation of Selective Availability (SA) in GPS satellites. With SA, GPS timing is degraded as a way of limiting the navigation

\*Work of the U.S. Government not subject to copyright.

accuracy available to the standard positioning service (SPS) user. This follows since navigation in GPS is accomplished using measurements of time as received from satellites. If common-view time transfer is performed strictly, that is, with measurements taken on identical seconds, and with receivers which process the signals and the data identically, then the GPS satellite clocks cancel completely. SA makes this need for strict common-view even more important. We include in this paper some direct satellite data with SA and predict the effects on common-view time transfer due to differences in receivers. Thus, a standard can improve time transfer by allowing common-view time transfer to be done with different receivers and still cancel the effects of the satellite clock.

The new format has potential to improve GPS common-view time transfer due to a number of elements: (1) the standard specifies the method for treating short term data, (2) it presents data in consistent formats including needed terms not previously available, and (3) includes a header of parameters important for the GPS common-view process. Essential to common-view time transfer is that stations track satellites according to a common schedule. In coordination with the release of firmware conforming to this new format the Bureau International des Poids et Mesures (BIPM) will release future international track schedules consistent with the new standard. In this paper we summarize information about the short-term data processing, the header and the data format. When developing the standard for a receiver, one should obtain all the detailed information as reported in the Technical Directives<sup>[4]</sup>.

## SHORT TERM DATA PROCESSING

Data processing is performed as follows:

1. Pseudo-range data are recorded for times corresponding to successive dates at intervals of 1s. The date of the first pseudo-range data is the nominal starting time of the track. It is referenced to UTC and appears in the data file under the acronyms MJD and STTIME.
2. Least-squares quadratic fits are applied on successive and nonoverlapping sets of 15 pseudo-range measurements taken every second. The quadratic fit results are estimated at the date corresponding to the midpoint of each set.
3. Corrections are applied to the results of (2) to obtain estimates of the local reference minus the Satellite Vehicle (SV) clock (REFSV) and of the local reference minus GPS time (REFGPS) for each 15 second interval.
4. The nominal track length corresponds to the recording of 780 short-term measurements. The number of successive and nonoverlapping data sets treated according to (2) and (3) is then equal to 52. For full tracks, the track length TRKL will thus equal 780 s.
5. At the end of the track, least-squares linear fits are performed to obtain and store the midpoint value and slope for both REFSV and REFGPS. Since these two are related deterministically by nearly a straight line they will have the same rms deviation around the fit, which is also stored as DSG. In addition, least-squares linear regression gives the midpoint and slope of the ionospheric and tropospheric model values, and the ionospheric measurements if they exist.

## THE EFFECTS OF SA

We investigate the effects of SA by taking measurements every 15 s of GPS – UTC(NIST) tracking different satellites from horizon to horizon. We took data sequentially from three different satellites on two consecutive days, November 21–22, 1994. The satellites had pseudo-random code numbers (PRN's) 20, 22, and 25. Figures 1–3 show the data from the three satellites, and Figures 4–6 show the time deviation TDEV of the three, respectively.

The new standard will cancel all the clock dither when used for common-view GPS time transfer, provided that each of the two receivers involved track the same satellites over the same time periods. If there is a difference of 15 s in the tracking, for example if one receiver tracks 15 s less than the other, then the clock dither of SA will corrupt the common-view time transfer. We can estimate this by looking at the expected dispersion in time at due to SA at 15 s. The rms of the three TDEV values for  $\tau=15$  s is 11 ns. From the TDEV plots we see that the slope on the log-log plots starts consistent with a model of  $\tau^0$  from 15–30 s. If we assume a model of flicker phase modulation (PM) for  $\tau=15$  s this implies an expected time dispersion of 13 ns<sup>[5]</sup>. Over a 13 min track there are 52 estimates of REFGPS and REFSV each from a quadratic fit over 15 s of data. Let us consider the case where one track is a full-length track and the matching track in another receiver is 15 s short. If we can assume that the effects of one 15 s point average down in the linear fit as the square root of the total number of points, then we can expect the effect on the common-view time transfer to be

$$\frac{13\text{ns}}{\sqrt{52}} = 1.8 \text{ ns.} \quad (1)$$

Thus SA could add approximately 2 ns to a common-view uncertainty budget with only a mis-match of 15 s from exact common-view. With a goal of 1 ns we see the reason why a standard for data taking can help common-view time transfer.

Many users receive GPS time directly from the satellites without using the common-view method to compare with another lab. From considering the TDEV of SA, we can design a filter that averages SA optimally, to allow users to obtain the best possible restitution of GPS time<sup>[6]</sup>. From the three TDEV analyses we see a bump rising from 1 min and dropping at 16 min. This effect could be due in part to a periodic behavior with a period of approximately 16 min<sup>[7,8]</sup>. Averaging can improve the GPS restitution if the TDEV values drop with increasing <insert 4>. Yet there is no indication in these data that the TDEV values drop significantly beyond 16 min. This may be due to effects at the beginning and end of the tracks when the elevation is low. This suggests limitations on the potential for filtering SA. Yet our data were taken using a single channel receiver. A multi-channel receiver could improve on filtering. It may be that the combination of SA signals still drop in TDEV, allowing improvement from averaging.

## THE DATA FORMAT

The data format consists of:

1. a file header with detailed information on the GPS equipment,
2. a line header with the acronyms of the reported quantities,
3. (3) a unit header with the units used for the reported quantities,
4. (4) a series of data lines, one line corresponding to one GPS track. The GPS tracks are ordered in chronological order, the track reported in line n occurring after the track reported in line (n-1). Each line of the data file is limited to 128 columns and is terminated by a carriage-return and a line feed. The format for one line of data can be represented as follows:

### No measured ionospheric delays available

```

0000000000000000000000000000000000000000000000000000000
0000000001111111112222222222333333333334444444
1234567890123456789012345678901234567890123456
PRN*CL**MJD**STTIME*TRKL*ELV*AZTH***REFSV*****
*****hmmss**s** .1dg*.1dg****.1ns*****
*12*12*12345*121212*1234*123*1234**1234567890*

```

```

00000000000000000000000000000000000000000000000000000011
444555555555556666666666777777777788888888889999999990
7890123456789012345678901234567890123456789012345678901
*SRSV*****REFGPS****SRGPS**DSG*IOE*MDTR*SMDT*MDIO*SMDI*
.1ps/s*****.1ns****.1ps/s*.1ns*****.1ns.1ps/s.1ns.1ps/s
+12345**1234567890**12345*1234*123*1234**123*1234**123*

```

```

11111111111111111111111111111111
00000000111111111222222222
234567890123456789012345678
CK
**
12optionalcommentsoptionalc

```

### Measured ionospheric delays available

```

0000000000000000000000000000000000000000000000000000000
0000000001111111112222222222333333333334444444
1234567890123456789012345678901234567890123456
PRN*CL**MJD**STTIME*TRKL*ELV*AZTH***REFSV*****
*****hmmss**s** .1dg*.1dg****.1ns*****
*12*12*12345*121212*1234*123*1234**1234567890*

```

0011  
444555555555555666666666677777777778888888888999999999900  
7890123456789012345678901234567890123456789012345678901  
\*SRSV\*\*\*\*\*REFGPS\*\*\*\*\*SRGPS\*\*DSG\*IOE\*MDTR\*SMDT\*MDIO\*SMDI\*  
.1ps/s\*\*\*\*\*.1ns\*\*\*\*\*.1ps/s\*.1ns\*\*\*\*\*.1ns.1ps/s.1ns.1ps/s  
+12345\*\*+1234567890\*\*+12345\*1234\*123\*1234\*\*+123\*1234\*\*+123\*

11111111111111111111111111111111111111  
0000000011111111112222222222  
234567890123456789012345678  
MSIO\*SMSI\*ISG\*CK  
.1ns.1ps/s.1ns\*\*  
1234\*\*+123\*123\*12optcomments

The following is an example of what the data looks like, using fictitious data.

Example (fictitious data)

GGTTS GPS DATA FORMAT VERSION = 01  
REV DATE = 1993-05-28  
RCVR = AOA TTR7A 12405 1987 14  
CH = 15  
IMS = 99999 or IMS = AIR NIMS 003 1992  
LAB = XXXX  
X = +4327301.23 m  
Y = +568003.02 m  
Z = +4636534.56 m  
FRAME = ITRF88  
COMMENTS = NO COMMENTS  
INT DLY = 85.5 ns  
CAB DLY = 232.0 ns  
REF DLY = 10.3 ns  
REF = 10077  
CKSUM = C3 or CKSUM = 49

No measured ionospheric delays available

PRN	CL	MJD	STTIME	TRKL	ELV	AZTH	REFSV	SRSV	REFGPS	SRGPS	DSG		
IOE	MDTR	SMDT	MDIO	SMDI	CK						.1ns	.1ps/s	
			hhmmss	s	.1dg	.1dg	.1ns	.1ps/s	.1ns	.1ps/s	.1ns	.1ns	.1ps/s
3	8D	48877	20400	780	251	3560	-3658990	+100	+4520	+100	21	221	64 +90
-27	BBhello												
18	02	48877	35000	780	650	910	+56987262	-5602	+5921	-5602	350	123	102 +61
281	+26 52												
15	11	48878	110215	765	425	2700	+45893	+4892	+4269	+4890	306	55	54 -32
+15	A9												
15	88	48878	120000	780	531	2850	+45992	+4745	+4290	+4745	400	55	57 -29
+16	18receiv. out of operation												

Measured ionospheric delays available

PRN	CL	MJD	STTIME	TRKL	ELV	AZTH	REFSV	SRSV	REFGPS	SRGPS	DSG		
IOE	MDTR	SMDT	MDIO	SMDI	MSIO	SMSI	ISG	CK			.1ns	.1ps/s	
			hhmmss	s	.1dg	.1dg	.1ns	.1ps/s	.1ns	.1ps/s	.1ns	.1ns	
3	8D	48877	20400	780	251	3560	-3658990	+100	+4520	+100	21	221	64 +90
-27	480	-37	18	F4hello									
18	02	48877	35000	780	650	910	+56987262	-5602	+5921	-5602	350	123	102 +61
281	+26 9999 9999 999 89no meas ion												
15	11	48878	110215	765	425	2700	+45893	+4892	+4269	+4890	306	55	54 -32
+15	599 +16 33 29												
15	88	48878	120000	780	531	2850	+45992	+4745	+4290	+4745	400	55	57 -29
+16	601 +17 29 00rec out												

The definitions of the acronyms used in the data format follow. Note that a \* stands for a space, ASCII value 20 (hexadecimal). Text to be written in the data file is indicated by ' '.

### File header

- Line 1: 'GGTTS\*GPS\*DATA\*FORMAT\*VERSION\*='\*01, title to be written.
- Line 2: REV\*DATE\*='\* YYYY'-'MM'-'DD, revision date of the header data, changed when 1 parameter given in the header is changed. YYYY-MM-DD for year, month and day.
- Line 3: 'RCVR\*='\* MAKER'\*TYPE'\*SERIAL NUMBER'\*YEAR\*', maker acronym, type, serial number, first year of operation, and eventually software number of the GPS time receiver.
- Line 4: 'CH\*='\* CHANNEL NUMBER, number of the channel used to produce the data included in the file, CH = 01 for a one-channel receiver.
- Line 5: 'IMS\*='\* MAKER'\*TYPE'\*SERIAL NUMBER'\*YEAR\*', maker acronym, type, serial number, first year of operation, and eventually software number of the Ionospheric Measurement System. IMS = 99999 if none.
- Line 6: 'LAB\*='\* LABORATORY, acronym of the laboratory where observations are performed.
- Line 7: 'X\*='\* X COORDINATE '\*m', X coordinate of the GPS antenna, in m and given with at least 2 decimals.
- Line 8: 'Y\*='\* Y COORDINATE '\*m', Y coordinate of the GPS antenna, in m and given with at least 2 decimals.
- Line 9: 'Z\*='\* Z COORDINATE '\*m', Z coordinate of the GPS antenna, in m and given with at least 2 decimals.
- Line 10: 'FRAME\*='\* FRAME, designation of the reference frame of the GPS antenna coordinates.
- Line 11: 'COMMENTS\*='\* COMMENTS, Any comments about the coordinates, for example the method of determination or the estimated uncertainty.
- Line 12: 'INT\*DLY\*='\* INTERNAL DELAY '\*ns', internal delay entered in the GPS time receiver, in ns and given with 1 decimal.
- Line 13: 'CAB\*DLY\*='\* CABLE DELAY '\*ns', delay coming from the cable length from the GPS antenna to the main unit, entered in the GPS time receiver, in ns and given with 1 decimal.
- Line 14: 'REF\*DLY\*='\* REFERENCE DELAY '\*ns', delay coming from the cable length from the reference output to the main unit, entered in the GPS time receiver, in ns and given with 1 decimal.

Line 15: 'REF\*=' REFERENCE, identifier of the time reference entered in the GPS time receiver. For laboratories contributing to TAI it can be the 7-digit code of a clock or the 5-digit code of a local UTC, as attributed by the BIPM.

Line 16: 'CKSUM\*=' XX, header check-sum: hexadecimal representation of the sum, modulo 256, of the ASCII values of the characters which constitute the complete header, beginning with the first letter 'G' of 'GGTTS' in Line 1, including all spaces indicated as \* and corresponding to the ASCII value 20 (hexadecimal), ending with the space after '=' of Line 16 just preceding the actual check sum value, and excluding all carriage returns or line feeds.

Line 17: blank line.

## Acronyms

The following are the definitions of the acronyms

PRN:	Satellite vehicle PRN number.
CL:	Common-view hexadecimal class byte.
MJD:	Modified Julian Day.
STTIME:	Date of the start time of the track in hour, min and second referenced to UTC.
TRKL:	Track length, 780 for full tracks, in s.
ELV:	Satellite elevation at the date corresponding to the midpoint of the track in 0.1 degree.
AZTH:	Satellite azimuth at the date corresponding to the midpoint of the track in 0.1 degree.
REFSV:	Estimate of the time difference of local reference minus SV clock at the middle of track from the linear fit, in 0.1 ns.
SRSV:	Slope of the linear fit for REFSV 0.1 ps/s.
REFGPS:	Estimate of the time difference of local reference minus GPS time at the middle of the track from the linear fit, in 0.1 ns.
SRGPS:	Slope of the linear fit for REFGPS 0.1 ps/s.
DSG:	[Data Sigma] Root mean square of the residuals to the linear fit for REFGPS in 0.1 ns.
IOE:	[Index of Ephemeris] Three digit decimal code (0-255) indicating the ephemeris used for the computation.
MDTR:	Modelled tropospheric delay at the middle of the track from the linear fit, in 0.1 ns.
SMDT:	Slope of the modelled tropospheric delay resulting from the linear fit in 0.1 ps/s.
MDIO:	Modelled ionospheric delay resulting from the linear in 0.1 ns.
SMDI:	Slope of the modelled ionospheric delay resulting from the linear fit in 0.1 ps/s.
MSIO:	Measured ionospheric delay resulting from the linear fit in 0.1 ns.
SMSI:	Slope of the measured ionospheric delay resulting from the linear in 0.1 ps/s.
ISG:	[Ionospheric Sigma] Root mean square of the residuals to the linear fit in 0.1 ns.
CK:	Data line check-sum: hexadecimal representation of the sum, modulo 256, of the ASCII values of the characters which constitute the data line, from column 1 to space preceding the check-sum. (both included). There can be optional comments on the data line after the check sum out to the 128 character line length. These characters are not included in the line check-sum.

## CONCLUSIONS

The new GPS data format, along with the prescription for processing short term data, can help improve common-view time transfer. Especially with the implementation of SA, common-view tracks can be significantly degraded if the two receivers tracking in common view do not work identically. The new standard can help us move toward a goal of 1 ns time transfer accuracy across intercontinental distances using GPS time transfer in common-view.

## REFERENCES

- [1.] Allan D.W. and Weiss M.A., "Accurate Time and Frequency Transfer During Common-View of a GPS Satellite," In Proc. 34th Ann. Symp. on Frequency Control, 1980, 334-346.
- [2.] Lewandowski W. and Thomas C., "GPS Time Transfer," Proc. IEEE (Special Issue on Time and Frequency), vol.79, 1991, pp.991-1000.
- [3.] Lewandowski W., Petit G. and Thomas C., "Precision and Accuracy of GPS Time Transfer," IEEE Trans. Instrum. Meas., vol. IM42, 1993, pp.474-479.
- [4.] Allan D.W. and Thomas C., "Technical Directives for Standardization of GPS Time Receiver Software," Metrologia, 1994, vol. 31, pp. 69-79.
- [5.] Allan D.W., "Time and Frequency (Time-Domain) Characterization, Estimation, and Prediction of Precision Clocks and Oscillators," IEEE Trans. UFFC, vol. UFFC-34, 1987, pp.647-654.
- [6.] Thomas C., "Real-Time Restitution of GPS Time," Proc. 7th European Forum on Time and Frequency, 1993, pp.141-146.
- [7.] Rutman J. and Walls F. L., "Characterization of Frequency in Precision Frequency Sources," Proc. IEEE (Special Issue on Time and Frequency), vol.79, 1991, pp. 952-960.
- [8.] Allan D. W. and Dewey W., "Time-Domain Spectrum of GPS SA," Proc. Institute of Navigation GPS Meeting, Sept. 1994.

## QUESTIONS AND ANSWERS

**DAVID ALLAN (ALLAN'S TIME):** I would like to just highlight the importance of the paper you presented on this new standard. Just to tell everybody, we believe, as we go through the theory of all the errors in common view, that with this new standard that an accuracy of one ns is achievable. To date, only about four ns has been documented just by way of where we are versus where we think the standard can take us. So I think it's very important work for the operational aspects, for clock input to TAI and UTC. So thank you for sharing it with us.

The other point that I would like to make is on the TDEV plot, that it is not a necessary and sufficient condition that if you have a hump in the data that it's due to a periodic event. There are at least two, and probably more, basic processes in the essay spectrum, and if one looks at longer-term data, in fact, this is confirmed; and there is not necessarily just the 60-minute type periodic phenomena. It's really two pretty much separate parallel processes; and, in fact, period modeling is not the best model that one would want to use.

I simply want to point out that it's not a necessary and sufficient condition, given a hump, that there is a periodic event.

**M.J. VANMELLE (ROCKWELL):** A couple of things. The rubidium is on 20 and not on 25. So it's hard to tell between rubidiums and cesiums there.

Also, did you ever do the experiment on the satellites that don't have SA on them, like number ten? Do you get that same two ns error with 15 seconds separation?

**MARC A. WEISS (NIST):** No, it's lower. I'm sorry, at 15 seconds, I'm not sure. There should be very short-term -- I'm not sure what we were trying.

**HAROLD CHADSEY (USNO):** A quick question for you. You were talking about the fact that when you do the common view that everything drops out. What about geometrical effects? Also, the fact that speed of the wave is not constant through the atmosphere, and you'll be effected more through a thick atmosphere than through a small atmosphere?

**MARC A. WEISS (NIST):** What I said that the effects of Selective Availability cancel completely if you do exact common-view time transfer and use a post-process ephemeris. Of course, the effects of ionosphere and troposphere are still there. Those need to be dealt with. The ionosphere, by measuring, and the troposphere can be helped also with measurements. They need to be if we're going to get the best we can.

**GERNOT M. WINKLER (USNO):** I think the time has come to start a little controversy, because we are all too peaceful down here. You have somehow attacked obliquely one of the tenants of my gospel which I have been preaching for 10 years. That is the melting pot method can average out by having a sufficient amount of data -- it can average out the effects of Selective Availability. Your comment was that you cannot be sure that biases are averaging out.

I want to remind you that the common view -- that's true; I mean, the common view cancels the effect of Selective Availability; but in the Selective Availability, the satellites themselves are not correlated; and the noise, which is superimposed, is strictly bounded. So if you have these

conditions and a sufficient amount of data collection, you completely suppress the individual noise. It just depends on how much data you need. And it turns out that if you have an eight-channel receiver and you average about six hours, that you cannot distinguish the resulting time transfer data from what we obtain with the keyed receiver.

The great advantage of a melting-pot method, compared to the common view, is that it is a robust method. You obtain perfection just commensurate with the effort that you have. You have internal checks on the result which you have, because we have a statistic of the variations. In a case of the common view, you have nothing. We know that in practice your one ns or two ns accuracy cannot be achieved. The question is, how do you check operation in an automatic system? How do you check that you really can rely on a single data point in comparison to the melting pot where you always have lots of data? Whatever happens, it will produce an outlier which is rejected.

So, I wanted to bring that out because there is a great difference in the basic philosophy. In the common view, theoretically you have a superior method; but in practice, I maintain there are weaknesses; and do you lack a measure of performance as compared to the melting-pot method where you have everything you need? Do you have really a robust method which protects you against outliers of whatever magnitude in fact?

**MARC A. WEISS (NIST):** I would like to respond to that. Thank you, Dr. Winkler. I know for years now we've had differences on this. It's going to wake people up a little bit. One point is that we don't have only a point in common view. We can do pretty much everything with common view that you do with a melting pot, and more. That with the melting pot, if you have a eight-channel receiver at two locations, then why not take the eight channels of data simultaneously at the two locations and cancel all the effects of SA, and then use robust statistics on the resulting data where all the biases have been cancelled, and all that's left is the noise? So I think all the statistics that you do with melting pot are still there with common view.

The other thing is that because data are bounded does not in itself imply that averaging brings you down to a single correct number. It may, in fact -- I don't doubt that it has worked on many occasions; but simply saying that they're bounded does not -- there's no reason that it should average down correctly.

**GERNOT M. WINKLER (USNO):** But we have a check, because you look at the distribution of your measurement points. On that you simply add all that area, which we have to do to obtain the competence of that area.

**MARC A. WEISS (NIST):** I don't agree with that. You can have all the data averaging down to the wrong number. I understand that that is not what you've found by doing it. But there's no guarantee that that always will happen.

**CLAUDINE THOMAS (BIPM):** Of course, I will have some words. For TAI, we have 46 contributing laboratories, I mean, laboratories keeping local UTC; and most of them are using GPS now. First of all, all of these laboratories, except maybe USNO, have only one channel CA code receiver. That is to say, except for USNO, no one has one channel receivers which are given reliable measurements. So obviously, we have no data to do the measurements at

the present time. Maybe it will come, but that's not the case for the moment. That's the first point.

The second point is that view of the BIPM for the computation of TAI has always been to try to reduce errors in the physical phenomena which are invoked; for instance, for the ionospheric delay, we like to use measured ionospheric delays as they are labelled. For the position of the satellite, we like to use precise satellite ephemerides. For the antenna coordinates, huge work was done some years ago by my colleague, Dr. Lewandowski (he can speak about that) in which he found accurate positions for the antennas. So we have always tried to phase all our sources and trying to reuse them. That was our viewpoint and that is what we did until now. That was the way we worked.

The last point, of course, common-view time transfer is done, it's computed. To find time difference between two local UTCs, we have a range, of course, for a long-distance time link, like between NIST and OP; we have a range common view for, let's say, two or three days. So we have some kind of average of course. For a smaller distance, like between Paris and PTB, Germany, we have a range, let's say, of less than one day. So that is to say we have some kind of average too.

I would say that what we are doing at the present time is the best we can do with the data we have.

**RICHARD KEATING (USNO):** You've stated that with common view, you're eliminating all these errors. I assume that's because of symmetry. But that's a theoretical position. When you get down to actual practice, reality doesn't always follow theory. I just have to ask you, how confident are you that you have no biases in common view? Can you really say that you can average and you are not getting any biases?

**MARC A. WEISS (NIST):** Well what would a bias be due to?

**RICHARD KEATING (USNO):** Well, for example, I'll give you an example. I have seen estimates of precise ephemeris accuracies. They've ranged from anything from one meter to 20 meters. There is a real possibility there that your precise ephemerides may not be as accurate and may contain real biases.

**MARC A. WEISS (NIST):** I think that's a good point in fact. Biases have to be due -- if you look at the common-view process, you have the satellite and then you have the ground stations on the earth; and then you have the atmosphere. So if you measure it exactly at the same time -- the only thing I'm claiming that cancels exactly is Selective Availability. In fact, the only thing I know for sure that cancels is clock dither. The ephemeris cancels to the extent that an error is perpendicular to the line between the satellites. If there is an error in the satellite position, it will add an error to common-view time transfer. And in fact, with precise ephemerides, prior to having the laser reflector, we had no way of knowing if they were accurate. They were simply consistent.

Errors can also come in the atmosphere due to ionosphere and due to troposphere, due to multi-path at the stations, and due to coordinate errors. So all of those things can add errors. It's going to be true whether you're using melting pot or common view or anything. Those are

all in GPS. Whenever you do GPS, you're concerned about ephemeris, ionosphere, troposphere, and multi-path, and coordinates.

I think a point that I would really like to stress about that -- and I think your point is well made -- is that it's the difference between accuracy and stability; that you can have numbers that agree perfectly, that are extremely well consistent and are consistently wrong. For example, if you took a commercial cesium clock -- and this is the difference between a commercial cesium and a laboratory primary standard. If you have a commercial cesium and it's produced by a manufacturing technique, and there's a millimeter error in the end-to-end phase shift in the cavity, all the clocks will have that; and they'll all be off in frequency because of that, in exactly the same way; and all the other effects will average down and you'll end up with a bias that does not average.

That's an example of the difference between stability and accuracy. I think we need to be very careful when we use the word "accuracy." We're not talking about something that you can average; we're talking about something that you have to prove.

**GERNOT M. WINKLER (USNO):** Your example is making my point. How do you find out that all of these cesiums have a bias?

**MARC A. WEISS (NIST):** You evaluate them.

**GERNOT M. WINKLER (USNO):** You evaluate them and you look at the statistical distribution of what their frequencies are; and you compare them with a standard. You found out how it is.

**MARC A. WEISS (NIST):** But you don't compare with another standard. You evaluate them independently; you measure the effects through something that's completely independent.

**CLAUDINE THOMAS (BIPM):** There's a very big question of the difference between stability, precision and accuracy of course. There were some fundamental and formal papers about that at the BIPM. We consider that an accuracy is characterized by an uncertainty given as a one sigma value which was from the quadratic sum of the different uncertainties which are estimated from the different sources of errors which appear within common-view time transfer. I have already at the BIPM tried to do that, and I think that we can estimate an uncertainty of about 10 ns, it's eight to ten ns, one sigma for long-distant GPS common view, using precise satellite ephemerides from the IGS, and ionospheric measurements and with the hypotheses that the receivers themselves are correctly calibrated, which may not be the case; and which could add, of course, a bias. So let's say eight to ten ns, one sigma as the accuracy of GPS common views.

# SOME PRELIMINARY RESULTS OF THE FAST CALIBRATION TRIP DURING THE INTELSAT FIELD TRIALS

W.J. Klepczynski (USNO)  
US Naval Observatory  
Washington D.C., USA

J.A. Davis (NPL)  
National Physical Laboratory  
Teddington, UK

D. Kirchner (TUG)  
Technical University of Graz  
Graz, Austria

H. Ressler (SRI)  
Space Research Institute  
Graz, Austria

G. De Jong (VSL)  
NMI, Van Swinden Laboratories  
Delft, The Netherlands

F. Baumont (OCA)  
Observatoire de la Côte d'Azur  
Grasse, France

P. Hetzel (PTB)  
Physikalisch-Technische  
Bundesanstalt  
Braunschweig, Germany

A. Soering (FTZ)  
Forschungs- und  
Technologiezentrum  
DBP Telekom  
Darmstadt, Germany

Ch. Hackman (NIST)  
National Institute of  
Standards and Technology  
Boulder, Colorado, USA

M. Granveaud (LPTF)  
Observatoire de Paris  
Paris, France

W. Lewandowski (BIPM)  
Bureau International  
des Poids et Mesures  
Sèvres, France

## Abstract

*At the beginning of 1994, field trials for an international two-way time transfer experiment using the INTELSAT V-A(F13) satellite at 307°E were started. The experiment was set up to last one year and involved six European time laboratories and two North-American time laboratories. Three times a week, 5-minute time transfer sessions were scheduled. At each of these laboratories, GPS common-view time observations were also performed.*

*From September 22 to October 22, 1994 a calibration trip which visited participating laboratories in Europe was organized. It involved a portable Vertex 1.8 meter two-way station (Fly Away Station [FAST]), belonging to USNO, and a portable GPS time transfer receiver, belonging to BIPM. The*

*calibration trip was conducted by members of the staff of USNO and Observatoire de la Cote d'Azur (OCA). It provided differential delays of the satellite Earth stations and GPS receivers. The initial analysis of this calibration campaign are reported here.*

## **I. Introduction**

The TWSTT technique has developed the reputation of being one of the most accurate and precise methods for time transfer<sup>[1,2]</sup>. One of the goals of the FAST Calibration Trip was to evaluate the quality of this measurement technique. While quality implies a somewhat nebulous expression, attempts can be made to quantitatively express the quality of the technique as a function of its capability. Its capability being defined in terms of its accuracy and precision. Obviously, a technique, where the accuracy is identical to the precision of measurement, is a technique which has reached its full capability. This relation can be shown as:

$$\text{FULL CAPABILITY} \quad \text{Accuracy} = \text{Precision}$$

If the accuracy of a measurement process is significantly less than its measurement precision than systematic errors are still affecting the process. The technique is, then, not yet of high quality.

In regard to TWSTT, estimates for the inherent precision of measurement for this technique range from 100–500 ns.<sup>[3]</sup> It is possible to adopt 250 ps. as the current level of precision. Various estimates for the achievable accuracy range from 25 to 1 ns. This means that significant systematic errors are still affecting the results of TWSTT. It is the reason for undertaking this FAST Calibration Trip. It is hoped that, by careful measurements, more insight into the errors affecting TWSTT will be gained. It is assumed that one of the factors contributing to this error is our inability to measure the delays that signals undergo as they pass through the spacecraft. This thought to be one of the greatest contributors to the systematic errors affecting the measurement process.

## **II. FAST Calibration Trip**

With regard to calibrating or determining delays through a system, there are three approaches. One is to design and develop equipment which will inject a signal into the system and consequentially trace its path throughout the station. This is the approach of Gerrit de Jong at VSL<sup>[4]</sup>. One can then take this calibration station around to different laboratories and measure the delays through other similar stations. This procedure could be called absolute calibration (AC).

Another approach would be to measure the delays throughout a small portable station and then transport this station to other laboratories in order to make side-by-side measurements with the station to be calibrated. This approach could be called absolute system calibration (ASC).

Still another approach would be to carry a transportable station around to different laboratories and make side-by-side measurements and refer all measurements to one primary reference

station. This is the approach adopted for this experiment since operational absolute calibration equipment has not yet been fully developed. This approach could be called relative system calibration (RSC)

Planning for the FAST calibration started at the Second Meeting of the CCDS Working Group on TWSTT held at NPL on 22 October 1994[5].

### III. Observational Plan

The plan for RSC is rather simple. One makes initial measurements of the calibration station with respect to one fixed base station. A record of the difference is made. Similar measurements will be made at subsequent base stations and the differences also noted. At the same time, measurements are also made with respect to all other base stations participating in the experiment. Then, relative calibration with regard to any base station can be deduced.

The observation sequence followed at each laboratory visited by the FAST Team consisted of making side-by-side measurements between the FAST and visited laboratory for at least half an hour. Next, the FAST and laboratory base station each did time transfers with all other participating labs. This observation period usually spanned several hours. Finally, The FAST made side-by-side observations with the visited laboratory base station before going on to the next laboratory.

Also, at each base station, sufficient documentation of known, measured delays were made in order to correct for as many systematic offsets as possible.

### IV. Data Analysis

The observed data obtained at VSL are presented in Tables 1, 2 and 3. Several consistency checks can be performed with this data. Because the FAST had not yet returned to its initial starting point at the time of the writing of this paper, a closure error or verification that nothing happened to the FAST during the trip has not yet been performed.

An initial analysis that can be done is to set up a three cornered hat method to see if there is consistency among the readings [6]. By differencing the data in Tables II and III, one can compute a value for the time difference between the FAST at VSL and the base station at VSL [FAST(VSL)-VSL(Base Station)]. These differences are given in Table IV. Next, one can compute the differences between the observed values for FAST(VSL)-VSL(Base Station) and the computed one. This is given in Table V. The data in Table V indicates that the two procedures agree to within about a nanosecond.

### V. Discussion

The consistency check performed in Section IV points to another fact that has been the subject of some speculation. The data in Table I was obtained by going through the spot transponder on INTELSAT V-A (F13) which covers Europe. The data exhibited in Tables II and III was

obtained through the transponder which connects Europe to North America. Since the data measured for the difference between the FAST located at VSL and the VSL Base Station and the data computed from the set of measurements obtained using USNO as an intermediary is so close together, it seems that the delays through the different transponders are not that much different. This is not conclusively proven by this procedure. In any event, this is a notable observation. Once a permanent routine evolves in TWSTT, it is easy to visualize that data exchange may not always occur through the same transponders of the satellite being used. This observation merits further corroboration because it is a possible source contributing to the systematic errors of the measurement process.

## VI. Conclusions

Preliminary analysis of some of the data obtained during the FAST Calibration Trip to Europe indicate that the equipment performed reasonably well. After additional data is obtained when the FAST is returned to USNO, it will be possible to verify this conclusion. It will also then be possible to establish a calibrated path between the stations which participated in the experiment. This will be an essential step to precede the next round of international time transfers.

## References

- [1] Veenstra, L., Kaiser, J., Costain, C., Klepczynski, W. and Allan, D. "*Frequency and time coordination via satellite*", COMSAT Technical Review, Vol. 11, No. 2, 369-401, Fall 1981.
- [2] Howe, D.A., Hanson, D.W., Jespersen, J.L., Lombardi, M.A., Klepczynski, W.J., Wheeler, P.J., Miranian, M., Powell, W., Jeffries, J. and Myers, A. "*NIST-USNO Time Comparisons using Two-Way Satellite Time Transfers*", 43rd Annual Symposium on Frequency Control, 193-198, 1989.
- [3] Hanson, D.W. "*Fundamentals of Two-Way Time Transfer by Satellite*", 43rd Annual Symposium on Frequency Control, 174-178, 1989.
- [4] de Jong, G. and Polderman, C. "*Automated Delay Measurement System for an Earth Station for Two-Way Satellite Time and Frequency Transfer*," European Forum for Time and Frequency, 1994.
- [5] Minutes of the Meeting of the BIPM Working Group of the CCDS on Two-Way Satellite Time Transfer, 20-21 October 1993.
- [6] Winkler, G.M.R. "*Intermediate Term Frequency Measurements with the HP Computing Counter in the USNO Time System*", Proceedings of the 4th Annual PTTI Planning Meeting, 152-167, 1972.

<b>Table I Observed Time Differences [FAST(VSL)-VSL(Base Station)]</b>		
MJD	49625.52419	49626.35815
Observed (FAST-VSL)	-667.28 ns	-669.31 ns.

<b>Table II Observed Time Differences [USNO(Base Station) - VSL(Base Station)]</b>		
MJD	49624.62534	49626.48090
Observed (USNO-VSL)	122.13 ns.	130.32 ns.

<b>Table III Observed Time Differences [USNO(Base Station) - FAST(VSL)]</b>		
MJD	49624.62327	49626.46942
Observed (USNO-FAST)	790.14 ns.	797.97 ns.

<b>Table IV Computed Time Differences [FAST(VSL)-VSL(Base Station)]</b>		
MJD	49625	49626
Computed (FAST-VSL)	668.01 ns.	667.65 ns.

<b>Table V Observed-Computed Time Differences of FAST(VSL)- VSL(Base Station)</b>		
MJD	49625	49626
(O-C) FAST-VSL	0.73 ns.	-1.67 ns.



## PANEL DISCUSSION ON WORKSHOPS

Moderator: Raymond L. Filler  
US Army Research Laboratory

**RAY FILLER:** Welcome to Part II of the audience moderator discussion which occurred yesterday. Today we're going to have our three session chairpersons (one is missing in action) give us a brief summary of what transpired at their session yesterday. Then for the rest of the time, we'll have audience questions. We're going to start with Joe White from the NRL whose session was entitled "Real Time Automated Systems."

**JOE WHITE (NRL):** We had a good crowd yesterday, we had about 30 or so people, pretty much a roomful. And we started off trying to define what a real-time automated system was, and basically came up with this kind of thing — that it was system that provided time or frequency, or both, to the user specification actually in real time; that it might include some sort of a historical calibration feature; but that basically what he wanted, he got out of the spigot right when he asked for it.

The other thing about the automated part, in particular, was there was not a frequent operator action required. In fact, in many cases, there wouldn't be an operator around it at all; we talked about fully-unattended and remotely-controlled type applications. The applications of these systems would typically include things like national time scales, remote time stations, and, as embedded pieces of equipment in military systems, telecommunication systems.

The class of performance that we were looking at for these systems, as far as time went, was on the order of 100 ns or better time accuracy; frequency accuracy to at least a part in  $10^{11}$ ; and again, this depended with some of them being as good as part in  $10^{14}$ ; and frequency stability, ranging from hydrogen maser systems, like a radio observatory system, to parts in  $10^{13}$  at a second to other systems that might only be in parts in  $10^{13}$  at a day. The other factor in this performance was that we required a synchronization to some national standard, or at least some network standard, and usually by a GPS or two-way time transfer measurements.

When we talked about the measurements, one of the things that came out that people thought was important there was that the measurements be accurately time-tagged when they're collected. Those of you that played with these systems, particularly things run by PCs, know that those time tags can often be in large error. And we talked about means of doing that, including having a hardware clock in the measurement system that provided very accurate time; or, alternatively, using one of the telephone or network time synch mechanisms for the control computer to keep it on time to the millisecond range.

Naturally, we all wanted nice quiet, unambiguous measurements, and we decided, in general, that meant making time measurements — or frequency measurements, I should say — at

5 MHz to get the smoother performance there. While one pps measurement was certainly necessary for things like GPS measurements, two-way time transfer measurements, in general, there were a lot of problems with those, as far as having a clean pulse to measure, establishing the right triggering levels, the effects of long cables, those kinds of things.

We next talked about distribution systems, and we started off talking about the effects of the local environment on the distribution; that is, that the temperature, humidity, those kinds of things, often had an effect. The other thing that went with that is having a good way of connecting to it, that the connectors that were used and the types of cable were very important to achieving a good distribution, that just the distribution amplifier alone didn't really cover everything. We were typically looking for isolation of at least 100 dB between ports, and also 100 dB from output to input, which we have seen some systems not doing.

The other thing that was kind of interesting in distributions, we talked about widely-distributed systems, for instance, a communications network where the real-time automated system wasn't two racks sitting on one site, but a rack here, and a rack 100 miles away, and another that really is — in the terms of the way that system worked, really that was the system that they wanted to have as a real-time automated system. So sometimes the whole interconnection and distribution gets to be a pretty large problem.

From there, we went to software, or actually, robustness, which got us to software pretty quickly. Sam Stein gave what I thought was a nice definition of robustness; and that is that the small error in the system caused only small problems to the system operation. For instance, losing one device in the system shouldn't cause it all to die. That got us immediately to computers, and we decided there that you really need both stable user software, the specific software you wrote to make that system work, and stable underlying operating systems for the computer itself. A lot of times that's UNIX or OS-2, or something like that; that there often was great peril in changing versions of operating systems that ran the whole thing.

Also, in the robustness area, we talked about the trade-off between single point failures and the things that you do to try to avoid single point failures; there is a point of diminishing marginal returns as you add more and more redundancy and put in the switches to put the redundant sides together, that often you actually got to a system that was worse than what you started with; and that one of the solutions to that was to encourage your user of the system, the people that take the time and frequency outputs, to design their systems to be tolerant of small glitches; so that you really had a robust system in total, not just in the time and frequency part, but also in the piece that used the time and frequency.

We ended the robustness part with trying to define how you put robustness in the specification. And I think we came to the conclusion it was difficult to define that. There are really two problems. One was that you had to define what the users environment was, because what was robust for one environment may not be robust at all for another. And the other problem was that it's awfully hard to think of everything that can go wrong. You try to come up with very blanket-type statements that will cover everything; and when you field the system, you almost always find out there is something you left out. So I think we wound up agreeing that we had a difficult problem that we didn't quite know how to define.

We ended up talking about maintenance and testing. The general consensus, as far as maintenance went, was that we thought that systems should be maintained generally at the box level in the field; that the modern hardware is simply too complex to deal with in the field; that no matter how well you train your technicians, it's very difficult, it's very expensive; that, in general, you ought to have a lot of spares and rotate them around and let the manufacturer or at least some highly-trained depot deal with most of those issues. To support determining when we had problems, we talked about built-in tests; and also, about a remote diagnostics capability.

That's pretty much it.

**RAY FILLER:** Thank you. Next, we'll have Dick Sydnor from JPL. His session was entitled "Real World User Requirements."

**RICHARD SYDNOR:** None of us seemed to know exactly what that title meant, so it took a little bit to get the thing going and we sort of wandered over a large area.

The first part of the discussion was sort of a *déjà vu*; we have talked about this many times in the past, and it's the problem of communication between the supplier and the user. We had a number of examples of a user having incomplete specifications. He forgets that he's going to take the spacecraft oscillator and launch it. So it has to have a shock and vibration specification, and he's left that out. Then he comes and says "Gee, it broke." That kind of thing happens more often than you might think.

Also, on the other hand, sometimes the oscillator or frequency standard supplier doesn't have a really complete set of specifications in his catalog. He doesn't say what effect vibration has on phase noise, for example; so sometimes it's difficult to figure out exactly what this particular item is going to do in your environment.

It was suggested that the supplier who gets a set of specifications from a user should question those requirements. He knows more about his oscillators than the user does probably. And if something looks a little bit awry, then he should question that and find out if the user means what he says, or if he has left something out. Many times the user is not very familiar with the oscillator and how it works, and its problems. And so there is a misunderstanding of what some of the specifications need. So there is a need for user education.

But who is responsible for that? That was kicked around for quite awhile. And John Vig had some comments about availability of literature that would outline tests and give information to the user. Some users say there is no information out there. And it just means that they haven't really looked very much.

I think the best suggestion, but probably the hardest to implement in that area, was that the supplier should be involved in the procurement from the very beginning. And that's a little hard to do with the present legal situation where you have competitive bids, how you get all these suppliers involved in it. But still, it looks like the most logical way to handle some of those problems. Those problems have been discussed many times in the past, and no solution has been forthcoming as yet.

Then we sort of wandered away from that area, and we started talking about problems,

various specific problems in terms of, say, distribution systems, time delay variations in cables, fiberoptics, how you stabilize fiberoptic systems, good connectors, that sort of thing; how you make sure that if you have a large network and you distribute it in time to, say, a bunch of people that are all various distances away from your main control clock, how they all have the same time, rather than varying all over the place due to the length of the cables. We had quite a bit of discussion on that.

Somebody asked what do the margins mean in a specification; and there is 90 percent probability that it will do such-and-such. Do people really understand that? I think the answer on that one was that nobody really knows exactly what is meant by that margin statement, and most people would rather have a specification that says it's guaranteed to do no worse than such-and-such.

There were some comments about various problems with crystal oscillators. It was brought to our attention that crystal oscillators stored at a very low temperature sometimes comes back out of that as a completely different crystal oscillator than the one you put in. There are aging rate changes and everything else.

That pretty much handles it. We had a large group in here. I would say the room was half full. But we had only five or six people that really contributed. Thank you.

**RAY FILLER:** I'm sorry that our third session chairman is not here. But if anybody who was there wants to make some comments, that's fine.

We're going to open the floor now to anybody for questions, comments, discussion of any sort, on this topic or maybe any other.

**GERNOT M. WINKLER (USNO):** It may be useful to elaborate a little bit more on your comments about margins and specifications. It's a problem which comes up over and over again; and that is that a system, whatever kind, has certain system performances; and then you have accidents. The two come from different distributions. And I think they should be separated.

It makes no sense to include accidents in a system specification; if you separate them, you can put a limit on how many you will tolerate per year, or per month, or whatever. But the system should be characterized after these accidents have been separated; because otherwise, you characterize two different processes with one number.

**RICHARD SYDNOR:** The margin discussion would have more to do with things like radiation exposure; after a certain number of rads of radiation, the probability is ninety percent that it will be within a certain range. That sort of thing is typically what you get with radiation exposure, for example. The specs you see in manufacturers' catalogs on something says, for example, at a second, a part in  $10^{13}$ . To me, that means that it's no worse than that, under any condition. A benign environment, obviously.

But if you are talking about systems, then you have to know not only, say, an upper limit, you have to know what the spread, what the distribution of the things are. And that's not in the manufacturers' catalogs. And many of them probably don't even know what it is. Some manufacturers will supply that information, if it's available, and they give it in terms of a

histogram or something like that, a performance of the different ones that were produced. And that's essential if you're doing a system design. But that wasn't discussed during our meeting.

**DICK KLEIN (LOCKHEED AT KENNEDY SPACE CENTER):** One of the things we've noted with more than one vendor, they'll take the specification, particularly a short-term specification of an oscillator, and publish it as the short-term specification of the GPS receiver, ignoring the perturbation of the circuitry within the receiver itself. And we found that to be a problem in more than one vendor. Particularly one problem, you could almost see a IRIG A on the 1 MHz output. And it turned out that they were able to correct it. But apparently, it wasn't tested at the factory, only the specification that the oscillator manufacturer gave.

**JOE WHITE:** I think that happens.

**FRED WALLS (NIST):** One of the limitations and specifications for almost all oscillators and synthesizers, and things of that sort, is a lack of specification for AM noise. And in many system applications, it is the AM noise that limits noise floor for residual measurements on amplifiers and other things; you have AM to PM conversion in your amplifiers and on mixers and on non-linear things. You can have two oscillators with the same phase noise, and yet different AM; and one will work and one won't work. And so, we need to raise the consciousness of both manufacturers and users to insist on AM noise specifications.

**RICHARD SYDNOR:** That's a good point. Many manufacturers don't even know what the AM noise performance of the oscillators are, because they measure just the phase component and not the AM component.

**JOHN VIG:** In our experience in the Army, many of the problems that come to us originate from the fact that people who are assigned the job of writing a specification, and this often involves major systems – people just sit down and write specifications in isolation, without regard to what's been written before; and they invent their own definitions, invent their own way of measuring certain parameters for which others have already worked out the details. For example, Ray came back from a meeting recently on a major radar system. He was asked to review the specification for the oscillator, and he found several things that were just basically wrong with the specification; one, of which, was that a frequency of zero –

**RAY FILLER:** Yeah, a frequency of zero. The frequency aging specification was plus or minus F zero, I think, or something.

**JOHN VIG:** Yes, totally nonsensical specifications are being written by people who don't know what they're doing. And this is for multi-billion dollar systems. So I think the manufacturers probably could perform a service by including in their literature a list of existing specifications that people could at least start with. There are IEEE specifications, there are military specifications, there are IEC specifications; we have a set of definitions in a CCIR<sup>1</sup> glossary. That means they are all internationally recognized and accepted documents.

If somebody has a job of writing a specification, it's so much easier to go to the existing document and just call out a paragraph of an existing document rather than to sit down and scratch your head, 'How should I define 'aging,' how should I define 'phase noise?' ” and

---

<sup>1</sup>International Radio Consultative Committee, now named the ITU-R.

invent things when there is no need for that.

**JIM DeYOUNG (USNO):** I think you said that Dr. Hellwig wasn't here. I took some notes, and so maybe I could give a short synopsis of what happened in our group, "User Environmental Effects."

Dr. Hellwig introduced a document that is going to be published, I believe, in the spring of '95, discussing user environmental effects, including radiation, acceleration, temperature, humidity, et cetera. It's going to be IEEE Standard 1193-1994.

Our group — after Dr. Hellwig gave this little bit of introduction to get us going, he also introduced three areas he thought were important, which is fitness of use. Does your device or system really meet your requirements that you originally had formed? He had another consideration: "How do I characterize this?" or, optimize the design is the bottom line on that. And then he discussed liability and survival of systems that are important in your timing or frequency.

We talked about complex systems, as that's getting to be a problem. We have specifications on individual devices, but then how do you merge those specifications on those devices and get a global picture of how the system is going to perform? We decided communication; in my few years in PTTI, that's always been one of the things we discussed in most of these forums, is communication as one of the most important things that can happen.

There were a few specifics that we discussed, and that happens to be related GPS clocks on board the satellites. At least one gentleman — I'm not sure of his name — mentioned something about the Block II-R clocks where, in the early incarnations of the GPS clocks, they were doing frequency stability measurements; I believe it was temperature variation in a vacuum. Those tests were done and they found some problems with specific clocks. But those tests aren't even being done now in the Block II-R clocks. So that was pointed out as possibly a problem.

Then one final thing we discussed was that the design materials and the components are very important; therefore, you want the highest quality of those things. That's pretty much everything I have in my notes from that group.

**RAY FILLER:** Anybody have anything else to add to that or to any other topic of discussion? Thank you.

52281  
P-10

# EUROPEAN PLANS FOR NEW CLOCKS IN SPACE

Sigfrido Leschiutta\*# and Patrizia Tavella\*  
 \*Istituto Elettrotecnico Nazionale, Torino, Italy  
 #Politecnico di Torino, Elettronica

## Abstract

*An outline of the future European space research program where precise clocks are necessary is presented, pointing out how space applications are posing impressive requirements as regards clock mass, power, ruggedness, long life, accuracy and, in some cases, spectral purity.*

*The material presented was gathered in some laboratories; useful information were obtained from the Space Agencies of France (CNES), Germany (DARA) and Italy (ASI), but the bulk is coming from a recent exercise promoted inside ESA (the European Space Agency) and aimed to prefigure space research activities at the beginning of the next millennium. This exercise was called Horizon 2000 plus; the outcomings were summarised in two reports, presented by ESA in may 1994.*

*Precise clocks and time measurements are needed not only for deep-space or out-ward space missions, but are essential tools also for Earth oriented activities. In this latter field, the European views and needs were discussed in October 1994, in a meeting organized by ESA and devoted to Earth Observation problems.*

*By a scrutiny of these reports, an analysis was performed on the missions requiring a precise clock on board and the driving requirements were pointed out, leading to a survey of the necessary PTTI developments that to some extent are in the realm of possibility but that pose serious challenges. In this report the use of frequency standards in the satellite navigation systems is not considered.*

## 1. INTRODUCTION

A large number of frequency standards are used in every spacecraft, mostly for telecommunication purposes or as time reference for the on-board computers. In some cases clocks are required for the time-tagging of data, but in other instances the mission of the spacecraft itself requires the availability of precise frequency standards or clocks. Well known examples are the navigation satellites in which the frequency stability or accuracy play a fundamental role in all the methods, conical as ARGOS, hyperbolic, as one way TRANSIT and TSIKADA and DORIS <sup>1</sup>, and circular, as one way GPS and GLONASS or two-way PRARE <sup>2</sup>.

<sup>1</sup>DORIS - is a satellite based radio positioning system, designed and operated by CNES, France. It is an "inverted" TRANSIT, operating at higher carrier frequencies and with transmitters on ground and reception and data collection on board.

<sup>2</sup>PRARE - Precision Range And Range-rate Experiment, is a satellite based tracking system, following, at the same time, the conical, hyperbolic and two way circular navigation system. The system was designed at the University

Being satellite navigation requirements, as regards frequency standards, covered adequately in the literature, the aim of this paper is to deal with less known topics, such as the use of precise frequency standards in space research. Also the "precise" navigation of these satellites, if required, is not here considered, because methods and devices are similar to those of navigation or geophysical satellites or are using instruments, such as the star tracker, not based on frequency standards.

The occasion of this study was offered by the results of a request of proposals called by the European Space Agency in 1993. That call for ideas was devoted to Space research beyond 2000; the resultant activity was called **Horizon 2000 plus**, since it should be the continuation in time of the program **Horozon 2000**, now in implementation, with a number of missions launched between 1995 and 2005.

The second section of this paper is devoted to an outline of the program **Horizon 2000 plus**, limited to the satellites having special requirements as regards time and frequency Metrology in order to fulfil their mission while the third section deals with the **Earth Observation** topics. This latter section relies on the conclusions of an ESA-sponsored meeting, held in October 1994.

The fourth section covers the principal methods used, the fifth lists the "precision" requirements, while the last one presents some actions, researches and goals to be performed and reached in the next years, in order to make feasible the bold program of Space research.

To complete the panorama, not only the on board clocks and standards are considered, but also the related devices used on ground, moreover also laser sources, when used as frequency reference or timing devices, are considered in this survey.

It appears that PTTI and in particular precise clocks will play a fundamental role in space mission, particularly when verifications of fundamental physics are involved. Such needs of precise clocks and PTTI technology challenge our current technology and practice and, by turn, will give insight to the PTTI community of possible improvements

## 2. THE ESA HORIZON 2000 PLUS SURVEY

In 1993, ESA launched a call for proposals for the realm of "Space Sciences", and for the next Century. In ESA jargon Space Sciences are formed by :

- - astronomy
- - solar system
- - fundamental physics.

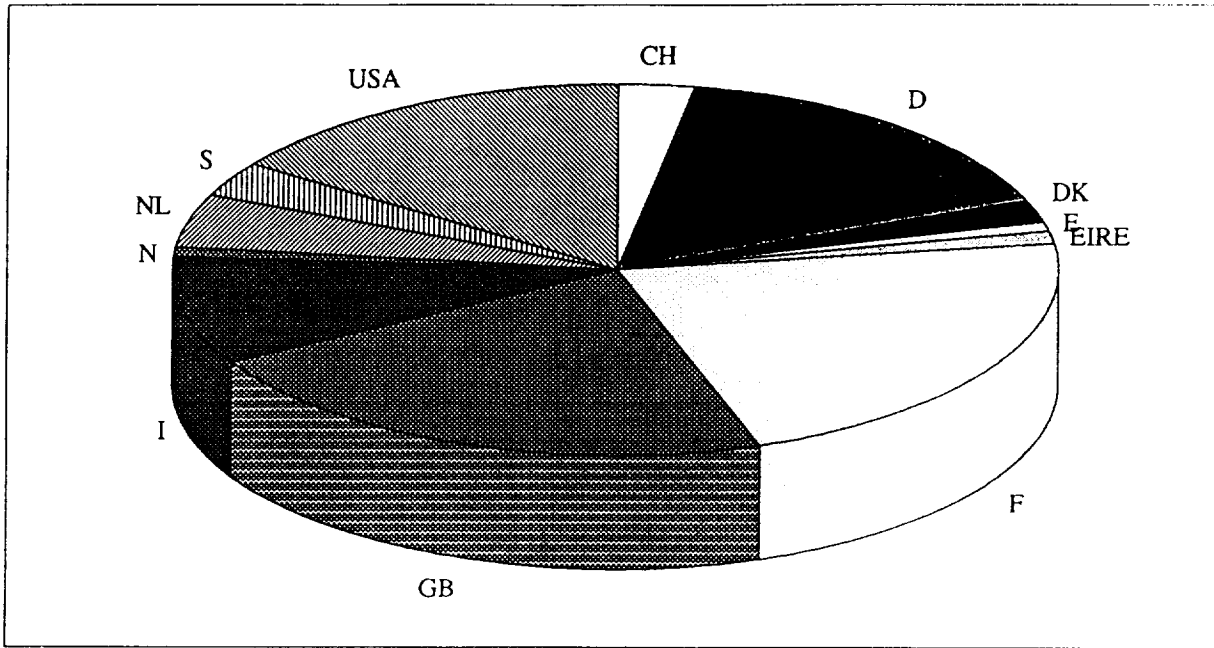
By the end of 1993 about one hundred Laboratories, from both sides of the Ocean, answered to the call for ideas [1]; as a matter of record for the three above mentioned areas, the proposals

---

of Stuttgart, Germany, it is presently under test on Meteor III and it will be flown also on ERS-2 with launch planned in 1995. The use of PRARE is proposed also for other missions.

were respectively 35, 41, and 30. It's interesting to note that of the 106 proposed ideas, almost 90 came from European institutions while the remaining part came from USA (considering the project leader). The inputs arrived from different countries as visualized in the table and drawing below.

CH	D	DK	E	EIRE	F	GB	I	N	NL	S	USA
3	17	2	1	1	23	23	10	1	5	3	16



To assess the value of the proposals, ESA formed five “topical teams” or groups of experts, whose conclusions and recommendations were presented to the scientific community during a meeting held in Italy in May 1994 [2,3].

Out of the 30 odd proposals presented in the Fundamental Physics sector, 12 are considering the use of frequency standards, clocks of frequency-stabilized lasers as the key component of the mission. In the other sectors, some proposals were considering the use of “precise” frequency standards inside the positioning, navigation or telecommunication systems. As pointed out in Section 1, these missions are disregarded in this survey.

## 2.1 MISSIONS IN THE FUNDAMENTAL PHYSICS SECTOR

After receiving the proposals, the topical team specifically devoted to fundamental physics mission analysis stated that:

- - a cornerstone mission should be the detection of gravitational waves in space;

- - three scientific topics are of foremost importance: gravitational waves, universality of free fall, and the relation between space–time curvature and matter. The following projects were selected as the best proposals in these areas respectively:
  - LISA Laser Interferometry Space Antenna,
  - STEP Short Range Equivalence Principle experiment,
  - SORT Solar Orbit Relativity Test;
- - some existing technologies need developments, among them: lasers, frequency standards and time transmission.

During a recent meeting (Oct. 1994), three additional missions have been recommended among which one concerns an interferometric observatory and an other a gravitational wave observatory. The missions requiring PTTI devices on board, are listed in Table I, with their acronyms, a brief synthetic description, the originating Laboratory and Nation, and the characteristics of the needed frequency standards.

Some other proposals involving the use of “precise” clocks are circulating now in Europe, and are listed with the same criteria in Table II.

Mission	Aims	Source	Needed Clocks	
			why	which
CASP Close Approach Solar Probe	relativity test	Smithsonian Astrophysical Observatory USA	1st and 2nd order red–shift measurement	H maser
CRONOS on MILLIMETRON Clock Relativity Observations of Nature of Space–time	relativity and gravitational test (based on RADIOASTRON II)	Observatory of Neuchatel CH	red–shift and gravitational background radiation measurement	2 H masers on board + 1 on Earth in future: cold H maser or cold microgravity clocks
ORT Orbiting Radio Telescope	radioastronomy VLBI in space	Onsala Space Observatory Sweden	high resolution angular measurements	H maser on board? GPS receiver on board?
SMRPM Small Mercury Relativity and Planetology Mission	around Mercury relativity test Limit on $\dot{G}$	Interplanetary Space Physics Institute Italy	delay measurement	H maser
SORT Solar Orbit Relativity Test	relativity test	Observatory of “Cò d’Azur” France	red–shift measurement	H maser (ESA and and Russia) or cooled atomic clocks (CNES)

TABLE I continued				
STUFF Strong Test on the Universality of Free Fall	similar to SMRPM	Montana State University USA	delay measurements ?	H maser?
VULCAN solar probe	similar to CASP	University of London UK	red-shift measurement	H maser (or cooled atom/ trapped ions)
Needed stable Lasers				
ISLAND Inverse square Law using iNertial Drift	verification of the inverse square law of gravitation	University of Strathclyde Scotland UK	displacement measurement linewidth 1 Hz @ 532 nm	1 Nd YAG laser @ 1.064 $\mu\text{m}$ frequency doubled
LARGO Long Armlength Relativistic Gravitational Observatory	detection of gravitational	Jet Propulsion Laboratory, California USA	spacecraft baseline variation detection	10 Watt Nd YAG laser
LISA Laser Interferometer Space Antenna	Gravitational wave detection	Max-Planck Institut für Quantumoptik, Garching D JPL USA	interferometer length variation	3 Watt stabilized Nd YAG laser @ 1.064 $\mu\text{m}$ , stability $= 10^{-13} / \sqrt{Hz}$ @ f=1 mHz
Needed System Timing				
LATOR Laser Astrometric Test of Relativity	Sun gravitational deflection of light	Rutherford Appleton Laboratory Didcot UK	sending "laser flashlight" in solar orbit	suitable time measurement system
VLO Very low frequency Lunar Observatory	Exploring the 100 kHz - 30 MHz window	Observatoire Paris, France	pulsar studies	suitable time reference system

Mission	Aims	Source	Needed Clocks	
			why	which
CASSINI	gravitational wave detection and	Jet Propulsion Laboratory, CA USA	Doppler shift measurement	Rb clock $\sigma_y \approx 10^{-12}$ @ 100s; acceleration sensitivity $\approx 10^{-12}/g$
QUASAT	VLBI interferometry	ESA		H masers on ground
LAGEOS III LAsEr GEODETic Satellite	relativity tests on gravitomagnetic field	Italian Space Agency ASI, NASA	orbit determination	Cs clocks on Earth (laser ranging)
EXTRAS Experiment on Timing Ranging and Atmospheric Sounding	geodesy atmosphere physics and relativity tests on METEOR M	Russian Space Agency ESA Obs. Neuchatel	position measurement; low phase noise reference	2 H maser; time transfer with precision of 10 ps
CRONOS on RADIOASTRON I (similar to the Japanese VSOP)	Space Very Long Baseline Interferometry	Russian Space Agency ESA Obs. Neuchatel	high resolution angular meas.; $10^{-6}$ accuracy red-shift measurement	one H maser on board + several on Earth

### 3. EARTH OBSERVATION NEEDS

Also in the case of Earth-oriented satellites, the Navigation requirements, in some cases very stringent, are disregarded in this survey. From the meeting held at ESTEC, Noorwijk, Holland, in October 1994, quite unexpectedly the major request for better "navigation and positioning" and consequently "better frequency standards", went from the community of Oceanographers.

It seems that the models of oceanic currents circulation require near one order of magnitude improvement in the High harmonics of the Geopotential, i.e. the very accurate tracking of satellites in circular orbit, flying at about 160 km, for a period of half or one year. This craft, named ARISTOTELES, will pose difficult problems of navigation, since every fortnight the satellite should be re-boostered. The use of GPS system is planned, with differential corrections coming from ground.

Other Frequency and Time requirements come from the short term frequency stability of the radar-altimeters and of the reference sources for space borne Synthetic Aperture Radars.

### 4. WHY "PRECISE" CLOCKS ARE NEEDED

The topics to be investigated and consequently the measurements to be performed are listed in Table III.

**TABLE III**

topic		measurement
relativity effects	equivalence principle	frequency variation time advance
	photon trajectories (bending of light)	propagation time variation
	gravitomagnetic field (Lens-Thirring effect)	spacecraft position
	gravitational wave detection	spacecraft position (with reference to the Earth) interferometry
reference frames		spacecraft relative positions
pulsar timing		time of arrival versus TAI (models of time scales)
ranging to interplanetary spacecrafts		time of propagation (relativity corrections)
radioastronomy geodesy		phase measurements (extra long baseline interferometry)

Most of these activities are moreover requiring the introduction of relativistic effects [4]. For instance, in 1983 it has been shown [5], that the bending of light by the sun can amount to as much as 36 ns of additional time delay.

Out of General Physics, quite a deal of investigations are possible with “precise” clocks on board, such as Earth limb sounding (the ionospheric gradients around the Earth), or measurements on the interplanetary or the interstellar medium.

A new brand of Space Activities requiring “precise” clocks are planned on the very special satellite formed by the Moon. In the far side of the Moon currently ESA-sponsored studies are in progress in Europe, investigating, between the others, the concept and the feasibility of a Very Low Frequency Array (VLFA project), in the band 100 kHz – 30 MHz ( for radioastronomers 100 kHz is a very low frequency ...) for interferometric operations.

Consequently, coming back to Table III, the kinds of measurements to be performed are well known activities of the Frequency and Time Metrology; the problems to be solved are the utmost accuracies or stabilities to be offered and the need to fulfil formidable requirements, as regards mass, unattended operation, life, power and general reliability, and in some cases

harsh environment.

## 5. FREQUENCY AND TIME REQUIREMENTS

With reference to Tables I and III, the general "precision" i.e. accuracy and stability requirements were calculated or gathered from the existing literature; in some cases, assumptions were made. As regards the environment and life requirements, information was usually not available in the literature and consequently the estimates are responsibility of the authors.

Results and estimations are gathered in the last two columns of Table I, in which, when possible, an indication of the proposed device is provided.

## 6. RECOMMENDED ACTIONS

As regards the science and technology developments to be planned for the next years, as a logical prerequisite to the implementations of the proposed post 2000 scientific space missions, information can be gathered from two ESA documents [1, 3], from which the following list is extracted:

- drag free systems
- position sensors
- acceleraometers
- lasers for interferometry
- lasers for transmission of time signals
- active optics technology
- frquency standards + clocks
- time transmission and comparison methods
- lightweight materials
- cryogenics also applies to clocks (cold H maser)
- high speed data transmission
- cooled atomic frequency standards

From discussions with experts in the field, it seem that the most desirable strives should be toward the following devices:

- a frequency standard with mass less than 25 Kg, stability  $10^{-15}/d$ , life 5 years, power 15—20 W, accuracy not critical (for interferometric operations)

- a frequency standard with mass less than 50 Kg, stability  $10^{-17}/\text{d}$ , life 5 years, power 15—20 W
- frequency stabilized solid state lasers, with stability of  $10^{-15}/1000\text{s}$ , mass a few Kg, power 5 W (for long range interferometric operations)
- time transfer and comparison methods with a resolution of about 10 ps

The use of accurate (and stable) clocks on deep space probes or orbiting satellites could allow a one-way measurement of the velocity of light. This measurement would be an important test of the isotropy of  $c$ , but it would require the development of

a frequency standard with mass less than 25 Kg, stability  $10^{-14}/\text{d}$ , accuracy  $10^{-14}$ , life 5 years, power 10 W.

The revised interest for the Space Station and its attached Columbus module, would offer the very promising possibility to test in space atomic clocks, without stringent mass requirements and with the possibility of servicing directly on the craft.

Along these technical developments, parallel improvements must be reached in propagation time models, relativistic corrections, interplanetary (in the far future interstellar) plasma effects, and, for Earth based measurements, ionospheric and tropospheric effects.

## ACKNOWLEDGEMENTS

The cooperation of Dr. R. Bonnet and Dr. G. Cavallo of ESA – Space Science Directorate – and of Dr. P. Emiliani of ESA – Earth Observation Programme - in making available the quoted documents, and of Prof. G. Busca is gratefully acknowledged.

## REFERENCES

- [1] ESA European Space Agency, “*Mission concepts*”, tome I and II, 4/11/1993
- [2] ESA European Space Agency, “*HORIZON 2000 PLUS: inputs from the working groups*”, 16/5/1994
- [3] ESA European Space Agency, “*HORIZON 2000 PLUS: Preliminary reports from the topical teams*”, draft 2, 16/5/1994
- [4] R. W. Hellings, “*Relativistic Effects in Astronomical Timing Measurements*”, *Astron. J.* 91, 650 (1986).
- [5] Richtner, R.A. Matzner, *Phys.Rev. D*, 3007 (1983).

## QUESTIONS AND ANSWERS

**PETER WOLF (BIPM):** To test the isotropy of speed of light, you don't necessarily need accuracy in your frequency standard. If it is sufficiently stable and you watch it during a certain period, you can syntonize it and determine its frequency offset – and correct for it. I will say more about this in my paper tomorrow.

**SIGFRIDO LESCHIUTTA:** Thank you. You are completely right. You and your colleagues will cover that tomorrow.

56-70

5.27.32

p. 15

## TIME ACTIVITIES AT THE BIPM

Claudine Thomas  
Bureau International des Poids et Mesures  
Pavillion de Breteuil  
32312 Sèvres Cedex  
France

### Abstract

*The generation and dissemination of International Atomic Time, TAI, and of Coordinated Universal Time, UTC, are explicitly mentioned in the list of the principal tasks of the BIPM, recalled in the Comptes Rendus of the 18th Conférence Générale des Poids et Mesures, in 1987. These tasks are fulfilled by the BIPM Time Section thanks to international cooperation with national timing centers, which maintain, under metrological conditions, the clocks used to generate TAI. Besides the current work of data collection and processing, research activities are carried out in order to adapt the computation of TAI to the most recent improvements occurring in the time and frequency domains. Studies concerning the application of general relativity and pulsar timing to time metrology are also actively pursued. This paper summarizes the work done in all these fields and outlines future projects.*

## INTRODUCTION

The Comité International des Poids et Mesures, CIPM, discussed the role of the Bureau International des Poids et Mesures, BIPM, in the 1980s and its conclusions were made known in the Convocation to the 18th Conférence Générale des Poids et Mesures [1], in the following terms:

*“The purpose of the BIPM is to provide the physical basis necessary to ensure worldwide uniformity of measurements. Therefore, its principal tasks are:*

- *to establish and disseminate the International Atomic Time, and, in collaboration with the appropriate astronomical organizations, Coordinated Universal Time;*
- *to furnish whatever help is possible in the organization of [those] international comparisons which, although not carried out at the BIPM, are carried out under the auspices of a Comité Consultatif;*
- *to ensure that the results of international comparisons are properly documented and, if not published elsewhere, are published directly by the BIPM...*”

The definition of TAI was approved by the Comité International des Poids et Mesures in 1970, and recognized by the Conférence Générale des Poids et Mesures, CGPM, in 1971. It reads as follows:

*International Atomic time (TAI) is the time reference coordinate established by the Bureau International de l'Heure on the basis of the readings of atomic clocks operating in various establishments in accordance with the definition of the second, the unit of time of the International System of Units.*

In 1988, responsibility for TAI was transferred to the Time Section of the BIPM, according to one of the explicit missions recalled above.

From its definition, TAI is the result of a collective effort. It calls for the maintenance of atomic clocks in national timing laboratories, and for international comparisons between these clocks. One has thus established an exchange in which: \* timing centres produce time transfer and clock data and send it to the BIPM, \* the Time Section of the BIPM produces TAI, distributes it as time corrections to national time scales, and then publishes international time comparisons.

*The efficiency of this organization and the quality of its results rely upon the care and the rigor of the work effected in the contributing laboratories and at the BIPM, and upon a continuous, positive, and fruitful dialogue between both parties.*

The Time Section of the BIPM is helped in its work in two ways:

- The Comité Consultatif pour la Définition de la Seconde, CCDS, creates working groups on specific topics such as Improvement of TAI, GPS Standardization, and Two-Way Satellite Time Transfer. The membership of these groups includes experts and members of the staff of the Time Section. Recommendations are issued and proposed for adoption to the CCDS, and then the CIPM and the CGPM, after extended discussions. This procedure makes it possible for the Time Section to keep itself informed about new techniques or studies. The Recommendations which are passed also give a formal guide to its work.
- The Time Section of the BIPM has at its disposal a time laboratory including two caesium clocks and several GPS time receivers. Most of this equipment is on loan from private companies or from national timing centres. Data taken at the BIPM are not introduced in the TAI computation, but are simply analyzed for specific studies. This work provides a background of practical experience which sensitizes the Section to the problems of gathering data and allows it to make better use of that reported from outside.

The organization of the work at the Time Section is described in Fig. 1. The main objectives are perfectly clear and concern, as already stated, the generation and dissemination of TAI and UTC. However, they can easily be extended to the production of good realizations of the Terrestrial Time, TT, as defined by the International Astronomical Union, IAU, in 1992

[2]. These objectives imply that current activities centre on the regular production of TAI and on clock comparisons. More fundamental investigations are also carried out about time scale algorithms, time transfer methods, pulsar timing, and general relativity. This is described in the following sections.

## GENERATION OF TAI AND UTC

As is well known, TAI is obtained through the computation of a weighted average of clock readings [3]. The main algorithm, optimized for long-term stability, treats as a whole blocks of data collected over a two-month period, and produces in deferred-time a free time scale, EAL. External to this main algorithm, accuracy is ensured by frequency steering corrections, which are applied to EAL to obtain TAI, after comparison with the best primary frequency standards.

The 230 contributing clocks are kept in 46 national time centers spread world-wide. At present, all but four of these laboratories are compared using the Global Positioning System, GPS. Rough data are sent to the BIPM and treated according to strict common views in order to overcome Selective Availability effects [4, 5]. The general organization of the international GPS network used by the BIPM is shown in Fig. 2. It comprises:

- two long distance lines, linking three nodes: the NIST (USA), the OP (France), and the CRL (Japan), where GPS antenna coordinates are known accurately, and where ionospheric measurements are available. In addition, GPS data are corrected in post-processing with precise satellite ephemerides available from the International Geodynamics Service, IGS. For these two long-distance links (*ge* 6000 km) clock comparison noise is smoothed out for averaging times of order three days, and the overall accuracy is of order 6 ns to 8 ns ( $1 \sigma$ ) [6].
- local stars on a continental scale. Ionospheric measurements and precise satellite ephemerides are not used for these short-distance links (*le* 1000 km), but accurate GPS antenna coordinates help to improve the accuracy obtained. Typically, clock comparison noise is smoothed out for averaging times of order 12 hours to 24 hours, and the overall accuracy is of order 2 ns ( $1 \sigma$ ) [6].

The reference time scales TAI and UTC have been regularly computed and published in the monthly *Circular T* since the 1st January 1988, the date of official transfer of this responsibility from the old BIH to the BIPM. Annual reports are also produced by the BIPM Time Section, and have been available, in the form of computer-readable files, in the BIPM INTERNET anonymous FTP since 5 April 1994.

For years, the TAI scale interval has been regularly compared with the best realizations of the SI second provided by the primary frequency standards maintained at the PTB (Germany), PTB CS1 and CS2, which operate continuously as clocks. Their stated accuracies are respectively  $3 \times 10^{-14}$  and  $1.5 \times 10^{-14}$  ( $1 \sigma$ ). Recently, two newly designed caesium frequency standards, using optical production and detection of atoms have been evaluated:

- NIST 7, developed at the NIST (Boulder, Colorado, USA) reaches an accuracy of  $1 \times 10^{-14}$ [7].
- JPO (Jet à Pompe Optique), developed at the LPTF (Paris, France) attained an accuracy of  $1.1 \times 10^{-13}$  when evaluated for the first time in May 1993[8].

The deviation of the TAI scale interval, to the SI second as realized by PTB CS1, PTB CS2, and NIST 7, is shown in Fig. 3 for the last three years. The JPO is not included because its uncertainty is much larger than that of other primary frequency standards. On average, this deviation is estimated to be of order  $0.2 \times 10^{-14}$ , with an uncertainty of  $11 \times 10^{-14}$  ( $1 \sigma$ ) for the two-month interval July–August 1994. Since April 1993, the TAI frequency has remained constant with respect to the best primary standards, so no frequency-steering corrections have been applied.

## ALGORITHMS FOR TIME SCALES

The quality of the timing data used for TAI computation is rapidly evolving thanks to the wide use of GPS time transfer, and to the extensive replacement of older designs of commercial clocks by the new HP 5071A clocks and active auto-tuned hydrogen-masers. White measurement noise of distant time comparisons is thus smoothed out by averaging data on periods shorter than 10 days. In addition, the use of very stable clocks leads to a large improvement in the stability of TAI and UTC. By application of the N-cornered hat technique to the data obtained in 1993 and at the beginning of 1994, for the comparisons between TAI and the best independent time scales of the world (maintained at the NIST, the VNIIFTRII, the USNO and the PTB), one obtains the following estimates of stability (expressed in terms of Allan standard deviation and shown in Fig. 4):

$$\begin{aligned}\sigma_y TAI (\tau = 10\text{days}) &= 3.9 \times 10^{-15}, \\ \sigma_y TAI (\tau = 20\text{days}) &= 3.2 \times 10^{-15}, \\ \sigma_y TAI (\tau = 40\text{days}) &= 3.5 \times 10^{-15}, \\ \sigma_y TAI (\tau = 80\text{days}) &= 4.9 \times 10^{-15}.\end{aligned}$$

The stability of TAI and UTC lies thus below  $5 \times 10^{-15}$ . It also appears that the basic interval of computation, at present 60 days, can be reduced. This, if done, will help to shorten the delay of access to TAI. We are thus testing a new version of the algorithm ALGOS for the definitive computation of TAI each month, using real data from the beginning of 1992. Results are encouraging and it has been decided that the CCDS working group on Improvements to TAI should meet in March 1995 to discuss this new algorithm.

An interesting point is that the same stability study carried out using EAL instead of TAI gives the following results:

$$\begin{aligned}\sigma_y EAL(\tau = 10\text{days}) &= 3.9 \times 10^{-15}, \\ \sigma_y EAL(\tau = 20\text{days}) &= 3.2 \times 10^{-15}, \\ \sigma_y EAL(\tau = 40\text{days}) &= 3.1 \times 10^{-15}, \\ \sigma_y EAL(\tau = 80\text{days}) &= 4.0 \times 10^{-15}.\end{aligned}$$

A degradation of the stability of TAI, for averaging times ranging from 40 days to 80 days, is apparent when compared with the stability values obtained for EAL. This is probably due to the single frequency steering correction of  $5 \times 10^{-15}$  carried out in April 1993. Clearly the amplitude of this frequency step was too large, given the size of EAL fluctuations. It follows that steering corrections should be small (probably of order 1 to  $2 \times 10^{-15}$ ), and are useful only for modification of the TAI frequency in the very long term.

Given the high stability of recently designed commercial clocks and hydrogen-masers, it appears that it is now time to consider fundamental modification of the TAI algorithm. The next meeting of the CCDS working group on Improvement to TAI, scheduled for March 1995, is a good opportunity to discuss this topic. We are therefore studying, on real data, the following points:

- computation of TAI every 30 days instead of 60 days,
- introduction of a frequency drift evaluation in the frequency prediction of hydrogen-masers,
- change of the upper limit of weights,
- change of the weight determination procedure, which is at present based on the observation of systematic frequency changes with annual signature, a phenomenon which tends to disappear,
- danger of excessive dependence on a single clock type (HP 5071A),
- advantages of changing the basic measurement cycle from 10 days to 1 day,
- advantages of increasing or decreasing the number of participating clocks.

These studies have been partly reported<sup>9, 10</sup>, and it is already expected that the shortening of the period of definitive computation and a better use of hydrogen masers will be recommended by the working group.

## TIME LINKS

The BIPM Time section is interested in any time comparison method which has the potential for nanosecond accuracy. We are thus involved in the development of GLONASS, LASSO, two-way time transfer via geostationary satellites, and ExTRAS (Experiment on Timing, Ranging and Atmospheric Soundings, also named "hydrogen maser in space"), although GPS strict common-views remain the time transfer means used for current TAI computation.

### Global Positioning System, GPS

Among its current activities, the BIPM issues, twice a year, GPS international common-view schedules, produces international GPS comparison values, and also publishes an evaluation of the daily time differences between UTC and GPS time. These differences were obtained by treatment of data from Block I satellites only. Since April 1994, only one Block I satellite has

been observable, and daily values have been obtained by smoothing data taken from the Block II satellites viewed at angles of elevation greater than 30°. The results are less precise than before (daily standard deviations of order 12 ns, against 3 ns) because Selective Availability is currently implemented. Although we have shown that precise restitution of GPS time is possible using multi-channel P-code GPS time receivers<sup>[11]</sup>, this method cannot be used because reliable and regular data from such a receiver is not yet available.

An important part of our current work is to check the differential delays between GPS receivers which operate on a regular basis in collaborating timing centres, by transporting a portable GPS time receiver from one site to the other. Exercises in differential calibration of GPS receivers carried out in 1994 concerned the links between the OP ( France) and the NPL (United-Kingdom)<sup>[12]</sup>, the NIST (USA)<sup>[13]</sup>, the USNO (USA)<sup>[14]</sup>, and a European round-trip OP to OP successively through the OCA (France), the TUG (Austria), the FTZ (Germany), the PTB (Germany), the VSL (The Netherlands), and the NPL (United Kingdom)<sup>[15]</sup>.

Since 1983, several differential calibrations have been performed between the NIST and the OP. The results are shown in Table 1.

Date $t$	$\delta/\text{ns}$	$\sigma/\text{ns}$
July 1983	0.0	2.0
January 1985	-7.0	13.0
September 1986	+0.7	2.0
October 1986	-1.4	2.0
January 1988	-3.8	?
April 1988	+0.6	?
March 1994	+1.4	2.0

*Table 1. Results of 7 exercises in the differential calibration of the GPS time equipment in operation at the NIST and at the OP. The quantity  $\delta$  is the time correction to be added to the values  $UTC(NIST)(t) - UTC(OP)(t)$ , obtained at date  $t$  from raw GPS data, in order to ensure the best accuracy of the time link. The quantity  $\sigma$  is the estimated uncertainty ( $1 \sigma$ ) in the value  $\delta$ .*

In 1983 the internal delay of the OP GPS time receiver was determined at the NIST, before shipping to the OP, so that the time comparison values between  $UTC(NIST)$  and  $UTC(OP)$  could be obtained from GPS data without any systematic correction. This accuracy is maintained by applying time corrections  $\delta$  which compensate for variations with time in the internal delays of the two pieces of GPS equipment. The values of  $\delta$  remain inferior to their stated uncertainty ( $1 \sigma$ ) even after 10 years of continuous operation, which indicates the excellent long-term stability of the equipment.

For several years, GPS accuracy has also been studied by testing the closure condition through a combination of three links, OP-NIST, NIST-CRL and CRL-OP, using precise GPS satellite ephemerides and ionospheric delays measured at the three sites<sup>[6]</sup>. As shown in Fig. 5, the closure condition presents a residual bias of a few nanoseconds on daily averages which can

be determined with a precision of less than 2 ns. With the passage of time, the IGS precise satellite ephemerides continue to improve, which results in a corresponding improvement in the determination of the deviation from the closure. The residual bias now probably originates from errors in station coordinates and errors in ionospheric measurements. Results from codeless dual-frequency ionospheric measurement systems are sensitive to multipath effects which induce biases in particular directions<sup>[16]</sup>: these biases are not averaged when testing the closure condition if the observations selected are directed towards the East and West. Work is under way to evaluate these biases.

Within the group on GPS Time Transfer Standards, GGTTS, the BIPM has made a considerable effort to formulate technical directives for the standardization of GPS time-receiver software, together with a new format for GPS data files<sup>[17, 18]</sup>. The implementation of such directives and of the new data format should help to provide sub-nanosecond accuracy for GPS common-view time transfer. Practical development of the standardized software is in hand at the NIST and it is intended that it will be available for world-wide use from beginning of 1995<sup>[19]</sup>.

Another issue is the estimation of the tropospheric delay. At present, GPS time-receivers use simple models of the troposphere which, as was believed until recently, should provide an estimation of tropospheric delay with an uncertainty of 1 ns to 2 ns. Recent comparisons of these models with a semi-empirical model based on weather measurements show, however, differences of several nanoseconds for hot and humid regions of the world<sup>[20]</sup>. Further investigations of the tropospheric delay will continue at the BIPM.

## **GLOBAL NAVIGATION SATELLITE SYSTEM, GLONASS**

Values of comparison between UTC and GLONASS time, provided from observations of GLONASS satellites by Prof. P. Daly, University of Leeds, are currently published in the *BIPM Circular T*. The BIPM intends to issue an experimental international GLONASS common-view schedule in 1995, and to test it through an experiment with the RIRT, Russia. For this purpose, the BIPM will receive a GLONASS time receiver on loan from Russia.

## **TWO-WAY SATELLITE TIME TRANSFER, TWSTT**

Two-way time transfer through a geostationary satellite is potentially more accurate than one-way methods such as those using GPS or GLONASS, essentially because there is no need to evaluate the range between ground station and satellite. No two-way time transfer experiment has been conducted at the BIPM, which does not possess the necessary heavy equipment, however, the BIPM does chair the CCDS working group on Two-Way Satellite Time Transfer, which meets every year, and was involved in the comparison between the two-way technique and the GPS common-view method which used the link between the TUG (Austria) and the OCA (France)<sup>[21]</sup>. The BIPM was also involved in the field-trial which was organized in 1994. This is an international two-way time transfer experiment through the INTELSAT V-A(F13) satellite at 307°E, which involves both European and North-American laboratories. This began in January 1994 and should last one year. During the summer of 1994, the Earth stations involved have been calibrated using a portable station. At the same time, the GPS equipment in these laboratories was differentially calibrated using a portable GPS time receiver provided

by the BIPM. These calibration exercises should allow previous estimates of the accuracy, of order 2 ns ( $1 \sigma$ ), of the two-way technique to be verified<sup>[15]</sup>.

### Laser Synchronization from Satellite Orbits, LASSO

The BIPM has been involved in an experiment to compare time transfer by LASSO with GPS common-view time transfer between Texas and France<sup>[22]</sup>. The results of the calibration of laser equipment at the two sites should be available at the end of 1994 and will allow, for the first time, an estimation of the accuracy of the LASSO technique, which is expected to be of order 1 ns ( $1 \sigma$ ).

### Experiment on Timing Ranging and Atmospheric Soundings, ExTRAS

The Experiment on Timing Ranging and Atmospheric Soundings, ExTRAS, calls for two active and auto-tuned hydrogen masers to be flown on board a Russian meteorological satellite Meteor-3M, planned for launch at the beginning of 1997. Communication between the on-board clocks and ground stations is effected by means of a microwave link using the PRARE technique, Precise Range And Range-rate Equipment, and an optical link operating using the T2L2 method, Time Transfer by Laser Link. The PRARE and T2L2 techniques are upgraded versions of the usual two-way and LASSO methods. Associated with the excellent short-term stability of the on-board hydrogen masers, these should make it possible to solve a number of scientific and applied problems in the fields of time, navigation, geodesy, geodynamics and Earth-atmosphere physics. The impact of ExTRAS in the time domain, has been studied<sup>[23]</sup> in terms of anticipated uncertainty budgets: the potential accuracy of this experiment is characterized by uncertainties below 500 ps ( $1 \sigma$ ) for satellite clock monitoring and ground clock synchronization.

## APPLICATION OF GENERAL RELATIVITY TO TIME METROLOGY

An investigation of the application of the theory of relativity to time transfer has been completed<sup>[24]</sup>. Explicit formulae have been developed, which make it possible to compute, to picosecond accuracy, all terms describing the coordinate time interval between two clocks situated in the vicinity of the Earth, and linked through *i*) a one-way technique (GPS), *ii*) a two-way method via a geostationary satellite (TWSTT), or *iii*) a two-way optical signal (LASSO).

Current work centers on the application of the theory of relativity to the frequency syntonization of a clock with respect to the Geocentric Coordinate Time (TCG) at an accuracy level of  $10^{-18}$ . For Earth-bound clocks, this is limited to some parts in  $10^{17}$  due to poor knowledge of some geophysical factors (essentially the potential on the geoid). However, for clocks on terrestrial satellites, all terms can be calculated with  $10^{-18}$  accuracy. The results of this work will allow the establishment of a complete relativistic framework for the realization of TCG at a stability of  $10^{-18}$  and picosecond TCG datation accuracy. This should be sufficient to accommodate all expected developments in clock technology and time transfer methods for some years to come.

The work of the CCDS working group on the Application of General Relativity to Metrology was supported by numerous discussions with Prof. B. Guinot, Chairman of the working-group, and participation in the preparation of a text to be used as part of the final report of this group.

## **PULSARS**

Millisecond pulsars can be used as stable clocks to realize a time scale by means of a stability algorithm. Work has been carried out with a view to understanding how such a pulsar time scale could be realized and how it could be used for monitoring very-long instabilities of atomic time. An important feature of this work is that a pulsar time scale could allow the transfer of the accuracy of the atomic second from one epoch to another, thus overcoming some of the consequences of failures in atomic standards<sup>[25]</sup>.

## **CONCLUSIONS**

The Time Section of the BIPM produces time scales which are used as the ultimate references in the most demanding scientific applications. They serve also synchronization of national time scales and local representations of the Coordinated Universal Time, upon which rely all time signals used in current life. This work is thus in complete accordance with the fundamental missions of the BIPM.

Timing data used to generate the International Atomic Time comes from national metrological institutes where timing equipment is maintained and operated in the best conditions. An international collaboration is thus necessary and requests from the contributing laboratories to follow guides given by the BIPM. In return, the BIPM has the duty to process data in the best way in order to deliver the best reference time scales. For this purpose, it is necessary for the BIPM to examine in detail timing techniques and basic theories, to propose alternative solutions for timing algorithms, and to follow advice and comments expressed inside the CCDS working groups.

## References

- [1.] "BIPM Comptes Rendus 18e Conférence Générale des Poids et Mesures, BIPM Publications, 1987, p 23.
- [2.] IAU, *Information Bulletin* 67, 1992, p 7.
- [3.] TAVELLA P. and THOMAS C., "Comparative Study of Time Scale Algorithms," *Metrologia*, 1991, 28, 57-63.
- [4.] ALLAN D.W. and WEISS M.A., "Accurate time and frequency transfer during common-view of a GPS satellite," *Proc. 34th Ann. Symp. on Freq. Control*, 1980, p 334.
- [5.] ALLAN D.W., GRANVEAUD M., KLEPCZYNSKI W.J., and LEWANDOWSKI W., "GPS Time Transfer with Implementation of Selective Availability," *Proc. 22nd PTTI*, 1990, 145-156.
- [6.] LEWANDOWSKI W., PETIT G., and THOMAS C., "Precision and Accuracy of GPS Time Transfer," *IEEE Trans. Inst. Meas.*, 42, 1993, 474-479.
- [7.] LEE W.D., SHIRLEY J.H., LOWE J.P., and DRULLINGER R.E., "The accuracy Evaluation of NIST-7," *IEEE Trans. Instr. Meas.*, 1995, accepted.
- [8.] ROVERA D., DE CLERCQ E., and CLAIRON A., "An Analysis of the Major Frequency Shifts in the LPTF Optically Pumped Primary Frequency Standard," *IEEE Trans. Ult. Fer. and Freq. Cont.*, 41, 1994, p 245.
- [9.] THOMAS C. and ALLAN D.W., "A real-time prediction of UTC," *Proc. 25th PTTI meeting*, 1993, 217-229.
- [10.] AZOUBIB J. and THOMAS C., "The Use of Hydrogen Masers in TAI Computation," *Proc. 9th EFTF*, 1995, accepted.
- [11.] THOMAS C., "The use of the AOA TTR-4P GPS receiver in operation at the BIPM for real-time restitution of GPS time," *Proc. 25th PTTI*, 1993, 183-194.
- [12.] THOMAS C. and MOUSSAY P., "Determination of differential time correction between GPS time receivers located at the Observatoire de Paris, Paris, France, and the National Physical Laboratory, Teddington, United Kingdom," *Rapport BIPM-94/2*, 1994, 12 pages.
- [13.] THOMAS C., MOUSSAY P., "Determination of differential time correction between GPS time receivers located at the Observatoire de Paris, Paris, France, and the National Institute of Standards and Technology, Boulder, Colorado, USA," *Rapport BIPM-94/3*, 1994, 12 pages.
- [14.] LEWANDOWSKI W., "Determination of the differential time correction between GPS time equipment located at the Observatoire de Paris, Paris, France, and the United States Naval Observatory, Washington D.C., USA," *Rapport BIPM-94/11*, 1994, 14 pages.

- [15.] KLEPCZYNSKI W.J., DAVIS J.A., KIRCHNER D., DE JONG G., BAUMONT F., HETZEL P., SOERING A., HACKMAN C., GRANVEAUD M., and LEWANDOWSKI W., "Comparison of Two-Way Satellite Time Transfer with GPS Common-View Time Transfer during the Intelsat Field Trial," *Proc. 9th EFTF*, 1995, accepted.
- [16.] THOMAS C., PETIT G., and MOUSSAY P., "Comparison between different dual-frequency GPS receivers measuring ionospheric delay for time and frequency applications," *Proc. 8th EFTF*, 1994, 1012-1028.
- [17.] ALLAN D.W. and THOMAS C., "Technical Directives for Standardization of GPS Time Receiver Software," *Metrologia*, 1994, 31, 69-79.
- [18.] THE GROUP ON GPS TIME TRANSFER STANDARDS, "Technical Directives for Standardization of GPS Time Receiver Software," *Rapport BIPM-93/6*, 1993, 32 pages.
- [19.] WEISS M.A. and THOMAS C., "Implementation and Release of a Standard Format for GPS Common View data," *Proc. 26th PTTI*, 1994, accepted.
- [20.] LEWANDOWSKI W., GRUDLER P., and BAUMONT F., "Study of tropospheric correction for GPS common-view time transfer between the BIPM and the OCA," *Proc. 8th EFTF*, 1994, 981-997.
- [21.] KIRCHNER D., RESSLER H., GRUDLER P., BAUMONT F., LEWANDOWSKI W., HANSON W., KLEPCZYNSKI W., and UHRICH P., "Comparison of GPS and Two-Way Satellite Time Transfer Over A Baseline of 800 km," *Metrologia*, 1993, 30, 183-192.
- [22.] LEWANDOWSKI W., PETIT G., BAUMONT F., FRIDELANCE P., GAIGNEBET J., GRUDLER P., VEILLET C., WIAN T.J., KLEPCZYNSKI W.J., "Comparison of LASSO and GPS time transfers," *Proc. 25th PTTI*, 1993, 357-365.
- [23.] THOMAS C., WOLF P., UHRICH P., SCHAEFER W., NAU H., and VEILLET C., "Anticipated Uncertainty Budgets of PRARE and T2L2 Techniques as Applied to ExTRAS," *Proc. 26th PTTI*, 1994, accepted.
- [24.] PETIT G., WOLF P., "Relativistic theory for picosecond time transfer in the vicinity of the Earth," *Astronomy and Astrophysics*, 1994, 286, 971-977.
- [25.] PETIT G., TAVELLA P., and THOMAS C., "How can Millisecond Pulsars improve the Long-Term Stability of Atomic Time Scales?," *Proc. 6th EFTF*, 1992, 57-60.

Acronyms of the laboratories quoted in the text

CRL	Communications Research Laboratory, Tokyo, Japan
FTZ	Forschungs – und Technologiezentrum, Darmstadt, Germany
LPTF	Laboratoire primaire du Temps et des Fréquences, Paris, France
NIST	National Institute of Standards and Technology, Boulder, CO, USA
NPL	National Physical Laboratory, Teddington, United Kingdom
OCA	Observatoire de la Côte d’Azur, Grasse, France
OP	Observatoire de Paris, Paris, France
PTB	Physikalisch–Technische Bundesanstalt, Braunschweig, Germany
RIRT	Russian Institute of Radionavigation and Time, St. Petersburg, Russia, Austria
TUG	Technische Universität, Graz, Austria
USNO	U.S. Naval Observatory, Washington D.C., USA
VSL	Van Swinden Laboratorium, Delft, The Netherlands

## QUESTIONS AND ANSWERS

**GERNOT M. WINKLER (USNO):** In your presentation, you showed the definition of TAI. I find it remarkable, the sentence which I forgot in the meantime, and that is in conformance with the definition of the second. That has, of course, direct implications regarding the use of hydrogen masers. Could you maybe comment on that?

**CLAUDINE THOMAS (BIPM):** This is the first definition from 1971. Of course, there were other definitions which have been -- this definition has been updated in time. Now it is exactly stated that the scale unit of TAI must be as close as possible to the SI second as realized on the rotating geoid. So the word "in accordance" -- but that's a question. You know that we have national laboratories which think that we shouldn't use hydrogen masers in computing TAI because they are using the hydrogen atomics instead of the cesium atom. That's something to be discussed.

**FRED WALLS (NIST):** I would like to address that. Using a hydrogen maser is no different than using the commercial cesium standard which does not have the same accuracy of the primary standards in the national labs. What you need for the short term are flywheel oscillators that are stable; it doesn't matter if they're based on calcium, if they're based on mercury, if they're based on hydrogen or any other atom, if you have something which is very stable. They're just a flywheel. The definition of the second comes at the present time from large primary standards and national laboratories. That can be used to establish frequency in the long term, as you do now.

So I do not see any conflict at all.

**CLAUDINE THOMAS (BIPM):** Atomic hydrogen masers are very stable. And, of course, they cause the stability of TAI. But they must be used carefully in the particular case where they show a drift relative to some primary system frequency standards. This drift, should be evaluated and calculated in the algorithm, of course.

**FRED WALLS (NIST):** Yes, I agree with that. But something quite serious which you only partially alluded to is we must agree internationally on whether or not to include the black body radiation. That is something that's on the order of  $2 \rightarrow 4 \times 10^{14}$ ; and it's quite serious at the level of accuracy that the national scales are now. We must come to some agreement. I think it should be included, in my opinion.

**CLAUDINE THOMAS (BIPM):** Well this is something which will be discussed next March during the meeting of the working group on the improvement of TAI. There are many questions to discuss, and, in particular, using data from these new test tables and accurate primary frequency system standards and how to correct them.

**HARRY PETERS (SIGMA TAU STANDARDS):** The National Radio- astronomy has 12 hydrogen masers, 10 of them are stationed from the Hawaiian Islands to the Virgin Islands; they are operating continuously and many of them have been going since 1987. I have been encouraging them to try to keep a record of time; they don't vary their synthesizers. And it seems to me that this is an asset that could possibly be included in the international time scale if they could just improve the record-keeping and perhaps transmit the information to you.

Thank you.

**GERNOT M. WINKLER (USNO):** I would like to come back to the question of the black body radiation. Because, this is an extremely important point, and it should be discussed as much as possible. An objection has been raised to the inclusion of that at the present time, before any experimental verification exists. The question is, is there an effort going on anywhere to demonstrate, at least in a quantitative way, the existence of that effect? Since the effect goes with the fourth power of temperature, it shouldn't really be too difficult to make a test, even within obtainable laboratory conditions -- different between, for instance, an operation of 10 degrees C. and 40 degrees C. should be substantial. Do you have any comments on that?

**THOMAS PARKER (NIST):** I'm not really the person to be doing this, but they're beginning to think about how to try and do that with NIST 7. It's pushing the limits of what we can do, but they are beginning to make some plans to try and see how far they can make an evaluation of the black body radiation. It's not clear that we're in position to really get a good number on that yet.

**DAVID ALLAN (ALLAN'S TIME):** Actually two comments, I guess. Maybe one is a question. I believe the linear mercury ion trap at JPL, because of its excellent long-term stability, is in a good position to measure the black body radiation. So I put a question to JPL in that regard.

The other point I wish to make is picking up on Dr. Winkler's question about hydrogen masers. Very often, even with cavity servos, in very long term we see frequency drift, as you alluded to. And it's one thing to include it, it's another thing to ask what is the uncertainty on the estimate. And that has not been addressed well. But these are important questions for TAI because of the need for long-term performance.

**CLAUDINE THOMAS (BIPM):** We use it on real data at the BIPM for the moment. And it appears that it is not always easy to detect a minor drift.

**FRED WALLS (NIST):** If you look at the drift that's been estimated for a lot of the hydrogen masers, it's within one or two sigma of what the accuracy claimed at the national labs for their primary cesium standards averaged over one or two years. It's so small that at this point I find it very difficult to believe the estimate on the drift on the hydrogen masers. The drift may, in fact, be zero for some of them, maybe for many of them.

So even though there is some difference -- and you say parts in  $10^{17}$  per day averaged over a year or two, that's within the one sigma limit of accuracy claimed at PTB and at NIST, and NRC and whatever.

**CLAUDINE THOMAS (BIPM):** The thing I can tell you about that is that we have tried to compute another version of EAL at various times, without any hydrogen maser. And it gives something which seems to have a lower drift. So maybe hydrogen masers adds some drift to EAL. But, of course, we are missing about 30 clocks when we do not use hydrogen masers. So, that's another point.

**SIGFRIDO M. LESCHIUTTA:** Before I give the floor to Dr. Winkler, I want to make a comment. There are a huge numbers of questions, and some of those questions are double

questions. I think the time is right for discussions for the people inside the national laboratories to talk about the next meeting to be held in Paris. If I remember correctly, that meeting will be convened by Dr. Winkler, since you are chairman of that activity. Do you want, Dr. Winkler, to add some additional remarks?

**GERNOT M. WINKLER (USNO):** Yes. In fact, thank you for these comments, because these are essentially the main points which will be discussed. And that meeting would be more productive if the participants coming from the laboratories receive any ideas which exist in regards to these points.

Coming back to the question of drifts, on the basis of a considerable number of clocks -- and 12 of them are Sigma Taus at the Observatory -- I have come to the conclusion that there is no zero. There is no clock which has a zero drift. In other words, any clock has sometimes changes in its structure or any observation which sometimes comes up as different values; so that at a level of our capability today, it is impossible to state that there is any clock which has zero drift.

Going back to the hydrogen maser, for instance, it is quite possible that the process which controls the cavity tuning, which is based on the measurement of the hydrogen line itself, is disturbed by effects which come from the cavity coating. And that is an effect which possibly has to do with chemistry changes in the surface. There are all kinds of things. In other words, as we go down in our level of precision to smaller and smaller values, we find more and more effects which can make a change and which do not always exist. And we have to realize that there is a difference between our ideas, which are ideal, of course, and to reality, which is infinitely complex and which you have to remember.

**HARRY PETERS (SIGMA TAU STANDARDS):** I think one point that is a serious point is that one should possibly look at this from an astrophysical point of view or a structure-of-the-universe point of view; after all, the universe is suppose to be expanding at a part of  $10^{10}$ ; or effectively, we are shrinking, as another view of it, at a part of  $10^{10}$  per day. There is no absolute knowledge of whether the relative frequency of hydrogen and cesium are not changing fundamentally, due to conventional changes or whatever. I mean, we don't know that hydrogen absolutely does not change them slightly or change them in regard to cesium at  $10^{-14}$ , well, maybe 13 or 15. So there is that absolute question of are all these transitions really constant and you must choose one, I suppose..

**SIGFRIDO M. LESCHIUTTA:** Certainly, Dr. Peters, you are opening quite a large program. I know that some activities are underway in some laboratories comparing fine transitions with hyperfine transitions. And some activities are now in Europe, and most in the United States. Basic physics is a wonderful thing. I fully agree with you that the program you described is opening new question marks.

**CLAUDINE THOMAS (BIPM):** I would like to make a comment about the last point made by Dr. Winkler. Of course, before the meeting I will write down all studies which have been done at the BIPM on real data. It does not cover all the questions, but we will make reports and send those reports to people who will be there. This might be a first attempt to answer these questions.



62-53  
P-13

# ANTICIPATED UNCERTAINTY BUDGETS OF PRARETIME AND T2L2 TECHNIQUES AS APPLIED TO ExTRAS

C. Thomas<sup>1</sup>, P. Wolf<sup>1,2</sup>, P. Uhrich<sup>3</sup>, W. Schäfer<sup>4</sup>  
H. Nau<sup>5</sup>, and C. Veillet<sup>6</sup>

<sup>1</sup>Bureau International des Poids et Mesures, Sèvres, France

<sup>2</sup>Queen Mary and Westfield College, London, United Kingdom

<sup>3</sup>Laboratoire Primaire du Temps et des Fréquences, Paris, France

<sup>4</sup>Institut für Navigation, Stuttgart, Germany

<sup>5</sup>Deutsche Forschungsanstalt für Luft und Raumfahrt e.V.,  
Oberpfaffenhofen, Germany

<sup>6</sup>Observatoire de la Côte d'Azur, Grasse, France

## Abstract

*The Experiment on Timing Ranging and Atmospheric Soundings, ExTRAS, was conceived jointly by the European Space Agency, ESA, and the Russian Space Agency, RSA. It is also designated the 'Hydrogen-maser in Space/Meteor-3M project'. The launch of the satellite is scheduled for early 1997. The package, to be flown on board a Russian meteorological satellite includes ultra-stable frequency and time sources, namely two active and auto-tuned hydrogen masers. Communication between the on-board hydrogen masers and the ground station clocks is effected by means of a microwave link using the modified version for time transfer of the Precise Range And Range-rate Equipment, PRARETIME, technique, and an optical link which uses the Time Transfer by Laser Link, T2L2, method. Both the PRARETIME and T2L2 techniques operate in a two-directional mode, which makes it possible to carry out accurate transmissions without precise knowledge of the satellite and station positions.*

*Due to the exceptional quality of the on-board clocks and to the high performance of the communication techniques with the satellite, satellite clock monitoring and ground clocks synchronization are anticipated to be performed with uncertainties below 0.5 ns (1  $\sigma$ ). Uncertainty budgets and related comments are presented.*

## INTRODUCTION

The Experiment on Timing Ranging and Atmospheric Sounding, ExTRAS, was conceived jointly by the European Space Agency, ESA, and the Russian Space Agency, RSA. It is also designated the "Hydrogen-Maser in Space/Meteor-3M project", and is scheduled for early 1997. The experiment calls for ultra-stable frequency and time sources, two active and auto-tuned hydrogen masers, to be flown on board a Russian meteorological satellite, Meteor-3M.

Communication between the on-board hydrogen masers and the ground stations is effected by a microwave link using the Precise Range And Range-Rate Equipment modified for time transfer, PRARETIME, technique, and an optical link which uses the Time Transfer by Laser Link, T2L2, method. The combination of ultra-stable time and frequency sources with precise and accurate tracking equipment should help to solve a number of scientific and applied problems in the fields of navigation, geodesy, geodynamics and Earth atmosphere physics. It should also allow timing measurements with accuracies never reached before.

## ON-BOARD HYDROGEN MASERS

Compared with other atomic frequency standards, passive hydrogen masers offer improved short-term stability<sup>[1]</sup>. They are generally used as short-term references in timing laboratories, but cannot serve as time-keepers because of the huge drift they generate over averaging times longer than several hours. However, recent developments of active hydrogen masers operating according to specific auto-tuning modes for the cavity reduce frequency drift while causing a negligible degradation of the short-term stability<sup>[2]</sup>. This type of hydrogen maser already contributes, on the ground, to short-term internal time comparisons and to long-term time keeping in national timing centres concerned with time metrology.

Rubidium and caesium clocks are currently used in navigation systems, for example in the Global Positioning System, GPS, where all Block II satellites are equipped with caesium standards. To date, no hydrogen maser has ever been flown with the exception of a hydrogen maser belonging to the Smithsonian Astrophysics Observatory which was sent into parabolic flight in 1976<sup>[3]</sup>. Space hydrogen masers are also planned as future on-board clocks for the Russian GLObal NAVigation Satellite System, GLONASS, in order to improve the short-term stability of the flying standards.

The active auto-tuned hydrogen masers scheduled for flight on Meteor-3M are a Russian-designed hydrogen maser, proposed by the Institute of Metrology for Time and Space, VNI-IFTRII, Mendeleev (Russia), and a Swiss Space Hydrogen Maser, SHM, proposed by the Observatoire de Neuchâtel, ON, Neuchâtel (Switzerland). These two units are of a weight ( $\leq 50$  kg), volume ( $\leq 0.1$  m<sup>3</sup>) and power consumption ( $\leq 60$  W) compatible with an on-board installation. In addition they will be compared continuously and are interchangeable. Their short-term stability is characterized by the Allan deviation given in Table 1.

Averaging time	Allan Deviation
$\tau/s$	$\sigma_y(\tau)$
1	$1.5 \times 10^{-13}$
10	$2.1 \times 10^{-14}$
100	$5.1 \times 10^{-15}$
1000	$2.1 \times 10^{-15}$
10000	$1.5 \times 10^{-15}$
100000	$\leq 1 \times 10^{-14}$

*Table 1: Allan deviation  $\sigma_y(\tau)$ , versus the averaging time  $\tau$ , of the Space Hydrogen Maser (SHM) developed by the Observatoire de Neuchâtel, ON, Neuchâtel (Switzerland), for flying on board Meteor-3M. Numbers are provided by Dr G. Busca, of the ON, in his proposal for ExTRAS (1993).*

The first consequence is that the comparison of ground clocks with the on-board hydrogen maser ensures access to a stable and slowly drifting time scale for synchronization of local

time scales used for real-time dating of events on the Earth. In a complementary process, the time scale to be delivered by the on-board clock can be closely steered in real-time on any reference time scale, such as a local representation of UTC, UTC(k), kept by laboratory k: for this purpose, it is sufficient to distribute, in the satellite message, a time correction between the on-board and ground time scales. The experiment ExTRAS thus serves all the functions of time dissemination.

The specifications of Table 1 have another impact on time metrology when flying such hydrogen masers on Meteor-3M. This is linked to particular features of the satellite orbit: its polar orbit and its altitude, of order 1000 km, lead to a period of revolution around the Earth of order  $T = 100$  min, and to possible observation of the satellite at least four times a day from any location on the Earth. The total error ( $1 \sigma$ ) accumulated by the on-board hydrogen maser during one revolution can be estimated as<sup>[4]</sup>:

$$\sigma \approx \sigma_y(\tau) \cdot T, \quad (1)$$

which leads to the value 12 ps. If two observations are distant by 3 hours, the error ( $1 \sigma$ ) accumulates to less than 50 ps.

It follows that comparisons between remote clocks on the Earth can be performed by differential observation of the time scale provided by the on-board hydrogen maser when it is visible from the stations. This is the clock transportation method, and there is no need to organize common views, as is done with GPS and GLONASS, the uncertainty caused by the on-board clock during its flight between the two stations being typically of order 50 ps.

To conclude, ExTRAS provides a means of time transfer based upon the transportation, via satellite, of an ultra-stable clock able to keep its time very precisely throughout the period of transportation. This time transfer method, the simplest imaginable, is thus of major interest to the timing community. Full advantage of the qualities of hydrogen masers on board Meteor-3M can be taken only if very accurate methods are used to ensure the connection between observing stations on the ground and the spacecraft. Specific features of two-direction links, such as via PRARETIME and T2L2 are discussed in the following sections.

## **PRARETIME: PRECISE RANGE AND RANGE-RATE EQUIPMENT, MODIFIED VERSION FOR TIME TRANSFER**

The Precise Range And Range-Rate Equipment, PRARE, is a high precision and fully automated facility for microwave link between clocks on board a satellite and ground stations. Its primary function consists of range and range-rate measurements, but a modified version of PRARE devoted to time transfer, PRARETIME, has also been developed. The modification concerns some hardware details and an additional time interval measurement at the ground station site. The PRARE equipment operates with a down-and-up link in the X-band (8489 GHz for down-link and 7225 GHz for up-link) between the ground and the satellite, together with a down-link in the S-band (2248 GHz)<sup>[5, 6, 7]</sup>. The PRARE X-band up-link exists only if the ground station is equipped with a ground transponder and its 60 cm parabolic dish. In this

case, the only one considered in this paper, the PRARE system operates in a two-way mode, which can be used for timing purposes such as:

- time comparisons between one ground clock and the on-board clock: this is known as satellite clock monitoring, and
- time comparisons between two ground clocks through transportation of the on-board clock: this is known as ground clock synchronization.

## Timing applications through ExTRAS via PRARETIME

### Satellite clock monitoring

A signal is emitted by the satellite S and retransmitted immediately by the Earth station E. The time interval  $t_{SE}$  between emission and reception on board the satellite,  $t_{SE} = t_1 - t_0$ , is recorded. The time difference between the clocks  $\Delta t$  is given by<sup>[8]</sup>:

$$\Delta t = t_{SE}/2 + \delta. \quad (2)$$

With  $T_1$  and  $T_2$  the individual transmission times for the down-link and the up-link, the time correction  $\delta$  is written as:

$$\delta = (T_1 - T_2)/2, \quad (3)$$

which may be expressed as<sup>[8]</sup>:

$$\delta = [\delta_{e,d} - \delta_{e,u} + \delta_{i,d} - \delta_{i,u}]/2 - \mathbf{v}_S(t_0) \cdot \mathbf{R}_{ES}(t_0)c^{-2} + \mathbf{O}(c^{-3}), \quad (4)$$

where  $\delta_e$  and  $\delta_i$  are external (ionospheric and tropospheric) and internal (cables, ...etc) delays respectively, subscripts 'd' and 'u' refer to the down- and up-links,  $\mathbf{R}_{ES}(t_0)$  is the station to satellite vector at date  $t_0$ ,  $\mathbf{v}_S$  is the satellite velocity in a geocentric inertial frame and  $c$  is the speed of light in vacuum.

## Ground clock synchronization

The satellite S emits signals to each ground station A and B which are immediately re-transmitted to the satellite. Three time intervals are recorded by the satellite:

- $t_S = t_3 - t_0$ , the time elapsed between the emission of the two signals,
- $t_{SA} = t_2 - t_0$  and  $t_{SB} = t_4 - t_3$ , the times elapsed between the emission and reception on-board the satellite of the signals received in stations A and B.

The time difference between the ground clocks  $\Delta t$  is given by<sup>[8]</sup>:

$$\Delta t = (t_{SB} - t_{SA})/2 + t_S + \delta. \quad (5)$$

The time correction  $\delta$  is written as:

$$\delta = [(T_3 - T_4) - (T_1 - T_2)]/2, \quad (6)$$

where  $T_1$ ,  $T_2$ ,  $T_3$ , and  $T_4$  are the individual transmission times for the down-links and the up-links.

Using (4),  $\delta$  is expressed as:

$$\delta = [\delta_{e,d} - \delta_{e,u} + \delta_{i,d} - \delta_{i,u}]_B/2 - [\delta_{e,d} - \delta_{e,u} + \delta_{i,d} - \delta_{i,u}]_A/2 - \mathbf{v}_S(t_3) \cdot \mathbf{R}_{BS}(t_3)c^{-2} + \mathbf{v}_S(t_0) \cdot \mathbf{R}_{AS}(t_0)c^{-2} + \mathbf{O}(c^{-3}), \quad (7)$$

in a notation following that of (4).

In (4) and (7) no range estimations are involved in terms of order  $c^{-1}$ , which is typical of a two-way method. Terms of order  $c^{-2}$  can amount to 300 ns and can be calculated at the picosecond level even with a poor knowledge of satellite ephemerides and velocity (accuracies of these quantities should be of order 12 m and 0.02 m/s respectively). Terms in  $c^{-3}$  contribute a few picoseconds.

It follows that the time comparison value between the ground clock and the on-board clock, or between the two ground clocks, can be deduced from measurements of time intervals on-board the satellite, and from the estimations of differential delays in the up- and down-paths. No accurate estimation of the range between the satellite and the station is needed.

It is important to note that tropospheric delays totally cancel in the up- and down-paths because the troposphere is a non-dispersive medium which yields the same delay for the PRARE up

and down carrier frequencies. In contrast, the ionosphere is a dispersive medium and the corresponding differential delays do not cancel in (4) and (7). The up- and down-links from the stations to the satellite do not necessarily pass through the same internal electronic circuits and cables, so internal differential delays remain in (4) and (7).

## **Sources of uncertainties for timing applications through ExTRAS via PRARETIME**

The uncertainties affecting timing observations come from the on-board hydrogen-maser, signal transmission through the atmosphere, and the equipment which is used to emit and transmit the signals. All the uncertainties given in the following are  $1 \sigma$  estimations: they are summarized in Table 2.

### **Uncertainty due to the on-board hydrogen maser**

The uncertainty brought by the on-board hydrogen maser is deduced from its stability. This is negligible for the quantities  $t_{SE}$ ,  $t_{SA}$ , and  $t_{SB}$  and thus has no impact on satellite clock monitoring. It must be taken into account, however, for the quantity  $t_S$  since this depends on the time duration which separates the observations of the satellite from the two stations being compared. A conservative estimate is of order 50 ps ( $1 \sigma$ ).

### **Uncertainty on the atmospheric delay of the signal**

The frequency separation between the S-band and X-band PRARE down-links makes it possible to measure the ionospheric delay of the signal. One expects a very low level of uncertainty, of order 20 ps ( $1 \sigma$ ), for the measurement of the difference between down and up ionospheric delays. For ground clock synchronization, this uncertainty appears twice (in quadratic).

### **Uncertainty on the calibration of equipment**

The on-board payload, the Earth stations, and the PRARETIME modems and counters must be very carefully calibrated before launch. One expects an uncertainty in the calibration of order 50 ps ( $1 \sigma$ ) for each of these elements. These uncertainties appear twice (in quadratic) for ground clock synchronization. However, the on-board payload is known to remain very stable between adjacent observations. It follows that the corresponding uncertainty partly disappears for ground clock synchronization. One estimates a total residual uncertainty of 20 ps ( $1 \sigma$ ) for this particular case.

The uncertainty associated with PRARETIME modems and counters arises from error sources such as instrumental delays (temperature, calibration of electronic components,  $C/N_o$  influence, ...etc), timer resolution, multipath transmission, and problems related to the antenna phase centre. It may not be possible to separate this uncertainty from those coming from the on-board payload and the Earth station calibrations.

## Uncertainty due to the links to local 1 pps signals

The PRARETIME technique only uses the high frequency (5 MHz) signals from the on-board and ground clocks. Time transfer, however, usually takes place between time scales which take the form of a series of local signals at 1 pulse per second, 1 pps. It is thus necessary to take into account uncertainties arising in the links to the local 1 pps signal. Passing from 5 MHz signals to 1 pps signals requires cables and electronic circuits for frequency division and pulse formation. It generates uncertainties which are generally estimated to be of order 300 ps ( $1 \sigma$ ). In the PRARETIME system, no 1 pps signal is physically available on board the satellite, so this class of uncertainty arises only in the timing circuitry of the ground stations.

## Anticipated uncertainty budgets for timing applications through ExTRAS via PRARETIME

The anticipated uncertainty budgets for satellite clock monitoring and ground clock synchronization are given in Table 2. Those parts of uncertainty arising from the method itself and from the links to the local 1 pps signal are shown separately. The uncertainty of the method itself amounts to 89 ps ( $1 \sigma$ ) for satellite clock monitoring, and 117 ps ( $1 \sigma$ ) for ground clock synchronization. The total uncertainties of 313 ps and 440 ps ( $1 \sigma$ ), largely dominated by uncertainties due to local links to the 1 pps signals in the ground stations, are well below 0.5 ns ( $1 \sigma$ ), which represents a major improvement for time metrology. In addition, the PRARETIME instrument makes it possible to disseminate any time scale maintained on the ground thanks to additional information contained in the S-band downward signal. The achievable uncertainty of this particular timing mode is to be further investigated.

## T2L2: TIME TRANSFER BY LASER LINK

The Time Transfer by Laser Link, T2L2, technique provides an optical time link between the on-board hydrogen masers and ground clocks. It may be seen as a continuation of the LASER Synchronization from Satellite Orbit (LASSO) technique, which was successfully carried out between the McDonald Observatory in Texas, USA, and the Observatoire de la Côte d'Azur, France, in 1992, through the geostationary satellite Meteosat-P2. Very few LASSO time comparison points were obtained during this experiment<sup>[9, 10]</sup>. They show a precision of order 200 ps, which is a major improvement over other methods, but, unfortunately no accuracy evaluation has been made so far now. The LASSO experiment also showed the possibility of monitoring the on-board clock with a precision of order 50 ps. This could serve time dissemination purposes, but again the corresponding uncertainty has not yet been evaluated.

The specific and principal difficulties of the LASSO experiment are:

- the rather poor stability of the oscillator on board Meteosat-P2. The consequence is that the stations to be synchronized must both shoot the laser onto the satellite within a time window equivalent of common-view conditions.
- the weather conditions must be excellent to avoid excessive light dissipation which prevents the ground observer from counting an adequate number of return photons.

Problems with on-board oscillators should largely be resolved using T2L2, because ultra-stable sources are used. In addition, as the Meteor-3M satellite orbit is far lower altitude than that of the geostationary Meteosat-P2 satellite, the effects of weather conditions should be less severe.

The T2L2 equipment can easily be installed on board the satellite. The principal elements in this equipment are a light detector linked to an event timer, and an Optical Retroreflector Array (ORA). The Earth sites concerned with this experiment require to have at their disposal facilities for high-power pulsed-laser shooting, together with a telescope. Very few sites meet these requirements and it may be necessary to increase the number of laser stations to take full advantage of the ExTRAS experiment.

## Timing applications through ExTRAS via T2L2

The T2L2 time transfer system can serve satellite clock monitoring and remote ground clock synchronization according to schemes symmetrical to those already presented for the PRARETIME technique.

### Satellite clock monitoring

A signal is emitted by the Earth station E with  $T_1$  and is reflected immediately by the satellite S. The time interval  $t_{ES}$  between emission and reception at the station,  $t_{ES} = t_1 - t_0$ , is recorded. The time difference between the clocks  $\Delta t$  is given by<sup>[8]</sup>:

$$\Delta t = t_{ES}/2 + \delta. \quad (8)$$

$T_2$  the individual transmission times for the up-link and the down-link, the time correction  $\delta$  is written as:

$$\delta = (T_1 - T_2)/2. \quad (9)$$

Using (4), this is expressed as:

$$\delta = [\delta_{i,u} - \delta_{i,d}]/2 + \mathbf{v}_E(t_0) \cdot \mathbf{R}_{ES}(t_0)c^{-2} + \mathcal{O}(c^{-3}), \quad (10)$$

with notations similar to that of (4).

## Ground clock synchronization

Laser pulses are emitted from the ground stations A and B, and reflected by the satellite S. Three time intervals are recorded:

- $t_S = t_3 - t_1$ , the time elapsed between the reflection of the two signals (recorded on the satellite),
- $t_{AS} = t_2 - t_0$  and  $t_{BS} = t_4 - t_0 - \Delta t$ , the times elapsed between the emission and reception (recorded in stations A and B).

The time difference between the ground clocks  $\Delta t$  is given by<sup>[8]</sup>:

$$\Delta t = (t_{AS} - t_{BS})/2 + t_S + \delta. \quad (11)$$

The time correction  $\delta$  is written as:

$$\delta = [(T_1 - T_2) - (T_3 - T_4)]/2, \quad (12)$$

where  $T_1$ ,  $T_2$ ,  $T_3$ , and  $T_4$  are the individual transmission times for the up-links and the down-links.

Using (10), this is expressed, with a notation similar to that of (4), as:

$$\delta = [\delta_{i,u} - \delta_{i,d}]_A/2 - [\delta_{i,u} - \delta_{i,d}]_B/2 + \mathbf{v}_A(t_0) \cdot \mathbf{R}_{AS}(t_0)c^{-2} - \mathbf{v}_B(t_0 + \Delta t) \cdot \mathbf{R}_{BS}(t_0 + \Delta t)c^{-2} + \mathbf{O}(c^{-3}). \quad (13)$$

In (10) and (13) no range estimations are involved in terms of order  $c^{-1}$ , which is again typical of a two-way method. Terms of order  $c^{-2}$  may amount to 20 ns and can be calculated at the picosecond level even with a poor knowledge of satellite-station ranges and station velocities in an inertial frame (accuracies in these quantities should be of order 100 m and 0.02 m/s respectively). Terms in  $c^{-3}$  contribute a few picoseconds.

It follows that the time comparison value between the ground clock and the on-board clock, or between the two ground clocks, can be deduced from measurements of time intervals on-board the satellite and in the ground stations, and from the estimations of differential delays in the up- and down-paths. No accurate estimation of the range between the satellite and the station is needed.

It is important to note that atmospheric delays totally cancel in (10) and (13) since the T2L2 up and down frequencies are equal. The up- and down-links from the stations to the satellite do not necessarily pass by the same internal electronic circuits and cables, so internal differential delays remain in (10) and (13).

## Sources of uncertainties for timing applications through ExTRAS via T2L2

The uncertainties affecting timing observations come from the on-board hydrogen-maser, and from the different equipment which is used for emitting and reflecting the optical pulses. Similar comments apply to the estimation of uncertainties as were given for PRARETIME, but two points should be noted:

- no uncertainties are to be taken into account for atmospheric delays, and
- only counters, and no modems, are used in the T2L2 technique, which reduces the corresponding uncertainty to 10 ps ( $1 \sigma$ ).

## Anticipated uncertainty budgets for timing applications through ExTRAS via T2L2

The anticipated uncertainty budgets are given in Table 3 for satellite clock monitoring and ground clock synchronization through ExTRAS via T2L2. Again, the parts of the uncertainty coming from the method itself and from the links to the local 1 pps signals are separated. One obtains an uncertainty for the method of 71 ps ( $1 \sigma$ ) for satellite clock monitoring, and 90 ps ( $1 \sigma$ ) for ground clock synchronization. The total uncertainties of 308 ps and 434 ps ( $1 \sigma$ ) are again largely dominated by terms arising from the local links to the 1 pps signals in the ground stations.

To conclude, the estimates of the T2L2 anticipated uncertainty budgets are very close to those obtained with PRARETIME: the main uncertainty is not due to the method itself, and the overall accuracy of time transfer is characterized by an uncertainty well below 0.5 ns ( $1 \sigma$ ). In terms of the method itself, T2L2 is slightly more accurate than PRARETIME and may be considered as the reference technique. In addition, studies about the calibration of the on-board payload are being carried out, which may show that the tentative estimate of the corresponding uncertainty, which is given in Table 3, is too pessimistic. Unfortunately, however, T2L2 depends on clear weather and on specific laser equipment of a kind not available in many time laboratories.

## CONCLUSIONS

The ExTRAS experiment could provide a time transfer method based on satellite transportation of ultra-stable hydrogen masers. Two-way connections with the satellite are ensured by two techniques, PRARETIME and T2L2, both potentially accurate at a level about 300 ps ( $1 \sigma$ ) and both able to provide satellite clock monitoring and ground clocks synchronization. This could represent a very interesting improvement in the accuracy of time transfer methods when compared to GPS common views, achieved with an uncertainty of order 2 ns ( $1 \sigma$ ) over short distances ( $\leq 1000$  km) and 5 ns ( $1 \sigma$ ) over long distances ( $\geq 5000$  km), and to Two-Way Satellite Time Transfer via geostationary satellite, for which the best accuracy achieved is at present 1.7 ns ( $1 \sigma$ ). This would be of major interest for time metrology, in particular for comparison of future clocks designed for frequency uncertainties of some parts in  $10^{16}$ .

## REFERENCES

- [1] VANIER J., and AUDOIN C., The Quantum Physics of Atomic Frequency Standards, Adam Hilger, 1989.
- [2] DEMIDOV N.A., EZHOV E.M., SAKHAROV B.A., ULJANOV B.A., BAUCH A., and FISHER B., Proc. 6th EFTF, p 409, 1992.
- [3] VESSOT R.F.C., MATTISON E.M., NYSTROM G.U., COYLE L.M., DECHER R., FELTHAM S.J., BUSCA G., STARKER S., and LESCHIUTTA S., Proc. 6th EFTF, p 19, 1992.
- [4] ALLAN D.W., IEEE Trans. on Ultr. Ferr. and Freq. Cont., 34, 6, p 647, 1987
- [5] SCHÄFER W., and WILMES H., Workshop on Advances in Satellite Radio Tracking, 1986, Austin, Texas, USA.
- [6] SCHÄFER W., Proc. 6th EFTF, p 41, 1992.
- [7] HARTL P., SCHÄFER W., CONRAD M., REIGBER C., FLECHTNER F., HÄRTING A., and FÖRSTE C., Workshop on Navigation Satellite Systems, 1994, ESOC, Darmstadt, Germany, 1994.
- [8] PETIT G., and WOLF P., Astronomy and Astrophysics, 286, p 971, 1994.
- [9] GAIGNEBET J., HATAT J.L., MANGIN J.F., TORRE J.M., KLEPCZYNSKI W., MCCUBBIN L., WIANT J., and RICKLEFS R., Proc. 25th PTTI, p 367,1993.
- [10] LEWANDOWSKI W., PETIT G., BAUMONT F., FRIDELANCE P., GAIGNEBET J., GRUDLER P., VEILLET C., WIANT J., and KLEPCZYNSKI W.J, Proc. 25th PTTI, p 357,1993.

Table 2: Anticipated uncertainty budgets for satellite clock monitoring and ground clock synchronization through ExTRAS via PRARETIME. All uncertainties are in picoseconds and correspond to a 1 sigma statistical analysis. No uncertainties on time comparison arise from range estimation.

Uncertainty source	Satellite clock monitoring	Ground clocks synchronization
Range	0	0
Hydrogen maser	0	50
Atmospheric delay	20	$20\sqrt{2}$
On-board payload	50	20
Earth station	50	$50\sqrt{2}$
Modems & counters	50	$50\sqrt{2}$
Method accuracy	89	117
Ground link to 1 pps	300	$300\sqrt{2}$
Total accuracy	313	440

Table 3: Anticipated uncertainty budgets for satellite clock monitoring and ground clocks synchronization through ExTRAS via T2L2. All uncertainties are in picoseconds and correspond to a 1 sigma statistical analysis. No uncertainties on time comparison arise from range estimation and atmospheric delays.

Uncertainty source	Satellite clock monitoring	Ground clocks synchronization
Range	0	0
Hydrogen maser	0	50
Atmospheric delay	0	0
On-board payload	50	20
Earth station	50	$50\sqrt{2}$
Counters	10	$10\sqrt{2}$
Method accuracy	71	90
Ground link to 1 pps	300	$300\sqrt{2}$
Total accuracy	308	434

## QUESTIONS AND ANSWERS

**SIGFRIDO M. LESCHIUTTA:** I was saying that we shall aim to the 10 ps resolution. So, this experiment is aiming to 300 ps.

**CLAUDINE THOMAS (BIPM):** Maybe I must add that funding is not yet voted for this experiment. So, I'm not so sure it will happen, but let's hope.



52584

## PTTI Applications at the Limits of GPS P. 11

R.J. Douglas  
Time and Frequency Standards Group  
Institute for National Measurement Standards  
National Research Council of Canada  
Ottawa, Canada K1A 0R6  
(613) 993-5186, Fax (613) 952-1394

J. Popelar  
Geodetic Survey Division  
Geomatics Canada  
Department of Natural Resources  
615 Booth Street  
Ottawa, Canada K1A 0E9  
(613) 943-2354, Fax (613) 995-3215

## Abstract

*Canadian plans for precise time and time interval services are examined in the light of GPS capabilities developed for geodesy. We present our experience in establishing and operating a geodetic type GPS station in a time laboratory setting, and show sub-nanosecond residuals for time transfer between geodetic sites.*

*We present our approach to establishing realistic standard uncertainties for short-term frequency calibration services over time intervals of hours, and for longer-term frequency dissemination at better than the  $10^{-15}$  level of accuracy.*

The state-of-the-art for applying GPS signals to geodesy is more advanced in some ways than is the common practice by national time and frequency laboratories for applying GPS signals to PTTI work. The Geodetic Survey of Canada's positioning capabilities have benefitted greatly from the application of GPS techniques [1], which include GPS Inferred Positioning System (GIPSY) software developed at the Jet Propulsion Laboratory, with a capability for sub-nanosecond clock synchronization [2], [3]. Currently, GPS techniques for time transfer between national time laboratories have not exploited the more advanced global geodetic capabilities.

In national time laboratories, common practice has been to use single-channel C/A code receivers in the common-view mode where 13 minute tracks (about 40 per day) are taken on its regional tracking schedule. The tracking schedule is issued for each region by the International Bureau of Weights and Measures (BIPM), and with a delay of several weeks the common-view differences are post-processed (with the measured ionospheric corrections, when available) using the precise ephemerides determined for geodesy. One major refinement to this process is possible by using

GPS receivers which can make comparisons with the GPS carrier phase, and use this information for interlaboratory frequency comparisons. Geodetic receivers can do this, producing significantly higher precision measurements than the usual timing receivers. Geodetic receiver networks also track signals simultaneously from multiple satellites (up to 8) to obtain 10-20 times more data from each station than is specified in the BIPM tracking schedule. Geodetic receivers track C/A code, carrier phase, and P code on the L1 and L2 frequencies (when Anti-Spoofing, or AS, is off and the P code is transmitted), measuring them all with respect to the receiver clock, locked to the station's frequency reference. Ionospheric corrections are measured for all satellite tracks from the difference in arrival time of the L1 and L2 signals, determined from L1 and L2 P-code measurements (AS off) or from cross-correlation of the L1 and L2 signals (AS on). Tropospheric corrections are also modelled for each station [2]. Daily satellite orbit solutions, based on these observations from around the globe, determine the space coordinates of the GPS receivers at the level of about 3 cm or 100 ps; and benefit from station frequency references derived from modern masers.

Despite remarkably good time residuals of well under a nanosecond [2], [3] reported using these techniques, they have not yet been widely embraced by national time laboratories. Subnanosecond timing precision might lead to improved short-term accuracy of interlaboratory frequency comparisons and facilitate the use of the next generation of primary frequency standards. Benefits would also accrue for remote frequency calibrations of hydrogen masers (particularly free-running hydrogen masers), or frequency calibrations of compact hydrogen masers, or calibrations of cryogenic superconducting and/or dielectric frequency standards, or perhaps even providing short-term calibration commensurate with the  $10^{-13}$  1000s-stability of the best crystal oscillators [5].

In Canada, the geodetic spatial reference system is the responsibility of the Geodetic Survey Division (GSD) of the Federal Government's Department of Natural Resources (NR Can), and the time reference is the responsibility of the Time and Frequency Standards Group of the National Research Council of Canada (NRC). The two organizations have begun preliminary work on evaluating the possibilities and benefits of collaboration. This paper will focus on the precise time and time interval aspects, and possible PTTI applications.

## **The Global Geodetic GPS Network**

The International Association of Geodesy formally established the International GPS Service for Geodynamics (IGS) in 1993. It started operations in 1994, with over 40 participating agencies from more than 20 countries. Over 50 continuously operating stations are now collecting and exchanging data (mostly using Rogue GPS receivers), with many more planned. Of these stations, some use a hydrogen maser frequency reference; and of these some take part in VLBI observations for geodesy and time transfer. The IGS data are archived in three Global Data Centres, and analyzed by seven Analysis Centres which forward their results to the Global Data Centres for archiving and on-line access.

The Geodetic Survey of Canada operates one of these Analysis Centres, and the data analyses reported here are drawn from their routine processing [1]. The daily routine analysis is based on the data from about 24 globally distributed GPS tracking stations (Figure 1). The data from each station, sampled at 30 s intervals, are validated to monitor the receiver clock and tracking including

cycle slip detection), code multipath and ionospheric activity levels, and to compute differential satellite range corrections. One GPS receiver with a hydrogen maser frequency reference is used as a master reference clock, and other stations' clocks are reported with respect to this master clock. GIPSY II software uses carrier phase and pseudo-range measurements to generate, from each day's data, precise GPS satellite ephemerides, satellite and station clock corrections, Earth orientation parameters (EOP), station coordinate corrections and satellite orbit predictions for the next 24 hour period. The full solutions are then used for geodetic positioning, and for the station clock intercomparisons.

GSD processes each day's data independently, without overlaps (unlike other Analysis Centres), using the previous day's predictions as only the initial estimates for satellite orbits. Comparisons of the precise orbits from different Analysis Centres show RMS differences of around 20 cm [4]. Station residuals, on 7.5 min observations, show RMS deviations typically under 1 m for range, 1 cm for phase and less than 300 ps between the receiver clocks of two stations with hydrogen maser frequency standards. The repeatability of the daily averages for the station coordinates is typically 1 to 2 cm. GSD uses AS range bias modelling which shows station and satellite dependences.

The small variations in mean space coordinates mainly reflect *differentials* in reception time, and it cannot be expected that the time coordinate would be as stable on average, since common-mode delays which affect all satellites (and which can largely cancel for the space coordinates) will be included with the station clock in the solutions. The time variances of systematic errors in tropospheric delay variations, uncorrected ionospheric delay variations, multipath pulling systematics, temperature related variations of delay in antennas, cables and receivers; variations in receiver timing due to amplitude variation of the 5 MHz reference, or the 5 MHz reference's cable delay variation all add to the variances of the two station clocks (particularly small for masers) filtered by the whole adjustment process, and warrant careful study at better than the 300 ps level of precision exhibited by the station clock residuals.

Another concern might be that the clock residuals could be deceptively low: that the fitting process is so optimized that the effective bandwidth for clock variations is smaller than we believe. However, in the work presented here, the effective bandwidth of the solutions every 7.5 minutes allows for white phase noise on the receiver clocks of up to 1 ms. This allows the solution to cope with receiver clock resets. The station clock solutions are normally more than  $10^7$  times smoother than this, and show Allan deviations at 7.5 minutes as small as  $3.7 \times 10^{-14}$ . The broad bandwidth for the station clocks is confirmed in that known clock anomalies are quickly reproduced in time intercomparisons by this method. Independent clock and baseline comparisons between several IGS stations are made by VLBI, and are reassuring [2], [3]. Other independent techniques such as two-way time transfer for time synchronization and frequency calibration will also be used for comparison. Techniques for measuring systematic time delay effects, and where possible correcting their causes, are also planned.

## GPS Station at NRC

For the GPS station at NRC, both ground level and rooftop antenna locations were evaluated for multipath and radio interference, and the convenient rooftop location was found more suitable.

The ground level site (the two-way time transfer antenna compound) would also require continuous monitoring of the loop delay ( $1.2\mu\text{s}$ ). Three matched triax lines and three matched coax lines were installed, cut to minimize phase perturbations (length a multiple of  $\lambda/4$  or 50 ns) for the 5 MHz reference from the maser distribution amplifiers. The three lines permit individual cable delays to be determined. Two Turborogue SNR-8000 receivers were installed to provide redundancy and a capability for evaluating possible systematic effects. For the results presented here, one antenna fed both receivers through a microwave splitter. When the receivers are fed from the same maser, this zero baseline setup shows periods when the clock solution differences are well under 50 ps, although occasional day-to-day variations of 100 ps have been observed. To monitor the receivers clocks and to recover absolute timing, the 1 pps outputs of the two receivers are measured each hour with respect to a 1 pps derived from the maser.

The receivers' 5 MHz frequency reference is supplied by the NRC-built hydrogen maser H4, a low-flux maser with a fluoroplast F-10 coated bulb, operated with cavity autotuning. Its average drift rate is less than  $3 \times 10^{-17}$  per day. The rest of the NRC ensemble consists of two other masers, three NRC-built high-stability primary cesium clocks ( $\sigma_y(\tau) \leq \times 10^{-12}/\tau^{1/2}$  out to  $\tau = 10^5$  seconds) and two commercial cesium clocks (HP5071A). The other masers are H3: similar to H4, but with a FEP-120 Teflon bulb coating, and an average drift rate of  $3 \times 10^{-16}$  per day, and H1: a free-running NRC-built maser which has been operating since 1967. High-resolution (0.2 ps) phase measurements between clocks of the ensemble are used in an algorithm for generating the ensemble time scale, optimized for stability over several days. The stabilities of all the ensemble clocks are monitored routinely. The Allan deviation attributed to H4 is typically less than  $2 \times 10^{-15}$  over periods of 1-10 days. Thus time transfer, between NRC and other laboratories with similar masers, could reliably measure time transfer instability of a few hundred ps over 24 hours or less; but for investigating the longer term stability limit of GPS time transfer, even the best masers' stability will not suffice and comparisons with other techniques such as two-way time transfer will have to be employed.

## Operational Experience

The long-term behaviour of the two Turborogue receivers over the past year has given excellent time residuals, as will be shown below. They have been integrated into the NRC time laboratory operations with only minor problems. The receiver 1 pps outputs have exhibited two types reset, which are somewhat inconvenient. The most common is the receiver software reset, where the receiver software resets its time by  $n$  cycles of the analog-to-digital converter clock (48.885 ns at the 20.456 MHz ADC clock frequency) - often by several microseconds - without affecting the coherence of the 5 MHz to 20.456 MHz synthesis. These 1 pps resets present a processing problem only, and when resolved do not affect the precise time and frequency intercomparisons. The rarer type of power-down reset does affect the coherence of the ADC clock synthesis, altering the state of the receiver's synthesizer with respect to the station's 1 PPS. Thus resets after a receiver lock-up (e.g. lightning strike), or after cabling changes or following operator "finger trouble" need to be measured carefully, with respect to the time laboratory's UTC(k). Neither type of reset presents any technical difficulty for a time laboratory, where differences between 1 pps signals are measured and logged automatically.

The receiver GPS data sampling rate is 30 s (C/A pseudorange, C/A phase, and P2-P1 differential delay, by cross-correlation with AS, or P1 and P2 pseudo-ranges and phases with AS off), and the data is extracted regularly by GSD. GPS data from about 24 IGS sites were used in GIPSY II processing of each 24 hour period, to determine precise GPS ephemerides, Earth orientation parameters and daily station mean coordinates. Station coordinate solutions provide daily mean positions in the ITRF (ITRF92). The daily solutions also provide, in 7.5 minute intervals, receiver clock differences with respect to the reference station, and each station's tropospheric corrections. The receiver clock differences are evaluated allowing for a wide bandwidth white phase noise of 1 ms, and have no further smoothing. No data overlap is used from one day to the next, except that the initial orbit estimates are extrapolated from the precise ephemerides of the previous day's solution. The independence of each day's solution, and its clock intercomparisons, can be used to simplify our preliminary analysis of the frequency stability of this powerful method of clock intercomparisons.

## Stability

Operationally, geodesy can tolerate occasional receiver clock resets (of the two kinds discussed above) as well as receiver clock variations in frequency which are undesirable for PTTI stability analysis. For our initial stability analyses, we select periods (of up to several weeks) that are largely free from the unmistakable signatures of these perturbations, and apply the classical techniques of stability analysis. There are other good techniques for examining the stability of the clock difference solutions, such as observing the time residuals on closure checks from solutions over different groups of stations [2] - but we prefer the standard method for quantifying and presenting the method's stability for frequency transfer.

Figures 2 through 6 show receiver clock differences between maser-equipped stations for 20 consecutive daily global solutions, starting at 1994-10-25 00:00 UTC. Figure 2 shows the clock difference for this period along the shortest baseline (200 km), between the NRC time laboratory in Ottawa and the Algonquin Park observatory. In Figure 2, the rapid change in frequency at the end of day 4, of  $23 \times 10^{-14}$ , is associated with a large temperature excursion in the Algonquin maser room, which was fixed on day 7. The rapid response of the solution is noteworthy, and confirms the broad bandwidth allowed by the solution.

Figure 3 shows the maser comparisons between NRC and Goldstone (CA). Figure 4 shows the maser comparisons between NRC and Madrid (Spain). These are long baselines ( $4 \times 10^3$  and  $6 \times 10^3$  km), but the stations still have common view satellites in the global solutions. In Figure 5 is plotted a maser intercomparison with a longer baseline ( $1.7 \times 10^4$  km) between NRC and Tidbinbilla (Australia) which have no common view satellites. Figure 6 shows an intermediate case ( $10^4$  km), the difference between the Figures 3 and 4, a comparison between Goldstone and Madrid.

The performance is strikingly good. The daily solutions are not forced to smooth day-to-day maser comparisons, and have to re-solve for the carrier phases from one day to the next. Nonetheless on many days only small discontinuities can be seen between solutions. The largest discontinuities are for the end of days 16 and 18, and are clearly associated with the NRC station bias. Within each day's solution, the maser comparisons are even more stable. For the smoothest comparison,

Figure 3, the Allan deviation  $\sigma_y(\tau = 450s)$  is  $1.9 \times 10^{-13}$ , and  $3.7 \times 10^{-14}$  if the effects of the discontinuities are removed from the analysis. Clearly the effects of systematic uncertainties will be more important for real applications than this level of the solutions' stability. One example of such systematics can be seen in Figure 4, where there is a  $\pm 10^{-13}$  short-term frequency variation.

Earlier Algonquin to NRC comparisons are shown in greater detail in Figure 7. The magnitude of the time discontinuities between daily solutions are emphasized in the Figure, and can be used to determine the RMS residual of the clock comparisons at each 00:00 UTC. In the absence of any uncertainty in the solutions, one day's solution should extrapolate (forward in time) to the same clock difference as the next day's solution (extrapolated backwards in time). Since the daily solutions are independent, the time offset in the solutions should average to  $\sqrt{2}$  times the residual. Thus the end-point residual can be determined from the RMS average time offset (divided by  $\sqrt{2}$ ). The estimate does not include the full long-term effects of time-dependent variation of the satellite orbits, the station equipment and the atmosphere, which must be accounted for in any estimate of the frequency-transfer stability, however it does account for these effects acting on successive daily solutions, including the redetermination of the carrier phases. Figure 8 shows a histogram of the time discontinuities between NRC's maser and masers at five other stations (Algonquin, Yellowknife, Goldstone, Madrid and Tidbinbilla) for the 20 day period shown in Figures 2-6. The RMS residual is 880 ps, but appears to have outliers from a central peak, which has an RMS of 310 ps.

The zenith tropospheric correction solutions, which are smoothed for each site with a  $33 \text{ ps}/\sqrt{\text{hour}}$  random-walk, for this 20-day period show an Allan deviation of  $\sigma_y(\tau = 1\text{day}) = 1.2 \times 10^{-15}$  for the NRC-Algonquin link and up to twice this for the longer baselines. For the results presented here, these small corrections have been applied; for other methods it presents useful insight into one term in the time transfer error budget.

The independence of each day's processing can also be used to determine an Allan deviation from each day's average frequency:  $(2M - 1)^{-1} \sum_{i=1}^M (Y_{i+1} - Y_i)^2$ . The results of this Allan deviation, comparing the NRC maser to remote clocks via the geodetic network's clock solution clearly shows clock noise for some stations: For St. John's (Newfoundland), using a Rb clock,  $\sigma_y(\tau = 1\text{day}) = 7.7 \times 10^{-13}$ ; for Penticton (BC), using a cesium clock,  $\sigma_y(\tau = 1\text{day}) = 3.6 \times 10^{-14}$ ; for Algonquin, using a maser with a misbehaving maser room thermostat,  $\sigma_y(\tau = 1\text{day}) = 3.8 \times 10^{-14}$ ; for the remaining four stations equipped with masers, at Yellowknife  $\sigma_y(\tau = 1\text{day}) = 1.1 \times 10^{-14}$ ; at Tidbinbilla  $\sigma_y(\tau = 1\text{day}) = 7.0 \times 10^{-15}$ ; at Madrid  $\sigma_y(\tau = 1\text{day}) = 5.0 \times 10^{-15}$  and at Goldstone  $\sigma_y(\tau = 1\text{day}) = 4.9 \times 10^{-15}$ .

These results are quite encouraging, but further work is required to study possible systematic time and frequency biases present. The short-term stability of frequency transfer also warrants further study. The results shown in the NRC-Madrid comparison (bottom graph in Figure 3) show a residual double-hump structure, within each day's solution, which is not likely due to the intrinsic behaviour of the Madrid maser and could be associated with GPS satellite constellation geometry. Clearly this behaviour could generate biases on hour-long frequency calibrations by GPS which could be up to  $\pm 10^{-13}$ . The long-term statistics of the comparisons, including the time offsets between daily solutions, need to be considered and compared with other high-accuracy methods such as two-way time transfer. Post-processed frequency and time dissemination within Canada will benefit if these questions can be addressed for periods of  $10^3$  to  $10^4$  seconds. One can imagine

calibration services that provide traceable frequency calibrations for crystal oscillators at accuracy levels of  $10^{-12}$  and better. If the longer term accuracy (for time intervals longer than one day) can also be established, the GPS geodetic-style time transfer might be helpful in comparing the next generation of high-accuracy frequency standards [6], particularly on baselines where two-way time transfer is more difficult. To establish the random component of the standard uncertainty associated with this type of frequency transfer, we would like to apply the techniques we have developed for standard power-law noise models [6]. These techniques can be applied to the continuous clock solutions within the day, but require further development to be applied for longer time periods. The frequency transfer capabilities of operational GPS systems, developed for geodesy, appears to be a strong candidate both for interlaboratory frequency comparisons and for frequency dissemination applications.

## Acknowledgements

The authors would like to thank particularly J. Kouba and P. Tétreault for their major contributions in improving the GIPSY clock solutions; D. Hutchison for establishing the appropriate data base, and the Canadian Active Control System (CACs) operating team which is responsible for the CGS daily acquisition and processing. The world-wide collaboration organized by the IGS is essential for providing the data for the PTTI applications presented here.

## References

- [1] J. Kouba, P. Tétreault, R. Ferland and F. Lahaye, *IGS Data Processing at the EMR Master Control System Center*, **Proceedings of the 1993 IGS Workshop**, Edited by G Beutler and E. Brockmann, International GPS Service for Geodynamics (IGS), University of Berne, pp. 123-132 (1993).
- [2] C.E. Dunn, S.M. Lichten, D.C. Jefferson and J.S. Border, *Sub-nanosecond Clock Synchronization and Precision Deep Space Tracking*, **Proc. 23rd Annual PTTI Applications and Planning Meeting**, pp. 89-99 (1991).
- [3] C.E. Dunn, D.C. Jefferson, S.M. Lichten, J.B. Thomas, Y. Vigue and L.E. Young *Time and Position Accuracy Using Codeless GPS*, **Proc. 25th Annual PTTI Applications and Planning Meeting**, pp. 169-179 (1993).
- [4] G. Beutler, J. Kouba and T. Springer, *Combining the Orbits of the IGS Processing Centres*, *Bull. Geodesic* in press, (1994).
- [5] J.R. Norton, *Performance of Ultrastable Quartz Oscillators using BVA Resonators* **Proc. 8th European Time Forum** pp. 457-465 (1994).
- [6] D. Morris, R.J. Douglas and J.-S. Boulanger, **The Role of the Hydrogen Maser Frequency transfer from Cesium Fountains**, *Japanese Journal of Applied Physics*, **33**, pp. 1659-1668 (1993).

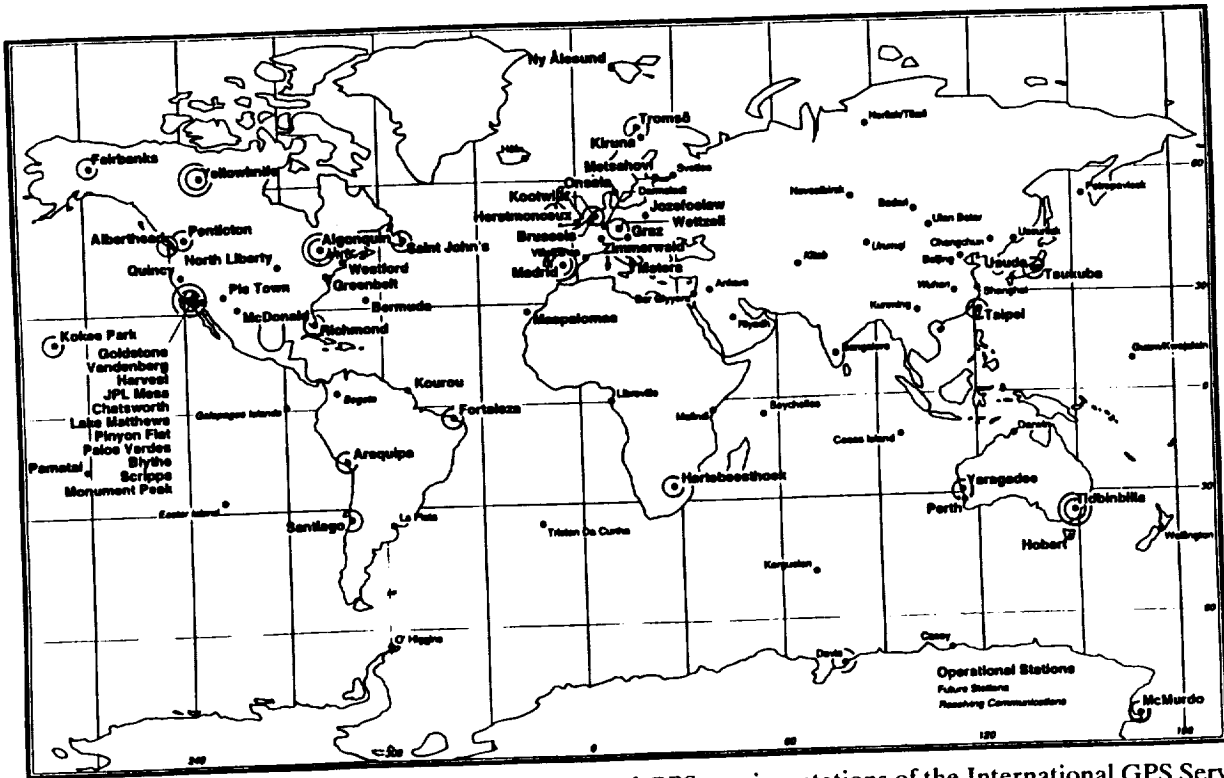


Figure 1. Map showing locations of existing and planned GPS receiver stations of the International GPS Service for Geodynamics. Stations mentioned in the text have double circles. The global GPS solutions whose timing results are described in the text, use up to 24 stations - such as the set shown circled here.

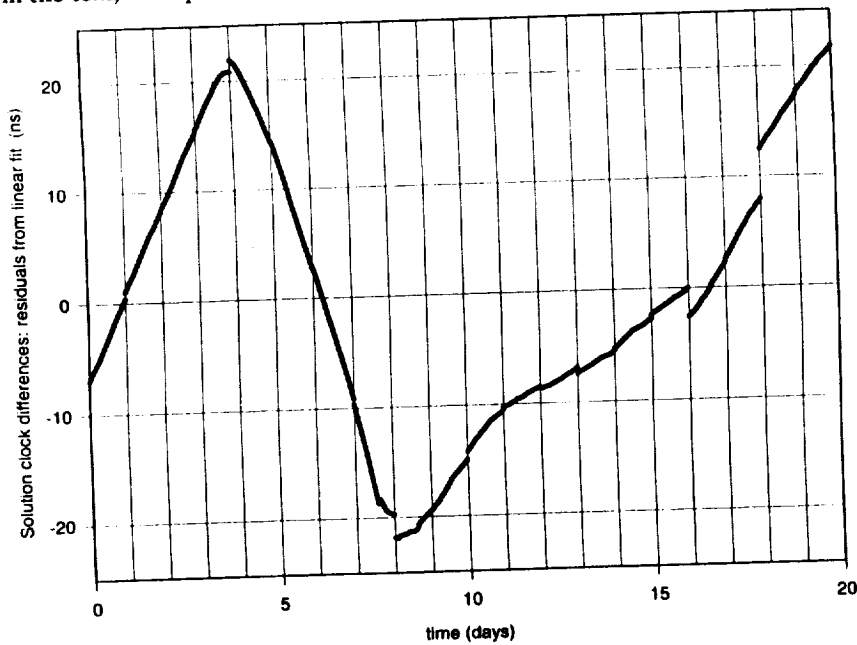
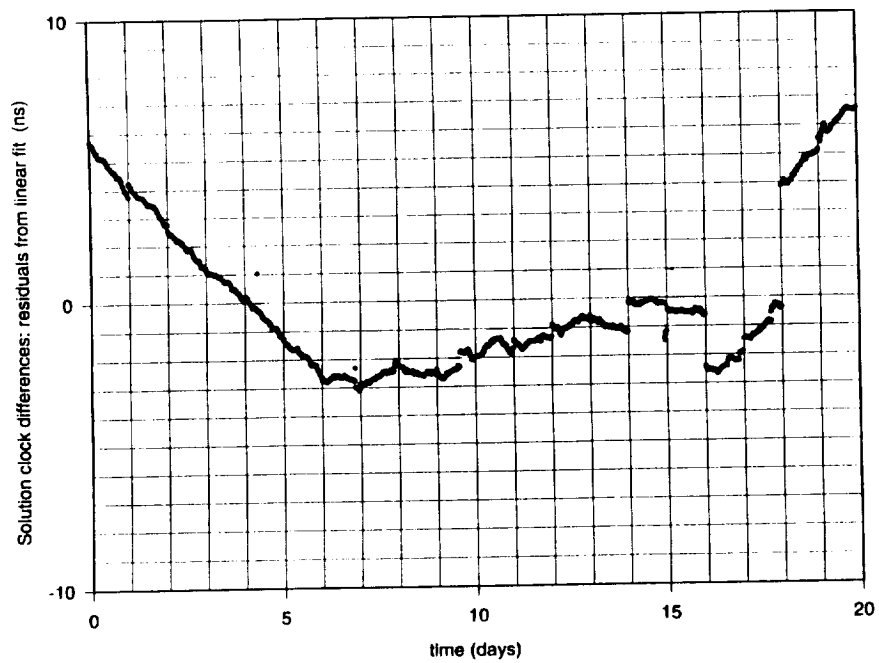
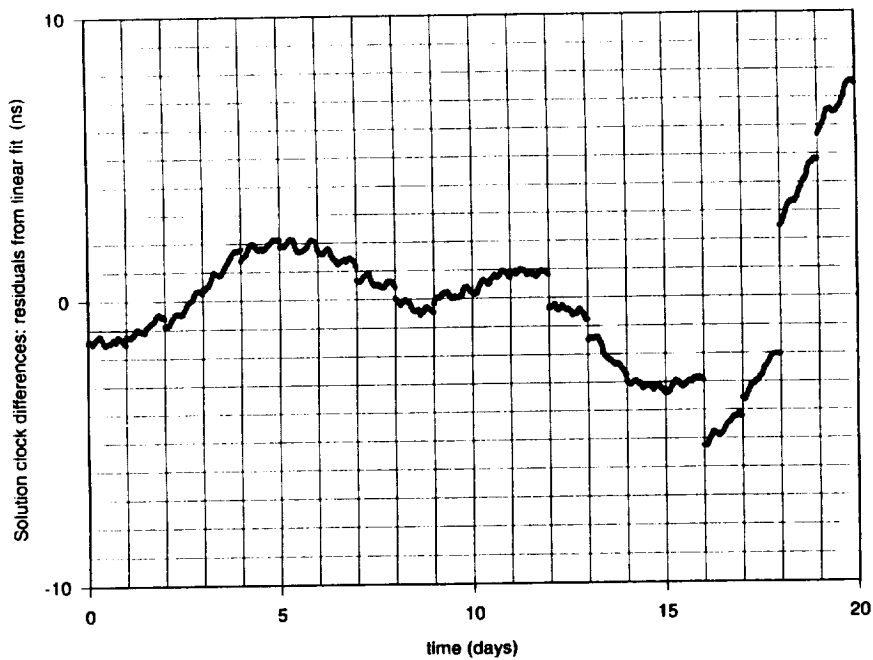


Figure 2. Maser clock differences between Algonquin and NRC (200 km baseline), obtained from the global GPS solution. Each day is treated independently.

ORIGINAL PAGE IS  
OF POOR QUALITY



**Figure 3.** Maser clock differences between Goldstone and NRC, obtained from the global GPS solution. Some direct common view satellites exist for this  $4 \times 10^3$  km baseline.



**Figure 4.** Maser clock differences between Madrid and NRC, obtained from the global GPS solution. Some direct common view satellites exist for this  $6 \times 10^3$  km baseline.

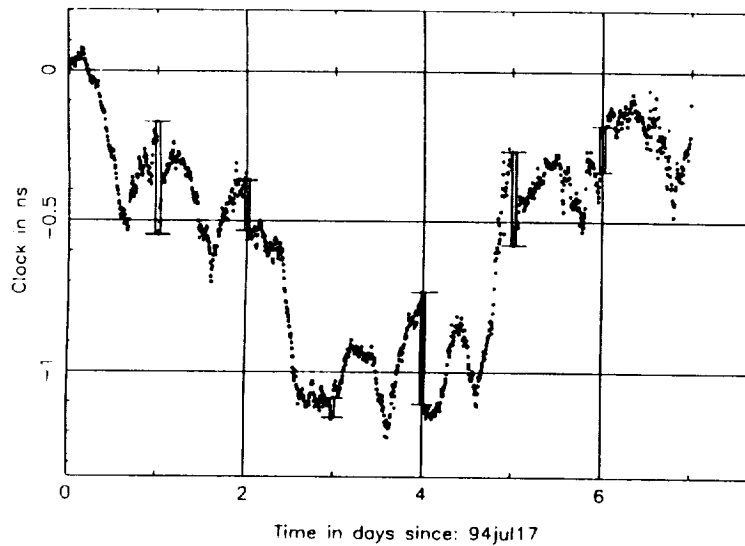


**Figure 7.** Daily global GPS solutions showing the Algonquin - NRC maser clock differences, with the discontinuities emphasized by the “bars” at 00:00 each day.

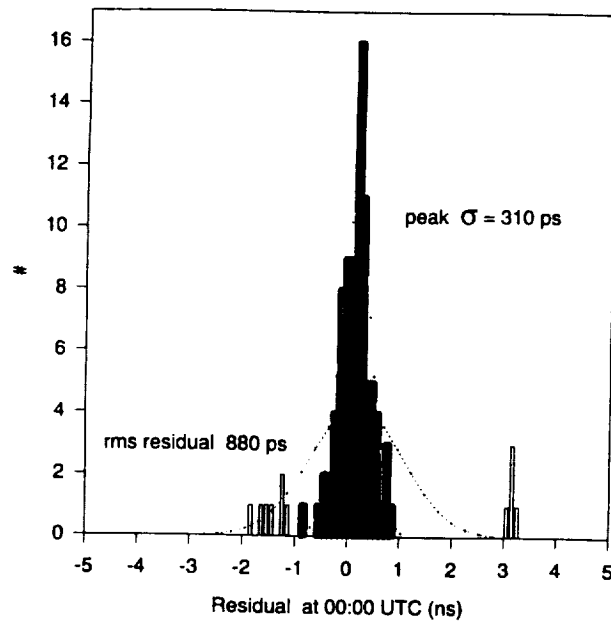


**Figure 8.** Histogram of daily solution discontinuities for the 20 days of Figs.2-6, between NRC and five IGS stations using masers, scaled by  $1/\sqrt{2}$  to reflect the residual at the ends of the daily solutions. The open bars represent values included in the determination of the “rms” value, and excluded from the “peak  $\sigma$ ” value.

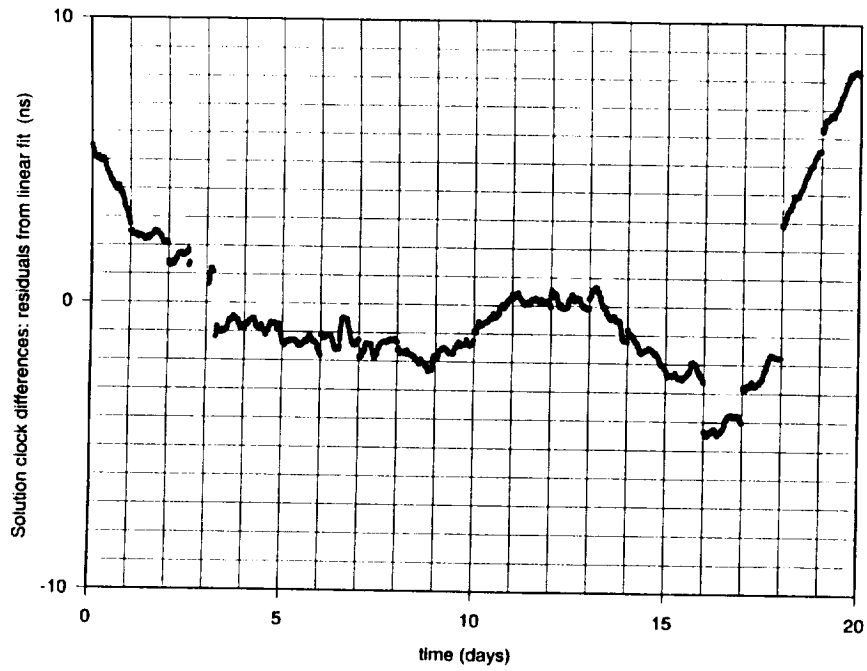


**Figure 5.** Maser clock differences between Tidbinbilla and NRC, from the global GPS solution. No common view satellites exist for this  $1.7 \times 10^4$  km great circle baseline.

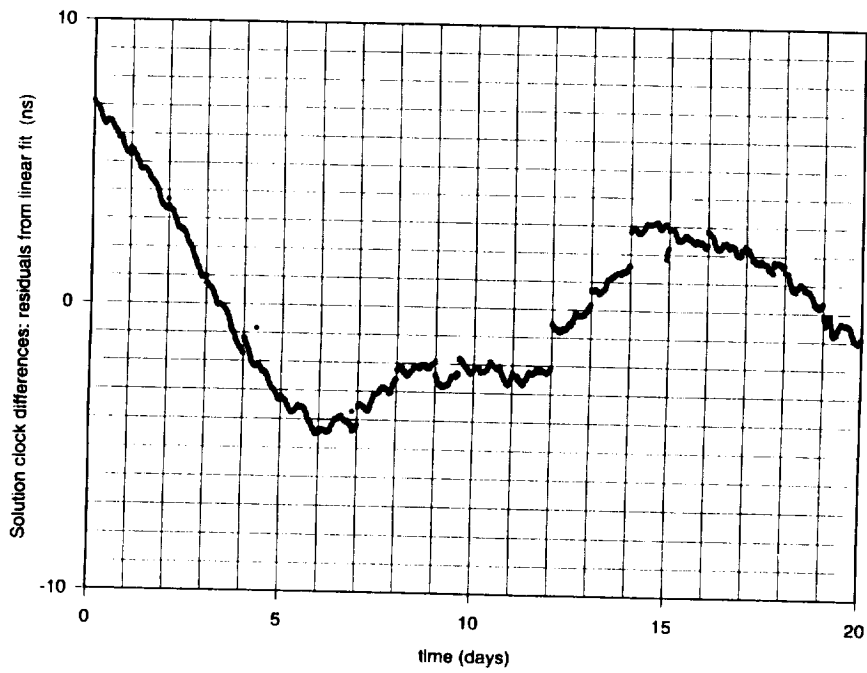


**Figure 6.** Maser clock differences between Madrid and Goldstone, a  $10^4$  km baseline.



153/15  
P. 17

# TIME ASPECTS OF THE EUROPEAN COMPLEMENT TO GPS: CONTINENTAL AND TRANSATLANTIC EXPERIMENTAL PHASES

P. Uhrich, B. Juompan, R. Tourde  
Laboratoire primaire du temps et des fréquences [LPTF]  
Observatoire de Paris, Bureau national de métrologie  
Paris, France

M. Brunet, J-F. Dutrey

Centre national d'études spatiales [CNES]  
Toulouse, France

## Abstract

*The CNES project of a European Complement to GPS [CE-GPS] is conceived to fulfill the needs of Civil Aviation for a non-precise approach phase with GPS as sole navigation means. This generates two missions: a monitoring mission – alarm of failure –, and a navigation mission – generating a GPS-like signal on board the geostationary satellites. The host satellites will be the Inmarsat constellation. The CE-GPS missions lead to some time requirements, mainly the accuracy of GPS time restitution and of monitoring clock synchronization.*

*To demonstrate that the requirements of the CE-GPS could be achieved, including the time aspects, an experiment has been scheduled over the last two years, using a part of the Inmarsat II F-2 payload and specially designed ground stations based on 10 channels GPS receivers. This paper presents a review of the results obtained during the continental phase of the CE-GPS experiment with two stations in France, along with some experimental results obtained during the transatlantic phase (three stations in France, French Guyana, and South Africa). It describes the synchronization of the monitoring clocks using the GPS Common-view or the C- to L-Band transponder of the Inmarsat satellite, with an estimated accuracy better than 10 ns ( $1 \sigma$ ).*

## INTRODUCTION

The 'Centre national d'études spatiales' (CNES, France) is the French Space Agency. The CNES project of a European Complement to GPS (CE-GPS in the following) is dedicated to the needs of the Civil Aviation community to achieve the requirements of a non-precision approach phase with GPS used as sole navigation means. Many functions have to be fulfilled by such a system, for which the time requirements are reaching the state of the art of the techniques used by the Time Metrology community. The whole CE-GPS project started more than four years ago, and the experimental part more than two years ago.

At this point of the CE-GPS project, all experimental stages have been performed, with a great amount of collected data to be processed. The results presented in this paper concern only the time aspects of the experiment, the calibrations of the ground stations and the synchronization of the monitoring clocks during the continental and transatlantic phases. Both Common-view GPS and Two-way time transfer through geostationary satellite have been used, the processing of the data being carried out by the 'Laboratoire primaire du temps et des fréquences' (LPTE, France). The results obtained are compared to the requirements of the CE-GPS project.

## SHORT REMINDER OF THE CE-GPS PROJECT

The concept of the CE-GPS and the experimental system were presented at the EFTF 93<sup>[1]</sup>. The CNES project of a European Complement to GPS is mainly dedicated to the needs of the Civil Aviation community. It can be considered as the first step of a French design for a Global Navigation Satellite System (GNSS). The reference mission adopted by the CNES will:

- achieve the requirements of a non-precision approach phase.
- enable GPS to be used as sole navigation means.

The functions to be fulfilled by such a system are:

- a monitoring mission: alarm of a failure on a GPS satellite within 10 seconds.
- a navigation mission: to increase the GPS availability by eliminating coverage gaps.

Following the proposals of satellite operators, it was agreed that the space segment would be provided by the Inmarsat III geostationary satellites. Because one of the system specifications is to minimize modifications on the existing GPS receivers, the signal transmitted by the geostationary payload shall be similar to a GPS signal. In addition it has to carry specific CE-GPS informations. This and other specifications have many consequences, among which only the time aspects are described in this paper.

To prove the feasibility of such a Complement to GPS, and to help estimating the performances and the limits of an operational system, the CNES has organized an experiment of which main objectives are:

- to confirm the ability of transmitting a GPS-like signal from a geostationary satellite.
- to demonstrate the feasibility of synchronizing with the GPS time a virtual clock on board the geostationary satellite.
- to demonstrate the capability of GPS receivers to process the CE-GPS signal.
- to evaluate the User Equivalent Range Error (UERE) [2] when using the geostationary satellite.
- to synchronize the ground stations following the requirements.

The space segment of the CE-GPS experiment, beside the GPS NAVSTAR constellation, is the Inmarsat II F2 geostationary satellite of which part of a transponder in the payload was made available free of charge to the CNES for the duration of the experiment. The ground segment is made of three specially designed ground stations based on 10 channels navigation GPS receivers, whose development has been entrusted to the IN-SNEC (Caen, France), and of a computer processing station for the collected data located at the CNES space center of Toulouse (France).

The CE-GPS experimentation was divided into three stages: a first stage in May-June 1993, with two stations located at the IN-SNEC (Caen, France) in parallel with the same clock, called the "calibration phase", a second stage from September to November 1993 with one station at the LPTF (Paris, France) and another one at the CNES space center of Toulouse (France), called the "continental phase"; a third stage from May to June 1994, with three stations located at the CNES space centers of Toulouse (France), Kourou (French Guiana) and Hartebeeshoek (South Africa), called the "transatlantic phase". The acronyms used for these three stations are TLS, KRU, and HBK, with obvious meanings.

## TIME ASPECTS OF THE CE-GPS

The time requirements concerning the navigation mission to be fulfilled by the system are the synchronization with respect to GPS satellites. The standard deviation of the time difference between an event issued from the geostationary payload and an equivalent event issued from any GPS satellite should be less or equal to 120 ns with Selective Availability (S.A.) on [2]. With S.A. off, these requirements drop to 20 ns. Concerning the monitoring mission, the time requirements deal with the relative synchronization of the monitoring clocks, which should be within 10 ns (1 s) in accuracy if they are in view of the same geostationary satellite, or within 15 ns (1 s) if not.

The description of the system architecture, of the ground stations, and the discussion about time and frequency servo-control techniques, or orbitography aspects, have been made elsewhere [1,3]. Only the experimental set-up and some of the calibration results are presented here. The method for restituting the GPS time following the requirements, based on the statistical behaviour of the S.A. noise, is described in a paper presented at the EFTF 94 [4], along with some experimental results obtained with a four-channel time dedicated GPS receiver: over an averaging period of 2 h 24 min, and with the simultaneous use of the four channels, it has been demonstrated that the GPS time could be restituted on the ground with an accuracy of 14 ns (1 s). A possible method for achieving a clock synchronization is to use the results of the GPS time restitution separately calculated in remote stations [1,4].

The time aspects of the CE-GPS presented in this paper are the synchronization of the ground stations clocks, either by GPS Common-view or by Two-way satellite time transfer (TWSTT) through the geostationary payload. The well known method for the synchronization of remote atomic clocks is the GPS Common-View technique [5]. Because GPS time dedicated receivers are included in the CE-GPS ground stations, it was decided to use the Common-View technique with the BIPM schedule as the reference for clock synchronization, provided that a calibration of the remote receivers is done, and that atmospheric measurements are made available. Until

now, TWSTT was performed using Eutelsat or Intelsat telecommunication system, or domestic satellites. When using MITREX Modems over short bases ( 800 km), an accuracy of 1.7 ns (1 s) has been estimated, and directly compared to the equivalent GPS Common-view results [6]. It was proposed to use the Inmarsat C- to L-Band transponder, and the spare C/A GPS gold pn-codes [1,2].

## EXPERIMENTAL SET-UP

The description of the ground stations will be limited to the basic equipments involved and to the items and techniques related to the results presented in this paper. The complete presentation of the stations of the CE-GPS experiment can be found elsewhere [1].

Inmarsat II F2 is located -15.5 E. The Sagnac effect for all links is easy to determine with an uncertainty within 0.01 ns (1 s). All stations are identical in terms of a spatial link:

Antenna diameter C-Band: 0.6 m  
Uplink frequency: 6428.475 MHz (C-Band)  
Uplink S/C G/T: -14 dB/K  
Antenna diameter L-Band: 1.2 m  
Downlink frequency: 1533.475 MHz (L-Band)  
Downlink on axis G/T: 1.3 dB/K  
Maximum EIRP: 39.8 dBW

At the start of the experiment, no data were available concerning TWSTT performances when using an Inmarsat transponder, C/A gold codes, and GPS receivers as Modem. The basic sampling period of the data inside these GPS receivers is 0.6 s. It was decided to schedule four sessions per day, each lasting 15 min, to allow statistical analysis on a sufficient amount of data, and to detect any influence of atmospheric parameters on the performances. The sessions took place at 1:15, 7:15, 13:15, and 19:15 TU.

Inside each ground station (figure 1) are implemented two SERCEL NR106, which are ten-channel GPS navigation receivers. They are related, thanks to the switcher 1, either to a common GPS antenna (L1 carrier), or to the receiving antenna of the Inmarsat signal (L-Band) converted to L1 before the switcher. The GPS antenna is also connected to a GPS receiver SERCEL NRT2, which is a 4 channels time dedicated receiver. The NRT2 is directly supplied with the 1pps output of the Cesium clock of the station. This is the classical set-up for the GPS Common-view technique.

Because the navigation receivers NR106 have no input for dating external events, like the 1 pps from the Cesium clock, it was necessary to build up a so-called 'GPS signals generator', which has two functions. It generates a sequence of C/A code synchronized with the 1 pps output of the clock, which modulates a L1 carrier in order to be dated by the internal counter of both NR106. This signal is denoted '1 pps L1-C/A'. The C/A code chosen for this internal link for all CE-GPS stations is numbered 33: it is a spare for the operational GPS, not to be used until further notice. For referring any external signal to the Cesium clock of the station, the dating of this internal 1 pps L1-C/A signal has to be done simultaneously with the dating of the external signal. The other function of this 'generator' is to output the servo-controlled signal related to

the 1 pps of the clock to the transmitting antenna towards Inmarsat (C-Band carrier). This is similar to the transmitting part of a Modem used for the TWSTT, like MITREX for instance. The equivalent to the receiving part of a classical TWSTT Modem are the NR106 receivers.

There are opportunities for test links, short loop, and changes of the role of each NR106 receiver. There are other possible station configurations to be considered [1], but for the time aspects of the CE-GPS, a stable configuration was chosen for the whole period of data collection. The Cesium clocks monitoring the CE-GPS stations were a HP 5071 A option 1 at the LPTF, a HP 5061 A option 4 at TLS and KRU, and an Oscilloquartz at HBK. All types have proven to remain stable enough to evaluate properly the performances of the CE-GPS stations.

Either the GPS or the C- to L-Band radiowave techniques need estimations of the atmospheric delays. Models for tropospheric delays are working reasonably well at the nanosecond level. For ionospheric delays, ionospheric calibrators are needed. Ten channels codeless receivers (not on figure 1) were used at all CE-GPS stations for measuring the ionospheric delays on the GPS satellites signals. A polynomial mapping method was scheduled to be used to determine the ionospheric delays in the direction of the Inmarsat geostationary satellite. But many problems occurred during the running of the ionospheric calibrators. Considering the small distance between both stations involved in the continental phase ( 800 km), it was decided to use the STANAG results as the ionospheric delays in the direction of GPS satellites, and a Bent model for the C- and L-Band ionospheric delays in the direction of the Inmarsat satellite. Because the lines of sight of the Inmarsat satellite from both TLS and LPTF stations were very close, the difference of the C-Band ionospheric delays was negligible at the nanosecond level.

For the transatlantic phase, because the ionospheric calibrators have worked well only part of the time, the LPTF proposed to compute the ionospheric delays as following:

- for each 15 s sampled measurements in the direction of GPS satellites, a VTEC (vertical total electronic content) is calculated.
- a mean value of these VTECs is estimated, and projected in the direction of the geostationary satellite.
- for each TWSTT 15 min session, a mean value of the ionospheric delays is computed.
- during the whole periods where TWSTT measurements have been made continuously an average value of the ionospheric delays in the direction of the geostationary satellite is computed, separately for the 4 daily sessions. Three periods of 5 to 7 days duration, where the CE-GPS stations have worked continuously, have been identified during the transatlantic phase of the experiment.

It was proposed to consider as an uncertainty on these values the highest standard deviation of the computed average values, which was 5.1 ns (1 s). This is of course not a state of the art value. It was also proposed to try to use some IGS ( International GPS Service for geodynamics) post-processed data, but the results are not available yet.

## CALIBRATIONS

All internal delays of the ground stations were either measured (cables) or estimated (electronic components) following the manufacturers data sheets with a good uncertainty. A short loop performed during the calibration stage of the experiment, along with TWSTT sessions with both stations connected to the same clock, have shown that the measured differential delays were in good agreement with the estimated values, given the estimated global uncertainty. One of the critical issues is the calibration of the 'GPS signal generators'. Examining the synchronization equations, it appears that the 1 pps signal group delay through each generator must be monitored. Frequent calibration sessions were scheduled in all stations during the whole experiment. A calibration consists roughly in measuring the time delay between the arrivals into the NRT2 of two homologous 1 pps signals: a direct 1 pps signal from the Cesium clock and the 1 pps L1-C/A signal supplied through the generator output. This procedure was possible because the NRT2 have proven to remain quite stable all over the experiment.

The results of the successive calibrations during the continental phase are presented on figure 2. The calibrations at CNES station appear more stable than the LPTF station measurements. Moreover the CNES station was switched off for a while on MJD 49266 (October 6): there are obviously two sets of data before and after this MJD, each scattered within 4 ns. On the contrary the LPTF data are much more scattered within 25 ns. It has been shown by the manufacturer of the stations that, owing to the components used for this experiment, the signal generator could exhibit stepwise varying delays, each step being a multiple of 2.44 ns. By processing in deferred time the dating of the 1 pps L1-C/A performed continuously by both NR106 of each station, those variations could be identified, summed and compared to the day to day calibrations of figure 2. With the analysis of these records, some improvements could be achieved, but a lot of discrepancies are remaining, mainly due to missing data. This is why these discontinuities in the delays are disregarded. The average values of the calibration sessions are adopted along with the relevant standard deviations as uncertainties, giving for the signal generators delays:

- at TLS (continental phase): mean value = 1007.5 ns; standard deviation = 4.8 ns.
- at LPTF: mean value = 998.5 ns; standard deviation = 7.1 ns.

A similar behaviour of the signal generators was observed during the transatlantic phase of the experiment (Figure 3). The generator of the HBK station, formerly located at the LPTF, remained the most perturbed one, compared to the generator of the KRU station, which has never been switched off during the whole experiment. The manufacturer of the stations believes that the generator of the KRU station has reached the best achievable stability, with the components used for the building of it. The average values of the calibration sessions were adopted along with the relevant standard deviations as uncertainties, as for the continental phase, giving for the signal generators delays:

- at TLS (transatlantic phase): mean value = 1009.4 ns; standard deviation = 6.3 ns.
- at HBK: mean value = 986.1 ns; standard deviation = 7.6 ns.
- at KRU: mean value = 1025.8 ns; standard deviation = 1.4 ns.

A calibration by transportation of two GPS receivers was organized during the continental phase of the experiment, so that three round-trips were performed between the LPTF and the TLS station. It has worked remarkably well, except for some local problems too long to explain here, giving the usual uncertainty of 1.5 ns (1 s) on the differences between the two time scales. An other control of the results was possible thanks to the operational GPS Common-view link between the two stations involved, used continuously for the computation of the TAF ('Temps atomique francais').

No temperature effect was noticeable on the sets of data.

## CONTINENTAL EXPERIMENTAL PHASE

An analysis of the data by the Modified Allan deviation showed that white phase noise is preponderant on each 15 min session over a period long enough to allow the computation of an average value. The precision of one 0.6 s sampled CE-GPS observation is about 9 to 10 ns, as can be deduced from the Modified Allan deviation. It could be compared to the MITREX observations that are ten times better [6], but it remains consistent with the magnitude expected when using C/A code along with standard discriminators on signals affected by a measured C/No of about 40 dB(Hz).

On Figure 4 are presented the average values of the TWSTT 15 min sessions, compared to the Common-view GPS daily averages between the GPS time receivers connected to the CE-GPS stations. One can see that the TWSTT points are well distributed around the GPS curve, even though they are scattered. It appears that many sessions have suffered from the above mentioned stepwise varying delays compared to the average values of the generators delays. This is a logical consequence of the choice to use an average of the calibration measurements. The uncertainties of the generators delays are obviously the most degrading part for the accuracy of this experiment of TWSTT through Inmarsat. We propose the following uncertainty budget in nanoseconds (1 s):

Inmarsat transponder	0	[Global coverage]
Sagnac effect	0.0	
Ionospheric delays	2.0	[Differential/Bent model]
Differential delays (LPTF-CNES)	6.2	[1ppsL1-C/A generator]
UTC(LPTF)-1 pps REF	0.5	[short line]
UTC(CNES)-1 pps REF	1.0	[long line]
<hr/> Two-way accuracy	<hr/> 6.6	<hr/> [Quadratic sum]

This accuracy is given for each session averaged result, and remain well below the upper limit of the CE-GPS requirements (10 ns). It surely will drop to a more interesting value compared to the MITREX results [6] if the behaviour of the generators could be withdrawn from the measurements. The uncertainty of the comparison between GPS Common-view and TWSTT can be estimated in nanoseconds (1 s) by:

TWSTT (CE-GPS continental)	6.6	
GPS Common-view [5]	3.4	[800 km baseline]
Uncertainty of the comparison	7.5	

This uncertainty appears consistent with the data plotted on Figure 4.

## TRANSATLANTIC EXPERIMENTAL PHASE

A statistical analysis of the transatlantic data showed that a white phase noise behaviour is observed, as for the continental phase. Until now, no GPS Common-view data are available to be compared to the TWSTT results, and a lot of TWSTT data are missing, due to local problems in the equipments. On figures 5, 6 and 7 are plotted the TWSTT results on each link. The regular behaviour of the two different types of atomic clocks used can yet be recognized. In a very similar way as for the continental phase, we propose the following uncertainty budgets in nanoseconds (1 s) for each link:

Ionospheric delays	5.1 [average computed from GPS measurements]		
Equipment delays	TLS - HBK	HBK - KRU	KRU - TLS
7.0	5.5	4.6	
UTC(k)-1 pps REF		1.0	[two stations]
TWSTT accuracies	8.7	7.6	6.9

These accuracies are near the upper limit of the CE-GPS requirements (10 ns). One of the possible tests of the consistency of the results, along with a check of the computation options, is to calculate the deviation from the closure between the three stations. For this purpose, daily independent TWSTT results have been built up, for two of the three TWSTT links, by interpolation between two separated measurements sessions, centered on the date of the third link result. The deviations from the closure are plotted on figure 8. Even if only few points are available, there is obviously a bias between the three different sets of data. Again the behaviour of the generators of the stations is suspected to be the most important part of this bias. The results are scattered between - 8.0 ns and 15.3 ns. These values are consistent with the estimated accuracies given above. But the weak number of computed values do not allow us to realize a more complete statistical analysis.

If one could consider that the behaviour of the 1 pps L1-C/A generator in the KRU station would be the regular behaviour of an operational CE-GPS ground station, and if the ionospheric delays could be measured with a better uncertainty, by using the IGS post-processed data for instance, one could estimate the following uncertainty budget:

Ionospheric delays	2.0
Equipment delays	1.5
UTC(k)-1 pps REF	1.0 [two stations]
TWSTT accuracy	2.7

This could be the best achievable accuracy of the method, with similar stations more than 10,000 km apart, as far as the global coverage of the satellite's antenna is realized.

## CONCLUSION

It has been demonstrated that the time requirements of the CE-GPS could be fulfilled with ground stations comparable to those built up for the purpose of the experiment presented in this paper, either for a distance between the stations inferior to 1000 km, or for stations more than 10,000 km apart. Even with the calibration problems related to the signal generators as conceived for this experiment, the monitoring clock synchronization could be done by the TWSTT technique through an Inmarsat geostationary satellite, with C/A gold codes and GPS receivers, with an accuracy of 7 to 9 ns (1 s). The best achievable accuracy is estimated within 2.7 ns (1 s).

The software for computing the timing data from the pseudo-range measurements made by the NR106, which are only GPS navigation receivers, is nearly completed. It will allow in the future the computation of GPS Common-view data the same way as in GPS receivers dedicated to time measurements, making the NRT2 receivers connected to the CE-GPS stations useless. Because NR106 are 10 channels receivers, it will supply data for the restitution of GPS time with the highest number of GPS satellites available simultaneously, reducing the averaging period for a similarly reduced S.A. noise.

Beside TWSTT, other techniques are scheduled to be tested with signals transmitted by the Inmarsat transponder. Among others, the servo-control could be the most interesting due to its near real-time time transfer capability. In this case however the synchronization is less accurate than the best achievable with post-processed data.

## ACKNOWLEDGEMENTS

The authors gratefully acknowledge Dr C. Thomas (BIPM) for many fruitful discussions. Co-workers on the CE-GPS experiment at the LPTF, G. Fréon and P. Blondé, at the CNES, J. Barbier, M. Deleuze, J-L. Issler, D. Berges, J-P. Lefèvre, N. Suard, T. Trémas, R. Tribes, and C. Yven, and at the IN-SNEC, F. Varieras and F. Saffre, are here acknowledged. The authors thank J. Berthier (Observatoire de Paris) for his help in the processing of the raw data.

## REFERENCES

- [1] J. Barbier, T. Tremas (CNES). *"European Complement to GPS: presentation of the concept and experimental system."* Proceedings of the 7th EFTF, Neufchâtel, March 93.
- [2] STANAG. Technical characteristics of the NAVSTAR GPS. June 91.
- [3] J. Barbier, M. Deleuze, J-L. Issler (CNES), P. Uhrich, B. Juompan (LPTF), et al. *"European Complement to GPS: main experimental results."* Proceedings of the ION-GPS 94 (to be published).

- [4] P. Urich, B. Juompan, G. Fréon, R. Tourde, P. Blondè (LPTF), M. Brunet, J-F. Dutrey, J. Barbier, J-L. Issler, N. Suard, T. Trémas (CNES). "*Time aspects of the European Complement to GPS: some experimental results.*" Proceedings of the 8th EFTF, Munich, March 94.
- [5] W. Lewandowski, G. Petit and C. Thomas (BIPM). "*Precision and Accuracy of GPS Time Transfer.*" IEEE Trans. on Instr. and Meas. Vol. 42, No. 2, 1993, 474-479.
- [6] D. Kirchner (TUG), H. Ressler (IWF), P. Grudler, F. Baumont, C. Veillet (OCA), W. Lewandowski (BIPM), W. Hanson (NIST), W. Klepczynski (USNO), P. Urich (LPTF). "*Comparison of GPS Common-view and Two-way Satellite Time Transfer Over a Baseline of 800 km.*" Metrologia 1993, 30, 183-192.

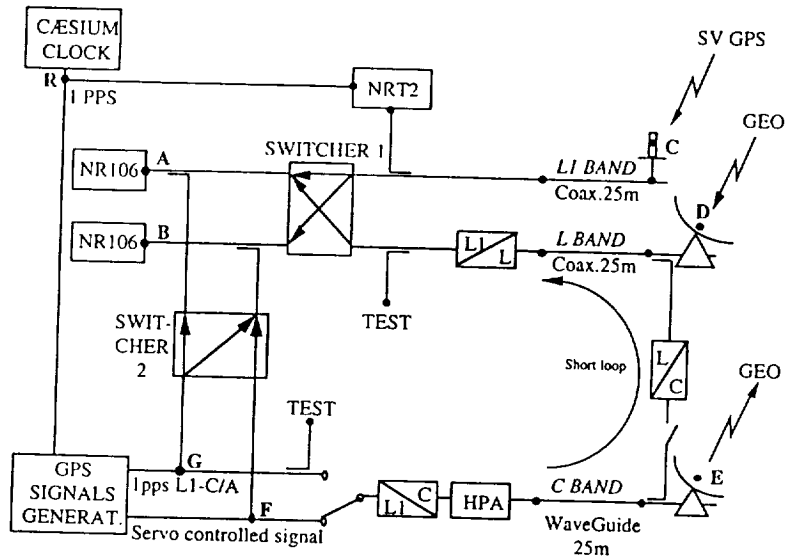


Figure 1. Diagram of a CE-GPS ground station.

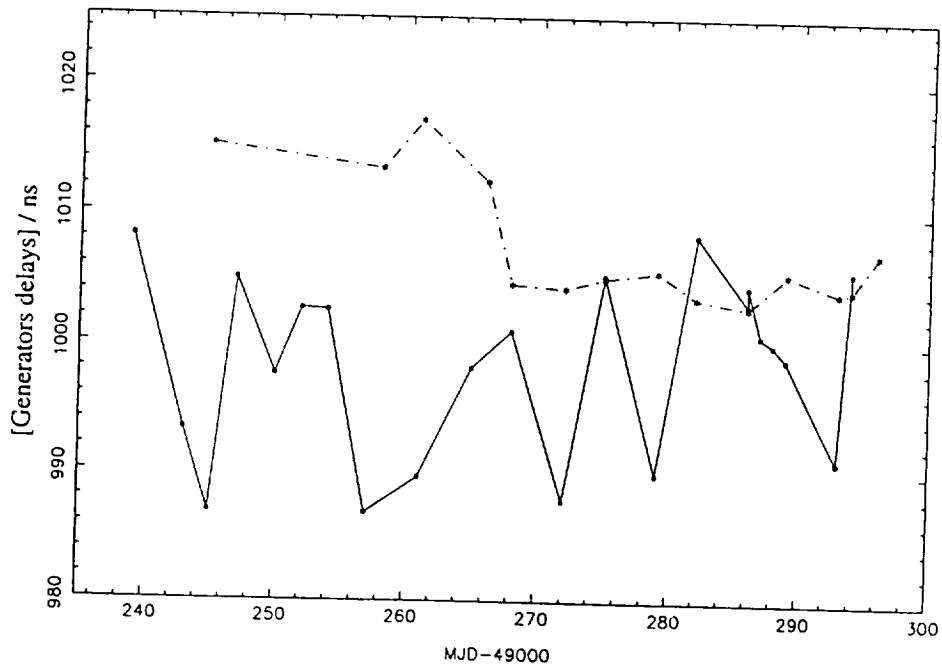
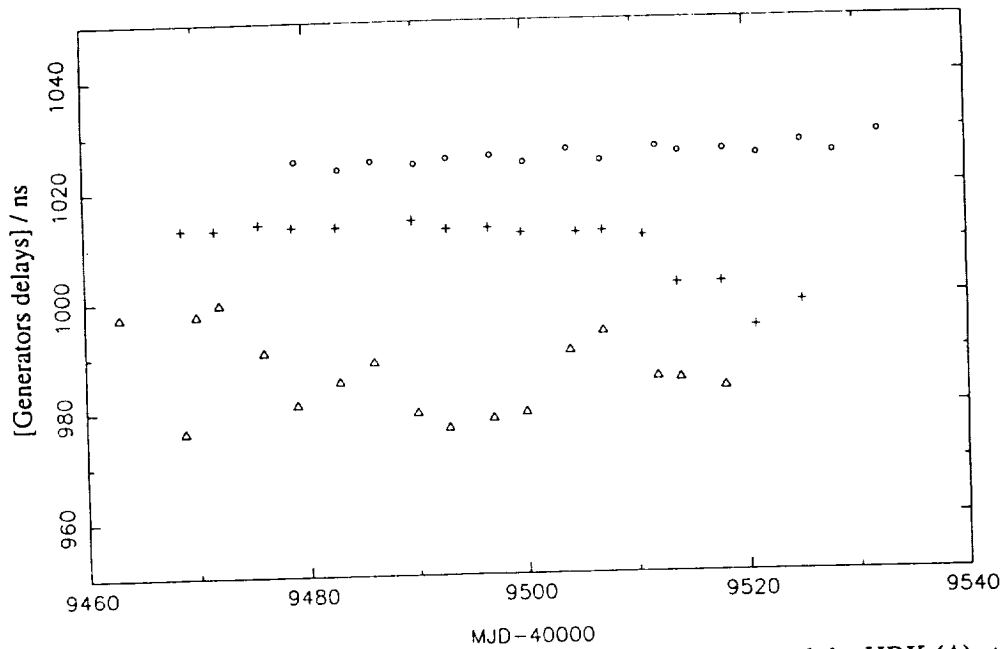
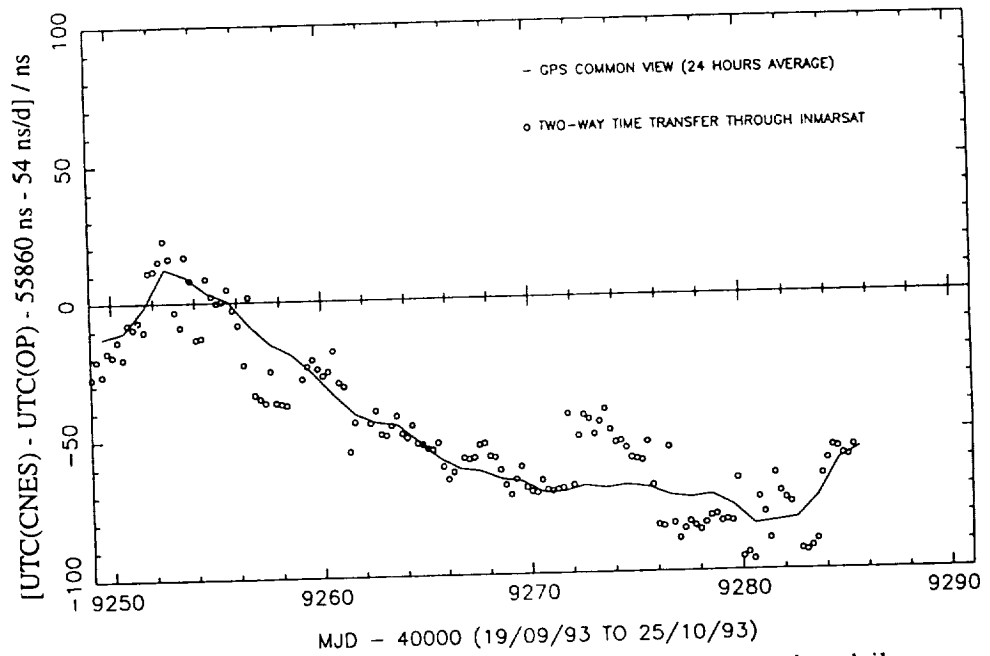


Figure 2. Calibration of the generators at the LPTF (\*) and at TLS (•) during the continental phase of the experiment.



**Figure 3.** Calibration of the generators at the KRU (°), the TLS (+), and the HBK (Δ) stations during the transatlantic phase of the experiment.



**Figure 4.** TWSTT 15 min averaged sessions and GPS common-view daily averages (CE-GPS continental phase).

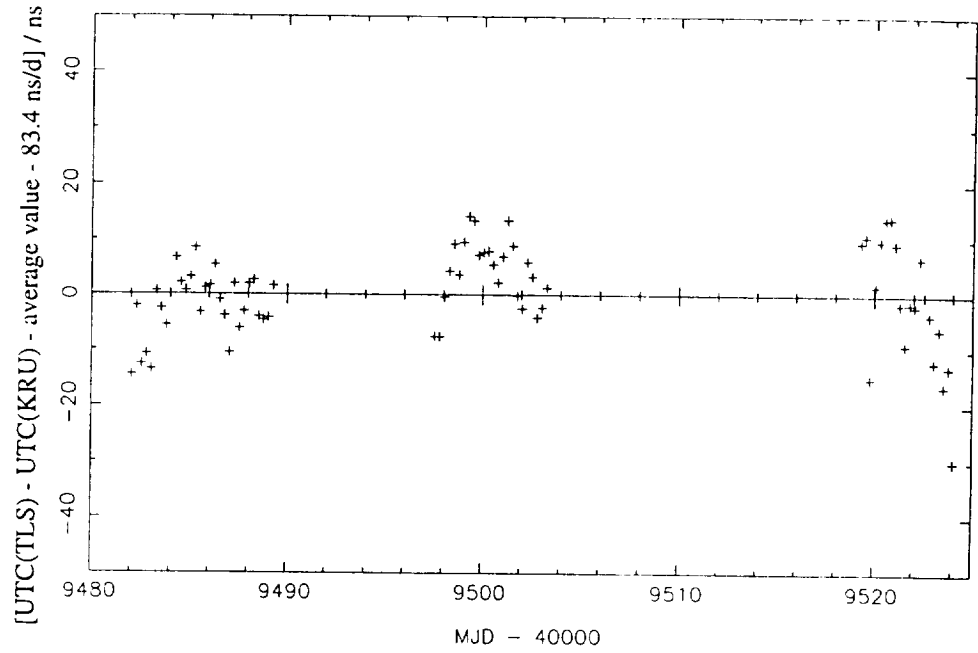


**Figure 5.** TWSTT 15 min averaged sessions between TLS and KRU (CE-GPS transatlantic phase).

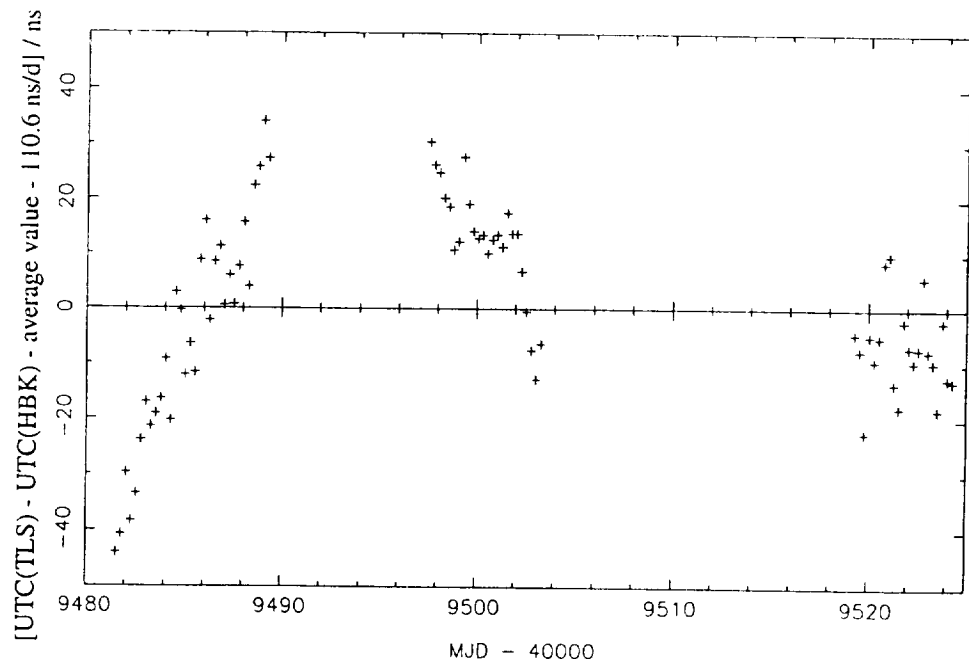


**Figure 6.** TWSTT 15 min averaged sessions between TLS and HBK (CE-GPS transatlantic phase).

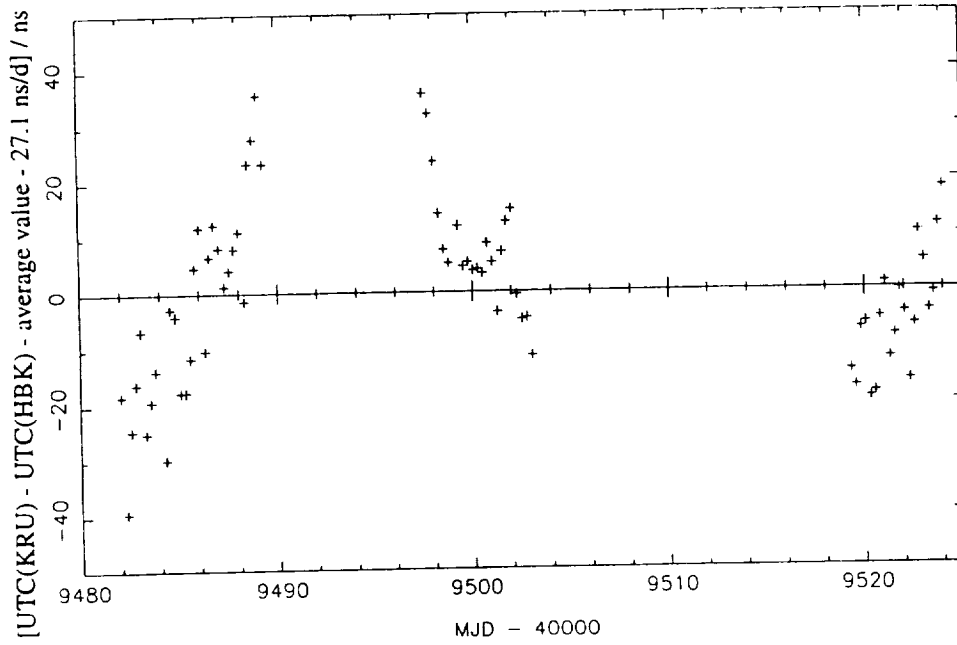


**Figure 7.** TWSTT 15 min averaged sessions between KRU and HBK (CE-GPS transatlantic phase).

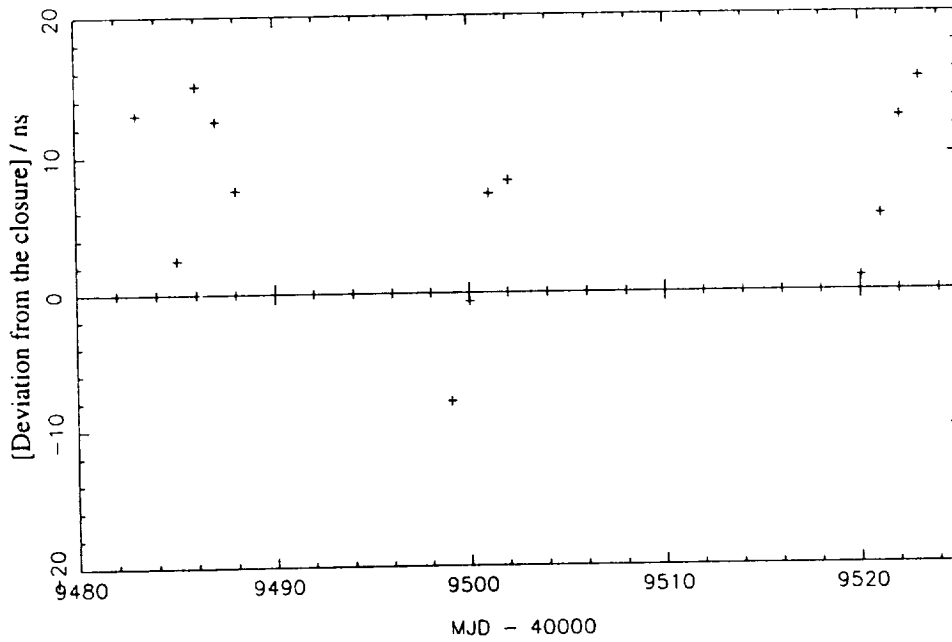


**Figure 8.** Deviation from the closure TLS - KRU - HBK (CE-GPS transatlantic phase).

# LASSO EXPERIMENT INTERCALIBRATION TRIP FOR THE TWO LASSO RANGING STATIONS

J. Gaignebet and J.L. Hatat  
Lunar Laser Ranging Team  
P. Grudler  
Observatoire de la Côte d'Azur

W.J. Klepczynski and L. McCubbin  
U.S. Naval Observatory

J. Wiant and R. Ricklefs  
McDonald Observatory, Texas

## Abstract

*In order to achieve the accuracy of the LASSO time transfer between OCA, Grasse, France and McDonald Observatory, Texas, USA, an intercalibration of the two Laser Ranging Stations was made.*

*At the same stations, GPS receivers were set up and the GPS to Laser epoch differences were also monitored.*

*In addition to the principle and the results of the measurements, the cause of the difficulties met during the campaign will be described.*

## INTRODUCTION

After a successful LASSO Ranging Campaign by the two Lunar Laser Ranging (LLR) Stations, University of Texas at Mc Donald and Observatoire de la Côte d'Azur in Grasse, which took place from April 1992 to January 1993, an intercalibration trip for the participating stations has been set up.

The principle of this intercalibration (Fig. 1) is to use a common vector on both sites, in order to determine the emission delay difference. The common vector is a specially designed laser ranging station, transportable and able to be set up close to each telescope. The range limit of such a station is of a few kilometers on simple ground targets (corner cube).

## CONFIGURATIONS

At each site two configurations were scheduled:

- emission by the LLR local station and reception by both LLR local station and calibration station (Fig.2).
- emission by the calibration station and reception by both stations (Fig. 3). These configurations allow to write a set of redundant relations from which we can derive the difference of the emission delays. This difference is called the LASSO calibration. For the LASSO calibration to be valid, it is necessary that the delays of the calibration station and the cables for the 5 MHz and the 1 Hz remain stable. A special design of the calibration station allows to monitor any change in the internal delays and the cables being considered as part of the equipment thereof. The same set of cables will be used at every site.

Outside of the LASSO calibration, another calibration is needed in the Lasso synchronization relations. It is the ranging calibration of each LLR Station.

This is routinely surveyed by the ranging teams and could be also determined from the two way flight time of the laser beam of the calibration station.

## CALIBRATION TRIP

The calibration started in April 1993 at LLR OCA Station. The transportation of the calibration station was easy since a van had been purchased for that purpose. Setting the station near the LLR telescope was quite easy, we only had to solve a Radio Frequency Interference, probably caused by the iron sheet cover of the dome of the LLR station. In June of the same year, we moved the station to the LLR station at McDonald. The transportation of the calibration station was done by air, from Nice to Houston, then by truck, from Houston to El Paso and finally by car, from El Paso to the Observatory.

At the station our equipment had to be set up outside as the shelter of the LLR station was already quite crowded. This occurred to be somewhat of a problem as the weather was unusually bad (heavy rain and wind) for such an area as Texas at that time of the year. After some hardware adjustments (laser, telescope focus) the calibration station was ready to work in less than two days in what we would call an expected nominal mode. However, because we did not have any oscilloscope that we could use, we were unable to control the level of the discriminators and actually for some reason they were not set as they were for the calibration at OCA.

We have to mention here that we encountered some problems, which are not unusual when you carry material to different countries. The ATA Carnet, for example is not commonly used in some areas as El Paso, and of course it can be of a risk to go through customs on an official Holiday.

## CALIBRATION SESSIONS

- The LLR OCA station was designed with LASSO in mind, therefore outside of the Radio Frequency Interference problem, no other difficulties appeared. The data files are very

stable for successive and close together sessions, but not for day to day sessions with a noise around 150 ps up to 300 ps (Fig. 4).

- The LLR McDonald station, in spite of some difficulties saved the LASSO experiment, as it was the only other station ready and in position to make LASSO sessions at that time.

The station had been designed with only the goal of ranging and later on adapted for LASSO observations.

Consequently we have encountered some limitations at McDonald station:

1. Processing the data in real time was impossible, as a preprocessing of the data at University of Texas at Austin was absolutely necessary to make the files readable. This led to the impossibility of scheduling any other session in case that something would fail. An example is that we could not discover that a range gate had been adjusted in the wrong way, rejecting the real data and recording the adjacent noise (Fig. 5).
2. The design of the equipment is such that the same interpolator is used for both the emission and the reception. Ranging the Moon or satellites is very efficient in this way, as any variation in the interpolator slope cancels. For LASSO the emission delay, relying on a single path in the interpolator, may and actually does change from day to day (estimated to up 5 ns). For calibration sessions, ranging on a close target is impossible, because the dead time of the interpolator is far too large (Fig. 6). As the system is computer driven in a synchronous mode, the LLR station is then also unable to record emissions from the calibration station (Fig. 7).

Back to OCA LLR station we discovered that the calibration equipment delay had changed during the trip, most likely during the hardware tuning at McDonald station and because we did not have a oscilloscope, we could not readjust the constant fraction discriminator at the ideal level. This adds an uncertainty of 1 ns. Taking into account the previous remarks, the data files recorded at McDonald station have the same discrepancy than the ones of OCA. The short term stability is rather good (1 to 3 hours) but the values drift from session to session.

The overall calibration is computed at 136,999 ps. It is obvious that this is meaningless due to the long term unstability of a part of the Lunar Laser Ranging station equipment at McDonald, which was not fully designed for LASSO experiment.

The estimated discrepancy could be up to  $\pm 2.5$  ns.

## CONCLUSION

Considering what we have learned during this first intercalibration trip, we think that the equipment as it is designed, could provide a value with an accuracy of a few hundreds picoseconds (200 to 300 ps).

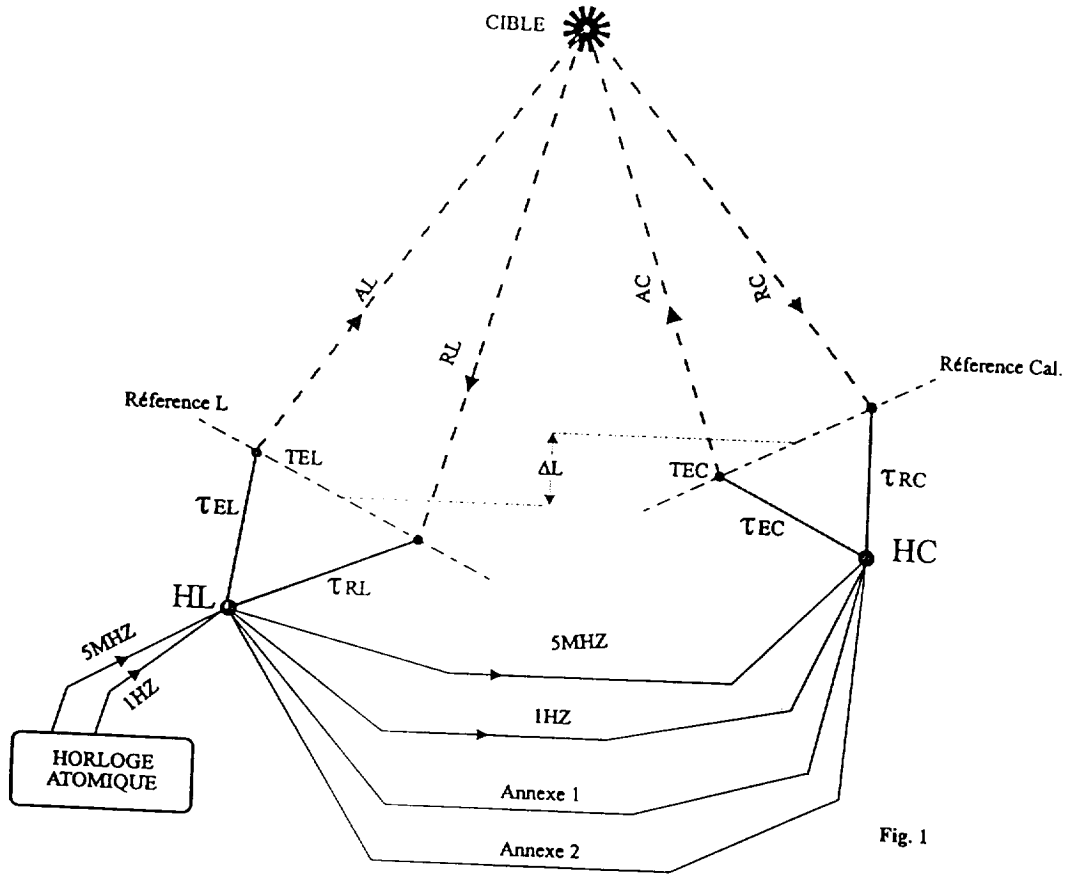
It has to be noticed that the stations willing to participate in such campaigns have to be designed for time transfer and need event timers reaching at least the same accuracy.

With some changes, such as fast photodetectors, a new event timer and new discriminates, the level of 30 to 10 picoseconds could be reached.

## **REFERENCE**

J. Gaignebet et al., "*LASSO Experiment: Intercalibration of the LASSO Ranging Stations*", Proceedings 25th Annual Precise Time and Time Interval Applications and Planning Meeting, December 1993.

# INTERCALIBRATION LASSO CONFIGURATION GENERALE



## STATION LASER LUNE :

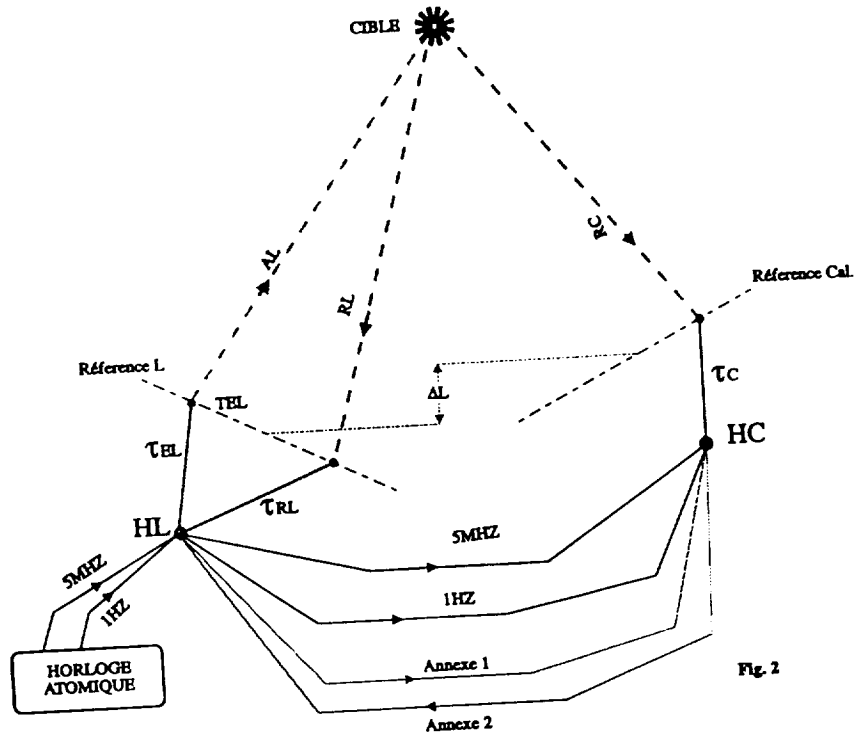
HL = Dateur Laser Lune  
 Ref.L = Référence station Laser Lune  
 TEL = Heure passage laser au point de ref  
 AL = Temps aller Ref.L / cible  
 RL = Temps retour cible / Ref.L.  
 $\tau_{EL}$  = Ecart Réf.L / Dateur HL.  
 $\tau_{RL}$  = Ecart Dateur HL / Réf.L.  
 $CCLL = \tau_{EL} + \tau_{RL}$  (Constante de calibration LL)  
 $AL = RL$

## STATION DE CALIBRATION :

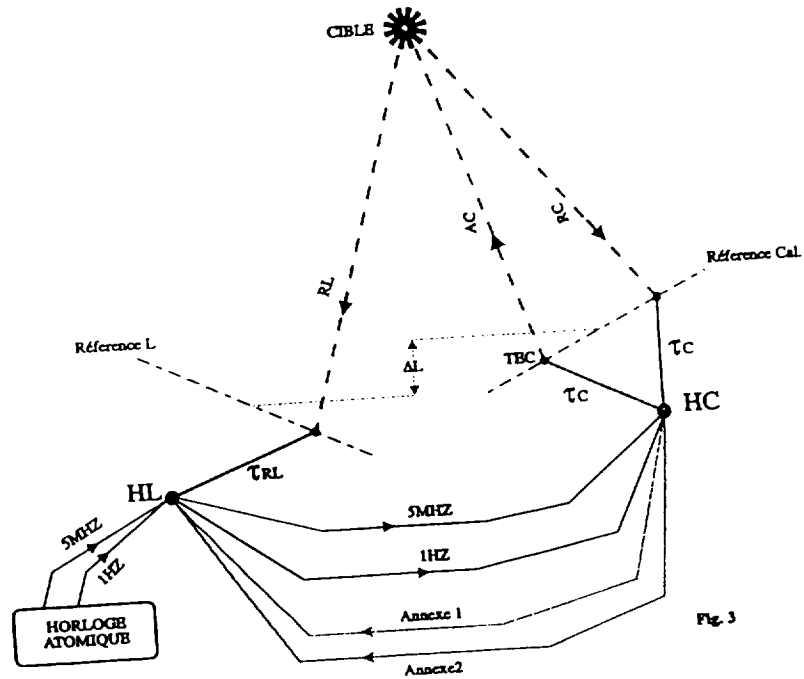
HC = Dateur station de calibration  
 Réf.Cal. = Référence stat. de Calib.  
 TEC = Heure au point de Réf.  
 AC = Temps aller Réf.Cal/cible  
 RC = Temps retour cible/Réf.Cal.  
 $\tau_{EC}$  = Dateur Réf.Cal. / Dateur HC  
 $\tau_{RC}$  = Ecart Dateur HC / Réf.Cal.  
 $\tau_{EC} = \tau_{RC} = \tau_C$   
 $AC = RC$

5MHZ, 1HZ, Annexe1, Annexe2 = Câbles coaxiaux

## INTERCALIBRATION LASSO CONFIGURATION PHASE1 GRASSE



## INTERCALIBRATION LASSO CONFIGURATION PHASE2 GRASSE



# LASSO INTERCALIBRATION PHASE 1 GRASSE

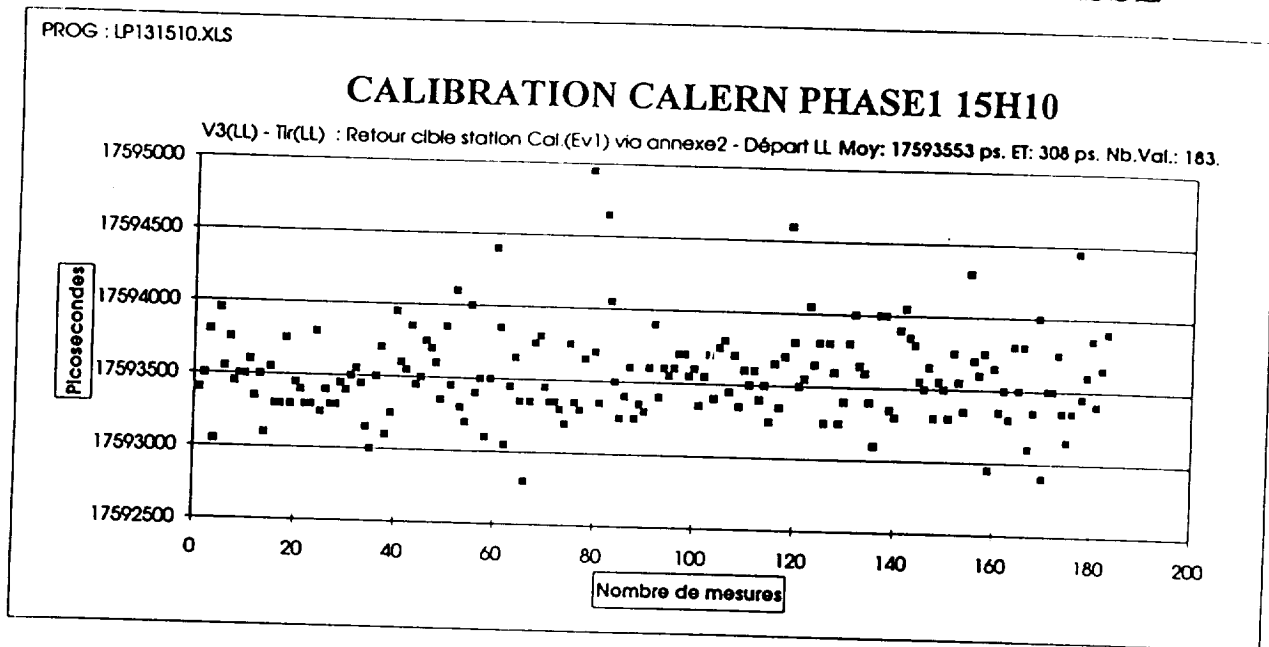


Fig. 4

# LASSO INTERCALIBRATION PHASE2 TEXAS

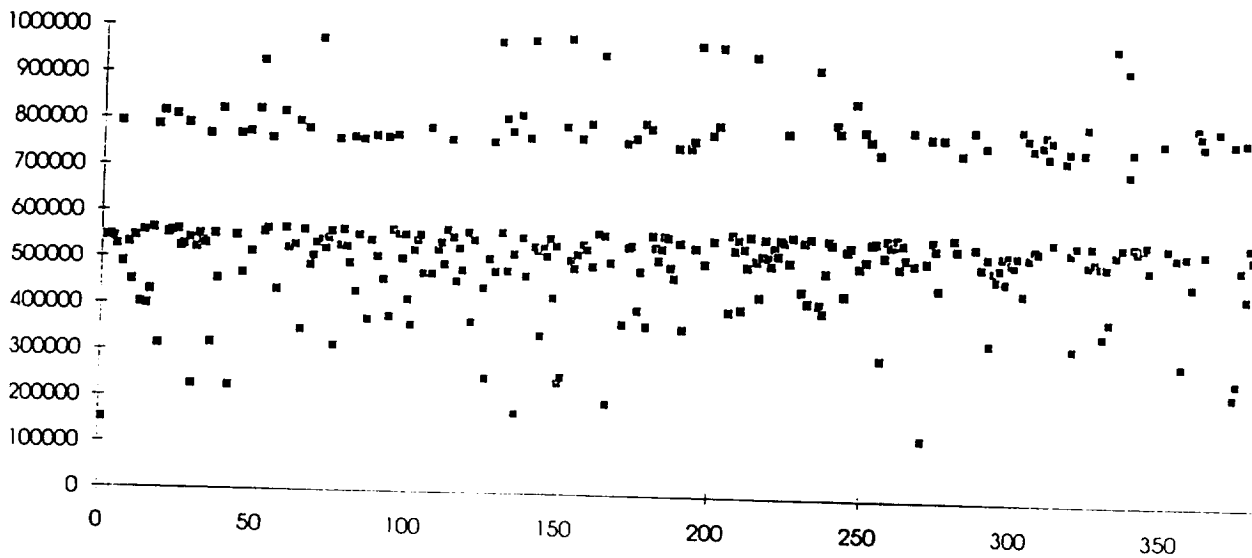


Fig. 5

# INTERCALIBRATION LASSO CONFIGURATION PHASE1 TEXAS

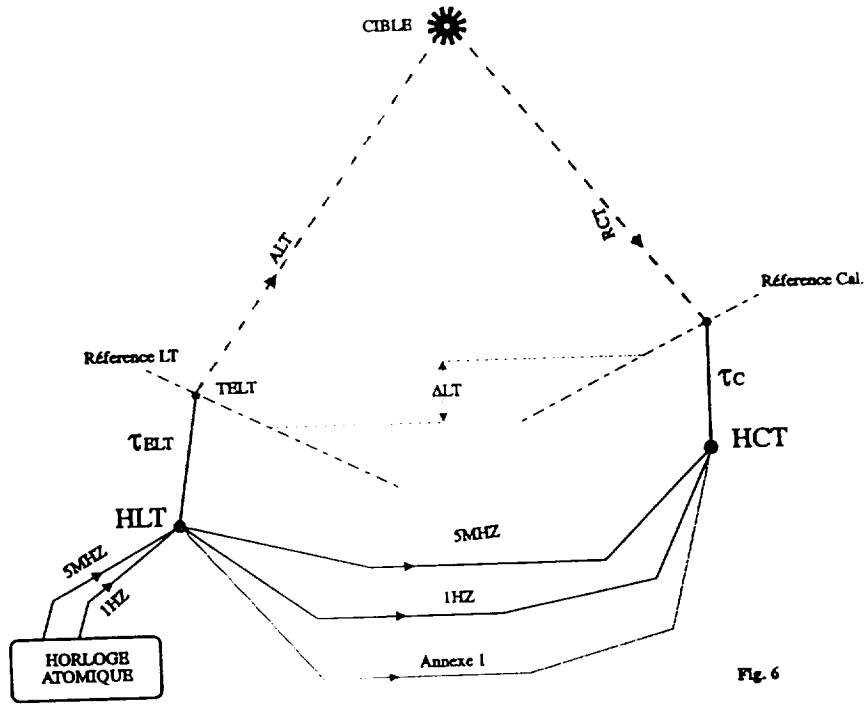


Fig. 6

# INTERCALIBRATION LASSO CONFIGURATION PHASE2 TEXAS

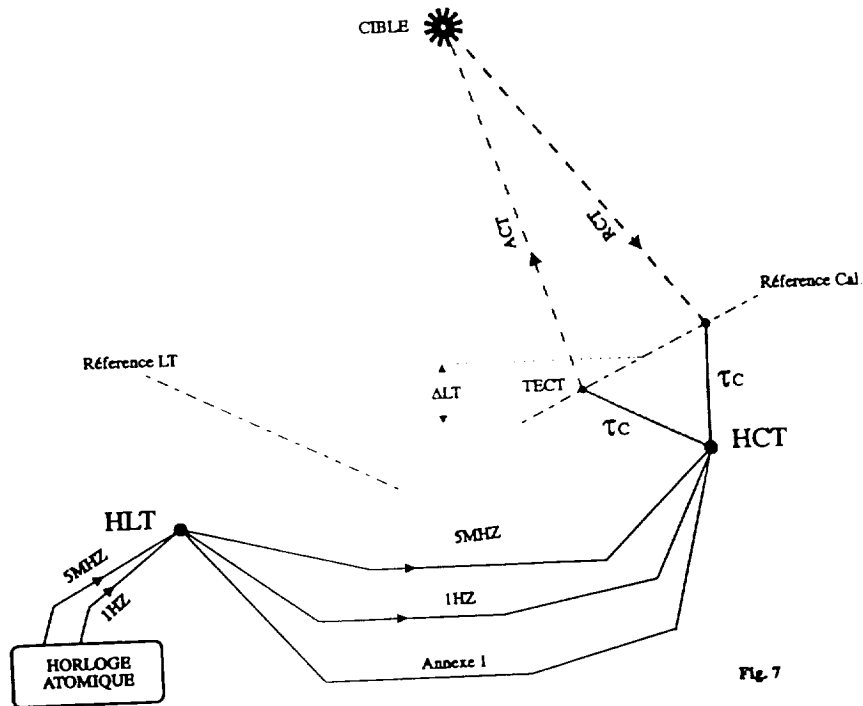


Fig. 7

52276

P. 9

# Network Time Synchronization Servers at the U. S. Naval Observatory

R. E. Schmidt  
Directorate of Time  
Time Scales Division  
U. S. Naval Observatory  
Washington, DC 20392

## Abstract

*Responding to an increased demand for reliable, accurate time on the Internet and Milnet, the U.S. Naval Observatory Time Service has established the network time servers, tick.usno.navy.mil and tock.usno.navy.mil. The system clocks of these HP9000/747i industrial work stations are synchronized to within a few tens of microseconds of USNO Master Clock 2 using VMEbus IRIG-B interfaces. Redundant time code is available from a VMEbus GPS receiver.*

*UTC(USNO) is provided over the network via a number of protocols, including the Network Time Protocol (NTP) [DARPA Network Working Group Report RFC-1305], the Daytime Protocol [RFC-867], and the Time protocol [RFC-868]. Access to USNO network time services is presently open and unrestricted.*

*An overview of USNO time services and results of LAN and WAN time synchronization tests will be presented.*

In October, 1994, the Internet consisted of 3,864,000 hosts in 56,000 domains over 37,022 networks. This represents a growth rate in number of hosts of 61% over 12 months<sup>[1]</sup>. A number of networked time servers are providing time to this population voluntarily, using the Network Time Protocol (NTP) and other protocols, but the top of the timing pyramid, the domain of the stratum-1 servers, is sparsely populated. The current list of primary servers<sup>[2]</sup> includes:

Region	Time Synchronization Source				
	Atomic	GPS	WWV/DCF77	GOES	Other
US West	-	1	8	1	
US Mountain	2	-	1	-	
US Midwest	-	-	3	-	
US East	2	2	6	-	
Hawaii	-	-	1	-	
Canada	-	-	-	2	
Japan	-	4	-	-	
France	-	-	1	-	
Germany	-	1	3	-	
Australia	1	-	-	-	
United Kingdom	-	-	2	-	1 Omega
Netherlands	-	-	1	-	
Switzerland	-	-	1	-	
Norway	1	1	1	-	1 Loran-C

The two U.S. East servers with atomic clock links are new additions, the USNO network time servers tick.usno.navy.mil and tock.usno.navy.mil. They are Hewlett-Packard HP9000/747i industrial VME bus workstations. Each hosts a Datum bc635vme synchronized generator, which is fed from a Time Systems Technology Model 6460 IRIG-b generator receiving 5MHz from USNO Master Clock #2.

Redundant time is provided by a TrueTime GPS-VME board in one system, which feeds IRIG-b to a TrueTime VME-SG synchronized generator in the second host. Network Time Protocol (NTP) clock drivers were written for these interfaces.

Tick and tock operate as stratum-1 servers of the NTP network time protocol<sup>[3]</sup>. Clients exchange timestamp packets with the servers to measure delay, clock offset, and network and operating system dispersion. NTP then corrects the local system clock via step offsets or, more commonly, by slewing the UNIX system clock. The adjtime routine the value of the tick increment to be added to the kernel time variable at each hardware timer interrupt. Frequency and phase offsets of the local server UNIX system clocks from their synchronized generators are measured by NTP at 64-second update intervals.

With this off-the-shelf hardware we keep the servers' system clocks to within 100 microseconds of UTC(USNO). (Other NTP hosts do better than this, but our goal is to synchronize UNIX system clocks to tolerable levels, with a minimum of effort. NTP clients synchronize to a few milliseconds of UTC(USNO), and long-distance clients to tens of milliseconds.

## TESTING NTP TIME TRANSFERS

For the past six months we have synchronized to our servers a number of local hosts and one distant source, an HP9000/425t located at the Naval Observatory Time Substation near Miami, FL. To converse with the latter system from Washington, we must route packets through six or seven intervening NASA sites. Pings take from 100 to 3400 ms, depending on the level of net traffic. Yet we are able to do quite satisfactory system time synchronization, as the figures demonstrate.

One measure of the success of network time synchronization is TDEV, the "time domain stability measure" as described by D. W. Allan et. al. at the 1994 Frequency Control Symposium<sup>[4]</sup>

$$\sigma_x = [1/6 \langle (\Delta^2 \bar{x})^2 \rangle]^{1/2} \quad (1)$$

In the following "sigma-tau" diagrams, one is able to distinguish types of noise, decorrelation timescales, and even diurnal modulation of workstation crystal clocks<sup>[5]</sup>.

## FUTURE WORK

The success of the USNO network time servers, which are now processing about 155,000 NTP packets per month, establishes them in the ranks of the few stratum-1 servers. But clearly Washington, DC-based servers are of limited usefulness nationally. The growing availability of low-cost GPS receivers, and even integrated, standalone GPS/NTP servers, provides the potential for an ensemble of geographically dispersed time servers with sources of reliable and accurate time traceable to UTC(USNO) via GPS. It would take only about a dozen GPS/NTP servers, located on the ANSnet T3 backbone, to provide nationwide network time services that would be dependable and accurate<sup>[6]</sup>, and a similar number for the Defense Information Systems Network (DISN).

The USNO will upgrade its Internet link to a T1 line from its present 56kb connection in December, 1994<sup>[7]</sup>. This should smooth some of the serious time warps seen by our WAN clients. ISDN promises further potential for wide-area timing links. USNO plans to be active in time synchronization via ISDN in 1995.

## NETWORK TIME SERVICES

UTC(USNO) is provided over the network via a number of protocols.

### 1. RFC-1305 NETWORK TIME PROTOCOL

The USNO time servers are stratum 1 servers for the Network Time Protocol (NTP) [DARPA Network Working Group Report RFC-1305].

### 2. TELNET ASCII TIME

The U.S. Naval Observatory Master Clock is accessible in low-precision mode via telnet to one of the time servers on port 13. The time server will ping your system and estimate the network path delay. It will then send Modified Julian Date, Day of Year, and UTC time as ASCII strings followed by an on-time mark (\*) which will be advanced by the estimated network delay. The uncertainty in the network delay estimate can reach hundreds of milliseconds, but is typically good to a few tens of milliseconds.

### 3. RFC 868 TIME PROTOCOL

The "time" protocol [RFC-868] is supported on TCP and UDP port 37. This service returns a 32-bit binary number, in network byte order, representing the number of seconds of time since 1 Jan. 1900 UT. The "rdate" program uses TCP port 37 and is supported on our servers.

### 4. RFC 867 DAYTIME PROTOCOL

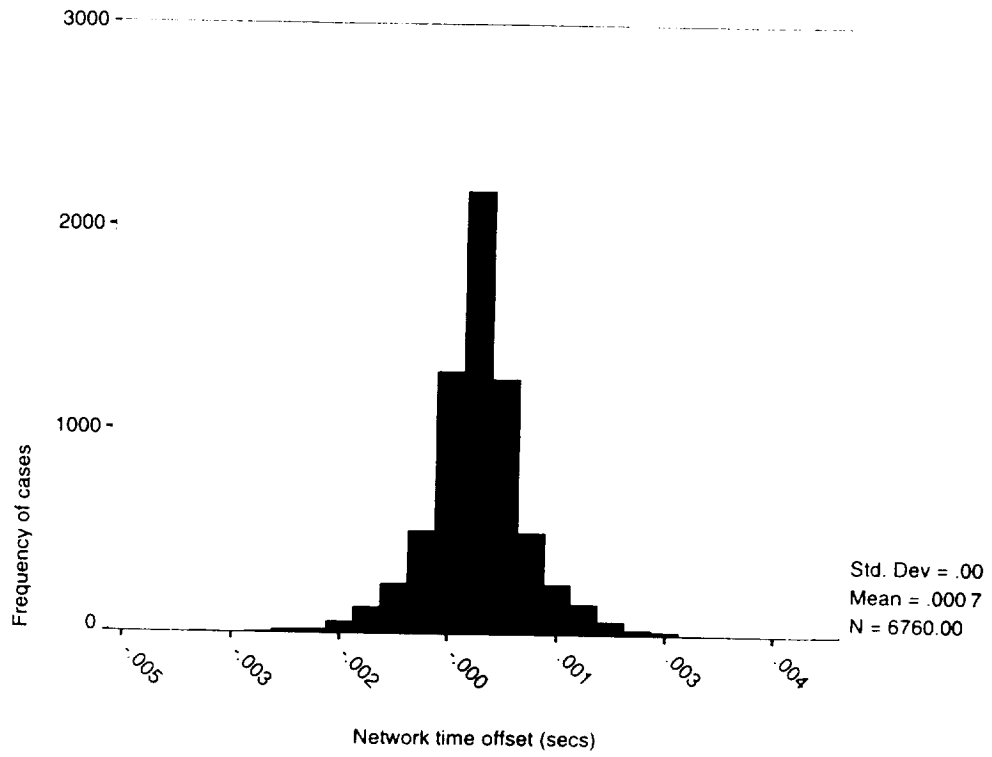
The ASCII "daytime" protocol is supported only on UDP port 13. The TCP implementation has been replaced by the telnet ASCII time protocol above.

## REFERENCES:

- [1] Lottor, Mark, Internet Domain Survey, Oct. 1994
- [2] Mills, D.L., Information on NTP Time Servers and Radio Timecode Receivers, 3 Nov. 1994
- [3] Mills, D.L., Network time Protocol (Version 3) specification, implementation, and analysis. DARPA Network Working Group Report RFC-1305, University of Delaware, March 1992, 113 pp.
- [4] Allan, D. W., Time-Domain Instability Measures in Time and Frequency and for Telecommunications, lecture notes, Frequency and Control Symposium, 1994.
- [5] DeYoung, J. A., private communication.
- [6] ANSnet T3 Backbone Map, Advanced Network & Services
- [7] Withington, F. N., private communication.

# NTP Synchronization

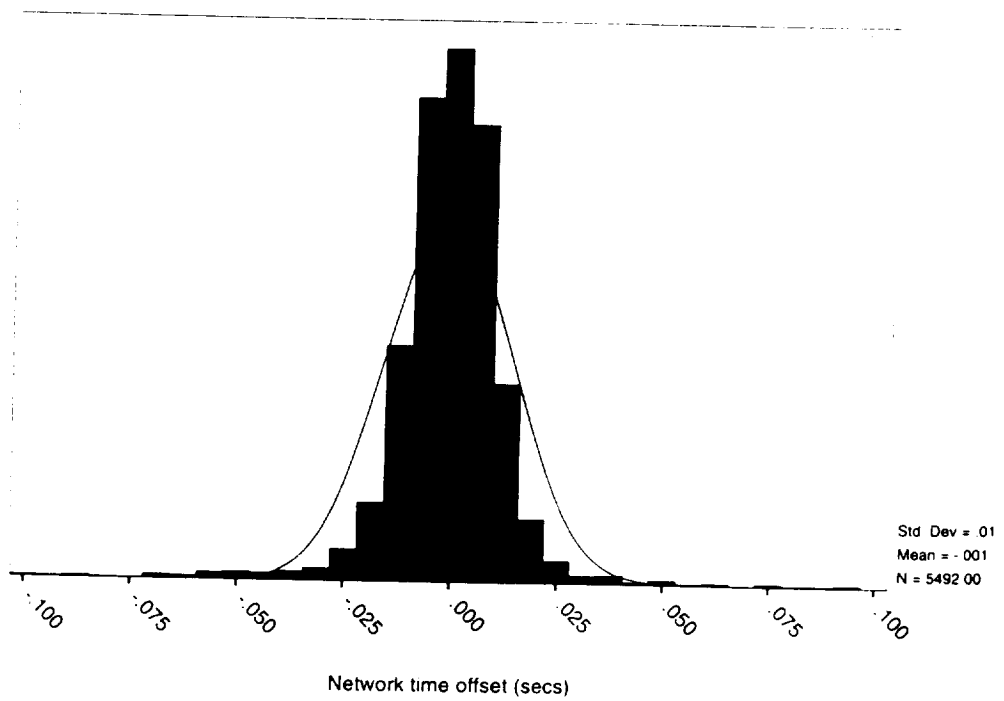
USNO Local LAN



# NTP Time Synchronization

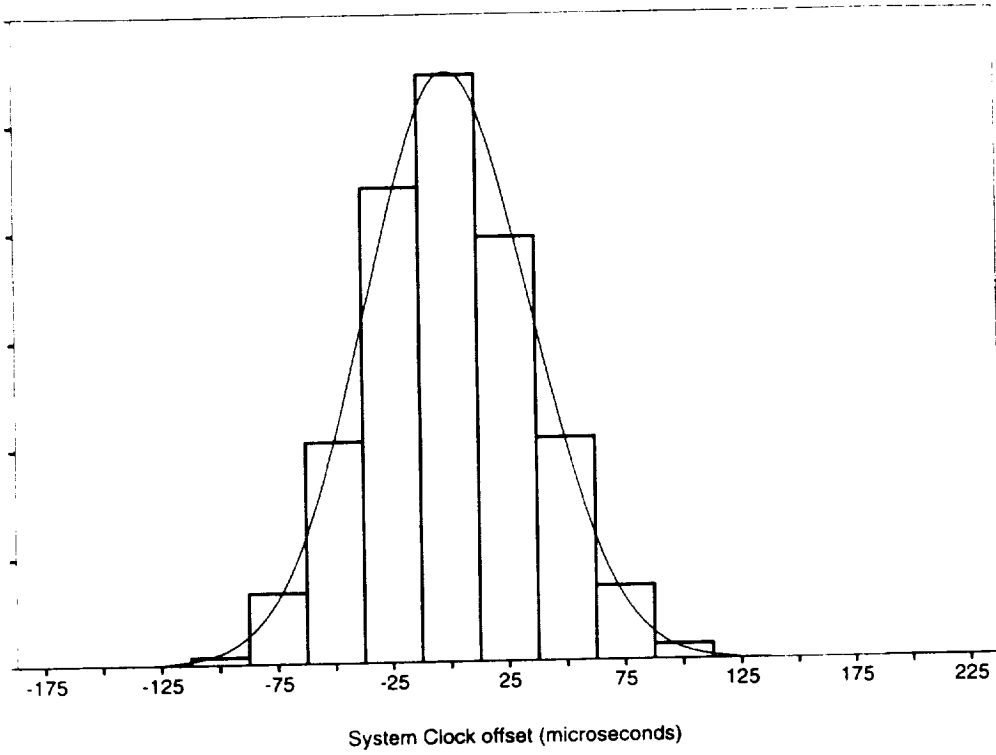
Washington, DC - Miami, FL

Aug. - Nov. 1994



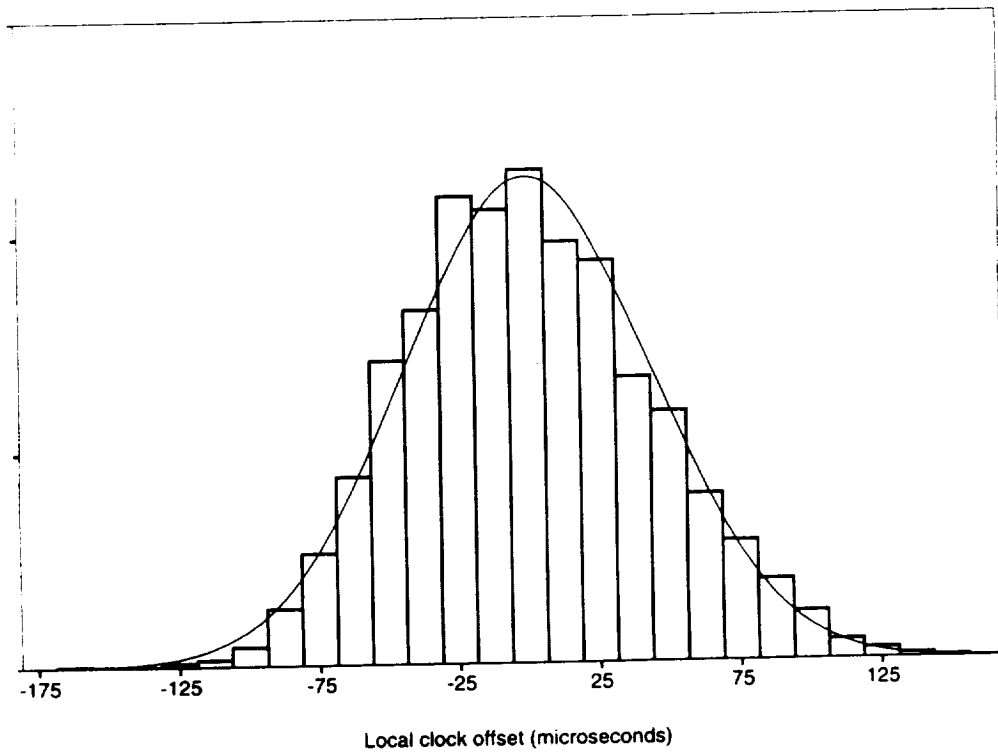
### Server Clock - UTC(USNO)

tick.usno.navy.mil



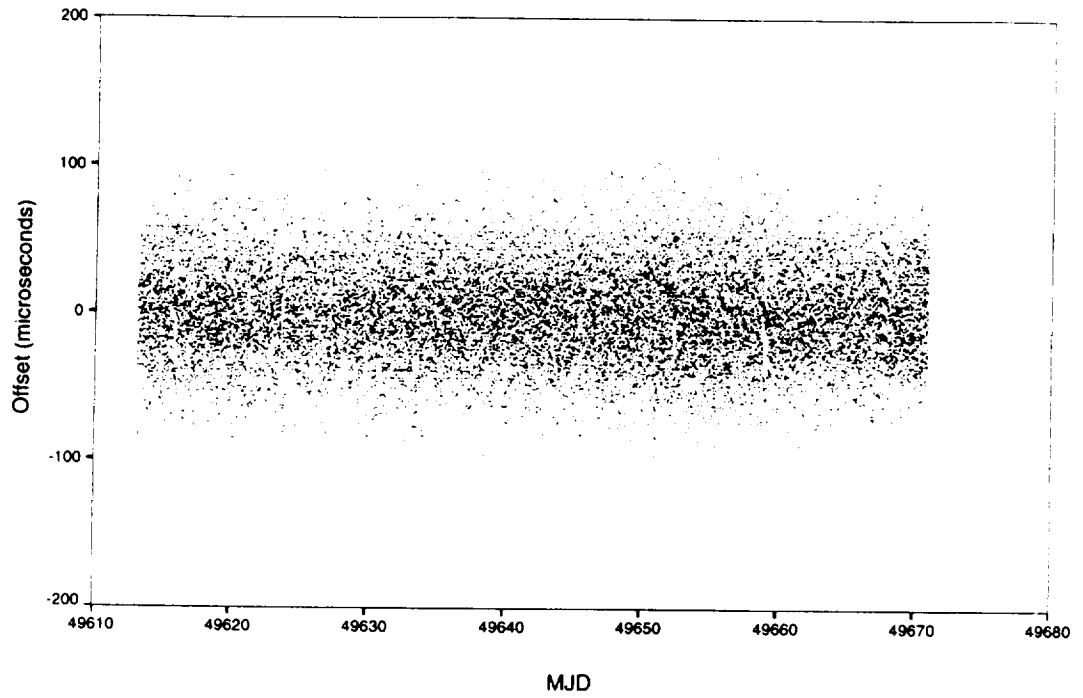
### Server Clock - UTC(USNO)

tock.usno.navy.mil



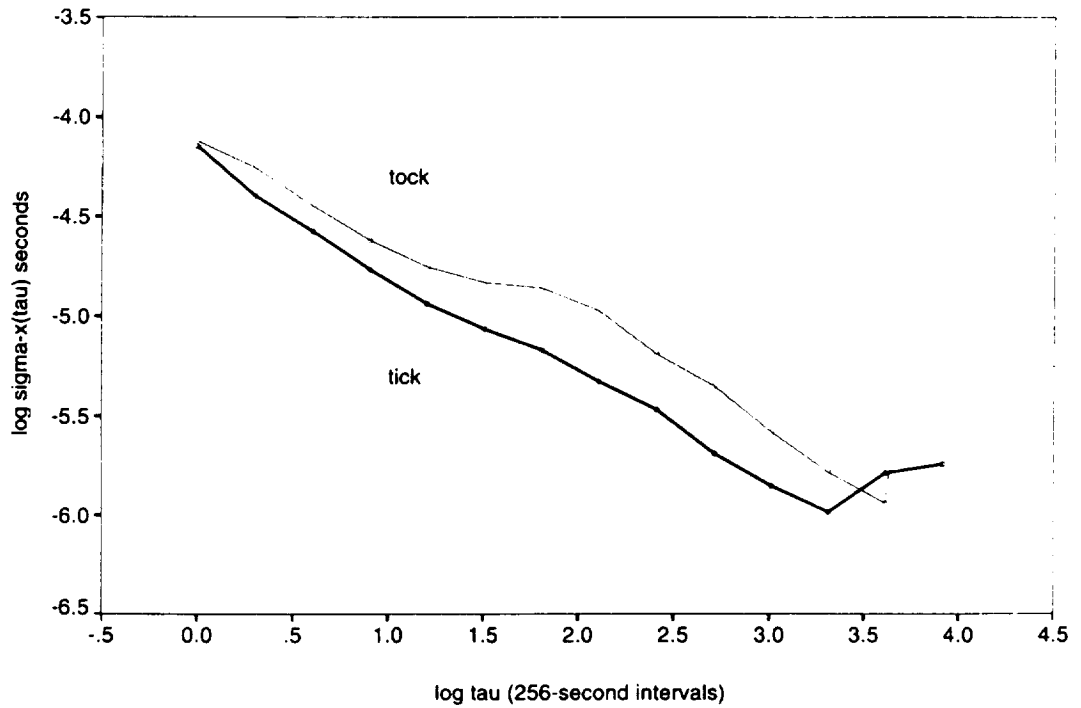
# Server Local Clock Offset

## Tick - UTC(USNO)



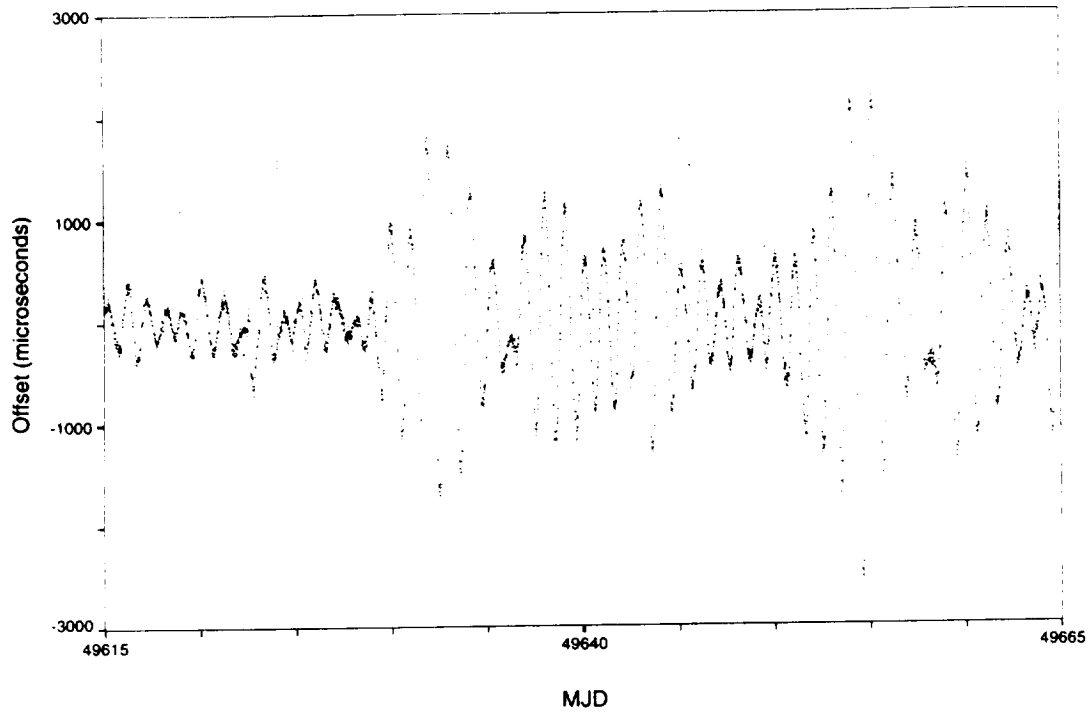
# TDEV Stability, NTP Servers

Time Servers' Local Clock - UTC(USNO)



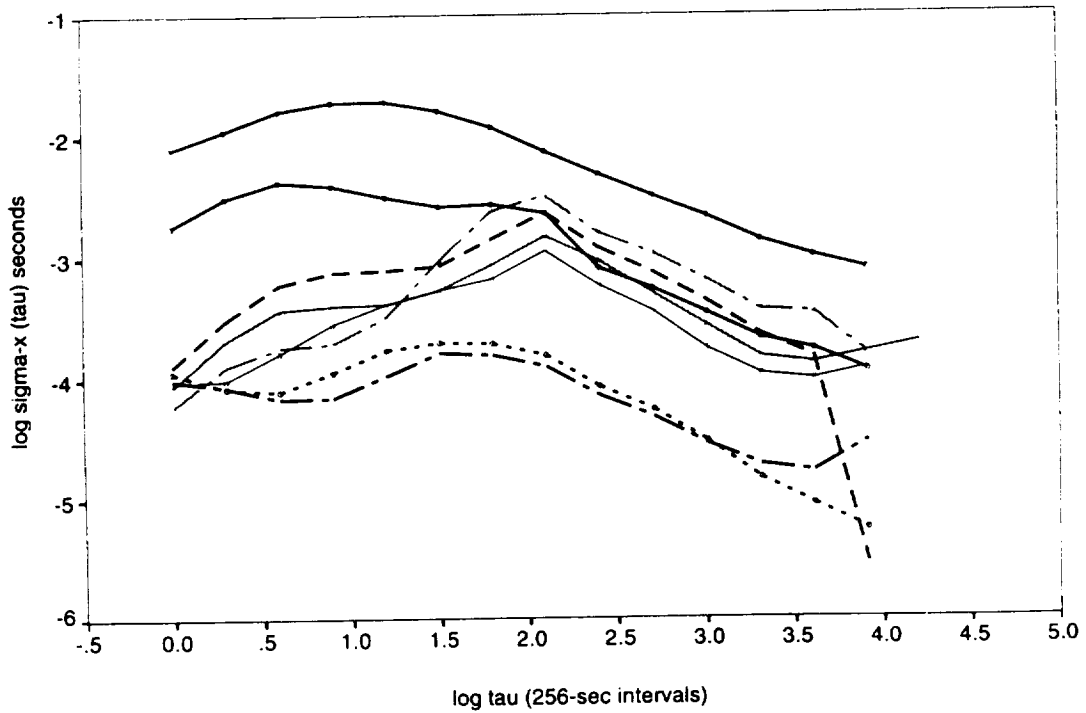
# Diurnal Modulation of Local Client

cassini.usno.navy.mil



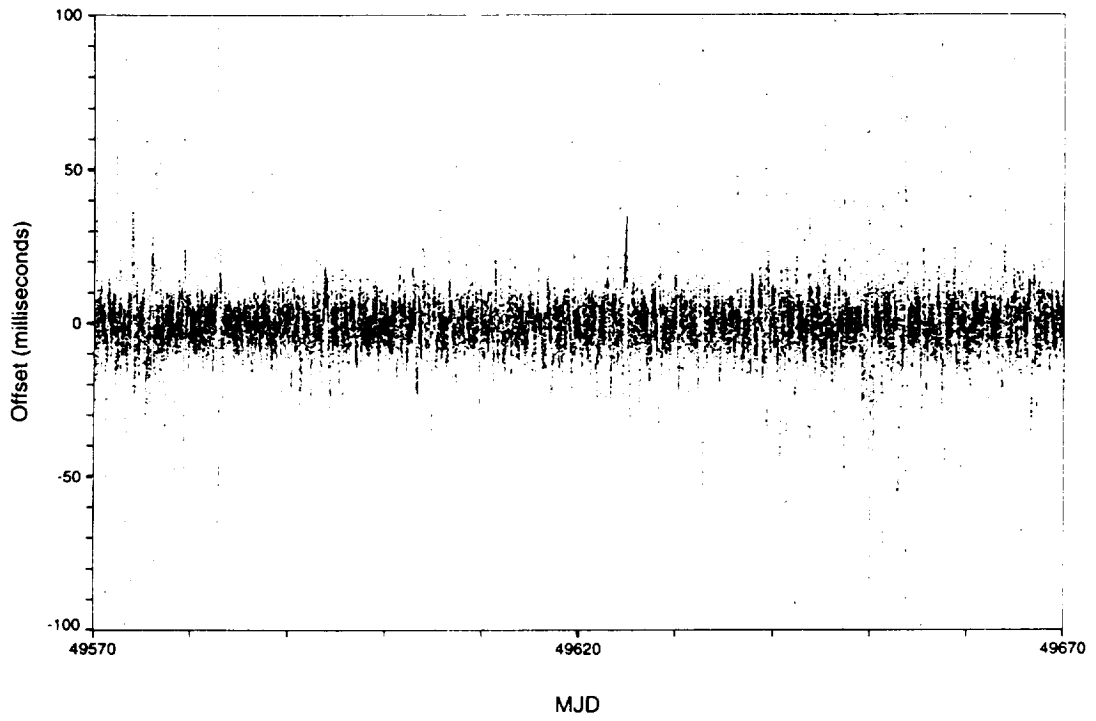
# TDEV Stability, NTP Clients

Local USNO Lan Clients



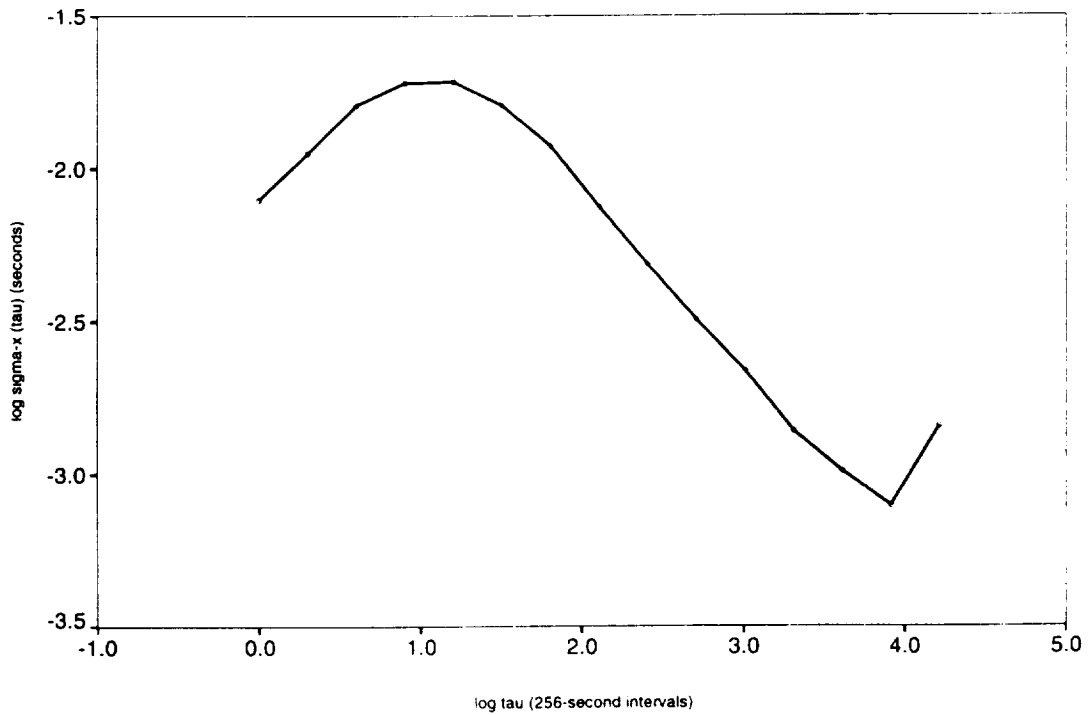
# Long-distance NTP Synchronization

Washington, DC - Miami, FL



# TDEV Stability, Long-distance NTP

Washington, DC - Miami, FL





# CUSTOM TURNKEY TIME & FREQUENCY SYSTEMS

## A STRUCTURED, EXPANDABLE APPROACH

David F. Wright  
Radiocode Clocks Ltd.  
Kernick Road  
Penryn  
Cornwall, TR10 9LY.  
United Kingdom.

### Abstract

*Radiocode Clocks Ltd. have developed a Turnkey Time and Frequency Generation and Distribution System strategy based upon a bus of three, "core" signals from which any Time code, Pulse rate or Frequency can be produced. The heart of the system is a ruggedized 19 inch, 3U Single Eurocard chassis constructed from machined 10mm aluminum alloy plate and designed to meet stringent Military, Security and Telecommunications specifications. The chassis is fitted with an advanced multilayer backplane with separate ground planes for analog and digital signals ensuring no degradation of low noise frequency references in the proximity of high speed digital pulse transmissions.*

*The system has been designed to be used in three possible configurations:*

- a) As a stand alone generation and distribution instrument.*
- b) As a primary distribution unit in a turnkey Time and Frequency system.*
- c) As a secondary distribution unit at a remote location from the Turnkey Time and Frequency System providing regeneration of core signals and correction for transmission delays.*

*When configured as a secondary distribution unit the system will continue to provide usable outputs when one, two or even all three of the "core" signals are lost.*

*The instrument's placement within a system as a possible single point of system failure has required the development of very high reliability translator, synthesizer, phase locked loop and distribution modules together with a comprehensive alarm and monitoring strategy.*

## INTRODUCTION

The requirements for sources of Precise Time and Frequency have grown substantially in recent years, not just in the number of projects but also in their complexity. An increasing number of users are specifying redundancy, high reliability, expandability and a plethora of Time code, Pulse rate and Reference frequency outputs in their systems. In dual or triple

redundant configurations the switching, monitoring and alarm management of such a myriad of signals can become technically complex, commercially expensive and, in many cases, can reduce system availability. This, coupled with the tightening of international standards with regard to electromagnetic compatibility, electrical safety and product quality, has led to the development of a new strategy for Time and Frequency distribution.

## SYSTEM ARCHITECTURE

Traditionally, when designing a turnkey distribution system, two or three master clocks, frequency standards or time code generators are fitted with one of each required system output. In some complex cases an atomic frequency standard will provide a stable reference frequency to a pair of low noise quartz oscillators via individual frequency or phase locked loops. These oscillators then produce one of each of the required frequency outputs which are fault detected and switched to a frequency distribution unit, while a GPS or Off-air master clock synchronizes two or three time code generators, each of which produces one of every required time or time interval output. These in turn, are majority voted, fault detected and switched to a timing buffer or distribution unit.

The addition of features such as secondary power supplies, alarms and output monitoring quickly make the system difficult to use, very inflexible, costly to manufacture and support and inefficient in terms of spares ranging.

Our solution to these problem has been to reduce the number of switched signals to an absolute minimum and to use these "core" signals as references with which to generate the required system outputs. Using conventional copper or fiber optic technology the minimum "core" signal count is three, a 1 Pulse per second (1 PPS) epoch marker, a 10MHz reference frequency and a proprietary format RS422 time message.

These "core" signals are generated by one or more Time and Frequency Standards such as GPS or Off-Air receivers, free running atomic or quartz clocks or a combination of the above. The "core" signals, plus alarm and status signals from the master time and frequency source are fed to an intelligent monitor and changeover unit which will fault detect, majority vote and switch between sources. This unit also acts as a system alarm manager. The selected "core" signals are then fed to a high reliability, modular distribution chassis based upon a single Eurocard format and fitted with dual power supplies, an alarm management module, an input/expansion module and a backplane accommodating the "core" signals, power lines, alarm signals and inter-module control signals.

Because there are also smaller applications, where a single distribution chassis is sufficient and the use of an external source of time and frequency is not always necessary, a range of "core" signal generation modules, which could obtain time from an external reference, has been developed for the distribution system. These modules now include GPS, Loran, WWVB, MSF and DCF receivers, together with free-running master time and frequency sources.

Historically, the distribution of low noise frequencies and digital signals has been undertaken using two separate chassis. As this approach was considered cumbersome, a single chassis architecture was developed for the distribution of all time and frequency signals while maintaining

the quality of the outputs. This has been achieved by developing an advanced multilayer backplane with high isolation and separate ground planes for analog and digital signals allowing high speed pulse trains and low-noise frequencies to be processed in close proximity without any significant degradation in signal quality.

High reliability modules have also been developed which accept the required signals from the backplane and translate, synthesize and distribute virtually any Time and Frequency signal. Most modules are 4E wide and provide five isolated outputs of each signal. The Input module has been developed to provide expansion outputs of the “core” signals so that when the chassis is fully populated, additional modules can be added by simple connection of further chassis allowing virtually infinite expansion capabilities without having to modify or reconfigure all the instruments in the system.

Another important design consideration was the provision of high stability, very low noise reference frequencies within the distribution system. Good long and medium term stability can be achieved by using a Cesium standard or GPS-disciplined Rubidium atomic oscillator but typical specification requirements of  $1 \times 10^{-12}$  over 24 hours,  $1 \times 10^{-11}$  over 1 second, and phase noise below 110 dBc/Hz at 1 Hz offset from carrier could only be achieved by the use of a high quality ovenized quartz oscillator phase locked to the “core” 10 MHz signal.

Our standard PLL module uses a number of novel techniques to implement the well proven second order phase locked loop that has the required characteristics. In the short term, up to some tens of seconds, the phase locked loop’s ovenized oscillator frequency can be more stable than the “core” signal; for this reason the phase locked loop is designed to have a time constant of about one minute. For longer time periods the loop holds the oscillator in phase with the 10MHz reference. Time constants of that order can be realized using analog techniques but when the requirement for “holdover” operation on loss of reference is considered the use of digital control becomes mandatory. A microprocessor controlled loop provides sophisticated solutions for all of the control problems but has inferior reliability performance. Worse still, the processor generates a broad spectrum of noise signals which are unwelcome in a module whose primary purpose is to provide high quality, low noise analog signal outputs.

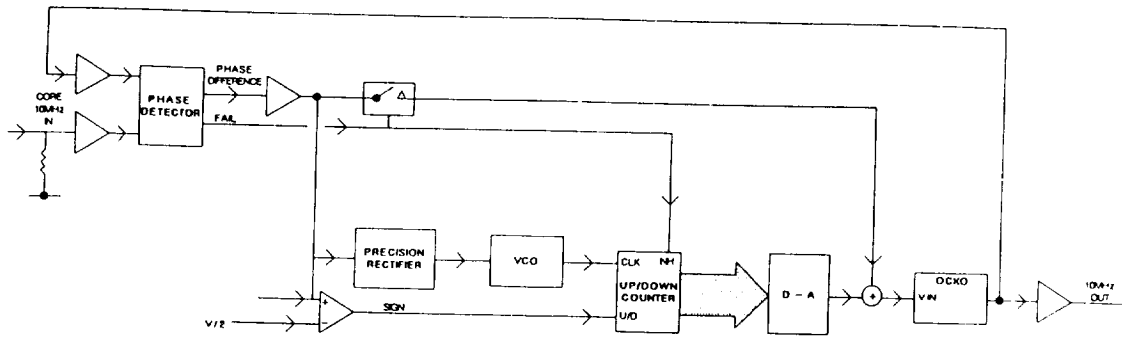
The solution we have developed for this system is part analog, part digital proportional and integral control. The control loop error signal is formed by direct phase comparison of the 10MHz “core” signal and the local ovenized oscillator in a circuit which is effective over more than 320 degrees of phase, almost a whole cycle at 10MHz. The magnitude of the phase difference provides the control signal for a low frequency voltage controlled oscillator which clocks a 16 bit up/down counter. The sign of the phase difference determines the count direction. The counter outputs connect to a 16 bit DAC which provides the integral part of the loop control signal. When the phase difference has been driven to zero in a steady state condition the up/down counter ceases to be clocked and no other clock signals are active in the control system.

The integrator can set the ovenized oscillator control voltage anywhere in it’s entire range but the largest proportional control contribution required has only a fraction of the value of the control range. This signal is a fraction of the loop error signal already derived from the phase detector; it is fed through an analog switch and summed with the signal from the DAC to form

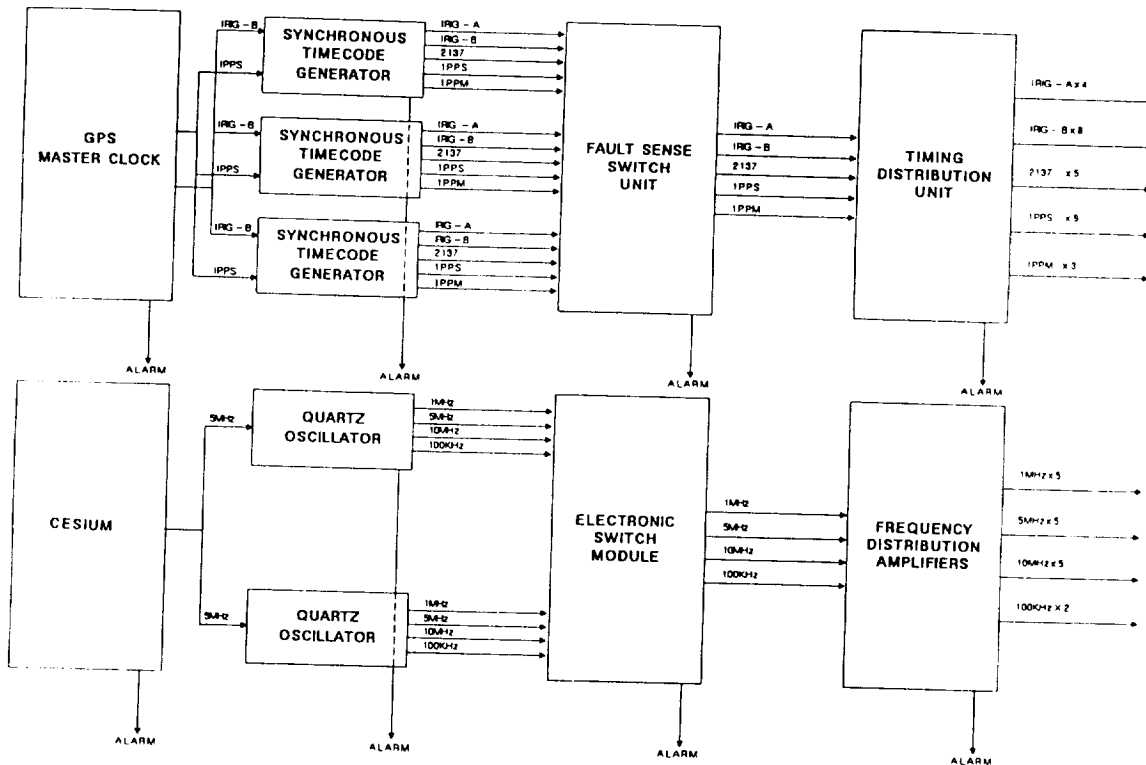
the ovenized oscillator control voltage.

The proportional control is immediately active at a low level in response to a loop error; the integral control works to drive the phase to zero in the longer term. If the “core” 10MHz reference is lost then the integrator has the correct value to hold the oscillator at the last best control value indefinitely. The digital parts of the circuit fit readily into programmable logic and the controller adds no clock noise to the OCXO output.

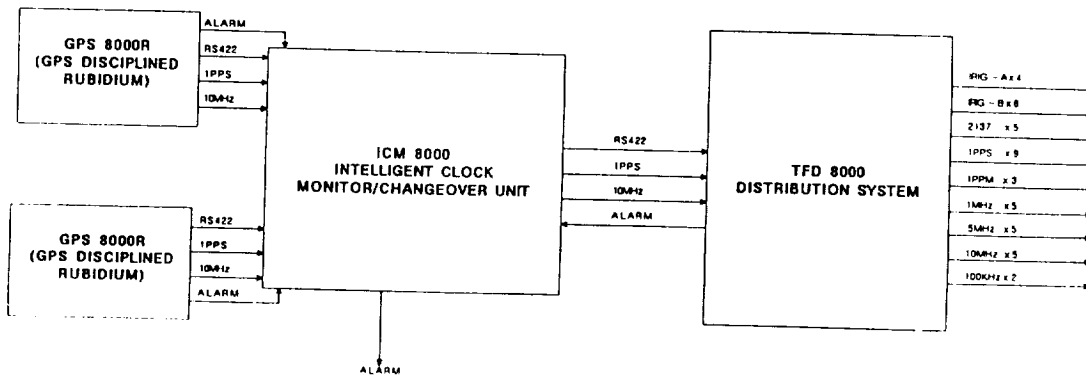
Development of the Low Noise Phase Locked Loop Oscillator Module has provided us with a new time and frequency distribution sub-system, the TFD8000. This is now considered not only a product but a new strategy providing a structured, expandable approach to turnkey system design which has already proved cost-effective, reliable and easy to maintain in applications within the Defense, Security and Telecommunications Industries.



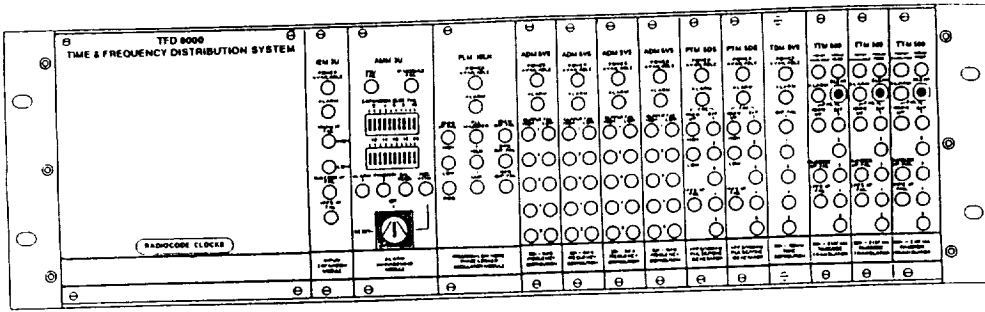
PHASE - LOCKED LOOP MODULE



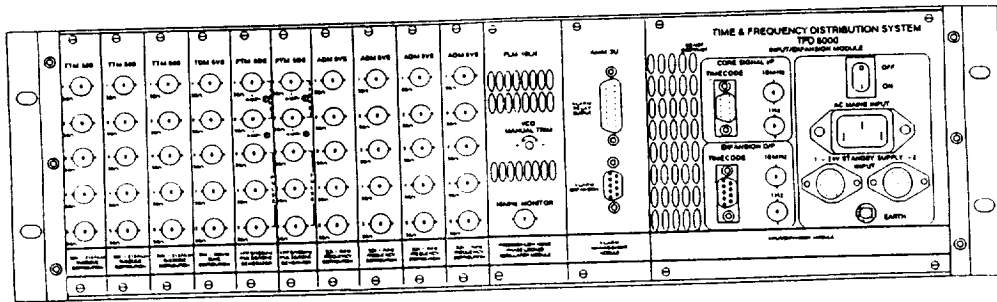
TRADITIONAL TIME & FREQUENCY SYSTEM



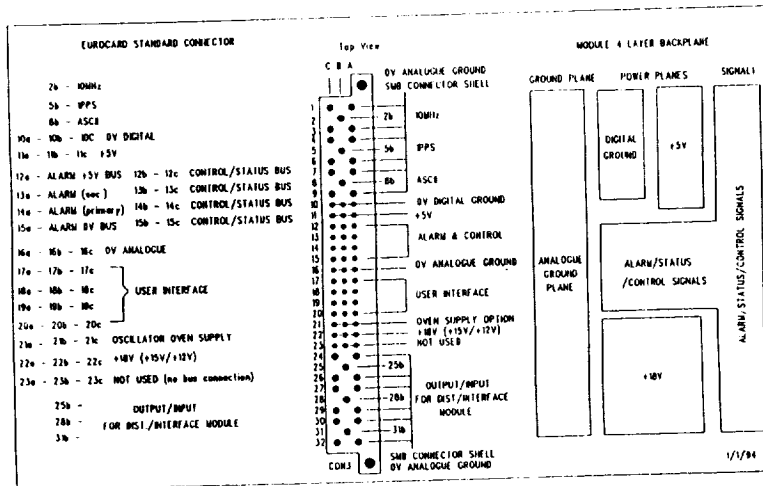
MODERN TIME & FREQUENCY SYSTEM



FRONT PANEL TYPICAL SYSTEM CONFIGURATION



REAR PANEL TYPICAL SYSTEM CONFIGURATION



TYPICAL BACKPLANE CONFIGURATION

# High Resolution Time Interval Counter

Victor S. Zhang, Dick D. Davis, Michael A. Lombardi  
Time and Frequency Division  
National Institute of Standards & Technology  
325 Broadway, Boulder, CO 80303

## Abstract

*In recent years, we have developed two types of high resolution, multi-channel time interval counters. In the NIST two-way time transfer MODEM application, the counter is designed for operating primarily in the interrupt-driven mode, with 3 start channels and 3 stop channels. The intended start and stop signals are 1 PPS, although other frequencies can also be applied to start and stop the count. The time interval counters used in the NIST Frequency Measurement and Analysis System are implemented with 7 start channels and 7 stop channels. Four of the 7 start channels are devoted to the frequencies of 1 MHz, 5 MHz or 10 MHz, while triggering signals to all other start and stop channels can range from 1 PPS to 100 kHz. Time interval interpolation plays a key role in achieving the high resolution time interval measurements for both counters. With a 10 MHz time base, both counters demonstrate a single-shot resolution of better than 40 ps, and a stability of better than  $5 \times 10^{-12}$  ( $\sigma_x(\tau)$  after self test of 1000 seconds). The maximum rate of time interval measurements (with no dead time) is 1.0 kHz for the counter used in the MODEM application and is 2.0 kHz for the counter used in the Frequency Measurement and Analysis System. The counters are implemented as plug-in units for an AT-compatible personal computer. This configuration provides an efficient way of using a computer not only to control and operate the counters, but also to store and process measured data.*

## Introduction

Time interval measurements are essential not only to the analysis of a time scale or a frequency standard, but also to the synchronization of time scales at remote locations. Many of these measurements require a time interval counter with better than 100 ps resolution. The technology advancement in electronics and in personal computers makes it possible to have such high resolution time interval counters at fairly low costs.

Two types of high resolution, multi-channel time interval counters have been developed at NIST in recent years. One of them is used in the NIST spread spectrum two-way time transfer MODEM<sup>[1]</sup> (MODEM counter); the other one operates in the NIST Frequency Measurement and Analysis System<sup>[2]</sup> (FMAS counter). Both counters are designed to make time interval measurements on more than one pair of start/stop signals input from different channels. The measurements are taken at rates ranging from 1 Hz to a maximum of 100 kHz. Instead of having a microprocessor for each counter, the counters are implemented as plug-in units for an

AT-compatible personal computer. The counters are controlled by software. This configuration provides an efficient way of using a computer not only to control and operate the counters, but also to process and store data. Although the two counters are designed for a specific application, the software can be easily re-programmed so that the counters can perform as a universal time interval counter, or for customized applications. To obtain accurate and stable measurements, a stable reference frequency of either 1 MHz, 5 MHz or 10 MHz is required for both counters. The estimated cost of parts for either a MODEM counter or a FMAS counter is around \$500.

The MODEM counter and the FMAS counter are different in some respects; the FMAS counter offers more capability in terms of simultaneous time interval measurements. However, they have one thing in common. Both use time interval interpolation to achieve the high resolution time interval measurements. This paper presents a discussion of the time interval interpolation technique, and a description of each counter's operation and performance.

## Time Interval Interpolation

Every digital time interval counter uses an oscillator (counter clock) to provide a time base for the time interval measurement. The time interval between start-count and stop-count signals  $\Delta t$  is measured by the counter as an integer multiple of the time base period; that is,

$$\Delta t = NT, \quad (1)$$

where  $N$  is the number of clock periods recorded by the digital counter in the interval and  $T$  is the period of the counter clock or the time base of the time interval measurement. In general,  $NT$  is only an approximation (the main portion) of  $\Delta t$ , because the start-count and stop-count signals are not in phase with the counter clock, as illustrated in Figure 1. Because both  $\delta t_1$ ,  $\delta t_2$  are less than  $T$ , they can not be measured directly by the digital counter. Therefore, the resolution of the digital counter measurement is dictated by the frequency of the time base. The resolution can be improved by increasing the frequency  $f = 1/T$  of the counter clock. However, this approach puts greater demands on the electronic devices and makes implementation more difficult.

Both the MODEM counter and the FMAS counter estimate the time intervals  $\delta t_1$ ,  $\delta t_2$  to achieve the high resolution time interval measurement. The estimations of  $\delta t_1$ ,  $\delta t_2$  are accomplished by two interpolators. The interpolator scales  $\delta t_1$  or  $\delta t_2$  into a magnified time interval and then estimates the interval with the time base  $T$ .

A block diagram of a simplified start-count interpolator is depicted in Figure 2. The interpolator consists of two integrators, a delay cell, a voltage comparator, and a digital counter. Both integrators are charged with a constant current  $I_{REF}$ . The delay cell introduces a delay  $\delta t_1 + T$ , where  $T = 100$  ns and  $\delta t_1 < 100$  ns for the 10 MHz time base used in the counters. The function of the integrators and the delay cell is to scale  $\delta t_1$  into a larger time interval. The digital counter, together with the 10 MHz time base, is used to estimate the scaled  $\delta t_1$ . The arrival of the start-count signal turns on the charging current  $I_{REF}$  to Integrator A. At this

time, the digital counter begins to count the periods of the 10 MHz time base. Integrator A is charged in the period of  $\delta t_1 + T$  and the charging current  $I_{REF}$  is then switched to Integrator B. The voltage  $U_R$  developed on Integrator A is held as a reference voltage for the comparator during the course of Integrator B being charged. When  $V_B > U_R$ , the comparator blocks the connection between the 10 MHz clock and the digital counter. Figure 3 shows a timing diagram of the start-count interpolator, where  $C_A$  and  $C_B$  ( $C_A < C_B$ ) are the ramping capacitances used in Integrator A and Integrator B, and  $K = (C_A/C_B)$  is the scaling factor of the interpolator.

Because the 10 MHz time base is connected to the digital counter during the magnified time interval

$$K \cdot (\delta t_1 + T) = K \cdot T + K \cdot \delta t_1 , \quad (2)$$

the number of 10 MHz pulses recorded by the digital counter during that interval,  $N_{st}$ , is linearly proportional to the time interval of  $\delta t_1$ . The relationship between  $\delta t_1$  and  $N_{st}$  can be expressed by the linear equation

$$\delta t_1 = A \cdot N_{st} + B , \quad (3)$$

where the slope A and the intercept B are determined through the interpolator calibration. During the calibration, the minimum  $N_{st}$  and the maximum  $N_{st}$  are obtained by slewing the phase of a test signal with respect to the 10 MHz time base to simulate the different values of  $\delta t_1$ . Because the minimum  $N_{st}$  corresponds to  $\delta t_1 = 0$  and the maximum  $N_{st}$  corresponds to  $\delta t_1 = T$ , the slope and intercept of the interpolation are

$$A = \frac{T}{\max[N_{st}] - \min[N_{st}]}, \quad B = \frac{\min[N_{st}] \cdot T}{\max[N_{st}] - \min[N_{st}]} . \quad (4)$$

Therefore,

$$\delta t_1 = A \cdot N_{st} + B = \frac{N_{st} - \min[N_{st}]}{\max[N_{st}] - \min[N_{st}]} \cdot T . \quad (5)$$

This result is illustrated in Figure 4. Because

$$K = \left( \frac{C_B}{C_A} + 1 \right) = \max[N_{st}] - \min[N_{st}] , \quad (6)$$

the resolution of the interpolation is given by  $T/K$ . With  $T = 100$  ns,  $C_A = 150$  pF,  $C_B = 0.47$   $\mu$ F the resolution is

$$\frac{T}{\frac{C_B}{C_A} + 1} = \frac{100 \times 10^{-9}}{3134} = 32 \times 10^{-12} . \quad (7)$$

The function of the stop-count interpolator is the same as that of the start-count interpolator. It is applied to estimate the interval of  $T - \delta t_2$ . Because of this, the main digital counter takes one more 10 MHz pulse after the arrival of stop-count signal. By combining the main digital counter measurement  $NT$  and measurements of the two interpolators together, the time interval counter presents the measurement as

$$\Delta t = NT + \frac{N_{st}T}{\max[N_{st}] - \min[N_{st}]} - \frac{N_{sp}T}{\max[N_{sp}] - \min[N_{sp}]}, \quad (8)$$

where  $N_{sp}$  is the digital counter measurement of the stop-count interpolator.

The time interval interpolation has a side-effect of reducing the maximum sample rate of the time interval measurements. Assume that both start-count and stop-count interpolators have the same scaling factor so that  $\max[N_s] = \max[N_{st}] = \max[N_{sp}]$ . Because it takes  $\max[N_s] \cdot T$  to complete an interpolation, the time interval measurements can be made only at a rate  $< 1/(\max[N_s] \cdot T)$  in order to avoid dead time.

## The MODEM time interval counter

The NIST spread spectrum two-way time transfer MODEM is developed for synchronizing remote time scales through geostationary satellites. The accuracy of the two-way time transfer is expected to achieve sub-nanoseconds. This requires a high resolution time interval counter for the measurements. The MODEM counter is designed with two functions, and it is installed in an AT-compatible personal computer. The interface of the MODEM counter is used to link the transmit (TX) and receive (RX) of the MODEM to the computer which controls the operation of the MODEM and the counter. The time interval counter portion of the MODEM counter is configured to measure the 1 PPS from TX, RX, and local time scale. The characteristics of the MODEM counter are similar to that of the FMAS counter in terms of the time interval measurement, except that the MODEM counter has only three input channels and a maximum sample rate of 1.0 kHz.

## The FMAS time interval counter

The Frequency Measurement and Analysis System (FMAS) is a new frequency calibration and characterization tool developed at NIST in the past year. It is designed to be used at calibration laboratories or other institutions to perform on-site high-level frequency calibrations traceable to NIST. All the frequency measurements are made by the FMAS counter in terms of the phase differences between the oscillators being calibrated and their corresponding reference frequency source<sup>[3]</sup>. Table 1 lists the FMAS specifications which

Table 1.	
Number of measurement channels	5
Input frequencies accepted by system: Start-count channel (with Frequency Divider) Other Start-count channel and Stop-count channel	1, 5, and 10 MHz $\leq 100$ kHz
Primary Oscillator Frequency	1, 5, 10 MHz
Single Shot Measurement Resolution	$< 40$ ps

are relevant to the FMAS counter. A block diagram of the simplified FMAS counter in a typical FMAS application is given in Figure 5.

The FMAS counter offers 7 start-count channels and 7 stop-count channels for connection to the secondary oscillators. Four of the 7 start-count channels are designed for oscillators with 1, 5, or 10 MHz output frequencies. A frequency divider is used on each of these 4 channels to divide the 1, 5, 10 MHz input down to 1, 5, or 10 kHz. The time interval measurement can be started with any of the start-count channels and stopped with any of the stop-count channels by the control of start-count channel select and stop-count channel select. The time interval between the start-count and stop-count signals is measured by the main counter and the two interpolators with a 10 MHz time base. The 10 MHz time base VCXO is locked to a primary oscillator of 1, 5, 10 MHz. Because it takes approximately 0.4 ms for the FMAS counter's interpolators to complete a time interval interpolation, the FMAS counter is able to make the time interval measurements of a single pair of start-count and stop-count signals at the rate of 2.0 kHz with no dead time. The maximum time interval of the main counter is about 429 s. Besides resolution, stability is another important characteristic of the counter. Figure 6 and Figure 7 show a typical result of the FMAS counter stability through self test measurements. Resolution of the time interval measurement should not be confused with the absolute accuracy of the time interval measurement. The accuracy of a time interval counter is influenced by many factors including the resolution. Our test results have shown both the MODEM counter and the FMAS counter have an accuracy estimated to be in the range of 200 ps to 300 ps, when used with a high quality primary oscillator.

According to the FMAS specification, the counter is configured to provide up to 5 of the 7 start-count channels for the secondary oscillators. The phase of a 1, 5, 10 MHz input signal can be shifted by integer multiples of  $10 \mu\text{s}$  with respect to the time base. The phases of all the secondary oscillators can also be shifted with respect to the phase of the time base by multiples of 100 ns. The phase shift is necessary in order to avoid the underflow or overflow measurements caused by the fast drift of the secondary oscillator. One of the direct (without the divider) start-count channels and one of the stop-count channels are connected to the 500 kHz output of the 10 MHz time base for the diagnostic purposes. Because all the secondary oscillators are calibrated with respect to the primary oscillator, and because the 10 MHz time base is locked on the primary oscillator, all the time interval measurements are stopped by the 10 kHz signal derived from the 10 MHz time base. The counter's operation and measurements are fully controlled by the FMAS software. Up to 5 secondary oscillators can be calibrated simultaneously.

## Summary

Time interval measurement is critical in the field of time and frequency standards. By combining today's technologies in electronics and personal computers, we have developed two types of high resolution time interval counter at low cost. Both counters have demonstrated a sufficiently high stability performance. Although the counters are designed for their specific applications, they can be readily to be modified for other applications.

## References

- [1] Dick D. Davis and Dave A. Howe, "*A Direct Sequence Spread Spectrum Modem Design*", 5th European Frequency and Time Forum, Besancon, March, 1991, pp. 89 - 95.
- [2] Michael A. Lombardi, "*The NIST Frequency Measurement Service*", unpublished paper submitted to Measurement Science Conference, Jan., 1995.
- [3] D. B. Sullivan, D. W. Allan, D. A. Howe, and F. L. Walls, editors, **Characterization of Clocks and Oscillators**, NIST Technical Note 1337, 1990.

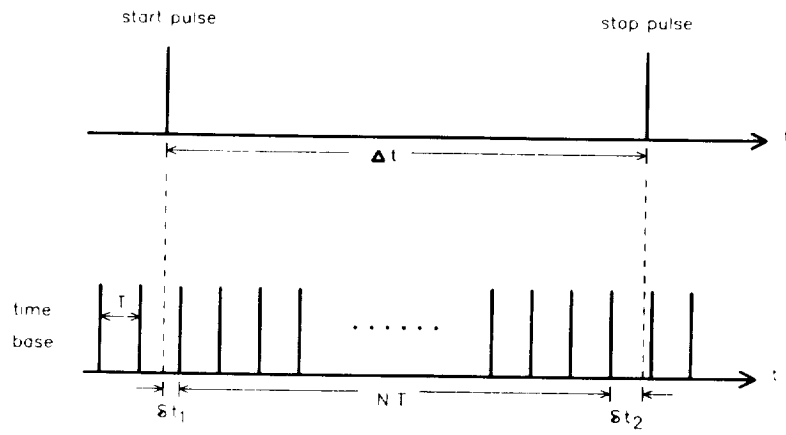


Figure 1. Time interval measurement by digital counter

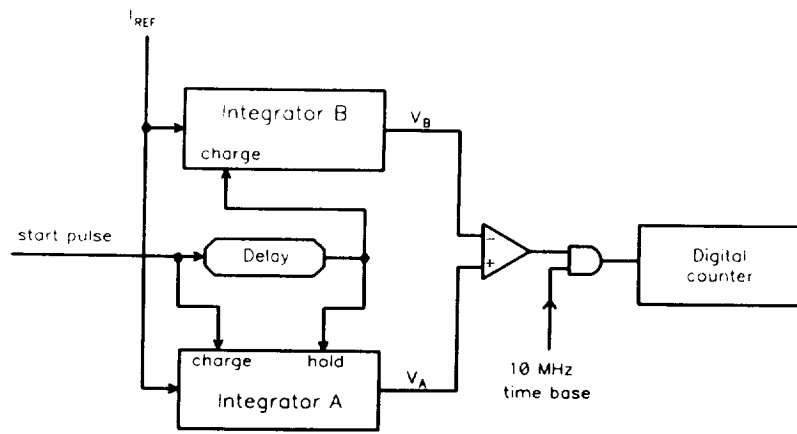


Figure 2. Block diagram of start-count interpolator

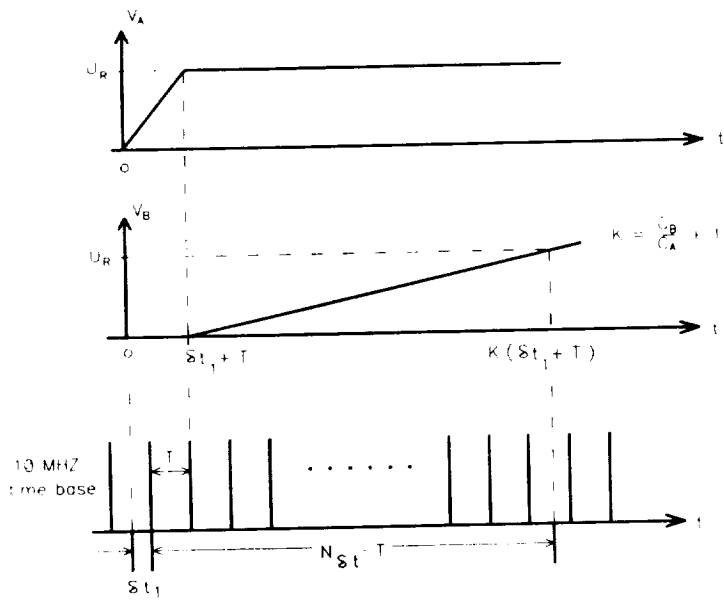


Figure 3. Timing diagram of start-count interpolator

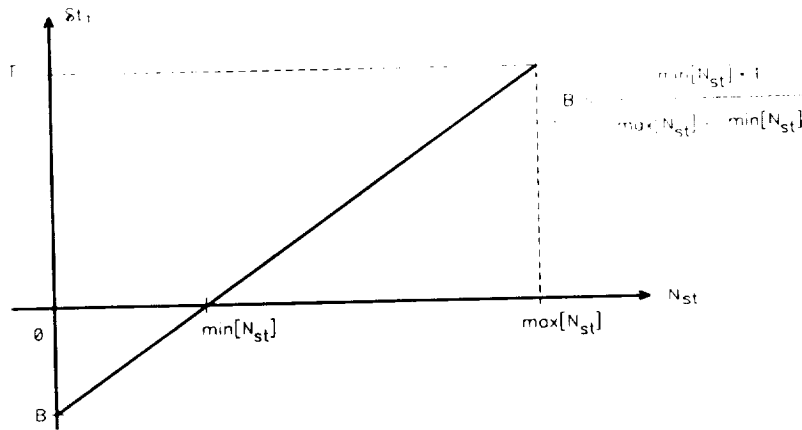


Figure 4. Time interval interpolation

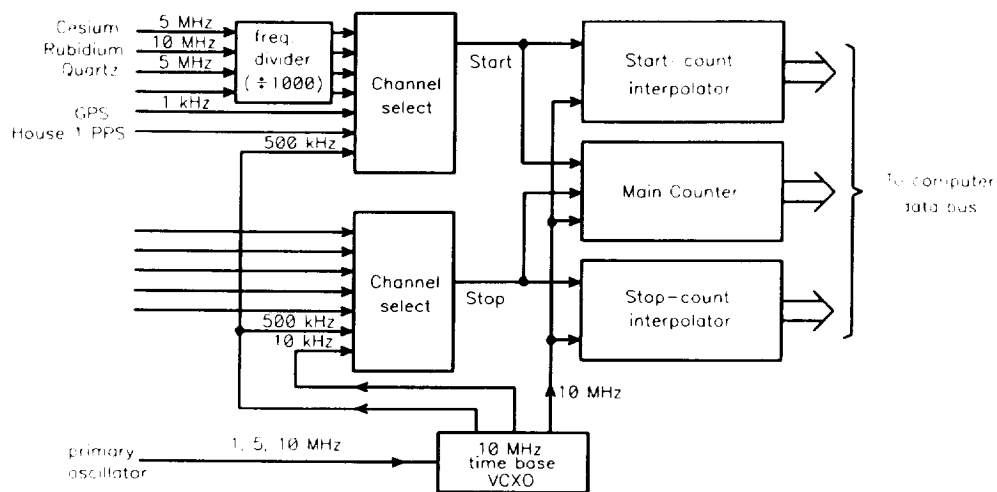


Figure 5. Block diagram of FMAS counter

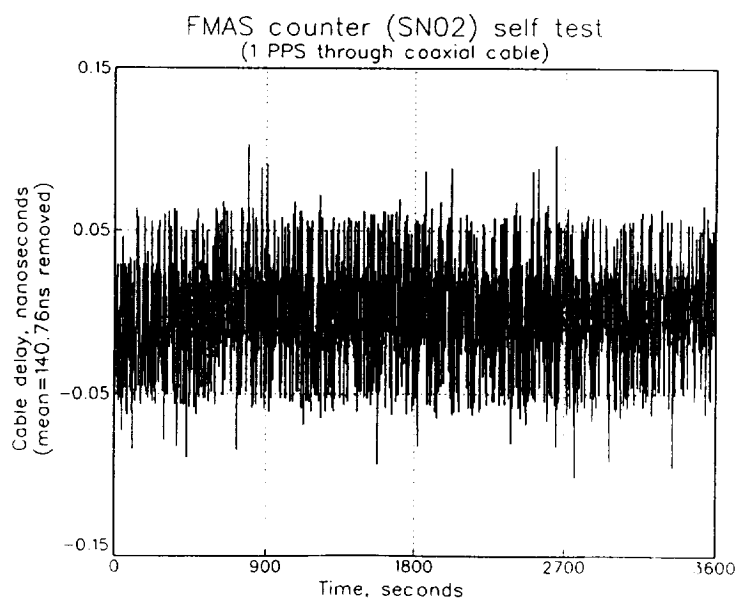


Figure 6. FMAS counter self test measurements

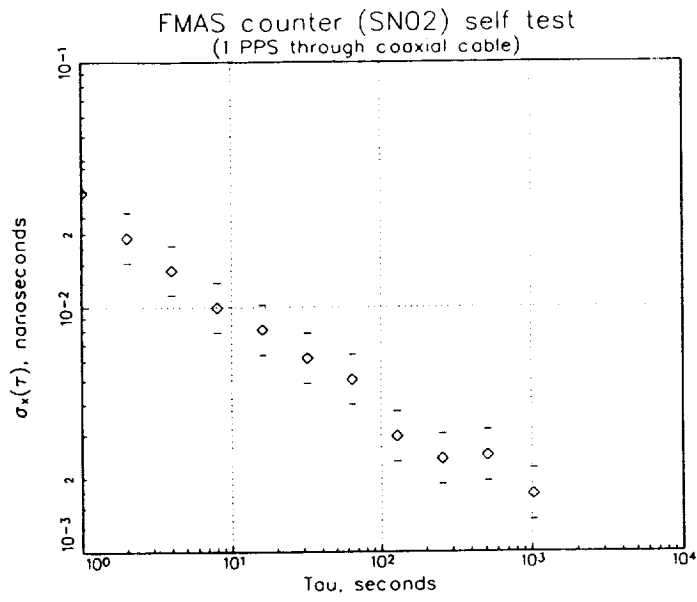


Figure 7.  $\sigma_x(\tau)$  of FMAS counter self test

2017  
P 8

# INVESTIGATION INTO THE EFFECTS OF VHF AND UHF BAND RADIATION ON HEWLETT-PACKARD (HP) CESIUM BEAM FREQUENCY STANDARDS

Andrew Dickens  
United States Naval Observatory  
and  
University of Virginia

## Abstract

*This paper documents an investigation into reports which have indicated that exposure to VHF and UHF band radiation has adverse effects on the frequency stability of HP cesium beam frequency standards. Tests carried out on the basis of these reports show that sources of VHF and UHF radiation such as two-way hand held police communications devices do cause reproducible adverse effects. This investigation examines reproducible effects and explores possible causes.*

## I. INTRODUCTION

The need for a reliable frequency standard is common for both Department of Defense and industrial applications. The Hewlett-Packard 5061A and 5061B Cesium Beam Frequency Standards have widespread use fulfilling the need for these frequency standards.

The DoD Timing Operations Division of the U.S. Naval Observatory (USNO) undertakes the delivery and installation of cesium beam frequency standards on select Navy vessels. During some of these installations, the installed clock was observed to jump unexpectedly. On occasion, the alarm lamp would illuminate. After searching for a possible cause for these events, it was noted that these fluctuations could be correlated with instances where personnel had used hand held transceivers in the proximity of the clock. The suspicion that electromagnetic radiation may be responsible for a change in the performance of the Hewlett-Packard frequency standards led to the decision to embark upon a more thorough investigation of this phenomenon.

## II. PRIMARY EFFECTS OF VHF AND UHF BAND RADIATION

The first task undertaken in the course of this research was to ascertain if radio frequency (RF) radiation had a noticeable and reproducible effect on the frequency stability of the HP cesium

beam frequency standards. Since the hand held transceivers were the suspected interfering devices, an experiment was formulated to imitate this situation.

In order to evaluate the effect on frequency stability, it was desired to see how the time interval between the clock and a known stable reference varied when RF radiation was introduced. An HP 5061B was obtained and placed in the test configuration shown in Figure 1. The 5 MHz output of this clock was compared with a 5 MHz signal derived from the USNO Master Clock (USNO MC). The time interval between these two signals was measured with an HP 5370B time interval counter (which utilized a reference frequency also derived from the USNO MC) and recorded on a desktop computer. This test setup is shown in Figure 3.

A two watt hand held UHF radio, operating on a frequency of 462.575 MHz, was obtained. This radio is of the type often used for job site communication. After obtaining the natural rate of the clock, the UHF radio was placed five feet from the front of the clock and keyed. The time interval between the clock under examination and the USNO MC was recorded several times per second by the data acquisition system (DAS). The collected time interval data clearly showed that the rate of the clock accelerated dramatically from the normal rate when the UHF radiation was applied, and returned to its normal rate after the radiation ceased. This response of the 5061B is shown in Figure 2. The time offset that had been acquired while the RF was present remained. Repeated tests of varying lengths were conducted and produced similar results.

In order to ensure that the data collected was indicative of the effect of the RF on the clock, not on the counter, the effect of the RF energy on the counter's measurements had to be recorded. The start and stop inputs to the counter were fed with different lengths of cable connected to the USNO derived 5 MHz source. The different lengths of cable provided a stable, fixed time interval (TI) to measure. The TI data output of the counter was recorded for five minutes to record any natural fluctuations. Then the UHF radio was placed in contact with the counter and keyed as the computer continued to record the time interval measurements. After ten minutes, the radio was turned off and the counter was observed for five more minutes. Fluctuations in the TI data were seen while the RF was present, but they were well below the levels of fluctuation seen when recording the time interval between the clock and the reference frequency. The counter did not acquire a permanent offset from the Master Clock as the HP frequency standard had. In order to minimize the effect of the RF on the accuracy of the counter's measurements, precautions were taken to keep the counter on a grounded surface at least ten feet away from the radiation source and shielded from direct RF exposure by the metal cases of other equipment. Care was also taken to keep the coaxial connections short and away from the source of radiation.

The above experiment was repeated with the VHF radios used by the USNO Police, operating on a frequency of 140.3MHz, and similar results were observed. Unfortunately, it was only possible to borrow these radios for a short length of time.

### III. FREQUENCY AND POWER DEPENDENCE

Having established that the HP 5061B cesium standard was sensitive to RF radiation, it was of interest to explore the dependence of this effect on the frequency and power of the RF energy. A Fluke 6080 RF signal generator was used as the source of RF energy. The output of the signal generator was fed to a straight wire antenna one foot five inches in length, placed two feet in front of the clock under examination. The DAS program was modified to perform the following procedure. First, the clock was monitored for a length of time with the RF output silenced. Then, the program activated the signal generator and set the frequency to the first frequency of interest. After monitoring the clock for a specified period of time, the program changed the frequency of the signal generator to the next frequency of interest. When all the selected frequencies had been monitored, the signal generator output was silenced and the clock was monitored for a specified period of time. The power of the signal was left constant throughout the sweep. All program parameters were entered by the user, making this a very flexible DAS. This experiment setup is shown in Figure 4.

In order to know the real RF strength that was incident upon the clock for any frequency, the frequency response of the antenna needed to be calculated. A matched straight antenna was fabricated and was placed two feet away, parallel to the transmitting antenna. The receiving antenna was connected to an HP 8562 spectrum analyzer. The magnitude of the signal at this antenna was recorded as the signal generator was swept across the frequency band of interest. The matched nature of these antennas allows correction to be made for the characteristics of the antenna. The frequency response plot is shown in Figure 5.

It was found that the clock exhibited sharply accelerated rates around two particular frequencies (Figure 1). The first was at 128 MHz, and the second was around 150MHz.

### IV. INVESTIGATION OF POSSIBLE CAUSES

The investigation now turned to isolating areas within the clock that are sensitive to RF radiation. The general strategy was to observe the signals at various points within the clock both under normal conditions and while the clock was exposed to RF radiation. The nature of some of these signals made observation on an analog oscilloscope difficult, necessitating the use of a digital oscilloscope (HP 54504). In order to isolate stages of the control feedback loop, the links between subassemblies were removed as required. The test points of interest could then be observed both before and during radiation. Particular care was taken to discriminate between those effects that were caused by the RF radiation and those that were caused by the modification of the feedback circuits. Such discrimination was made easy by the fact that the RF source could be turned on and off at will.

The following sections describe the effects noted at several points within the clock and the causes that they tend to imply.

#### A DC Control Voltage and Synthesized Frequency.

The DC control voltage took on a very large negative value when the UHF radio was placed near the clock. When the UHF radio was at a distance of two feet, the control

voltage was measured at approximately -300mV. The output from the external Synth jack did not appear to be affected even when the radio was in very close proximity to the clock. The Fluke signal generator was used to trigger the scope in order to determine if there was a phase shift in the synthesizer test point signal when the RF was applied. No such phase shift was observed, even after the clock's alarm light was illuminated.

#### B A7 AC Amplifier Assembly and A8 Phase Detector Assembly.

The AC error signal at test point J6 on the A7 AC amplifier module was seen to produce a large sinusoidal wave form of greater than 1.9 V peak-to-peak when the handheld radio was keyed nearby. The 274 Hz monitor point J2 normally showed a sinusoidal wave form which became mixed with an irregular sawtooth wave form with many transients when the radio was keyed.

The error signal available at test point J1 on the A8 phase detector assembly jumped to a peak voltage of nearly 3 V when the RF was applied. When the link between point J4 on the A7 assembly and J3 on the A8 assembly was removed, the A8 module showed much less response to RF, even when the handheld radio was placed nearly in direct contact.

An A7 assembly identical to that in the clock was obtained. The output from this unit, which was powered by two DC power supplies, was observed. The unit showed a very strong response to RF energy. When RF was applied, a sinusoidal signal of approximately 137 Hz was obtained at test point J6. The unit drew a large amount of current when RF was applied. The current peaked when a +20 dBm signal from the straight wire antenna was placed one inch away, reaching nearly 3 amps. Even at a distance of three feet, a current of 0.5 amps was still drawn from the power supplies.

#### C Cesium Beam Tube.

Proceeding one more step backwards in the control loop, the signal output of the cesium beam tube was examined. When radio frequency radiation from the signal generator was applied to the clock, a sinusoidal component with the same frequency as the RF source was seen at the output. This output signal was very noisy as viewed on the oscilloscope. With the oscilloscope set to repetitive mode, a wave form that was much more clearly defined was built up. At 200 MHz, the output RF voltage was about 63 mV peak-to-peak. At 150 MHz, the maximum voltage was seen at 150 mV peak-to-peak. There was no apparent change in the RF voltage when the A1 assembly was removed from the feedback loop. There was also no apparent change in RF voltage when the link between the A3 Frequency Multiplier and the A4 Harmonic Generator was removed.

From these observations, it seems reasonable to conclude that the RF radiation is being introduced to the feedback loop through the cesium tube assembly. It is quite possible that the high-voltage power supplies provide the means by which incoming RF radiation is transported into the cesium beam tube. While there is capacitive coupling to ground, it is in parallel with an inductance formed by the transformer. The combined reactance of these elements may form an oscillator at certain radio frequencies. At the frequencies of resonance, these capacitors would offer no protection against the transport of RF energy.

## V. POSSIBLE MODIFICATIONS TO EXISTING 5061 CLOCKS

To prevent radio frequency pickup in the cesium beam tube, it might be possible to place an RF choke coil in series with the DC outputs of the high-voltage supply modules. This will substantially increase the resistance seen by RF signals, and may decrease the RF component introduced into the tube. A high-voltage low-value capacitor placed after the choke coil would act to short any RF signal to ground while leaving the DC current unaffected. This modification would not affect the DC rectification circuit.

A more extensive modification would be to replace the transformer with a semiconductor-based voltage multiplication circuit, eliminating the inductive effect of the transformer coils. This may be a superior solution from an RF rejection standpoint.

It is probably not a practical option to filter the RF from the output of the cesium beam tube. In order to reject RF after the tube, an RF shunt capacitor could be run to ground. Unfortunately, this could affect the operation of the clock by introducing a phase shift in the signal. A more reasonable approach might be to use parallel narrow-band bandpass filters to allow only the desired signals to pass. The most reasonable way to protect the A7 AC against RF pickup and amplification may be through the addition of extra shielding.

# Clock Rate vs. Frequency and Power

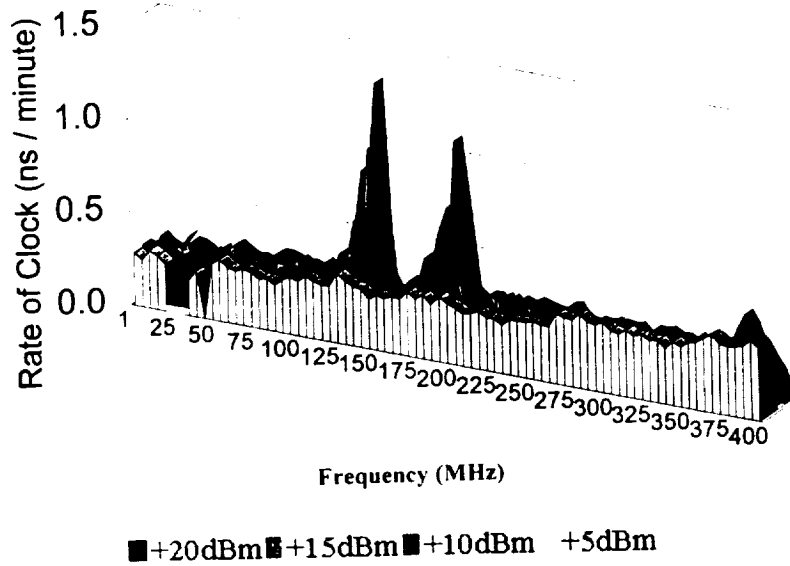


Figure 1 : Clock Rate vs. Frequency and Power

## 5061B Offset

2 Watt UHF Radio Five Feet Away

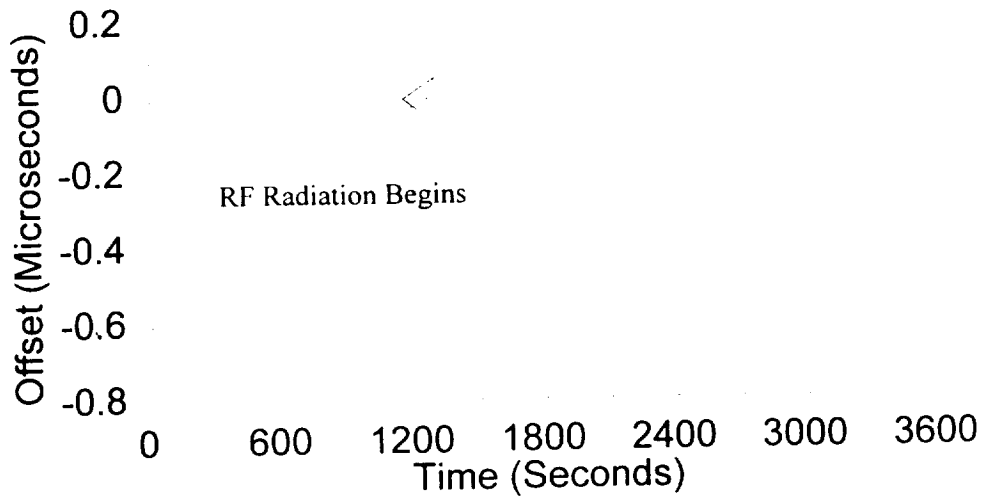
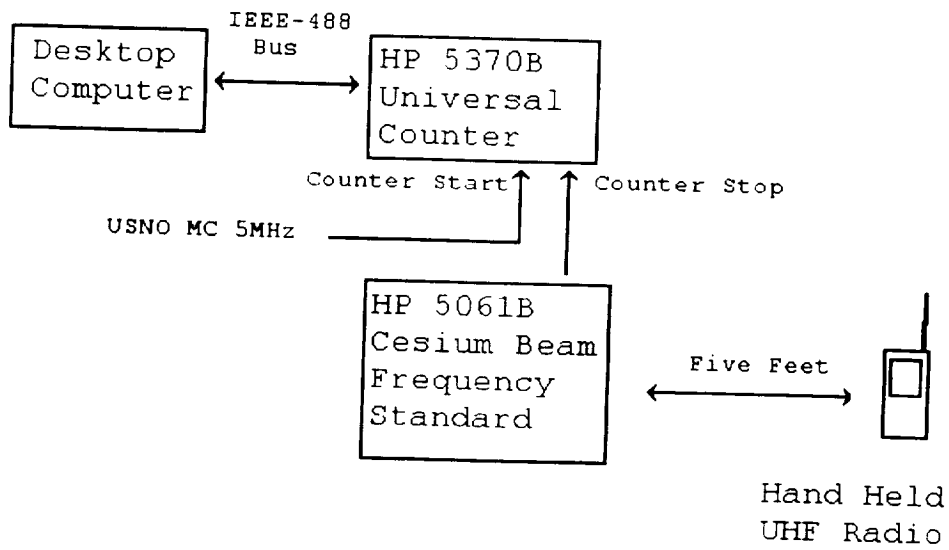
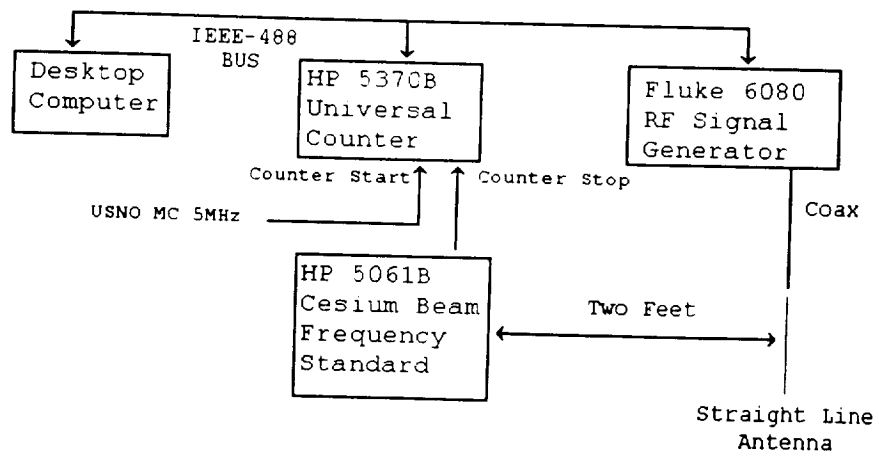


Figure 2 : UHF Response



**Figure 3 : UHF Experiment Setup**



**Figure 4 : VHF Experiment Setup**

# Antenna Frequency Response

+20dBm Two Feet Separation

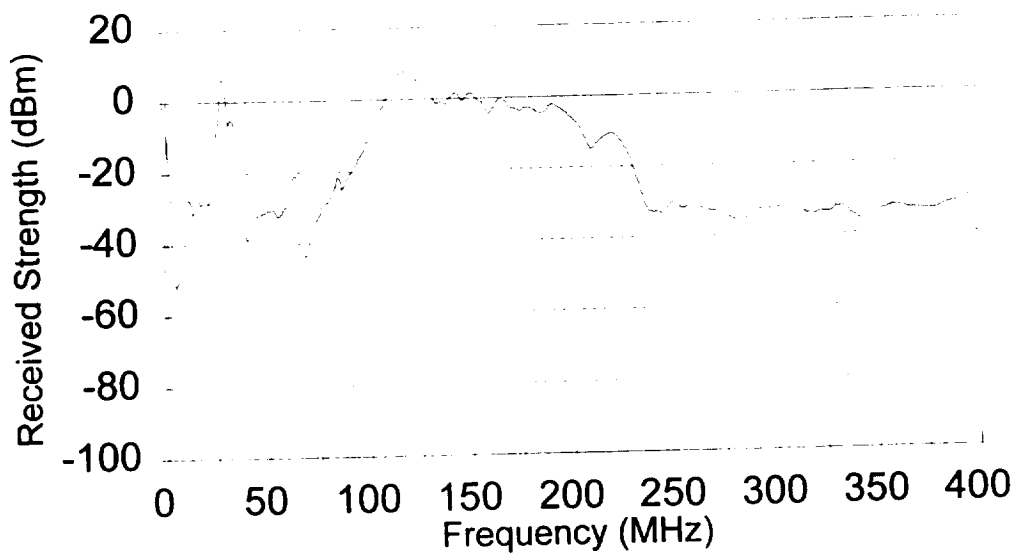


Figure 5 : Antenna Frequency Response

# Relativistic Timescale Analysis Suggests Lunar Theory Revision

Steven D. Deines  
Collins Avionics and Communications Division  
350 Collins Road NE  
Cedar Rapids, Iowa 52498

Dr. Carol A. Williams  
Department of Mathematics  
4202 East Fowler Avenue  
University of South Florida  
Tampa, Florida 33620

## Abstract

*The International Standard (SI) second of the atomic clock was calibrated to match the Ephemeris Time (ET) second in a mutual four year effort between the National Physical Laboratory (NPL) and the United States Naval Observatory (USNO). The ephemeris time is "clocked" by observing the elapsed time it takes the Moon to cross two positions (usually occultation of stars relative to a position on Earth) and dividing that time span into the predicted seconds according to the lunar equations of motion. The last revision of the equations of motion was the Improved Lunar Ephemeris (ILE), which was based on E. W. Brown's lunar theory. Brown classically derived the lunar equations from a purely Newtonian gravity with no relativistic compensations. However, ET is very theory dependent and is affected by relativity, which was not included in the ILE. To investigate the relativistic effects, a new, noninertial metric for a gravitated, translationally accelerated and rotating reference frame has three sets of contributions, namely (1) Earth's velocity, (2) the static solar gravity field and (3) the centripetal acceleration from Earth's orbit. This last term can be characterized as a pseudogravitational acceleration. This metric predicts a time dilation calculated to be -0.787481 seconds in one year. The effect of this dilation would make the ET timescale run slower than had been originally determined. Interestingly, this value is within 2 percent of the average leap second insertion rate, which is the result of the divergence between International Atomic Time (TAI) and Earth's rotational time called Universal Time (UT or UT1). Because the predictions themselves are significant, regardless of the comparison to TAI and UT, the authors will be rederiving the lunar ephemeris model in the manner of Brown with the relativistic time dilation effects from the new metric to determine a revised, relativistic ephemeris timescale that could be used to determine UT free of leap second adjustments.*

## Introduction

Time is measured by counting cycles or fractions of cycles of any physical repeatable phenomenon. The oldest method is based on the rotation of the Earth to define the timescale called Universal Time (UT or UT1 to be more specific). The actual solar day varies by the angles sunlight strikes the Earth as it moves in its inclined elliptical orbit. Through mathematics, the concept of a mean solar day can be established in terms of the sidereal day that Earth takes to rotate  $2\pi$  radians. As the Earth's rate of rotation was discovered to vary somewhat, a more precise time standard was developed by monitoring the motion of the heavenly bodies and comparing them to the theory of motion for that body. Similar to hands of a clock passing the numbered positions on the clockface, the observed position or ephemeris of a heavenly body against the stellar background determines the timescale, called Ephemeris Time (ET). Unfortunately, ET is very theory dependent. The actual Ephemeris Time of an event was determined well after it occurred due to postprocessing of the observations.

In the mid 1950s, precise atomic frequency standards were developed for ultrastable, long term operation. The atomic vibrations would be monitored so that the number of elapsed cycles could provide the conversion to establish an atomic clock. The primary atomic timescale is currently the International Atomic Time (TAI). The length of the atomic SI second was defined by Markowitz et al. (1958) by an observationally determined value of the ET second obtained from the Improved Lunar Ephemeris (ILE). However, a timing problem surfaced when it was seen that UT ran at a different rate than TAI. Based on conversations with personnel at the US Naval Observatory (USNO) into the derivation of the ILE, it was determined that relativity effects were not incorporated into Brown's lunar theory. Preliminary relativity calculations have yielded a time dilation effect in the lunar ephemeris with a value that is within 2% of the observed divergence between UT and TAI. Work is ongoing to rederive a relativistic lunar ephemeris and obtain a relativistic ET timescale, which will be compared to the TAI and UT timescales.

## Development of the Ephemeris and Atomic Timescales

The International Atomic Time (TAI) scale is based on the rate of time defined by the Système International (SI) second. Since 1967, the SI second has been the standard unit of time in all timescales. The calibration study that utilized the ILE to define the SI second averaged the cycles tabulated over 4 years from the cesium standard and compared them to the length of the ET second.<sup>[1]</sup> So, the SI second matches an ephemeris second very closely and provides continuity between the ET and TAI timescales.<sup>[2]</sup>

The ILE is a classically derived lunar ephemeris, which is based on E. W. Brown's classical lunar theory as derived from Newtonian gravitation. Brown's original theory as documented in his memoirs<sup>[3,4,5,6,7]</sup> was finished before general relativity was published in 1916. General relativity theories prior to 1950 using standard spherically symmetric metrics for a single mass produce relativistic corrections well below the level of precision of the empirical corrections applied to the ILE.<sup>[8]</sup> Therefore, relativistic corrections to the ILE were not considered necessary.

The very first version of ET was defined by Clemence, who used Newcomb's classical theory

for the Tables of the Sun from 1896. Since Einstein published his special and general relativity theories in 1904 and 1916, respectively, it is obvious that ET had no intentional relativistic corrections incorporated in the first ET timescale. From the observational results of Spencer Jones (1939),<sup>[9]</sup> Clemence derived the fluctuation factor  $\Delta = ET - UT$  to convert UT to a time measure defined by Newcomb's tables.<sup>[10]</sup> Because the year was so long, which then took months after an event to determine ET, the Moon's orbit was the best object to study because it had the shortest period. The best lunar theory available was Brown's methodical derivation. But, Brown had to adopt an empirical term from other sources to get better agreement between his lunar theory and the lunar observations used to get the constants of integration for his theory. Clemence determined the correction to Brown's lunar theory so that the independent time variable in the lunar theory would be the same as that in Newcomb's Table of the Sun.<sup>[11]</sup> Following Clemence's computations published in 1948, the International Astronomical Union agreed to remove Brown's empirical term and to rescale Brown's lunar theory by correcting the mean longitude,  $L$ , with the following equation:

$$\Delta L = -8.72'' - 26.74''T - 11.22''T^2 = \Delta L_0 + \Delta nT + \frac{1}{2}\Delta \dot{n}T^2 \quad (1)$$

where  $T$  is measured in Julian centuries from 1900 January 0 at Greenwich Mean Noon.

The equation to correct the mean longitude of the Moon can be considered a correction to the mean motion rate of  $\dot{n}$  by a value of  $\Delta \dot{n} = -22.44''/cy^2$ . This modification to the mean longitude agreed with the observations of Spencer Jones (1939). Brown's lunar theory with this correction to the mean longitude and a minor aberration correction term made up the ILE used to compute ET. Recently, Markowitz reported<sup>[12]</sup> that the SI second and the ILE second were still consistent to a part in  $10^{10}$ , which effectively establishes that the SI and ET seconds are equivalent.

## Evidence of Timescale Problem

There has been considerable evidence of timescale inconsistencies between UT and ET. Ephemeris timescales based solely on the orbital periods of the planets appeared to run faster than UT. Data from Spencer Jones showed that the lunar orbital secular acceleration was  $5.22''/cy^2 = \Delta \dot{n}_{\text{Moon}}$  and the apparent secular acceleration of the solar orbit was  $1.23''/cy^2 = \Delta \dot{n}_{\text{Sun}}$ . Spencer Jones attributed the cause to tidal friction slowing down Earth's rotational rate.<sup>[13]</sup> It also appears that Clemence computed the secular acceleration of Earth's rotation,  $\dot{\omega}$ , using the secular orbital acceleration of the Moon and Mercury to get  $\Delta \dot{\omega} = -11.22''/cy^2$ . Munk (1963) computed the secular acceleration of Earth's rotation from Spencer Jones' numbers with the following formula for the "weighted discrepancy difference," in which any dependence to a variable Earth rotation was removed.<sup>[14]</sup> The attempt here was to extract the contribution due to any lunar errors in the timing problem from other sources. So, the weighted discrepancy difference (WDD) is the weighted difference of the secular orbital accelerations between the Moon and Sun that has not been accommodated in the lunar ephemeris used for defining the lunar ET.

$$WDD(t) = \int \int \left[ \dot{n}_{\text{Moon}}(t) - \left( \frac{n_{\text{Moon}}}{n_{\text{Sun}}} \right) \dot{n}_{\text{Sun}}(t) \right] dt dt \quad \text{which implies that} \quad (2)$$

$$\frac{d^2}{dt^2} WDD(t) = \left[ \dot{n}_{\text{Moon}}(t) - \left( \frac{n_{\text{Moon}}}{n_{\text{Sun}}} \right) \dot{n}_{\text{Sun}}(t) \right] = 5.22''/cy^2 - 13.37(1.23''/cy^2) = -11.22''/cy^2 \quad (3)$$

Based on Clemence's results, WDD(t) could be computed by using Mercury instead of the Sun. Munk assumed that WDD is due to the secular acceleration of Earth's rotation, which will affect values of the independent variable t. He ruled out the alternative option, which is  $\dot{n}_{\text{Mercury}} n_{\text{Mercury}} = \dot{n}_{\text{Sun}} n_{\text{Sun}}$ , because these secular orbital accelerations are empirical and have no explanation from classical gravitation theory. Lambeck did basically the same thing as Munk using solar, Mercury and Venus data.<sup>[9,15,16,17]</sup> Using Spencer Jones' work plus three other sources, Lambeck concluded<sup>[18]</sup>

$$\frac{\dot{n}_{\text{Sun}}}{n_{\text{Sun}}} = \frac{\dot{n}_{\text{Mercury}}}{n_{\text{Mercury}}} = \frac{\dot{n}_{\text{Venus}}}{n_{\text{Venus}}} \quad (4)$$

Again, Lambeck reached the same result as Munk and stated that the empirically derived acceleration has to be caused by a secular deceleration in Earth's rotation as the only plausible mechanism under classical theory.

All of these authors would get the same value for what is interpreted as the secular acceleration of Earth's rotation,  $-11.22''/cy^2$ . Notice this is exactly the value for the quadratic term in the equation used to correct Brown's lunar theory for the ILE. This value corresponds to a corrected secular acceleration in the Moon's mean longitude of  $-22.44''/cy^2$ . A very recent observation using lunar laser ranging gives  $-26.0'' \pm 1.0''/cy^2$  for the Moon's secular acceleration.<sup>[19]</sup>

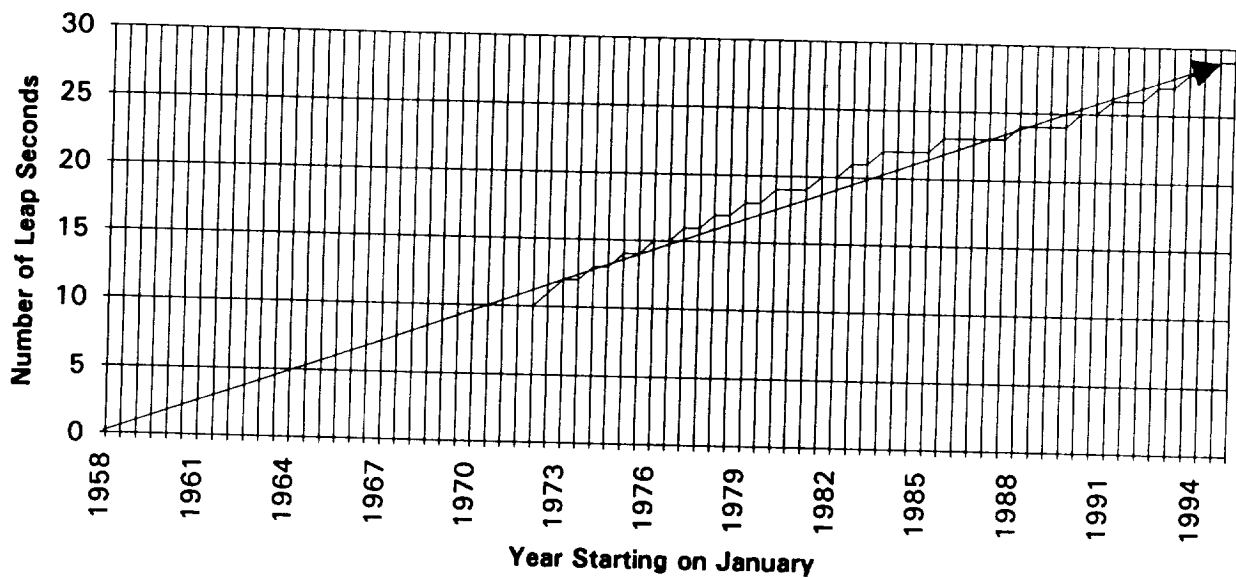
When a divergence occurs between two time standards, either the first standard is running slower than the second or the second standard is running faster than the first. All of the authors mentioned in the previous section have identified that there is a timing problem between a timescale based on Earth's rotation and ephemeris time. One option is that ET is running a bit too fast, which could be caused by not including sufficient relativity corrections to lengthen the time unit interval appropriately in the orbital equations of motion. The original ET standard used Earth's orbit to measure one year, which was then divided into ephemeris seconds based on the classically derived theory of the Sun. If the ephemeris second interval were a bit smaller than the proper second interval in a relativistic theory, the ET standard would predict that Earth would complete one entire orbit before Earth actually traveled  $2\pi$  radians of mean anomaly. Let M represent the observed mean anomaly and T, the orbital period of the Earth. Then,  $\Delta M = M - nT$ . As  $T = 2\pi/n$ , then  $\Delta M = M - 2\pi$ . This discrepancy is often interpreted as a secular acceleration,  $\Delta M = \frac{1}{2}\dot{n}T^2$ . If  $\Delta M$  is caused by an annual, fixed timing error,  $\Delta T$ , then one may write  $\Delta M = n\Delta T$ . The correction between the secular acceleration, and the timing error is given by

$$\frac{\dot{n}}{n} = \frac{2\Delta T}{T^2} = \text{constant} \quad (5)$$

Munk and others have attributed the source of the problem to tidal friction that slows down the Earth's rate of rotation, which then makes the UT timescale run slower, whereas the above ratios suggest that the timing problem is attributed to ET running slightly fast. If the computed ET is running faster than the actual ET,  $\Delta M$  will be negative. This is confirmed when inserting the negative value of  $\dot{n}$ .

There has been a general divergence between UT and TAI timescales over the past 30 years. Since the epoch for both UT and TAI is 0 hour of 1958 January 1, UT (as modeled by Universal Coordinate Time UTC as based on the SI second) has trailed behind TAI by 29 seconds.<sup>[20]</sup> The leap seconds inserted into the UTC timescale, which closely follows UT, are plotted in Figure 1. Leap seconds are inserted at midnight of either December 31 or June 30, depending when it is decided that an update is needed.

**Leap Second Insertion**



Looking at Figure 1, there is a periodic variation in the overall trend as UT and TAI steadily diverge. Fluctuations in the Earth's rotation over timescales of less than a few years are dominated by atmospheric effects,<sup>[21,22,23]</sup> which affect the atmospheric angular momentum and Earth's moment of inertia and rotation. The average leap second insertion rates for three recent intervals show the effect of the granularity in the data caused by the periodic behavior of the atmosphere and the constraint of inserting leap seconds on the approved dates of June 30 and December 31. The three slopes can also be used to determine the excess length of a mean solar day in terms of SI seconds.

Average Length of Mean Solar Day in SI Seconds	
1992-1958	86400.00214
1993-1958	86400.00216
1994-1958	86400.00218

Subtracting 24 hours of seconds from the average length of day and then inverting gives the

average leap second insertion rate in days as shown in the table below:

Average Leap Second Insertion Rate	
1958-1992	466.6667 day/sec
1958-1993	463.0357 day/sec
1958-1994	459.6551 day/sec

The intent of the cesium clock calibration experiment in 1958 was to calibrate the SI second so that it would be as close as possible to the ET second. It is obvious from the figure that the rates of UT and TAI do not match.

## Relativity Effects on Time Standards

Relativity theory has shown that velocity and accelerations affect time, which classical physics does not predict. Relativity requires that a distinction between proper time and coordinate time be made. Proper time is the time kept by an ideal clock attached to the observer, much like a wristwatch tells the observer his time. Coordinate time is equivalent to the instantaneous readout of the master time standard, wherever it may be located, and the output time is communicated instantaneously to the observer at his coordinate position. Any moving, accelerated observer will have a slower proper time than if he was stationary and not gravitated. The Earth is not only rotating, so that an observer on its surface experiences tangential rotational velocity and centripetal acceleration, but it also has orbital dynamics that give Earth, as well as an observer on its surface, additional velocity, centripetal acceleration and gravitational acceleration from the Sun.

For the observer on Earth's geoid (surface where the sum of rotational centripetal acceleration and local gravity from Earth is a constant), a timescale can be defined by Earth's rate of rotation (e.g. UT). This standard does suffer from periodic variations in the atmospheric angular momentum due to expanding and contracting air masses. In general, the rotational time standard is fairly consistent and usable for timekeeping over the long term. Because Earth experiences orbital dynamics and solar gravity, UT slows down (experiences the time dilations that lengthen the second interval compared to operating at a stationary, nongravitated location where no relativity effects exist). Therefore, UT is a proper timescale that has the same time dilations as any fixed place on Earth. So, UT is actually a noninertial time standard, because Earth's reference frame is accelerated.

Ephemeris Time is determined by an Earth observer viewing the position of a heavenly body, like the Moon, and comparing it to a classically predicted orbital position. Postprocessing of the equations of motion will produce a value of the time, a time tag, for the observed position, which is used to define the timescale for ET. With no relativistic perturbations included, the predicted positions are appropriate only for a stationary, gravity-free observer. This is the only location where proper and coordinate times are equivalent which constitutes what we call inertial time. Such a time interval derived by only classical physics is as short as possible.

The equations of motion should be in terms of the observer's own reference frame, which requires that the problem be treated relativistically. Classical equations of motion have no

relativistic time dilations so that the observer's reference frame is interpreted as being stationary and nongravitated. The classical equations of motion establish an inertial time standard. However, the Earth bound observer experiences orbital velocities and associated accelerations that constitute a noninertial reference frame and a noninertial time standard. So, the observers' own proper time rate is slower than classical physics predicts. The time tags given to the observed angular position of a heavenly body is essentially equivalent to Earth's proper time, namely UT. Since ephemeris time was defined with equations of motion that assumed the observer would be stationary and nongravitated, the ET time intervals are a bit short. This would explain why ET would run faster than UT over the long term.

Atomic time standards are defined to operate on Earth's geoid. The atomic clocks are at the same location as the observer on Earth's surface, so that an atomic clock experiences the same relativity effects as a clock in Universal Time.<sup>[24]</sup> However, atomic clocks were carefully calibrated to match the rate of the ET timescale, which assumed an unaccelerated, stationary frame for the observer. Thus, TAI and ET do not have the same common rate as the UT timescale. Neither TAI, ET nor UT operate in an inertial reference frame. If the complete relativity compensations were included in the lunar ephemeris, then the relationships between these three time rates should be closer.

## Noninertial Relativistic Metric and New Time Dilation Effects

Since the Earth and Moon define noninertial systems orbiting each other, then the choice of a relativistic metric must accommodate all relativistic terms for a noninertial dynamical system. Just as measurements taken in noninertial reference frames require that extra classical terms (e.g. centripetal and Coriolis forces) must be taken into account when transforming to inertial frames, then relativistic measurements taken in a noninertial frame must have extra correction terms that would not be found in an inertial frame. Many metrics, such as the Schwarzschild metric, assume the massive object is stationary or nonrotating or inertial. The Nelson metric is an exact, noninertial metric appropriate for a nongravitationally accelerated, rotating reference frame.<sup>[25]</sup> Deines has extended the exact Nelson metric for nongravitationally accelerated frames to include Newtonian gravity. The inclusion of the Newtonian gravity with the nongravitational accelerations should encompass all significant relativistic terms to second order, since the post-Newtonian approximation from general relativity has the Newtonian gravity as the only second order contribution. The noninertial relativistic contributions are the velocity factor from special relativity, the Newtonian gravitational term from the second order post-Newtonian approximation from general relativity, and a new nongravitational potential contribution that can be treated in general relativity as an effective pseudogravitational factor to account for the centripetal acceleration. The new metric is defined below:

$$g_{ij} = \delta_{ij} = \begin{cases} 1 & \text{if } i = j \\ 0 & \text{if } i \neq j \end{cases} \quad (6)$$

$$g_{0j} = \frac{1}{c}(\vec{\omega} \times \vec{R})_j \quad (7)$$

is equivalent to 469.0343 days per leap second. This prediction is within 2% of the average time between leap seconds accumulated between 1994 and 1958. It is also within 0.5% of the observed average time between leap seconds if the average was taken between 1992 and 1958. These preliminary computations indicate that a relativistic lunar ephemeris timescale may well be close to UT.

Also, very preliminary calculations applied to the lunar ephemeris have been made with the time dilation equation. When the total relativistic contributions as calculated to second order are not accommodated in the lunar ephemeris, an apparent secular acceleration in the lunar orbit of  $-25.66''/cy^2$  is predicted, which is about 1.3% of the observed value.

## Conclusion

As discussed already in this paper, astronomers and geophysicists have, for many years, identified a timescale divergence between Universal Time (UT) and Ephemeris Time (ET). This problem has carried over to the observed divergence between UT and International Atomic Time (TAI), which the latter timescale has a rate defined by the current SI second that was calibrated carefully to the ET second. Previous scientific opinions are that UT is slowing down due to tidal friction. An equally plausible option is that ET had been running slightly faster than UT. The lack of a physical cause has kept this option from serious consideration until now.

An in-depth study of the historical development of our current timescales reveals that the equations of motion that defined the former standard of Ephemeris Time did not include any relativity compensations. Since ET is based on the length of the yearly orbit that was subsequently divided into ET seconds as prescribed by those equations of motion, the ET timescale could be running slightly faster than Earth's proper time standard. Without the relativistic time dilation effects that would "stretch" the ET second slightly, there will be slightly more seconds marked off per year than there should be. In that case, time predictions based on a complete revolution will be ahead compared to when the heavenly body will actually complete an orbit. Studies have shown the planets all lag behind the ET predictions with equal ratios of mean motion rate divided by mean motion. Classical gravitational theory can not explain the existence of these empirical ratios. However, relativity seems to be a possible source of this phenomena.

Because the Earth and Moon are not sufficiently inertial, a relativistic metric that deals with a generalized noninertial reference frame has been developed. Deines has extended the noninertial Nelson metric with Newtonian gravity to satisfy the requirement for modeling a noninertial system in gravity. In noninertial reference frames, three sets of relativistic contributions occur: velocity, gravitational and nongravitational terms. Preliminary research indicates the new relativistic metric will give an updated, theoretical expression for the lunar mean motion and, thereby, a new effect on the lunar timescale to be used for ET. A new time dilation equation has been derived from this new metric and has been used to estimate the time dilation effects of Earth's proper time compared to an inertial coordinate time. Assuming UT typifies Earth's proper time and assuming TAI with the SI second establishes Earth's coordinate time, then the time dilation equation predicts that UT should trail behind TAI by .7787481 seconds per year, which is within 2% of the observed divergence between UT and TAI. Also,

$$g_{oo} = - \left( 1 + \frac{\vec{A} \cdot \vec{R} + \Phi}{c^2} \right)^2 + \frac{(\vec{\omega} \times \vec{R})^2}{c^2} \quad (8)$$

where  $\vec{A}$  is the time-dependent translational, nongravitated acceleration of the observer's frame relative to a nongravitated inertial frame,  $\Phi$  is the Newtonian gravitational potential independently existing in the neighborhood of the observer,  $\vec{\omega}$  is the time-dependent angular velocity vector of the observer's spatial frame rotating relative to the inertial frame, and  $\vec{R}$  is the range vector of the accelerated observer's origin from the inertial frame.

Using the fact that the Nelson metric preserves flat space-time, Deines has rigorously derived a new time dilation equation for a rotating reference frame that is accelerated both nongravitationally and gravitationally.

$$d\tau = \sqrt{\left( 1 + \frac{\vec{A} \cdot \vec{R} + \Phi}{c^2} \right)^2 - \left( \frac{V^2}{c^2} \right)} dt \quad (9)$$

with  $\vec{V}$  being the time-dependent velocity of the observer's frame relative to the inertial frame. If proper time  $\tau$  is associated with UT as Earth's proper time and coordinate time  $t$  is considered as TAI with its SI second, then the square root term is the time dilation factor between the UT and TAI seconds.

To estimate the expected time dilation of Earth in its orbit around the Sun, integrate the time dilation equation over one year by the following process. Assume the inertial frame is sufficiently far from the Sun as to experience no gravitational red shift with its ideal master clock (e.g. fixed somewhere on the celestial sphere). Draw the displacement vector  $\vec{R}$  from the inertial frame to the barycenter located at the Sun and continue on to the Earth-Moon barycenter. Since the first leg of this vector sum is fixed and assumed sufficiently stationary, the problem now reduces by a transformation to evaluating the time dilation equation from the Sun to Earth. Expand the radical in powers of  $c^2$  and retain only the first order terms. Assume Earth's orbit is a perfect ellipse. Substitute the Newtonian potential with the classical representation of the reduced mass divided by the new  $\vec{R}$  vector. Derive the expression for the centripetal acceleration due to the elliptical orbit and substitute directly for the dot product term. Give  $V^2$  its value for elliptical orbits. Obtain the differential form of Kepler's equation to express  $dt$  as a function of  $dE$  where  $E$  is the eccentric anomaly.

Collect terms as a function of  $E$  and integrate over  $2\pi$  radians for one anomalistic year (i.e. perigee to perigee or 365.259635 days) to get the effective rate difference between proper and coordinate time as given below:

$$\tau - t = - \frac{\mu}{2ac^2} \sqrt{\frac{a^3}{\mu}} \int_0^{2\pi} (5 + e \cos E) dE = - \frac{\sqrt{\mu a}}{2c^2} 5E \Big|_0^{2\pi} = -0.778748084 \quad (10)$$

seconds per anomalistic year

The result from this integration is that UT will trail TAI by .7787481 seconds in one year, which

very preliminary computations using this time dilation equation indicate that the total relativity effects when ignored can produce an apparent lunar acceleration of  $-26.66''/cy^2$ , which is within 1.3% of the current observed value of the lunar secular acceleration in mean longitude.

Our future research work will generate a relativistic lunar ephemeris by following Brown's methodical development and using the new noninertial metric. The ongoing project will compare the original ephemeris timescale to a relativistic one. It is expected that the comparison will match the comparison between UT and TAI. One outcome of this effort may be the precise determination of a UT timescale by an appropriate conversion factor applied to an atomic timescale based on the SI second. This could allow an ultraprecise definition of a new UT timescale free of any leap second insertions.

This research effort is funded by the Office of Naval Research contract N00014-94-1-1021.

## References

- [1] W. Markowitz, R. Hall, L. Essen and J.V.L. Parry, "Frequency of Cesium in Terms of Ephemeris Time," *Physical Review Letters*, Vol 1, No. 3, August 1, 1958, p. 105-107.
- [2] Explanatory Supplement to the Astronomical Almanac, P. K. Seidelmann (ed.), University Science Books, 1992, p. 84.
- [3] E.W. Brown, "Theory of the Motion of the Moon: Part I," *Memoirs of the Royal Astronomical Society for 1896-1898*, Vol. 52, (1899) p. 39-116.
- [4] E.W. Brown, "Theory of the Motion of the Moon: Part II," *Memoirs of the Royal Astronomical Society for 1896-1898*, Vol. 53, (1899) p. 163-202.
- [5] E.W. Brown, "Theory of the Motion of the Moon: Part III," *Memoirs of the Royal Astronomical Society for 1899-1901*, Vol. 54, (1904) p. 1-64.
- [6] E.W. Brown, "Theory of the Motion of the Moon: Part IV," *Memoirs of the Royal Astronomical Society*, Vol. 58, (1908) p. 51-146.
- [7] E.W. Brown, "Theory of the Motion of the Moon: Part V," *Memoirs of the Royal Astronomical Society for 1908-1910*, Vol. 59, (1910) p. 1-104.
- [8] For example, Schwarzschild's secular advance in the perigee of the Moon is  $0.06''/cy$ , which is well below the corresponding term in the ILE correction to the tabular mean longitude of  $-26.74''/cy$ . See J. Lestrade et al., *High-Precision Earth Rotation and Earth-Moon Dynamics*, D. Reidel Publishing Co., 1982, p. 217-225.
- [9] H. Spencer Jones, "The Rotation of the Earth, and the Secular Accelerations of the Sun, Moon and Planets," *Monthly Notices of the Royal Astronomical Society*, Vol. 99, No. 7, 1939, p. 541-558.
- [10] See note 2, p. 79.
- [11] *Ibid.*

- [12] W. Markowitz, "*Comparisons of ET(Solar), ET(Lunar), UT, and TDT,*" *The Earth's Rotation and Reference Frames for Geodesy and Geodynamics*, 1988, p. 413–418.
- [13] See note 9, page 554.
- [14] W.H. Munk, "*Variation of the Earth's Rotation in Historical Time,*" *The Earth–Moon System*, B.G. Marsden and A.G.W. Cameron (eds.), Plenum Press, New York, 1966, p.52–54.
- [15] R.L. Duncombe, (1958). *Motion of Venus 1750–1949*, *Astron. Pap. Am. Ephem. Naut. Alm.*, XVI, 1–258.
- [16] L.V. Morrison and C.G. Ward (1975). *The Analysis of the Transits of Mercury*, *Mon. Not. R. Astron. Soc.*, 173, 183–206.
- [17] R.R. Newton (1976). *Ancient Planetary Observations and the Validity of Ephemeris Time*, Johns Hopkins University Press, Baltimore, MD., pp. 749.
- [18] K. Lambeck, *The Earth's Variable Rotation: Geophysical Causes and Consequences*, Cambridge University Press, Cambridge, 1980, p. 69–71.
- [19] J.G. Williams, X.X. Newhall and J.O. Dickey, "*Lunar Laser Ranging: Geophysical Results and Reference Frames,*" *Americal Geophysical Monograph: Space Geodesy and Geodynamics*, February 1993 preprint.
- [20] *The Astronomical Almanac*, U.S. Government Printing Office, 1994, page K9.
- [21] R.D. Rosen and D.A. Salstein, "*Variations in Atmospheric Angular Momentum on Global and Regional Scales and the Length of Day,*" *J. Geophys. Res.*, 88, 5451–5470, 1983.
- [22] T.M. Eubanks et al., "*A Spectral Analysis of the Earth's Angular Momentum Budget,*" *J. Geophys. Res.*, 90, 5385–5405, 1985.
- [23] R. Hide and J.O. Dickey, "*Earth's Variable Rotation,*" *Science*, 253, p. 629–637, 1991.
- [24] N. Ashby and D. Allen, *Radio Science*, 14, p. 649–669 (1979).
- [25] R. A. Nelson, *J. Math. Phys.*, 28, 2379, (1987)



623/1  
p. 13

# THE DEEP SPACE NETWORK STABILITY ANALYZER

Julian C. Breidenthal, Charles A. Greenhall,  
Robert L. Hamell, Paul F. Kuhnle  
Jet Propulsion Laboratory  
California Institute of Technology  
4800 Oak Grove Dr.  
Pasadena, California 91109

## Abstract

*A stability analyzer for testing NASA Deep Space Network installations during flight radio science experiments is described. The stability analyzer provides realtime measurements of signal properties of general experimental interest: power, phase, and amplitude spectra; Allan deviation; and time series of amplitude, phase shift, and differential phase shift. Input ports are provided for up to four 100 MHz frequency standards and eight baseband analog (>100 kHz bandwidth) signals. Test results indicate the following upper bounds to noise floors when operating on 100 MHz signals:  $-145$  dBc/Hz for phase noise spectrum further than 200 Hz from carrier,  $2.5 \times 10^{-15}$  ( $\tau = 1$  second) and  $1.5 \times 10^{-17}$  ( $\tau = 1000$  seconds) for Allan deviation, and  $1 \times 10^{-4}$  degrees for 1-second averages of phase deviation. Four copies of the stability analyzer have been produced, plus one transportable unit for use at non-NASA observatories.*

## Introduction

The Deep Space Network (DSN) is called upon to attain high levels of frequency stability for scientific purposes. For instance, the upcoming Cassini mission to Saturn will use the DSN to attempt detection of gravitational radiation, and to observe properties of Saturn's rings, atmosphere, and satellites<sup>[1]</sup>.

These and related investigations<sup>[2]</sup> measure small perturbations on a radio signal passing between the earth and a distant spacecraft. The Cassini applications are fairly typical, requiring frequency stability of a few parts in  $10^{15}$  (Allan deviation for sampling time  $\tau = 100$  to 10,000 s) and single-sided phase noise around  $-60$  dBc/Hz (1 to 10 kHz offset from an 8.4 GHz carrier).

It is challenging to achieve such stabilities in the operational environment faced by the DSN. That environment includes months-long periods of duty; spatially distributed, outdoor, and moving equipment; and competition for observing time. We have found that stability failures can remain hidden in the bulk of DSN activities, only to surface when the scientific experiment is undertaken. This is troublesome because most mission experiments cannot be repeated.

Therefore the DSN has, in the past, tested its systems using instrumentation suitable for use by specially trained personnel. This approach was expensive, however, and the time to analyze data has often allowed additional diagnostic evidence to disappear, necessitating repeated tests.

We developed a stability analyzer to enable operations personnel to rapidly measure stability in various ways, in order to lower costs and reduce response time. The particular measurements made are: power, phase, and amplitude spectra; Allan deviation; and time series of amplitude, phase shift, and differential phase shift. Our analyzer provides inputs for up to four 100 MHz frequency standards and eight baseband analog (>100 kHz bandwidth) signals, with the possibility of expanding to accept digital inputs over a local area network. Four copies of the stability analyzer have been produced, plus one transportable unit for use at non-NASA observatories.

## Instrument Overview

The DSN stability analyzer has two major components: 1) the RF and Analog Assembly, and 2) the Controller Assembly, as depicted in Figure 1.

The RF and Analog Assembly provides the conditioning and conversion of the input analog signals into a signal the controller can analyze. The equipment is installed in two parts: the 100 MHz Interface Assembly and an RF Cabinet Assembly.

The 100 MHz Interface assembly resides as close as possible to the DSN primary frequency standards, usually hydrogen masers (H-masers). Intentionally, this location is isolated from routine personnel access, as well as from as many environmental influences as possible. The assembly receives four 100 MHz inputs, which are compared in pairs. The comparison (described further below) results in a 100 kHz signal that is sent over a fiber-optic interface to the RF cabinet. The RF assembly resides in a convenient location for access by test personnel. It provides reference frequency synthesis and distribution, switching among the possible input sources, signal conditioning in the form of amplification, and optional downconversion with detection of zero crossings.

The Controller Assembly resides next to the RF assembly, and provides an operator interface for selection of the test type and hardware configuration, and for presentation of results. The Controller also controls details of switches and instrumentation, acquires data by means of analog-to-digital (A-D) converters and a time interval counter, and analyzes the data acquired. Originally, the RF assembly was housed in one rack and the controller equipment was housed in a second rack. These cabinets have since been bolted together to form a double cabinet, and components of each have been swapped to improve ergonomics for the operator. See Figure 2 for a photograph of the double cabinet.

# Analog Electronics Design

## 100 MHz Interface Assembly

This assembly selects the pair of 100 MHz signals to be analyzed, and converts the selected signals into a form that can be transported to the low frequency equipment. Figure 3 shows a block diagram.

Output from the 100 MHz assembly is sent on fiber optics to the low frequency equipment to prevent ground loop currents that could induce spurious signals or noise into signals being measured, or could contaminate the frequency standard's outputs. The 100 MHz Interface has four 100 MHz input ports. Two input ports are connected to H-Maser outputs, and one other port is normally used for comparing the station's coherent reference generator 100 MHz output against the H-masers. The 100 MHz signals are selected for measurement using RF relays followed by high reverse isolation amplifiers cascaded with output matrix switches. The combined isolation of both sets of switches and 60 dB reverse isolation of the amplifiers provides more than 150 dB crosstalk isolation between signals.

Switch control commands are sent over fiber optics to the 100 MHz Interface using commercial modems and digital I/O boards to address switch decoders that operate the switches.

The selected pair of inputs are frequency multiplied by 99 and 100 respectively with phase-locked cavity multipliers. The multiplier outputs at 9.9 GHz and 10.0 GHz are mixed to generate 100 MHz. The result is frequency translated to 100 kHz in an offset frequency generator, and sent on a fiber-optic link to the low frequency assembly.

The frequency conversion process yields a single 100 kHz carrier with a phase spectrum containing the relative stability of the 100 MHz inputs, with a 40 dB margin above what would be obtained from direct mixing of one input with the other input, offset by 100 kHz. Amplitude information is lost. Frequency translation to 100 kHz is necessary for the A-D converter, and allows the signal to be transported to the low frequency assembly over low-cost multimode fiber optics.

## Low Frequency Interface Assembly

This assembly contains switches that select among baseband receiver signals and the 100 kHz signal from the 100 MHz assembly. The selected signals are routed to measurement ports of the computer system. Figure 4 shows a block diagram.

Baseband signals are selected by matrix switches and sent to programmable attenuators that set levels into the interface amplifiers. Another matrix switch outputs the selected signals to the desired output ports. The frequency translated 100 MHz maser-pair signal is input to the low frequency assembly on multimode fiber. The fiber-optic receiver output is  $\pm 15$  kHz bandpass filtered to eliminate aliasing of spectral components, then routed to the output matrix switches. One output of the matrix switch feeds a zero crossing detector for 1-second phase measurements. The zero crossing detector generates a 1 PPS output that is routed over fiber optics to the frequency counter. The other outputs of the matrix switch are sent on coax

488 bus is used to communicate with two frequency synthesizers and a time interval counter. (One synthesizer supplies the local oscillator for the last downconversion to 1 Hz as shown in Figure 4, while another supplies the sample clock for A–D conversion.) The VME chassis contains a Skybolt 8116–V vector processor and an Analogic DVX 2503 16–bit, 400 kHz A–D converter.

The Skybolt computer is delivered with its own Unix–based operating system, which allows the execution of one user program. We have written the one user program to provide custom real–time multitasking and digital signal processing. The program is designed to accommodate one test at a time, in the form of an execution script including the digital signal processing, along with some small Skybolt system tasks. The code is written in C and Fortran.

The software on the Sun runs with the Unix operating system using a Motif–style window manager environment. Custom screens allow operators to use the stability analyzer with only occasional reference to an instruction manual. Unique test script files are compiled at run–time to control test tasks, which are started in the Sun and executed in the Skybolt. The scripts are written in a custom language, similar to Structured Query Language (SQL), including higher–level operations such as Define, DoWhile, If, etc. The Sun code is written in C, some of which is computer generated by programming tools and utilities, mainly Builder Xcessory, Lex, and Yacc.

The signal processing software supports tests for Allan deviation of phase and differential phase, time series of phase and amplitude, and spectra of signal, phase, and amplitude. Each of 17 distinct tests can be selected by the operator with a single mouse click on the display. The test configuration parameters (input source, sample rate, averaging time, etc.) are automatically loaded from editable configuration files, and can also be modified at the display by the operator.

The sample clock for A–D conversion comes from a Hewlett Packard 3325A synthesizer, referred to 10 MHz from the Reference Frequency Distribution Assembly. Although the A–D converter can handle 400 kHz, the limit of the current implementation is 230 kHz. Nevertheless, this rate is adequate to handle two of the widest baseband signals (bandwidth 45 kHz) from the Deep Space Network Radio Science open–loop receiver. The frequency span of spectra can vary from 50% of the sample rate down to an arbitrarily small band about the carrier.

## **Digital Signal Processing (DSP) Algorithms**

### **Vectorized Processing**

The signal processing routines run on a single–board computer, the 40 MHz Skybolt, containing an Intel I860, a floating–point vector processor with its own high–speed data cache. To achieve the best computational throughput on this processor, we avoided recursive operations, such as phase–locked loops and recursive digital filters, in favor of sequential, nonrecursive operations on large arrays, such as element–by–element vector arithmetic, inner products, finite–impulse–response (FIR) digital filters, and the fast Fourier transform (FFT), all of which are supported by Sky Computer’s vector library and compiler. Throughputs of 25–30 million floating–point operations per second were achieved.

cable to A–D converters in the VME Assembly for other measurements of signal, phase, and amplitude. A digital I/O assembly receives RS232 switch commands from the computer to address the switch decoders that actuate the matrix switches and set attenuation values.

### **Zero Crossing Detector**

The stability analyzer employs two methods for phase detection: one method using software processing of A–D samples, and another using a time interval counter<sup>[5]</sup>. For the second method, we use a new design of zero crossing detector that has reduced time jitter compared to previous designs<sup>[4]</sup>. In operation, the zero crossing detector heterodynes the signal to 1 Hz, then processes the 1 Hz output to produce 1 Hz rate, 30 microsecond–wide pulses that are sent over fiber optics to the time interval counter.

### **Time Interval Counter**

A HP 5334B Counter is modified to accept inputs from the rear panel, and to accept the fiber–optic signal from the zero crossing detector and a 10 PPS signal from the reference distribution assembly.

### **Reference Frequency Distribution**

This assembly distributes a high–stability 10 MHz station reference to the frequency synthesizers and the time interval counter, and also generates a 10 pulse per second signal used by the time interval counter for phase detection.

### **Environmental Concerns**

The stability analyzer has been designed to minimize influence of the environment on measurements. The most environmentally sensitive equipment is placed in the frequency standards room where ambient temperature stability is better than  $\pm 0.1^\circ\text{C}$ . All signals between the 100 MHz assembly and the stability analyzer racks are connected through fiber optics to eliminate groundloops that could induce powerline spurious into measured output. The analog electronics of the 100 MHz and low frequency assemblies are temperature stabilized with a thermoelectric control system that reduces room temperature variations by a factor of 20. Magnetic shields around the electronics attenuate magnetic fields by more than 20 dB, thereby minimizing pickup of AC powerline harmonics.

### **Controller and Software Design**

The Controller Assembly consists of a Sun Microsystem Sparc 2 general purpose computing system, with an attached VME computer chassis. The Sparc 2 performs the user interface function, hardware control, and the display and logging of test results. The computer includes an Integrix SBus expansion unit, a 1.2 GByte hard disk, a 5.0 Gbyte Exabyte tape drive, a CD ROM reader, along with the usual monitor, keyboard, mouse, and laser printer. Serial ports are used for communication with the analog hardware and a time code translator, and an IEEE

## Sampling the Video Signal

We discuss here only the processing of the signal through the A–D converter; the processing of 1-Hz zero-crossing signals through the counter has previously been documented<sup>[5]</sup>. The analog “video” signal is specified to be a sinewave with weak sidebands in a known frequency band about the carrier. (The total sideband power should not exceed about  $-30$  dBc.) First, this signal has to be sampled at a such a rate that the sidebands of the digitized signal faithfully reproduce the sidebands of the analog signal. For example, the output of the 100 MHz Interface Assembly is a 100 kHz signal with sidebands between 85 kHz and 115 kHz. If this is sampled at 80 kHz, the sampled signal, which lives in a 40 kHz band, has a carrier at 20 kHz and sidebands between 5 and 35 kHz. The 16-bit A–D necessarily adds its own noise and distortion; fortunately, by adjusting the sample rate one can reduce their effects on measurement results by whitening the noise and moving the aliased harmonic distortion images away from the frequency band of interest.

## Overview of Signal Processing

To allow the user to check the overall quality of the signal, we supply a test called “full band spectrum”. This test simply computes a spectrum of the sampled signal in the maximum frequency span available, namely, half the sample rate  $f_s$ . Also provided are snapshot plots of A–D samples vs time.

The main job of the DSP is to extract the phase and amplitude modulations from the digitized video signal within a user-selected frequency  $B$  of the carrier. Two processes for this are supplied, called medium band and narrow band. Medium band is used for  $B$  from  $f_s/4$  down to  $f_s/256$ . Narrow band is used for smaller values of  $B$ , with essentially no lower bound except that implied by the user’s patience. These processes are described below. First, however, we describe a vectorized algorithm for sinewave analysis that underlies much of the processing.

## The Pony Computation

At the heart of the DSP is a simple vectorized algorithm for estimating the frequency, phase, and amplitude of one batch of a sampled sinewave. It was obtained by adapting Prony’s method of harmonic analysis<sup>[6]</sup> to the case of just one harmonic component, the carrier itself. Given an  $N$ -point data vector  $(x_n, n = 0, \dots, N-1)$ , we wish to fit a sampled sinewave  $c_n = A \cos(\omega n + \theta)$ . The computation is divided into two parts: Pony 1, which estimates frequency  $\omega$ , and Pony 2, which estimates  $A$  and  $\theta$ . The Pony 1 computation uses the observation that the noiseless sinewave  $c_n$  satisfies the difference equation  $c_{n-1} + c_{n+1} = (2 \cos \omega)c_n$ . Accordingly, we estimate  $2 \cos \omega$  as the regression coefficient of the vector  $(x_{n-1} + x_{n+1})$  on the vector  $(x_n)$ , where  $n$  runs from 1 to  $N-2$ . This computation requires only two inner products, of form  $\sum x_n^2$  and  $\sum x_n x_{n+1}$ , plus some scalar arithmetic. For use in Pony 2 and elsewhere, we also generate a complex vector of powers  $u^n$ , where  $u = \exp(-i\omega)$ , by means of a vectorized “powers” algorithm that takes advantage of the Skybolt architecture.

Pony 2 uses  $\omega$  to estimate  $A$  and  $\theta$  by solving the two-parameter least-squares problem  $x_n = a \cos \omega n - b \sin \omega n$  for the unknowns  $a$  and  $b$ . The only vector computation needed is

are combined by subtraction (with some adjustments) to give differential phase, which can be post-processed in the same way as single-channel phase residuals.

## Spectral Estimation

Direct FFT-based spectral estimation methods are used<sup>[9]</sup>. The sequence of operations applied to a data buffer is detrending, tapering, zero-padding to a power-of-2 FFT size, applying a real or complex FFT, squaring the magnitude, equalizing the lowpass decimation filter, and scaling. Some of these elements are discussed below. A sequence of spectral estimates can be averaged to produce a run spectrum with greater statistical stability.

Spectral density of signal, phase, or fractional amplitude deviation is displayed in units of dBc/Hz, *i.e.*, single-sideband power per Hz relative to total (carrier) power, expressed in decibels. Thus, a phase spectrum shows  $\mathcal{L}(f) = S_\varphi(f)/2$ . A signal spectrum shows both sidebands.

Each spectrum produced by the analyzer has an associated resolution bandwidth  $b$ , which is just the two-sided noise bandwidth of the spectral window. The power of a narrow spectral line in dBc equals its displayed level in dBc/Hz plus  $10 \log_{10} b$ . Both  $b$  and  $10 \log_{10} b$  are reported to the user.

## Detrending

Before applying the FFT to a data array, this analyzer preconditions the array by subtracting a linear fit obtained by drawing a straight line between the centroids of the first sixth and the last sixth of the graph of data vs time. This procedure removes both the level and slope divergencies characteristic of certain processes with stationary second increments<sup>[10]</sup>, and allows the average of many array spectra to converge to a stable run spectrum. This avoids a problem noticed by Walls, Percival, and Irelan<sup>[11]</sup>, who preconditioned their data by subtracting the mean; they found that the estimated spectrum for noise with a true  $f^{-4}$  spectrum depended on the number of array spectra that were averaged. For full band spectrum, no detrending is needed because most of the energy is in the carrier.

## Data Tapering

To avoid problems of energy leakage from high portions of a spectrum into lower portions, each data array is multiplied by a tapering sequence drawn from a family of functions called discrete prolate spheroidal sequences (DPSS). (Actually, we use a set of convenient approximations, the “trig prolates” developed by Greenhall<sup>[13]</sup>.) For full band and medium band spectra, we use a single bell-shaped taper from this family. For narrow band spectra we use a nonadaptive, unweighted version of Thomson’s multiple-taper method<sup>[12, 9]</sup>. An array of detrended data is tapered by four orthogonal tapering sequences, giving rise to four distinct “eigenspectra”,  $S_0(f)$  through  $S_3(f)$ . These are averaged to produce the spectral estimate  $S(f)$  for the array. In a broadband noise region, the  $S_k(f)$  are approximately uncorrelated, and hence  $S(f)$  has about one-fourth the variance of each  $S_k(f)$ . For a given frequency resolution, the desired statistical stability is achieved from fewer data arrays.

$\sum x_n u^n$ . Then  $A$  and  $\theta$  are obtained from  $A \exp(i\theta) = a + ib$ .

### Medium Band Processing

This mode of processing operates by a sequence of mixing and filtering to extract the complex-valued analytic signal, containing only the power from the positive-frequency side of the original waveform<sup>[7]</sup>, from which the amplitude and phase modulations can be extracted by a rectangular-to-polar operation. The Pony 1 calculation estimates the carrier frequency  $f_c$ , and a mixing signal  $\exp(-i2\pi f_c t)$  is generated by the powers algorithm. After the right-hand part of the carrier is mixed to zero frequency, a FIR lowpass decimation filter is applied to eliminate the other part of the carrier and to select the desired frequency span  $(-B, B)$ . The result is the desired analytic signal within  $B$  of the carrier, shifted to zero frequency.

The analytic signal is the basis of all further processing. If a signal spectrum is wanted, then a two-sided spectrum is generated after removing the DC component (the shifted carrier). If amplitude or phase are wanted, then a rectangular-to-polar operation is applied and the phase sequence unwrapped from  $(-\pi, \pi)$ . (Wan, Austin, and Vilar<sup>[8]</sup> give a more efficient unwrapping method.)

### Narrow Band Processing

In this mode of computation, the A-D data for the whole run are processed in contiguous batches of size  $N$ , each of which is analyzed by both parts of the Pony computation to produce a sample of batch-averaged frequency, amplitude, and phase. The bandwidth of the extracted amplitude and phase samples is  $f_s/(2N)$ . Because of the efficiency of the Pony computation, the DSP can keep up with the stream of A-D samples at the highest rate of the A-D converter, 400 kHz, although, as mentioned above, the analyzer is currently limited to a total sample rate of 230 kHz.

For computational efficiency,  $N$  has to be at least 200. To save storage, we allow batches no greater than a designated maximum batch size (now 8192). Because we also wish to allow arbitrarily small analysis bandwidths, the batch averages can themselves be averaged together in groups of arbitrary size  $r$  to produce samples with bandwidth  $f_s/(2Nr)$ . In choosing this crude lowpass decimation method, we accepted some aliasing problems to gain simplicity, consistency, and efficiency.

The phase information computed by Pony 1 and 2 is local to each batch, and is known modulo  $2\pi$  only. We have devised an algorithm to process these local data into a sequence of global phase residuals; it is essentially the same as the algorithm used for processing the 1 Hz zero crossing counter readings<sup>[5]</sup>. For the algorithm to succeed, the frequency must be changing slowly enough from batch to batch so that the current batch phase can be predicted from earlier ones within  $\pi$ . The algorithm issues an alarm if any prediction error exceeds  $\pi/2$  in absolute value.

The low-rate sequence of amplitude and phase residuals extracted by the narrow band process can be subjected to a variety of post-processing functions, including time-series display, spectral estimation, and Allan deviation. For a two-channel test, the phase residuals of the two channels

## Allan Deviation

From a stream of narrow band or 1 Hz zero crossing phase residuals, the analyzer produces estimates of Allan deviation with estimated drift removed, using the simple three-point drift estimator recommended by Weiss and Hackman<sup>[14]</sup>. The required  $\tau$ -overlapped sums for first and second moments of second  $\tau$ -differences of phase are accumulated in real time.

To generate conservative error bars for plus or minus one standard deviation of Allan variance, we assumed a random-walk-frequency model of phase noise. Using a method of Greenhall<sup>[15]</sup>, we carried out a numerical computation of  $\nu$ , the equivalent degrees of freedom of the drift-removed Allan variance estimator, as a function of  $M$ , the number of summands. The sequence of  $\nu$  vs  $M$  was fit with a simple empirical formula. Then, if  $\sigma$  is the estimated Allan deviation, the reported error bar is

$$\sigma(1 \pm (2/\nu)^{1/2})^{1/2}.$$

Because of severe negative bias of the drift-removed estimator for small  $M$ , results are reported only for  $M \geq 4$ .

## Test Methods

A series of tests of the stability analyzer were conducted at JPL's Frequency Standards Laboratory in order to demonstrate first, that the results of the stability analyzer agree with those of other measurement equipment, and second, that it meets its noise floor requirements. Noise floor results are given in Table 1.

Allan deviation runs of at least 24 hours duration were carried out on pairs of 100 MHz frequency standards. The results were compared to those from an existing FSL Allan Deviation test set and found to agree within 5%. The noise floor was measured by splitting the single output of an H-maser and applying it to two inputs of the stability analyzer. These tests were carried out in both zero crossing detector mode and the narrow band phase modes.

Time series of differential phase were tested using a HP 3326 dual channel synthesizer as the input source. The two outputs of the synthesizer were manually steered in frequency to produce phase drifts of known amplitude. Comparison was made to the results from a HP 8508 phase meter, and also to a strip chart recording the phase difference. This last signal was developed by simple mixing between the two outputs of the synthesizer. These tests were also run with both channels of the synthesizer set at the same frequency for at least 15 hours, to observe the noise floor.

## References

- [1] A.J. Kliore et al, "*Investigation description and science requirement document, Cassini radio science team*", pp 6 & 13, private communication, 10 Feb 1993
- [2] S.W. Asmar and N.A. Renzetti, "*The Deep Space Network as an Instrument for Radio Science Research*", Publication 80-93, rev 1, Jet Propulsion Laboratory, Pasadena, CA, 15 Apr 1993
- [3] P.F. Kuhnle, "*NASA/JPL Deep Space Network frequency and timing*", Proceedings of the 21st Annual Precise Time and Time Interval (PTTI) Applications and Planning Meeting, pp 479-490, 1989
- [4] G.J. Dick, P.F. Kuhnle, and R.L. Sydnor, "*Zero crossing detector with submicrosecond jitter and crosstalk*", Proc 22nd PTTI Meeting, pp 269-282, 1990
- [5] C. Greenhall, "*A method for using a time interval counter to measure frequency stability*", IEEE Trans UFFC, vol 6, pp 478-480, 1989
- [6] S. Marple, **Digital Spectral Analysis with Applications**, Prentice-Hall, 1987
- [7] D. Vakman, "*Computer measuring of frequency stability and the analytic signal*", IEEE Trans Instrum Meas, vol 43, pp 668-671, 1994
- [8] K.-W. Wan, J. Austin, and E. Vilar, "*A novel approach to the simultaneous measurement of phase and amplitude of oscillators*", Proc 44th Freq Control Symp, pp 140-144, 1990
- [9] D. Percival and A. Walden, **Spectral Analysis for Physical Applications**, Cambridge, 1993
- [10] P. Lesage and C. Audoin, "*Characterization and measurement of time and frequency stability*", Radio Science, vol 14, pp 521-539, 1979
- [11] F. Walls, D. Percival, and W. Ireland, "*Biases and variances of several FFT spectral estimators as a function of noise type and number of samples*", Proc 43rd Freq Control Symp, pp 336-341, 1989
- [12] D. Thomson, "*Spectrum estimation and harmonic analysis*", Proc IEEE, vol 70, pp 1055-1096, 1982
- [13] C. Greenhall, "*Orthogonal sets of data windows constructed from trigonometric polynomials*", IEEE Trans ASSP, vol 38, pp 870-872, 1990
- [14] M. Weiss and C. Hackman, "*Confidence on the three-point estimator of frequency drift*", Proc 24th PTTI Meeting, pp 451-460, 1992
- [15] C. Greenhall, "*The fundamental structure function of oscillator noise models*", Proc 14th PTTI Meeting, pp 281-294, 1982

Table 1. Stability Analyzer Noise Floors			
Test	Input Source		
Allan Deviation	100 MHz	tau	sigma
		1 sec	$6 \times 10^{-15}$
		10 sec	$2 \times 10^{-15}$
		100 sec	$2 \times 10^{-16}$
		1000 sec	$3 \times 10^{-17}$
Phase Spectrum	100 MHz	Freq.	Spectral Density
		1 Hz	-126 dBc/Hz
		10 Hz	-135 dBc/Hz
		>100 Hz	-142 dBc/Hz
Signal Spectrum	baseband	1 Hz	-92 dBc/Hz
		10 Hz	-97 dBc/Hz
		>100 Hz	-98 dBc/Hz
Phase Spectrum		1 Hz	-98 dBc/Hz
		10 Hz	-104 dBc/Hz
		>100 Hz	-105 dBc/Hz
Amplitude Spectrum		1 Hz	-70 dBc/Hz
		10 Hz	-85 dBc/Hz
		>100 Hz	-88 dBc/Hz
Diff. Phase	baseband	Avg. Time	Phase Error
		1 sec	<0.001 deg rms
		1000 sec	<0.04 deg rms

Spectra were tested in a variety of ways. The signal sources were two H-masers for the 100 MHz inputs, one H-maser and an HP 8662 synthesizer, or one or two HP 3325 synthesizers for the baseband analog inputs. In the latter two cases, one synthesizer was modulated either by another synthesizer to simulate spurious signals, or by a HP 3561 noise source to simulate phase noise. The spectrum was then compared to the results from a HP 3589 or 3561 spectrum analyzer. The results agreed within a typical 2 dB peak-to-peak variation between spectral bins. For noise floor tests, a single H-maser signal was divided and applied for comparison at two inputs.

## Acknowledgments

We would like to thank Gerard Benenyan, Michael Grimm, Diana Howell, Nancy Key, Barron Latham, Beverly St.Ange, Eric Theis, and John Vitek for their contributions to this project.

The work described in this paper was performed by the Jet Propulsion Laboratory, California Institute of Technology, under a contract with the National Aeronautics and Space Administration.

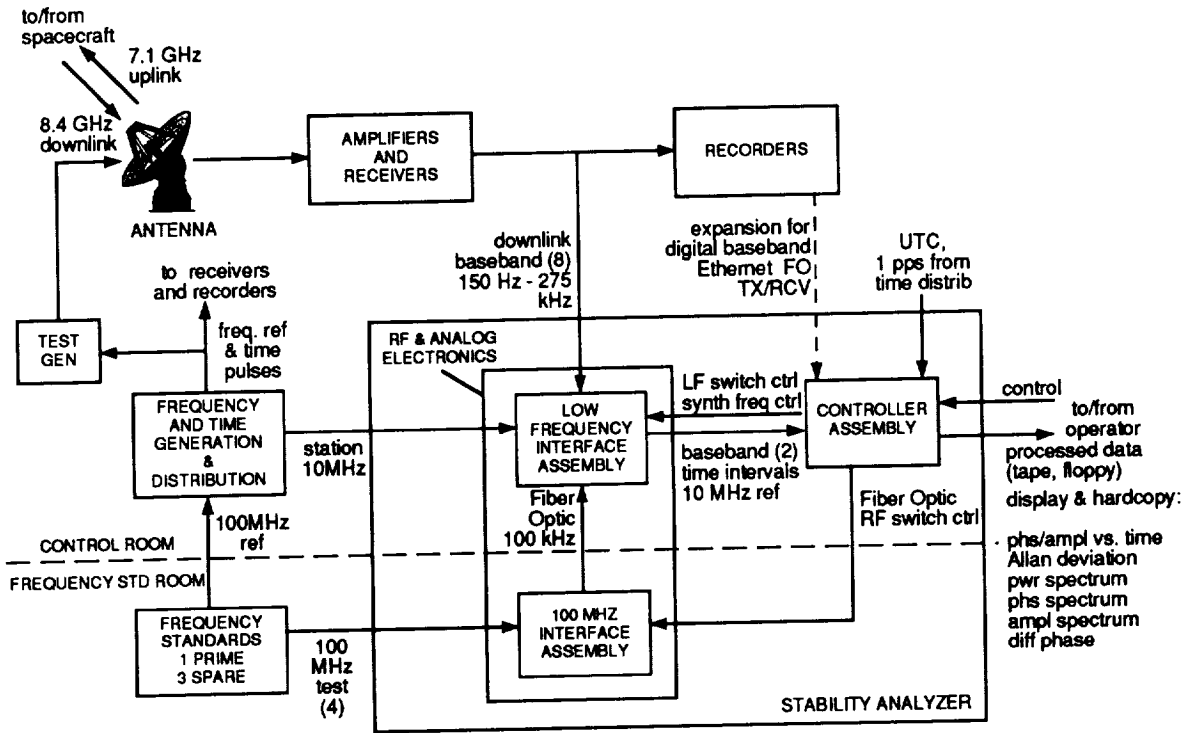


Fig. 1. Stability analyzer in a typical DSN installation.

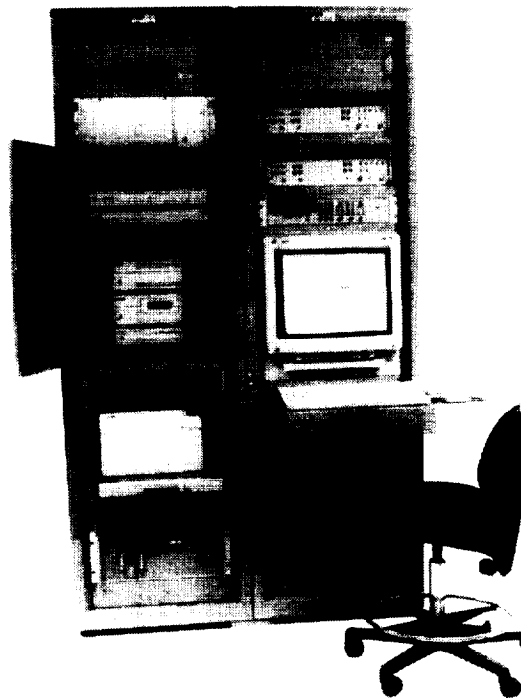


Fig. 2. Stability analyzer rack arrangement.

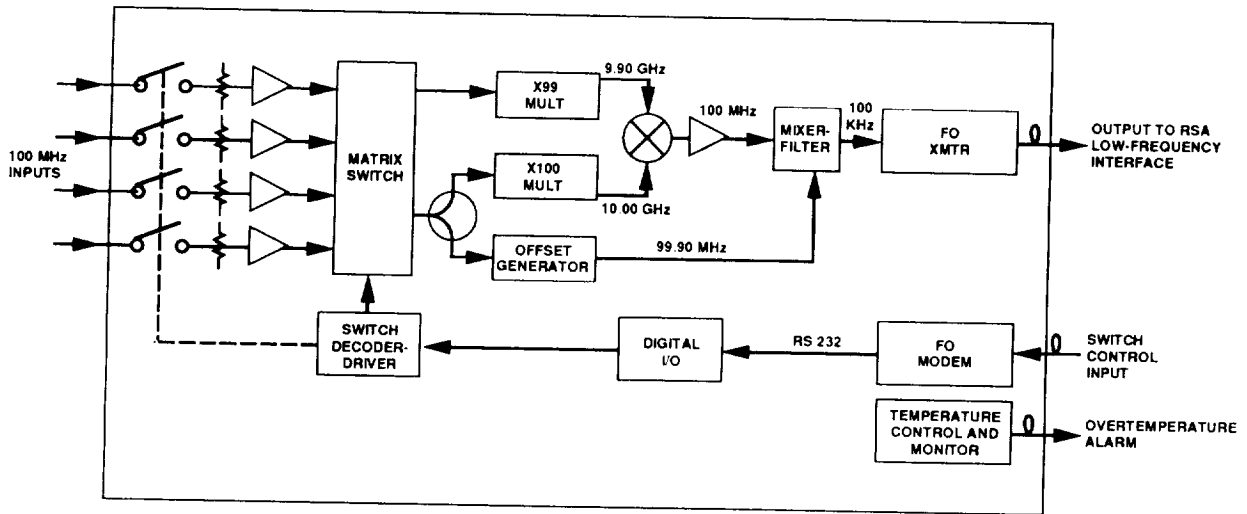


Fig. 3. 100 MHz interface block diagram.

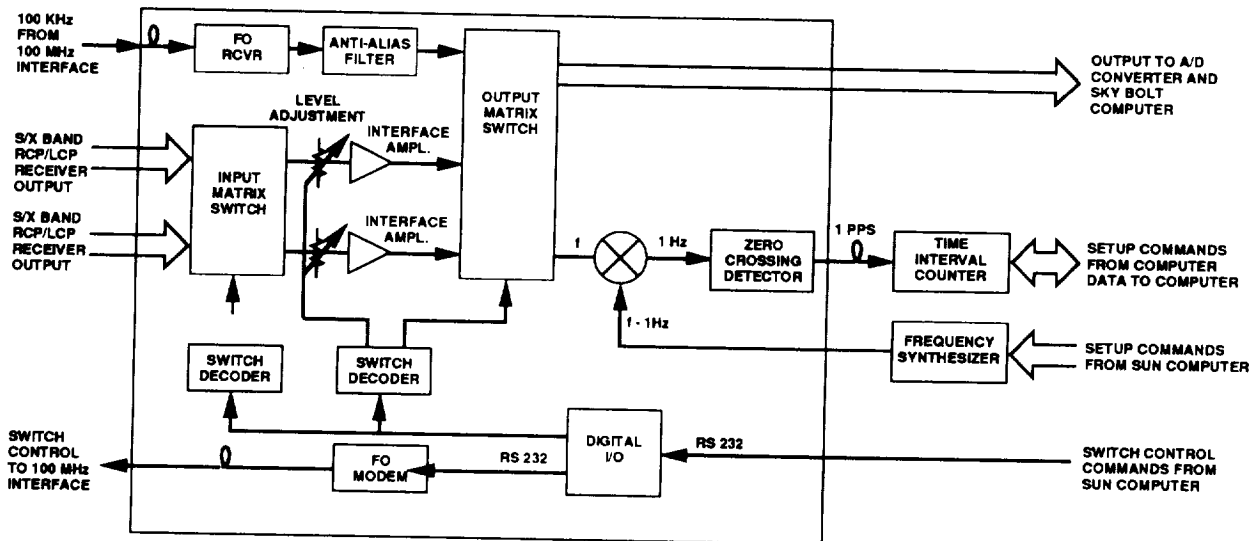


Fig. 4. Low frequency interface block diagram.



5/6-70

62292

# A Globally Efficient Means of Distributing UTC Time & Frequency Through GPS

John A. Kusters, Robin P. Giffard and Leonard S. Cutler  
Hewlett-Packard Co.  
David W. Allan, Allan's TIME  
Mihran Miranian, U.S. Naval Observatory

## Abstract

*Time and frequency outputs comparable in quality to the best laboratories have been demonstrated on an integrated system suitable for field application on a global basis. The system measures the time difference between 1 pulse-per-second (pps) signals derived from local primary frequency standards and from a multi-channel GPS C/A receiver. The measured data is processed through optimal SA Filter algorithms that enhance both the stability and accuracy of GPS timing signals.*

*Experiments were run simultaneously at four different sites. Even with large distances between sites, the overall results show a high degree of cross-correlation of the SA noise. With sufficiently long simultaneous measurement sequences, the data shows that determination of the difference in local frequency from an accepted remote standard to better than  $1 \times 10^{-14}$  is possible. This method yields frequency accuracy, stability, and timing stability comparable to that obtained with more conventional common-view experiments. In addition, this approach provides UTC(USNO MC) in real time to an accuracy better than 20 ns without the problems normally associated with conventional common-view techniques.*

*An experimental tracking loop was also set up to demonstrate the use of enhanced GPS for dissemination of UTC(USNO MC) over a wide geographic area. Properly disciplining a cesium standard with a multi-channel GPS receiver, with additional input from USNO, has been found to permit maintaining a timing precision of better than 10 ns between Palo Alto, CA and Washington, DC.*

## Introduction

Because GPS provides time traceable to Coordinated Universal Time (UTC), and its rate is syntonized with the international definition of the second, it provides a world-wide resource for time and frequency with heretofore unprecedented accuracies and precisions.

Although selective availability (SA) limits navigation and position accuracy to slightly better than the 100 meter specification, a method of filtering the SA noise has been developed for timing during the past year. This method provides enhanced GPS (EGPS) operation<sup>[1]</sup>. The EGPS approach has been shown to provide a real-time UTC(USNO MC) with stabilities of a few nanoseconds and frequency stabilities of  $1 \times 10^{-14}$ . The EGPS timing technique is a systems approach. The quality of the output will depend on the clock used with the receiver.

An EGPS clock based on a high quality quartz oscillator has demonstrated timing stabilities of 20 ns rms, long-term frequency stability of better than  $1 \times 10^{-13}$ , and elimination of frequency drift and reduction of environmental effects on the system output<sup>[1]</sup>.

GPS timing is becoming extremely important to society and to science. Major users include the Bureau International des Poids et Mesures (BIPM), which provides the standard for time and frequency, UTC; 45 national timing centers; NASA JPL's Deep Space Network; the world-wide measurement of the rapid-spin rates of the millisecond pulsars; NIST's global time service; NASA's timing of space platforms; and numerous other calibration and timing laboratories.

Of the six different methods of using GPS for timing<sup>[2]</sup>, three are the most popular. These are GPS direct, EGPS, and GPS Common-View. Of these, EGPS has by far the best performance/cost ratio.

GPS common-view requires that the clock sites participating use single satellites according to a pre-arranged schedule and exchange data. A different approach (EGPS) will yield essentially the same data almost in real-time, but with a simplified procedure. A multi-channel GPS receiver approach permits looking at all satellites in view. Even at continental distances, common satellites are viewed most of the time. Thus, a high degree of correlation can be expected, even with sites on opposite sides of a continent. Rather than using a single satellite for a relatively short period of time and sharing raw data to determine frequency and time changes, EPGS uses proper processing of data from all available satellites to obtain time comparison between the local site and UTC(USNO MC), as broadcast by GPS. The frequency of the remote clock can be compared directly with the broadcast value of UTC(USNO MC) or with similar data received directly from USNO. These comparisons have accuracy uncertainties of  $10^{-14}$ , or less than  $10^{-14}$ , respectively.

Long integration times require the use of clocks that exhibit sufficient long-term stability to maintain stable time and frequency. Presently, commercially available primary cesium-beam frequency standards exhibit typical accuracy of  $\approx 2 \times 10^{-13}$ , long-term stability (better than  $1 \times 10^{-14}$  beyond 1 week), with minimal environmental sensitivity.<sup>[3]</sup> A feature of these standards is that they operate as steerable clocks. The output time and frequency can be controlled by known amounts so that they agree with an external reference. These clocks may be ensembled together to improve robustness of the system.<sup>[4]</sup> The ensemble output can be shown to be better than the best physical clock in the system. Reliability is enhanced since the system continues uninterrupted with only some loss in performance should any one of the clocks fail.

Timing signals are now available from the full GPS constellation of 24 or more satellites offering world-wide, multiple satellite timing information referenced to UTC(USNO MC) with a high level of redundancy, reliability, and robustness. In addition, low-cost commercial multi-channel GPS C/A receivers with 1 pps outputs are available.

## SA Filtering

Until now, a significant problem with using GPS has been the imposition of Selective Availability (SA). SA is an intentional modulation added to the satellite clock signal such that a non-secure receiver cannot achieve full dynamic position accuracy. The recent development of effective,

optimal, SA filtering techniques based on the spectral characteristics of SA permits receiving UTC(USNO MC) time as broadcast by GPS almost as if SA were not present.<sup>[5]</sup>

These techniques provide no assistance in determining dynamic positioning, but are a major enhancement in determining time and frequency. Since UTC(USNO MC) is currently steered to UTC within  $\pm 60$  ns, and the broadcast correction from GPS has a documented accuracy of about  $\pm 20$  ns with respect to UTC(USNO MC), the system described provides a real-time access to UTC. Accurate measured values of the time difference between UTC (via GPS) and UTC(USNO MC) are available after a 48 hour delay. These can be used to improve further the timing accuracy to better than 10 ns.

## Experimental Results: Part I

During April and May 1994, time difference data were taken at four sites. These were: the US Naval Observatory (USNO), Washington, DC, the National Institute of Standards and Technology (NIST), Boulder, CO, Hewlett-Packard Laboratories (HPL), Palo Alto, CA, and the Hewlett-Packard Santa Clara Division (SCD), Santa Clara, CA.

At each site, the same, low-cost commercially available, 6-channel GPS C/A timing receiver was installed. The time difference between the 1 pps signal derived from the GPS receiver and the 1 pps from the local primary frequency standard was measured using conventional time-interval measurement techniques. Used in this experiment were: the Master Clock at USNO, the output from Microstepper B (tied to UTC(NIST) at NIST, a single HP5071A cesium-beam frequency standard at HPL, and an active ensemble of three HP5071A standards at SCD.

No attempt was made to synchronize the GPS 1 pps signals to the local signals. The receiver time delays were not calibrated, but as all receivers were identical, a reasonable assumption is that the delays were approximately the same. Finally, except for USNO, no attempt was made to correct for all of the known fixed time delays either in the GPS antenna or in the 1 pps delay from the local standard. As a result, the data obtained can be used to determine frequency accuracy, frequency stability, time stability, but not time accuracy between the various sites.

The experimental results are shown in Figures 1 through 4. Each plot presents 300 second averaged data for each data point, since 300 seconds was the shortest common measurement time of the four sites involved. At three of the sites, data points were taken every second, then 100 consecutive values were averaged and the 1 second data discarded. At the fourth site, 1 second data points were averaged every 60 seconds. Also shown as a white line in each plot are the SA filtered data, obtained by post-processing the original experimental data with the SA filter algorithm. The mean value has been subtracted from all data in the plots. The SA filter algorithm used was such that in an on-line system, the same outputs could be obtained in real time.

The filtered data in Figure 1 was compared with the output of a secure two-frequency keyed GPS receiver. This receiver used the measured rather than the broadcast value for the ionospheric delay correction. The rms of the time difference between the filtered estimate and the secure receiver was 1.5 ns.

The improvement in time-domain stability obtained through the use of this optimum filtering routine is shown in Figure 5. The upper line shows the modified Allan Deviation (MDEV) of the NIST time difference data before filtering. The data are dominated by SA noise, and the slope is about  $-3/2$ , indicating a white-phase noise process. The lower line is the MDEV of the filtered NIST data. The amplitude of the noise has been reduced to approximately the noise level expected of a cesium standard. At 200,000 seconds, outside the stop-band of the SA filter, the value of MDEV observed is of the same order as the noise of the UTC-corrected GPS. The improved time domain stability is obtained at the cost of a longer response time.

Table 1 presents some of the experimental results obtained after all data have been corrected for constant frequency offsets and slopes. The correction factors are shown. Significant is an almost 500-fold improvement in time-domain stability at 300 seconds and the uniformity from site to site.

A close examination of the data in Figures 3 and 4 (HPL and SCD) indicates a high degree of correlation. Given that the two sites are less than 25 km apart, this is not unexpected since both sites see the same GPS satellites at essentially the same time. A difference plot of the data is shown in Figure 6. As the data for the four sites share a common binning scheme, the cross-correlation coefficients were calculated for several selected pairs over the period of common data bins between the sites. The results are shown in Table 2. As expected, correlation decreases with distance between observation sites. This is undoubtedly due to differences in the tropospheric and ionospheric correction factors and a decreasing number of satellites common to both sites.

## Experimental Results: Part II

An experimental GPS tracking loop was set up to demonstrate the use of EGPS for dissemination of UTC(USNO MC) at a slightly improved accuracy over that from Part I. The experiment consisted of steering a cesium clock at Hewlett-Packard Laboratories in Palo Alto CA using the output of a multi-channel GPS receiver. The effects of the GPS-to-UTC(USNO MC) time-difference, and un-modelled receiver delays were minimized by using the readings from an identical receiver at USNO in Washington, DC the output of which was compared with the USNO master clock.

In order to avoid uncertainties due to the broadcast GPS to UTC(USNO MC) corrections, which could be as large as 100 ns, both receivers operated in the "GPS" timing mode.

At USNO the 1 pps output of a 6-channel receiver in the "position-hold mode" was timed with reference to UTC(USNO MC). Average time differences were computed using data extending over two days, evenly weighted. The averages were assigned to the modified Julian date (MJD) corresponding to the center of gravity of the data, and placed in a computer data file which could be read by ftp over Internet. The data file was automatically copied daily by the computer at HPL that managed the tracking loop. On receipt, the data in the file was usually between one and two days old.

At HPL the 1 pps output of an identical receiver in the same operating mode was compared with the 1 pps output of an HP 5071A cesium standard. Each hour, the readings taken in the

preceding 60 minutes were averaged and placed in a data file. A second-order feedback loop was used to steer the cesium standard. The inputs to the feedback calculation were the averaged time difference between the local clock and the output of the GPS receiver, and the averaged, delayed, data from USNO. The USNO data was processed by a simple predictor to estimate the current value of the GPS-UTC(USNO MC) time-difference. This value was subtracted from the local time difference and used to calculate a proportional frequency correction for the cesium standard.

The USNO data was subtracted from corresponding 2-day averages of the local time differences and summed into an integral that was scaled to give the frequency correction for the cesium standard. Effectively, over 90% of the 1 pps pulses at each site were used in the algorithm in order to minimize SA and quantization noise in the receiver. A block diagram of the tracking system is shown in Figure 7.

Initial operation of the tracking loop extended over 40 days. No independent check on the system accuracy with comparable resolution was available, so the results were analyzed on the basis of self-consistency. Figure 8 shows a histogram of the local two-day time differences, with the USNO two-day averages subtracted. The distribution is acceptable, with an rms value of 4 ns. This data shows the tracking error and is not affected by noise at frequencies lower than the loop cut-off, or noise that is coherent at both locations. This noise level compares quite well with the estimate of the cesium standard noise given by  $\tau * \sigma_y(\tau)$  calculated for 2 days, which is 3.5 ns. The noise in the tracking loop is shown in Figure 9, which shows the Allan deviation calculated for the frequency corrections applied each 6 hours to the cesium standard. The deviations are compatible with the noise expected from the cesium standard, when the loop transfer function is taken into account. At 4 days the Allan deviation of the frequency corrections is  $1.5 \times 10^{-14}$ . This represents the rms total of the cesium standard noise and the noise introduced by the GPS tracking loop including SA.

This performance suggests that excellent results can be obtained with time-tracking loops using multi-channel GPS receivers, even in the presence of SA. For good time resolution, a high quality local clock is essential. The performance of the loop described could be improved by better algorithms for estimating the real-time GPS-UTC(USNO MC) difference, and for minimizing diurnal effects in the GPS data. The performance of this loop will also depend on the dynamics and magnitude of the GPS-UTC(USNO MC) time difference, which was comparatively small during this experiment.

## Summary

The full set of data indicates that the EGPS technique permits a stable local clock to be steered accurately to UTC(USNO MC) using the GPS timing signal. The experimental results indicate that over a one month time period, frequency transfer accuracies of a few  $\times 10^{-15}$  are possible. Although no attempt was made to correct for fixed time delays in these experiments, it appears that sufficient accuracy can be obtained to maintain a local time scale close to the performance limits of the GPS system if the system delays are carefully determined.

## Acknowledgments

The authors sincerely acknowledge the active assistance of personnel from the United States Naval Observatory, and Victor Zhang and Marc Weiss of the Time and Frequency Division of the National Institute of Standards and Technology.

## References

- [1] J.A. Kusters, et.al., "A No-drift and less than  $1 \times 10^{-13}$  Long-term Stability Quartz Oscillator Using a GPS SA Filter," Proceedings of the 1994 IEEE International Frequency Control Symposium, IEEE Catalog No. 94CH3446-2, pp. 572-577, June 1994.
- [2] D.W. Allan, et.al., "Civil GPS Timing Applications," presented at the 1994 ION GPS-94 Conference, Salt Lake City, Sept. 1994.
- [3] J.L. Johnson and J.A. Kusters, "A New Cesium Beam Frequency Standard — Performance Data," Proceedings of the 1992 IEEE Frequency Control Symposium, IEEE Catalog No. 92CH3083-3, pp. 143-150, June 1992.
- [4] S.R. Stein, "Advances in Time Scale Algorithms," Proceedings of the Precise Time and Time Interval Applications and Planning Meeting, NASA Conference Publication 3218, pp. 289-302, Dec. 1992.
- [5] D.W. Allan and W.P. Dewey, "Time-Domain Spectrum of GPS SA," Proceedings of the ION GPS-93, Sixth International Technical Meeting of the Satellite Division of the Institute of Navigation.

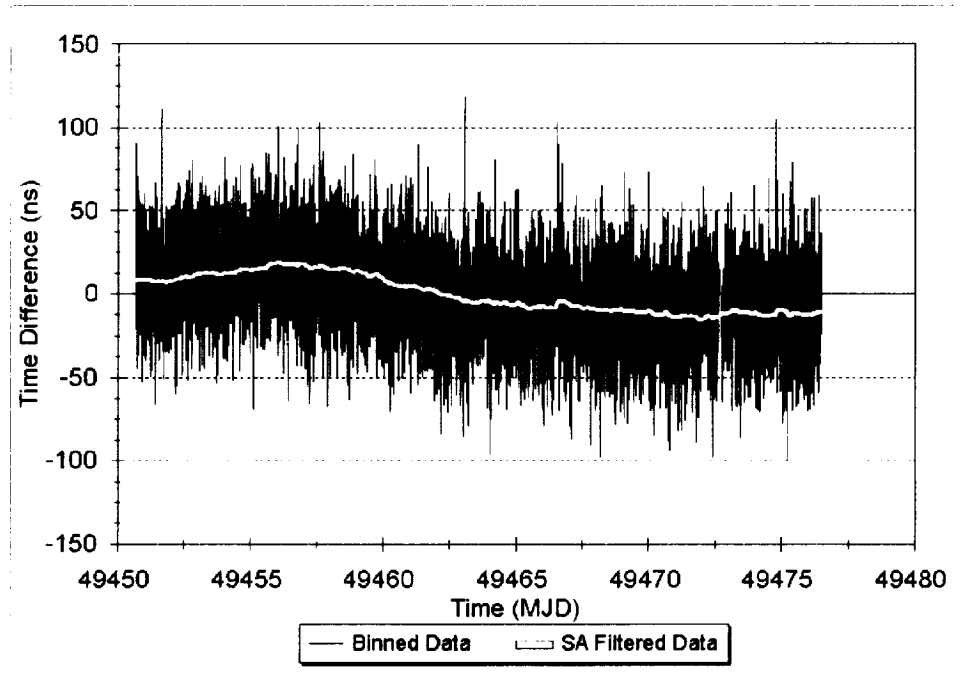


Figure 1. GPS vs. USNO Master Clock -- 300 second binned data

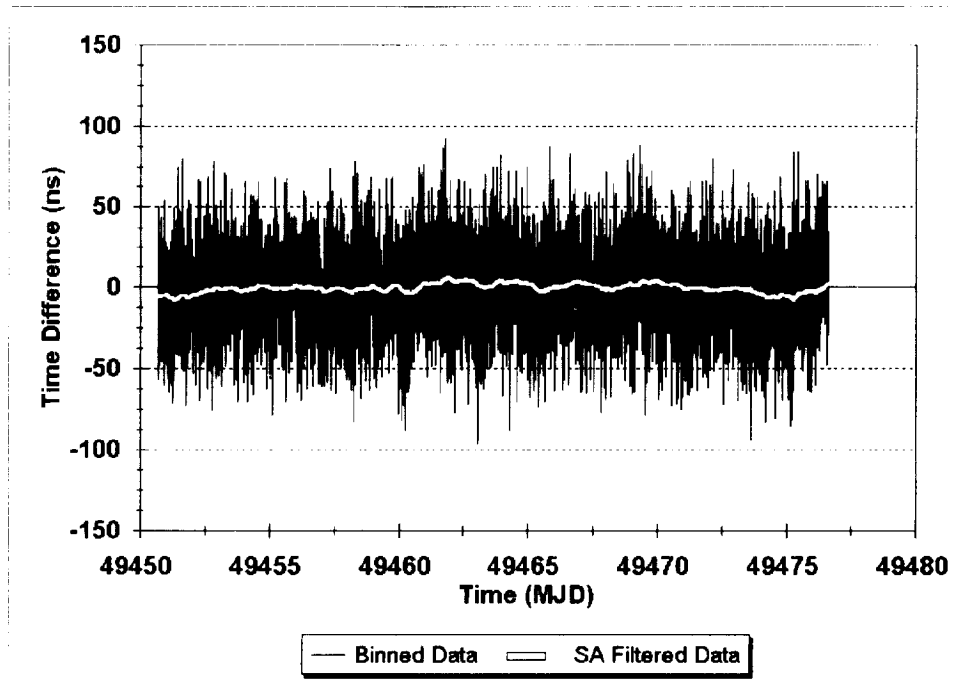


Figure 2. GPS vs. NIST Microstepper B -- 300 second binned data corrected for offset and slope.

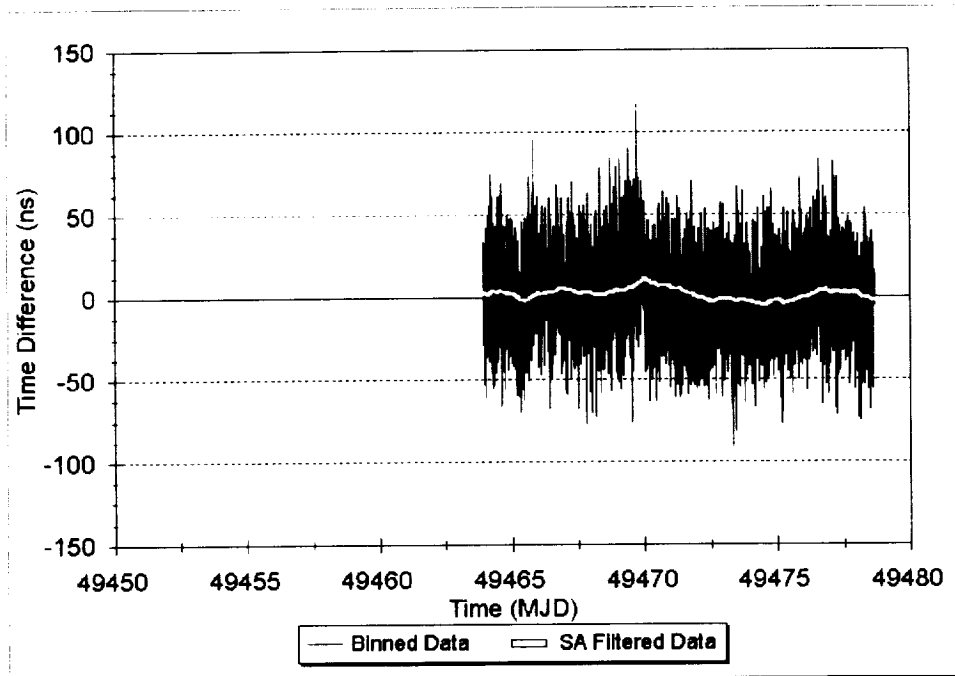


Figure 3. GPS vs. HPL HP5071A -- 300 second binned data

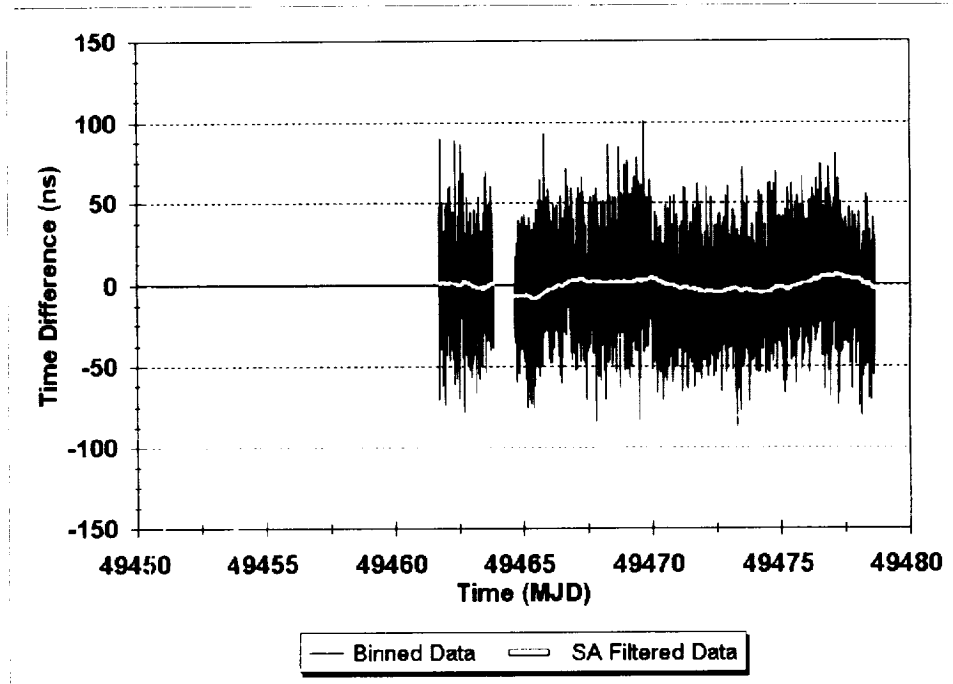


Figure 4. GPS vs. SCD HP5071A Ensemble -- 300 second binned data corrected for offset and slope

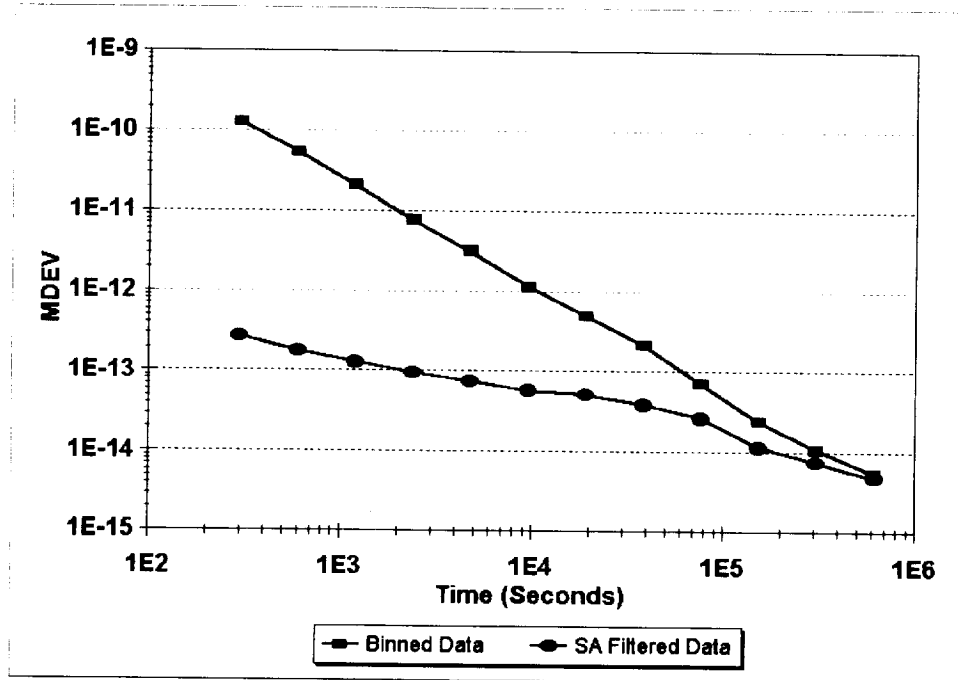


Figure 5. Modified Allan Variance, NIST Data

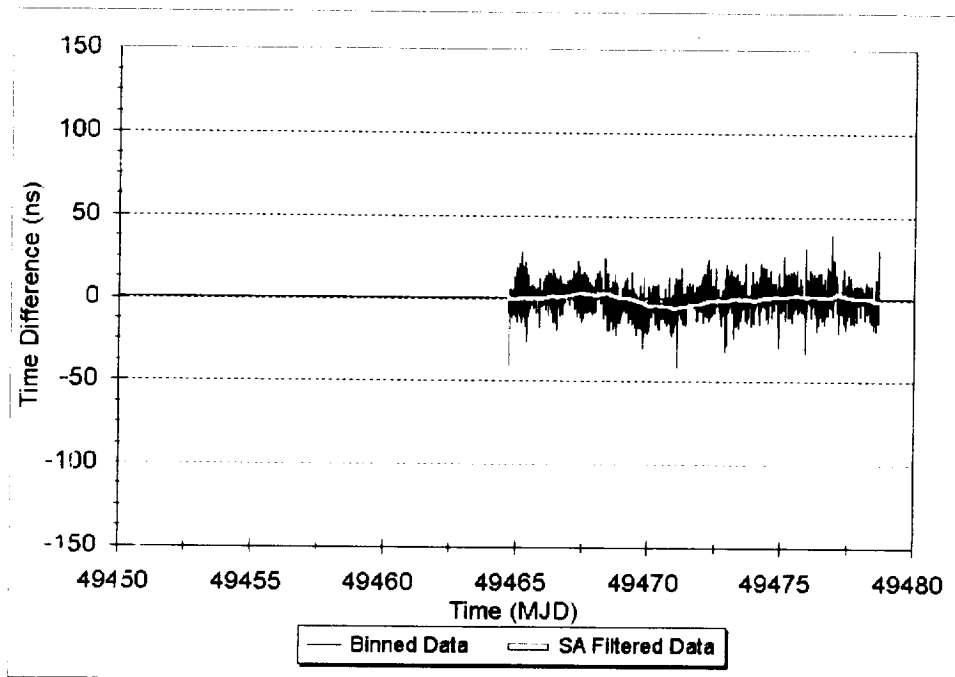


Figure 6. Difference data, SCD - HPL

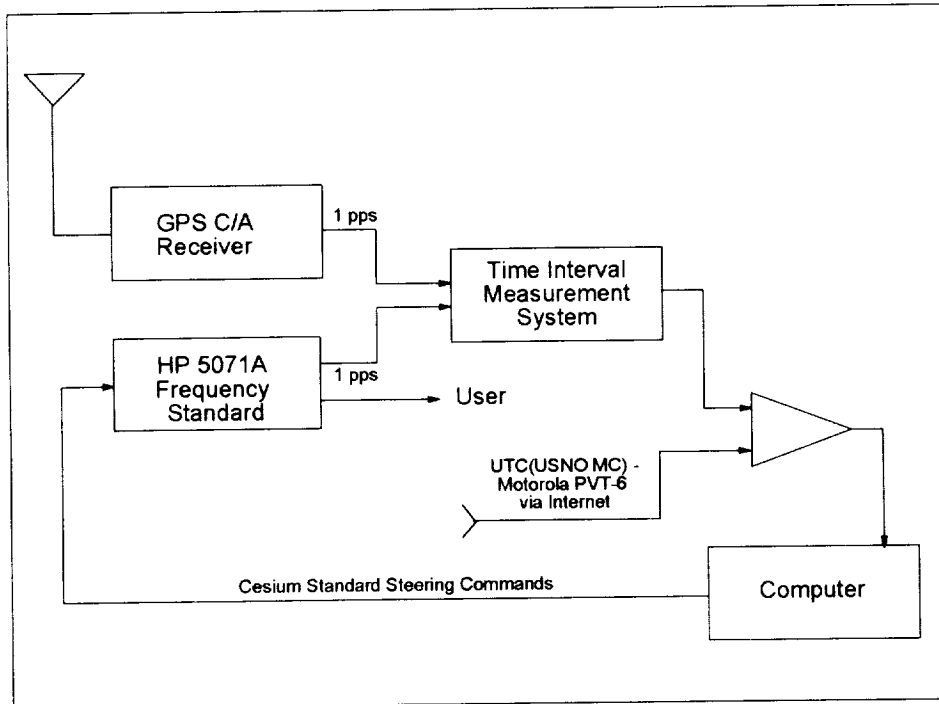


Figure 7. Block Diagram, GPS Disciplined Cesium Standard

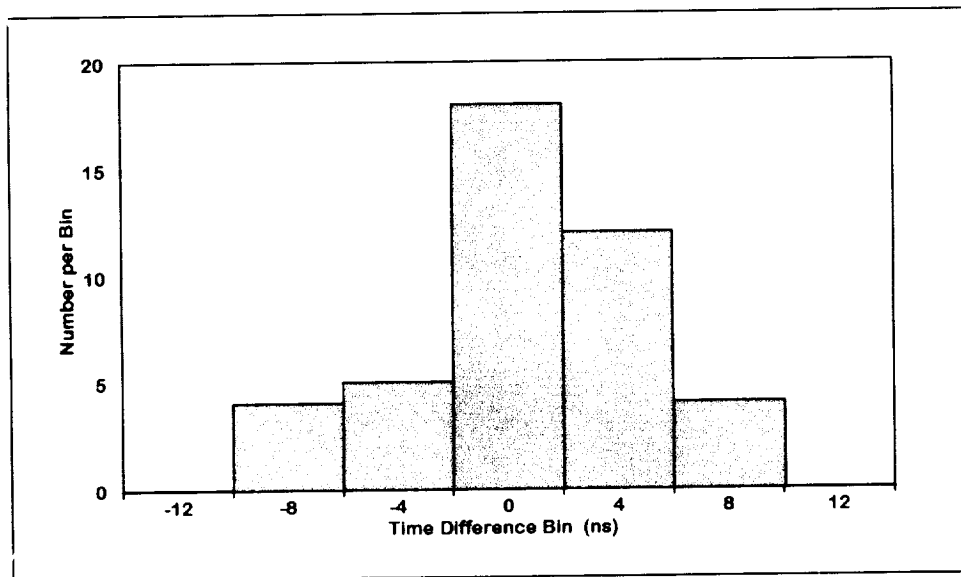


Figure 8. Histogram, HP5071A Disciplined to UTC(USNO MC) Local Two-day Time Differences,

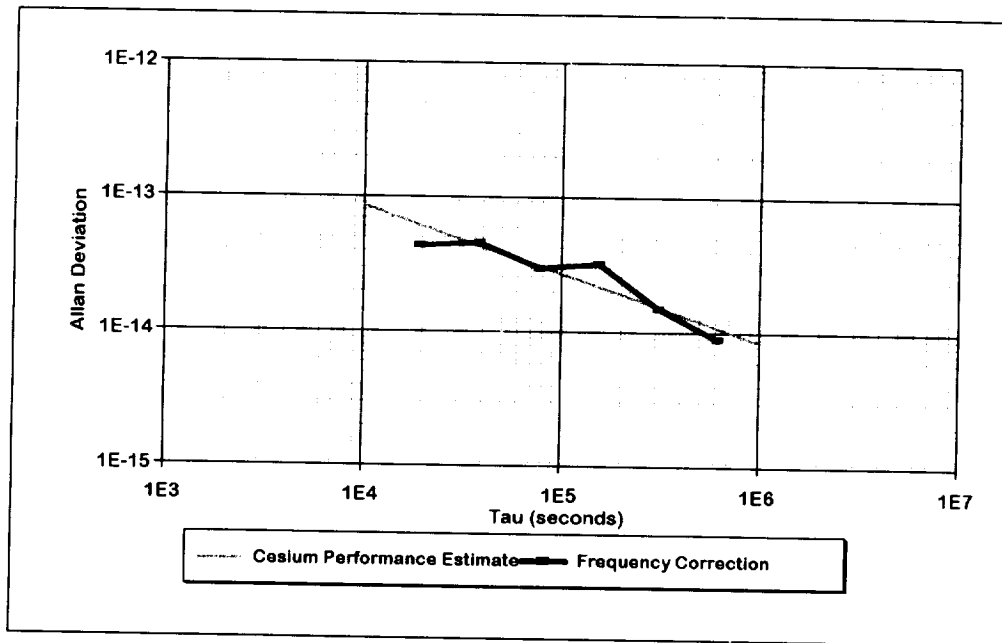


Figure 9. Allan Deviation, HP5071A Disciplined to UTC(USNO MC), steering data

	USNO	NIST	SCD	HPL
Offset (ns)		1146	579	571
Rate (ns/day)		1.8	8.9	-0.3
$\sigma_y(\tau=300 \text{ sec})$ - original data	$1.30 \times 10^{-10}$	$1.28 \times 10^{-10}$	$1.26 \times 10^{-10}$	$1.26 \times 10^{-10}$
$\sigma_y(\tau=300 \text{ sec})$ - filtered data	$2.71 \times 10^{-13}$	$2.69 \times 10^{-13}$	$2.63 \times 10^{-13}$	$2.63 \times 10^{-13}$

Table 1. Experimental Results, Part I

USNO -- NIST	0.67
NIST -- SCD	0.76
SCD -- HPL	0.96

Table 2. Normalized Cross-correlation Coefficients, Part I

## TUTORIAL PTTI MEASUREMENT TECHNOLOGY

CHAIRMAN: DR. FRED L. WALLS, NATIONAL INSTITUTE FOR STANDARDS AND TECHNOLOGY

This workshop is divided into three parts. The first part teaches the fundamentals and the basics of AM and PM noise measurements. The second part uses this background in the basic measurements to develop error models for PM and AM measurements. These models are then illustrated by selected practical examples. The emphasis is on identifying parameters to monitor and pitfalls to avoid. A few examples of PM and/or AM noise in selected components are presented. Fractional frequency stability in the time domain is easily calculated from phase noise measurements. This approach is particularly powerful for short measurement times or when there are significant spurious signals.

The third part details some approaches to the measurement problems that extend the frequency range and improve the accuracy and/or speed of the measurements.

## I. FUNDAMENTAL CONCEPTS AND DEFINITIONS IN PM AND AM NOISE METROLOGY

Eva Pikal  
NIST/University of Colorado

- A. Fundamental concepts
- B. Simple PM noise measurement systems
- C. Simple AM noise measurement systems

## II. DISCUSSION OF ERROR MODELS FOR PM AND AM NOISE MEASUREMENTS

Fred L. Walls  
NIST

- A. Error model for PM noise measurements
- B. Error model for AM noise measurements
- C. PM and AM noise models
- D. Conversion of PM data to  $\sigma_y(\tau)$  and  $\text{mod}\sigma_y(\tau)$

## III. STATE-OF-THE-ART MEASUREMENT TECHNIQUES FOR PM AND AM NOISE

Craig W. Nelson  
SpectraDynamics

- A. Ultra wideband measurements ( $f = 0.1$  Hz to 1 GHz)
- B. Integral AM and PM noise standards
- C. Ultra low-noise PM and AM measurement systems  
 $S(f) \leq -190$  dBc/Hz)

# FUNDAMENTAL CONCEPTS AND DEFINITIONS IN PM AND AM NOISE METROLOGY

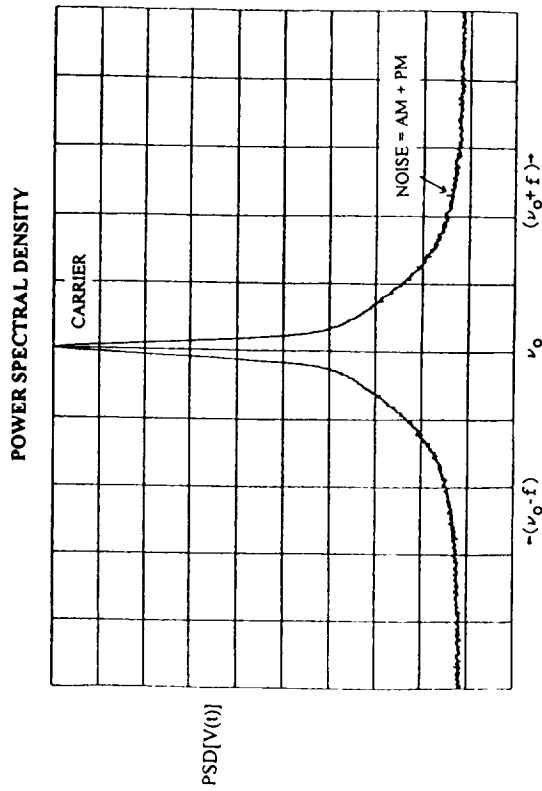
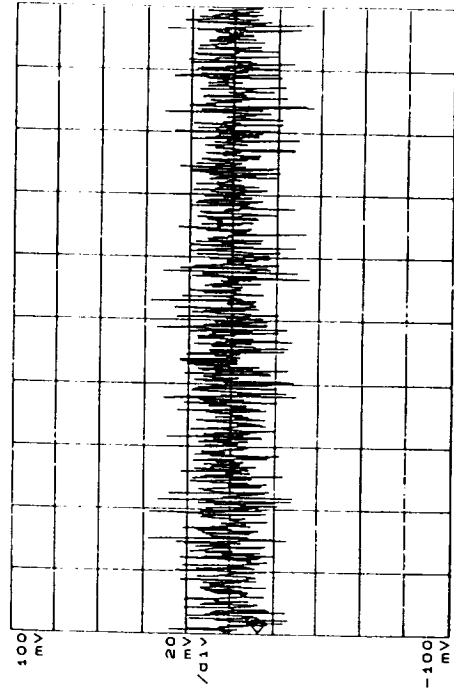
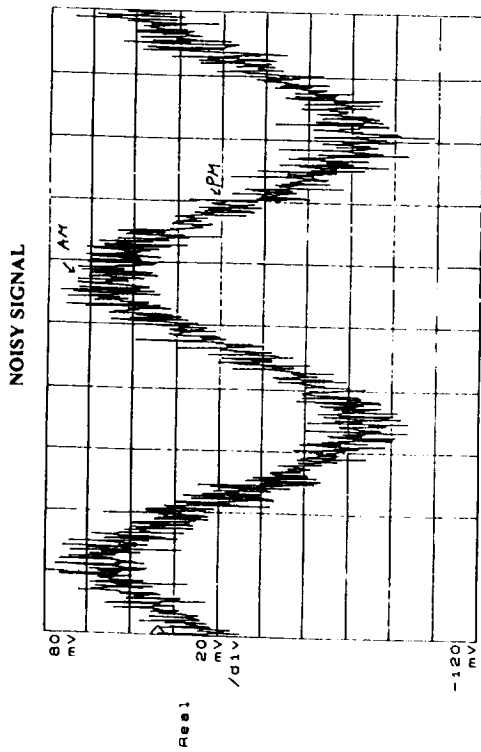
Eva F. Pikal  
NIST/University of Colorado

## FUNDAMENTAL CONCEPTS

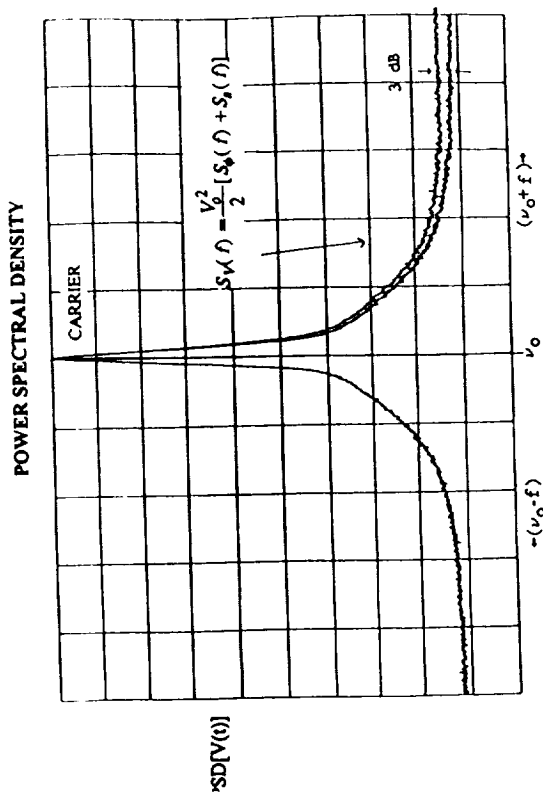
### SIMPLE PM NOISE MEASUREMENT SYSTEMS

- TWO OSCILLATOR METHOD
- DELAY LINE
- CAVITY DISCRIMINATOR

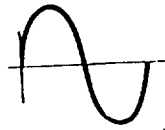
### SIMPLE AM NOISE MEASUREMENT SYSTEMS



WAVE THEORY REVIEW



perfect signal

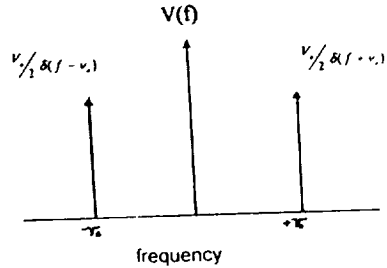


$$V(t) = V_o \cos(2\pi\nu_o t)$$

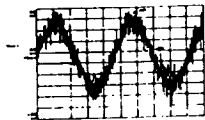
$$\text{phase} = 2\pi\nu_o t$$

$$T = \text{period} = 1/\nu_o$$

Fourier Transform:



PHASE AND AMPLITUDE FLUCTUATIONS



$$V(t) = [V_o + \epsilon(t)] \cos(2\pi\nu_o t + \phi(t))$$

$$\text{phase} = 2\pi\nu_o t + \phi(t)$$

$$\omega(t) = \frac{d}{dt} [\text{phase}]$$

$$\nu(t) = \frac{1}{2\pi} \frac{d}{dt} [2\pi\nu_o t + \phi(t)]$$

$$\nu(t) = \nu_o + \frac{1}{2\pi} \frac{d}{dt} \phi(t)$$

Fractional frequency deviation

$$y(t) = \frac{\nu(t) - \nu_o}{\nu_o} = \frac{1}{2\pi\nu_o} \frac{d}{dt} \phi(t)$$

PHASE/AMPLITUDE NOISE RELATIONSHIPS

$$S_\phi(f) = [\Delta\phi(f)]^2 \frac{1}{BW} \quad 0 < f < \infty \quad \left[ \frac{\text{rad}^2}{\text{Hz}} \right]$$

$$S_\epsilon(f) = \frac{[\Delta\epsilon(f)]^2}{V_o^2} \frac{1}{BW} \quad 0 < f < \infty \quad \left[ \frac{1}{\text{Hz}} \right]$$

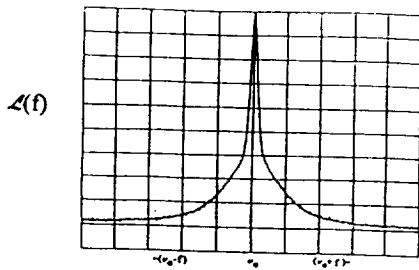
$$y(t) = \frac{1}{2\pi\nu_o} \frac{d}{dt} \phi(t)$$

derivative in time = multiplication by  $\omega$  in freq  
= multiplication by  $\omega^2$  in spectral density

$$S_y(f) = \frac{1}{[2\pi\nu_o]^2} (2\pi f)^2 S_\phi(f)$$

$$S_\phi(f) = \left[ \frac{\nu_o}{f} \right]^2 S_y(f) \quad 0 < f < \infty$$

$$S_{\phi}(f) = \mathcal{L}(v_o - f) + \mathcal{L}(v_o + f)$$



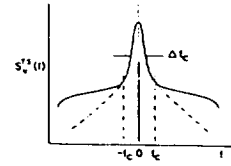
$$\mathcal{L}(f) = \frac{1}{2} S_{\phi}(f)$$

$$\text{dBc/Hz} = 10 \log(\mathcal{L}(f))$$

#### RMS PHASE DEVIATION

$$\phi^2(f)_{BW} = \int_{f-BW/2}^{f+BW/2} S_{\phi}(f) df \text{ rad}^2$$

#### POWER SPECTRAL DENSITY OF A NOISY SIGNAL



Double side-band spectral density:

$$S_v(f) \cong \frac{V_o^2}{2} [e^{-I(f_c)} \delta(f) + S_{\phi}(f) + S_{\phi}(f)]$$

$$0 \leq f \leq \infty$$

$$I(f) = \int_{f_c}^{\infty} S_{\phi}(f) df$$

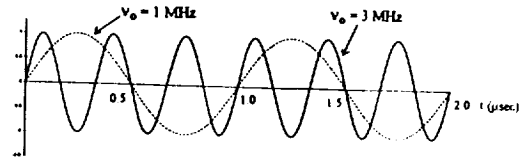
$I(f)$  = integrated phase modulation due to pedestal

$\delta(f)$  = carrier with frequency  $\pm f_c$

$$\text{Power in carrier} = \frac{V_o^2}{2} e^{-I(f_c)} \approx \frac{V_o^2}{2} \text{ for } I(f_c) \ll 1$$

#### FREQUENCY MULTIPLICATION/DIVISION EFFECTS ON PM NOISE

Frequency Multiplication



$$\nu_{o2} = N \nu_{o1} \quad \Delta \phi_2 = N \Delta \phi_1$$

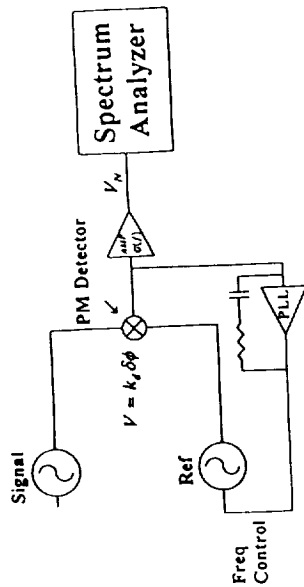
$$S_{\phi_2}(f) = \frac{[\Delta \phi_2]^2}{BW} = \frac{N^2 \Delta \phi_1^2}{BW} = N^2 S_{\phi_1}(f)$$

FREQUENCY DIVISION:

$$\nu_{o2} = \frac{\nu_{o1}}{N}$$

$$S_{\phi_2}(f) = \frac{S_{\phi_1}(f)}{N^2}$$

# Simple PM Measurements



$\frac{PSD V_n}{[k_d G(f)]^2}$  measures  $S_\phi(f)$  of the signal plus the system noise.

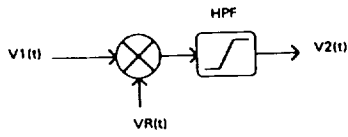
It is difficult to separate the system noise from a signal with low PM noise. Results uncorrected for PLL and gain variations with Fourier frequency.

NOISE TERMS INCLUDED IN  $\frac{PSD(V_n)}{K_d^2 G(f)^2}$

$$S_\phi(f) = \frac{[\Delta\phi_A(f) - \Delta\phi_B(f)]^2}{BW} + \frac{V_n(f)^2_{mixer}}{K_d^2 BW} + \frac{V_n(f)^2_{amp}}{K_d^2 BW} + \frac{V_n(f)^2_{SA}}{K_d^2 G(f)^2 BW} + S_{det}(f)\beta_A^2 + S_{sub}(f)\beta_B^2$$

$$S_\phi(f)_{pair} = S_{det}(f) + S_{sub}(f) + \frac{V_n(f)^2_{system}}{K_d^2 BW} + S_{det}(f)\beta_A^2 + S_{sub}(f)\beta_B^2$$

## FREQUENCY TRANSLATION



$$S_\phi(f, v_2) = S_\phi(f, v_1) + S_\phi(f, v_R) + S_{\phi T}(f)$$

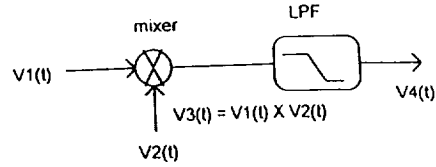
WHERE  $v_2 = v_1 + v_R$

$S_\phi(f, v_R)$  = PM NOISE OF REFERENCE SIGNAL

$S_{\phi T}(f)$  = PM NOISE ADDED BY THE TRANSLATOR

$S_\phi(f, v_2)$  DEPENDS ON THE DETAILS OF THE TRANSLATION

## BASIC CONFIGURATIONS OF NOISE MEASUREMENTS



$$V_1(t) = [V_1 + \epsilon_1(t)] \cos[2\pi\nu_o t + \phi_1]$$

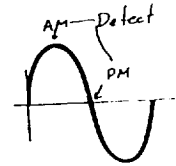
$$V_2(t) = [V_2 + \epsilon_2(t)] \cos[2\pi\nu_o t + \phi_2]$$

$$V_3(t) = \frac{A_1 A_2}{2} \{ \cos[2\pi(2\nu_o)t + \phi_1 + \phi_2] + \cos[\phi_1 - \phi_2] \}$$

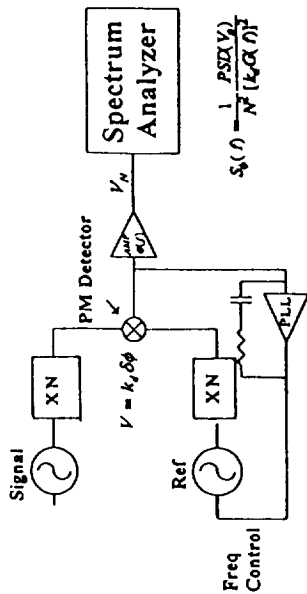
$$V_4(t) = \frac{A_1 A_2}{2} \{ \cos(\phi_1 - \phi_2) \}$$

$$AM \Rightarrow \phi_1 - \phi_2 = \pi n$$

$$PM \Rightarrow \phi_1 - \phi_2 = \frac{\pi}{2} + \pi n$$



**NOISE FLOOR IMPROVEMENT USING FREQUENCY MULTIPLIERS**



TO GET NOISE FLOOR SET A = B

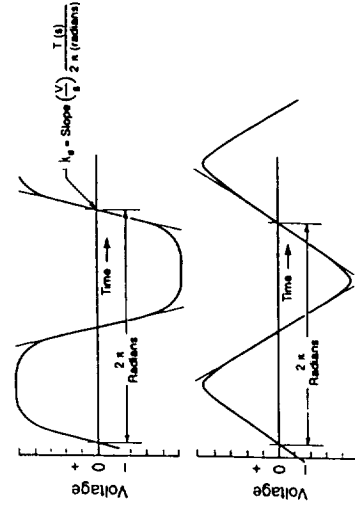
$$S_{\psi}(f)_{Noise Floor} = (2\pi f \tau_{delay})^2 S_{\psi A}(f) + \frac{V_n(f)^2_{system}}{K_d^2 BW} + S_{\psi A}(f) \beta_A^2 + S_{\psi}(f)_{power splitter}$$

$$\tau_{delay} = \frac{n\pi}{2} \frac{1}{\omega_0}$$

TO CALCULATE INDIVIDUAL PM NOISE FOR AN OSCILLATOR

$$S_{\psi}(f)_{AB} + S_{\psi}(f)_{AC} - S_{\psi}(f)_{BC} = 2S_{\psi A}(f) + \frac{V_n^2}{K_d^2 BW} + 2S_{\psi A}(f) \beta_A^2$$

**CALIBRATION FACTOR k<sub>d</sub>**



**DISCUSSION OF DIRECT PHASE COMPARISON**

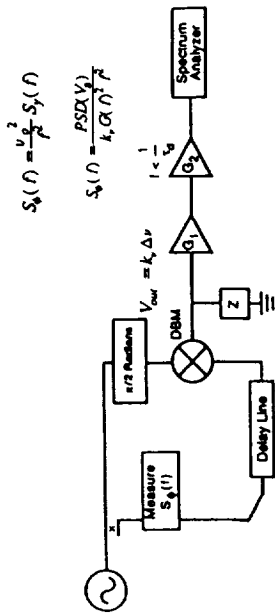
**ADVANTAGES**

- HIGHEST RESOLUTION (LOWEST NOISE FLOOR)
- NOISE FLOOR MEASURED WITH INFERIOR OSCILLATOR
- VERY WIDE BAND PERFORMANCE
- INEXPENSIVE

**DISADVANTAGES**

- REQUIRES A REFERENCE OF COMPARABLE STABILITY
- REQUIRES PHASE-LOCKED-LOOP (PLL) TO MAINTAIN  $\delta\phi < 0.1$  rad
- CALIBRATION DIFFICULT FOR  $f \ll$  PLL BW
- SENSITIVE TO HARMONIC DISTORTION
- FREQUENCY RESPONSE DEPENDS ON POWER & LOAD

MEASUREMENT OF  $S_{40}$  USING A DELAY LINE



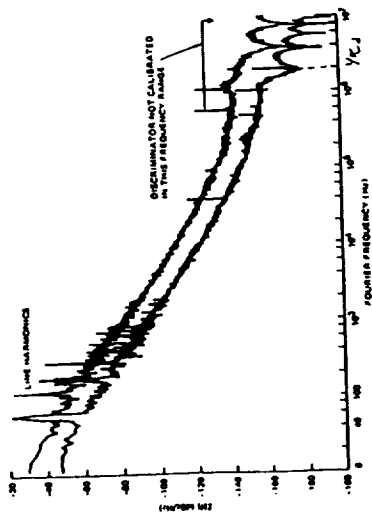
$$S_4(\omega) = \frac{v^2}{P} S_g(\omega)$$

$$S_4(\omega) = \frac{FSD(V)}{k_c \alpha \eta^2 P}$$

$$V_{out} = k_c \Delta v$$

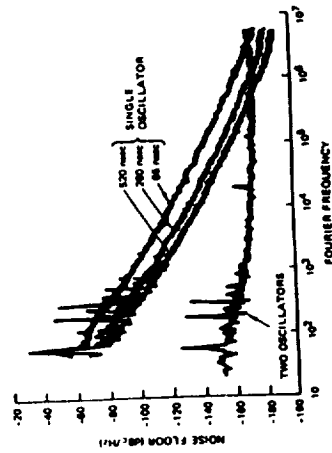
$$G_2 < G_1$$

DETERMINATION OF  $T_d$



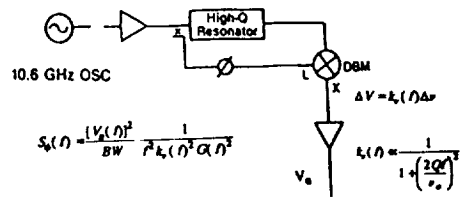
From Infrared and Millimeter Waves, Vol. 11, pp. 235-259, 1964 (also in NIST Technical Note 1337)

NOISE FLOOR COMPARISON FOR TWO MEASUREMENT SYSTEMS:  
DELAY LINE SYSTEM VS. TWO OSCILLATOR SYSTEM



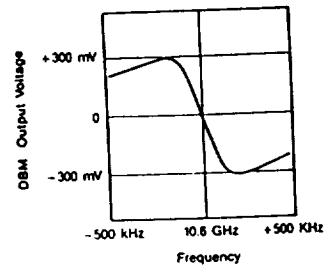
From Infrared and Millimeter Waves, Vol. 11, pp. 235-259, 1964 (also in NIST Technical Note 1337)

MEASUREMENT OF PHASE NOISE USING A HIGH-Q CAVITY



$$S_{\phi}(\omega) = \frac{(V_o(\omega))^2}{BW} \frac{1}{k_c(\omega)^2 \alpha \eta^2}$$

$$k_c(\omega) = \frac{1}{1 + \left(\frac{2Q\omega}{\omega_0}\right)^2}$$

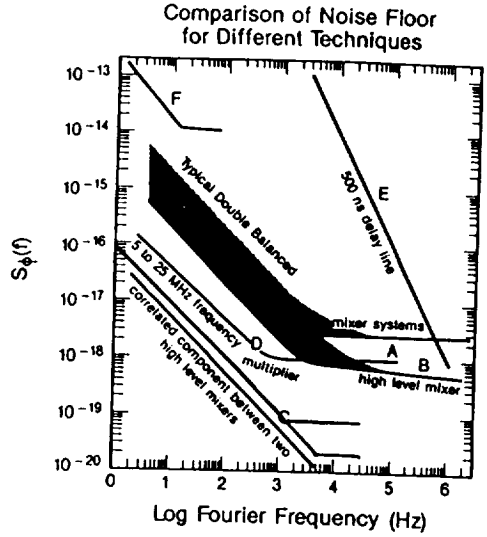


**DIRECT PHASE COMPARISONS**

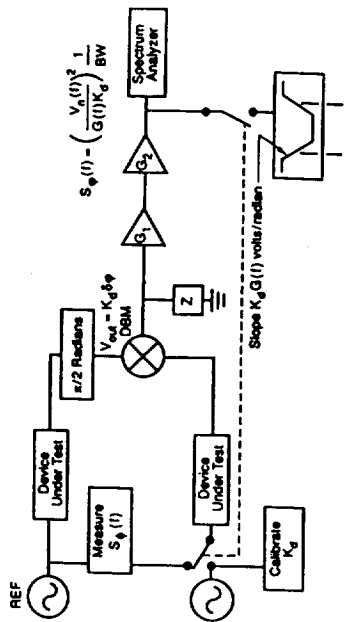
- ADVANTAGES:**
- DOES NOT REQUIRE SECOND SOURCE
  - SYSTEM TRACKS FREQUENCY CHANGES IN SOURCE
  - NO PLL EFFECTS
  - SIMPLE CALIBRATION  $V = G \cdot \Delta\phi$
- DISADVANTAGES:**
- NOISE FLOOR SCALES AS 1/2 NEAR CARRIER
  - NOISE FLOOR DIFFICULT TO MEASURE
  - DIFF. CAVITIES REQUIRED FOR EACH  $\omega$
  - DIFF. CAVITIES/DELAY LINES FOR DIFF.  $f$
  - DIFFICULT TO MEASURE BEYOND CAVITY BW OR BEYOND DELAY LINE TIME
- LOWEST NOISE FLOOR**
- NOISE FLOOR MEASURED WITH INFERIOR OSCILLATOR**
- VERY WIDE BAND PERFORMANCE**
- INEXPENSIVE**
- REFERENCE OF COMPARABLE STABILITY**
- REQUIRES PLL TO MAINTAIN  $\Delta\phi < 0.1$  rad**
- CALIBRATION DIFFICULT FOR  $f \ll$  PLL BW**
- SENSITIVE TO HARMONIC DISTORTION**
- FREQUENCY RESPONSE DEPENDS ON POWER & LOAD**

**DIRECT FREQUENCY COMPARISONS**

- ADVANTAGES:**
- DOES NOT REQUIRE SECOND SOURCE
  - SYSTEM TRACKS FREQUENCY CHANGES IN SOURCE
  - NO PLL EFFECTS
  - SIMPLE CALIBRATION  $V = G \cdot \Delta\phi$
- DISADVANTAGES:**
- NOISE FLOOR SCALES AS 1/2 NEAR CARRIER
  - NOISE FLOOR DIFFICULT TO MEASURE
  - DIFF. CAVITIES REQUIRED FOR EACH  $\omega$
  - DIFF. CAVITIES/DELAY LINES FOR DIFF.  $f$
  - DIFFICULT TO MEASURE BEYOND CAVITY BW OR BEYOND DELAY LINE TIME



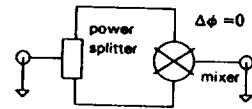
Measurement of  $S_{\phi}(f)$  for Two Amplifiers



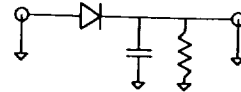
**AM NOISE DEFINITION**

$$S_s(f) = \left( \frac{\Delta\epsilon}{V_o} \right)^2 \frac{1}{BW}$$

**AM DETECTORS**

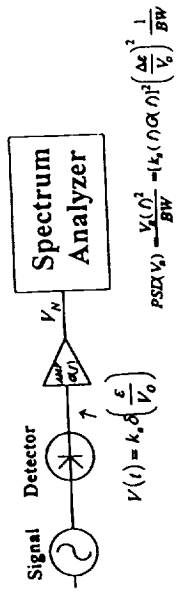


Mixer Detector



Diode Detector

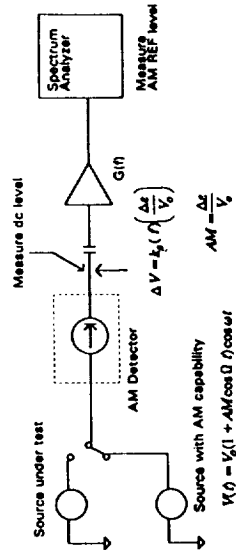
# Simple AM Measurement



$\frac{PSD V_n}{[k_a G(f)]^2}$  measures  $S_x(f)$  of the signal plus the system noise.

It is difficult to separate the system noise from a signal with low AM noise.

## Determination of $[k_a(f)G(f)]$ for AM Measurement Systems



AM at the input signal:  $\frac{1}{2} \left(\frac{\% AM}{100}\right)^2$

AM at output: AM REF level

$$\frac{[k_a(f)G(f)]^2}{AM \text{ at Input}} = \frac{AM \text{ at Output} \cdot (AM \text{ REF level})^2}{\frac{1}{2} \left(\frac{\% AM}{100}\right)^2}$$

# Fundamental Concepts and Definitions in PM and AM Noise Metrology

## TUTORIAL – QUESTIONS AND ANSWERS

### Note from the editor

The questions were asked at various points during the presentation. They were transcribed and are presented here at the end of each tutorial.

**JIM COMPARO (AEROSPACE CORP.):** So  $S_v$  is the power spectrum density of that full voltage signal?

**EVA PIKAL (NIST):** Yes.

**JIM COMPARO (AEROSPACE CORP.):** And the first you said was what?

**EVA PIKAL (NIST):** The carrier.

**JIM COMPARO (AEROSPACE CORP.):** I see three terms there. One is contribution due to the phase noise; one is a contribution to the amplitude noise; and then there's a term out in front. And what is that?

**EVA PIKAL (NIST):** That's just a carrier, right? That's – you know, if it were ideal, it would just be a delta function at the frequency of oscillation.

**JIM COMPARO (AEROSPACE CORP.):** I guess my question is – and maybe I'm getting way ahead, but if there is some correlation between the amplitude noise and the phase noise, then the power spectrum of the voltage wouldn't necessarily be symmetric, would it? And so would it be fair to sort of consider these things as folded over on top of one another?

**EVA PIKAL (NIST):** I believe this assumes there is a correlation between AM noise and PM noise in the signal.

**MARC A. WEISS (NIST):** I am looking at "requires a reference of comparable stability." I thought you said we could use the oscillator under test as a reference as well.

**EVA PIKAL (NIST):** That's to measure the noise floor. You need a different reference to measure phase noise of the test oscillator. You need another oscillator. To measure the noise floor, you need to use the single oscillator to get rid of the noise of the source and the reference.

## II. DISCUSSION OF ERROR MODELS FOR PM AND AM NOISE MEASUREMENTS

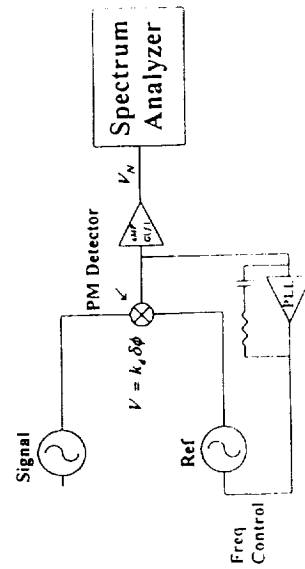
Fred L. Walls  
Group Leader for Phase Noise  
NIST

(303) 497 3207-Voice, (303) 497 6461-FAX.

walls@bldrdoc.gov-Internet

- A. Error model for PM noise measurements
- B. Error model for AM noise measurements
- C. PM and AM noise models
- D. Conversion of PM data to  $\sigma_y(t)$  and  $\text{mod}\sigma_y(t)$

## Simple PM Measurements



$\frac{PSD V_n^2}{[k_p G(f)]^2}$  measures  $S_{\phi}(f)$  of the signal plus the system noise.

It is difficult to separate the system noise from a signal with low PM noise. Results uncorrected for PLL and gain variations with Fourier frequency.

TIME AND FREQUENCY DIVISION, NIST

PTTI 1994

### ERROR MODEL FOR PM MEASUREMENTS

- 1 DETERMINATION OF K
- 2 DETERMINATION OF AMPLIFIER G(f)
- 3 PLL EFFECTS (IF ANY)
- 4 CONTRIBUTION OF AM NOISE
- 5 HARMONIC DISTORTION
- 6 CONTRIBUTION OF SYSTEM NOISE FLOOR
- 7 CONTRIBUTION OF REFERENCE NOISE
- 8 STATISTICAL CONFIDENCE OF DATA
- 9 LINEARITY OF SPECTRUM ANALYZERS
- 10 ACCURACY OF PSD FUNCTION

### I. DETERMINATION OF K

#### TRANSDUCER SENSITIVITY DEPENDS ON

- A. Frequency
- B. Signal power and impedance, reference power and impedance
- C. Mixer termination at all three ports
- D. Cable lengths

#### ACCURACY OF DETERMINATION DEPENDS ON DEGREE ABOVE PARAMETERS HELD CONSTANT PLUS

- A. Symmetry of waveform
- B. Signal-to-noise-ratio
- C. Phase deviation from 90°-depends on noise level, dc offset-may depend on f

#### CALIBRATION CONDITION MUST REPLICATE THE MEASUREMENT CONDITION AS CLOSELY AS POSSIBLE

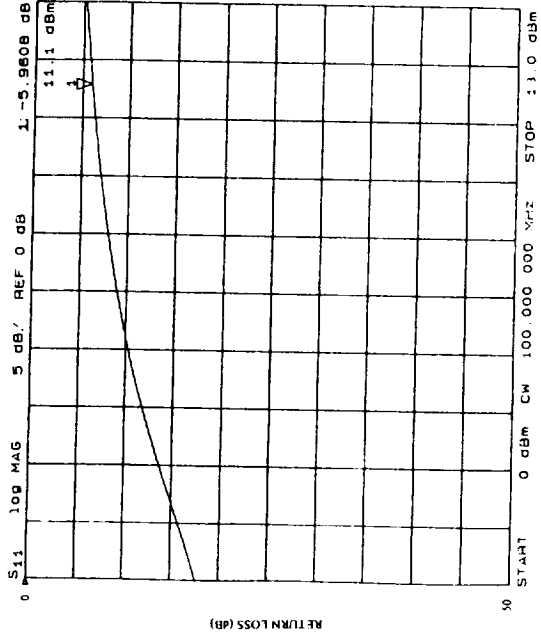
TIME AND FREQUENCY DIVISION, NIST

PTTI 1994

TIME AND FREQUENCY DIVISION, NIST

PTTI 1994

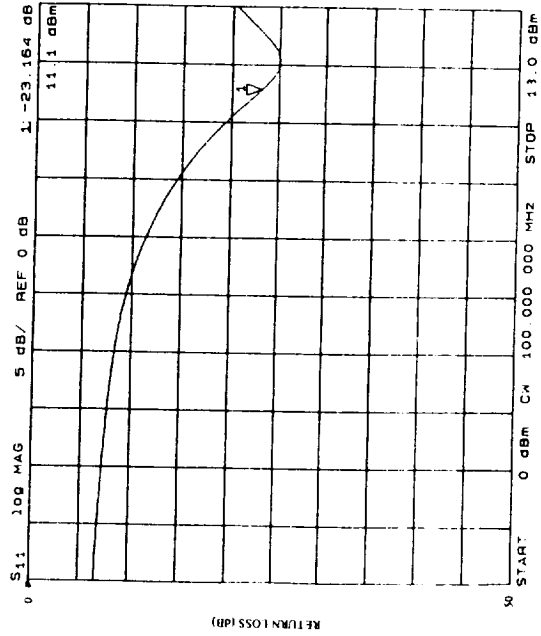
MIXER B RETURN LOSS VERSUS RF POWER AT 100 MHz AND A LO OF 15 dBm



TIME AND FREQUENCY DIVISION, NIST

PTTI 1994

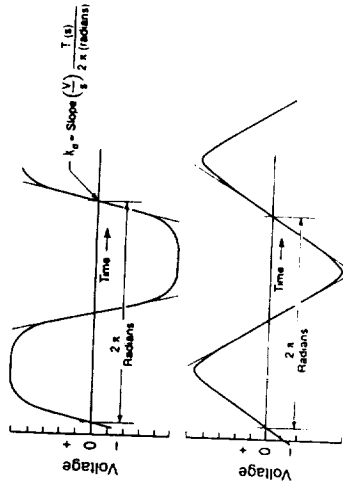
MIXER B RETURN LOSS VERSUS RF POWER AT 100 MHz AND A LO OF 15 dBm



TIME AND FREQUENCY DIVISION, NIST

PTTI 1994

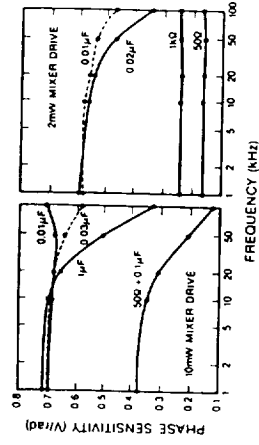
MIXER OUTPUT VOLTAGE VERSUS PHASE (TIME)



TIME AND FREQUENCY DIVISION, NIST

PTTI 1994

MIXER SENSITIVITY  $K_d$  VERSUS IF LOAD



TIME AND FREQUENCY DIVISION, NIST

PTTI 1994

## 2. DETERMINATION OF AMPLIFIER GAIN VERSUS FOURIER OFFSET

G(f) DEPENDS ON

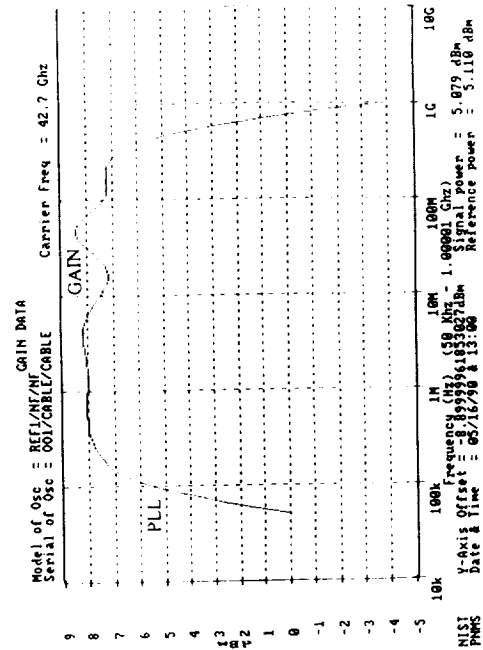
- A Intrinsic amplifier G(f)
- B Mixer output impedance
- C Signal power, impedance, and cable length through B
- E Reference power, impedance, and cable length through B

ACCURACY OF DETERMINATION DEPENDS ON THE DEGREE ABOVE PARAMETERS HELD CONSTANT PLUS

- A Linearity and slewing rate of amplifier

CALIBRATION CONDITION MUST REPLICATE THE MEASUREMENT CONDITION AS CLOSELY AS POSSIBLE

### PLL AND GAIN EFFECTS ON G(f) Kd



TIME AND FREQUENCY DIVISION, NIST

PTTI 1994

TIME AND FREQUENCY DIVISION, NIST

## 3. PLL EFFECTS (IF ANY)

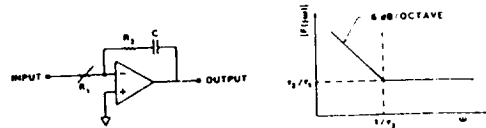
ATTENUATION OF THE LOW FREQUENCY PHASE DEVIATION CAN BE REDUCED BY

- A Normal PLL loop Results may be altered by additional filters in electronic frequency control (EFC) path
- B Signals that propagate through the power sources of the two oscillators
- C Signals that propagate through the air to pull the frequency of one or both signals
- E Signals that propagate through the measurement system (mixer) to pull the frequency
- F Injection lock feedback from the cavity discriminator or delay line discriminator

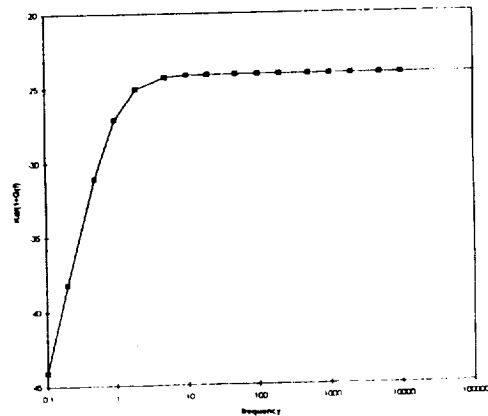
PLL EFFECTS SHOULD BE MEASURED IN SITU SINCE MANY EFFECTS IN THE EFC PATH ARE HIDDEN.

ERRORS IN PARAMETERS I-J ARE OFTEN CORRELATED

### PLL RELATIONS



$$G(f)_{PLL} = C \frac{(1 + j\omega R_2 C)}{j\omega R_1 C} \quad V_d = \frac{K_d (\Delta\phi_{test} - \Delta\phi_{ref})}{1 + G(f)_{PLL}}$$



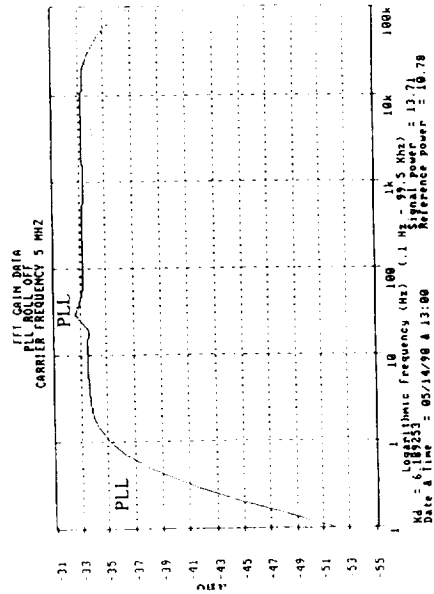
TIME AND FREQUENCY DIVISION, NIST

PTTI 1994

TIME AND FREQUENCY DIVISION, NIST

PTTI 1994

PLL EFFECTS ON G(f) Kd



PTTI 1994

4. CONTRIBUTION OF AM NOISE

AM TO PM CONVERSION IS UNIVERSAL

- A. Occurs via non-linear process
- B. Typically -15 to -25 dB in double balanced mixers
- C. Can reach -3 dB in some amplifiers
- D. Sets the noise floor in many measurements

TIME AND FREQUENCY DIVISION, NIST

TIME AND FREQUENCY DIVISION, NIST

PTTI 1994

MEASUREMENTS OF  $S_{\phi}(f)$  @ MHz SYNTHESIZER VS OSCILLATOR

f (Hz)	$S_{\phi}(f)  _{AB}$ (dB/Hz)	$S_{\phi}(f)  _{AB}$ (dB/Hz)	$S_{\phi}(f)  _{A \beta^2 A}$ (dB/Hz)	Measured Noise Floor dB rel Rad <sup>2</sup> /Hz	Actual Noise Floor
32	-119.8	-126.0	≈ -151.0	-154.0	-160.0
100	-124.2	-127.0	≈ -152.0	-154.0	-165.0
1 K	-132.1	-132.0	≈ -157.0	-158.0	175.0
10 K	-137.3	-133.0	≈ -158.0	-158.0	175.0
100 K	-136.8	-133.0	≈ -158.0	-158.0	175.0

PTTI 1994

5. HARMONIC DISTORTION

- A. Harmonics of signal and reference contribute to K and detected noise
- B. PM noise on harmonics may not be same as fundamental
- C. Sensitivity depends on power, impedance, harmonic number

TIME AND FREQUENCY DIVISION, NIST

TIME AND FREQUENCY DIVISION, NIST

PTTI 1994

TO GET NOISE FLOOR SET A = B

$$S_{\phi}(f)_{\text{Noise Floor}} = S_{\phi A}(2\pi f \tau_{\text{delay}})^2 + \frac{V_n(f)^2_{\text{system}}}{K_d^2 BW} + S_{\text{sub}}(f)\beta_A^2 + S_{\phi}(f)_{\text{power splitter}}$$

$$(2\pi f \tau_{\text{delay}})^2 S_{\phi}(f) = \left(\frac{f}{20}\right)^2 S_{\phi}(f) \quad \text{for } f = \frac{V}{10} \tau_{\text{delay}} = \frac{f}{2}$$

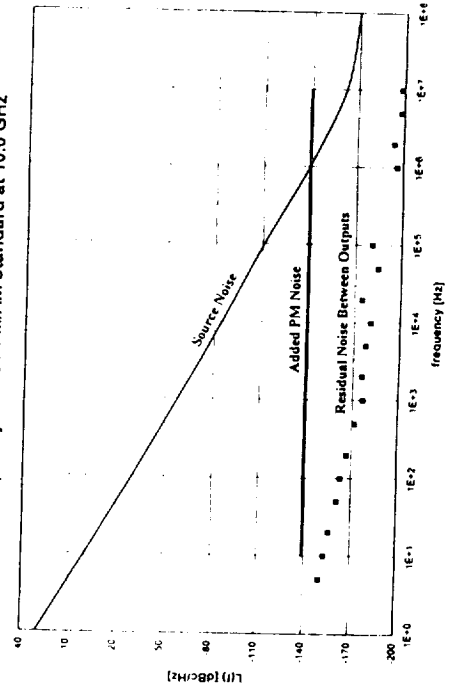
TO CALCULATE INDIVIDUAL PM NOISE FOR AN OSCILLATOR

$$S_{\phi}(f)_{AB} + S_{\phi}(f)_{AC} - S_{\phi}(f)_{BC} = 2S_{\phi A}(f) + \frac{V_n^2}{K_d^2 BW} + 2S_{\text{sub}}(f)\beta_A^2$$

TIME AND FREQUENCY DIVISION, NIST

PTTI 1994

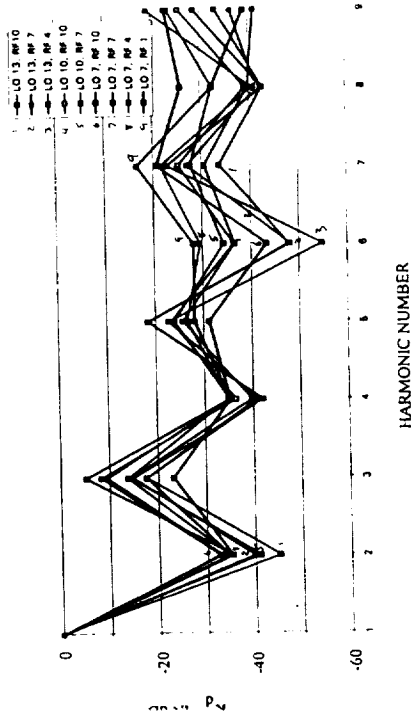
L(f) vs Frequency of NIST PM/AM standard at 10.6 GHz



TIME AND FREQUENCY DIVISION, NIST

PTTI 1994

HARMONIC SENSITIVITY OF MIXER VS RF AND LO POWER IN dB



TIME AND FREQUENCY DIVISION, NIST

PTTI 1994

### 6. CONTRIBUTION OF SYSTEM NOISE FLOOR

NOISE TERMS INCLUDED IN  $\frac{FSD(V_n)}{K_d^2 G(f)^2}$

$$S_{\phi}(f) = \frac{[\Delta\phi_A(f) - \Delta\phi_B(f)]^2}{BW} + \frac{V_n(f)^2_{\text{mixer}}}{K_d^2 BW} + \frac{V_n(f)^2_{\text{amp}}}{K_d^2 BW} + \frac{V_n(f)^2_{SA}}{K_d^2 G(f)^2 BW} + S_{\text{sub}}(f)\beta_A^2 + S_{\text{sub}}(f)\beta_B^2$$

$$S_{\phi}(f)_{\text{pair}} = S_{\phi A}(f) + S_{\phi B}(f) + \frac{V_n(f)^2_{\text{system}}}{K_d^2 BW} + S_{\text{sub}}(f)\beta_A^2 + S_{\text{sub}}(f)\beta_B^2$$

TIME AND FREQUENCY DIVISION, NIST

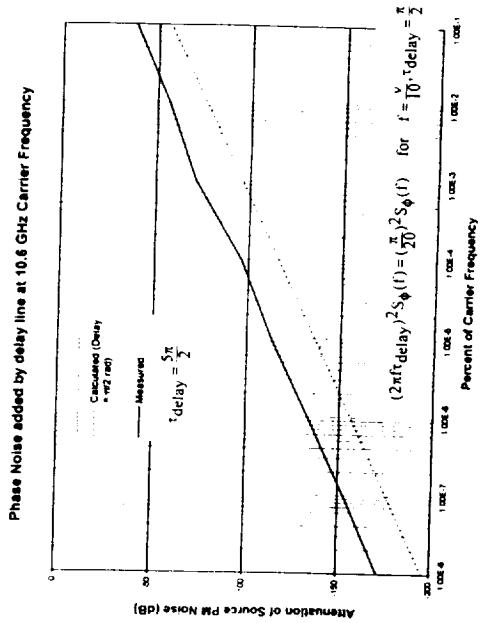
PTTI 1994

### 8. STATISTICAL CONFIDENCE OF THE DATA

Table 1. Approximate 68% confidence intervals for FFT Spectral Estimates  $N > 10$

power law noise type	uniform	window		flattened peak
		Hanning		
$f^0$	$1.02/\sqrt{N}$	$0.98/\sqrt{N}$		$0.98/\sqrt{N}$
$f^{-2}$	$1.02/\sqrt{N}$	$1.04/\sqrt{N}$		$1.04/\sqrt{N}$
$f^{-3}$	unusable	$1.04/\sqrt{N}$		$1.04/\sqrt{N}$
$f^{-4}$	unusable	$1.04/\sqrt{N}$		$1.04/\sqrt{N}$

$$S = S_m \left( 1 \pm \frac{B}{\sqrt{N}} \right)$$



TIME AND FREQUENCY DIVISION, NIST

PTTI 1994

TIME AND FREQUENCY DIVISION, NIST

PTTI 1994

TIME AND FREQUENCY DIVISION, NIST

PTTI 1994

### 7. CONTRIBUTION OF REFERENCE AM AND PM NOISE

NOISE TERMS INCLUDED IN  $\frac{PSD(V_a)}{K_d^2 G(f)^2}$

$$S_\phi(f) = \frac{L \Delta\phi_A(f) - \Delta\phi_{BT}(f)}{BW} + \frac{V_n(f)^2_{mixer}}{K_d^2 BW} + \frac{V_n(f)^2_{amp}}{K_d^2 BW} + \frac{V_n(f)^2_{SA}}{K_d^2 G(f)^2 BW} + S_{sub}(f) \beta_A^2 + S_{sub}(f) \beta_B^2$$

$$S_\phi(f)_{pair} = S_\phi(f) + S_{sub}(f) + \frac{V_n(f)^2_{system}}{K_d^2 BW} + S_{sub}(f) \beta_A^2 + S_{sub}(f) \beta_B^2$$

TIME AND FREQUENCY DIVISION, NIST

PTTI 1994

### STATISTICAL UNCERTAINTY OF FFT SPECTRAL DENSITY MEASUREMENTS

$$S_m(t) = S(t) (1 \pm k/N^*)$$

$$k = 1 - 68\%, k = 1.9 - 95\% \text{ CONFIDENCE } N \geq 10$$

$N$  = number of samples averaged

Number of Samples	$k = 1$ (approx. 68%)			$k = 1.9$ (approx. 95%)		
	$S_m - \sigma(1+k)$	$S_m$	$S_m + \sigma$	$S_m - \sigma(1+k)$	$S_m$	$S_m + \sigma$
4	0.54	2.	+3.3	2.5	3	+6
6	0.42	1.5	+2.3	1.4	2.5	+5
10	0.32	1.2	+1.7	0.61	2.1	+4
30	0.18	-0.72	+0.86	0.35	1.3	+1.8
100	0.1	-0.41	+0.46	0.19	-0.76	+0.92
200	0.058	-0.24	+0.25	0.14	-0.46	+0.51
1000	0.032	-0.13	+0.13	0.06	-0.26	+0.28
3000	0.018	-0.08	+0.08	0.035	-0.15	+0.15
10000	0.01	-0.04	+0.04	0.019	-0.08	+0.08

D. B. Percival and A. T. Walden, 'Spectral Analysis for Physical Applications,' Cambridge Univ. Press, 1993

B. N. Taylor and C. E. Kuyatt, NIST Technical Note 1 (NIST) 1993

STATISTICAL UNCERTAINTY OF SWEEP  
RF SPECTRAL DENSITY MEASUREMENTS

$$S_{\rho}(f) = \sqrt{S(f) + k(\text{VIDEO}_{\rho})^2 / \text{RES}_{\rho}^2}$$

k = 1 - 68% CONFIDENCE, k = 1.9 - 95% CONFIDENCE, N ≥ 10

VIDEO<sub>ρ</sub> = video bandwidth

N = number of sweeps averaged

RES<sub>ρ</sub> = resolution bandwidth ≤ f/10

kRES <sub>ρ</sub> /VIDEO <sub>ρ</sub>	k = 1 (approx. 68%)			k = 1.9 (approx. 95%)		
	S <sub>ρ</sub> - S(1+δ)	S <sub>ρ</sub> + δ	S <sub>ρ</sub> ± dB	S <sub>ρ</sub> - S(1+δ)	S <sub>ρ</sub> + δ	S <sub>ρ</sub> ± dB
	δ	γ	β	δ	γ	β
4	0.54	2	+1.1	2.5	3	+6
6	0.42	1.5	+2.3	1.4	2.5	+5
10	0.32	1.2	+1.7	0.61	2.1	+4
30	0.18	0.72	+0.86	0.35	1.3	+1.8
100	0.1	0.41	+0.46	0.19	0.76	+0.92
200	0.058	0.24	+0.25	0.14	0.46	+0.51
1000	0.032	0.13	+0.13	0.06	0.26	+0.28
1000	0.018	0.08	+0.08	0.035	0.15	+0.15
10000	0.01	0.04	+0.04	0.019	0.08	+0.08

1) B. Percival and A.T. Walden "Spectral Analysis for Physical Application," Cambridge Univ. Press, 1993

2) N. Taylor and C. E. Kuyatt, NIST Technical Note TN1297, 1993

9. LINEARITY OF SPECTRUM ANALYZER

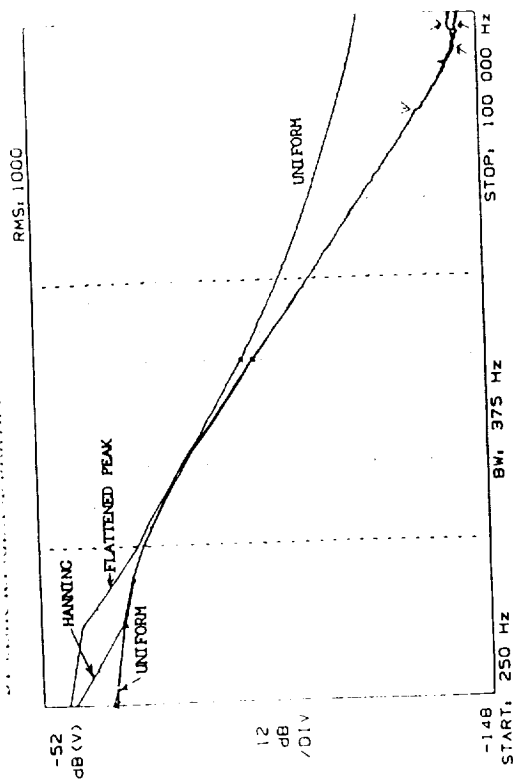
- A. Accuracy of wide dynamic range
- B. Digitizing errors
- C. Need to segment spectrum with filters

TIME AND FREQUENCY DIVISION, NIST

PTTI 1994

TIME AND FREQUENCY DIVISION, NIST

PTTI 1994



PTTI 1994

TIME AND FREQUENCY DIVISION, NIST

10. ACCURACY OF THE PSD FUNCTION

DEPENDS ON

- A. Signal type
  - Use flat top window for bright lines
  - Use Hanning window for noise
- B. Window function and Fourier frequency (leakage)
  - f should be less than span/23 for Flat top window
  - f should be less than span/75 for Flat top window

TIME AND FREQUENCY DIVISION, NIST

PTTI 1994

ORIGINAL PAGE IS  
OF POOR QUALITY

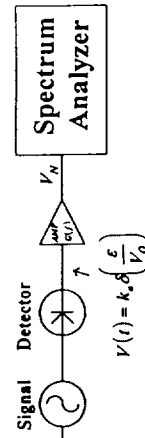
APPROXIMATE BIASES IN FFT SPECTRAL DENSITY ESTIMATORS

Channel #	Noise Type $f^*$			Noise Type $f^*$		
	Flat Top	Hanning	Uniform	Flat Top	Hanning	Uniform
1	20.1 dB	19.6 dB	19.6 dB	10.0 dB	8.6 dB	Uniform
2	16.7	Small	Small	9.1	0.4	Not Useable
3	7.22	↓	↓	4.0	0.4	
4	Small			1.2	Small	
5	↓			1.1	↓	
6				1.1		
7				1.0		
8				0.8		
9				0.6		
10				0.6		
11				0.5		
12				0.4		
13				0.4		
14				Small		
15				↓		

TIME AND FREQUENCY DIVISION, NIST

PTTI 1994

# Simple AM Measurement

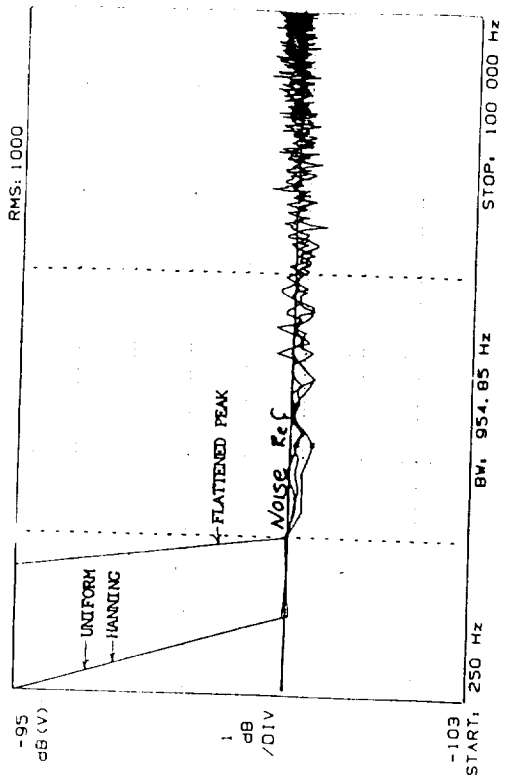


$\frac{PSDV_N}{[k_a G(f)]}$  measures  $S_s(f)$  of the signal plus the system noise.

It is difficult to separate the system noise from a signal with low AM noise.

TIME AND FREQUENCY DIVISION, NIST

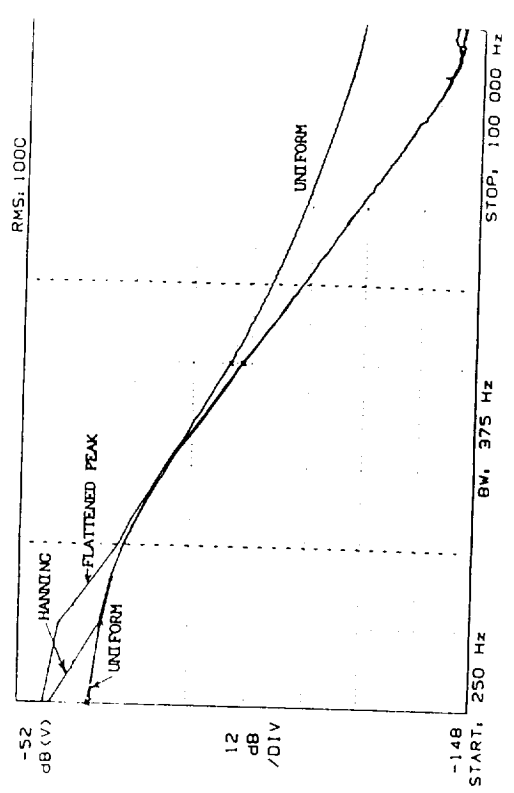
PSD OF  $f^*$  NOISE



TIME AND FREQUENCY DIVISION, NIST

PTTI 1994

PSD OF  $f^*$  NOISE



TIME AND FREQUENCY DIVISION, NIST

PTTI 1994

**ERROR MODEL FOR AM MEASUREMENTS**

- 1 DETERMINATION OF K
- 2 DETERMINATION OF AMPLIFIER G(f)
- 3 CONTRIBUTION OF SYSTEM NOISE FLOOR
- 4 STATISTICAL CONFIDENCE OF DATA
- 5 LINEARITY OF SPECTRUM ANALYZERS
- 6 ACCURACY OF PSD FUNCTION

**1. DETERMINATION OF  $K_a$**

**DETECTOR SENSITIVITY DEPENDS ON**

- A Carrier frequency
- B Signal power and impedance
- C Detector termination both ports
- D Cable lengths
- E Fourier frequency

Sensitivity to Fourier frequency is often difficult to measure due to bandwidth of most AM modulators

**CALIBRATION CONDITION MUST REPLICATE THE MEASUREMENT CONDITION AS CLOSELY AS POSSIBLE**

TIME AND FREQUENCY DIVISION, NIST

PTTI 1994

TIME AND FREQUENCY DIVISION, NIST

PTTI 1994

**2. DETERMINATION OF AMPLIFIER G(f)**

**Depends on**

- A Detector output impedance
- B Signal power, impedance, and cable length through A
- C Fourier frequency

**CALIBRATION CONDITION MUST REPLICATE THE MEASUREMENT CONDITION AS CLOSELY AS POSSIBLE**

**3. CONTRIBUTION OF AM SYSTEM NOISE FLOOR**

- A Noise floor difficult to measure in single channel systems
- B Cross-correlation can be used to determine noise floor (part III)

**CALIBRATION CONDITION MUST REPLICATE THE MEASUREMENT CONDITION AS CLOSELY AS POSSIBLE**

TIME AND FREQUENCY DIVISION, NIST

PTTI 1994

TIME AND FREQUENCY DIVISION, NIST

PTTI 1994

MODEL FOR PM IN AMPLIFIERS

$$S_{\phi}(f) = \left[ \frac{\alpha_E}{f} + \frac{2kTFG}{P} \right] \Rightarrow \sum_a (f) \quad \text{AM}$$

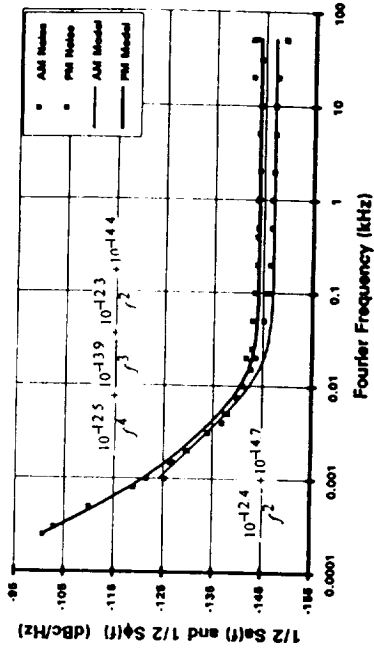
NEW

LEESON'S MODEL FOR PM IN OSCILLATORS

$$S_{\phi}(f) = \left( \frac{v_o}{2Q_L} \right)^2 \frac{1}{f^2} \left[ \frac{\alpha_E}{f} + \frac{2kTFG}{P} \right] + \left[ \frac{\alpha_E}{f} + \frac{2kTFG}{P} \right] + \left( \frac{v_o}{2Q_L} \right)^2 \frac{1}{f^2} \left[ \frac{\alpha_A}{f} \right]$$

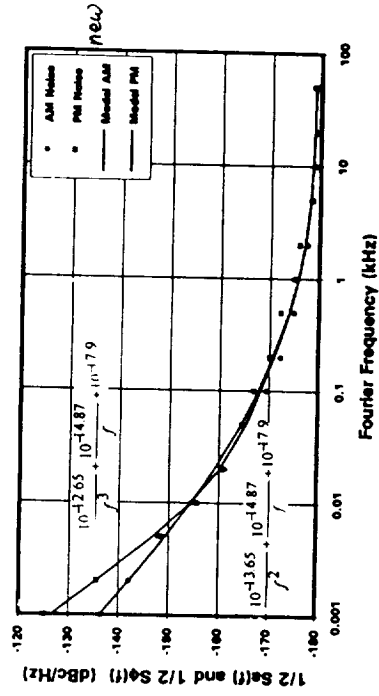
BW =  $v_o/2Q_L$       f < BW      Amplifier      f > BW      Resonator      f < BW

5 MHz AM and Phase Noise

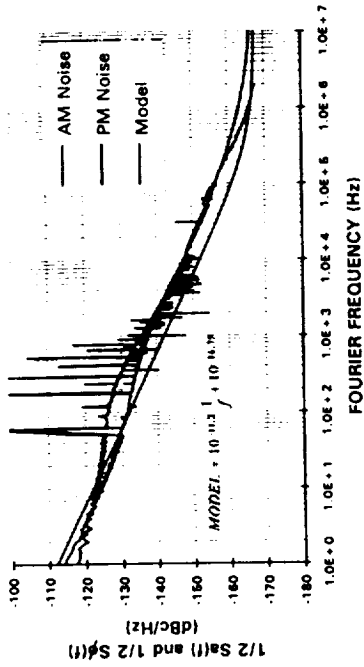


- NOISE MODEL OF AMPLIFIERS
- AM and PM similar 1/f + thermal
- NOISE MODEL OF OSCILLATORS
- PM complicated-see examples
- PM typically includes 1/f<sup>3</sup> + thermal
- AM depends on circuit and degree of limiting
- AM sometimes 1/f + attenuated thermal
- NOISE MODEL OF PM MEASUREMENT SYSTEMS
- 1/f + thermal for two oscillator type
- 1/f<sup>3</sup> + thermal for single oscillator type
- NOISE MODELS OF AM DETECTORS
- 1/f + thermal

5 MHz AM and PM Noise

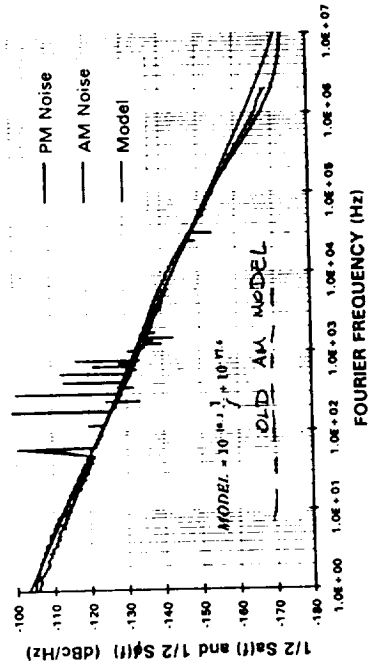


### AM AND PM NOISE IN AMPLIFIER #2

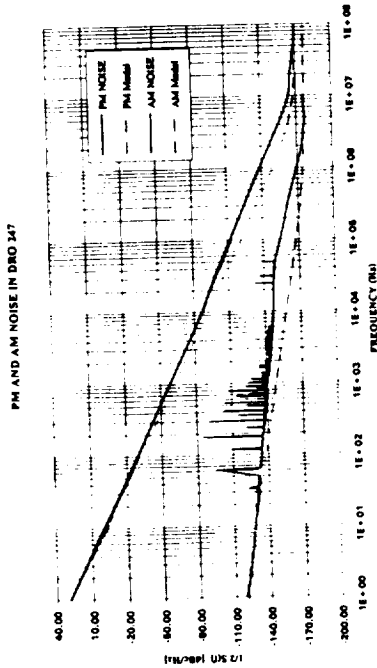


$$\frac{1}{2} S_{\phi}(f) = \frac{1}{2} S_{\phi}(f) = a_{\phi} f^{-1.26} \frac{2kTfG(f)}{P_c}$$

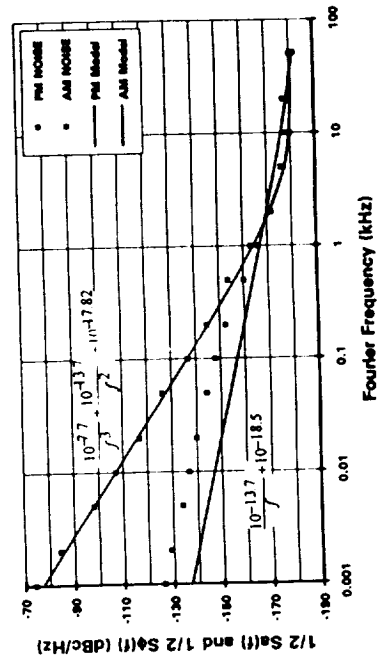
### AM AND PM NOISE IN AMPLIFIER #1



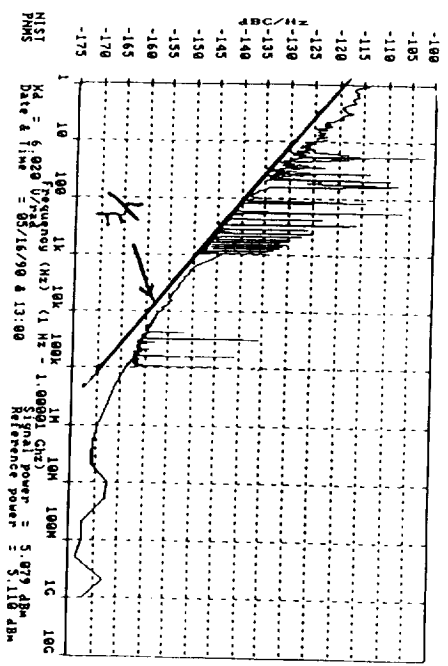
$$\frac{1}{2} S_{\phi}(f) = \frac{1}{2} S_{\phi}(f) = a_{\phi} f^{-1.26} \frac{2kTfG(f)}{P_c}$$



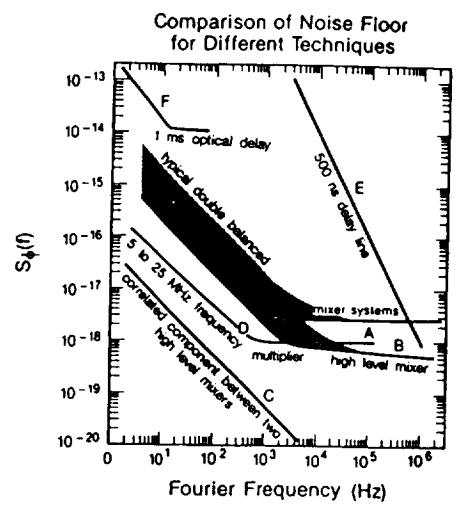
### 100 MHz AM AND PHASE NOISE



ORIGINAL PAGE IS  
OF POOR QUALITY



NOISE FLOOR OF WIDE-BAND NIST PM MEASUREMENT SYSTEM AT 42 GHz



PHASE NOISE RELATIONSHIPS

$$S_p(f) = \mathcal{L}(v_o - f) + \mathcal{L}(v_o + f)$$

$$\text{dBc/Hz} = 10 \log \mathcal{L}(f)$$

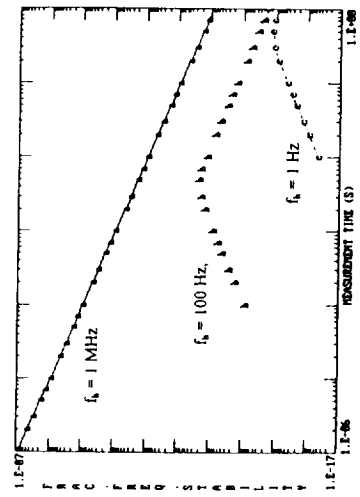
$$S_p(f) = \frac{v_o^2}{f^2} S_y(f) \text{ rad}^2/\text{Hz} \quad 0 < f < \infty$$

$$\sigma_y^2(\tau) = 2 \int_0^\infty df S_y(f) \frac{\sin^4(\pi f \tau)}{(\pi f \tau)^2}$$

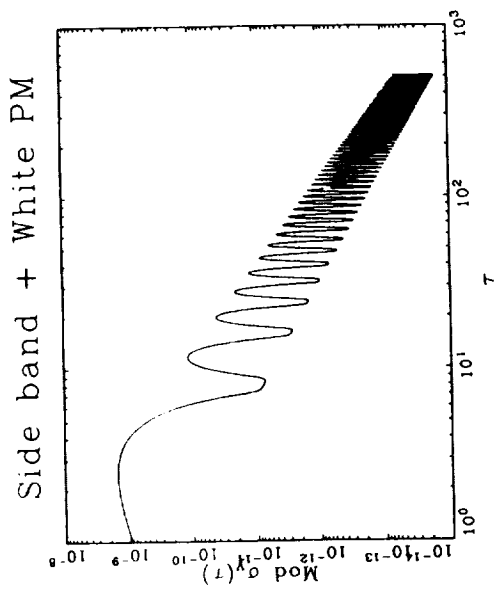
$$\text{Mod } \sigma_y(n\tau_o) = \left( \frac{2}{n^2(\pi n\tau_o)^2} \int_0^\infty S_y(f) \frac{\sin^6(\pi f n\tau_o)}{f^2 \sin^2(\pi f \tau_o)} df \right)^{1/2}$$

CONVERSION OF  $S_p(f)$  TO  $\sigma_y(\tau)$  FOR

$$S_p(f) = 4 \times 10^{-16} f^{-1} + 1 \times 10^{-17} \text{ AT } 100 \text{ MHz}$$



ORIGINAL PAGE IS OF POOR QUALITY



# Discussion of Error Models for PM and AM Noise Measurements

## TUTORIAL – QUESTIONS AND ANSWERS

### Note from the editor

The questions were asked at various points during the presentation. They were transcribed and are presented here at the end of each tutorial.

**RICHARD KEATING (USNO):** I have a problem with what you mean by “harmonic distortion.” Do you mean just simply the amount of power in the upper harmonics? Do you mean that a harmonic is just something that is some integer multiple of the fundamental? Or, do you refer to it as a partial? Do you mean something like that which is used in audio terminology where they talk about the “total power in the upper harmonics as being a distortion?” In short, what do you mean by “harmonic distortion?” Am I being clear?

**FRED WALLS (NIST):** Yeah, you’re being perfectly clear. And I wasn’t very clear on purpose. And the reason for that is convenience I guess. You can say “harmonic distortion,” or you can say “The second harmonic is minus 25 dBc, the third harmonic is minus dBc,” etcetera; and I’m just trying to show you this is the relative  $K_d$ . The sensitivity of the mixer to read out those harmonics in the signal, given an LO of a particular size, as a power ratio, relative to the fundamental. I’ve normalized the sensitivity of the fundamental to be zero dB or one.

And so you can see that I can change the sensitivity to, say, the third harmonic by 20 dB, depending how I tune LO and RF. And it’s easy to see here, it’s very clear that there’s an even/odd-kind of symmetry, namely the even orders are typically much less sensitive than the odds; but I can point this one out to you where, in fact, the fifth and sixth have about the same sensitivity. And the other thing that’s clear is, as you go to higher and higher harmonics, that the difference between odd and even tends to kind of wash out. And by tuning, you can make quite a difference here, 20, 25 dB. And some mixers will be better than others, low-level mixers will be different than high-level mixers, etcetera. And it’s a complicated structure, but it’s something you need to be aware of.

Now you can use it to your advantage. Sometimes you want to measure the phase noise of signal up here, and that’s the LO that you have. And if you tune it, you can see that you can do the ninth harmonic with a penalty of only 20 dB. Maybe that’s enough to get it done, maybe it isn’t. And, in some cases, you can actually run up to the 25th or the 45th, or whatever; what you pay is in the noise floor.

## NIST PM/AM noise measurement system

- Separates PM from AM noise
- Measures carrier frequencies from 5 MHz to 75 GHz
- Extends Fourier analysis to 1 GHz
- Measurement accuracy: 0.3 - 3 dB
- Calibrates most PM/AM measurement error models

PTTI 1994

3

## STATE-OF-THE-ART MEASUREMENT TECHNIQUES FOR PM AND AM NOISE

Craig Nelson  
SpectraDynamics Inc  
(303) 497-3069  
email: [nelson@boulder.nist.gov](mailto:nelson@boulder.nist.gov)

PTTI 1994

1

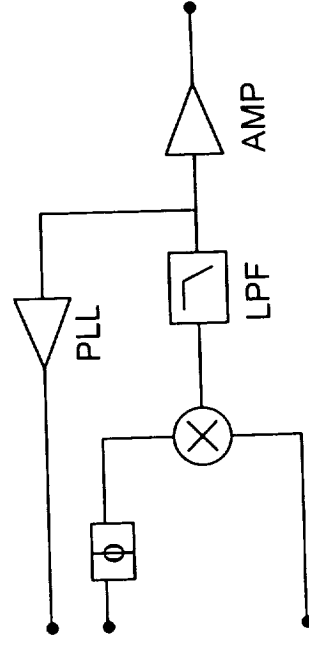
## State-of-the-art measurement techniques for PM and AM noise

- Ultra wideband measurements (Fourier frequencies 0.1Hz to 1 GHz)
- Integral PM and AM noise standards
- Ultra low-noise PM and AM measurement systems ( $S(f) \leq -190$  dBc/Hz)

PTTI 1994

2

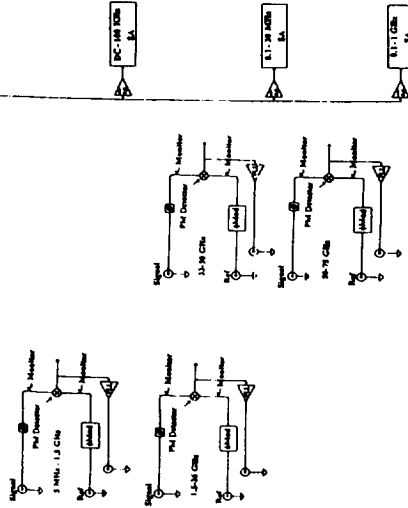
## Basic phase noise measurement



PTTI 1994

4

## NIST wideband measurement system



PTTI 1994

5

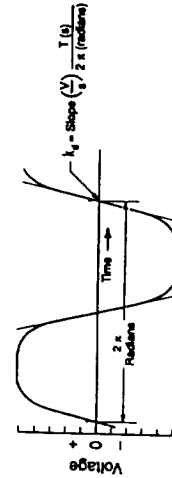
## NIST modulator

- Can be adjusted for pure PM or AM modulation
- Extremely flat frequency response
- Calibrates  $K_d(f)$  with system locked

PTTI 1994

7

## Determination of $K_d$

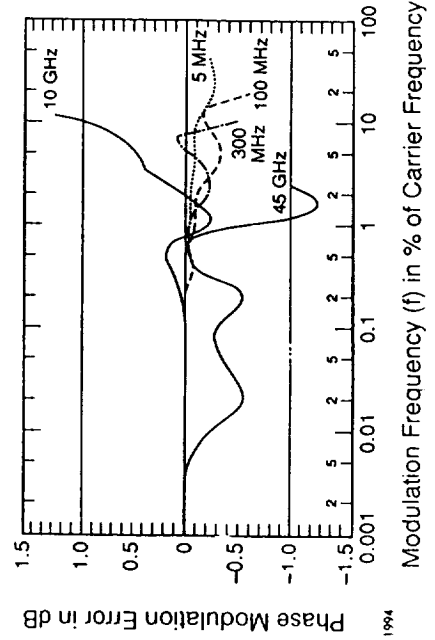


- Determines Gain at single frequency
- Does not calibrate pll effects

PTTI 1994

6

## Errors in the NIST modulator



PTTI 1994

10

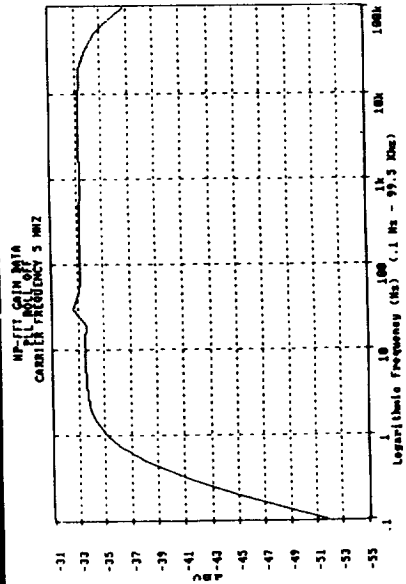
## Tips for measuring gain Vs Fourier frequency

- Measure power spectrum not PSD
- Use flattop windows for FFT
- Only small number of averages required
- Use zero span width on spectrum analyzers
- 3-5 points per decade
- create gain curve with cubic spline

PTTI 1994

11

## Sample gain curve at X-band



PTTI 1994

12

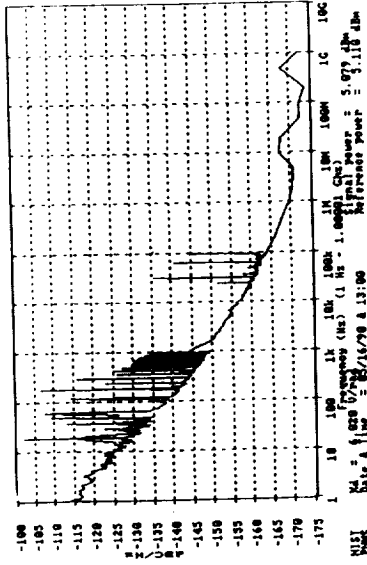
## Tips for measuring noise

- Use PSD on FFT
- Using Hanning window
- Confidence interval depends on number of averages
- Confidence interval depends also on resolution and video bandwidth for swept analyzers
- Keep level of system noise floor in mind

PTTI 1994

13

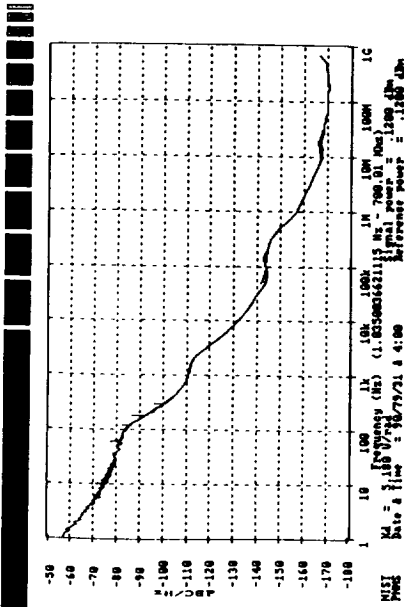
## Noise floor of NIST system at 42 GHz



PTTI 1994

14

## Phase noise of X-band synthesizer



PTTI 1994

15

## Current performance of NIST phase noise measurement system

Noise Floor	Accuracy
5 to 1500 MHz	$\pm 0.5$ dB 1 Hz to 32 MHz
-140 dBc/Hz at 1 Hz	$\pm 1$ dB 32 MHz to 150 MHz
-173 dBc/Hz Floor	
1.5 to 26 GHz	$\pm 1$ dB 1 Hz to 500 MHz
-135 dBc/Hz at 1 Hz	$\pm 2$ dB 500 MHz to 1 GHz
-170 dBc/Hz Floor	

PTTI 1994

16

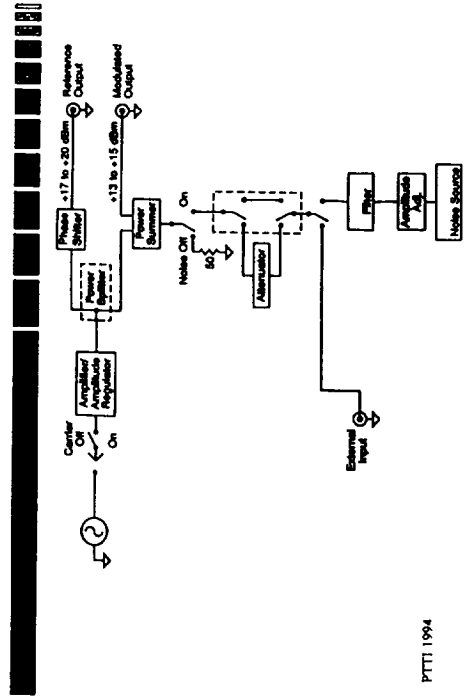
## Integral PM and AM noise standards

- Low noise signal source
- Two outputs with extremely low differential AM and PM noise
- Calibrated noise source
- Greatly simplifies AM and PM measurements

PTTI 1994

18

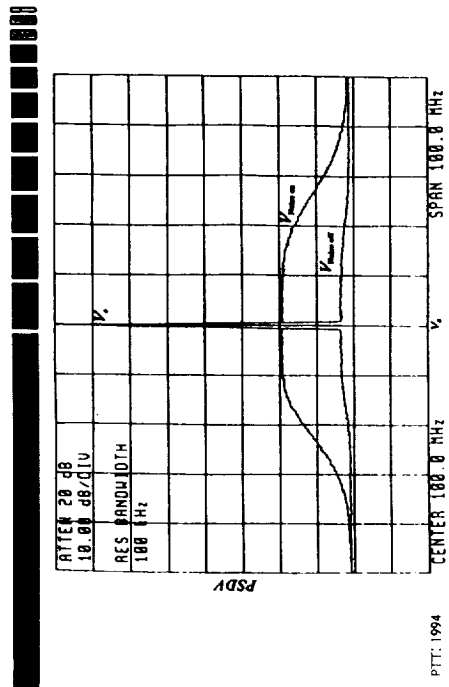
## Block diagram of NIST PM/AM noise standard



PTTI 1994

19

### Addition of noise to carrier



PFTI 1994

20

Added noise appears as equal amounts of AM and PM

While

$$S_a(f) = S_p(f) = \frac{PSDV_n(v_0 - f) + PSDV_n(v_0 + f)}{2V_0^2}$$

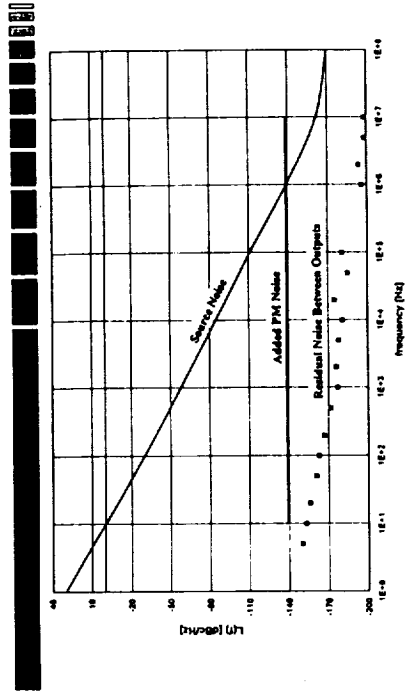
and

$$\int_{-\infty}^{\infty} S_p(f) << 0.1$$

PFTI 1994

21

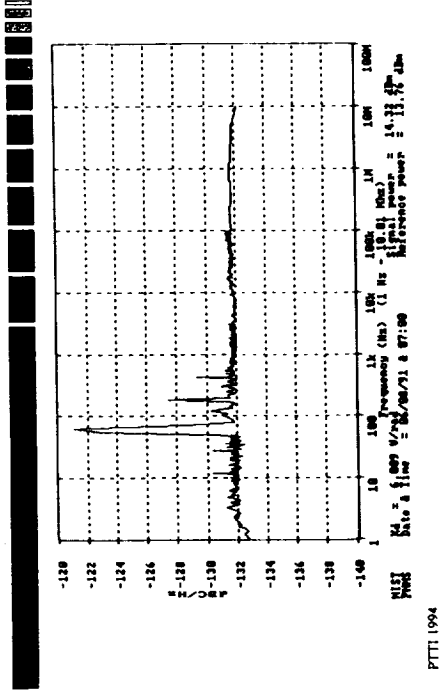
### Phase noise of NIST X-band PM/AM standard



PFTI 1994

22

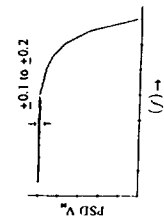
### Added PM noise at 100 MHz



PFTI 1994

23

## Stability of noise standard



$$\frac{dS(f)}{dTemp} < 0.02 \text{ dB/}^\circ\text{C}$$

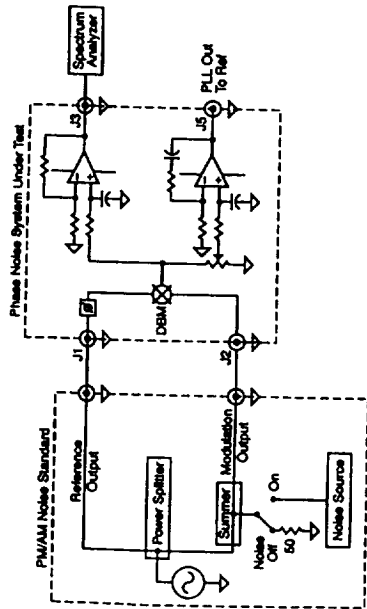
$$\frac{dS(f)}{dtime} < 0.2 \text{ dB/year}$$

$$\text{accuracy} / \text{calib.} \pm 0.15 \text{ dB}$$

PTTI | 1994

24

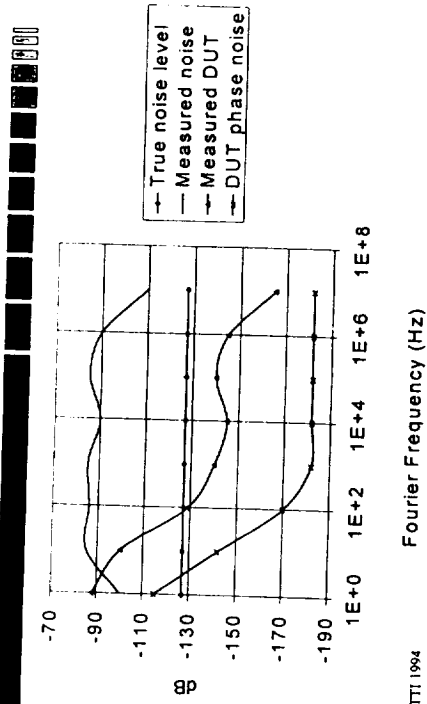
## System noise floor for PM



PTTI | 1994

25

## Use of noise calibration level



PTTI | 1994

26

## Calibration of noise floor and system accuracy

Table showing Maximum Residual Noise Between Channels and Differential PM/AM Noise Level.

SOURCE FREQUENCY	MAXIMUM RESIDUAL NOISE BETWEEN CHANNELS dB/Hz							
	1 Hz	10 Hz	100 Hz	1 kHz	10 kHz	100 kHz	1 MHz	10 MHz
5 MHz	-162	-172	-182	-190	-194	-191		
10 MHz	-161	-176	-183	-191	-197	-194		
100 MHz	-152	-162	-172	-182	-193	-194		
10.6 GHz		-153	-163	-173	-181	-181	-196	-198

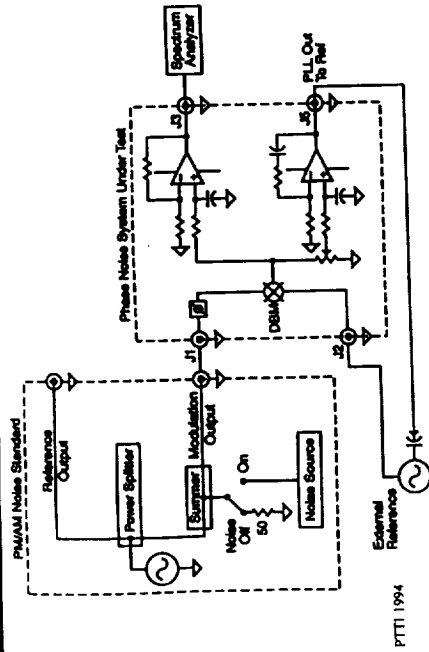
  

DIFFERENTIAL PM/AM NOISE LEVEL $\pm 0.2$ dB/Hz								
5 MHz	-127.3	-127.3	-127.3	-127.3	-127.3	-127.3	-127.3	-127.3
10 MHz	-128.4	-128.4	-128.4	-128.4	-128.4	-128.4	-128.4	-128.4
100 MHz	-129.5	-129.5	-129.5	-129.5	-129.5	-129.5	-129.5	-129.5
10.6 GHz		-138.9	-138.9	-138.9	-138.9	-138.9	-138.9	-138.9

PTTI | 1994

27

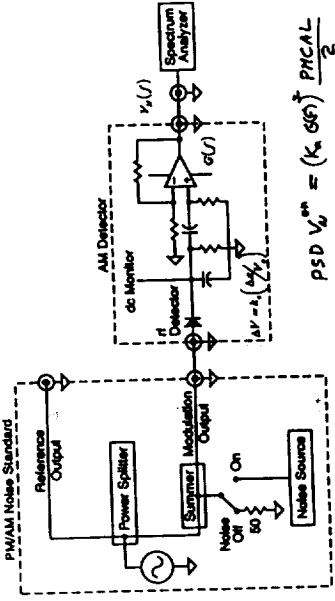
# Measurement of an external oscillator



PTTI 1994

28

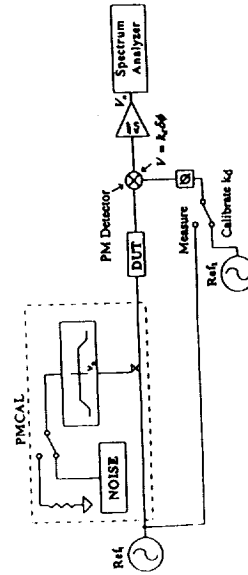
# Calibration of a simple AM measurement



30

PTTI 1994

# Measurement of other devices

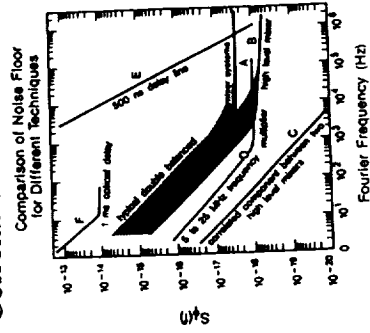


PTTI 1994

29

# Ultra low PM and AM measurement systems

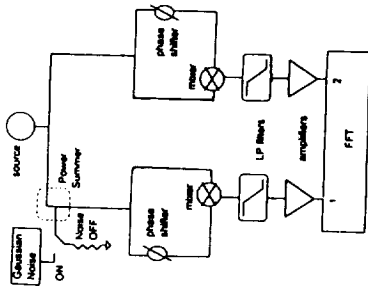
## Cross-Correlation



PTTI 1994

31

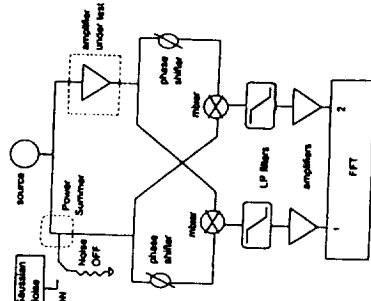
## Cross-correlation PM noise floor measurement



PTTI 1994

32

## Cross-correlation PM noise system for amplifier measurements



$$PSD_1 = P_{M_{amp1}}(f) \cdot \text{NOISE}_{channel1}$$

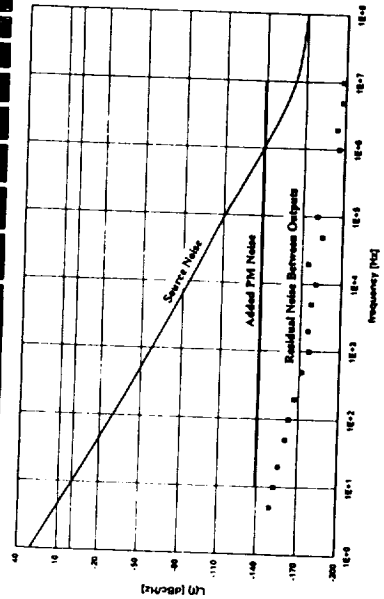
$$PSD_2 = P_{M_{amp2}}(f) \cdot \text{NOISE}_{channel2}$$

$$PSD(\text{CROSS}) = P_{M_{amp}}(f)$$

PTTI 1994

34

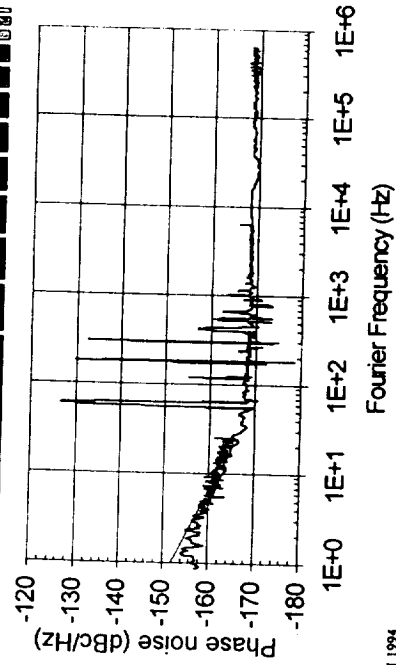
## Residual noise between channels of NIST phase noise standard



PTTI 1994

33

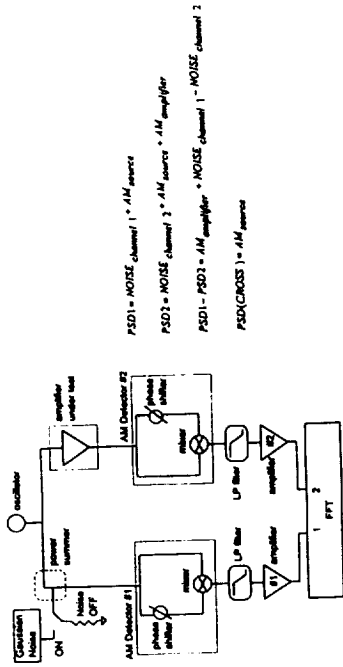
## Ultra-low noise amplifier measurement



PTTI 1994

35

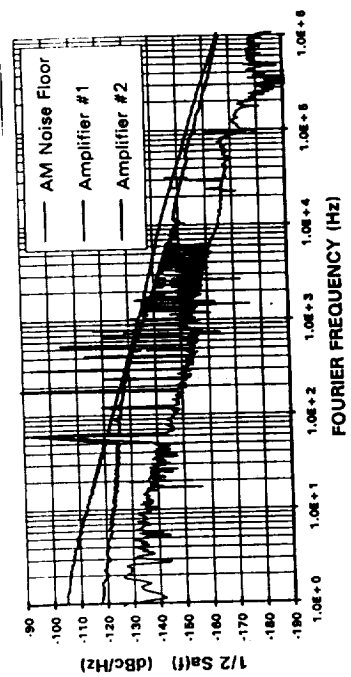
# Cross-correlation AM amplifier measurements



38

PTTI 1994

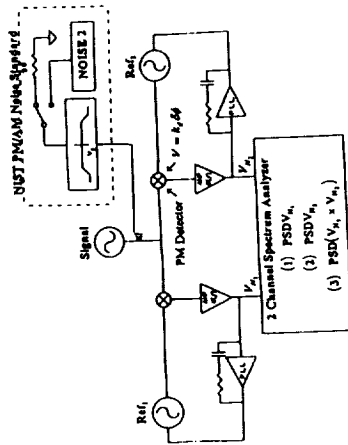
# Noise floor of AM measurement system



39

PTTI 1994

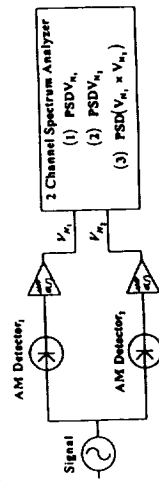
# Cross-correlation oscillator measurements



36

PTTI 1994

# Cross-correlation AM measurements



(1)  $\frac{PSDV_n}{[k_s \sigma(f)]^2}$  measures  $S_s(f)$  of the signal plus System, noise.

(2)  $\frac{PSDV_{n_s}}{[k_s \sigma(f)]^2}$  measures  $S_s(f)$  of the signal plus System, noise.

(3)  $\frac{PSDV(V_n \times V_{n_s})}{[k_s \sigma(f)]^2}$  measures  $S_s(f)$  of only the signal since System, noise is uncorrelated with System, noise.

37

PTTI 1994

## Conclusions

- To increase Fourier range a modulation technique (PM or FM) can be used.
- Using an added noise source greatly simplifies PM and AM measurements as well as decreases measurement times.
- For ultra-low noise floors cross-correlation techniques must be used.

# State-of-the-Art Measurement Techniques for PM and AM Noise

## TUTORIAL – QUESTIONS AND ANSWERS

### Note from the editor

The questions were asked at various points during the presentation. They were transcribed and are presented here at the end of each tutorial.

**JEFF INGOLD (ALLIEDSIGNAL TECHNICAL):** Does each spectrum analyzer have its own amplifier?

**CRAIG NELSON (SPECTRADYNAMICS):** Yes. We use a different amplifier for all of the spectrum analyzers.

**JEFF INGOLD (ALLIEDSIGNAL TECHNICAL):** And what kind of noise figure?

**CRAIG NELSON (SPECTRADYNAMICS):** I'm not sure on the actual noise figures of the separate amplifiers. But that all, in a sense, washes out, when we do the noise floor of the amplifier. Well, it's important in the design, obviously.

**JEFF INGOLD (ALLIEDSIGNAL TECHNICAL):** The overlap in the data, is that the cross-correlation between spectrum analyzers?

**CRAIG NELSON (SPECTRADYNAMICS):** Yes. Actually, we generally use several frequency spans in the measurements. For this measurement, we probably use a 25 Hz span that covers about to here on the FFT; then we probably use the 400 Hz span, a 1 kilohertz (kHz) span, and a 100 kHz span. And at this point, you can see the selective level meter takes over; and then finally, here the spectrum analyzer takes over.

Now when we sweep the space-modulated signal across, we measure it on all different instruments on the different analyzers. And we measure the same point. And then we can use that to cross the calibration over to different instruments. Then you can see they match up extremely well with this method.

**RALPH PARTRIDGE (LOS ALAMOS):** You seemed quite confident that you knew that those larger errors were due to the non-linearity in the analyzer. How do you come about that?

**CRAIG NELSON (SPECTRA DYNAMICS):** Well the error terms are error terms that we calculate, they're not absolute error terms. We measure value; we don't absolutely know what the true value is. So, it's an error analysis that we do through all the system. We figure there is a certain error budget to each term, and we sum those up.

**FRED WALLS (NIST):** The column there on the right is the confidence for the measurements, not the errors. Because if they were errors and we knew about them, we just back them out and measure it. But that's the sum of the errors from the modulator, the demodulator, the amplifier gains, POLs – wouldn't affect that.

I know it's been a really long session, but do you have any more questions? The one thing that a phase noise standard does not handle is the AM to PM conversions. That's one of the errors that one would have to measure independently.

**JEFF INGOLD (ALLIED SIGNAL TECHNICAL):** Could you back up to, I think it was 36? I can see A to B and A to C; but I don't quite see B to C on the three-corner hat. Could you expand a little bit?

**CRAIG NELSON (SPECTRADYNAMICS):** Well the B to C doesn't really happen.

**FRED WALLS (NIST):** And it's not needed?

**CRAIG NELSON (SPECTRADYNAMICS):** It's not needed, because the noise – I'm not saying you get all three of those measurements. With this technique, you only get the noise of the signal source. If you want the noise of all three oscillators, you still have to end up doing measurements. But frequently, you have to measure three oscillators just to get the absolute noise of a single oscillator. Does that answer your question?

**JEFF INGOLD (ALLIED SIGNAL TECHNICAL):** Yes.

**FRED WALLS (NIST):** All right, basically the noise in this measurement system and the noise in this reference are uncorrelated with the noise in this measurement in this measurement system. And so when you do the PST of the cross, those noise terms average to zero as one over the square root of the measurements, and they simply drop out. And the fact that the measurements are made simultaneously, then fluctuations in the various ones also cancel better in the noise floors, quite a bit better than what you can get if you did the actual three-corner hat sequentially.

The other difference is when you do the three-corner hat sequentially, you end up subtracting large numbers to get a little one; and so, a small error gets magnified by how much better the oscillator is. In this case, a small error in the calibration here is a small error in the final result, and not magnified by the difference.

**MALCOLM CALHOUN (JPL):** Do you have any preference between high-level mixers and low-level mixers in your phase noise measurement systems?

**FRED WALLS (NIST):** It depends on the power of the source. If I have quite a bit of power, then a high-level mixer gives me a little lower noise floor. If I have a small signal, then a low-level mixer will give me a better noise floor.



**PANEL DISCUSSION:  
Joint Defense Laboratories (JDL)  
Timing Research Status**

**MODERATOR**

**Edward D. Powers, jr.  
U.S. Naval Research Laboratory**

**PANEL MEMBERS:**

**John R. Vig  
U.S. Army Research Laboratory  
and  
Ronald L. Beard and Frederick E. Betz  
U.S. Naval Research Laboratory**

**EDWARD D. POWERS (NRL):** Good morning, everyone. We're going to start this morning off with a panel discussion on the Joint Defense Laboratory (JDL) Timing Research Status. We're going to talk a lot about what is Reliance and what does "Reliance" mean.

Our panel today is going to be Fred Betz from the Naval Research Laboratory (NRL), Ron Beard from the NRL and John Vig from the U.S. Army Research Laboratory (ARL). Dr. Ken Johnson was unable to attend today. We're also going to leave the floor more or less open for questioning throughout the whole panel discussion.

Let me turn it over to Fred Betz to start the discussion on his experience with what is Reliance. He's been on many panels for Reliance over the last few years, and he has quite a bit of knowledge about that. Fred.

**FREDERICK E. BETZ (NRL):** I don't have a prepared speech. I did get involved in the Reliance Program when my manager volunteered me a couple years ago, in 1990, to pick up when the Navy finally decided to get aboard Reliance. I understand the Army and the Air Force had gone through a Reliance type of activity. Finally, the Navy decided that maybe this was going to happen, and they had better join with the Army and Air Force.

In reality, it kind of all started when the Office of the Secretary of Defense, back in 1990, prepared a draft memorandum that said that they would take over all Science and Technology (S&T) funding activities for the three services. Perhaps for the first and only time in history the three-service principal S&T flag officers stood up and screamed in unison "No, let us do

it. Give us the rope and let us form our own noose that we may hang ourselves.”

So they formed a Joint Directors of Laboratories, which is composed of the three principal S&T flag officers for the three-services panel to investigate how they could meet the Department of Defense (DoD) objectives, which were to eliminate redundancy, promote joint activity, and, of course, I guess the redundancy and the perception that everybody was going their own way in doing what they would like in research, science and technology, without any guidance. A taxonomy was established – I’m not exactly sure how that came about. I got to be on the Space Panel, being a representative from the Naval Center of Space Technology.

At that time, there was also an astrometry panel. That was seeded, at that point in time, as a result of the determinations by the Reliance groups to the Navy, and basically with the U.S. Naval Observatory (USNO) being the principal actor in astrometry. The NRL had retained space clocks, and Dr. Vig retained frequency control technology. He’ll talk about that.

That is kind of the history. We went on for about three years, as I remained on the Space Panel, and not doing any real planning (to a very large extent), but more or less documenting the execution of the funding of science and technology. There were not a large number of true joint programs developed, although there were a number of small programs; and there were a number of good relationships that developed between the three representatives of the three services, in their technical areas. Instead of an environment like this in conferences, it was actually going to the residences of the laboratories of three services; and meeting, and working together, and looking at what each other were doing.

**JOHN VIG (ARL):** When this Reliance was initially created, my lab director came back and told us what had happened. And basically, the pie supposedly got carved up in a way that the three services each had a significant activity and area, like solid state technology, for example. Then it became, I believe it was, the Category I Program, where each service will continue doing research in a certain area; and there will be very close collaboration; and “jointness” was the key word; everything would be done jointly; that there would no Army solid state program or Air Force solid state program or Navy solid state program. All the programs shall be planned jointly and executed jointly, even though the funding might come from only one of the three services. So we were to be one big happy family, without the actual combination of the three services laboratories.

In frequency control technology, the Army was given what was called “Category III” responsibility, which meant that the Army had lead laboratory status within DoD for frequency control technology. When we first heard that, we thought that it was great news for us, we’re golden, we’re going to be the lead laboratory. Unfortunately, it didn’t turn out that way. Because of that, the Air Force, about that time, completely got out of frequency control; the Navy’s funding, I guess, was cut to zero in frequency control; and the Army’s funding was cut also. So instead of it helping the technology, I think it actually hurt us quite badly.

We were given frequency control; the Navy, for example, was given vacuum electronics; technology was a Navy Category III program. The Air Force was given antenna technology as an Air Force Category III program. But each of the three services continued to do service specific research in those areas.

This summer at the annual reviews, all the different electrotonic devices programs presented an annual review before a high-level DoD person, Dr. Susan Turnbach. I gave the presentation for frequency control technology. I pointed out that the technology has declined substantially since Reliance was created. I mentioned that, for example, ten years ago there were somewhere between 50 and 100 researchers in this area, because all three services had a significant program. The Air Force had a large program in frequency control technology; they were growing quartz sponsoring research and rubidium standards and various other technologies. The Navy had a significant program and the Army had a significant program. Today, the Army is the only one with an in-house 6.1, 6.2 activity in frequency control technology. The Navy and the Air Force have no 6.1, 6.2 programs. 6.1 is basic research, 6.2 means exploratory development, applied research, basically.

Apparently my briefing caught Dr. Susan Turnbach's and AGED'S attention; and as a result, I learned recently – well, let me backtrack a second. Every year there are one or two technology areas selected for a special study, to determine what the DoD's investment strategy should be in those technologies. This year the AGED selected frequency control technology as one of two technologies. So there will be a very high-level study done on what the DoD's investment strategy should be for frequency control technology. I was asked to draft a statement of work for that study and to recommend people who should be participants in that study. I recommended some of you as participants. Potentially, this could be very helpful to us if we do a good job.

**RONALD L. BEARD (NRL):** I think the real significance in this overall effort is that the direction within DoD seems to be towards focused programs like this and joint operation, such that DoD isn't spending a lot of money in duplicative efforts, and things like that, which is one of the words that was used when this was initially formed. I think it is significant to point out that when it was initially formed, too, what they looked at was work that was actually being done in-house within the government, rather than contracted efforts. It was through that mechanism whether to assign the lead laboratories and the focus centers for this technology.

But in this role of combining and doing joint DoD-type procurement and development, where does the role of time and frequency fall? Well, it's almost slipped through the margins, I think, as John was pointing out. This technology is viewed by many authorities within DoD as just kind of a black-box thing that you buy off the shelf. Come to a conference like this and get a catalog from the vendor, and you just buy one. The care and feeding of the technology and development isn't really appreciated, I think, very much beyond this community. How this community can affect the long-range planning by DoD and other agencies can bear an important part on how well this technology flourishes.

I think that is one of the significant things that we need to discuss this morning, is where is this technology going; how does it contribute to the long-range plan; and should it be a significant thing to be pointed out in some of these high-level technology development areas? Otherwise, within DoD, it will get submerged behind the new extra smart sensor, the new weapon system that blows up asteroids, or things like that.

I personally think that it's a very significant technology that transcends the individual systems. It's an intersystem technology, if you will. Too many system developers and technology developers

look at individual systems and specific devices to do that mission, a new sensor, something where they can see trees from the other side of the world, or something like that. Time and frequency goes across all systems, and it's difficult to get people to appreciate that. Many of them simply take it for granted. And, as I think we all know, it's not something you can really take for granted; it needs to be nurtured and developed. Significant developments have been made in this area.

**FREDERICK BETZ (NRL):** Ron, one of the problems with the funding for science and technology that have been incorporated under the JDL Reliance is that it only addressed the service S&T funds, which were probably about one-third of the total defense research technology budget. The vast majority, the other two-thirds, went to both the Strategic Defense Initiatives Office (SDIO) at the time, and later, Ballistic Missile Defense Office (BMDO), and also, Advanced Research Projects Office (ARPA). There is a move afoot, at this point in time, towards getting more involvement of Director Defense Research & Engineering (DDR&E) ; it's largely in turmoil at this point in time. There was a meeting of the JDL in August where Mr. Brachkosky from DDR&E was there, and essentially agreed to be a major participant in not the JDL Reliance, but in Defense Science and Technology Reliance. So it may even have a new name before very long. That would, again, tend to centralize the control and centralize the funding, if, indeed, as proposed, ARPA and SDIO funds were swept into this area.

As was mentioned, the Navy funding of Science and Technology went away for the GPS area. Fortunately, we're a reimbursable laboratory, and Ron went out and found "customers," Space Command (SPACECOM), I guess, and some others to provide funds to keep the organization growing. His science and technology staff in precision timing are still quite robust.

I might also mention that Ron mentioned that the in-house staff was the basis for the formation of the establishment of the Reliance strengths. That was true to the extent that scientists and engineers in house included those involved running outside contracts, technical managers of outside contracts. The R&D funding that went to outside contracts through that channel was also included in the accounting of who had the lead laboratory status. It wasn't just how many true in-house S&T scientists were available, but also how much funding they could leverage through contracts.

**JOHN VIG (ARL):** Any questions from the audience?

**HAROLD CHADSEY (USNO):** You're talking about having a joint thing where one lab knows what another lab is doing. The Naval Observatory is not that large a lab in comparison to many others and to the entire DoD community. We have problems enough figuring out what the person in the other building is doing. If they have a program that they had already written and everything set up for, and we could use that program, sometimes it's quite by accident that we find out about it. How do you propose and implement at what time a communication between one lab and another lab happens, and prevent the idea of "empire building" and somebody saying "Well I'm not going to give you that information because it will tear away from my empire?"

**JOHN VIG (ARL):** You have no choice. Even long before Reliance was created, there was another panel called the AGED, the Advisory Group Electron Devices. Before we could initiate

any contractual programs, if not in-house, we had to do was called an "AGED write-up;" we had to describe in just two or three pages as to what the program goals were; what the rationale was for the program; what the projected funding levels are; and who's going to be in charge of running the program; and who are the probable contractors who will bid on the program. This went to the AGED panel, which consisted of outside DoD, high-level executives, like vice-presidents of corporations, senior professors at universities and such. The AGED panel would look at these programs and look at the programs submitted by the Air Force and the Navy, and made sure that there was no duplication of effort; and also it was distributed to all the laboratories to make sure everybody knew what the other guy was planning.

So there was a formal mechanism to make sure that at least contractual programs were pretty well coordinated. Now this Reliance was to take the next step, and that is to make sure that all programs, whether they are contractual or in-house, were well coordinated; and not only coordinated, but actually performed jointly. So whereas before, if I decide I wanted to do a program on a very low power compensated oscillator, we would create a program; and write up a work statement; and then do an AGED write-up; and then it would get coordinated; and then it would be sent to the Navy and the Air Force to make sure they knew what the Army was doing.

Now, even before we do anything, we are supposed to contact our counterparts in the Navy and Air Force and jointly decide what should be done, jointly write the work statement, jointly do everything in the process of creating this contractual program. That's the theory anyway. Has it happened that way in reality? Not really. In large part, because we just simply don't have much money for contracts. So since the Reliance was created, we haven't had many contracts.

**RONALD BEARD (NRL):** I think communication is a problem, though, even in these joint efforts. Certainly in large efforts like this, it's very difficult — as he pointed out, it's difficult to communicate across the lab. It's even more difficult to communicate from laboratory to laboratory, especially on a programmatic level. That is a significant problem.

**FREDERICK BETZ (NRL):** Yet, that was one of the fundamental purposes of forming the Reliance panel in the area of astrometry. In astrometry, there was a single service identified, and perhaps it's time to readdress the technology centers of excellence across all the services if there's going to be a reevaluation and the realignment of the technology panels, so that USNO could participate with the Army and the Air Force personnel who are doing work in frequency.

**JOHN VIG (ARL):** In our technology area, there is an additional coordination mechanism, and that's the PTTI coordination meetings that we have every year at the USNO. Under Dr. Winkler's leadership, all the government organizations that are involved in PTTI technology get together and share information.

**GERNOT M. WINKLER (USNO):** I just want to correct one impression that exists persistently, and that is that the USNO is not a laboratory. The distinction is very important. We are part of an operational part of the Navy. This is not under the research and development organization which, for instance, is, of course, the case with NRL, which is under the Chief of Naval Research. Similarly in the other services.

Therefore, we are not a competitor in any way. We are a user of results of research and

development. That is the function of the USNO. Independently and separately from that, of course, is our role as the PTTI managers for DoD. In that regard, we have a coordination function, as you just mentioned, Dr. Vig.

I just wanted to keep that separate as much as we can, because otherwise, if things are that way, you always get into wrong conclusions. So we are not a laboratory, and that distinction is very important.

**FREDERICK BETZ (NRL):** I just had an opportunity to look at the document that came out in September of this year called "The Defense Technology Plan." I couldn't find anything in here, at least in the major headings, that dealt with precision timing or frequency. It may be buried deep down somewhere in one of the panels or subpanels, but it certainly isn't addressed as part of the a technology S&T effort at the Director of Defense Research and Engineering level.

**JOHN VIG (ARL):** That is because that document doesn't go down to the sub-subpanel level. That's where frequency control sits. There is an electronic devices panel under which there are a number of subpanels, one of which is RF components. Frequency control is a sub-subpanel in RF components technology. I think that only goes down to RF components and not to the sub-subpanel level.

We are a very small part of the total DoD electronic devices effort. In solid-state technology, when you look at the funding charts, we are a little blip; solid-state technology is probably 50 times as large in funding levels.

**RONALD BEARD (NRL):** Well, I'm not so sure that we should be a major heading under "Science and Technology" per se. But on the other hand, we could be part of the sub-sub-sub-sub-subpanel that's absolutely totally forgotten.

That's something I think we shouldn't allow to happen; because, this technology is taken so much for granted that people just assume you know time; I mean, people are familiar with time, they look at their watches everyday so that they can be at work on time. But it's not really viewed as a technology; and from that perspective, it just can be "subbed" into oblivion. I think that's the issue that I would like to bring forth, so that people can be aware of this when they're communicating with developers and people who are doing contracts and developing systems and those sorts of things.

You just can't take time for granted. It has to be generated, it has to be nurtured, and it has to be taken care of.

**JOHN VIG (ARL):** We also have an image problem. I have heard frequency control and clock technology it referred to as "that old technology."

**JOE WHITE (NRL):** Let me encourage a little bit of speculation for a minute. You all have talked about, number one, that within the time and frequency community we have done a fair amount of coordination; there's a mechanism to it. I think there has always been kind of a division of labor, particularly between our group and John's group, in terms of who did what. You generally work in the crystal and the portable technology, we tend to do work in the space area.

I think also, as Fred has pointed out, a lot of these meetings at a higher level don't really reflect that kind of a coordination going on, not necessarily in our area, but in general. Do you think we're in some danger, either at the DoD level or even at the service level, of somebody deciding to merge functions and solve our problems for us? Even though we may not have any problems, are we going to be swept into laboratory mergers or whatever? Anybody have a feeling about that?

**JOHN VIG (ARL):** Some of the cynics think that the whole idea of JDL Reliance was to prevent what is called the "purple-ization of DoD laboratories." "Purple" means forming a single – you know, the Army is green, the Air Force is blue and the Navy is, I guess, white. So, "purple" is a term that people have been using as a merging of the three services' efforts.

I believe that even now there are serious proposals being considered for merging the three organizations and creating a single DoD laboratory structure. Perhaps Helmut Hellwig is in a position to address that question.

**HELMUT HELLWIG (AF OFFICE OF SCIENTIFIC RESEARCH):** Let me comment on a couple of these questions.

The issue of the old Reliance and the incubating defense investment strategy, which I think is the current best word and the official word – I think it's on your document too – the issue is not whether or not you work with the other lab; the issue is that you don't have enough money to do what you used to do. So you are questioning where do you put the money; several dimensions, where do you put it and topics. So the question for time and frequency is not USNO versus NRL versus whatever goes on in the Air Force. By the way, something still goes on in the Air Force, in the extramural program; we're on a very solid 6.1 program.

The issue is: Should there be time and frequency in any DoD activity? Should Ron Beard go out of existence? That is the issue. Why could he go out of existence? Don't get me wrong here, there's no proposal, to the best of my knowledge, of that nature on the table. So I'm just giving you a fictitious view of the world. But it is the kind of thinking I want to project. Why couldn't he go out of the existence in the thinking of defense managers? Because of NIST and Hewlett Packard? That's why.

I think the challenge for the time and frequency DoD community is to prove that they add something significant to defense, in view of the ongoing academic and commercial activities. The issue has graduated very much from being an issue of "Are you working together?", yes, no, to "Why do you exist in view of other efforts?" "Should we use the money you are earning for things where it is more needed?" That is the issue, and it will be with us for the rest of the century.

**PHILLIP E. TALLEY (RETIRED FROM AEROSPACE CORPORATION):** Along the line of this discussion, I think that one shortcoming is that potential contractors for various large systems don't really know where within the government to go for advice for time and frequency. I've been inclined to recommend going to see Dr. Winkler as a source of what's available, and possibly recommendations of how to approach the time and frequency problems. But people don't seem to appreciate that there is help out there. I think the integration of labs, or whatever happens, needs to address this and make it known to the various industrial

contractors that service is available; and we need to know this in order to direct the efforts in whatever laboratory activities are going on, but will satisfy the needs for the future contractors.

**JOHN VIG (ARL):** We spend a considerable portion of our time answering questions over the telephone and having visitors come to us and ask us about oscillators. That is an important function that we perform. But that's not what sells programs when we go for our annual reviews. To say that we have advised a corporation or have answered questions from industry does not buy us much. If we have developed a new gizmo that we can demonstrate increases battery life in a tactical radio, because the power consumption of this oscillator is ten times lower than before, that's the kind of thing that sells programs. Or, if you can make tiny little atomic clocks versus the 19 inch rack atomic clocks, and you can explain what the significance is in future military systems, that can sell programs.

But you are right. That's an important function that government laboratories can and do serve. But that's sort of a side issue.

**EDWARD POWERS (NRL):** One final question here. Speaking of the Aerospace Corporation, other government laboratories, are they following this anywhere?

**JOHN VIG (ARL):** Not that I know of, no.

**RONALD BEARD (NRL):** One final quick comment. I think Helmut made some very good points, specifically that my group wasn't targeted for extinction. But I think that is the key issue. Since the resources and funding is going to be much more limited than it has been in the past, what are the technologies doing for you, compared to what is available? And, does additional research need to be done? In the additional research, where can you get the best available? That is the key issue.

**JOHN VIG (ARL):** We have an image problem. I think when there are annual reviews, and people get up and talk about these micro-electromechanical devices, tiny, tiny microscopic motors and actuators and pumps and various other devices, those are considered to be the sexy technologies. It's hard to compete with that when you are talking about a new generation of clocks, for example.

**RONALD BEARD (NRL):** The "glitzy" technologies.

**Ed Powers (NSR):** I would to thank the panel and the audience for their participation in this discussion.

8.10.2  
1 13

# Monte Carlo Simulations of Precise Timekeeping in the Milstar Communication Satellite System

J. C. Camparo and R. P. Frueholz  
Electronics Technology Center  
The Aerospace Corporation  
PO Box 92957, Los Angeles, CA 90009

## Abstract

*The Milstar communications satellite system will provide secure antijam communication capabilities for DoD operations into the next century. In order to accomplish this task, the Milstar system will employ precise timekeeping on its satellites and at its ground control stations. The constellation will consist of four satellites in geosynchronous orbit, each carrying a set of four rubidium (Rb) atomic clocks. Several times a day, during normal operation, the Mission Control Element (MCE) will collect timing information from the constellation, and after several days use this information to update the time and frequency of the satellite clocks. The MCE will maintain precise time with a cesium (Cs) atomic clock, synchronized to UTC(USNO) via a GPS receiver. We have developed a Monte Carlo simulation of Milstar's space segment timekeeping. The simulation includes the effects of: uplink/downlink time transfer noise, satellite crosslink time transfer noise, satellite diurnal temperature variations, satellite and ground station atomic clock noise, and also quantization limits regarding satellite time and frequency corrections. The Monte Carlo simulation capability has proven to be an invaluable tool in assessing the performance characteristics of various timekeeping algorithms proposed for Milstar, and also in highlighting the timekeeping capabilities of the system. Here, we provide a brief overview of the basic Milstar timekeeping architecture as it is presently envisioned. We then describe the Monte Carlo simulation of space segment timekeeping, and provide examples of the simulation's efficacy in resolving timekeeping issues.*

## Introduction

Figure 1 shows the baseline timekeeping architecture for Milstar as presently envisioned. The constellation will consist of four satellites in geosynchronous orbit<sup>[1]</sup>, each carrying a set of four rubidium (Rb) atomic clocks, though at any one time only one clock will be operational on any given satellite. A satellite's active clock is labeled as either master (MSR), monitor (MON) or slave. The slave clock ties its time and oscillator frequency to the master via timing comparisons performed through the satellite crosslinks using a slaving procedure developed by Lockheed (the Milstar prime contractor)<sup>[2]</sup>. The monitor clocks are free-running, and are present in order to assess the health of the MSR again via the satellite crosslinks. Several times a day, during normal operation, the Mission Control Element (MCE) collects timing information on the Triplet of free-running clocks (i.e., MSR, MON1 and MON2), and after several days uses

this timing information to update the time and oscillator frequencies of the Triplet. The MCE maintains precise time with a cesium (Cs) atomic clock, which is synchronized to UTC.

In outline, Milstar timekeeping would appear to be straightforward and robust; however, in detail precise Milstar timekeeping is a complex matter. The time comparisons between satellites via the satellite crosslinks, and those using the uplink/downlink between the inview satellite and the MCE, are not perfect: un-accounted for equipment delays can introduce non-negligible timing errors into the system. Moreover, even if the communications links were perfect, there are limits as to the accuracy with which time and oscillator frequency corrections may be applied to the satellite clocks. These limits are a consequence of both the satellite hardware and Milstar operating procedures. Additionally, the diurnal temperature variations that the satellites experience introduce timing errors as a consequence of the Rb atomic clock's (albeit slight) temperature sensitivity<sup>[3]</sup>. Though individually these processes are straightforward, with regard to system timekeeping they act together in non-obvious ways as part of a "satellite-to-MCE feedback loop": these processes cause time differences between the satellite and MCE, which the MCE attempts to correct periodically. Finally, it must be recognized that even though the satellite Rb atomic clocks will introduce no more than about 4  $\mu$ s of timing error into the system in a week<sup>[4]</sup>, this requires the MCE to set them perfectly. As a consequence of these considerations, it should be recognized that cursory analyses of timekeeping performance may neglect important subtleties, and could lead to incorrect conclusions.

In order to accurately address system level timekeeping issues, several approaches may be taken. First, one might consider developing a hardware prototype of system timekeeping. This approach is impractical not only because it requires a large capital outlay for the various pieces of equipment, but also because investigations into system timekeeping over periods of months would have to be done in real time. Alternatively, one could attempt to solve the satellite-to-MCE feedback loop equations. This too is an impractical approach, because closed form solutions could not be obtained without significant approximation. Moreover, altering system characteristics slightly (e.g., system algorithms) could force a re-derivation of the entire set of feedback loop equations, requiring significant amounts of additional effort. Our approach to answering system level timekeeping questions has none of the above mentioned drawbacks, as it is based on Monte Carlo simulation<sup>[5]</sup>. With a Monte Carlo approach, the results are obtained without approximation; years of system timekeeping experience can be built up over the course of several hours, and changing system algorithms requires nothing more than the change of a subroutine.

Figure 2 is a functional diagram of the Monte Carlo concept, illustrating some of the important components of this simulation capability. The studies to be discussed below have focussed on the MCE's management of space timekeeping assets, and the performance of those assets under varied operational conditions. Generally, however, Milstar timekeeping also includes the process of synchronizing Milstar time, which is maintained at the MCEs, to UTC which is maintained by the Naval Observatory for DoD programs. Synchronizing Milstar time to UTC should be straightforward, and hence not require detailed Monte Carlo simulations for the resolution of timekeeping issues.

In the analysis of system timekeeping, we start by generating a time series of random frequency fluctuations for both a satellite and MCE atomic clock<sup>[6,7]</sup>. Additionally, whenever timing

comparisons take place between clocks, we simulate the appropriate communication link time-transfer noise (i.e., either uplink/downlink or crosslink), and make allowances for any limitations as to timekeeping corrections. Finally, we include in the simulation the diurnal temperature variations that a satellite clock might experience, and the resulting diurnal frequency variations. All of these stochastic and deterministic process realizations are generated in a 486-PC, and frequency variations are integrated and combined with other timing errors. The output of a single simulation is the satellite time error as a function of time, and this can be obtained for any one of the four satellite clocks (i.e., MSR, MON or Slave). By performing thousands of these simulations we generate statistics on Milstar's timekeeping performance.

## Simulation of Atomic Clock Noise

The success of a Monte Carlo analysis of system timekeeping requires the accurate simulation of various timekeeping fluctuations, and in this regard one of the most significant challenges is the simulation of an atomic clock's colored (i.e., flicker and random-walk) frequency fluctuations. The approach we employ may be referred to as a "recursive filter" approach<sup>[6]</sup>, and is best described by considering the spectral density of an atomic clock's random processes. Experimentally, if one had white noise, and one wanted to turn this into colored noise, then one would simply pass the white noise through a filter. The filter function would then shape the noise process's spectral density into some desired form. This is essentially the method we employ for simulating colored noise processes as illustrated in Fig. 3<sup>[8]</sup>.

In order to simulate a noise process with a spectral density that is an even function of Fourier frequency  $f$ , we start with computer generated random numbers. These numbers have a uniform probability distribution, but may be transformed into random numbers with a normal (i.e., gaussian) probability distribution using the standard Box-Mueller algorithm<sup>[9]</sup>. At this point, we have a simulation of a gaussian white noise process. These numbers are input to a numerical filter, described by a transfer function  $H(f)$ , and the spectral density of the filter output is  $|H(f)|^2$ . Thus, to simulate random-walk noise we just need to choose  $H(f) \sim 1/f$ .

Simulating a noise process that is an odd function of Fourier frequency is a bit trickier, as  $H(f)$  would then have to be a function of Fourier frequency to some fractional power. (If  $H(f)$  is a rational function, then the inverse of  $H(f)$  can be found by the method of partial fractions.) Since the MCE's Cs atomic clock noise has a flicker noise component, this portion of the simulation is important for properly modeling the MCE's timekeeping capability. Simulating noise processes with [INSERT 3] may be accomplished by cascading filters that are integral functions of Fourier frequency.<sup>[6]</sup> By a judicious choice of filter functions, the cascade can be made to approximate an overall filter that is not a rational function of Fourier frequency, which in turn yields an [INSERT 4] that is (approximately) an odd function of Fourier frequency

As a final point, it should be mentioned that in deriving the equations for the recursive filter, it is assumed that the filter's operation is in steady-state. This is tantamount to assuming that the filter has been processing data since  $t = -\infty$ . The fact that the recursive filter must be started at some finite time in the Monte Carlo simulations is called the "Initialization Problem."<sup>[10]</sup> Though a technical description of this problem and its solution is beyond the scope of the present discussion, suffice it to say that if the Initialization Problem is not handled properly,

the accuracy of system timekeeping simulations would have to be called into question. In the present simulations we include initialization of both the satellite Rb atomic clocks and the MCE's Cs atomic clock.

An example of our capability to simulate colored atomic frequency standard noise is illustrated in Fig. 4. Using the method outlined above, we simulated the frequency fluctuations that are expected for a Milstar satellite Rb atomic clock. We then performed an Allan standard deviation calculation on these simulated frequency fluctuations, and the results are shown as boxes in Fig. 4. The solid line represents the expected Allan standard deviation for the satellite Rb atomic clocks based on clock manufacturer data. Clearly, the agreement between our simulated frequency fluctuations and those truly generated by the Milstar satellite atomic clock is excellent.

Figure 4 represents only one validation test for our Monte Carlo simulation of Milstar timekeeping. However, at every stage in the development of the Monte Carlo simulation, tests were performed to establish the simulation's verity. These tests included an accurate simulation of the MCE's cesium atomic clock, specifically its flicker noise component, and a demonstration that the simulation would generate expected results under well defined, though not necessarily Milstar accurate, conditions.

## Applications

The Monte Carlo simulation of Milstar timekeeping outlined above includes the full range of timekeeping processes and elements associated with the MCE's management of Space Segment assets, and it has been extensively exercised to address topics in both the single and multi-satellite environments. In this section we provide examples of those applications. The first of the examples concerns work that was performed several years ago when the question of how the MCE would estimate satellite time and frequency offsets was unanswered. This example will illustrate how various system algorithms can be easily changed and examined for their effect on overall system timekeeping using a Monte Carlo approach. The second example deals with the question of how satellite temperature variations influence precise satellite timekeeping. This latter example illustrates the complicated fashion in which various processes combine to produce a non-obvious dependence of timekeeping capability on system parameters.

### A. MCE Estimation Algorithms

As discussed in the general description of Milstar timekeeping, the MCE will determine the time offsets of all the satellites in the constellation via the inview satellite and crosslinked data. This timing information will then be used by the MCE in an estimation algorithm in order to determine the time and frequency corrections that need to be supplied to the various free-running (i.e., Triplet) satellite clocks. One of the major timekeeping questions faced by Milstar system planners in the mid-eighties concerned the form that the estimation algorithm would take.

Figure 5 illustrates an MCE ranging on an inview satellite, and the timekeeping data that the

MCE would collect (i.e., satellite time error as a function of measurement time). The time error collected by the MCE will have the general form:

$$x(\tau) = x_0 + y_0\tau + \frac{1}{2}D\tau^2 + \alpha \int_0^\tau [T(t, \theta) - T_0]dt + \int_0^\tau y_r^{\text{sat}}(\tau)dt + \int_0^\tau y_r^{\text{MCE}}(\tau)dt + \epsilon(\tau) \quad (1)$$

Here,  $x(\tau)$  is the time offset between the satellite and MCE at some time  $\tau$ ,  $x_0$  is an initial time offset,  $y_0$  is a constant fractional frequency difference between the satellite Rb clock and the MCE Cs clock,  $D$  is the fractional frequency aging rate of the satellite Rb clock (parts in  $10^{13}$  per day<sup>[11]</sup>),  $\alpha$  is the temperature coefficient of the satellite clock,  $T(t, \theta) - T_0$  is the diurnal temperature offset of the satellite clock from some nominal value,  $T_0$ ,  $y_r^{\text{sat}}$  and  $y_r^{\text{MCE}}$  represent the random fractional frequency fluctuations of the satellite and MCE clocks, respectively, and  $\epsilon(\tau)$  is the measurement error associated with the MCE-to-spacecraft communication link. The parameter  $\theta$  in the satellite temperature term represents the phase relationship between the satellite's diurnal temperature cycle and the cycle of MCE corrections. The question addressed with our Monte Carlo simulation, was how the MCE could best use the time error data presented in Fig. 5 to periodically correct the satellite time and frequency. In the following, the update interval will be defined as the period of time between MCE corrections of the satellite clock.

On an examination of Eq. (1) for  $x(\tau)$ , several possibilities for employing the time error data of Fig. 5 present themselves. First, the MCE could restrict its consideration to data collected only at the beginning and end of an update interval. The time error at the end of the update interval would then be the time correction that the MCE needs to apply ( $\delta t$ ), while the frequency correction ( $\delta y$ ) would come from the estimated rate of time error build up based on the two time error measurements. If  $T_{\text{update}}$  is the length of the update interval, then the time and fractional frequency corrections to be applied by the MCE are:

$$\delta t = xT_{\text{update}} \quad (2)$$

$$\delta y = \frac{x(T_{\text{update}}) - x(0)}{T_{\text{update}}} \quad (3)$$

This is called the 2-Point estimation algorithm, and has the advantage of being very simple. An alternate procedure would be to take advantage of all the intervening data collected by the MCE during the update interval. The data could then be fit to a straight line in order to determine the appropriate time and frequency corrections:

$$\delta t = \delta y \cdot T_{\text{update}} + t_0 \quad (4)$$

Here,  $\delta y$  and  $t_0$  are the slope and intercept determined by the linear least squares. This is called the Linear estimation algorithm, and it is to be noted that the frequency correction is determined by the slope of the linear least squares fit. Finally, by examining the above equation

for  $x(\tau)$ , one might expect to do better at correcting the clock by fitting the data to a quadratic, which would essentially be attempting to account for the Rb clock's aging rate:

$$\delta t = t_0 + \hat{y} \cdot T_{\text{update}} + \frac{1}{2} \hat{D} \cdot T_{\text{update}}^2 \quad (5)$$

Here,  $\hat{y}$  is the linear coefficient of the least squares quadratic fit, which is essentially the initial frequency offset of the clock, and  $\hat{D}$  is the least squares estimate of the aging rate of the clock. This is called the Quadratic estimation algorithm.

Using our Monte Carlo simulation of Milstar timekeeping, we were able to investigate the performance of each of these estimation algorithms<sup>[12]</sup>. The parameters that were employed in the calculations are collected in Table I. To determine the efficacy of any estimation algorithm, we allowed the MCE to correct the satellite clock several times, essentially letting the system get into a steady state, and then examined the satellite time error after either 3 or 10 days of free-running operation. (Note from Table I that a 3 day free-running period corresponds to the time error the satellite would have just prior to receiving its normal MCE correction.) Hundreds of simulations were performed (each with a different satellite clock aging rate) to generate the statistics of Milstar timekeeping, and the results of that analysis are collected in Table II. In the table, the standard deviation of time error at the end of the free-running period is tabulated for the various estimation algorithms. Since the Linear estimation algorithm minimizes the spread of satellite time error, it is considered to be the best estimation algorithm among these three. Similar results comparing the Linear estimation algorithm against a Kalman Filter estimation algorithm eventually lead to the adoption of the Linear estimation algorithm for the Milstar MCEs due to its simplicity.

The fact that the Linear estimation algorithm is superior to the Quadratic estimation algorithm was initially something of a surprise. Since the Quadratic estimation algorithm more closely models the underlying performance of the satellite Rb atomic clock, one would typically expect it to result in less timing error. After some study of this issue, we found that the poor performance of the Quadratic algorithm derives from the influence of the measurement noise,  $\epsilon(\tau)$ , and the Rb atomic clock frequency noise,  $y_r^{\text{sat}}$ , on the estimated coefficients. Apparently, these noise processes strongly influence the estimated drift coefficient in the Quadratic algorithm, and of course any error in that estimate has a strong influence on timekeeping since it contributes to time error quadratically.

## B. Satellite Temperature Variations and MCE Control of the Satellite Clock

As any Milstar satellite orbits the Earth, its temperature will vary in a diurnal fashion, and in the mid-eighties thermal analysis of the satellite payload indicated that the satellite clock would experience peak-to-peak temperature variations of  $\sim 20^\circ\text{F}$ . The question arose as to how these temperature variations would influence satellite timekeeping, both for the crystal oscillator that would be launched on DFS-1 (the first Milstar satellite) and the Rb atomic clocks that would be launched on subsequent satellites. Specifically, there was interest at the time in knowing

how large the satellite oscillator's temperature coefficient could get without impacting system timekeeping performance.

Clearly, the MCE could choose to set up its cycle of satellite corrections anywhere within the satellite's diurnal temperature cycle. The quantity expressing this relationship in Eq. (1) is  $\theta$ . For example, the MCE could choose to correct the satellite clock when the satellite temperature is near its largest daily value; this would correspond to a value of  $\theta = 0$  in Eq. (1). Alternatively, the MCE could choose to correct the satellite clock when the satellite temperature is near its daily mid-range value; this would correspond to a value of  $\theta = \pi/2$  in Eq. (1). (For the reader's general information, analysis has shown that the diurnal temperature variations will be roughly sinusoidal. We note, however, that our calculations employ the expected diurnal temperature variations and not a sinusoidal approximation.) Thus, in order to study the influence of a satellite oscillator's temperature coefficient on system timekeeping, it is necessary to specify  $\theta$ . Since the actual value of  $\theta$  for any given satellite is an arbitrary quantity, we performed two sets of analyses, one with  $\theta = 0$  and the other with  $\theta = \pi/2$ .

Parameters for one illustrative study are collected in Table III, corresponding to a satellite clock with characteristics very near those of a crystal oscillator clock. As discussed in the previous example, our method was to allow the MCE to update the satellite clock through several update intervals, essentially reaching a steady-state of timekeeping, and then to calculate the satellite time offset at the end of a free-running period. For the case under discussion, the free-running period was chosen to be 24 hours (i.e., the update interval). Again, hundreds of simulations were performed, which allowed us to generate the statistics of Milstar system timekeeping, and the results are shown in Fig. 6. In the figure, the  $2\sigma$  time error at the end of 24 hours is plotted as a function of the satellite clock temperature coefficient. Two curves are shown, one with the diurnal phase angle  $\theta = 0$  and the other with  $\theta = \pi/2$ .

It is clear from the figure that there is a dependence of Milstar timekeeping on  $\theta$ . Though the strength of this dependence was unexpected, it could be rationalized as a consequence of optimally choosing the data points employed by the MCE's estimation algorithm. More surprising, however, were the specific results for  $\theta = \pi/2$ , where the satellite time error is actually found to be a decreasing function of clock temperature sensitivity (at least for temperature coefficients less than about  $1 \times 10^{-11} / ^\circ\text{C}$ ). It would appear that for  $\theta = \pi/2$ , Milstar system performance is enhanced by having a clock with a slightly larger temperature coefficient. This counter-intuitive result indicates that under certain conditions the effects of the diurnal temperature variations on the Linear estimation algorithm can (to some extent) compensate for the frequency aging of the standard. With regard to the question that motivated these studies, the results of Fig. 6 indicate that the satellite clock temperature coefficients can take on values up to  $\sim 1 \times 10^{-11} / ^\circ\text{C}$  (for arbitrary  $\theta$  without significantly changing Milstar system timekeeping. This value is large, and indicates that the Milstar constellation can be made relatively robust to satellite diurnal temperature variations. Moreover, if the MCE judiciously chooses the correction cycle for the satellites under its control, then the diurnal temperature variations might actually be beneficial to Milstar timekeeping.

Taking a broader view of the results shown in Fig. 6, these Monte Carlo simulations demonstrate the complicated interplay among: satellite temperature variations, communication link time-transfer noise, frequency aging rates, and all the other parameters that are important to satellite

timekeeping. The relationship between system-time-error, satellite-oscillator-temperature-coefficient and [INSERT 17] was not obvious prior to the Monte Carlo computations. Even now, knowing that the relationship exists, it is not obvious what the optimum  $\theta$  value is for the MCE's estimation algorithm. The important lesson to be learned is that intuitive predictions of satellite timekeeping performance must be accepted warily. How all the various timekeeping processes combine to yield the system performance is not always obvious, and in this regard a Monte Carlo simulation of system timekeeping has great value.

## Summary

The above discussion has reviewed a Monte Carlo simulation of Milstar timekeeping. Given the complexity of Milstar timekeeping issues, our experience with these simulations has shown that many results are non-intuitive, and that without a Monte Carlo simulation capability accurate predictions of system performance would be exceedingly difficult (if not impossible) to obtain. Though the simulation capability was developed with Milstar in mind, the capability is fairly general, and could easily be applied to timekeeping issues associated with other satellite systems, for example GPS.

## Acknowledgment

Over the course of the past six years our efforts have been supported by various organizations within The Aerospace Corporation's Milsatcom Program Offices. The authors would especially like to acknowledge: R. Covey, J. Cox, A. Dubin, A. Grossman, R. Meis, and S. Sokolsky. The encouragement and support of these individuals has been greatly appreciated.

## References

- [1] J. Fawcette, Milstar: "Hotline in the Sky", High Technology, Nov., 62-67 (1983); J. Schultz, "Milstar to Close Dangerous C3I Gap", Defense Electronics, March, 46-59 (1983).
- [2] Greg Hively and George Keirns, "The Predicted Performance of the Control Algorithms Used to Synchronize the MILSTAR Time and Frequency Standards (U)", 15 July 1989 (Presented at the 1989 MILCOM Conference.)
- [3] J. Vanier, R. Kunski, P. Paulin, M. Tetu, and N. Cyr, "On the Light Shift in Optical Pumping of Rubidium 87: The Techniques of "Separated" and "Integrated" Hyperfine Filtering", Can. J. Phys. 60, 1396 (1982).
- [4] C. Audoin and J. Vanier, "Atomic Frequency Standards and Clocks", J. Phys. E 9, 697 (1976).
- [5] See also: P. Kartaschoff, "Computer Simulation of the Conventional Clock Model", IEEE Trans. Instrum. Meas. IM-28, 193 (1979).

- [6] M. J. Levin, "Generation of Sampled Gaussian Time Series Having a Specified Correlation Function", IRE Trans. Inform. Theory IT-6, 545 (1960); J. A. Barnes and S. Jarvis, Jr., "Efficient Numerical and Analog Modeling of Flicker Noise Processes", NBS Technical Note 604 (US Government Printing Office, Washington DC, 1971); J. S. Meditch, "Clock Error Models for Simulation and Estimation", Aerospace Technical Report TOR-0076(6474-01)-2, (The Aerospace Corporation, El Segundo, CA, 1975); J. S. Meditch and W. A. Feess, "Performance Limits in Clock Error Prediction", Aerospace Technical Report TOR-0077(2475-10)-1, (The Aerospace Corporation, El Segundo, CA, 1977); S. M. Kay, "Efficient Generation of Colored Noise", Proc. IEEE 69, 480 (1981).
- [7] For an alternate technique of simulating clock noise, see: N. J. Kasdin and T. Walter, "Discrete Simulation of Power Law Noise", in Proc. 1992 IEEE Frequency Control Symposium (IEEE, Piscataway, NJ, 1992) pp. 274-283.
- [8] J. C. Camparo and P. Lambropoulos, "Monte Carlo Simulation of Field Fluctuations in Strongly Driven Resonant Transitions", Phys. Rev. A 47, 480 (1993).
- [9] J. H. Ahrens and U. Dieter, "Computer Methods for Sampling from the Exponential and Normal Distributions", Commun. ACM 15, 873 (1972).
- [10] C. A. Greenhall, "Initializing a Flicker-Noise Generator", IEEE Trans. Instrum. and Meas. IM-35, 222 (1986); R. F. Fox, "Numerical Simulations of Stochastic Differential Equations", J. Stat. Phys. 54, 1353 (1989).
- [11] J. C. Camparo, "A Partial Analysis of Drift in the Rubidium Gas Cell Atomic Frequency Standard", in Proceedings of the 18th Annual Precise Time and Time Interval (PTTI) Applications and Planning Meeting, Washington D. C. , 1986, pp. 565-588.
- [12] Personnel at Lockheed (the Milstar prime contractor) investigated the possibility of employing a Kalman filter as an estimation algorithm.

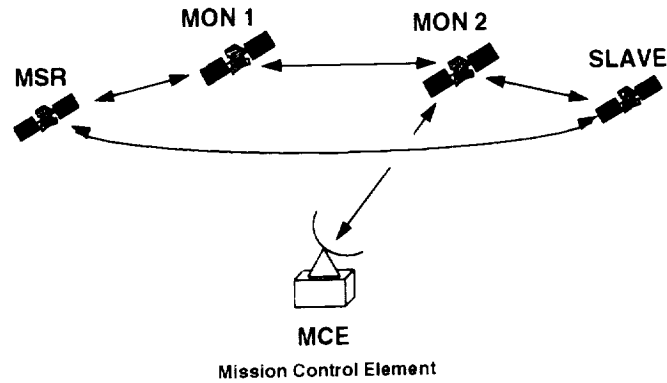


**Figure 1:** Operational diagram of the baseline Milstar timekeeping architecture. As discussed in the text, the constellation will consist of four satellites labeled: MSR (master), MON (monitor) or slave. The Mission Control Element (MCE) will periodically correct the time and oscillator frequency of the MSR and MONs.

### Process Realizations

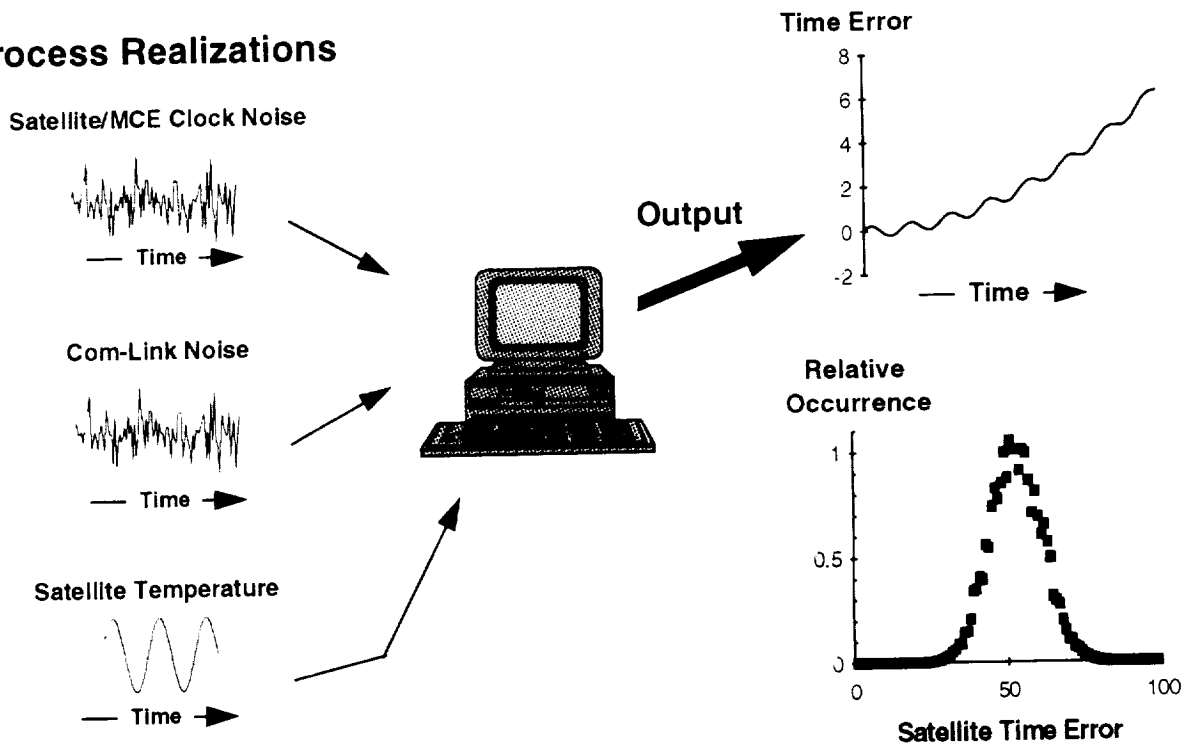
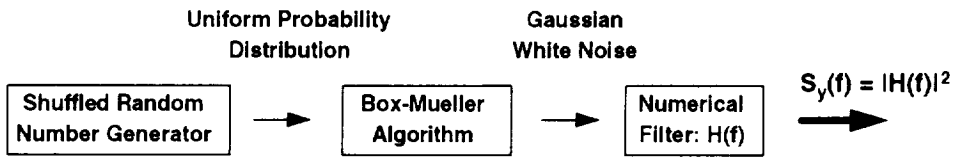


**Figure 2:** In the Monte Carlo simulation of Milstar timekeeping, realizations of *random* timekeeping processes as well as *deterministic* processes (e.g., satellite temperature variations) are generated. These fluctuations are combined to generate a single realization of a satellite clock's time-error history. By examining thousands of such simulations, the statistics associated with any clock's timekeeping performance may be built up for any set of parameters or operating scenario.

- Noise Generation for  $S_y(f) \sim 1/f^{2n}$ ,  $n=0,1,2,\dots$



- Noise Generation for  $S_y(f) \sim 1/f^{2n+1}$

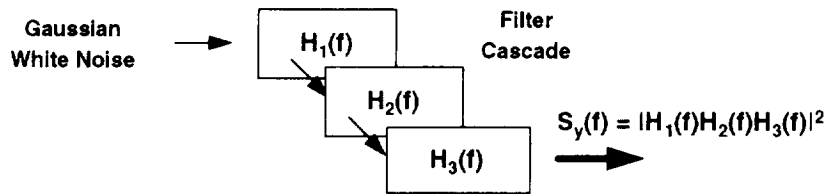


**Figure 3:** Method of simulating colored atomic frequency standard noise as discussed in the text.

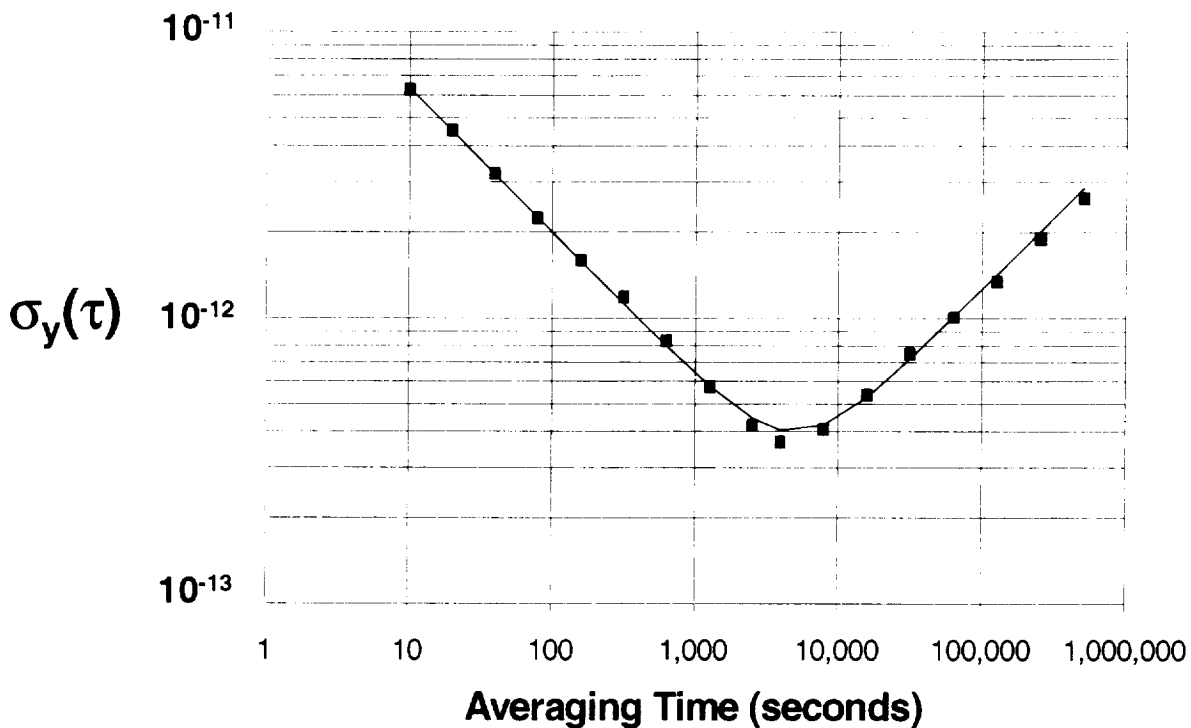


**Figure 4:** Allan standard deviation plot. The squares correspond to the Allan standard deviation obtained by analyzing the frequency fluctuations simulated by our Monte Carlo program for a Milstar satellite Rb atomic clock. The solid line represents the expected Allan standard deviation based on Milstar clock manufacturer data.

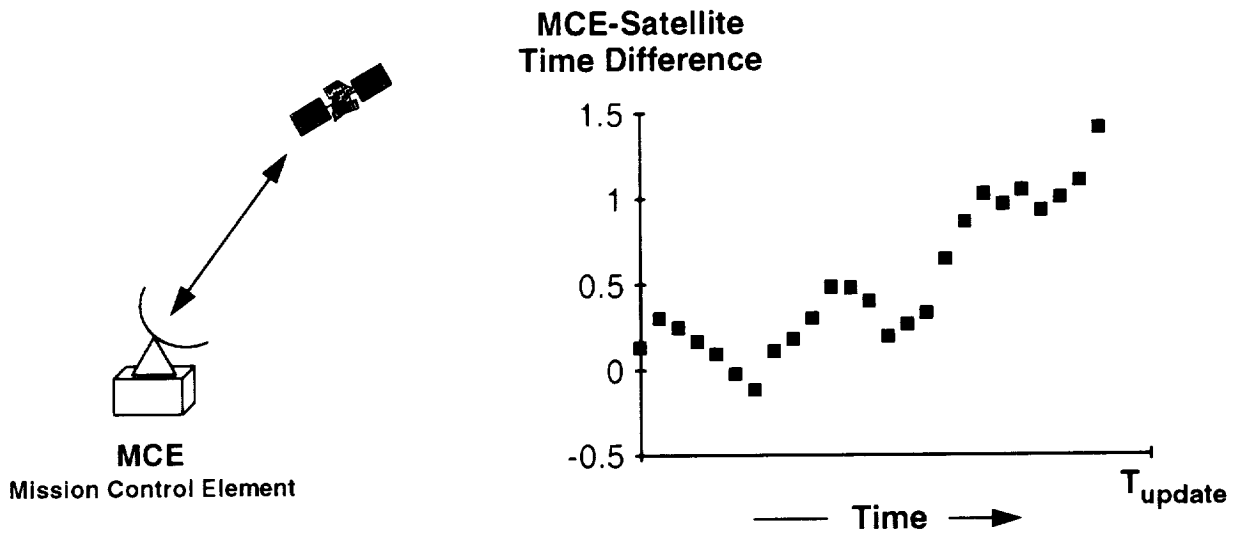


**Figure 5:** MCE ranging on an inview satellite and collecting time difference information. The MCE-to-Satellite time difference information is used to determine the time and frequency correction that the MCE should apply to the satellite.

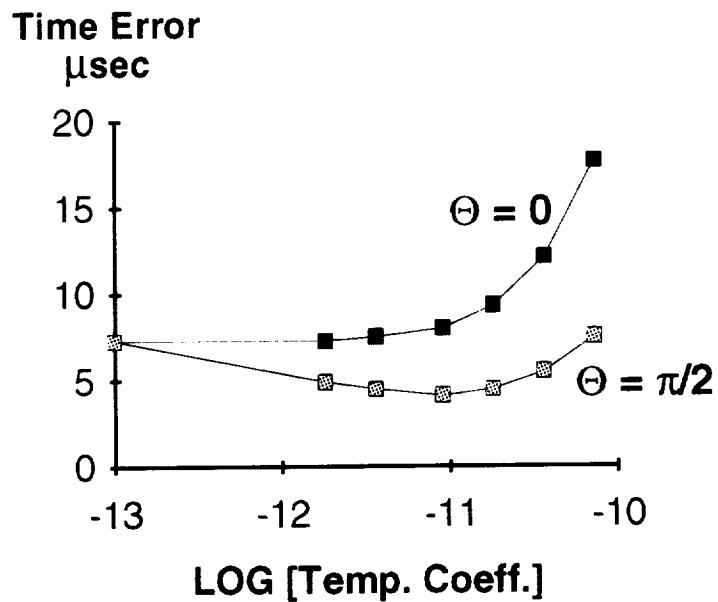


**Figure 6:** Satellite time error after 24 hours of free-running operation. Temperature coefficients for the satellite clock are per degree Celsius. The two curves labeled  $\theta = 0$  and  $\theta = \pi/2$  correspond to different phase relationships between the satellite's diurnal temperature cycle and the MCE's satellite correction cycle.

**Table I:** Parameters used in the Monte Carlo simulation of Milstar timekeeping for the question of which estimation algorithm is best for the Milstar system.

<u>Parameter</u>	<u>Value</u>
Satellite Rb Clock Allan Standard Deviation	$2 \times 10^{-11} / \sqrt{\tau} + 4 \times 10^{-15} \sqrt{\tau}$
Satellite Rb Clock Frequency Aging	$0.0 \pm 5.0 \times 10^{-13} / \text{day}$
Satellite Rb Clock Temperature Coefficient	$1.0 \times 10^{-12} / ^\circ\text{F}$
Diurnal Temperature Variation Phase Angle, $\theta$	0.0
Update Interval, $T_{\text{update}}$	3 days
MCE-to-Satellite Measurement Interval	8 hours

**Table II:** Results from Monte Carlo analysis of MCE estimation algorithms. The results show the standard deviation in microseconds of satellite time error at the end of a 3 day and 10 day free-running period.

<u>Estimation Algorithm</u>	<u>3-Day SD</u>	<u>10-Day SD</u>
2-Point	2.5	7.4
Linear	2.2	6.7
Quadratic	4.6	14.3

**Table III:** Parameters used in the Monte Carlo simulation of Milstar timekeeping for the question of how satellite temperature variations would influence satellite timekeeping.

<u>Parameter</u>	<u>Value</u>
Satellite Clock Allan Standard Deviation	$5 \times 10^{-13} / \sqrt{\tau} + 5 \times 10^{-14} \sqrt{\tau}$
Satellite Clock Frequency Aging	$2.0 \pm 0.5 \times 10^{-11} / \text{day}$
Satellite Clock Temperature Coefficient	0.0 to $4.0 \times 10^{-11} / ^\circ\text{F}$
Diurnal Temperature Variation Phase, $\theta$	0.0 and $\pi/2$ radians
Update Interval, $T_{\text{update}}$	24 hours
MCE-to-Satellite Measurement Interval	2 hours
MCE Estimation Algorithm	Linear



# AUTOMATED DELAY MEASUREMENT SYSTEM FOR AN EARTH STATION FOR TWO-WAY SATELLITE TIME AND FREQUENCY TRANSFER

Gerrit de Jong and Michel C. Polderman  
NMI Van Swinden Laboratorium  
P.O. Box 654  
2600 AR DELFT  
The Netherlands

## Abstract

*The measurement of the difference of the transmit and receive delays of the signals in a Two-Way Satellite Time and Frequency Transfer (TWSTFT) earth station is crucial for its nanosecond time transfer capability. Also, the monitoring of the change of this delay difference with time, temperature, humidity, or barometric pressure is important for improving the TWSTFT capabilities.*

*An automated system for this purpose has been developed from the initial design at NMI-VSL. It calibrates separately the transmit and receive delays in cables, amplifiers, upconverters, and downconverters, and antenna feeds. The obtained results can be applied as corrections to the TWSTFT measurement, when, before and after a measurement session, a calibration session is performed. Preliminary results obtained at NMI-VSL will be shown. Also, if available, the results of a manual version of the system that is planned to be circulated in September 1994 together with a USNO portable station on a calibration trip to European TWSTFT earth stations.*

## 1. Introduction

The Two-Way Satellite Time and Frequency Transfer (TWSTFT) method (Fig. 1) is used to compare two clocks or time scales which are often located at great distances from each other. The time scale events, normally the 1 pulse per second (1pps) signals, are simultaneously transmitted to the other clock by means of a transmission link through a satellite, normally a geostationary communication satellite. The delays in troposphere, ionosphere, satellite transponder and earth station equipment cancel in first order, the Sagnac correction can be calculated. The biggest source of asymmetry error is the sum of the transmit and receive equipment delay differences of the earth stations involved. For absolute time scale difference determination this sum has to be calibrated to the required uncertainty.

One method to accomplish this is to co-locate the two earth stations and do TWSTFT using a common clock.

If this is not feasible, a third earth station is subsequent co-located with both stations, and the relative delay difference of each of the two stations is calculated.

A third method is the separate measurement (calibration) at each earth station of the absolute transmit delay and the receive delay by using a special modified translator or Satellite Simulator in front of the antenna and some additional equipment. The required sum of the differences can then be calculated. This method was first described by De Jong (1989).

This paper addresses further progress. The method is developed by simplifying and enhancing the Simulator, a transportable equipment set has been constructed and finally an automated calibration method has been developed and realized.

## **2. Calibration principle with satellite simulator.**

### **2.1 Single frequency down converting satellite simulator**

The transmit frequency  $F_{up}$  of a earth station to a communication satellite (Fig. 2) for Ku-band is typical 14 GHz, the receive frequency  $F_{dn}$  is lower by a fixed amount, the translation frequency DF. This DF is for e.g. Intelsat in the USA 2295 MHz, in Europe 1495 MHz.

A double balanced mixer suitable for these frequency bands can be used for down conversion by feeding the translation frequency DF into the IF-port (Fig. 3a). When the transmit signal is fed into the RF-port then the LO-port contains the frequency difference ( $F_{up} - DF$ ), which is the receive frequency  $F_{dn}$ . The required power level for DF at the IF-port is 3 to 7 dBm. The conversion loss between the input signal at the RF-port and the output signal at the LO-port is normally less than 10 dB.

An antenna connected to the RF-port receives the transmitted signal in one polarisation and a similar antenna, but with orthogonal polarisation, at the LO-port sends the down converted signal back to the main antenna as receive signal. So this device simulates to what a satellite transponder does, but now the distance to the antenna is short and known.

When performing TWSTFT using this Satellite Simulator, in this case receiving the own signal back (ranging) (Fig. 4), the round-trip delay is measured from modem through cables, the up-converter, the power amplifier, the antenna feed, the distance to the satellite simulator (twice), the internal delay of the simulator, and the complete receive equipment path. The continued measurement of this sum delay already gives an impression of the instability of the equipment, but what we need is the difference between transmit and receive chain. The next chapter is a further step towards this.

### **2.2 Calibration with a dual frequency dual mixer simulator.**

The translation frequency DF can be obtained from a second mixer providing DF as the sum frequency of two other frequencies (Fig. 3b). For a reason we will see later, one of these frequencies is chosen to be equal to the 70 MHz IF frequency of the used modem. So the second frequency should be  $(DF-70)$  MHz. However, the output level of the second mixer is too low to excite the first mixer, and a wide band amplifier needs power, is active, and has a

delay to be measured. A solution is to place the RF and LO ports of the two mixers, as two down convertors, in series (Fig. 3c).

This works similar to the circuit (Fig. 4) of paragraph 2.1 (see Fig. 5): the transmitted signal is received back from the simulator, provided that 70 MHz and (DF-70) MHz signals of >3 dBm are fed into the IF-ports of the two mixers. The sum DLY1 of the transmit and receive delays  $TT(k)+TR(k)$  can be measured.

The 70 MHz Continuous Wave (CW) signal and the 70 MHz Transmit PN modulated signal from the modem are then interchanged (Fig. 6). The 70 MHz CW signal is up-converted to the transmit frequency  $F_{up}$ . The input to the mixers has become a unmodulated CW signal of e.g. 14 GHz. But the down conversion now uses a 70 MHz PN modulated signal, so the output signal from the satellite simulator is a PN modulated signal as before. Now the sum (DLY2) of the 70 MHz Reference Cable from modem TX output to the 70 MHz input of the simulator and the receive chain delay  $TR(k)$  is measured.

By using two other cables the delay of the used 70 MHz Reference Cable (DLY3) can be calibrated. Subtraction of DLY3 from DLY2 gives the receive delay  $TR(k)$ . Subtraction of  $TR(k)$  from DLY1 gives the transmit delay  $TT(k)$ . If this procedure is followed at both earth stations, and the values exchanged, the needed sum of transmit and receive delay differences can be calculated; the internal modem transmit delay should also be measured using a digital oscilloscope or the method described by De Jong (1989) and the resulting internal delay difference should be incorporated in  $TT(k)$  and  $TR(k)$ .

### 3. Improvement: dual frequency single mixer simulator

The simulator with two mixers in series works well. However, there are some disadvantages. Firstly the asymmetry: the mixer with the 70 MHz port is closer to one of the antennas, giving a small delay difference. Secondly, the 70 MHz signal is connected directly to the mixer IF-port which can give mismatch and consequently signal reflections leading to a "multi-path" effect. Thirdly the total conversion loss is doubled: 15 – 20 dB. Realizing that a mixer has its properties due to its non-linear characteristic, it was realized that a linear addition of two signals fed into a non-linear device should produce spectral components at the sum frequency as well as the difference frequency.

For addition of the 70 MHz and the (DF-70) MHz signals we have used a wide band (DC-12 GHz) resistive power combiner PD (Fig. 7). This device has 3 ports with equal properties and delay to the other ports. One disadvantage is the 6 dB insertion loss but the mismatch of the mixer IF-port to the cable is also reduced by this decoupling. Good results were obtained. The 70 MHz signal level for both the CW and the PN modulated signal should be at least at +8 dBm before the power combiner. An amplifier is added in the 70 MHz CW path for this purpose.

### 3.2 Construction of the Satellite Simulator

The resistive power combiner is placed in the satellite simulator box together with the mixer and the two antennas (Fig. 8). As inexpensive antennas we use two wave guide to coax adapters. They work fine, but might give some reflection back to the antenna dish.

The plastic material of the box is transparent to the frequencies concerned, so no hole was needed for the antennas. A nice symmetric component lay-out was adopted. Interconnections have been made (thanks to Mr. A. Trarbach, NMI Electronics Lab!) with semi-rigid coaxial cable and SMA connectors. The internal delay from antenna to antenna is 2 ns and matches the delay from the 70 MHz input to both antennas within 0.1 ns.

## 4. Portable Satellite Simulator Calibration equipment.

Two Satellite Simulators were built accordingly. One was placed in front of our fixed TWSTFT earth station. The other was used to assemble a portable earth station delay calibrator. This was used at several stations during the European TWSTFT Calibration Trip with the USNO movable earth station (FAST) in September and October 1994; it was also used to calibrate the FAST delays. The equipment was completed with two boxes (see Fig. 5), one containing a 5 MHz distribution amplifier and a 70 MHz source, both derived from the 5 or 10 MHz reference at the station and the other containing the 70 MHz amplifier and a source for (DF-70) MHz, which is 1425 MHz for Europe. This frequency was also phase locked to the 5 MHz reference at the stations. It is tunable in 5 MHz steps. When using the same translation frequency as in the satellite, the signal from the satellite is also present during calibration. To avoid possible interference, the antenna pointing should be changed to avoid pointing to the satellite or the source should be tuned to a slightly different translation frequency. Most stations have mechanical adjustment for azimuth and elevation, therefore the source was tuned to 1430 MHz. The receive frequency for the calibration was now 5 MHz lower than for the satellite. This is expected not to give a significant delay difference. Also a set of cables, up to 100 m length was included as well as the power supplies. The total mass was about 30 kg.

## 5. Automation of the Calibration

From TWSTFT experiments it is seen that at integration times greater than 200–300 s the Allan Deviation indicates an increase in instability. One of the reasons can be the change of the delays in the station equipment. Only if the delays in the transmit and in the receive equipment changes by the same amount at the same time, they cancel and do not influence the instability. The proposed method with the Satellite Simulator measures the TX and RX delays separately. So this method can be used for investigation of the delay changes but also to measure and then correct the data for possible changes. In the latter case the long term frequency transfer capability of TWSTFT would also improve. To do this, the calibration has to be automated.

NMI VSL has developed a automated measurement system for all equipment and cables. However, with exception of the internal 70 MHz TX and RX modem delays; this modem is in

a temperature and humidity controlled room and are expected to have the least change.

## 5.1 Design considerations

The automation should not disturb the correct termination of cables. When a cable carrying a signal temporarily is not used, it is to be terminated correctly. A solution for this is the use of so-called transfer switches: when a switch is activated the existing path is changed and a second path is substituted (Fig. 9). These switches are available in the form of coil-activated coaxial switches, relays. These relays are activated from a IEEE-488 bus through a relay adapter.

Our MITREX 2500 was already made programmable through such a device, and the same applies to the setting of the transmit frequency and the receive frequency. The calibration of the total delay of the 70 MHz reference path (the 70 MHz CW cable, the amplifier, and even the 70 MHz cable to the Satellite Simulator) is also included (Fig. 10).

## 5.2 Description of the measurements (Fig. 10).

### 5.2.1. Measurement of the sum of internal TX and RX modem delays.

Switch the modem into the TESTLOOP Mode. Now the TX output and the RX input of the modem are interconnected internally. The average Time Interval Counter (TIC) reading is stored as [1].

### 5.2.2 Measurement of the 70 MHz Reference path.

#### 5.2.2.1 Determination of sum of the delay of the 70 MHz TX and the 70 MHz RX cable.

Only the switches A and B are activated. Two ports of the power combiner PC are used to interconnect the far ends of the TX and RX cables, the third port is terminated in a termination T. The TIC reading is averaged and stored as [4].

subsubsubject5.2.2.2 Determination of sum of the delay of the 70 MHz CW + amplifier and the 70 MHz TX cable.

Only switches 1, 2, 3, C and A are activated. Two ports of the Power Combiner (PC) are used to interconnect the far ends of the CW and RX cables, the third port is terminated in a termination T. The TIC reading is stored as [5].

#### 5.2.2.3 Determination of sum of the delay of the 70 MHz CW + amplifier and the 70 MHz RX cable.

Only the switches 1, 3, C and B are activated. Two ports of the power combiner PC are used to interconnect the far ends of the CW and RX cables, the third port being terminated in a termination T. The TIC reading is stored as [6].

#### 5.2.2.4 Determination of sum of the delay of the 70 MHz CW + amplifier, the two cables to the Satellite Simulator and the 70 MHz RX cable.

Only the switches 1, D and B are activated. Two ports of the power combiner PC are used to interconnect the far end of the CW cable, the two Satellite Simulator cables and RX cables, the third port is terminated in a termination T. The two cables to the Satellite Simulator are

interconnected by a power combiner in the Satellite Simulator. The TIC reading is stored as [7].

#### **5.2.2.5 Calculation of the 70 MHz Reference path delay.**

The delay of the 70 MHz CW cable + amplifier is:  $0.5([5] - [1]) + ([6] - [1]) - ([4] - [1])$  [8]  
The delay of the sum of the two cables to the Satellite Simulator is  $[7] - [6]$ ; because of the fact that the two cables are co-located and of the same type the delay of one cable is calculated by the ratio R of the length of that cable compared to the sum of the lengths of both cables. In our case both cables have the same length, so  $R = 0.5$ , thus the delay [9] of one cable is:  $0.5([7] - [6])$ .

The total 70 MHz Reference path [10] is now:  $[8] + [9]$

#### **5.2.2. Measurement of the sum of all TX and RX delays.**

For this measurement all relays remain in the inactive position. However, the receive frequency is lowered by 5 MHz to receive the signal from the Simulator in stead of the signal from the satellite (otherwise the antenna should be pointed away from any satellite). The reading of the TIC is averaged and stored as [2].

#### **5.2.3. Measurement of the sum of 70 MHz reference cable and the RX delays.**

Now only switch 1 is activated, so the 70 MHz CW and the 70 MHz TX signals are interchanged. The average TIC reading is registered as [3].

#### **5.2.4 Calculation of the TX and RX delays.**

The RX delay is:  $([3] - [1]) - [10]$  [11] The TX delay is:  $([2] - [1]) - [11]$  [12]

### **5.3 Wiring Delays**

In the calculations in 4.2 the small and constant delays in the relays, power combiners and associated sort wirings were not mentioned, but these small delays of up to 1 ns were measured and are used as correction constants in the software. It appears that the length of a signal path through a high frequency device mostly is a good measure for its delay, the same as for coaxial cable: 5 ps for 1 millimeter.

## **6. Advantages of incorporation of Calibration sessions in regular TWSTFT measurements.**

The Calibration measurements as described in 4.2 can be performed in a calibration session. Such a session can precede and follow a TWSTFT session. From the delay change, a rate of change can be determined and the results from the TWSTFT sessions can then be corrected for that change.

Changes in cables and equipment are also detected and can be corrected for. Corrections could be done also during a long period; when both of a pair of TWSTFT stations do this,

then also the frequency transfer instability of the TWSTFT between them is improved because of a lower flicker floor. The remaining instrumentation instability source will then be restricted to the instability of the modems and the counters, apart from the reference clocks themselves.

## 7. Status and some results at NMI-VSL

Part of the system was installed and used since July 1994; the Relay system is now also installed (nov. '94), except the connections of the relays to the relay interface. Changes to our software will then be performed to incorporate the fully automated calibration in a Calibration session.

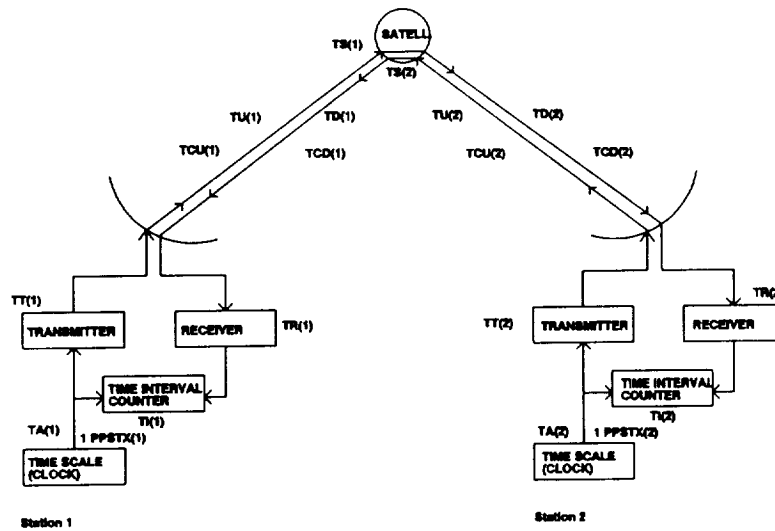
Fig. 11 shows the behaviour over about 4 months of our modem when TESTLOOP measurements are done. Fig. 12 shows results over the same period of Satellite Simulator loop (TX + RX delay) measurements. Results for the automated calibration system will become available next year. Also results from calibrations with the portable delay calibrator compared to the FAST calibration will be reported later.

## 8. Conclusion

The feasibility of this fully automated delay calibration system for a TWSTFT earth station using a special modified Satellite Simulator has been shown. It clearly detects and measures delay changes in the TX and RX path separately. It is a suitable and cost-effective tool to improve the instability of frequency and time transfer by means of the TWSTFT method.

## 9. References

- Jong, G de 1989, "Accurate Delay Calibration for Two-Way Time Transfer Earth Stations", Proc. 21th PTTI Meeting, Redondo Beach, pp. 107-115.
- Jong, G de 1993, "Two-Way Satellite Time Transfer: Overview and recent developments", Proc. 25th PTTI Meeting, Marina Del Rey CA, NASA Conf. Publication 3267, pp. 101-117
- Veenstra, L B 1990, "International Two-Way Satellite Time Transfer using INTEL-SAT space segment and small earth stations", Proc. 22nd PTTI Meeting, pp. 393-400.
- Kirchner, D 1991, "Two-Way Time Transfer Via Communication Satellites", Proceedings of the IEEE, Vol.79, No. 7, pp. 983-990.
- Davis, J A and Pearce, P R 1993, "Characterization of the signal delays in a ground station designed for satellite two way time transfer", Proc. EFTF 93, Neuchatel, pp. 113-118.



The timescale difference is given by:

$$\begin{aligned}
 TA(1) - TA(2) = & +0.5\{TI(1)\} && \text{(TIC reading at 1)} \\
 & -0.5\{TI(2)\} && \text{(TIC reading at 2)} \\
 & +0.5\{TS(1) - TS(2)\} && \text{(Satellite delay difference)} \\
 & +0.5\{TU(1) - TD(1)\} && \text{(Up/down difference at 1)} \\
 & -0.5\{TU(2) - TD(2)\} && \text{(Up/down difference at 2)} \\
 & +0.5\{TT(1) - TR(1)\} && \text{(TX/RX difference at 1)} \\
 & -0.5\{TT(2) - TR(2)\} && \text{(TX/RX difference at 2)} \\
 & -0.5\{TCD(1) - TCU(1)\} && \text{(Sagnac + sat. movement)} \\
 & +0.5\{TCD(2) - TCU(2)\} && \text{(Sagnac + sat. movement)}
 \end{aligned}$$

Figure 1. Two-Way Satellite Time and Frequency Transfer Method

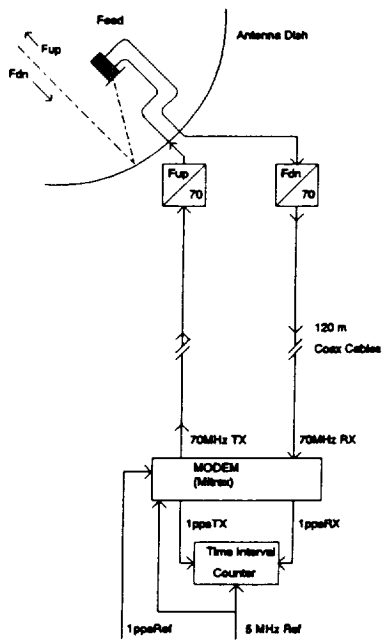


Figure 2. Typical TWSTFT Earth Station Configuration

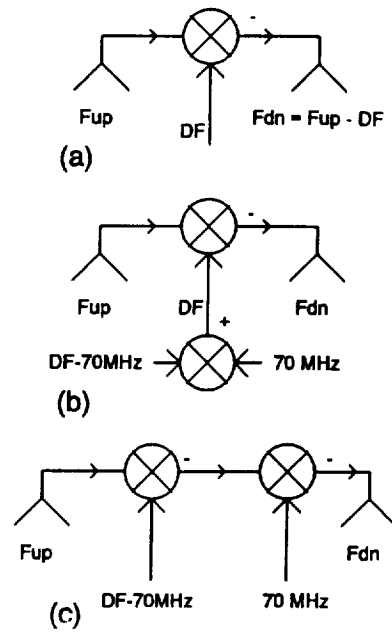


Figure 3. Different Translator Mixer Schemes

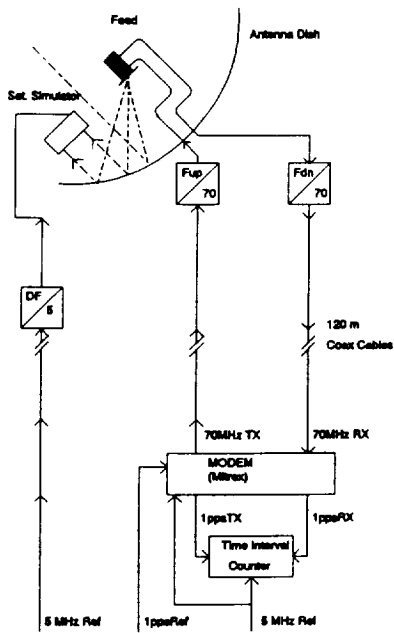


Figure 4. Ranging Using a Satellite Simulator

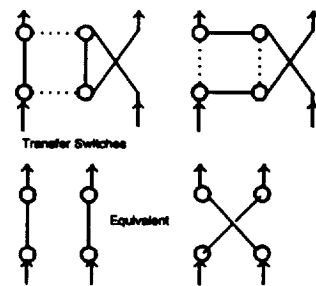


Figure 9. Transfer Switches

OFFICE OF THE  
DIRECTOR OF THE  
OFFICE OF THE  
DIRECTOR OF THE  
OFFICE OF THE  
DIRECTOR OF THE

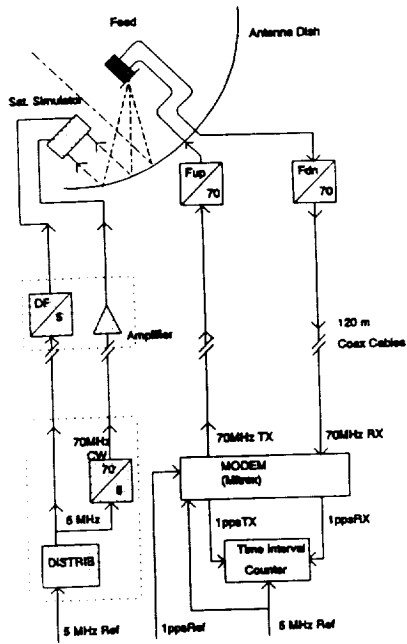


Figure 5. (Portable) Satellite Simulator for Measuring TR(k) + TT(k)

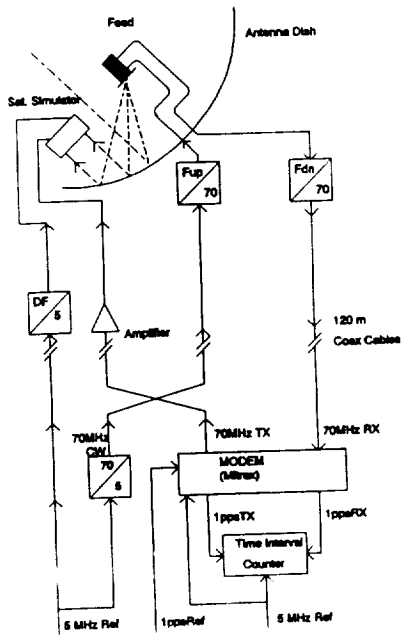


Figure 6. Satellite Simulator for Measuring TR(k) + Reference Path

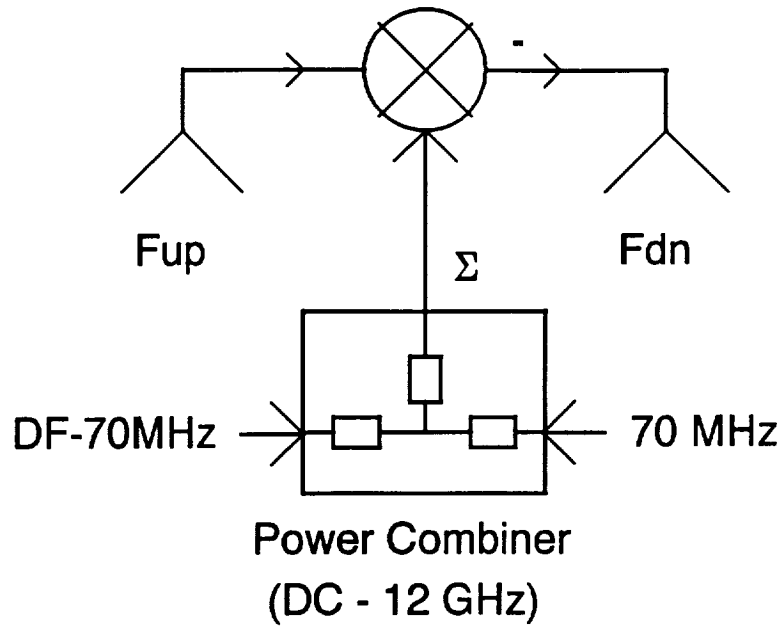


Figure 7. Use of Power Combiner and One Mixer

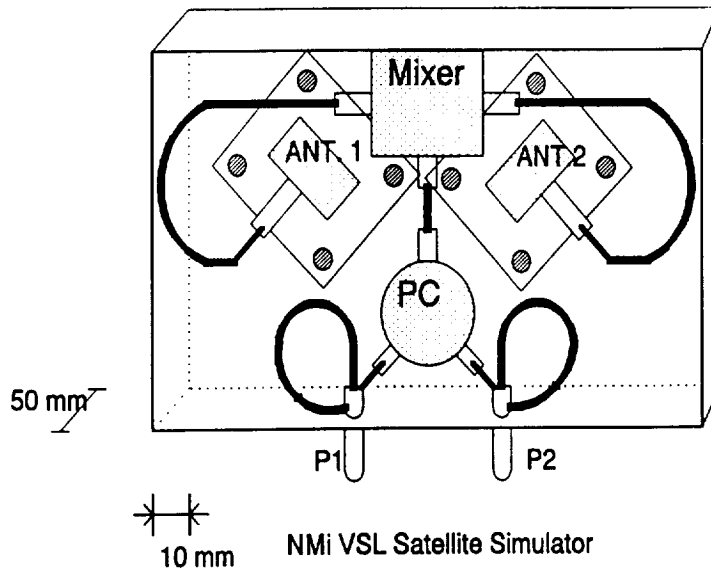


Figure 8. Layout of the NMi Satellite Simulator

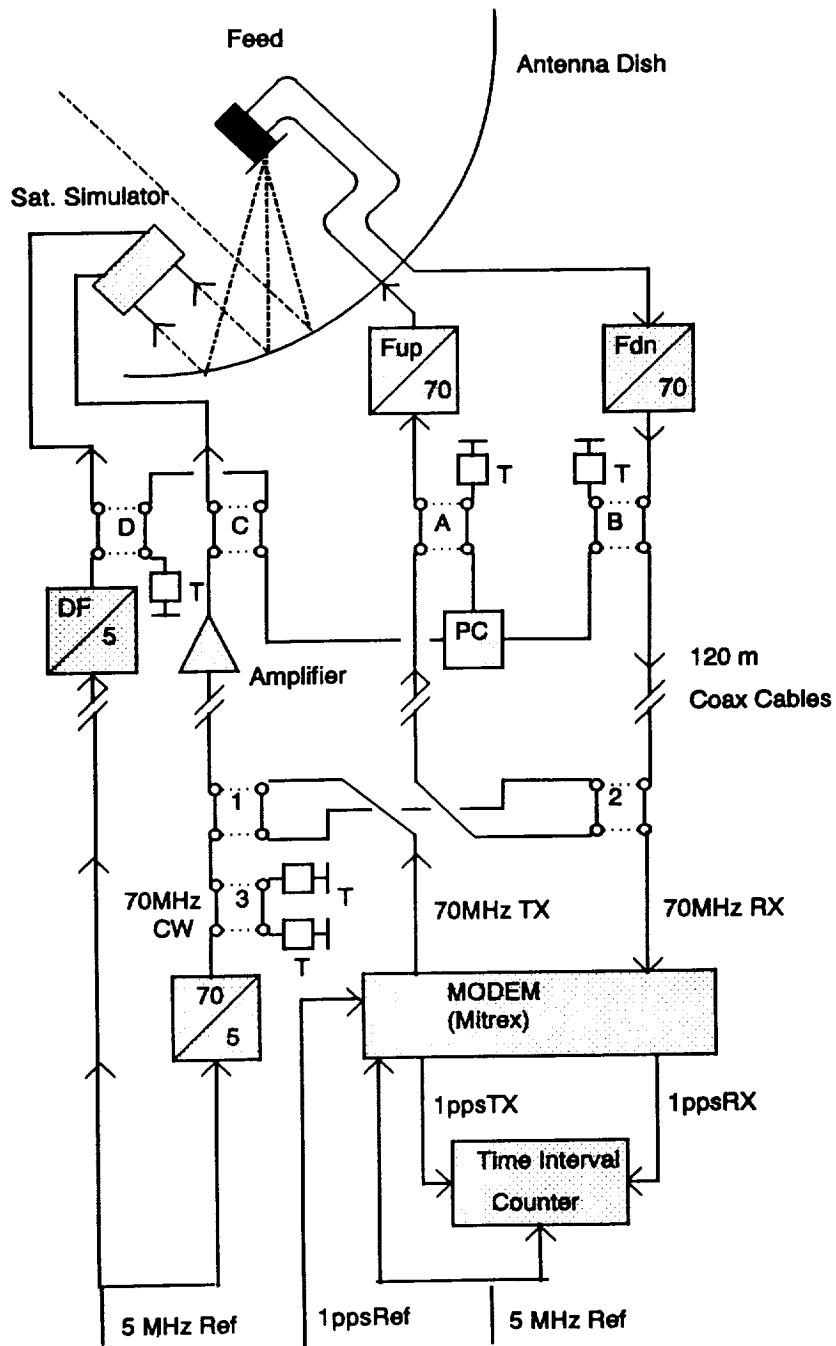


Figure 10. Automatic Delay Calibration System for TWSTFT Stations

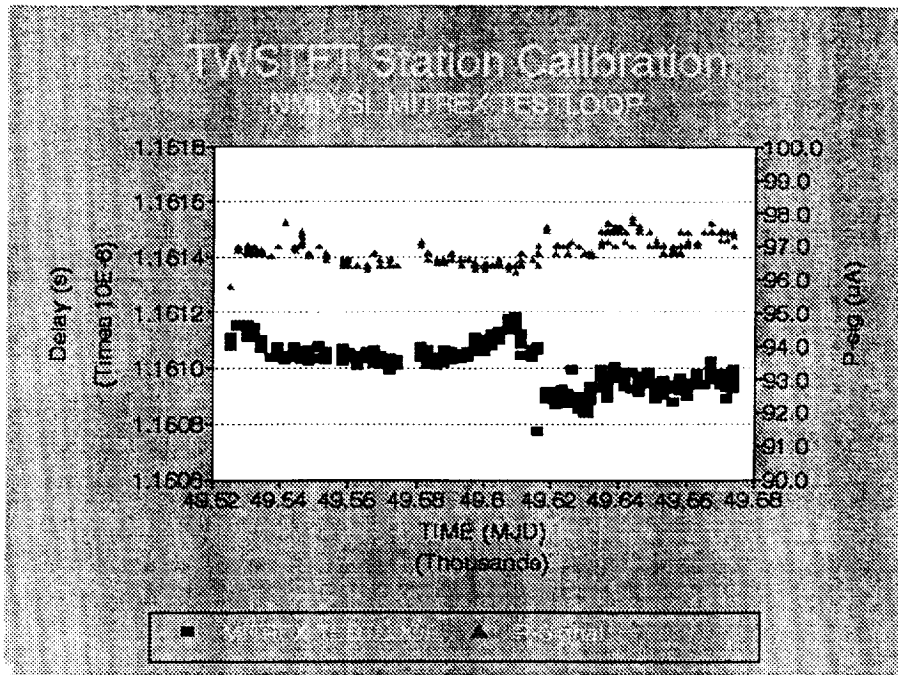


Figure 11. VSL MITREX Modem TESTLOOP Delay July - November 1994

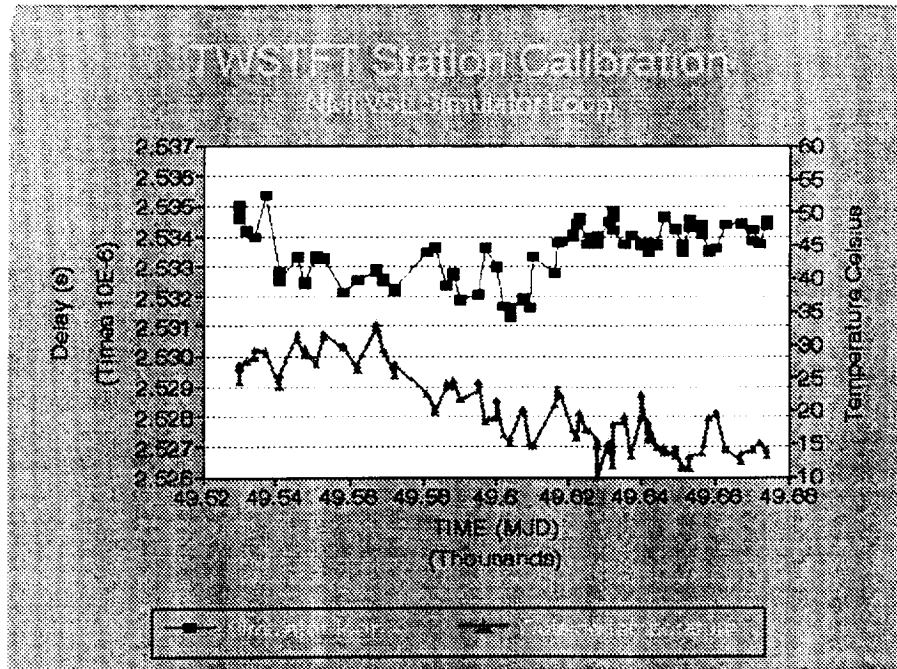


Figure 12. VSL RX+TX Delay July - November 1994



279-10  
522-15

# STUDY OF TROPOSPHERIC CORRECTION FOR INTERCONTINENTAL GPS COMMON-VIEW TIME TRANSFER

W. Lewandowski  
Bureau International des Poids et Mesures  
Pavillon de Breteuil  
92312 Sèvres Cedex, France

W.J. Klepczynski, M. Miranian  
United States Naval Observatory  
Washington, DC 20392-5420, USA

P. Grüdler, F. Baumont  
Observatoire de la Côte d'Azur  
Av. Copernic, 06130 Grasse, France

M. Imae  
Communications Research Laboratory  
Nukui Kita-machi, Koganei-shi, 184 Tokyo, Japan

## Abstract

*Current practice is to incorporate general empirical models of the troposphere, which depend only on the station height and the elevation of the satellite, in GPS time receivers used for common-view time transfer. Comparisons of these models with a semi-empirical model based on weather measurements show differences of several nanoseconds. This paper reports on a study of tropospheric correction during GPS common-view time transfer over a short baseline of about 700 km, and three long baselines of 6400 km, 9000 km and 9600 km. It is shown that the use of a general empirical model of the troposphere within a region where the climate is similar does not affect time transfer by more than a few hundreds of picoseconds. For the long distance links, differences between the use of general empirical model and the use of a semi-empirical model reach several nanoseconds.*

## INTRODUCTION

Among the improvements open to GPS common-view time transfer is increased accuracy in the estimation of the tropospheric delay. It has been assumed until recently that, for satellite elevations above 30°, a general empirical model, depending only on the station height and

satellite elevation, is sufficient. However, when carrying out common-view time transfer over long distances (9000 km), elevations as low as 20 are unavoidable. Also, different types of receivers use different tropospheric models which can differ by a few nanoseconds for angles of low elevation<sup>[1, 2]</sup>. Progress can be made by implementing recently established standards for receiver software which include a common model for estimating signal delays arising from tropospheric refraction<sup>[3]</sup>.

Recent comparisons of the models currently used by GPS time receivers with a semi-empirical model based on weather measurements show differences of several nanoseconds<sup>[4, 5, 6]</sup>. This discrepancy increases for observations performed in hot and humid regions of the world.

This paper reports on comparisons of GPS common-view time transfers performed using the tropospheric models incorporated in the receivers with transfers performed using a semi-empirical model. These comparisons have been carried out for one short baseline of about 700 km, and three long baselines of about 6400 km, 9000 km and 9600 km. It is shown that the use of the general empirical model of the troposphere within a region of similar climate does not affect time transfer by more than a few hundreds of picoseconds, while for the intercontinental GPS time links, differences between the general empirical model and a semi-empirical model reach several nanoseconds.

## TROPOSPHERIC DELAY AND ITS MODELS

The troposphere is the lower layer of the atmosphere extending from ground level to the base of the ionosphere. For radio frequencies, delay due to the troposphere ranges typically from about 10 ns for the zenith to about 100 ns for an elevation of 5° : it depends on the thickness of the troposphere and the content of water vapour along the line of sight. Tropospheric delay is commonly expressed as the sum of two components 'dry' and 'wet'. The 'wet' component is due to water vapour and can reach 15 % of the total correction.

At radio frequencies, unlike optical frequencies, the troposphere is a non-dispersive medium. Thus, the tropospheric delay cannot be estimated from two-frequency measurements as can the ionospheric delay. Instead, estimation of the delay relies on the use of one of a number of models<sup>[7]</sup>. The 'dry' component can be accurately estimated from models based on surface measurements of atmospheric pressure alone. The 'wet' component is more difficult to model, since measurements of meteorological conditions at the antenna site are generally not representative of conditions along the line of sight.

That several tropospheric models have been developed is mainly because of this difficulty in modelling the 'wet' component. Usually the delays are evaluated in the zenith direction. The zenith corrections are then 'mapped' down to lower angles of elevation using mapping functions. Models are either semi-empirical, based on surface measurements of the local temperature, atmospheric pressure and relative humidity, or empirical, based on a general reference atmosphere requiring only the station height and the angle of elevation to the satellite.

Of the semi-empirical models, some of the best known have been developed by Hopfield and Saastamoinen, and are widely used within the geodetic community. In this paper we use as reference a model developed by the Jet Propulsion Laboratory (JPL) for its deep space

missions<sup>8, 9</sup>. Evaluated against balloon measurements, it was found that this model is able to predict the zenith tropospheric delays with an accuracy at the subnanosecond level.

The tropospheric corrections currently used by the timing community are computed according to general empirical models which neglect the contribution due to the 'wet' component. Consequently, the errors resulting from these simple models may exceed 3 ns in a one-way range delay at 20° angle of elevation. The three models usually implemented are NBS<sup>[10]</sup>, STI<sup>[11]</sup> and STANAG<sup>[12]</sup>. The STANAG model is recommended in recently established standards for GPS time receiver software. In previous papers these models have been compared with one another and with semi-empirical models. Differences can reach several nanoseconds for low elevation angles.

## THE EXPERIMENT

To illustrate the possible impact on GPS common-view time transfer of the approximate models of tropospheric delay used in GPS time receivers, four time laboratories, listed below, were chosen. Several criteria contributed to this choice. The basic criterion was the availability of meteorological data recorded at the site. Next, two time laboratories had to be located in the same climatic zone (BIPM and OCA) and the other laboratories had to be situated as far away as possible and in climatic zones as different as possible. This last criterion was the most difficult to fulfil as can be seen from the table below, which lists the geographical latitudes of the sites.

Participating time laboratories in this experiment were:

BIPM, Bureau International des Poids et Mesures, Sévres, France, Lat. = 49 N, H = 127 m,

OCA, Observatoire de la Côte d'Azur, Grasse, France, Lat. = 43 N, H = 1322 m,

USNO, United States Naval Observatory, Washington D.C., U.S.A., Lat. = 39 N, H = 51 m,

CRL, Communications Research Laboratory, Tokyo, Japan, Lat. = 36 N, H = 130 m.

The GPS time receivers operating at the BIPM, the OCA and the CRL used the NBS type tropospheric model, and the receiver used at the USNO used the STI type tropospheric model.

Four GPS common-view time links, listed below, were considered. The short baseline link, BIPM-OCA, was analysed to see if there is any impact of approximated tropospheric delay on GPS common-view time transfer in the same climatic zone. The three long baseline links were considered for their climatic differences and low angles tracks.

BIPM - OCA, of 700 km, with 32 daily CV possible, according to Inter. GPS CV Sched. No 20,  
OCA - USNO, of 6400 km, with 18 daily CV possible, according to Inter. GPS CV Sched. No 20,  
OCA - CRL, of 9000 km, with 14 daily CV possible, according to Inter. GPS CV Sched. No 21,  
USNO - CRL, of 9600 km, with 8 daily CV possible, according to Inter. GPS CV Sched. No 21.

The BIPM–OCA link was analysed in terms of the available meteorological data for 22 and 23 April 1993, and three other links were analysed for 26 August 1993.

Elevation angles by track and location are given in Figures 1, 5, 9, and 13. For each link, the track was computed at both sites using both the simple empirical model in the receiver and the JPL semi-empirical model based on surface weather measurements. The results are given in Figures 2, 3, 6, 7, 10, 11, 14, and 15. Differences between the two models ranging from 0.4 ns to 1.1 ns for the short baseline link, and from 1 ns to 6 ns for long baseline links, can be observed. Next, the common views between the two sites were computed using the receiver and JPL models. The peak to peak differences between the two computations for individual common views do not exceed a few hundreds of picoseconds for the short baseline link (Figure 4) and reach 5 ns for the long distance links (Figures 8, 12, and 16). For two longest long links, OCA–CRL and OCA–USNO, a clear bias of a few nanoseconds may be observed. This is so because low elevation angles and limited number of common views were available. For the shortest of the long distance links, OCA–USNO, large discrepancies in the results may be seen (Figure 8). This is due to the large differences in the elevation angles at both sites (Figure 5).

## CONCLUSIONS

1. The use of a standardized tropospheric model in GPS time receivers is essential for accurate time comparisons.
2. For GPS time links within a region of similar climate, the use of a simplified standard tropospheric model is sufficient for 1 nanosecond accuracy.
3. For intercontinental GPS time links: common views should be performed at the same elevations at each side, the use of a more sophisticated model based on surface measurements should be considered and studied more closely.

## Acknowledgements

The experimental part of this work was done at the BIPM thanks to the loan of a commercial caesium clock from the USNO (Washington, DC, USA). The staff of the Time Section of the BIPM is grateful to the USNO for its generosity.

## References

- [1] D. Kirchner, H. Bessler, and S. Fassl, "Experience with two collocated C/A code GPS receivers of different type," in Proc. 3rd European Time and Freq. Forum, pp. 94–103, March 1989.
- [2] W. Lewandowski and C. Thomas, "GPS Time Transfer," Proc. IEEE, vol. 79, pp. 991–1000, July 1991.

- [3] The Group on GPS Time Transfer Standards, "*Technical Directives for Standardization of GPS Time Receiver Software*," Rapport BIPM-93/6, 1993.
- [4] W. Lewandowski, G. Petit and C. Thomas, "*GPS Standardization for the needs of Time Transfer*," in Proc. 6th European Time and Freq. Forum, pp. 243-248, 1992.
- [5] D. Kirchner, C. Lentz and H. Ressler, "*Tropospheric Corrections to GPS Measurements Using Locally Measured Meteorological Parameters Compared with General Tropospheric Corrections*," in Proc. 25th PTTI, pp. 231-248, 1993.
- [6] W. Lewandowski, P. Grudler and F. Baumont, "*Study of Tropospheric Correction for GPS Common-View Time Transfer between the BIPM and the OCA*", in Proc. 8th European Time and Freq. Forum, Vol II, 1994.
- [7] G.M.R. Winkler, "*Path delay, its variations, and some implications for the field use of precise frequency standards*" Proc. IEEE, vol. 60, pp. 522-529, 1972.
- [8] G.A. Madrid, C.C. Chao, et al., "*Tracking System Analytic Calibration Activities for Mariner Mars 1971 Mission* ," JPL Technical Report 32-1587, March 1, 1974.
- [9] H. F. Fliegel (The Aerospace Corporation, El Segundo, CA, USA), personal communication,
- [10] M. A. Weiss (NIST, Boulder, Co, USA), personal communication, 1989.
- [11] D. Kirchner (TUG, Graz, Austria), personal communication, 1991.
- [12] NATO Standardization Agreement (STANAG) 4294, Arinc Research Corporation, 2551 Riva Road, Annapolis, MD, 21401, USA, Publication 3659-01-01-4296, 1 August 1990.

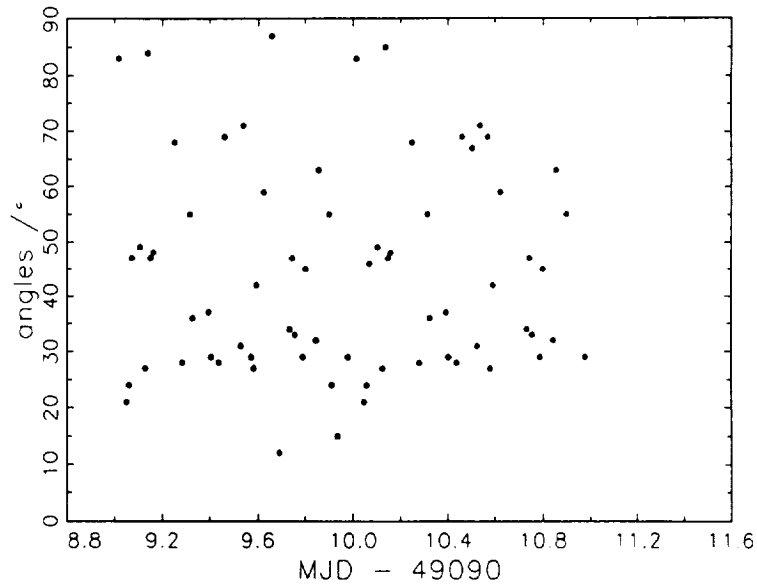


**FIGURE 1.** Elevation angles of each track on 22-23 April 1993 at the BIPM and OCA. They are the same within 1°.

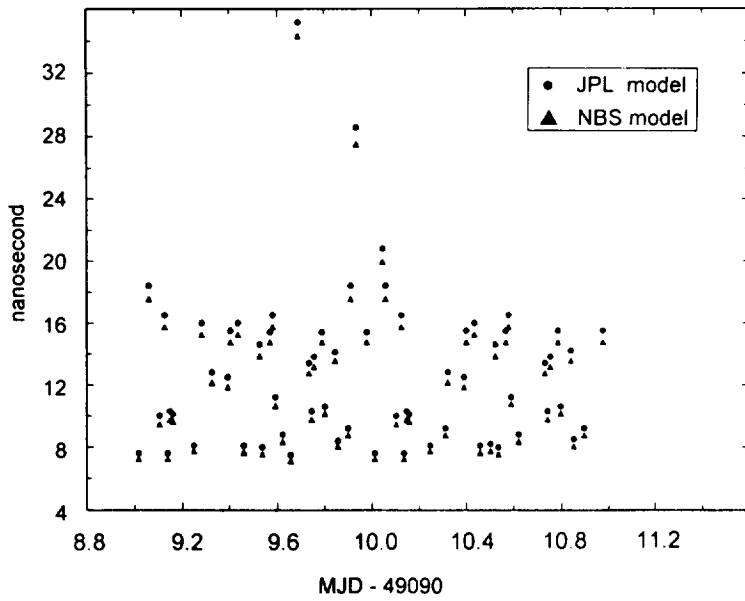


**FIGURE 2.** Tropospheric delays according to the JPL and the NBS models at the BIPM on 22-23 April 1993 for each track in the direction of the OCA.

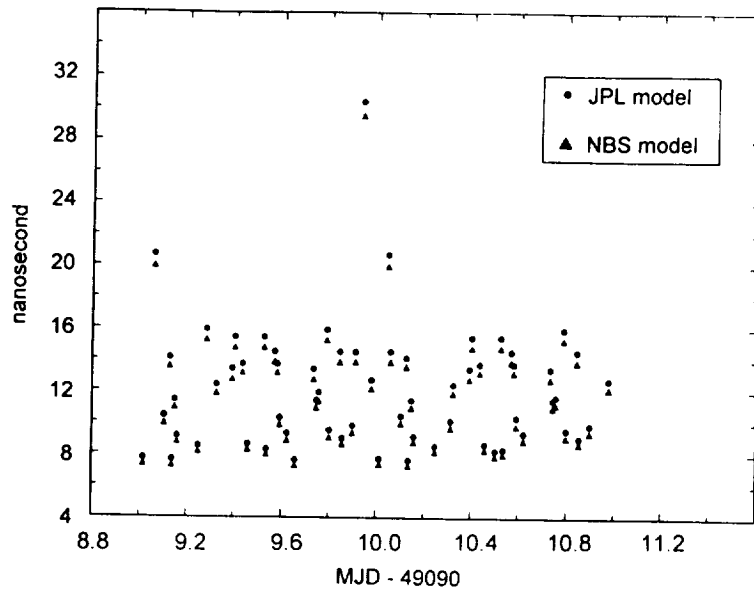


**FIGURE 3.** Tropospheric delays according to the JPL and the NBS models at the OCA on 22-23 April 1993 for each track in the direction of the BIPM.

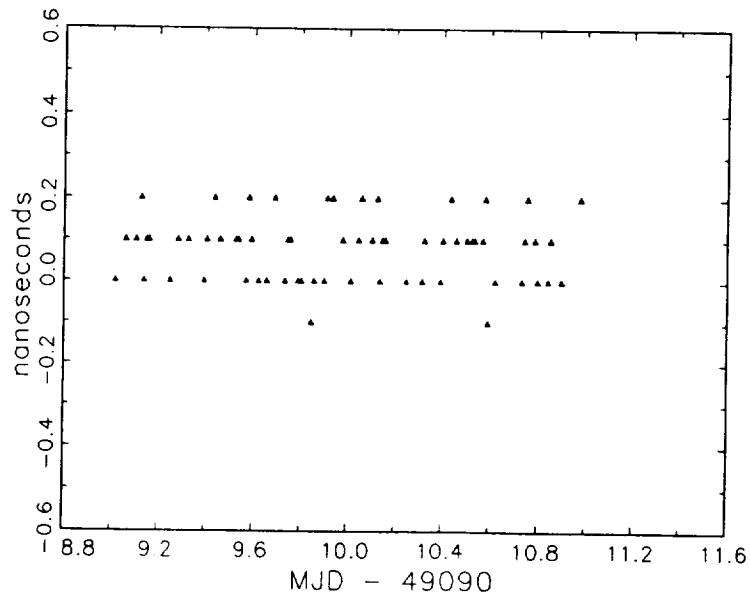


**FIGURE 4.** [BIPM Cs clock - OCA Cs clock] as obtained by GPS common views with the NBS tropospheric model minus [BIPM Cs clock - OCA Cs clock] as obtained by GPS common views with the JPL tropospheric model for each track on 22-23 April 1993.

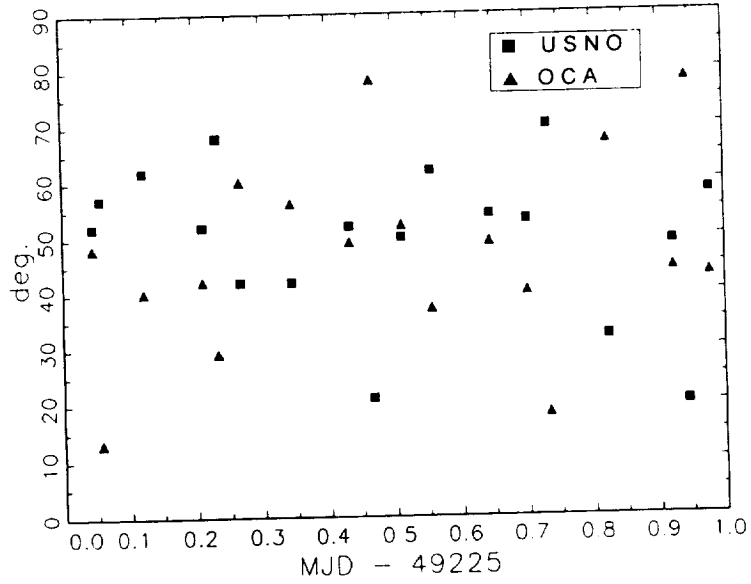


**FIGURE 5.** Elevation angles of each track on 26 August 1993 at the OCA in the direction of the USNO and at the USNO in the direction of the OCA.

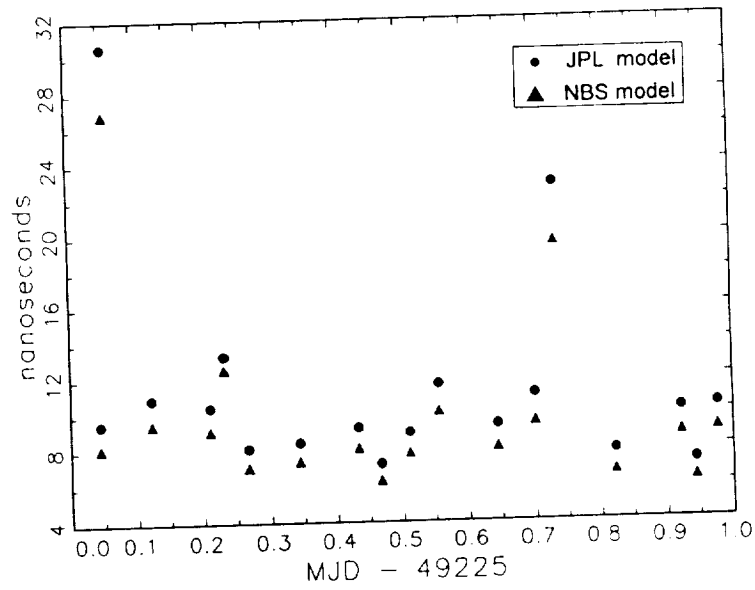


**FIGURE 6.** Tropospheric delays according to the JPL and the NBS models at the OCA on 26 August 1993 for each track in the direction of the USNO.

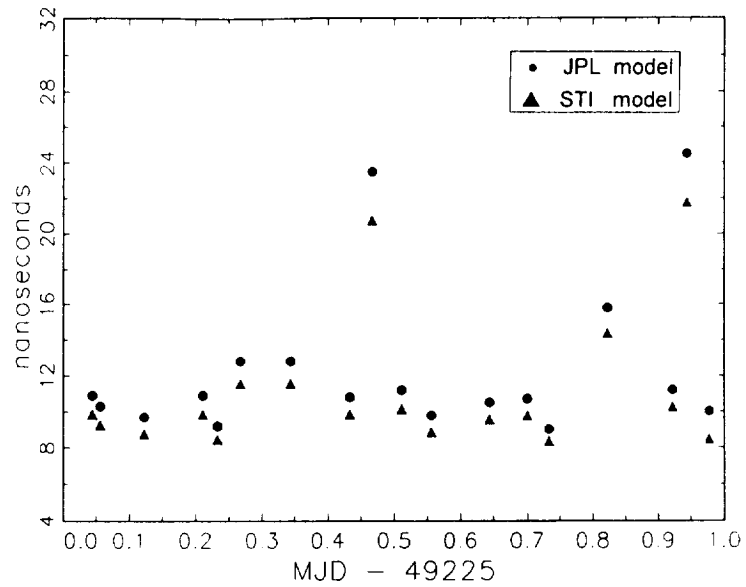


**FIGURE 7.** Tropospheric delays according to the JPL and the STI models at the USNO on 26 August 1993 for each track in the direction of the OCA.

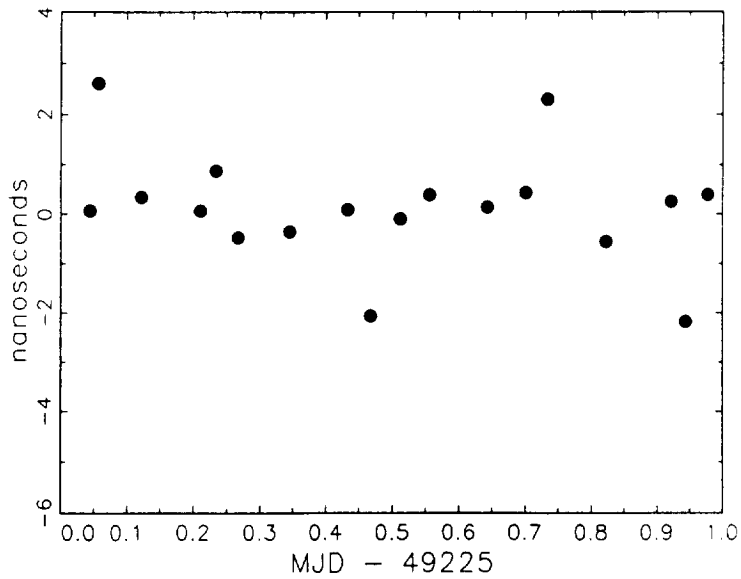


**FIGURE 8.** [OCA Cs clock - UTC(USNO Master Clock)] as obtained by GPS common views with the NBS and STI tropospheric models minus [OCA Cs clock - UTC(USNO Master Clock)] as obtained by GPS common views with the JPL tropospheric model for each track on 26 August 1993.

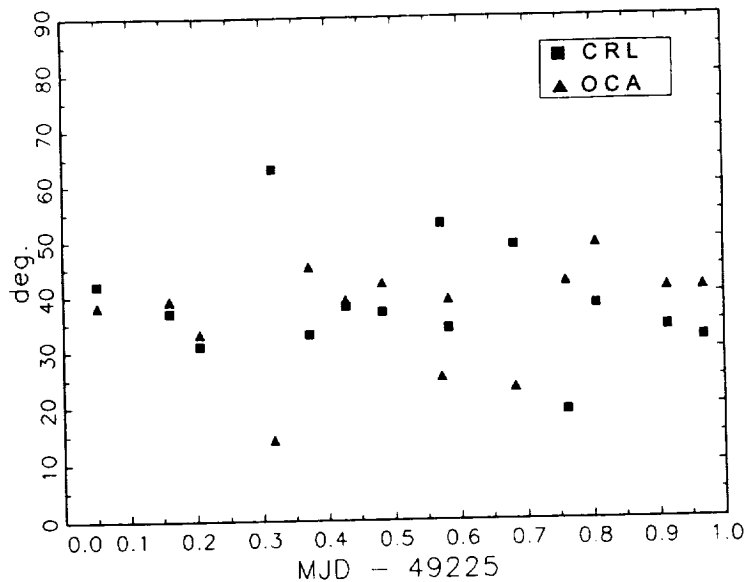


**FIGURE 9.** Elevation angles of each track on 26 August 1993 at the OCA in the direction of the CRL and at the CRL in the direction of the OCA.

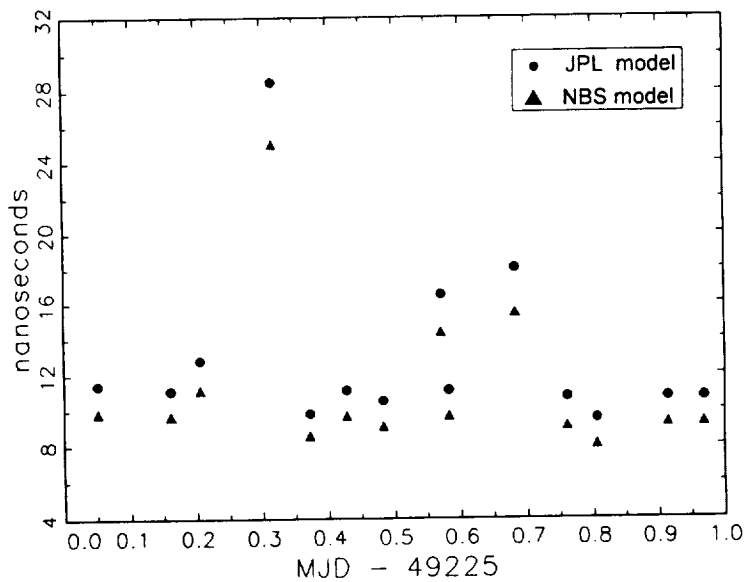


**FIGURE 10.** Tropospheric delays according to the JPL and the NBS models at the OCA on 26 August 1993 for each track in the direction of the CRL.

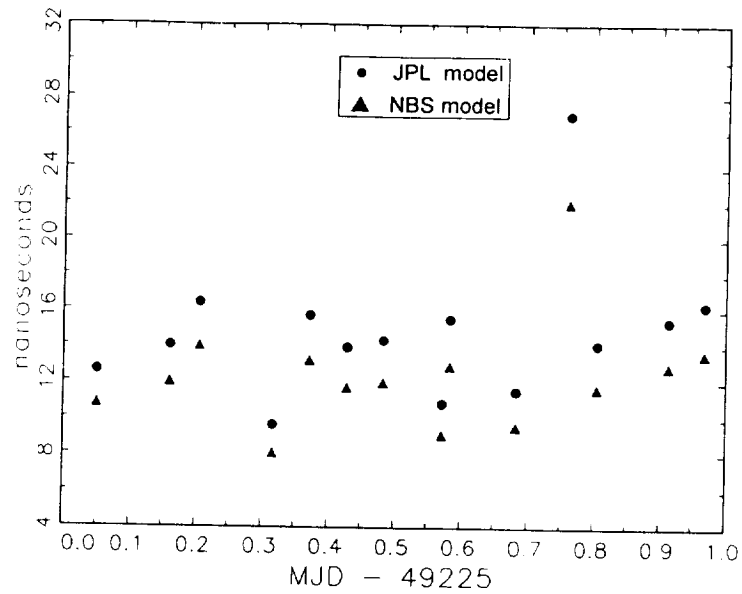


**FIGURE 11.** Tropospheric delays according to the JPL and the NBS models at the CRL on 26 August 1993 for each track in the direction of the OCA.

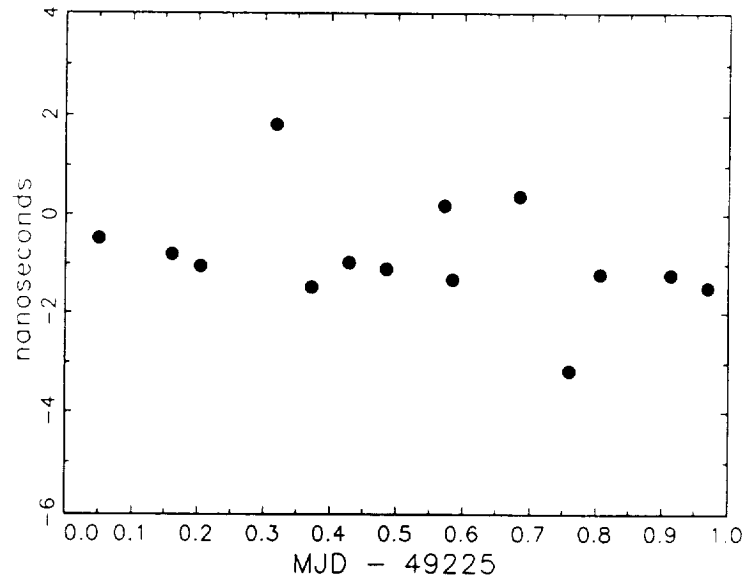


**FIGURE 12.** [OCA Cs clock - UTC(CRL)] as obtained by GPS common views with the NBS tropospheric model minus [OCA Cs clock - UTC(CRL)] as obtained by GPS common views with the JPL tropospheric model for each track on 26 August 1993.

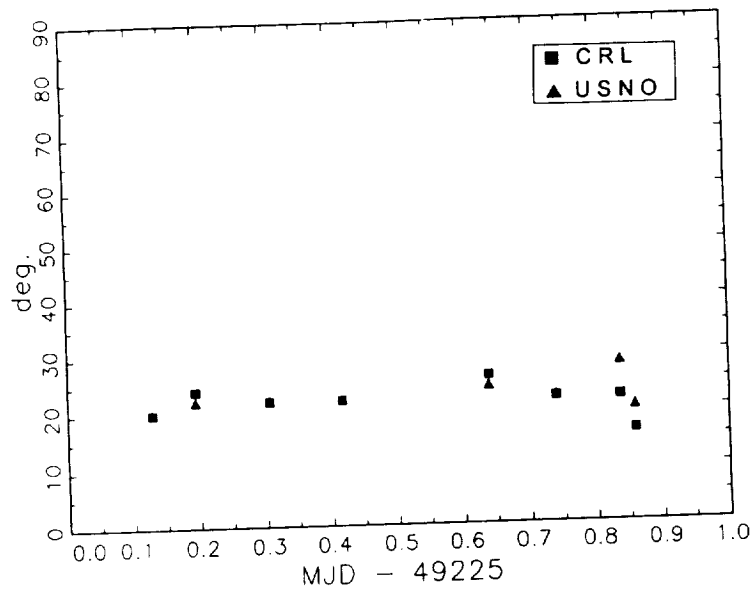


**FIGURE 13.** Elevation angles of each track on 26 August 1993 at the USNO in the direction of the CRL and at the CRL in the direction of the USNO.

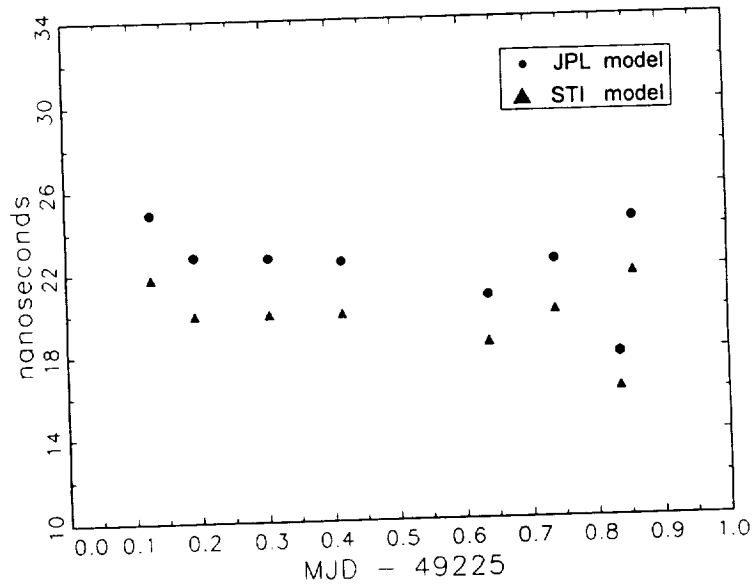


**FIGURE 14.** Tropospheric delays according to the JPL and the STI models at the USNO on 26 August 1993 for each track in the direction of the OCA.

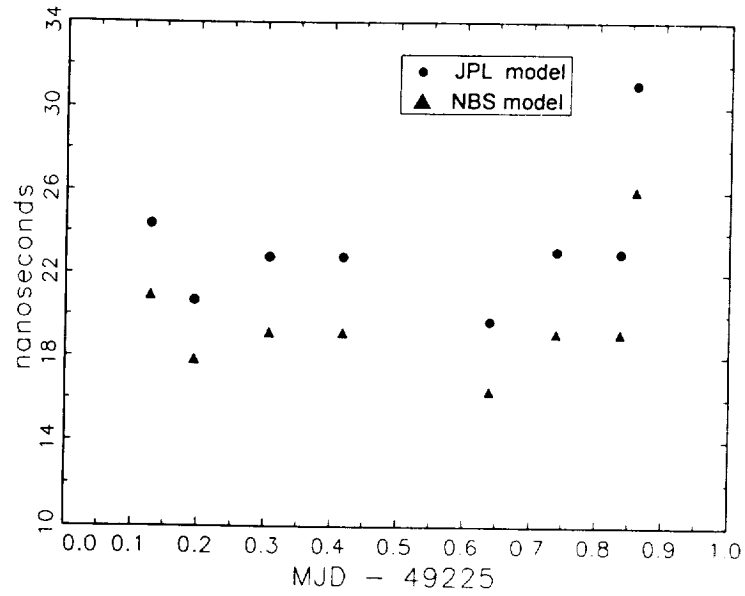


**FIGURE 15.** Tropospheric delays according to the JPL and the NBS models at the CRL on 26 August 1993 for each track in the direction of the USNO.

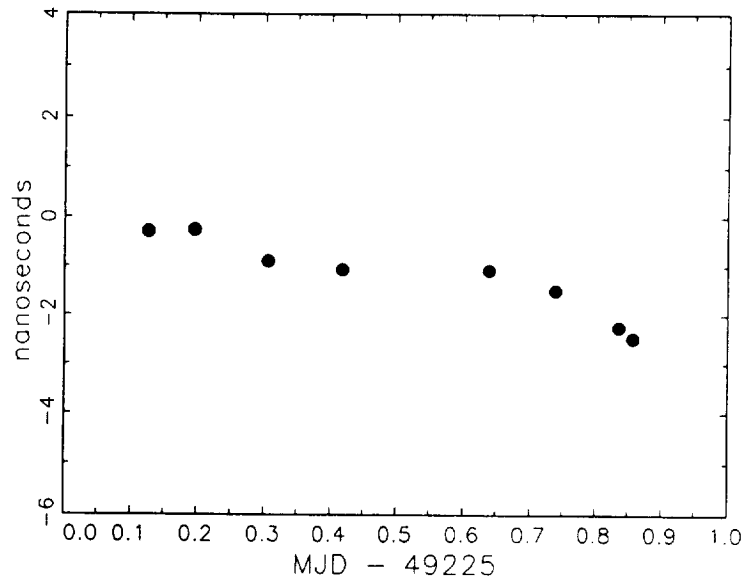


**FIGURE 16.** [UTC(USNO Master Clock) - UTC(CRL)] as obtained by GPS common views with the STI and NBS tropospheric model minus [UTC(USNO Master Clock - UTC(CRL))] as obtained by GPS common views with the JPL tropospheric model for each track on 26 August 1993.

## QUESTIONS AND ANSWERS

**MARC WEISS (NIST):** I wonder if you did a comparison of the effects of using measurements of humidity versus not using measurements of humidity, say, in the more accurate models, like the CHEL model? I'm asking this because even if we use the CHEL model, it's easy to use it in the receivers; but still, if we have to measure the humidity and have other measurements that go into it, that's a lot harder.

**DR. LEWANDOWSKI (BIPM):** It was considered to include in the standard format the measurement of humidity temperature. But this point was discussed, and finally the majority of the involved people decided not to do it, because of this external measurements to the receiver.

But there is a possibility to add additional columns with these measurements. But this issue of measuring meteor conditions comes in laboratories which measure international time links. So it's not of concern to many people; it's for those who want to do more accurate studies.

**MARC A. WEISS (NIST):** So my question is whether you compare using measurements versus not using measurements in the tropospheric model. What differences does that produce?

**W. LEWANDOWSKI (BIPM):** In measuring and not measuring? It was peak differences up to five ns in the intercontinental time links.

**DAVID ALLAN (ALLAN'S TIME):** I would like to actually make a comment in regard to the melting pot method which the USNO has introduced or has used, I think, quite effectively. In this case, of course, the satellites are at high elevation angles. And the question is -- and maybe this is really a question of Dr. Winkler -- one would like to do the same thing that has been done with common view, that is, go A to B, B to C, C back to A; and you get closure around the globe so you can test the around-the-world accuracy. And because of the high altitudes that you can achieve in using the melting pot method, it would be interesting to do the same thing, A to B, B to C, and go around the globe and check the closure on that. I don't know whether that's been done or not. Dr. Winkler, do you know?

**W. LEWANDOWSKI (BIPM):** Of course, using melting pot and high elevations improves the conditions. But again, for very accurate time links, measuring meteor conditions should be considered also, for any observations. If you want to go down under one ns.

At this moment, when we have troubles with receivers, they are noisy at the level of 10 ns, and this issue is not so urgent. But with future receivers, and if we want to go down under one ns, it should be gathered.

822  
P 13

# PROSPECTS FOR HIGH ACCURACY TIME DISSEMINATION & SYNCHRONIZATION USING CODED RADAR PULSES FROM A LOW-EARTH ORBITING SPACECRAFT

E. Detoma  
Fiat CIEI Div. SEPA  
Torino, Italy

C. Dionisio  
Alenia Spazio  
Roma, Italy

## 1 INTRODUCTION

The radar (an acronym for radio detection and ranging) is an instrument developed just before the WW-II to precisely measure the position of an object (target) in space. This is done by emitting a narrow pulse of electromagnetic energy in the RF spectrum, receiving the return echo and measuring the time of flight in the two-way path from the emitter to the target. The propagation delay provides a measure of the range to the target, which is not in itself sufficient to uniquely locate the position of the same in space. However, if a directional antenna is used, the direction of the echo can be assessed by the antenna pointing angles. In this way the position of the target can be uniquely determined in space. How well this can be done is a function of the resolution of the measurements performed (range and direction, i.e.: angles); in turn, the resolution will dictate the time and frequency requirements of the reference oscillator.

## 2 ANGULAR RESOLUTION

The angular resolution,  $\Delta\theta$ , of an antenna is a function of its beamwidth and, in principle, for an ideal antenna, is only limited by the laws of diffraction for an electromagnetic wave with a wavelength :

$$\Delta\theta[\text{rad}] = \frac{\lambda}{L} \quad (1)$$

where L is the linear dimension of the collecting area of antenna orthogonal to the direction of interest. For an antenna with a reflector, such as the ones used in radar, L is the linear dimension of the reflector. For a circular reflector,  $\Delta\theta$  is the same for any angle being measured (azimuth and elevation) since the linear dimensions are constant (L is the diameter) along these directions.

For a microwave Real Aperture Radar (RAR) working at X-band ( $f = 10$  GHz,  $\lambda = 0.03$  m), the angular resolution is primarily limited by the size of the antenna; for a 3 meter antenna, the resolution of the angular measurements is roughly  $0.510^{-2}$  rad (0.29 degrees), where the value of provided by eq. (1) has been halved, since the same antenna is used for transmission and reception. At a range of 50 km this translates in a position inaccuracy of about 500 m, which exceeds the ranging inaccuracy of most radars at the same distance. The large beamwidth prevents the microwave radar from being used for imaging purposes if the antenna dimensions are to be kept reasonable.

### 3 INTERFEROMETRIC TECHNIQUES

To overcome this limitation without increasing the size of the antenna, an interferometric configuration can be used instead, where two antennas are receiving the same return echo which is time-tagged with respect to the same time scale. This requires the use of the same frequency reference in the radar receivers in order not to introduce uncalibrated differential phase delays or of two frequency references coherent with each other. This arrangement is the basis of all the interferometric techniques, both for Connected Elements Interferometry (CEI, where the same local oscillator is fed to each element of the interferometric array) or for the Very Large Baseline Interferometry (VLBI, using separate coherent oscillators).

### 4 THE SYNTHETIC APERTURE RADAR

A different scheme was developed when engineers started to develop airborne radars for imaging purposes: the so-called Synthetic Aperture Radar, or SAR for short. In this scheme, the fact that the airborne radar was carried around by an aircraft was exploited, by considering that the same antenna was occupying different positions in space at different times, therefore acting as an array of spatially separated antenna of a large interferometer. These considerations apply only to a stationary target (since the return signals from each of the "virtual" antennas are taken at different times), but for surveying and imaging applications this technique works very well.

When spaceborne radars became a reality, it was easy to translate the SAR concepts in space, with the added advantage of a better stability, uniformity and predictability of the motion of the antenna, since, being bound to an orbiting spacecraft, its position vs. time is precisely set by the laws of the classical celestial mechanics.

In a SAR, the diffraction-limited resolution of a RAR can be improved with signal processing techniques, for example by Doppler-beam sharpening, where use is made of the incremental Doppler shift between adjacent points on the ground to increase the across-range resolution. The Doppler effect can be written (Fig. 1) as:

$$\frac{f_{Doppl}}{f} = \frac{2v \cos \theta}{c} \quad (2)$$

where  $f_{Doppl}$  is the Doppler shift (in Hz),  $f$  is the carrier frequency,  $v$  is the speed of the radar-carrying platform (this may be an aircraft or a spacecraft),  $\theta$  is the angle between the velocity vector  $v$  and the direction of observation,  $c$  is the speed of propagation of the electromagnetic radiation and the factor 2 accounts for the two-way propagation. Since:  $\lambda = c/f$ , eq. (2) can be rewritten as:

$$f_{Doppl} = \frac{2v \cos \theta}{\lambda} \quad (3)$$

By differentiation and neglecting the signs (ref. 1), we can derive the rate of change of the Doppler shift as:

$$\Delta f_{Doppl} = \frac{2v \cdot \sin \theta \Delta \theta}{\lambda} \quad (4)$$

Since the angular change  $\Delta \theta$  is related to the resolution  $R_y$  (see eq. (1) above):

$$\Delta \theta = \frac{R_y}{R} \quad (5)$$

eq. (4) becomes:

$$R_y = \frac{R \cdot \lambda}{2v \cdot \sin \theta} \cdot \Delta f_{Doppl} \quad (6)$$

If  $f_{Doppl}$  is measured down to 10 Hz, considering  $\theta$  close to 90 degrees, the satellite velocity being about 7 km/s and the range around 1000 km, then the  $R_y$  resolution drops to 21.5 m. (See para. 7 for an easy derivation of the satellite velocity in a circular orbit)

## 5 RANGING ACCURACY

The ranging resolution  $\Delta R$  (and accuracy) for a pulse radar is essentially a function of how well the round trip time of the transmitted pulse is measured:

$$\Delta R = c \cdot \frac{\Delta \tau}{2} \quad (7)$$

where  $c$  is the speed of propagation of the electromagnetic wave and  $\Delta \tau$  is the rise time of the received pulse. If the pulse is severely distorted by the propagation effects or by the reflection from the target, then it is better to consider  $\Delta \tau$  as the full width of the transmitted (received) pulse. For a depression angle  $\phi$  in the ZX plane, the resolution  $R_x$  along the x-axis (Fig. 1) becomes:

$$\Delta R = c \cdot \frac{\Delta \tau}{2 \cos \phi} = R_x \quad (8)$$

## 6 RANGING ACCURACY IN NOISE

From the information theory, for a signal affected by noise, it has been shown (ref. 4) that the accuracy of a time interval estimate is related to two parameters: the signal to noise ratio of the received signal (S/N) and the associated bandwidth BW (see ref. 2, page 5, and ref. 3, page 8):

$$\sigma(t) = \frac{1}{\beta \cdot \sqrt{R_o}}; \text{ and } R_o = \frac{2E}{N_o} \quad (9)$$

where  $R_o$  is the ratio of the peak signal to noise power and  $\beta = \beta_{[2]}$  is the normalized second moment of the signal energy spectrum:

$$\beta_{[2]} = \frac{\int_{-\infty}^{\infty} \left| \left[ \frac{\partial a(t)}{\partial t} \right]^2 \right| \cdot dt}{\int_{-\infty}^{\infty} |a(t)|^2 \cdot df} = \frac{\int_{-\infty}^{\infty} (2\pi f)^2 \cdot |A(f)|^2 \cdot df}{\int_{-\infty}^{\infty} |A(f)|^2 \cdot df} \quad (10)$$

and is a measure of the signal bandwidth. The larger the bandwidth, the better the determination of the time interval that can be obtained from the measurement.

## 7 TIME AND FREQUENCY REQUIREMENTS FOR A SPACEBORNE SAR RADAR

Spaceborne imaging radars are especially useful because of the characteristics of the electromagnetic portion of the spectrum in which they operate<sup>[1]</sup>: the atmosphere is a strongly absorbing medium in the visible and infrared region, especially in overcast or rainy weather, when visible or infrared detectors cannot operate. By providing their own source of radiation, radars can operate at night and penetrate the atmosphere with a smaller attenuation than optical sensors, thereby providing an all-weather imaging capability, even if they are not capable of the same detailed image resolution that can be provided by optical sensors.

The most interesting and diffused active microwave instruments are the Radar Altimeters (RAs) and the Synthetic Aperture Radar (SAR). In the near future, other instruments such as the Rain Observation Radar and the Cloud Radar will be developed and launched. The RA generates three measurements: (1) the height of the spacecraft over the Earth surface, (2) the sea waves standard deviation, (3) the wind speed at the sea surface based on reflectivity measurements. The RAs are nadir-looking instruments, generally operating at Ku-band (13.5–13.8 GHz), transmitting a linearly modulated (chirp) pulse with a typical bandwidth of 320 MHz. The transmitted power varies between 5 and 70 W, depending on the design and the application. The footprint is in the order of 15–20 km with an antenna of 1 m diameter. The interesting characteristic is that this instrument is maintained in operation along all the orbit (altitude:

500 – 1200 km), irrespectively of whether it is designed to track all the globe surface or the oceans only.

The SAR instruments are coherent radars which use the motion of the spacecraft to generate the synthetic aperture to increase the azimuth resolution and produce 2-dimensional images of the Earth surface. Spaceborne SARs are operating in the following bands: L, S, C, X, Ku; the transmitted pulses have bandwidths ranging from a few kHz to 300 MHz. The access area on the ground may vary from 50 km to more than 500 km in the more powerful SARs using steerable antenna beams. The transmitted peak power from a SAR can reach the 3–5 kW with antennas as large as 30 m<sup>2</sup>.

The geometry of RA and SAR electromagnetic illumination of the Earth surface during a typical mission is shown in Fig. 1, where the parameters of interest (access area, swath, height, etc.) are clearly identified. (The swath angle is equivalent to the instantaneous field of view for an optical instruments, defining the size of the image taken by the SAR; however, because of the peculiar technique used by SARs, the swath angle refers only to the across-track dimension of the image.) When we consider a satellite orbiting the Earth at about  $h = 1000$  km of height in a near circular, polar orbit, which is the typical orbit for a remote sensing SAR satellite, the linear velocity [in km/s] of the satellite in the orbit is given by:

$$v = 7.9 \cdot \sqrt{\frac{R}{R+h}} \quad (11)$$

and can be computed to be about 7 km/s, assuming for R (Earth radius) an average value of 6370 km. The orbital period P [in minutes] can be computed as:

$$P = 81.4 \cdot \sqrt{\left(1 + \frac{h}{R}\right)^3} \quad (12)$$

and comes out to be around 100–105 minutes for the previous parameters. On the subsatellite track, the SAR image moves at a linear velocity of about 6.35 km/s. If the image is to be located with a maximum error of 400 m, then the timing accuracy required to precisely correlate such an image to its position on the subtrack is only 63 ms. An overall synchronization accuracy of 5 to 10 ms seems more than justified to satisfy this requirement. However, if the single pixel of the image is to be correlated with its position on the subtrack, since the pixel corresponds roughly to the resolution cell of the SAR (a few meters), then the timing accuracy increases to 0.4 ms, and an overall synchronization accuracy in the range of 50 to 100  $\mu$ s must be achieved. This is generally beyond the capability of the bandwidth and delay stability of the command/telemetry data links, unless use is made of the wide bandwidth data link relaying back to Earth the data acquired by the spaceborne SAR.

The positioning and timing requirements can be easily satisfied with an onboard GPS receiver, but for the sake of providing a complete autonomy to the system, especially desirable if the SAR is used for national security purposes, we have investigated other possibilities to provide such a synchronization. As we are going to show thereafter, one interesting possibility can be provided by the use of the pulses of SAR itself; the possibility is interesting since, besides providing the desired accuracy in the synchronization of the onboard clock, the technique may have other interesting spinoffs.

Frequency accuracy and stability requirements are dictated mainly by the specified resolution of the SAR measurements. To perform good ranging measurements [see eq. (7)], it is important that the onboard frequency reference is stable (a few parts in  $10^{-8}$ ) and accurate for the full duration of the mission (2–3 years typical). Again, a measure of the frequency of the onboard oscillator can be easily derived in terms of time offset measurements (synchronization), if these are taken and recorded over a sufficient interval of time. Furthermore, the short term stability

of the on-board oscillator should be good, to insure a low jitter in the transmission of the pulse and reception of the echo (this can be degraded by the phase noise of the local oscillator), thereby insuring a good precision in the round-trip time interval measurement.

Frequency stability requirements are dictated mainly by eq. (5). Since frequency and time stability are equivalent:

$$\frac{\Delta f}{f} = \text{frac} \Delta t t \quad (13)$$

the short term stability of the oscillator over the round trip time interval (around 7 ms for a 1000 km range) must be capable of allowing the measurement of the rate of change of the Doppler shift: for a 10 Hz frequency resolution at X-band, this turns out to be around  $1 \cdot 10^{-9}$  at a sampling time  $\tau = 7$  ms. The characteristics of radar frequency sources used on operational spaceborne SARs designed by Alenia Spazio are listed in Table 1.

## 8 RANGING RESOLUTION (2-WAY) VERSUS TIMING CAPABILITY (1-WAY)

In order to evaluate the potential of the radar signal to transfer precise time, we must look again at the SAR specifications; for the SAR that we are considering the specified ranging accuracy is in the order of 3 to 10 meters: this translates to one-way time delay accuracies in the order of 20 to 60 ns worst case, since these figures can be further reduced by the consideration that they apply to a two-way measurement, and that for a one-way trip the signal to noise ratio is much, much better (since the RF power decreases as the square of the range and not with the fourth power, and the loss due to the target reflection [effective radar cross section] can be totally neglected).

Table 2 shows a comparison between the SAR and the well known GPS system; the comparison applies to several parameters relevant to the one-way time-transfer accuracy. Even if a full assessment of the capabilities of the SAR technique for time transfer has not yet been completed, nevertheless a quick inspection of the table 2 with reference to eq. (8) shows the potential of the technique.

Obviously, the well known limitations of the one-way technique (propagation delays) still apply, and they remain the main factor in determining the overall timing accuracy of the technique, presently limited by our knowledge of the troposphere and ionosphere behavior (propagation models); dual frequency operation (on new RAs) certainly will improve the ionospheric delay uncertainty by a direct measurement of the ionospheric delay.

## 9 PULSED AND CHIRPED RADARS

Early radars used pulses of RF energy for ranging purposes. While pulsed radars represent the easiest and historically older approach to range determination, since a pulse with a sharp rise time seems an ideal waveform because of its wide bandwidth, yet they suffer from other limitations. Multiple returns or widening of the pulse waveform because of the dispersive characteristics of the medium severely distort a narrow pulse; widening the pulse decreases the accuracy of the measurement. Moreover, the narrow RF pulses make inefficient use of the power available at the transmitter and of the bandwidth of the communication channel, providing a poor RF power density in the frequency domain over the spectrum of interest (the bandwidth BW of the transmitted pulse).

In general, the performance of narrow pulses as a time mark for ranging or synchronization purposes is poor with respect to other systems such as spread-spectrum (SS-PRN: Spread Spectrum Pseudo Random Noise) modulation techniques, nowadays widely used for the above

mentioned purposes. However, the latter method is complicated to implement, requires code synchronization to be acquired and maintained, and for these reasons is not well suited for ranging uncooperative targets, where the S/N ratio can be low, severely limiting the code tracking capability for SS-PRN systems.

Radar technology has developed another technique to overcome some of the previous limitations while making efficient use of the bandwidth available. (This technology is not limited to radars only, but it has been applied also to sonar ranging or to optical (laser) pulse compression.) This makes use of the compression of a wide pulse in the time domain exploiting the peculiar frequency domain characteristics of the pulse itself. The pulse can be compressed using analog (frequency modulation) or digital (Barker codes) methods. The pulse is coded in transmission and compressed when received using properly matched filters. Consider a transmitted pulse of duration  $\tau$ , linearly frequency modulated from  $f_1$  to  $f_2$  at a rate of

$$\frac{f_2 - f_1}{\tau} \quad (14)$$

(see Fig. 2). The received signal is fed to a frequency-dependent delay line, so that the low frequency portion of the spectrum (which is received first in the case shown in Fig. 3) is delayed of a greater amount than the higher frequency components (that are received later). Hence, at the output of the delay line all the components appear at the same time, effectively compressing the RF energy of the pulse in a very narrow interval in the time domain.

The final output is equivalent to a very narrow pulse even if the transmitted, reflected and received waveforms are of considerable duration in the time domain. For the conservation of the pulse energy, the amplitude of the compressed pulse will be higher than the amplitude of the received pulse. This pulse will have a  $\text{sinc}/x$  characteristic, with a maximum value of  $\sqrt{D}$  where  $D$  is defined as the dispersion factor, and is equal  $\tau \cdot (f_2 - f_1)$ . The compression ratio  $K_c$  is the ratio of the transmitted pulse width to the compressed pulse  $\tau'$ :

$$K_c = \frac{\tau}{\tau'} \quad (15)$$

Therefore, a one microsecond pulse with  $K_c = 100$  yields a compressed output pulse of 10 ns, with a range resolution capability of 1.5 m. A modern spaceborne SAR may work with higher values of  $K_c$ : typically, a 100  $\mu$ s pulse will offer the same level of performance with  $K_c = 100000$ , the main limitations being the capability to linearly modulate the transmitted pulse with minimum deviation from linearity, the phase delay flatness of the receiver and the linearity of the receiving delay line.

## 10 TIMING USE OF THE CHIRPED PULSE

The most common techniques to synthesize digitally a waveform include methods where samples of the waveform are precomputed and stored (typically in RAM), or where the values of circular functions (sine, cosine) are stored in memory (look-up table). The second approach offers many advantages: a signal wider bandwidth and higher center frequency, a reduction in the hardware complexity if different waveforms have to be generated, etc. The key element is the Numerical Controlled Oscillator (NCO) which, under external control, generates time-discrete sinusoidal samples (see Fig. 4). With an NCO-approach to the chirped pulse generation, the waveform can be modulated easily in amplitude (again, using a digital control or in analog form by acting on the reference voltage of the Digital-to-Analog Converter [DAC, see Fig. 4]), frequency or phase. Phase modulation, for example, will not disturb the frequency characteristic of the chirped pulse, while providing a mean to convey data superimposed to the RF carrier within the pulse width.

Working with a 100  $\mu$ s pulse at X band will provide a considerable time interval and bandwidth ( $\approx 300$  MHz) to superimpose data to the RF carrier in the pulse, using a suitable modulation

method. For instance, the data can be modulated in amplitude, frequency or phase on the chirped pulse, and recovered on reception prior the pulse compression. Alternatively, the synchronization data can be transmitted in dedicated pulses within the radar Pulse Repetition Period, without modifying the normally transmitted pulse.

If the information being coded includes the spacecraft position and time of transmission, then all the elements required to a one-way synchronization are present, and the pulse can be readily exploited for this purpose. The position of the spacecraft can be directly given in terms of its X, Y and Z coordinates in a suitable reference system; these can be provided by the onboard orbit processor or by a GPS receiver, if available. Alternatively, the spacecraft orbit elements can be transmitted, and the spacecraft position at the time of transmission computed on the ground. However, it is likely that future SAR spacecraft will compute their position with high accuracy in orbit, therefore the X, Y, Z coordinates will be directly available for transmission, minimizing the complexity of the ground equipment. The spacecraft local time scale will provide the time of transmission with adequate resolution, and this in turn can be referenced to UTC on the ground via the same synchronization technique.

## **11 SYNCHRONIZATION VIA THE CHIRPED PULSE**

The simplicity of the ground receiver, the high level of the receivable signal and its associated good S/N ratio make the method extremely attractive for very low cost synchronization and time dissemination. The user on the ground needs only to receive the transmitted pulses when the spacecraft orbits overhead. Since the level of the received pulse can be very high, the RF part of the receiver can be simple. The high frequency used limits the effects of the ionospheric delay and the tropospheric delay can be modeled or minimized using signals only when the satellite is at high elevation.

In the receiver, the received signal is split in two (see Fig. 5): one part is fed to the frequency-dependent delay line for pulse compression and range measurement; the other is fed to dedicated circuitry to extract the data coded on the pulse (spacecraft position and time of transmission message): these are used to recover the range information and, knowing the receiver position, to compute the synchronization offset.

If the user position is unknown, the system will allow some capability to precisely locate the user itself, with a method based on successive range measurements from the same satellite, as the satellite moves across in the sky in its orbit: this is exactly what was intended when the U.S. Navy TIMATION project was started many years ago. But navigation or positioning is not the purpose of the technique, however.

Since the synchronization result is just the offset between a ground clock and the spacecraft clock, the method can be inverted to obtain just what we were aiming for: a precise synchronization of the spacecraft clock to a ground reference (namely UTC) and a strict correlation of time and position of the spacecraft.

## **12 SAR SPACECRAFT PASSIVE RANGING**

Reversing the concept, we can use a limited array of ground antennas (3 to 4) in an interferometric configuration (CEI) to track the spacecraft itself with very high accuracy, providing the results of the orbit parameters determination to the onboard orbit processor via the command uplink. Four simultaneous ranges to four separate antennas whose location is known will provide the spacecraft position and the time offset of the onboard clock with respect to the ground references. In this way, the operation of the SAR satellite will be completely autonomous and independent of other navigation systems.

## 13 GEODETIC APPLICATIONS FOR THE PROPOSED SYSTEM

The system is capable of some interesting applications in other fields, notably in geodesy for crustal dynamics monitoring. Slight movements of the Earth crust can be precisely measured by an array of receivers tracking the orbiting SAR spacecraft. The low cost of the receivers and the high precision ranging and timing capability of the system make the technique suitable to implement large arrays over wide areas at reasonable cost. We have considered also the fact that, being a SAR satellite (usually on Earth observation satellite) in or near a highly inclined polar orbit, the system provides good coverage also of the polar regions, where the GPS satellites visibility is impaired by the GPS orbit inclination.

## 14 CONCLUSIONS

Spaceborne remote sensing Altimeters and Synthetic Aperture Radars (SARs) require a highly stable oscillator onboard and good synchronization for return echoes identification and SAR data processing. Therefore, one of the requirements in designing their onboard timing subsystem is to provide a precise synchronization to some ground reference, namely UTC, in order to precisely correlate the pulse time to the spacecraft position.

While this can be provided via the Navstar Global Positioning System (GPS), the capability exist to have an independent mean of synchronization using the transmitted radar pulse as a precise timing reference mark. The large bandwidth and extremely good signal to noise (S/N) ratio of the pulse received on the ground makes this approach extremely appealing for high-accuracy one-way time dissemination and synchronization.

The technique provides additional benefits, besides synchronization, in supporting the mission of the spacecraft. In fact, a small network of 3 to 4 ground receivers, operating as a Connected Elements Interferometer, may provide high accuracy tracking and position determination of the spacecraft for ranging and orbit determination by receiving and processing the same coded pulses. While synchronization and orbit determination can be supplied by an onboard GPS receiver, the proposed technique provides a high precision solution, in principle independent from GPS, to synchronize ground systems to the onboard clock and vice versa, extending the range of applications and possible users for the spacecraft and its instruments. The implementation is extremely attractive because of the low cost, since all the required components for the synchronization/ranging link are already available, but for the coding of the transmitted pulses.

In this paper we have presented a preliminary description and analysis of the potential of the technique to provide an alternative source of high precision timing to demanding users and a survey of the possible applications. Work is now in progress towards a full feasibility study aimed to evaluate the possibility to implement this concept on an advanced spaceborne SAR sensor being proposed by Alenia Spazio.

## 15 REFERENCES

- [1.] S.A. Hovanessian, "TACTICAL USES OF IMAGING RADARS", Microwave Journal (February 1984), pp. 109-123
- [2.] E.Byron, G.P.Gafke, J.W.McIntyre, "PHASE I STUDY AND DESIGN OF TECHNIQUES FOR PRECISE TIME TRANSFER VIA THE TRACKING AND DATA RELAY SATELLITE SYSTEM (TDRSS)", The Johns Hopkins University, Applied Physics Laboratory Special Report CSC-O- 322 (September 25, 1976)
- [3.] D.K. Barton, H.W. Ward, HANDBOOK OF RADAR MEASUREMENT, Artech House Inc. (1984)

- [4.] P.M. Woodward, PROBABILITY AND INFORMATION THEORY WITH APPLICATIONS TO RADAR, Pergamon Press (1957)
- [5.] C. Elachi, SPACEBORNE RADAR REMOTE SENSING: APPLICATIONS AND TECHNIQUES, IEEE Press (1988)
- [6.] S.A. Hovanessian, INTRODUCTION TO SENSORS SYSTEMS, Artech House (1988)
- [7.] Z. Borgarelli, R. Cortesini, C. Dionisio, "DIGITAL CHIRP GENERATOR SUITS SPACE APPLICATIONS", Microwaves & RF (June 1993)
- [8.] F. Nirchio, B. Pernice, L. Borgarelli, C. Dionisio, R. Mizzoni, CASSINI RADAR RADIO FREQUENCY S/S: DESIGN DESCRIPTION AND PERFORMANCE EVALUATION, JGRASS '93
- [9.] G. Angino, C. Dionisio, F. Rubertone, ERS-1 RADAR ALTIMETER SYSTEM DESCRIPTION, JGRASS '91

TABLE 1: Examples of SAR reference oscillators characteristics

Parameter	ERS-1 R (STALO)	CASSINI radar	X-SAR	ASAR
Frequency*[GHz]	7.35	12.96	8.415	5.331
Aging	$\pm 2$ [ppm/2yrs]	$\pm 0.2$ [ppm/yr]	$\pm 7$ [ppm/yr]	$\pm 1$ [ppm/4yrs] $\pm 0.001$ [ppm/100minutes]
Temperature drift[ppm/T]	$\pm 20/45^\circ\text{C}$	$\pm 0.4/55^\circ\text{C}$	$\pm 10/50^\circ\text{C}$	$\pm 0.04/50^\circ\text{C}$
Power level [dBm]	1	11	0	3
Harmonics [dBc]	< -50	< -50	< -60	< -60
Spurious [dBc]	< -60	< -60	< -60	< -60
Initial accuracy, Frequency [ppm]	$\pm 1$	$\pm 0.02$	$\pm 1$	$\pm 1$
Short term stability	-	$5.3 \times 10^{-13}$ $\tau = 1 \text{ s}$	-	$2 \times 10^{-11}$ $\tau = 7.5 \text{ ms}$
Phase noise [dBc/Hz] <sup>#</sup>	< -105 (f=1 kHz)	< -85 (f=1 kHz)	< -95 (f=300 Hz)	-

\*RF carrier frequency [transmission frequency]

<sup>#</sup>f=Fourier frequency

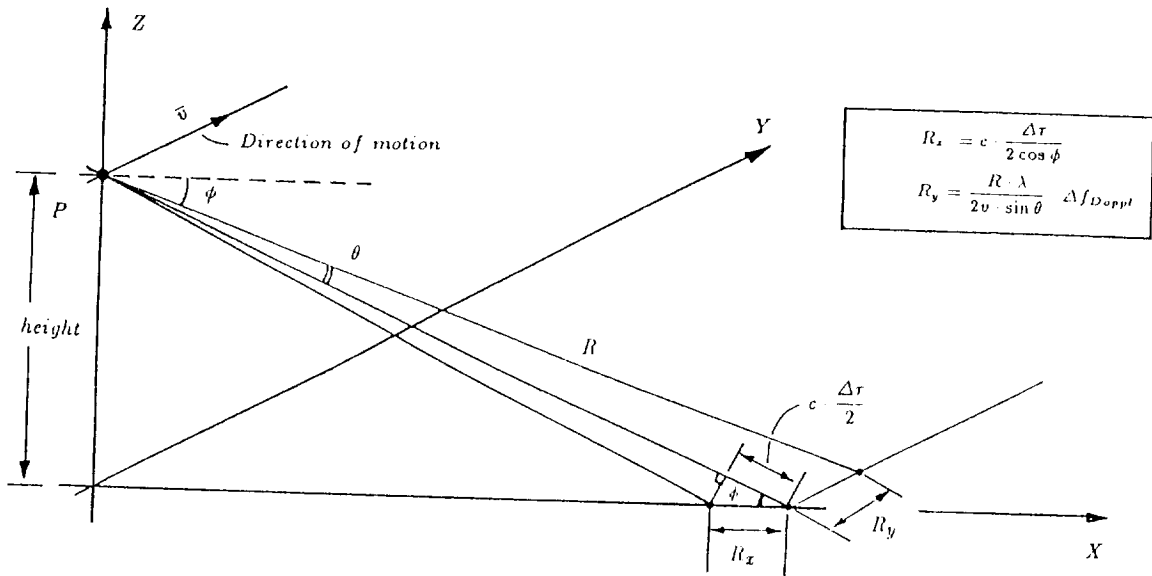
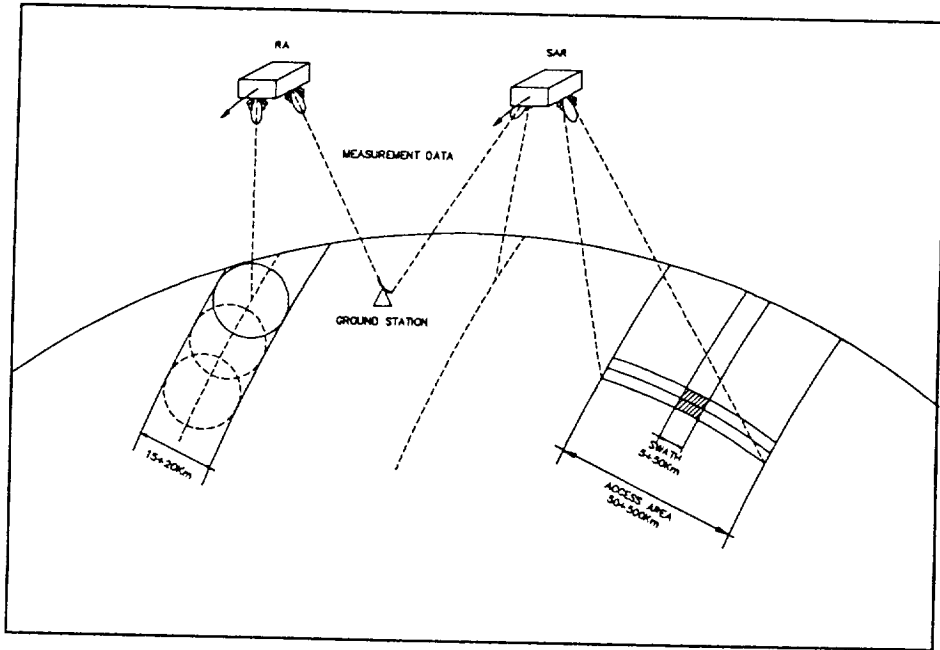
**TABLE 2: Comparison of parameters relevant to the one-way synchronization between GPS and a SAR system**

Parameter	GPS	SAR	Comments
RF Carrier	1.2, 1.5 GHz	10 GHz*	Ionospheric delays are smaller for higher RF carrier frequencies
RF Bandwidth	$\pm 10$ MHz	$\approx 300$ MHz	Available Bandwidth*
RF Power	$\approx 10$ W	$\approx 1 \div 5$ kW	Determines the (peak) S/N on reception*
Height	20000 km	1000 km	Determines the S/N on reception*
Modulation	Spreadspectrum	Chirped pulse	GPS modulation is more efficient in making maximum use of available bandwidth and link power budget
Orbit	Inclined	Polar	Coverage of polar regions for geodesy purposes is possible with the SAR concept
Availability	Continuous	About 4 $\div$ 6 passes per day	SAR in polar orbit does not provide a continuous coverage

\*See eq. (8)

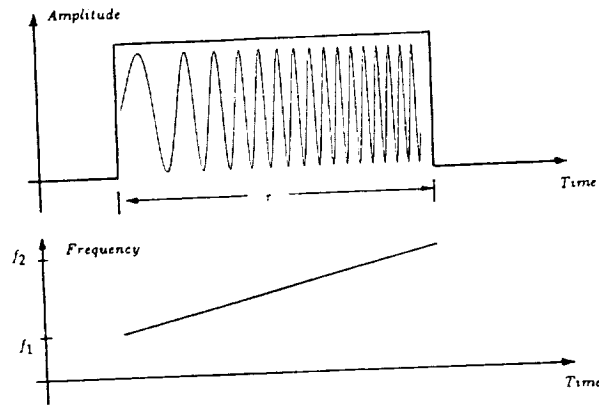
\*The sample figure refers to an X-band SAR

FIGURE 1: SAR Concepts

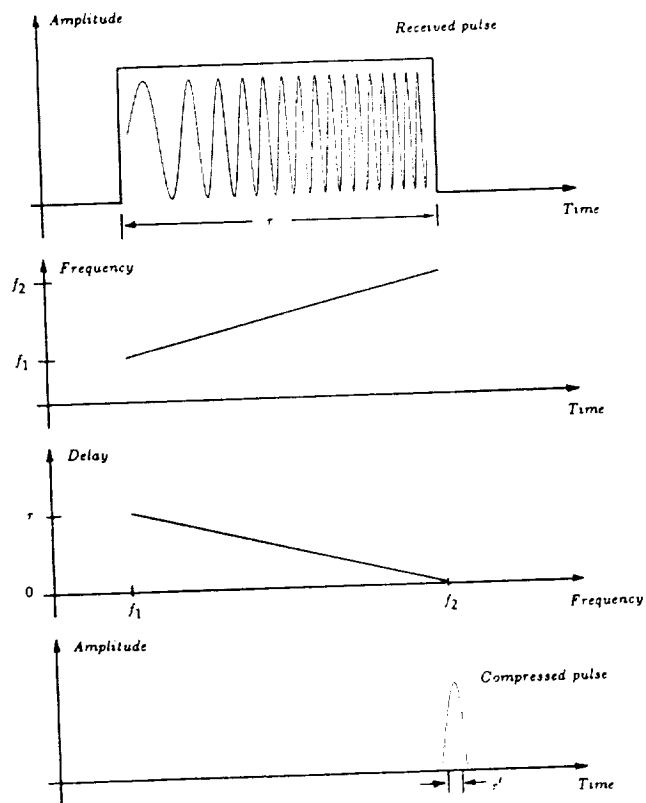


SAR GEOMETRY AND X-Y RESOLUTION

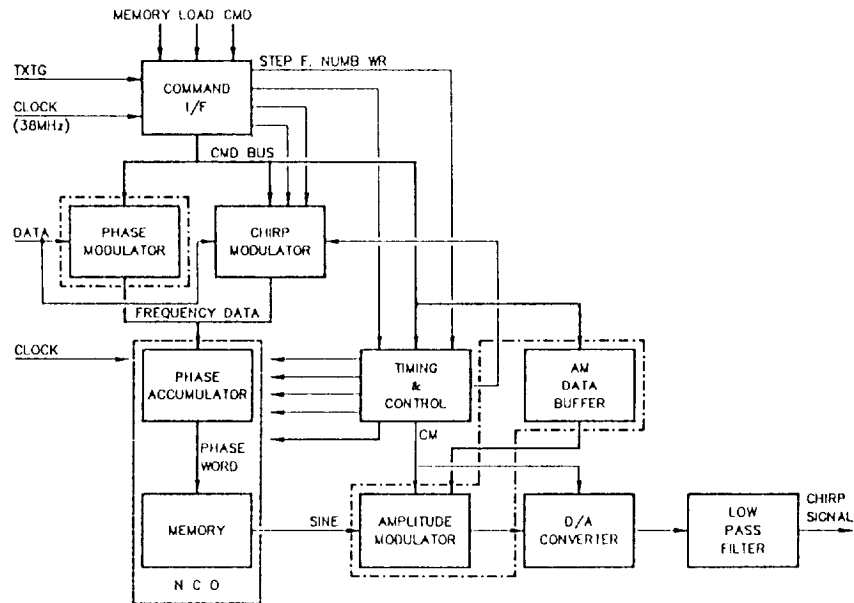
**FIGURE 2: Transmitted waveform of a linear FM pulse (chirp)**



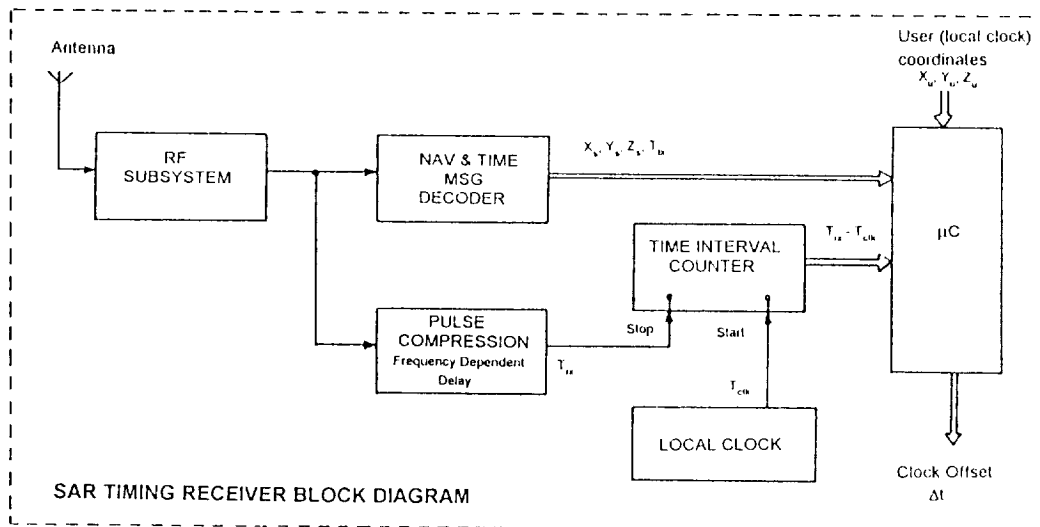
**FIGURE 3: Received waveform of a FM pulse and pulse compression**

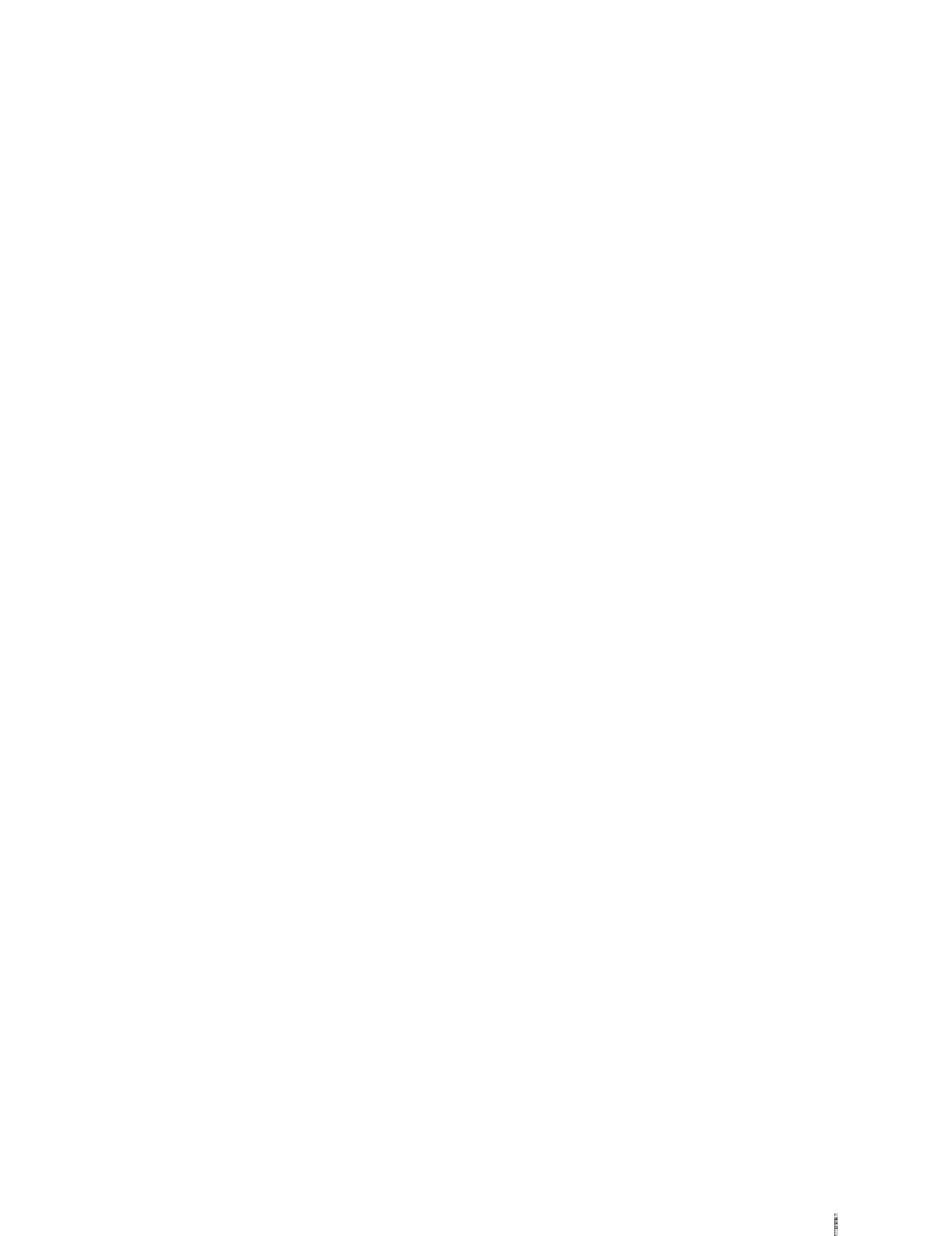


**FIGURE 4: Digital Chirp Generator (DCG) block diagram**



**FIGURE 5: Ground Timing Receiver block diagram**





# Metafitting: Weight Optimization for Least-Squares Fitting of PTTI Data

R.J. Douglas and J.-S. Boulanger  
Time and Frequency Standards Group  
Institute for National Measurement Standards  
National Research Council of Canada  
Ottawa, CANADA K1A 0R6  
(613) 993-5186, Fax (613) 952-1394

## Abstract

*For precise time intercomparisons between a master frequency standard and a slave time scale, we have found it useful to quantitatively compare different fitting strategies by examining the standard uncertainty in time or average frequency. It is particularly useful when designing procedures which use intermittent intercomparisons, with some parameterized fit used to interpolate or extrapolate from the calibrating intercomparisons. We use the term "metafitting" for the choices that are made before a fitting procedure is operationally adopted. We present methods for calculating the standard uncertainty for general, weighted least-squares fits and a method for optimizing these weights for a general noise model suitable for many PTTI applications. We present the results of the metafitting of procedures for the use of a regular schedule of (hypothetical) high-accuracy frequency calibration of a maser time scale. We have identified a cumulative series of improvements that give a significant reduction of the expected standard uncertainty, compared to the simplest procedure of resetting the maser synthesizer after each calibration. The metafitting improvements presented include the optimum choice of weights for the calibration runs, optimized over a period of a week or 10 days.*

## Introduction

In preparing to fit precision time comparison data, usually questions concerning "optimal" fitting strategies have been addressed in a generic rather than in a specific sense. It is interesting to examine whether, for specific cases, significant advantages might accrue from customizing the fitting strategy to the specific pattern of data points and the noise spectrum. In practice, many really important choices are made before any fit is finalized, and yet are not necessarily optimized as part of the fitting procedure. (a) A fitting metric and method must be chosen (such as least-squares fitting). (b) The set of parameterized basis functions must be chosen: basis function number and type (such as a second order polynomial). (c) An outlier removal method may be adopted (such as iteratively discarding a limited number of points having anomalously high residuals). (d) The relative weighting to be given to each data point must be determined (such as the use of end-point only linear fits vs unweighted linear least-squares fits). (e) A final "consistency of fit with data and noise model" parameter should be derived (such as the reduced  $\chi^2$  for a least-squares fit with

known noise). Many of these choices depend in subtle ways on the type of noise encountered, and here precise time measurements often provide details of the noise spectrum which are not trivial to incorporate into an optimal treatment of (a)-(e). Since the term “fitting” is generally interpreted as referring to the determination of a set of parameters from a particular data set, we use the term “metafitting” to encompass the optimization of the broader processes such as (a)-(e).

But in what sense is this “metafitting” to be judged? At first sight, there appear to be too many choices. The fitting might be optimized in an average sense, minimizing some metafitting metric function that sums over experimental residuals. If the autocorrelation function of the noise is known (or modeled) it is possible to calculate and minimize the metric function summing over the expected “residuals” at unmeasured times. Thus the fitting might be optimized in a local sense, minimizing a residual at a specific time (open to choice), or it might be optimized to minimize a residual of the average frequency over a specific interval (each end being open to choice). The point, points or interval must be chosen, and a procedure must be found to estimate the expected residual(s) at times other than those at which measurements have been taken.

Fortunately, international guidelines [1] now strongly suggest a good quantity to optimize: the “standard uncertainty”, which is the root-mean-square residual of the fit’s extrapolation or interpolation to a specific point, one not necessarily included in the fit. It is also a good quantity to optimize in that a standard method [2](the Wiener-Kolmogoroff theory) exists for any fitting procedure that uses a linear combination of the data. All least-squares fitting procedures with linear coefficients can be handled explicitly in this way [5]. For the purposes of time and frequency metrology, metafitting to minimize the standard uncertainty is a good choice - but it might not be as good a choice in other applications (where, for example it might be more appropriate to try minimizing the occurrence of outlier events having disastrous consequences). For frequency or time interval metrology, the standard uncertainty in the average frequency over an interval makes an even more attractive discriminant for metafitting.

The power law noise models appropriate for PTI phase comparisons can have low frequency divergences that appear to be worrying to some purists who wish to assure strict stationarity of any process **before** developing its formalism. In the development of computable forms [3],[5], it is straightforward to show that the standard uncertainty in the average frequency of a least-squares fit is not divergent for most commonly encountered power law noise spectra, with the exception of random walk frequency noise. However, the real question is more stringent than simple stationarity: have we enough long-term data on the system being modeled to obtain results which converge? We believe that this type of question can be rigorously handled by imposing a low-frequency cutoff (and thus ensuring a formal stationarity), and then verifying not merely that any results extracted from the model converge as the low frequency limit approaches zero - but also that the results have converged to the desired degree before the low frequency limit is sampling Fourier components of the noise which have not been measured.

## Choosing Weights in Weighted Least-Squares Fits

We present here a general strategy for evaluating and optimizing distributions of weights in a weighted least-squares fit to phase data. We will concentrate on optimizing fitting that compares the

frequency of a continuously operated oscillator with a frequency standard (perhaps intermittently operated), for the purposes of frequency calibration. The strategy is based upon the analytic expressions for the standard uncertainty in frequency, generally extrapolated over a wider interval than the calibration interval, where a dense set of high-precision phase comparisons would normally be available. A noise model is assumed which has wide applicability to a broad range of frequency standards. The degree of frequency control will be evaluatable for any set of weights in a weighted least-squares fit that is linear in the fitting coefficients (but fully general in the choice of basis functions).

As our metafitting metric we choose the standard uncertainty in the average frequency, evaluated over a general interval which could be considerably displaced from the fitting interval. This is the most appropriate metric for frequency metrology applications, since the standard uncertainty is now the internationally recommended [1] way of specifying calibration uncertainty. With our procedures the standard uncertainty in average frequency can be evaluated for a broad class of noise models, for any set of fitting points, for any extrapolation or interpolation interval, for any linear combination of arbitrary basis functions, and for any least-squares weighting. In particular, in any of the above cases our procedure can evaluate the standard uncertainty the equal-weight procedure (advocated for its robustness) to the end-point procedure (advocated for its “optimum” estimate of frequency for some pure classes of noise), as well as any intermediate case with higher weights near the end-points of the calibration interval. The procedure permits the evaluation of the trade-off of uncertainty for other procedures which are perceived as being more robust. As is shown below, even with large data sets, in some cases it appears to be feasible to choose the optimum set of weights which minimize the standard uncertainty in average frequency for the interval being considered.

## Noise Model

The noise model  $x_m(t)$  is the modeled phase difference between the master frequency standard and the standard being calibrated. The noise model is taken as being the sum of a deterministic part (which could include a phase offset, frequency offset and frequency drift) and a random noise part,  $x_0(t)$ . The random noise includes the “full” noise model that is usually used in discussions of frequency standard stability [9]: a sum of five noise processes, each normally distributed about the mean (but with variances which depend on the time sampled in different ways) that have spectral densities of phase noise ( $S_x(f)$ ) that are power laws which range from flat to increasingly divergent at low frequencies. Expressing the five terms in terms of the spectral density of the mean-square of the fluctuations in  $\frac{dx_0(t)}{dt}$  (or  $y_0(t)$ ) at a frequency  $f$ ,  $S_y(f)$ , each noise term is described by an amplitude  $h_\alpha$  which is taken to be independent of any time translations (stationarity and random phase approximations). The sum includes  $\alpha = 2$ , white phase noise in  $x$ ;  $\alpha = 1$ , flicker ( $1/f$ ) noise in  $x$ ;  $\alpha = 0$ , white frequency noise and random walk phase noise;  $\alpha = -1$ , flicker frequency noise; and  $\alpha = -2$ , random walk frequency noise. A low-frequency cutoff  $f_l$  and an upper frequency cutoff  $f_h$ . The spectral density of the mean-square fluctuations in  $x_0(t)$  is  $S_x(f)$ , and for this noise model

$$S_y(f) = \sum_{\alpha=-2}^2 h_\alpha f^\alpha \quad \text{and} \quad S_x(f) = \sum_{\alpha=-2}^2 \frac{h_\alpha f^{(\alpha-2)}}{(2\pi)^2} \quad (1)$$

For a given noise model of this type, the standard uncertainty of the fit at any given time can be calculated from the autocorrelation function  $\langle x_0(t)x_0(t+\tau) \rangle$ . It is divergent for four of our five types of noise unless a low-frequency cutoff is applied, and even then can challenge the accuracy and dynamic range capacities of classical computing. Analytic expressions for this autocorrelation function exist for each type of noise [5], and modern arbitrary-precision computer languages are able to cope directly with the autocorrelation function.

In our analysis of the uncertainty associated with any useful least-squares fit, we expect no divergences to infinity in the standard uncertainty, and so the combinations of the autocorrelation functions must have their divergent parts cancel, with the fitting itself acting as low-frequency cutoff. In considering the standard uncertainty of average frequency from a least-squares fit, we have found it helpful to use analytic expressions [5], [4], [3] for the less divergent general two-interval covariance of the random noise model, that is the covariance of the time-scale departure over the time interval  $[t_1, t_2]$  with the time-scale departure over the time interval  $[t_3, t_4]$ :

$$\begin{aligned} \mathcal{S} &= \langle [x_0(t_2) - x_0(t_1)] [x_0(t_4) - x_0(t_3)] \rangle \\ &= \int_{t_1}^{t_2} \int_{t_3}^{t_4} \langle y_0(t') y_0(t'') \rangle dt'' dt' \\ &= (t_2 - t_1)(t_4 - t_3) \langle \bar{y}_{[t_1, t_2]} \bar{y}_{[t_3, t_4]} \rangle \end{aligned} \quad (2)$$

where  $\langle \bar{y}_{[t_1, t_2]} \bar{y}_{[t_3, t_4]} \rangle$  is the general covariance of the average frequency: a generalization of the two-sample variance of the average frequency. The generalization includes the possibility of an overlap of the intervals (as well as the possibility of a “dead time” between the intervals), and incorporates the possibility of considering the frequency average over two time intervals of different duration. Just as for the two-sample variance of  $y$ , and for the autocorrelation function of  $x(t)$ , the covariance separates into the five terms of the noise model.

Analytic forms for the five terms of the autocorrelation function of  $x(t)$  and for the five terms of the general cross-correlation of  $\bar{y}$  are given in references [5], [4] and [3], derived with only the usual assumptions about high and low frequency limits to the noise bandwidth. The references also contain some comments on practical methods for computing values using these forms.

## Weighted Least-Squares Fits

Weighted least-squares fitting chooses the  $n$  linear coefficients  $d_l$  of the  $n$  basis functions  $g_l(t)$ , to arrive at a function  $x_p(t)$  which will be used for interpolation or extrapolation. In frequency standards work, we would usually fit a phase offset, a frequency offset, and sometimes a drift rate and higher terms such as daily or seasonal fluctuations.

$$x_p(t) = \vec{d} \cdot \vec{g}(t) = d_1 + d_2 t + d_3 t^2 + \sum_{l=4}^n d_l g_l(t). \quad (3)$$

The coefficient vector  $\vec{d}$  is chosen to minimize the sum over the  $N$  fitting points with phase difference values of  $x(t_i)$  at times  $t_i$

$$L_2^2 = \sum_{i=1}^N W_i [x(t_i) - \vec{d} \cdot \vec{g}(t_i)]^2 \quad (4)$$

where the weight  $W_i$  is applied to the square of the  $i^{\text{th}}$  residual. Least-squares fitting is done by setting the  $n$  derivatives of  $L_2^2$  equal to zero, which gives a set of  $n$  linear equations which can be solved for the  $n$  fitting coefficients of  $\vec{d}$ :  $\mathbf{G}\vec{d} = \vec{s}$ , where  $\mathbf{G}$  is an  $n \times n$  matrix with elements  $G_{qr} = \sum_{i=1}^N W_i g_q(t_i) g_r(t_i)$ , and  $\vec{s}$  is an  $n$ -dimensional vector with elements  $s_r = \sum_{i=1}^N W_i x_0(t_i) g_r(t_i)$ . For the purposes of modelling the standard uncertainty, we use  $x_0(t_i)$  to model  $x(t_i)$ , since it can be shown [5] that any general offset in phase, offset in frequency or a linear frequency drift is exactly absorbed by the fit.

## Metafitting with Time Uncertainty Metric

One candidate metric for judging weighted least-squares fits is the standard uncertainty in time, determined at a specific time  $t$ , relative to the set of fitting points  $\{t_i\}$ . We can explicitly calculate the effects of the weighted least-squares fit reacting to the noise model for this time  $t$ : we are not restricted to studying the variance at the fitting points. The expected variance in  $x(t)$  from the fit  $\vec{d} \cdot \vec{g}(t)$  can be calculated in terms of the autocorrelation function  $\langle x_0(t_i) x_0(t_j) \rangle$ ,

$$\left\langle [x(t) - \vec{d} \cdot \vec{g}(t)]^2 \right\rangle = \sum_{i=0}^N \sum_{j=0}^N D_i(t) D_j(t) \langle x_0(t_i) x_0(t_j) \rangle, \quad (5)$$

where  $D_0(t) = 1$  and  $D_i(t) = W_i \sum_{q=1}^n \sum_{r=1}^n (\mathbf{G}^{-1})_{qr} g_r(t_i) g_q(t)$ . For the standard noise model, the autocorrelation function  $\langle x_0(t) x_0(t) \rangle$  can be evaluated analytically [5], although the resulting expressions can challenge the dynamic range of conventional computing. The square root of this variance in  $x(t)$  would be the formal metric. The minimization problem, for optimizing this metric with respect to the weights  $W_i$ , looks intractable, but for cases of most interest it can be substantially simplified in the same way as is described below for the frequency uncertainty metric.

Variants of this  $L_2$  metafitting metric are also possible, summing variances over multiple test times. Other metafitting metrics of the  $L_p$ -norm (Holder norm) class, could also be constructed. The min-max ( $\lim p \rightarrow \infty$ ) norm would minimize the maximum expected time deviation amongst the test times. Metafitting with the  $p = 1$  metric would (for this class of metrics) give the most leeway in allowing a small number of test points to have large variances. All these metafitting variants are

substantially more intricate to use, and do not readily yield the major computational simplifications which can be found for the single-point  $L_2$  metric.

The method outlined above does not bring any great new insights into optimal ways of combining equivalent clocks, nor for the optimal use of continuously operated primary standards, however when a secondary time scale is to track a primary time scale where only intermittent intercomparisons are available, an optimal choice could be made in terms of the noise processes known to be present.

## Metafitting with Frequency Uncertainty Metric

For precise time interval work, where the average frequency is the chief quantity of interest, we wish to minimize the standard uncertainty in average frequency over an interval  $[t, t + \tau]$ , caused by the noise model as filtered by the weighted least-squares fitting procedure to the points  $\{t_i\}$ . Although the noise model is independent of time translations, clearly the standard uncertainty in average frequency,  $u_y$ , would be expected to depend on the offset of  $t$  from  $\{t_i\}$ , as well as the interval breadth  $\tau$ . It is defined by

$$u_y^2(t, \tau) = \left\langle \left[ \left\{ \frac{x_0(t + \tau) - x_0(t)}{\tau} \right\} - \left\{ \frac{\vec{d} \cdot (\vec{g}(t + \tau) - \vec{g}(t))}{\tau} \right\} \right]^2 \right\rangle. \quad (6)$$

We note that  $\{x_0(t + \tau) - x_0(t)\} = \sum_{j=1}^{N+1} [x_0(t_j) - x_0(t_{j-1})]$ , if we define  $t_{j=0} = t$  and  $t_{j=N+1} = t + \tau$ . Although it might be convenient to envisage the set of  $\{t_j\}$  as an ordered set with  $t_j > t_{j-1}$ , it is not necessary to do so. Ordering the fitting points does not detract from the generality in any way, but we do not wish to restrict the values of  $t$  or  $t + \tau$ . We would like to re-express the  $\vec{d} \cdot \{g(t + \tau) - g(t)\}$  as a sum over only differences of the form  $x_0(t_i) - x_0(t_j)$ . We note that we can expand  $x_0(t_i) = x_0(t_1) + \sum_{j=2}^i \{x_0(t_j) - x_0(t_{j-1})\}$ , so that  $\vec{d} \cdot \{\vec{g}(t + \tau) - \vec{g}(t)\}$  is equal to

$$\begin{aligned} \mathbf{G}^{-1} \sum_{i=1}^N W_i x_0(t_i) \cdot \{\vec{g}(t + \tau) - \vec{g}(t)\} = \\ \sum_{i=1}^N W_i \sum_{j=2}^i \{x_0(t_j) - x_0(t_{j-1})\} \sum_{q=1}^n \sum_{r=1}^n (\mathbf{G}^{-1})_{qr} g_r(t_i) \{g_q(t + \tau) - g_q(t)\} \\ + x_0(t_1) \sum_{i=1}^N W_i \sum_{q=1}^n \sum_{r=1}^n (\mathbf{G}^{-1})_{qr} g_r(t_i) \{g_q(t + \tau) - g_q(t)\} \end{aligned} \quad (7)$$

and the last term, multiplying  $x_0(t_1)$ , can be shown to be equal to zero. To show this, it is sufficient to show that  $\sum_{i=1}^N W_i \vec{g}(t_i) \mathbf{G}^{-1} \vec{g}(t)$  is independent of  $t$ , or that  $\sum_{i=1}^N W_i \vec{g}(t_i) \mathbf{G}^{-1}$  is equal to the vector  $[1, 0, 0, \dots, 0]$ . We observe that, from our definition of  $\mathbf{G}$  and since  $g_1 = 1$ ,  $\mathbf{G}[1, 0, 0, \dots, 0] = \sum_{i=1}^N W_i \vec{g}(t_i)$ , and premultiplying by  $\mathbf{G}^{-1}$  completes this proof, provided only that  $g_1$  is a constant. Thus  $u_y^2(t, \tau) \tau^2$  is equal to

$$\begin{aligned}
& < \left[ \sum_{j=1}^{N+1} \{x_0(t_j) - x_0(t_{j-1})\} \right. \\
& - \sum_{i=1}^N W_i \sum_{j=2}^i \{x_0(t_j) - x_0(t_{j-1})\} \sum_{q=1}^n \sum_{r=1}^n (\mathbf{G}^{-1})_{qr} g_r(t_i) \{g_q(t+\tau) - g_q(t)\} \left. \right]^2 > = \\
& < \left[ \{x_0(t_{N+1}) - x_0(t_0)\} - \sum_{i=1}^N W_i \{x_0(t_i) - x_0(t_{i-1})\} \sum_{q=1}^n \sum_{r=1}^n (\mathbf{G}^{-1})_{qr} g_r(t_i) \{g_q(t+\tau) - g_q(t)\} \right]^2 >
\end{aligned} \tag{8}$$

Collecting the expressions with the same difference term  $\{x_0(t_j) - x_0(t_{j-1})\}$  allows us to write a useful form, namely

$$u_y^2(t, \tau) \tau^2 = < \left[ \sum_{j=1}^{N+1} \tilde{D}_j(t, \tau) \{x_0(t_j) - x_0(t_{j-1})\} \right]^2 >, \tag{9}$$

where for  $2 \leq j \leq N$ ,  $\tilde{D}_j(t, \tau) = 1 - \sum_{i=j}^N W_i \sum_{q=1}^n \sum_{r=1}^n (\mathbf{G}^{-1})_{qr} g_r(t_i) \{g_q(t+\tau) - g_q(t)\}$ ;  $\tilde{D}_{j=1}(t, \tau) = 1$  and  $\tilde{D}_{j=N+1}(t, \tau) = 1$ . Multiplying the terms explicitly gives a computable form for the standard uncertainty in average frequency:

$$u_y^2(t, \tau) \tau^2 = \sum_{j=1}^{N+1} \sum_{k=1}^{N+1} \tilde{D}_j(t, \tau) \tilde{D}_k(t, \tau) < [x_0(t_j) - x_0(t_{j-1})][x_0(t_k) - x_0(t_{k-1})] >. \tag{10}$$

The utility of this form lies in the fact that it is a sum over functions of the general form of Eq. 2, which are easier to compute for our full noise model.

## Metafitting Weights for Large Data Sets

For a given noise model (defined by the 5 parameters  $\{h_\alpha\}$  used to define  $S_y(f)$ ), and a given distribution of fitting points  $\{t_j\}$ , and for a given interval  $[t, t + \tau]$ ; the standard uncertainty in average frequency over the interval can be calculated:  $u_y(t, \tau)$ . Thus a choice of weights can be determined which minimizes  $u_y(t, \tau)$ , the standard uncertainty due to the effects of the random noise. For each fitting point added, another weight must be determined. For small sets of fitting points, the minimization problem is tractable, but for larger sets the minimization appears much less straightforward. The weights could be parameterized to reduce the dimensionality of the problem, at the expense of generality.

The full generality can be retained by largely linearizing the problem. For  $N$  fitting points, there are also  $N$  weights to choose. Without loss of generality, the set of weights  $\{W_i\}$  can be normalized:  $\sum_{i=1}^N W_i = 1$ . If the partial derivative of  $\mathbf{G}^{-1}$  with respect to  $W_k$  can be constrained to be zero, then most of the  $N$ -dimensional search problem can be linearized, leaving a nonlinear search over at worst

$[(n(n+1)/2) - 1]$  dimensions.  $\mathbf{G}^{-1}$  will be independent of  $W_k$  if each element of  $\mathbf{G}$  is constrained to be a constant,  $G_{qr} = \sum_{i=1}^N W_i g_q(t_i) g_r(t_i)$ . Since  $G_{qr} = G_{rq}$ , and since normally  $g_1 = 1$ , there remain  $[(n(n+1)/2) - 1]$  values. These constraint equations are used in the linear solution, and the optimum values of  $G_{qr}$  can subsequently be found by nonlinear searching techniques.

For polynomial fitting, with  $n$  basis functions  $\{g_k(t) = t^{k-1}\}$ , the partial derivative of  $\mathbf{G}^{-1}$  with respect to  $[N - 2n + 2]$   $W_i$ 's there would be only  $[2n - 2]$  dimensions for the non-linear search, and if the problem can be set up symmetrically about the time origin, so that the first moment of the weights and all odd moments are zero, there would be only  $[n - 1]$  non-linear search parameters. The even moments of the weights (summed over the fitting times  $\{t_i\}$ ) would then be the  $[n - 1]$  non-linear search parameters. If the problem is intrinsically asymmetric, then there would be  $[2n - 2]$  moments to use as nonlinear search parameters. For extrapolation, it seems clear that there will be little likelihood of driving any  $W_i$  negative, but it remains a concern for the general case and must be guarded against.

Consider for example the case of choosing a weighted least-squares fit of a general quadratic to  $N$  phase comparison data points at a specific set of times  $\{t_i\}$ . For a specific noise model described by the coefficients  $\{h_\alpha\}$ , we want to choose the weights to minimize the standard uncertainty in the average frequency over the time interval  $[t, t + \tau]$ . By constraining weights to sum to 1, and by constraining the first through fourth moments of the weights to be independent of the first  $[N - 4]$  weights, we can ensure that  $\mathbf{G}^{-1}$  is independent of  $[N - 4]$  weights. By equating to zero the  $[N - 4]$  partial derivatives of  $u_y^2(t, \tau)$  with respect to  $W_i$  we can minimize the standard uncertainty in average frequency with respect to these  $[N - 4]$  weights. The easiest form to differentiate for this purpose is one like that of Equation 8, which has collected all the terms multiplied by any weight  $W_i$ . Including the constraint equations, we then have  $N$  linear equations in the  $N$  unknown weights  $\{W_i\}$ , parameterized in the 4 moments remaining to be searched. The optimized standard uncertainty for this set of four moments is evaluated, and a four-parameter search (each set of moments being optimized by re-solving the  $N$  linear equations) this search is tractable by the simplex method (for example). If the problem is symmetric about some time (symmetry for both  $\{t_i\}$  and  $[t, t + \tau]$ ), it can be set up so that the first and third moments are zero, and there would be only two parameters to search.

Choosing weights is simpler for a **linear** least-squares fit to  $N$  phase comparison data points, taken at a specific set of times  $\{t_i\}$ . To metafit the best weights that minimize the standard uncertainty in the average frequency over the interval  $[t, t + \tau]$  for the noise model of interest, described by the coefficients  $\{h_\alpha\}$ , we can again linearize the problem - but with only two search parameters (the first and second moments of the weights). We define three constraint equations  $\sum_{i=1}^N W_i = 1$ ,  $\sum_{i=1}^N W_i t_i = M_1$  and  $\sum_{i=1}^N W_i t_i^2 = M_2$ . The  $N$  partial derivatives, with respect to the weights, of the standard uncertainty in average frequency over the interval  $[t, t + \tau]$  give a set of  $N$  equations  $\mathbf{F} \cdot \vec{W} = \vec{r}$ , where  $F_{ij} = (t_i - M_1)\tau / (M_2 - M_1^2) < [x_0(t_i) - x_0(t_1)][x_0(t_j) - x_0(t_1)] >$  and  $r_j = < [x_0(t + \tau) - x_0(t)][x_0(t_j) - x_0(t_1)] >$ . The first column of  $\mathbf{F}$  is a column of zeros. Three of these equations are to be replaced by the three constraint equations: one replacement is for the most ill-conditioned equation  $j$  which has  $t_j$  closest to the centroid of the weights ( $M_1$ ) for this iteration, the other two replacements are more arbitrary. If the problem is symmetric about some time (symmetry for both  $\{t_i\}$  and  $[t, t + \tau]$ ), it can be set up so that the first moment is zero, and there would be only one parameter to search.

An even simpler case of metafitting is the choice of weights in a simple weighted average, for multiple calibration runs to minimize the standard uncertainty in the average frequency for a specific period, arbitrarily placed with respect to the calibration runs. We consider calibration intervals long enough to be in the regime where the two end point method is chosen for each calibration run, with  $M$  such calibration intervals  $[t_i, t_i + \tau_i]$ . For the weighted average of the  $M$  calibrations, the standard uncertainty in the average frequency over an interval  $[t, t + \tau]$ ,  $u_y^2(t, \tau)$  is

$$u_y^2(t, t + \tau) = \left\langle \left[ \frac{\{x(t + \tau) - x(t)\}}{\tau} - \sum_{i=1}^M w_i \frac{\{x(t_i + \tau_i) - x(t_i)\}}{\tau_i} \right]^2 \right\rangle. \quad (11)$$

Assigning a weight of  $-1$  to the interval  $[t, t + \tau]$ , defining  $\tau_0$  as being equal to  $\tau$ , Equation 11 can be rewritten as

$$u_y^2(t, t + \tau) = \left\langle \left[ \sum_{i=0}^M \frac{w_i}{\tau_i} \{x(t_i + \tau_i) - x(t_i)\} \right]^2 \right\rangle. \quad (12)$$

A solution for the optimum weighting procedure is relatively easy to find since the minimum value for  $u_y^2(t, t + \tau)$  is to be found for values of  $w_i$  satisfying  $\frac{\partial}{\partial w_k} [u_y^2(t, t + \tau)] = 0$ , so that after taking the derivative and separating out the  $i = 0$  term

$$\begin{aligned} \sum_{i=1}^M \frac{w_i}{\tau_i \tau_k} \langle [x(t_i + \tau_i) - x(t_i)][x(t_k + \tau_k) - x(t_k)] \rangle \\ = \frac{1}{\tau_k} \langle [x(t + \tau) - x(t)][x(t_k + \tau_k) - x(t_k)] \rangle. \end{aligned} \quad (13)$$

We use  $M - 1$  of these equations, and for the  $M^{\text{th}}$  equation we use the normalization equation of the weights:  $\sum_{i=1}^M w_i = 1$ . This gives  $M$  simultaneous linear equations in the  $M$  unknown weights. The general interval covariance has analytic forms for our noise model, in terms of the  $\mathcal{I}$ -function [4]. If we define the  $M \times M$  matrix  $\mathbf{F}$ :  $F_{1,j} = 1$  for  $j = 1..M$ ,  $F_{i,j} = \frac{1}{\tau_i \tau_j} [\mathcal{I}(t_i + \tau_i - t_j) + \mathcal{I}(t_j + \tau_j - t_i) - \mathcal{I}(t_i + \tau_i - t_j - \tau_j) - \mathcal{I}(t_i - t_j)]$  for  $i = 2..M$  and  $j = 1..M$ , and define  $\vec{r}$ :  $r_1 = 1$  and  $r_j = \text{frac}1\tau\tau_j [\mathcal{I}(t + \tau - t_j) + \mathcal{I}(t_j + \tau_j - t) - \mathcal{I}(t + \tau - t_j - \tau_j) - \mathcal{I}(t - t_j)]$  for  $j = 2..M$ . The  $M$  dimensional weights vector  $\vec{w}$  is  $\mathbf{F}^{-1} \cdot \vec{r}$ .

## Applications

For any given potential application of metafitting weights, we must consider whether metafitting is more than an interesting academic exercise: can metafitting find a reduction in the standard uncertainty which is a significant improvement? Since uncertainties are rarely established to better

than 10%, an improvement should be larger than this to be deemed significant. Therefore we have examined the simplest case, of linear extrapolation, discussed above, and for the five different power-law noise types we have considered distributions of weights with different moments [6]. We have examined the expected standard uncertainty for both symmetric extrapolation suited to time-scale calibration (where post-processing can be used to apply calibrations from the “future”) and to time-asymmetric extrapolation suited to real-time applications. For symmetric extrapolation intervals that are large compared to the calibration run’s duration, different common weight distributions gave similar uncertainties (differing by less than 10%) except for white phase noise. For one-way extrapolation for times much longer than the calibration run’s duration, the uncertainties are even more similar (less than 2% advantage for end-point fitting over equal weights, except for white phase and flicker phase noise). Thus for many PTTI applications, end-point fitting and equal-weight fitting give similar standard uncertainties, and the choice should be between the greater simplicity of the end-point fit and the greater robustness of the equal-weights fitting procedure.

In real-life PTTI work, robustness would often prevail over simplicity. For trying to optimize results from multiple calibration runs, simplicity is valuable to us while robustness is not needed in the model. The optimum processing of a number of calibration runs is expected to be largely independent of the processing within the run.

The main application which has attracted our attention is the optimal use of hydrogen masers, calibrated periodically in frequency with intermittently operated cesium fountain frequency standards [8], [6]. We consider two types of maser operation: free-running and autotuned. We use two power law models for the maser noise, representing a free-running hydrogen maser (type 1) with  $h_2 = 2.7 \times 10^{-24}$ ,  $h_1 = 2.9 \times 10^{-30}$ ,  $h_0 = 2.9 \times 10^{-27}$ ,  $h_{-1} = 2.6 \times 10^{-31}$  and  $h_{-2} = 7.2 \times 10^{-36}$ ; and an auto-tuned maser (type 2) with  $h_2 = 6.7 \times 10^{-23}$ ,  $h_1 = 2.9 \times 10^{-30}$ ,  $h_0 = 2.9 \times 10^{-27}$ ,  $h_{-1} = 7.2 \times 10^{-31}$  and  $h_{-2} = 4.9 \times 10^{-37}$ . NRC has two low-flux masers which would benefit from a metafitting optimization of the weights *within* a calibration run of an hour, since there is still some white phase noise contribution for this calibration interval. Preliminary analysis suggests that the end-point procedure is within 10% of the optimum. For phase data taken every 30 s for an hour, extrapolated to an interval of a day, the end point method is 1.2% better than the equal-weight linear least squares fit for our free-running maser model, and as good for the type 2 maser model. Thus we can use the simple two end points procedure to establish the best frequency transfer accuracy for multiple calibration runs. For this procedure the standard uncertainty for multiple calibration runs can be calculated more easily than in the general case.

Within the context of end-point fitting from each calibration run there are still metafitting choices to be made about the way in which the runs are to be used. One possible strategy is a loose lock in frequency: after a calibration run (an hour in duration, in our example) is complete, the frequency of the maser is reset (through the synthesizer control, for example), either immediately - or after some delay. Clearly the least delay is best, and we chose this procedure with zero delay as the reference procedure as we examine a series of possible improvements.

A slightly better possibility might be to have an output tightly locked in phase to the cesium fountain during the calibration run, followed by a frequency lock to the fitted frequency of the calibration run. The phase-lock type of frequency control removes the noise of the maser during the calibration run, giving it an advantage that remains noticeable for extrapolation intervals many times longer than the calibration interval. However, for extrapolations of an hour-long calibration

out to a period of a day or more, there is not a large advantage: 2.3% for the free-running maser and 2.4% for the autotuned maser model.

A more significant advantage comes from allowing postprocessing, as can often be tolerated in time-scale construction and for frequency intercomparisons. We consider a single calibration interval  $t_c$  and calculate the ratio of the standard uncertainty of the average frequency over an interval  $\tau$  for the best real-time frequency control to the symmetrically extrapolated time interval  $\tau$ . The quantitative postprocessing advantage will depend upon the specific processing scheme or schemes envisaged - the duration and frequency of calibration intervals. The postprocessing advantage is up to a factor of two [6].

A postprocessing advantage of two is really quite significant. To achieve the same improvement in the maser ensemble could be done - by increasing the maser ensemble size by four times. The postprocessing advantage of greatest interest to us is for  $\tau$  representing extrapolation to the time interval between calibrations - which we expect would be between 1 day and 1 week. Initial interlaboratory frequency intercomparisons between cesium fountains, before regular calibration schedules can be set up, may require extrapolation times longer than 1 week for minimum uncertainty.

Envisaging multiple frequency calibration runs per week, of either hydrogen maser type with a cesium fountain having a standard uncertainty of  $10^{-14}\tau^{-1/2}$  optimistically 5 per week, at the same time each working day, what is the best weighting procedure for using these calibrations in an algorithm to determine the frequency over a given interval? For the week's pattern, postprocessing extrapolation of each day's results independently, using the frequency from the nearest calibration interval gives a 77% improvement in accuracy for the free-running maser, and an improvement of 29% for the auto-tuned maser.

We have solved for the optimum weights of the maser calibrations to give the lowest standard uncertainty in average frequency over one week [6]. The week is best spanned by weighting Monday and Friday runs more heavily, to account for the weekend gap in calibrations. For the type 1 maser, the optimum weights follow the spanning times rather closely, and the optimum weights offer only a 1.1% improvement in average frequency. For a type 2 maser, there is a 4.7% improvement.

If adjacent weeks' calibration runs are also available, and the average frequency over a particular week is required, the optimum metafitting includes a small admixture from the preceding and the following weeks. For a type 1 maser, most of the weight comes from the preceding Friday and the following Monday. For an autotuned (type 2) hydrogen maser noise model, the optimum weights have a slower variation through the weeks, and the three-week optimum has several % of the weight on points that are a full week from the calibration runs of the central week. There is a 19% improvement to the type 1 maser, and an 18% improvement for the type 2 maser. The improvements are summarized in Table I, given with standard uncertainties and cumulative advantages as each improvement is applied. For either maser model, the optimization of weights to apply to each run over multiple weeks gives about a 20% improvement in accuracy from the equal-weight case. It is not a large improvement, but it is almost free - although it does give additional cross-correlation between each week's frequency processed in this way. Cascaded with the other advantages discussed earlier, it results in a factor of 2.2 improvement in the accuracy transferrable with a free-running (type 1) hydrogen maser; and an improvement of 64% for the auto-tuned (type 2) maser. For the free-running maser model, the metafitted optimum standard uncertainty is 6.8 times smaller than

method	Type 1			Type 2		
	$u_y(7d)$	Adv.	Cum. adv.	$u_y(7d)$	Adv.	Cum. adv.
I $f$ reset to unweighted fit	$1.79 \times 10^{-15}$		1.00	$1.15 \times 10^{-15}$		1.00
II $f$ reset to end points	$1.77 \times 10^{-15}$	1.2%	1.01	$1.15 \times 10^{-15}$	0%	1.00
III phase lock + II	$1.73 \times 10^{-15}$	2.3%	1.04	$1.12 \times 10^{-15}$	2.4%	1.02
IV daily postprocessed	$0.97 \times 10^{-15}$	77%	1.83	$0.87 \times 10^{-15}$	29%	1.32
V metafit 1 week	$0.97 \times 10^{-15}$	1.1%	1.85	$0.83 \times 10^{-15}$	4.7%	1.39
VI metafit 3 weeks	$0.81 \times 10^{-15}$	19%	2.21	$0.70 \times 10^{-15}$	18%	1.64
VII metafit 5 weeks	$0.81 \times 10^{-15}$	0%	2.21	$0.70 \times 10^{-15}$	.1%	1.64
$\sigma_y(7d)$	$5.48 \times 10^{-15}$			$1.72 \times 10^{-15}$		

Table 1: Reduction of standard uncertainty in average frequency at 7 days, for a free-running (type 1) maser, and an autotuned maser (type 2), when controlled by different methods from five 1-hour calibrations per week. The % advantage for each method is the accuracy improvement over the previous method. The last column gives each method's cumulative advantage over method I, a synthesizer reset to the least-squares calibration fit. The Allan deviation  $\sigma_y(\tau = 7d)$  is also given.

the Allan deviation at 1 week, and for the type 2 maser it is 2.5 times smaller than the Allan deviation at 1 week.

Other interesting strategies are beyond the scope of this work. Longer runs on Monday and Friday and/or early-Monday and late-Friday calibration runs could be invoked to further improve the performance. Our methods allow for weight optimization for any set of calibration runs, and for calculating the resulting standard uncertainty in average frequency.

For some applications, statistical independence of each week, or each 10-day period, may be highly valued - for example, the clock reports to BIPM each 10 days that are used for determining TAI (and UTC) should be independent of each other. Weights for data from the weekly calibration cycle could be re-optimized for the seven different 10-day cycles that would exist. The metafitted optimum weights for the two maser models are shown in Figure 1. For the free-running maser model, the 70-day standard uncertainty in average frequency is  $3.31 \times 10^{-16}$  for the combination of the seven independent optimized 10-day periods, as compared to  $3.07 \times 10^{-16}$  for the combination of 10 independent 7-day periods. For the autotuning maser model, the 70 day standard uncertainty in average frequency is  $2.72 \times 10^{-16}$  for the combination of the seven independent optimized 10-day periods, as compared to  $2.62 \times 10^{-16}$  for the combination of 10 independent 7-day periods.

## Conclusion

Our method for calculating the standard uncertainty for realistic noise models has allowed us to compare a wide variety of algorithms for treating one particular calibration schedule. We have metafitted the algorithm in several ways, and have identified ways to improve the accuracy of the maser frequency control by 2.2 and 1.64 times. We find that using the 10-day BIPM schedule, with independent processing of the calibrations for the 10-day periods, the expected asymptote for a

single auto-tuned (type 2) maser could reach  $1.2 \times 10^{-16}$  at 1 year. For a free-running (type 1) maser, the standard uncertainty at 1 year would be  $1.5 \times 10^{-16}$ . Thus a flicker floor and accuracy of  $10^{-16}$  for the cesium fountain is accessible for periods of a year with current masers carrying the time scale. Operating the masers at the stability level of the masers presents a challenge. Transferring  $10^{-16}$  frequency accuracy to a second laboratory also presents a challenge. The reliability of a cesium fountain which might do this seems to be a major challenge, perhaps comparable to the challenge of making a cesium fountain with a flicker floor and accuracy of  $10^{-16}$ . Perhaps the greatest value of this metafitting procedure is to show the very best performance which might be extracted from masers represented by these models. If greater accuracy is desired, then different approaches must be used.

## References

- [1] **Guide to the Expression of Uncertainty in Measurement**, International Organization for Standardization, Geneva, 1993. First edition. (Published in the name of BIPM, IFCC, ISO, IUPAC, IUPAP and OIML.)
- [2] A. Papoulis, **Probability, Random Variables, and Stochastic Processes**, McGraw-Hill, New York, 1965. First edition pp. 400-402. (Omitted from subsequent editions.)
- [3] R.J. Douglas and J.-S. Boulanger, **Local Oscillator Requirements for Timekeeping in the  $10^{-14}\tau^{-1/2}$  era**, *Proceedings of the 1992 IEEE Frequency Control Symposium*, pp. 6-26 (1992).
- [4] D. Morris, R.J. Douglas and J.-S. Boulanger, **The Role of the Hydrogen Maser Frequency transfer from Cesium Fountains**, *Japanese Journal of Applied Physics*, **33**, pp. 1659-1668 (1994).
- [5] R. J. Douglas., J.-S. Boulanger and C. Jacques, **Accuracy Metrics for Judging Time Scale Algorithms**, *Proc. 25th Annual PTTI Applications and Planning Meeting*, pp. 249-266 (1993).
- [6] J.-S. Boulanger and R.J. Douglas, **Frequency Control of Hydrogen Masers Using High Accuracy Calibrations**, *Proceedings of the 1994 IEEE Frequency Control Symposium*, pp. 695-708 (1994).
- [7] D.W. Allan, **Time and Frequency (Time-Domain) Characterization, Estimation, and Prediction of Precision Clocks and Oscillators**, *IEEE Trans. Ultrason., Ferroelec., Freq. Contr.* **UFFC-34**, pp. 647-654, (1987).
- [8] J.-S. Boulanger, D. Morris, R. J. Douglas. and M.-C. Gagné, **Hydrogen Masers and Cesium Fountains at NRC**, in *Proc. 25th Annual PTTI Applications and Planning Meeting*, pp. 345-356 (1993).
- [9] J.A. Barnes, A.R. Chi, L.S. Cutler, D.J. Healey, D.B. Leeson, T.E. McGunigal, J.A. Mullen Jr., W.L. Smith, R.L. Sydnor, R.C. Vessot and G.M.R. Winkler: **Characterization of Frequency Stability**, *IEEE Trans. Instrum. Meas.* **IM-20**, pp. 105-120 (1971).

Autotuned Maser —————  
 Free-running Maser ······

### Optimum Weights for Weekday Calibration of 10-day Average Frequency

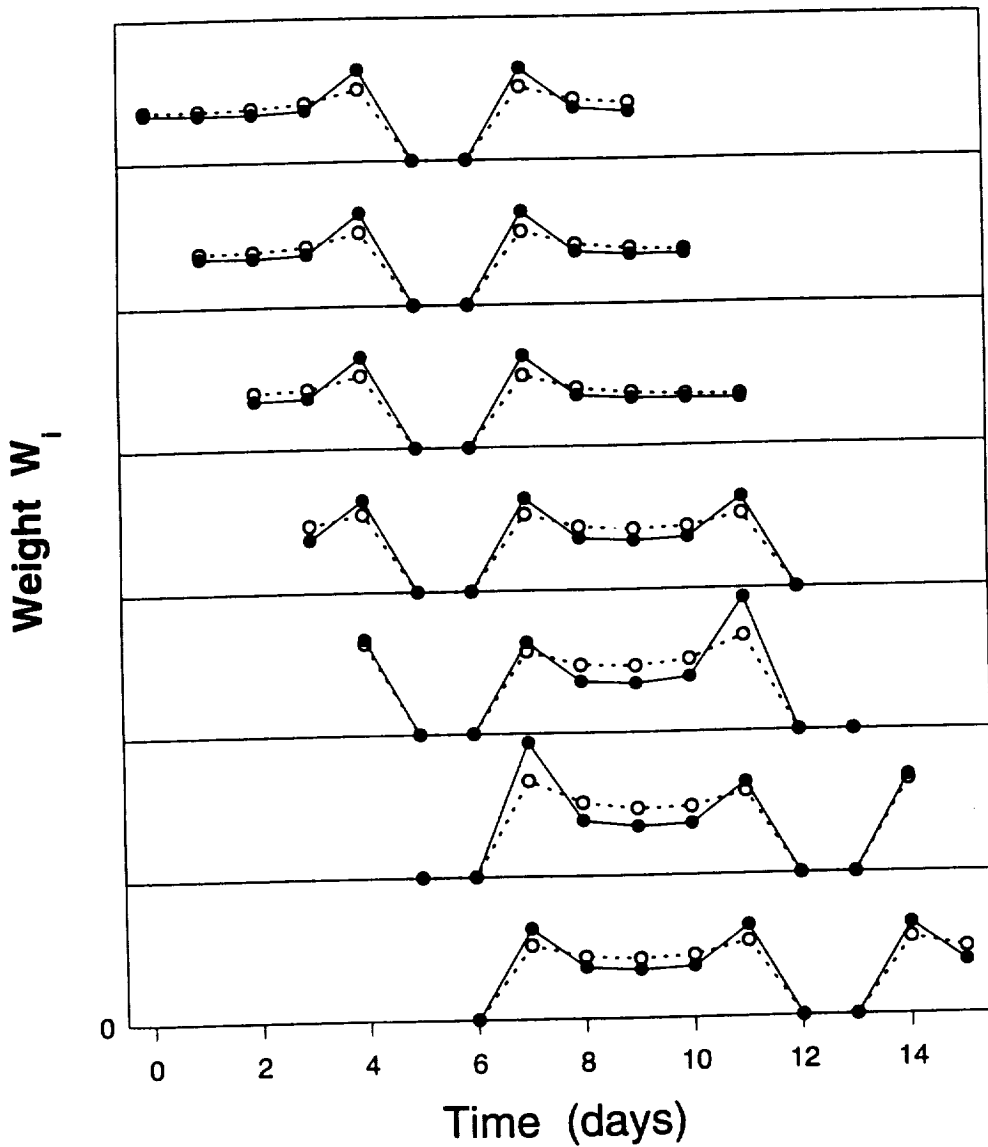


Figure 1. Optimum weights for combining weekday calibrations that give the minimum standard uncertainty in the average frequency over a 10-day interval. The calibrating reference standard is taken to be an ideal one, used for one hour, at the same time every working day. The optimum weights are shown for two flywheel oscillators: a free-running hydrogen maser model and an auto-tuned maser model. The optimum weights are shown for a the 10-day period starting on each day of the week.

# Methodologies For Steering Clocks

H. Chadsey, USNO

## Abstract

*One of the concerns of the PTTI community is the coordination of one time scale with another. This is accomplished through steering one clock system to another, with a goal of a zero or constant offset in time and frequency. In order to attain this goal, rate differences are calculated and allowed for by the steering algorithm. This paper will present several of these different methods of determining rate differences. Ideally, any change in rate should not cause the offset to change sign (overshoot) by any amount, but certainly not by as much as its previous absolute value. The advantages and disadvantages of each depend on the user's situation.*

## INTRODUCTION

Although control system theory is not new, it has been more highly developed in some fields than others. One good example is rocket science and the degree of control theory development needed for the US Space Shuttle to "catch" the Hubble Space Telescope in December of 1993. The trick was to meet up with the orbiting unit and grab it. If the control was wrong, the Shuttle would not reach the unit; pass by it; or, worse, crash into it. This approach to an offset (in position) is done through the precise firing of rockets. It is a very critical operation because the rockets have only two states: off and full thrust.

The same type of problem faces a laboratory trying to steer the frequency of a clock. The objective is to maintain a clock at zero (or some other fixed) time offset from some reference clock. While steering to the desired value, the offset should not be allowed overshoot by any amount, but most certainly not by the same or more than its previous maximum offset. An important difference is that more precise clock control can be obtained because a variable steer rate algorithm can be determined. This can be done by taking the principles of control theory as applied in other fields of operation and applying them to the control of clocks.

## REASON TO STEER

The need for steering may be understood by looking at what happens when no steering is attempted. A lab might only monitor the time offset of the clock to some standard periodically (hourly, daily, weekly, etc.). From these periodic measurements, missing values would be derived by interpolation, operations would be carried out with no controlling of the clock. For some applications, especially if they are performed over short periods of time, this is acceptable. However, all clocks have a rate which changes. This is called drift and it is not constant. As

a result, the clock will be very far ahead or behind and vary in offset amount when compared to the reference clock, creating problems for some operations. (See Figure 1.)

## STEERING METHODS

To correct for the drift of a clock, the most rudimentary of steering methods can be used. For example, the clock may be closely monitored and allowed to increase the offset value as compared to the standard. Once the clock has reached a predetermined offset, it may be time-stepped to a different value. Operations continue by using the varying offset values and interpolating between them as needed. This is much like the example of the Space Shuttle cited earlier, where the space craft is allowed to drift, controlled through the use of varying-length, full-throttle corrective actions. In the controlling of cesium clocks with this method, there are two major potential problems. First, operations can be disrupted when the clock is time-stepped. This can in some cases be avoided by performing the steps at times when the clock is not being used for operations. When the clock is adjusted, very close monitoring must be performed and methods developed to determine values of offset during the stepping procedure. Second, cesiums and many other types of clocks can have their characteristics changed when they are time-stepped. Cesium clocks have been known to change their drift rate when adjustments of any type are made to them. Again, it depends on how the clocks are being used whether this will have an adverse effect on operations. (See Figure 2.)

We turn now from the manipulation of the clock to controlling of the output from the clock. Timing is controlled, not by adjusting the clock itself, but through adjustment of its output with a phase microstepper or similar device.

The most efficient and drastic of these steering adjustments is commonly referred to as the "Bang-Bang" mode of operation. The crudest form is the two-stage steering algorithm. This is the method currently employed by the GPS Master Control Station to control GPS time. This methodology lets the clock(s) drift at its natural rate until a predetermined offset is reached. At that time, a frequency change is made to the output (using a phase microstepper, or adjustment of the clock, etc.). The new drift rate of the output is in the opposite direction and at a greater rate than the natural drift of the clock. This new rate is kept until the clock reaches another predetermined offset value, when the rate is again changed back to its first value. These rates are currently  $\pm 1.0 \times 10^{-19}$  seconds per second squared for the GPS system. As a result of this two value steering, the clock oscillates between the extreme offset values. Because the natural rate of the clock is in only one direction, the "wave" is asymmetric. (See Figure 3.)

The next step in complexity is the three-stage steering algorithm. Here, one has the additional state of a zero rate of steer to the system. The theory is that while the clock offset is within a narrow range of offset, a zero rate of steer is employed by the system. When the offset is outside this narrow range, the upper or lower steer rate is employed to move the clock to within the narrow offset range when the zero rate is again used. While this is very easy to perform programmatically, it still does not correct for the natural rate of the clock. It can also produce a wave pattern which may not be stable enough for the operational use of the clock output. (See Figure 4.)

The previous steering methods use a fixed, predetermined rate of adjustment. We next consider the possibilities of enhancement to a system when a variable rate adjustment is implemented. First, when the rate is not fixed, we will discuss how it is determined. Second, we will see how the rate correction is applied.

One of the first conclusions is that the clock can now be adjusted for its natural drift. We no longer have to hassle with an asymmetric wave of offsets. But how can the natural drift rate be determined?

One method would be to subtract the first data point collected after the last rate change was applied from the last data point collected and divide by the number of days in the interval between them. This would result in a rate per day which can easily be used to calculate an adjustment. This method, however, does have a potentially large fault. If the data are noisy, the rate determined could be of the wrong magnitude and/or sign.

A second method would be to take an average of the differences between successive days of data. This would reduce the likelihood of problems. For a well-behaved system, the taking of successive differences will allow one to construct where the next data point will lie. As a result, a rate change can be determined and tested before it is applied to the system. The problems here are that, depending on the precision of measurement and control desired, the clock system may not be a well-behaved system; large amounts of data are required which are not always available; and this method does not react well to sudden change, such as a clock jump.

A third method would be to perform some type of data analysis on the data points in order to find the slope of the values. A system of tracking the rate of change of a moving average or linear line fitting with slope determination over short time periods does very well. It is improved when, on larger data sets, a data filter is used to remove outlying points. After some testing, I chose the linear fit method because of its more direct approach, its flexibility to filter outlying points, and the fact that "one cannot design a filter better than the optimum linear filter".

Now that we have a way of determining the natural drift of the clock, we can use that to help in controlling it. This leads to a methodology I will refer to as graduated steering. It is graduated because the rate of correction applied is no longer fixed, but varies according to some algorithm. Because we can determine the natural drift of the clock by one of the methods previously discussed, it follows that we should use that as a starting point for the amount of the change.

For example, if the rate of the clock was found to be positive 30 nanoseconds per day, then we can apply a rate of -30 nanoseconds per day by use of a phase microstepper. The result would be a clock with a zero rate of change as compared to the reference standard. (The change can also be an adjustment of the C-field, but a phase microstepper allows for finer adjustments.)

Now that we have created a clock with a zero drift, we must get a zero offset to the reference clock in order for our operational requirements to be met. This could be done by time stepping ("banging") it back to zero. This would require the calculation and manual operation of the time step. It would also mean that our operation could be disrupted by the time

step. The long-term complication would be that if the natural rate of change for the clock was not determined exactly, after a period of time the procedure would have to be repeated. This requires constant monitoring of the system, training of personnel in how to make the corrections, and ascertaining that the corrections are made when they are needed.

The correction to a zero (or near zero) offset can be performed by modifying the rate determination program to also add a small amount to that required to achieve zero drift. But, how should this additional amount be determined? A method that was used at USNO based the additional amount on the clock drift. This was found to lead to some undesired effects. Using the offset value as a factor for additional calculation provides much better control of the clock. The idea of steering back to a zero offset should be based not only on the rate at which one is moving toward or away from it, but also on the present offset value. If, for instance, one's clock has a rate of 50 nanoseconds per day and the current offset is zero, one would then introduce a rate change of -50 nanoseconds per day to achieve zero offset. On the other hand, if one's clock has a rate of 50 nanoseconds per day and the present offset value is 100 nanoseconds, one would introduce a rate change of -50 nanoseconds per day to correct for the rate of the clock plus an additional amount to get back to zero offset. The additional amount could be the present offset value divided by some damping factor, say 4. In this case, the offset would be zero in 4 days time and another rate correction introduced to flatten the rate of the clock. This method of simple graduated steering will correct for the natural drift of the clock and if the clock is offset from a standard reference, it will adjust it back to zero offset. The USNO Master Clock is steered in a similar fashion.

Under ideal circumstances, this simple graduated steering method works fairly well. The complication arises when one is unable to make one or more of the rate corrections. This can be caused by the failure of one computer to instruct another controlling the microstepper to make a change (e.g. because of a faulty phone connection), by computer or microstepper failure, or, if the operation is performed manually, by the absence of required personnel. The magnitude of this error can be lessened if a damping factor is used or if the one in use is increased.

## **PRESENT USNO STEERING METHOD**

The present USNO method of steering remote clocks has developed into a very sophisticated process that is totally computer-controlled. Operator intervention is needed only in case of equipment failures or other extraordinary events (e.g. clock jumps or clock replacement). The process begins by a program determining the offset of the remote clock from the USNO Master Clock using GPS. This can be done using one of several methods. USNO currently uses the 48-hour running linear-fit melting-pot method. Once the offset for a series of days has been determined, the steering rate determination program begins to work.

The program to determine an adjustment to the phase microstepper performs several tests before the calculation is actually performed. The first test is to determine whether or not a steer correction is permissible. There is a big danger in calculating rate changes using data that contains a mix of data from before and after implementation of the last rate correction. Calculation using mixed data can lead to the steering process causing the clock offset values

to oscillate in a very extreme manner. (See Figure 5.) Because of this danger and the use at USNO of the two-day fit method of GPS data processing, the steer rate determination does not use any offset values two days following the implementation of the last correction.

The next test is to make sure that there are enough data to determine an accurate rate of the remote clock. This requires at least two days of data. The more data collected, the more accurate the determination will be. However, if too many days are used, problems such as fast reaction to clock jumps and clock replacement will be created. So, when possible, the minimum amount of days between steers is used.

As a result of the these first two tests performed by the program, rate changes to the remotely controlled clocks occur no sooner than once every four days. Combination of the avoidance of mixed data and use of sufficient data points can improve clock stability by a factor of ten.

The actual rate change is then determined. From the above tests and predictions of the offset, it is easy to determine whether the clock is moving toward or away from zero offset and whether the offset changed sign during the time between the last rate correction and the present or will change sign before the time of the next rate correction. Programmatically, this creates a four-state test switch:

1. All collected and predicted values are of the same sign and the trend is toward a zero offset. In this case, the steer rate change would be the predicted value divided by the damping factor and again divided by the number of days between steer rate changes. This double division prevents overcorrection of the clock.
2. All collected and predicted values are of the same sign and the trend is away from a zero offset. In this case, the rate change would be the rate of the clock away from zero to flatten the clock rate plus an additional amount to direct the clock back toward zero. This additional amount would be the predicted value divided by the damping factor. The number of days between steers is NOT used in the divisor, as this would not cause the clock to turn around its direction of offset travel. Overcorrection is kept to a minimum because of the time intervals at which events occur. The correction is applied when the clock has already moved further away from zero than the collected data indicate.
3. All collected values are of one sign and the predicted value is of the opposite sign. In this case, it was found from the many possible ways it can occur that the best correction is to make the rate change equivalent to the rate of clock, thus zeroing the clock rate.
4. Some of the collected values are of one sign and the rest of the collected values and the predicted value of the opposite sign. In this case, the rate change would again be the rate of the clock away from zero to flatten the clock rate, plus an additional amount to direct the clock back toward zero. This additional amount would be the predicted value divided by the damping factor. The number of days between steers is NOT used in the divisor, as this would not cause the clock to turn around its direction of offset travel. Overcorrection is kept to a minimum because of the time intervals at which events occur. The correction is applied when the clock has already moved further away from zero than the collected data indicate.

The correction is then placed in units of nanoseconds rate of change per day. Another program implements the change in the phase microstepper at the remote unit. The process is complete until the next correction is needed.

## **RESULTS OF STEERING**

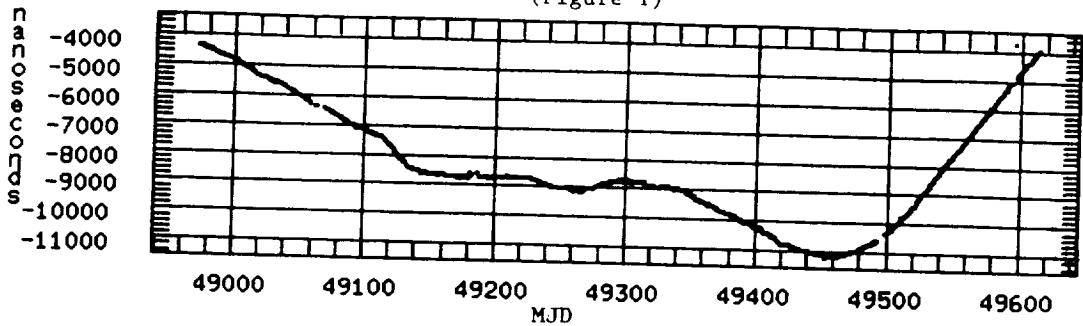
Figures 6 and 7 show the results of the implementation of the present control program for two sites. The clock being controlled in Figure 6 is located in the office area of an Air Force PMEL. The clock being controlled in Figure 7 is located in a controlled environment chamber. Both are using the same program for determining the rate adjustment for the phase microstepper.

## **CONCLUSION**

With some thought and investigation into the control theories used in other fields of operation, the timing community can develop programs to provide more accurate and precise control of time references. This can only lead to improvements in operations and an ultimate savings of money and personnel time. Control of a clock or system of clocks can range from a simple manual operation concerning the periodic readjustment of a clock to an elaborate computer program control operation. The computer control program can be as complicated as the programmer desires. "...intuition is at a premium in nonlinear design" and the control of a clock system in a changing environment is definitely a nonlinear operation. Beyond a certain point of complexity, the more that is added to a program, the more likely a control error will occur.

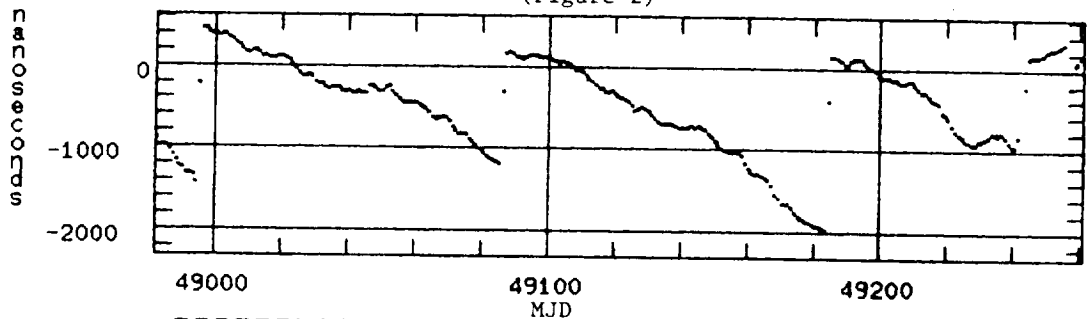
### USNO minus UNSTEERED CLOCK

(Figure 1)



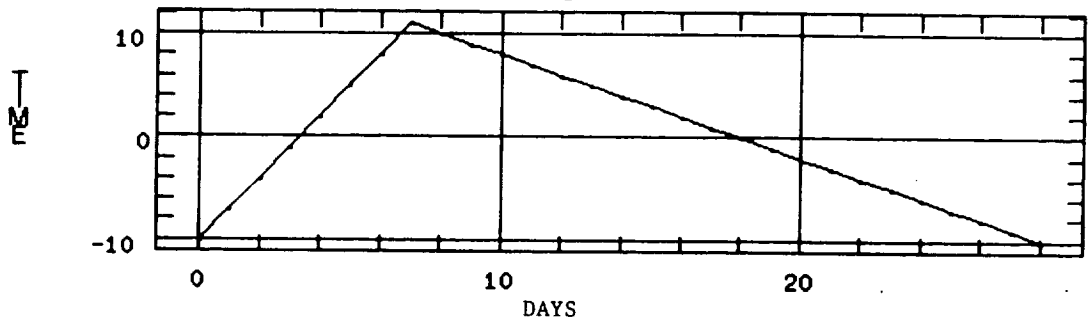
### USNO minus STEPPED CLOCK

(Figure 2)



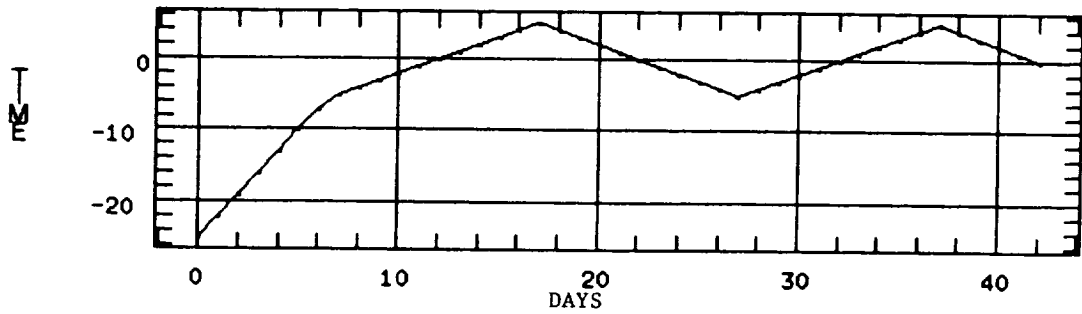
### REFERENCE minus CLOCK USING TWO-STAGE STEERING

(Figure 3)



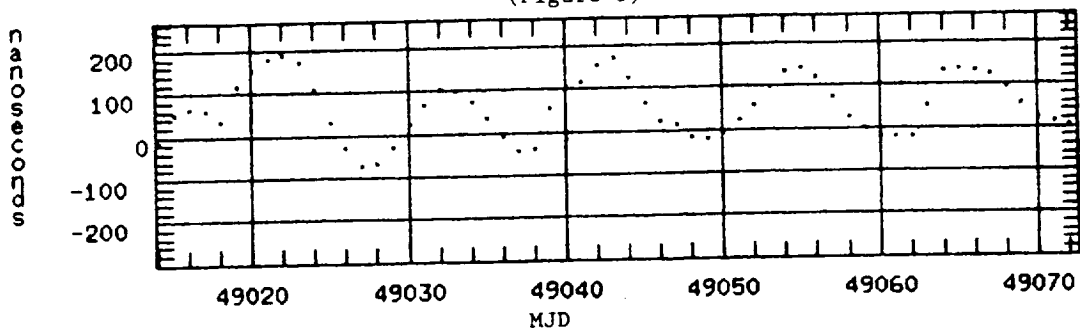
### REFERENCE minus CLOCK USING THREE-STAGE STEERING

(Figure 4)



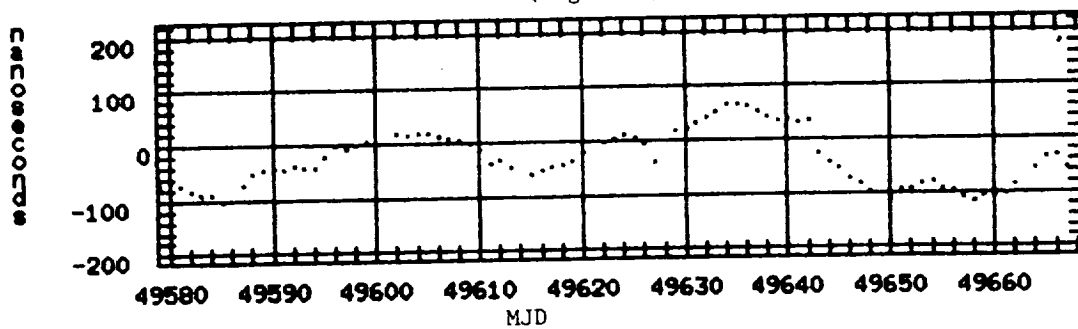
### USNO minus MIXED DATA STEERED CLOCK

(Figure 5)



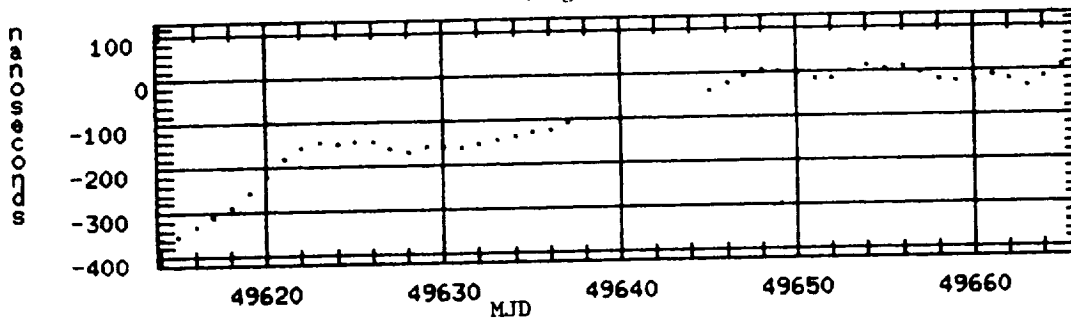
### USNO minus STEERED CLOCK IN OFFICE

(Figure 6)



### USNO minus STEERED CLOCK IN CONTROLLED AREA

(Figure 7)



350 27  
12

# THE EFFECTS OF CLOCK ERRORS ON TIMESCALE STABILITY

Lee A. Breakiron  
Directorate of Time  
U.S. Naval Observatory  
Washington, DC 20392

## Abstract

*The weighting scheme for the cesium clocks and hydrogen masers constituting the USNO timing ensemble is reexamined from an empirical standpoint of maximizing both frequency accuracy and timescale uniformity. The utility of a sliding-weight relation between the masers and the cesiums is reaffirmed, but improvement is found if one incorporates inverse Allan variances for sampling times of 12 and 6 hours for the cesiums and masers, respectively, with some dependence on clock model.*

## INTRODUCTION

Maximum timescale stability and efficient use of resources require the proper relative weighting of data from atomic clocks. This paper represents a continuation in our quest for an optimal weighting scheme as the U.S. Naval Observatory (USNO) clock ensemble has changed, first with the addition of hydrogen masers to our cesium-beam frequency standards and then with the introduction of the new-model HP5071A cesium standards, which are phasing out our HP5061 standards. The previous study of our weights was based on data from HP5061 cesiums and a few masers<sup>[1]</sup>. The lower noise of the HP5071A cesiums justifies a reexamination of our weighting procedures.

Since timescale algorithms are generally designed to optimize frequency stability, clocks are commonly weighted according to their individual frequency stabilities, as measured by inverse Allan variances  $1/\sigma_y^2$ . A previous study, however, found no significant improvement in our timescale if inverse Allan variances were used rather than equal weights, so the latter have been retained<sup>[2]</sup>. The performance of each USNO clock is closely monitored and any change in its rate precipitates total deweighting until its behavior is again satisfactory and its rate accurately redetermined. The deweighting is done automatically in the computation of the near-real-time mean timescale (done every hourly measurement) toward which the Master Clocks are steered; deweighting is done manually during the repeated postprocessing which ultimately results in the final timescale.

The incorporation of hydrogen masers, with their different noise characteristics, requires special treatment of their data. Some labs use a Kalman filter to handle data from such a heterogenous

ensemble<sup>[3]</sup>. We have obtained good results from a sliding-weight relation between the masers and the cesiums that mirrors their respective class average sigma-tau plots, with the sampling time  $\tau$  replaced by the time prior to the latest measurement<sup>[1]</sup>. This results in a time dependence of the weights, requiring recomputation of the entire timescale every hourly time step. The masers dominate the clock weights in the recent past, but are entirely phased out over a 75-day period, so only the last 75 days actually need to be recomputed. This zeroing of the maser weights prevents any drift of the timescale due to the masers, since even though the frequency drifts of all clocks are determined and removed from the data, some errors in these drift corrections might otherwise accumulate.

Still, as data collect, reconsideration of the sliding-weight relation might be worthwhile, as might that of assuming equal weights for the masers among themselves. Also, fitting average sigma-tau plots to a class of clocks is not a straightforward, and may be a questionable, procedure, so the approach taken here is to select clocks of homogeneous type for generation of test timescales whose sigma-tau plots may then be meaningfully compared.

## THE HP5071A CESIUMS

The new-model HP5071A commercial cesium frequency standards exhibit a significant reduction in noise level over the older HP5061 models and other cesiums due to improvements in electronics and careful allowance for environmental effects<sup>[4]</sup>. USNO currently has 50 HP5071A cesiums in 13 vaults or environmental chambers available for timescale data acquisition. In fact, they have been used in the timescale computation since February 1992. A preliminary scheme weighted an HP5071A cesium equal to 1.5 times that of an HP5061 cesium.

In order to further investigate their weights, twelve of the best HP5071A cesiums were selected which displayed constant rate and negligible drift over an interval of 200 days (MJD 49137–49337, when the reference maser changed rate). Fig. 1 is a sigma-tau plot for the twelve HP5071A cesiums relative to the Sigma-Tau maser NAV5 (in all such plots, a frequency offset has been removed). Approximating their weights with inverse Allan variances at a sampling time of 30 days (around the minimum), we find that the weights range over a factor of 3.1.

However, how valid are Allan-variance-based weights for these clocks, and what sampling time should be used? Though the theoretical answer to the latter for our algorithm is one hour, the true answers to both questions are affected by noise and systematics. In particular, the noise of our time-interval-counter measurement system is significant at one hour. A proper gauge of a clock's contribution to a timescale is:

$$\frac{1}{\sigma_{c,i}^2(\tau)} = \frac{1}{\sigma_{\text{twsi}}^2(\tau)} - \frac{1}{\sigma_{\text{twso}}^2(\tau)} \quad (1)$$

where  $\sigma_{c,i}^2(\tau)$  is the reduction in variance contributed by clock  $i$ ,  $\sigma_{\text{twsi}}^2(\tau)$  is the Allan variance of the timescale computed including clock  $i$ , and  $\sigma_{\text{twso}}^2(\tau)$  is the Allan variance of the timescale computed without clock  $i$ .

This assumes that the clocks involved are not significantly correlated. This has been found to

be the case for USNO clocks when the clocks are not disturbed by environmental and human influences<sup>[2,5]</sup>, which are minimized by the environmental control and maintenance procedures at USNO; data affected by such disturbances have been rejected from this study, as they are from the computation of UTC (USNO). While correlations may seem to be significant when clock frequency variations are intercompared<sup>[5]</sup>, unpublished USNO results indicate that few of these cannot be explained by the use of a common reference, as has been found by others<sup>[6]</sup>.

The intention was to use these clocks to generate test timescales, and twelve clocks were thought to be sufficient to produce a stable timescale, while still being few enough for such a timescale to show a measurable effect if one of the clocks was omitted. Test timescales were generated for all twelve clocks and every subset of eleven clocks, using equal weights; the clock contributions were then calculated via Eq. (1). An indication of the best Allan variance to weight by would be that which best predicts a clock's contribution to such a timescale. Unfortunately, a scatter plot showed only that an Allan variance for a sampling time of a few hours was better for weighting than one for a few days.

To better quantify this, a relative error parameter  $\phi$  was defined such that:

$$\phi_i^2(\tau) = \frac{|\sigma_{c,i}^2(\tau) - \sigma_{y,i}^2(\tau)|}{\sigma_{c,i}^2(\tau)} \quad (2)$$

where  $\sigma_{y,i}^2(\tau)$  is the Allan variance of clock  $i$ . Values of  $\log \phi$  are plotted vs.  $\log \tau$  for all the cesiums in Fig. 2. Some points are missing because  $\phi$  was not available when the computed clock contribution was negative, as it occasionally was, due to noise. Averages were not very stable, but the median minimum relative error occurred for a sampling time of 12 hours.

As a check, test timescales were generated for the same interval and clocks, weighting the clocks by inverse Allan variances over a range of sampling times from 1 hour to 30 days. The resulting sigma-tau plots are given in Fig. 3. There is little difference between most of them, but the worst are the long sampling times, as one would expect. The best sampling time was around 12 hours. Variances computed for  $\tau = 12$  hours would also reflect well the effects of any diurnal environmental perturbations. At  $\tau = 12$  hours,  $\sigma_{c,i}^2(\tau)$  varied over a factor of 2.8 and  $\sigma_{y,i}^2(\tau)$  varied over a factor of 2.0. Consequently, inverse 12-hour Allan variances will be our choice for weighting the HP5071A cesiums.

## THE HP5061 CESIUMS

At present, 14 HP5061A cesiums and two HP5061B cesiums in four vaults or environmental chambers are available for timescale data acquisition. The sigma-tau plots for ten HP5061A cesiums are given in Fig. 4 for from 80 to 169 days of data. A similar analysis was attempted of the clock contributions as was done for the HP5071A cesiums. Also, each HP5061A clock was substituted for a member of the HP5071A ensemble, and timescales were generated and analyzed for each. In both cases, the HP5061A data were too noisy to reach reliable conclusions.

Comparing the average 12-hour Allan deviations in Fig. 4 with those in Fig. 1 gives:

$$\langle \sigma_{5071} / \sigma_{5061} \rangle = 0.795$$

Comparing the median 12-hour Allan deviations gives:

$$\langle \sigma_{5071} / \sigma_{5061} \rangle = 0.785$$

Consequently, we will adopt a weight ratio of:

$$w_{5061} / w_{5071} = \sigma_{5071}^2 / \sigma_{5061}^2 = 0.62$$

for any HP5061 cesium relative to a typical HP5071A cesium.

As a check on whether equal weights should be retained for the HP5061A clocks, test timescales were generated for 104 days of data (MJD 49233–49337), weighting by inverse Allan variances for a range of sampling times. The results are presented in Fig. 5. While inverse 1-hour Allan variances make slightly better weights than those for somewhat longer sampling times, equal weights yielded significantly better stabilities than did any of the Allan-variance-based weights.

## THE MASERS

USNO currently has three SAO masers and ten Sigma-Tau masers in seven vaults or environmental chambers available for timescale data acquisition. During a 222-day interval (MJD 49404–49626) of constant drift and variance, four SAO masers (one has since left) and five Sigma-Tau masers were selected for analysis. Some rate corrections and occasional outlier rejections were required, but this is done routinely by the timescale algorithm. Some of these masers were steered in frequency, so their data were mathematically desteered.

An n-cornered-hat analysis was performed to obtain their absolute Allan deviations, which are plotted in Figs. 6 (for the SAO masers) and 7 (for the Sigma-Tau masers). (The analytical method, which produces identical results as the method commonly in use<sup>[7]</sup>, is described in the Appendix and is due, as far as we know, to Winkler<sup>[8]</sup>.) The curves for the Sigma-Tau masers differ systematically from those of most of the SAO masers, as might be expected, since the former are auto-tuned. The average  $\tau$  of minimum variance is 0.8 days for the SAO masers and 5.9 days for the Sigma-Tau masers. Approximating their weights with inverse Allan variances at the average  $\tau$  of their minimum variances, we find that the weights range over a factor of 166 for the SAO masers and 14 for the Sigma-Tau masers. This indicates that the weights of the two types of masers should be derived separately and that an upper limit on the weight of a clock will be necessary (more on this later).

Meaningful computations of clock contributions, then, will require unequal weighting. In order to determine the  $\tau$  of the Allan variances for such weights, test timescales were generated for the above interval and masers relative to the masers MC #1 and MC #2, weighting by

inverse Allan variances over a range of sampling times. A three-cornered-hat analysis was then done between each timescale relative to Master Clock (MC) #1, each timescale relative to MC #2, and the difference MC #1 – MC #2 in order to determine the absolute Allan variances of each timescale. The sigma-tau curves of these timescales are displayed in Fig. 8. At smaller sampling times (where the stability of the masers is of most interest to us), 6-hour Allan-variance-based weights are best.

On that basis, 6-hour Allan-variance-weighted timescales were generated for all nine masers and for every subset of eight. Clock contributions were next computed as they were for the cesiums. The corresponding values of relative error  $\phi$  are plotted in Figs. 9 (for the SAO masers) and 10 (for the Sigma-Tau masers). Again, some of the points are missing due to noise. The situation is less clear than for the HP5071A cesiums, but the sampling time of the median minimum relative error is also 6 hours. Hence, we will adopt 6-hour Allan-variance-based weights for the masers.

## THE MASERS RELATIVE TO THE CESIUMS

The rationale behind the sliding-weight scheme relating the masers to the cesiums is that: (1) it combines the short-term stability of the masers with the long-term stability of the cesiums; and (2) it retains the systematic frequency accuracy of the cesiums as an anchor to the final timescale, while maximizing the relative frequency stability of the timescale in the recent past, where it used to steer the Master Clocks. A Kalman-filter-based timescale algorithm can provide (1), but not (2). As noted above, the method requires recomputation of the timescale every time step, with the consequences that: (1) our timescale only becomes final 75 days in the past; and (2) UTC (USNO) at any given time may change by a few nanoseconds during those 75 days. The latter is logical because, as data accumulate, clock rates and drifts become more accurately determined, improving one's knowledge of the timescale at any point in the past.

As mentioned, HP5071A cesiums have been used in the timescale computation since February 1992. A preliminary scheme weighted the HP5071A cesiums and the hydrogen masers as follows:

$$w_{5071}(t) = 1/[\text{antilog}(0.130x^2 - 0.137x - 13.959)]^2 \quad (3)$$

$$w_{hm}(t) = 1/[\text{antilog}(0.309z^2 - 0.037z - 14.239)]^2 \quad (4)$$

where  $x = \log t - 5.9$ ,  $z = \log t - 5.2$ , and  $t$  is the time difference in seconds prior to the most recent measurement. At  $t = 0$ , the weight was arbitrarily set equal to  $t = 3600$  (not  $t = -1$ , as misstated in [1], p. 299).

In order to redetermine these relations using sigma-tau plots of timescales rather than those of clocks, test timescales were generated for: (1) the four SAO masers; (2) the five Sigma-Tau masers; and (3) five of the above HP5071A cesiums, all for the above 222-day interval. The masers were weighted by inverse 6-hour Allan variances and the cesiums by inverse 12-hour Allan variances. An upper limit of 33% of the total weight was placed on the individual

clock weights. Sigma–tau plots were computed for all three timescales. The ratio of the corresponding Allan variances for each maser timescale and the cesium timescale were taken and fitted with a second–order curve, as shown in Figs. 11 (for the SAO masers) and 12 (for the Sigma–Tau masers). The equations of these fits are:

$$w_{SAO/5071}(t) = [6.1 \pm 0.9](\log t)^2 - [79 \pm 9](\log t) + [257 \pm 22] \quad (5)$$

$$w_{ST/5071}(t) = [5.5 \pm 1.4](\log t)^2 - [76 \pm 14](\log t) + [261 \pm 34] \quad (6)$$

where  $t$ , the time in seconds prior to the latest measurement, has been substituted for  $\tau$ . The weights at  $t = 0$  are arbitrarily set equal to those at  $t = 3600$ . These relations reach minima at  $\log t = 6.5$  and  $6.9$ , respectively, at which point they can be ramped down to zero by  $t = 75$  days.

As a final test of the new weights, these sliding–weight relations, 6–hour maser weights, and 12–hour cesium weights were used for the same nine masers and nine of the HP5071A cesiums to generate timescales for the above 222–day interval. A single sigma–tau plot cannot properly characterize such a timescale because of the change in short–term stability relative to long–term stability with time. Since the cesiums dominate after 15 days in the past and it has been shown that the new weights provide some improvement over the old, the remaining question is whether the stability in the last 15 days has been enhanced. Accordingly, the interval was divided into fourteen 15–day segments and timescales were generated for each segment, with  $t$  reckoned from the end of each segment. The Allan variances of these timescales were then averaged and are presented in Fig. 13, where for comparison there have also been plotted the corresponding averages if one used the old weights<sup>[1]</sup> and the new weights but with no sliding relation. As can be seen, the new weights are a significant improvement on the short term over both the old and to not using the sliding relation at all.

## SUMMARY

The proper choice of timescale algorithm and clock weighting scheme depends on the purpose to which the resulting timescale is to be put. One objective of the USNO timescale is systematic frequency accuracy of the final timescale coupled with optimal relative stability in the recent past for the purpose of steering the Master Clocks. Compromise between these two aims is avoided by use of the sliding–weight relations between the masers and the HP5071A cesiums given in Eqs. (5) and (6). Adoption of inverse 6–hour Allan–variance weights for the masers and similar 12–hour weights for the cesiums will further improve UTC (USNO) by introducing responsiveness of the timescale to the performance of individual clocks beyond that already provided by careful monitoring and deweighting.

The new weights for an HP5071A clock  $i$  (of  $n$  such clocks) and an HP5061 clock  $j$  are, respectively:

$$w_{5071,i}(t) = \left[ \frac{\frac{1}{\sigma_{12,i}^2}}{\sum_{i=1}^n \frac{1}{\sigma_{12,i}^2}} \right] D_i(t) \quad (7)$$

and

$$w_{5061,j} = 0.62 \langle w_{5071} \rangle D_j(t) \quad (8)$$

where  $\sigma_{12}^2$  is the Allan variance for  $\tau = 12$  hours;  $D_i$  and  $D_j$  are deweighting factors in case of changes in performance, an uncertain rate, or an upper limit on the weight; and  $\langle \rangle$  denotes an average over all clocks. The new weight for a maser  $k$  (of a total of  $m$  such) is:

$$w_{hm,k}(t) = \left[ \frac{\sigma_{6,k}^2}{\sum_{k=1}^m \sigma_{6,k}^2} \right] D_k(t) w_{hm/5071}(t) \quad (9)$$

where  $\sigma_6^2$  is the Allan variance for  $\tau = 6$  hours,  $D_k$  is a deweighting factor, and  $w_{hm/5071}$  is given by Eq. (5) or (6). A upper limit on the weight prevents one or more superior clocks from dominating the timescale, which might lead to jolts of the timescale in the case of clock failure. The imposition of such a limit detracts from optimality, but is a requirement for reliability, which is another objective of the USNO timescale.

If the weights were based on stability relative to the mean timescale, a correction factor would have to be added to Eqs. (7), (8), and (9) for the so-called clock-ensemble effect, which would otherwise bias the timescale toward the best-performing clocks<sup>[9]</sup>. One may also question variances based on reference to a timescale whose own stability changes with time. Both problems may be avoided by referring the clocks to an unweighted, unsteered (or desteered) maser, rather than to the mean timescale.

Whether the adoption of gradual (robust), rather than instantaneous, deweighting would be a significant improvement remains to be tested; our large number of clocks has not made this a priority. Our short-term measurement noise should be appreciably reduced when our experimental Erbtec, or its successor the Steintech, system is reliable and capacious enough to be implemented, at which time the above weighting scheme will need to be reexamined. Further automation of the postprocessing procedure and more statistically rigorous treatment of rate and drift determination and rate and drift change detection are planned.

## REFERENCES

- [1] Breakiron, L. A., "Timescale algorithms combining cesium clocks and hydrogen masers," Proceedings of the 23rd Annual Precise Time and Time Interval (PTTI) Applications and Planning Meeting, 3-5 December 1991, Pasadena, California, pp. 297-305.
- [2] Breakiron, L. A., "The effects of data processing and environmental conditions on the accuracy of the USNO timescale," Proceedings of the 20th Annual Precise Time and

Time Interval (PTTI) Applications and Planning Meeting, 29 November–1 December 1988, Tysons Corner/Vienna, Virginia, pp. 221–236.

- [3] Jacques, C., Boulanger, J.-S., Douglas, R. J., Morris, D., Cundy, S., and Lam, L. F., “*Time scale algorithms for an inhomogeneous group of atomic clocks*,” Proceedings of the 24th Annual Precise Time and Time Interval (PTTI) Applications and Planning Meeting, 1–3 December 1992, McLean, Virginia, pp. 399–412.
- [4] Kusters, J. A., “*A new cesium beam frequency standard performance data*,” Proceedings of the 1992 IEEE Frequency Control Symposium, 27–29 May 1992, Hershey, Pennsylvania, pp. 143–150.
- [5] Breakiron, L. A., “*The effects of ambient conditions on cesium clock rates*,” Proceedings of the 19th Annual Precise Time and Time Interval (PTTI) Applications and Planning Meeting, 1–3 December 1987, Redondo Beach, California, pp. 175–184.
- [6] Tavella, P. and Thomas, C., “*Report on correlations in frequency changes among clocks contributing to TAI*,” BIPM Report 91/4, 1991.
- [7] Allan, D. W., “*Time and frequency (time-domain) characterization, estimation, and prediction of precision clocks and oscillators*,” IEEE Transactions on Ultrasonics, Ferroelectrics, and Frequency Control, vol. UFFC-34, 1987, pp. 647–654 = NIST Technical Note 1337, pp. TN121–TN128.
- [8] Winkler, G. M. R., 1994, private communication.
- [9] Tavella, P., Azoubib, J., and Thomas, C., “*Study of the clock-ensemble correlation in ALGOS using real data*,” Proceedings of the 5th European Frequency and Time Forum, 12–14 March 1991, Besancon, France, pp. 435–441.

## APPENDIX

An n-cornered-hat analysis for the individual variances of a set of uncorrelated clocks may be performed by writing the variance of the difference between the measurements of clocks i and j as the sum of their individual variances:

$$\sigma_i^2 + \sigma_j^2 = \sigma_{ij}^2$$

for all possible pairs of n clocks and then solving these as a system of n (n - 1)/2 simultaneous linear equations. The matrix equation could be expressed as:

$$\mathbf{M} \mathbf{X} = \mathbf{Y}$$

where, for four clocks:

$$\mathbf{M} = \begin{bmatrix} 1 & 1 & 0 & 0 \\ 1 & 0 & 1 & 0 \\ 1 & 0 & 0 & 1 \\ 0 & 1 & 1 & 0 \\ 0 & 0 & 1 & 1 \end{bmatrix} \quad \mathbf{X} = \begin{bmatrix} \sigma_1^2 \\ \sigma_2^2 \\ \sigma_3^2 \\ \sigma_4^2 \end{bmatrix} \quad \mathbf{Y} = \begin{bmatrix} \sigma_{12}^2 \\ \sigma_{13}^2 \\ \sigma_{14}^2 \\ \sigma_{23}^2 \\ \sigma_{24}^2 \\ \sigma_{34}^2 \end{bmatrix}$$

X may then be solved for by multiplying both sides by the Penrose pseudo-inverse of M, which here is:

$$\mathbf{M}^{-1} = \begin{bmatrix} 0.3\bar{3} & 0.3\bar{3} & 0.3\bar{3} & -0.1\bar{6} & -0.1\bar{6} & -0.1\bar{6} \\ 0.3\bar{3} & -0.1\bar{6} & -0.1\bar{6} & 0.3\bar{3} & 0.3\bar{3} & -0.1\bar{6} \\ -0.1\bar{6} & 0.3\bar{3} & -0.1\bar{6} & 0.3\bar{3} & -0.1\bar{6} & 0.3\bar{3} \\ -0.1\bar{6} & -0.1\bar{6} & 0.3\bar{3} & -0.1\bar{6} & 0.3\bar{3} & 0.3\bar{3} \end{bmatrix}$$

As with the standard n-cornered-hat method, the analysis fails if any of the variances solved for comes out negative. This generally occurs when the clocks are significantly intercorrelated, causing the variances to be underestimated.

## QUESTIONS AND ANSWERS

**MARC WEISS (NIST):** The result of that equally-weighted scale looks as good as a differently-weighted scale. It was rather surprising to me because we found results that are rather different.

Also, in general, using weights by themselves is really dependent on what algorithm you're using. And the tau that's used for determining the Allan Variance,  $\sigma_y(\tau)$ , the tau should come out of the algorithm; the algorithm should dictate the tau you use to determine weights. And using that kind of analysis, we found quite a difference when we used scales that are weighted differently for different clocks.

**LEE A. BREAKIRON (USNO):** It depends on exactly how you intend to use the time scale that you generate. We would like the highest systematic accuracy to determine our final time scale. That's why we phase out the masers, and we want the highest relative accuracy in the short term to steer our masers too. Yes, it depends what you are going to put the time scale to as to what tau you would weight by and whether it would make any difference.

**MARC A. WEISS (NIST):** What do you mean by "accuracy" in that context?

**LEE BREAKIRON (USNO):** We want the systematic accuracy of the time scale to be maximized, based only on the cesiums. So that's why we phase out the masers.

**MARC A. WEISS (NIST):** By accuracy, do you mean "frequency accuracy" or accuracy of time relative to some other scale?

**LEE BREAKIRON (USNO):** Right. The systematic frequency accuracy.

**JUDAH LEVINE (NIST):** I would just like to ask you to clarify your point of your recomputation of the data already submitted to the BIPM. Does that mean that the data in Circular T are, in fact, amended after the fact?

**LEE BREAKIRON (USNO):** Slightly.

**JUDAH LEVINE (NIST):** Is that amendment published subsequently? What I am saying is that if I look at Circular T and I copy a number down -- I'm trying to understand how it works.

**GERNOT M. WINKLER (USNO):** Two things. The Circular T values are determined from the individual clock readings which we submit to the BIPM. They are not changed. These are measurements which are made against a physical signal, which is the Master Clock; which is the same which is used to link to other laboratories.

What we are talking about here is the internal time scale which is used to steer the Master Clock. There is a very long time constant. We have to have something to steer to us. BIPM, of course, in a last analysis, is to panel for that. But for the day-to-day performance, we have an internal time scale, and that is the one which changes. Now that is the internal time scale which, again, has to be differentiated from the coordinated scale. The coordinated scale has additional frequency changes imposed because of our efforts to stay as close as we can to BIPM.

So the result is, the bottom line is that the Circular T values for the UTC, USNO are not changed.

**CLAUDINE THOMAS (BIPM):** Of course, UTC minus UTC USNO Master Clock is not changed, for sure. But I think that Gernot is speaking about the second page of Circular T which gives DI minus the individual TA; while what is called TA USNO is A.1 mean from USNO and for which we do not have the definitive values, as far as I understood with this thing with Dr. Breakiron last Friday. We do not have the definitive values; the values published are not the definitive values simply because definitive values are obtained 70 days after the fact, while USND values are before 70 days.

But it is true, we have not the definitive values. Maybe we can change this for the annual report. But that is something that I didn't know before coming here. But maybe we can change this.

**GERNOT M. WINKLER (USNO):** There is another point. And that is that TAI is not based on the contributions of the time scales. It is based on the contribution of individual clocks.

**CLAUDINE THOMAS (BIPM):** Yes, yes, of course. The independent time scales are not weighted in TAI. What are weighted is are the independent clocks supposed to be free-running.

But it's true that we are also publishing DI minus independent local TA on the second page of Circular T. And I think that Gernot was alluding to that particular publication, which has nothing to do with the first page which is UTC minus local UTCs. Thank you.

**LES BREAKIRON (USNO):** I thought of a better answer to Dr. Weiss. You have to realize that this data have been chosen because they are the highest quality that we have. And all things like rate corrections have already been either corrected for or the clock is removed for that reason.

So when you're dealing with data of that quality, and it's essentially been combed through like that, I think you would find results closer to ours.

**CLAUDINE THOMAS (BIPM):** Excuse me. I just want to add a small comment or question. On one of your transparencies, there is a difference, something like  $1$  over variance equals  $1$  over variance of something else, minus  $1$  of a variance of something else.

**LES BREAKIRON (USNO):** Right.

**CLAUDINE THOMAS (BIPM):** I'm very suspicious of doing differences of variances. If you have differences of one of a variance, it means you are able to do the sum of one of a variance. And this is only possible, of course, if the clocks are independent and if there is no limit of weight. As soon as you have a limit weight in any time scale, it is no longer true. That's an argument against TAI, which is very often said and discussed. Thank you.

**GERNOT M. WINKLER (USNO):** I think, since that is a planning meeting and requirements of great interest, I would like to hear of anyone who would be affected by these changes of the internal time scale, after the fact. We have been under the firm impression that it doesn't affect anyone, because it does not affect TAI, it does not affect the actual differences

which are reported on page one. It only affects the difference of DI minus internal time scale, which you published.

However I would like to hear from anyone who feels that this produces a difficulty.

**CLAUDINE THOMAS (BIPM):** Of course, the second page of Circular T, which gives DI minus TAK, is used only for laboratories which are giving TA. Of course, this has absolutely no impact on tau and users of UTC-K, which are published. The use is for you, in fact, to know it's doing your E.1 mean relative to TAI. Well, if anyone wants to make the same kind of thing, of course, if he has not the last updated values, he is mistaken, of course.

But the primary role of this answer is for the laboratories themselves.

**GERNOT M. WINKLER (USNO):** We have to ask ourselves.

**CLAUDINE THOMAS (BIPM):** Yes. All the users who would like to be linked for some reason to A.1 mean. Of course, if it only takes Circular T values, they do not have the last of this. So they may feel mistaken or have a distrust about that.

**JUDAH LEVINE (NIST):** My comment is that the most important aspect of the Circular T data is that I understand what it means. Speaking as a user of page two, the most important characteristic to me is that I understand exactly how those numbers are calculated. And now that I understand it, I understand it; and before, I didn't understand. And I think that is the most difficult aspect, is to know what the number actually means or how it was calculated.

**RANDY CLARKE (USNO):** I'm the one that does it. So just to let you know what you're facing, I would say that it's probably only a few nss. Because, we send in the reports after 30 days, so the major processing has already been done. So it's very rare that it's over five. If you're interested in what it is, it's something like five ns.

**CLAUDINE THOMAS (BIPM):** This can be done so simply in the new report of the BIPM. Just send me the last values when you have them, and I will publish them in the annual report; so everyone can get the updates after the fact, and that's all.

2200  
P. 9

# Relativistic Theory for Syntonization of Clocks in the Vicinity of the Earth

P. Wolf<sup>1,2</sup> and G. Petit<sup>1</sup>

<sup>1</sup>Bureau International des Poids et Mesures,  
Pavillon de Breteuil, 92312 Sèvres CEDEX, France

<sup>2</sup>Queen Mary and Westfield College, School of Mathematical Sciences,  
Mile End Road, London E1 4NS, Great Britain

## Abstract

*A well known prediction of Einstein's general theory of relativity states that two ideal clocks that move with a relative velocity, and are submitted to different gravitational fields will, in general, be observed to run at different rates. Similarly the rate of a clock with respect to the coordinate time of some spacetime reference system is dependent on the velocity of the clock in that reference system and on the gravitational fields it is submitted to. For the syntonization of clocks and the realization of coordinate times (like TAI) this rate shift has to be taken into account at an accuracy level which should be below the frequency stability of the clocks in question, i.e. all terms that are larger than the instability of the clocks should be corrected for. We present a theory for the calculation of the relativistic rate shift for clocks in the vicinity of the Earth, including all terms larger than one part in  $10^{18}$ . This, together with previous work on clock synchronization (Petit & Wolf 1993, 1994), amounts to a complete relativistic theory for the realization of coordinate time scales at picosecond synchronization and  $10^{-18}$  syntonization accuracy, which should be sufficient to accomodate future developments in time transfer and clock technology.*

## 1. Introduction

When using the concept of syntonization in a relativistic context certain ambiguities might appear which can lead to confusion and misunderstanding. It is therefore essential to first clarify the different meanings of the expression as used in time metrology within a relativistic framework.

Consider first the case where the relative rate of two distant clocks A and B is measured directly i.e. the frequencies of two signals coming from A and B respectively are compared by some observer 0. Taking the case where the observer is in the immediate vicinity of B and at rest with respect to B the measured relative rate is predicted as;

$$(d\tau_A/d\tau_B) - O = 1 + [(U_B - U_A) - v^2/2]/c^2 + O(c^{-4}) \quad (1)$$

in the first post-Newtonian approximation where  $(d\tau_A/d\tau_B)_O$  is the relative rate of the two clocks as observed by 0, U is the total gravitational potential at the location of the clock, v is

the relative speed of the two clocks and  $c$  is the speed of light in vacuum. Note that this result is completely dependent on the observer  $0$ . If, for example,  $0$  was in the immediate vicinity of  $A$  and at rest with respect to  $A$  the term in  $v^{\text{rel}}$  would change sign. Note also that (1) is independent of any reference frame or coordinate system. It is a coordinate independent, measurable quantity.

For the realization of coordinate time scales (like TAI) it is necessary to syntonize clocks with respect to the coordinate time in question, *i.e.* to determine the rate of a clock  $A$  with respect to an ideal coordinate time of some space-time reference frame. For example, using a geocentric non-rotating frame with TCG as coordinate time (as defined by the IAU (1991)) we obtain, again in the first post-Newtonian approximation;

$$d\tau_A/dTCG = 1 - [U(\mathbf{w}) + v^2/2]/c^2 + O(c^{-4}) \quad (2)$$

where  $(cTCG, w^k)$  are coordinates in the geocentric frame with  $\mathbf{w}$  representing the triplet  $w^k$ . The potential at the position of the clock  $U(\mathbf{w})$  is the sum of the Earth's potential and tidal potentials of external bodies, and  $v = ((dw^i/dTCG)(dw^i/dTCG))^{1/2}$  is the coordinate speed of the clock in the geocentric, non-rotating frame. Note that this rate depends entirely on the chosen reference frame. It is a coordinate quantity which cannot be obtained directly from measurement, but must be calculated theoretically using the definition of the reference frame in question with the appropriate metric equation.

When using repeated time transfers employing the convention of coordinate synchronization (Allan & Ashby 1986, Petit & Wolf 1994) for the determination of the relative rate of two clocks  $A$  and  $B$ , the resulting rate predicted by theory is simply:

$$dTA/dTB = (dTAdTCG)(dTCG/dTB) \quad (3)$$

with  $d\tau/dTCG$  given in (2). This is a combination of coordinate dependent quantities and not to be confused with the measurable quantity expressed in (1). The former is entirely dependent on the chosen reference frame and the convention of synchronization while the latter is specific to the measuring observer  $0$ . They will, in general, differ due to, essentially, the difference in the  $v^2/c^2$  terms. In sections 2 and 3 we will consider the syntonization of clocks with respect to coordinate times TCG (Geocentric Coordinate Time) and TT (Terrestrial Time, the ideal form of TAI) as defined by the IAU (1991) together with the transformation relating the two. The aim is to provide expressions in the form of (2) including all terms whose magnitudes exceed current and near future clock stabilities which are estimated to reach parts in  $10^{18}$ , as shown in Figure I (Maleki 1993).

When determining the relative rate of two distant clocks, one might be interested in time varying effects only (*i.e.* effects that influence the observed frequency stability), which, as will be shown, can be calculated at higher accuracies than constant frequency shifts. They are discussed briefly in section 5.

## 2. Syntonization with respect to TCG

Using the metric given in resolution A4 of the IAU (1991) the relation between the proper time of a clock T and TCG can be expressed as:

$$d\tau/dTCG = 1 - [U(\mathbf{w}) + \bar{U}(\mathbf{x}_E + \mathbf{w}) - \bar{U}(\mathbf{x}_E) - \bar{U}_{,k}(\mathbf{x}_E)w^k + v^2/2 + \mathbf{Q}_k]/C^2 + O(c^{-4}) \quad (4)$$

where coordinates in the barycentric frame are represented by  $(cTCB, x^k)$  with  $\mathbf{x}$  denoting the triplet  $x^k$  and the subscript E referring to the Earth's center of mass.  $U_E(w)$  and  $\bar{U}(\mathbf{x})$  are the Newtonian gravitational potentials of the Earth and of external masses respectively,  $v = ((dw^i/dTCG)(dw^i/dTCG))^{1/2}$ , the coordinate speed of the clock in the geocentric, non-rotating frame and  $Q_k$  is the correction for the non-geodesic barycentric motion of the Earth.

We find that in the vicinity of the Earth the term in  $Q$  and terms of order  $C^{-4}$  (given explicitly in Brumberg & Kopejkin 1990 and Kopejkin 1988) amount to a few parts in  $10^8$  or less. This implies that the specification of coordinate conditions (harmonic, standard post-Newtonian etc...) and the state of rotation of the frame (kinematically or dynamically non-rotating) is not significant for syntonization at the  $10^{-18}$  accuracy level.

All effects that need to be taken into account for the calculation of the remaining terms are listed in tables Ia and Ib, together with orders of magnitude and present day uncertainties of the associated corrections.

Syntonization with respect to TCG of Earth-bound clocks is limited at the  $10^{-17}$  accuracy level by uncertainties in the determination of the potential of the Earth at the location of the clock. Hence only effects whose influence on (4) is larger than this limit are considered in Table Ia.

The gravitational potential of the Earth,  $U_E(w)$  can be expressed as a series expansion in spherical harmonics. However, owing to mass irregularities such a series must be considered divergent at the surface of the Earth (Moritz 1961). Nonetheless, due to the predominantly ellipsoidal shape of the Earth, one can use the first two terms of this series expansion as a first approximation (Allan & Ashby 1986, CCIR 1990, Klioner 1992). Thus:

$$U_E(\mathbf{w}) = GM_E\alpha_1^2 J_2(1 - 3\cos^2\theta)/2w^3 \dots \quad (5)$$

where  $G$  is the Newtonian gravitational constant,  $M_E$  is the mass of the Earth,  $\alpha_1$ , and  $J_2$  ( $J_2 = 1.0826 \times 10^{-3}$ ) are the equatorial radius and the quadrupole moment coefficient of the Earth respectively and  $\theta$  is the geocentric colatitude of the point of interest.

Substituting (5) into the second term of (4) gives terms of the order of  $7 \times 10^{-10}$  and  $8 \times 10^{-13}$  respectively for points on the surface of the Earth.

The surface obtained when setting  $U_E(\mathbf{w}) + (\omega w \sin\theta)^2 = W_0$  in (5), with  $\omega$  representing the angular velocity of rotation of the Earth and  $W_0$  the gravitational + centrifugal potential on the geoid, differs from the ellipsoid of the Earth model by less than 10 m. Hence an estimate of the accuracy of (5) can be obtained by considering the maximal difference between the

geoid and the reference ellipsoid which can amount to  $\approx 100$  m (Vanicek & Krakiwsky 1986). Therefore expression (5) for the Earth's gravitational potential should not be used if accuracies better than one part in  $10^{14}$  are required.

On the coast the mean sea level can be determined using a tidal gauge. This level differs from the geoid by what is known as Sea Surface Topology (SST) which can amount to  $\pm 0.7$  m (Torge 1989). The SST can be determined with an accuracy of 0.1 m (Torge 1989) using oceanographic methods and satellite altimetry which induces an uncertainty of  $1 \times 10^{-17}$  in (4). The uncertainty in the knowledge of the potential on the geoid  $W_0$ , which is of the order of  $\pm 1 \text{ m}^2/\text{s}^2$  (Bursa 1992, 1993), contributes another part in  $10^{17}$ . The gravitational and centrifugal potential difference between mean sea level and an arbitrary point far from the coast can be obtained by geometrical leveling with simultaneous gravimetric measurements. The accumulated uncertainty when using modern leveling techniques and gravimetry is below  $0.5 \text{ mm}/\sqrt{\text{km}}$  (Kasser 1989) and does therefore not exceed a few centimeters even over large distances. In many countries leveling networks have been established at accuracies of 1–2  $\text{mm}/\sqrt{\text{km}}$  for primary points, the use of which would again induce errors at the centimetric level.

Therefore the constant part of the total potential at any point on the Earth's surface can be determined with an accuracy better than  $2.5 \text{ m}^2/\text{s}^2$  using a tidal gauge and good geometrical leveling. The main contributions to this uncertainty are due to inaccuracies in the determination of  $W$  and the SST. This limits the calculation of the second term in (4) at the level of  $2 \rightarrow 3 \times 10^{-17}$  which is the limit for syntonization of clocks with respect to coordinate time (TCG or TT) on the surface of the Earth.

Uncertainties in the potential model GEM-T3 (Lerch et al. 1992) and the determination of the satellite orbit (5 cm seems a realistic value) limit the accuracy of syntonization of satellite clocks at a few parts in  $10^{18}$  for low altitudes (semimajor axis  $< 15000$  km). For higher altitudes the effect of these uncertainties is below the  $10^{-18}$  level.

Therefore all terms necessary for the syntonization with respect to TCG of clocks on board high altitude satellites ( $a > 15000$  km) can be calculated to accuracies better than one part in  $10^{18}$ .

### 3. Transformation to TT

TCG is related to TT by a relativistic transformations, hence any clock that is syntonized with respect to TCG can also be syntonized with respect to TT. In this case the accuracy of syntonization may be limited by the uncertainty in the determination of the parameters participating in the transformation.

The IAU defined TT as a geocentric coordinate time scale differing from TCG by a constant rate, the scale unit of TT being chosen so that it agrees with the SI second on the geoid (IAU 1991). TT is an ideal form of the International Atomic Time TAI, apart from a constant offset. It can be obtained from TCG via the transformation:

$$dT/dTCG = 1 - L_g \quad (6)$$

with  $L_g = W_0/c^2 = 6.9692903 \times 10^{10} \pm 1 \times 10^{-17}$ .

It follows that at present the accuracy of syntonization with respect to TT is limited at the  $10^{-17}$  level due to uncertainties in the determination of the potential on the geoid  $W_0$ , even for clocks on board terrestrial satellites.

This limit is inherent to the definition of TT and can therefore only be improved by a reduction of the uncertainty in the determination of  $W_0$ . If highly stable clocks on board terrestrial satellites are to be used for the realization of TT at accuracies exceeding this limit it might prove necessary to change the definition. One possibility would be to turn  $L_g$  into a defining constant with a fixed value, which would at the same time provide a relativistic definition of the geoid (Bjerhammar 1985, Soffel et al. 1988).

#### 4. Time varying effects

For several applications of highly stable clocks, one is interested in the stability of the relative rate between two clocks, and therefore only time varying effects need to be considered, which can be calculated at the  $10^{-18}$  accuracy level even for clocks on the surface of the Earth. Table II gives a summary of all such effects estimated to exceed the  $10^{-18}$  limit.

Volcanic, coseismic, geodynamic and man-made (e.g. exploitation of oil, gas, geothermal fields) effects are highly localized and only need to be taken into account at some particular locations.

Polar motion and tidal effects are of periodic nature with essentially diurnal and semi-diurnal tidal periods, and the Chandler period (430 days) for the movement of the pole. If the clocks in question are syntonized using repeated time transfers (see (3)) at picosecond accuracy, tidal terms can be neglected as their short periods prevent their amplitudes in the time domain from reaching one picosecond (Klioner 1992).

For atmospheric pressure variations of  $\pm 10$  mbar on a global scale (corresponding to seasonal changes), the effect on the rate of a clock on the Earth's surface can reach  $\pm 2$  parts in  $10^{18}$  with local pressure changes ((anti)cyclones with pressure variations of up to  $\pm 60$  mbar) giving rise to a correction of up to  $\pm 2.7 \times 10^{-18}$  (Rabbel and Zschau 1985).

#### 5. Conclusion

We have presented a theory for the syntonization of clocks with respect to Geocentric Coordinate Time (TCG) including all terms greater than  $10^{-18}$  for clocks on board satellites at altitudes exceeding 15000 km. For this purpose terms of order  $c^{-3}$  and  $c^{-4}$  in the metric can be neglected, which implies that the specification of coordinate conditions and the state of rotation of the reference system is not necessary.

Syntonization with respect to Terrestrial Time (TT), an ideal form of TAI, is limited at the  $10^{-17}$  accuracy level due to the uncertainty in the determination of the potential on the geoid  $W_0$

inherent to its definition.

For clocks on the Earth's surface syntonization with respect to TCG or TT is limited at an accuracy of  $2 \rightarrow 3 \times 10^{-17}$  by uncertainties in the determination of the geopotential at the location of the clock.

We briefly discussed time varying effects that may influence the stability of the relative rate of two clocks. These can be calculated at the  $10^{-18}$  accuracy level even for clocks on the Earth's surface.

At present atomic clocks are approaching stabilities of the order  $10^{-18}$  (Maleki 1993) with further improvements expected in the near future. For comparisons of these highly stable clocks over large distances, and their application in experimental relativity, geodesy, geophysics etc. . . a sufficiently accurate relativistic theory for their syntonization, like the one presented in this paper, seems indispensable.

Together with a previous paper (Petit & Wolf 1994) the results obtained here amount to a complete relativistic theory for the realization of a geocentric coordinate time scale at a synchronization and syntonization accuracy of one picosecond and  $10^{-18}$  respectively.

## References

- Allan D.W. & Ashby N., 1986, in: Kovalevsky J., Brumberg V.A. (eds.), *Relativity in Celestial Mechanics and Astronomy*. Proceedings of the IAU Symposium No. 114 Leningrad 1985, Reidel, Dordrecht
- Bjerhammar A., 1985, *Bull. Géod.* 59, p.207
- Brumberg V. A. & Kopejkin, 1990, *Celestial Mechanics* 48, 23–44.
- Bursa M. et. al., 1992,, *Studia Geoph. et Geod.*, 36, 101–114.
- Bursa M., 1993, I.A.G. Special Commission SCR – Fundamental Constants (SCFC), Circular No 5.
- CCIR, 1990, *International Radio Consultative Committee, Reports, Annex to Volume VII*, p.150
- IAU, 1991, *IAU transactions Vol. XXIB, 1991, Proe. 21st Gen. Assembly Buenos Aires*, Kluwer Acad. Publ., Dordrecht, Boston, London.
- Kasser M., 1989, *C. R. Acad. Sci. Paris, t. 309, Sdrie 11*, p.695
- Klioner S.A., 1992, *Celestial Mechanics and Dynamical Astronomy* 53, p.81
- Kopejkin S.M., 1988, *Celestial Mechanics* 44, 87–115.
- Lerch F.J. et al., 1992, *NASA Technical Memorandum 104555*.
- Maleki L., 1993, *Proceedings 25th PTTI Meeting 1993, Nasa Conference Publication 3267*, 549–560.

- Moritz H., 1961, *Osterreichische Zeitschrift far Vermessungswesen*, v. 49, 11–15
- Petit G. & Wolf P., 1993, *Proceedings 25th PTTI meeting*, 205–215.
- Petit G. & Wolf P., 1994, *Astronomy and Astrophysics* 286, 971–977.
- Rabbel W. & Zschau J., 1985, *J. Geophysics* 56, p.81
- Soffel M. et al., 1988, *Manuscripta Geodetica* 13, p.143
- Torge W., 1989, *Gravimetry*, de Gruyter, Berlin
- Vanieek P. & Krakiwsky E., 1986, *Geodesy the Concepts*, North Holland.

Effect	Order of magnitude	Uncertainty
Earth's grav. pot.	$7 \times 10^{-10}$	$10^{-17}$
Centrifugal pot. ( $v^2/2/c^2$ )	$1 \times 10^{-12}$	$< 10^{-18}$
Volcanic and coseismic (highly localised)	$< 10^{-18}$	
External masses (moon, sun)	$10^{-17}$	$< 10^{-18}$
Solid Earth tides	$10^{-17}$	$< 10^{-18}$
Ocean tides	$10^{-17}$	$< 10^{-18}$

*Table Ia: Effects on syntonization with respect to TCG of clocks on the Earth's surface; Orders of magnitude and uncertainties of the corrections.*

Effect	Order of magnitude	Uncertainty
Earth's grav. pot.	$< 6 \times 10^{-10}$	few $10^{-18}$ (GEM-T3) $< 10^{-18}$ at $a > 10000$ km
2nd order Doppler ( $v^2/2/c^2$ )	$< 3 \times 10^{-10}$	few $10^{-18}$ (5 cm orbit uncertainty) $< 10^{-18}$ at $a > 15000$ km $< 10^{-18}$ at $a > 15000$ km
External masses: Moon	$4 \times 10^{-13}$	} $< 10^{-18}$
(at $a = 300000$ km) Sun	$4 \times 10^{-14}$	
Venus	$6 \times 10^{-18}$	
Solid Earth tides	} $10^{-18}$ (at low altitudes)	$< 10^{-18}$
Ocean tides		
Polar motion		
Atmospheric pressure		

*Table Ib: Effects on syntonization with respect to TCG of clocks on board terrestrial satellites; Orders of magnitude and uncertainties of the corrections.*

Effect	Order of magnitude	Uncertainty
Volcanic and coseismic (highly localised)	$< 10^{-16}$	
Geodynamic and man-made (localised and long-term $> 1$ year)	$< 10^{-16}$	
External masses (moon, sun)	$10^{-17}$	$< 10^{-18}$
Solid Earth tides	$10^{-17}$	$< 10^{-18}$
Ocean tides	$10^{-17}$	$< 10^{-18}$
Polar motion (long-term $\sim 430$ days)	$10^{-18}$	$< 10^{-18}$
Atmospheric pressure	$10^{-18}$	$< 10^{-18}$

Table II: Time varying effects on the Earth's surface for the determination of the relative rate of two clocks; Orders of magnitude and uncertainties of the corrections.

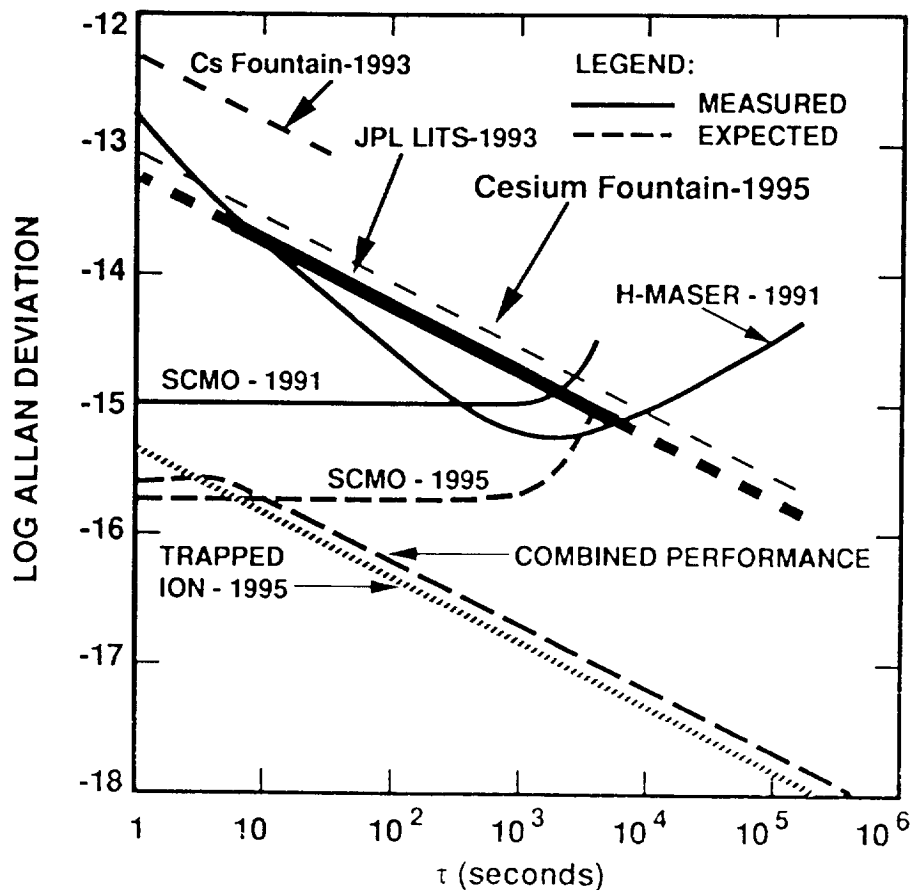


Fig. 1: Present and expected clock stabilities (from Maleki (1993)).

## QUESTIONS AND ANSWERS

**RICHARD KEATING (USNO):** I just have a comment. I don't think that the kind of presentation you just made is particularly useful. I think it's rather misleading. And I would like to say that because about seven years ago, I fired up an old pendulum clock at the request of a retired General Electric engineer. And if I had thought along the lines that you've just presented, I would not have expected to see any effects from, say, a lunar potential. In fact, the pendulum clock is highly sensitive. I could actually tell where the moon was, simply by the effect on the pendulum clock.

These are not relativistic effects, true. But they are far more dramatic, much larger, and they dominate the whole phenomena. So, just to concentrate solely on relativistic effects may be, I think, highly misleading. So, to talk about  $10^{-18}$ , which is a tenth of ps per day, when you actually in reality might have gravitational potential effects, which are the order of ms, I really think you've got bigger problems to worry about. And I think that this kind of paper is misleading.

**PETER WOLF (BIPM):** Okay, that's your opinion. Fine.

**R.J. DOUGLAS (NATIONAL RESEARCH COUNCIL OF CANADA):** I would like to come to Peter's defense and say this is one of the most useful kinds of things, because it tells where the limits are. It makes no sense to be thinking about designing optical frequency standards that are going to be useful for time keeping, that are alleged to be possibly stable to parts in  $10^{20}$ . Things that tell you where to stop the development are very useful for systems designers.

**GERNOT M. WINKLER (USNO):** I would raise the question about the semantics. You are using "syntonization," I believe, in the sense of the ability to absolutely calculate frequency differences. Because, you can always syntonize two standards to each other to see their signals. But you cannot compute the actual frequency difference on an absolute basis.

So, I think there is maybe a need to refine our semantics a little bit.

**PETER WOLF (BIPM):** I completely agree, yes. There is a big semantic problem concerning the word "syntonization." I have tried to consistently use it in two senses, "syntonization" of two clocks, one relative to another; "syntonization" with respect to coordinate time, which is an entirely different thing.

There might also be several other problems. I do think there's a semantic problem there, but that's only to be solved in time with people getting used to the different things going on.

**HENRY FLIEGEL (AEROSPACE CORP.):** I want to make one brief comment. I found your paper very useful and interesting. As far as terminology is concerned, I have one brief (almost theological) nit, and that is that I suppose the way to describe the gravitational series, the harmonic expansion, is as very slowly convergent, rather than divergent.

**PETER WOLF (BIPM):** On the surface of the earth?

**HENRY FLIEGEL (AEROSPACE CORP.):** I believe so, because if it were divergent, that

would mean that we ran eventually into a white noise regime.

**PETER WOLF (BIPM):** I have a paper which I can show you, which dates back to 1960, which does theoretically prove to show that you cannot be certain that on any point on the surface of the earth this vertical harmonic expansion will be convergent.

**HENRY FLIEGEL (AEROSPACE CORP.):** In that case, you have refuted all your critics. I would like to see your paper.

**PETER WOLF (BIPM):** I'm afraid it's in German, Doctor.

**HENRY FLIEGEL (AEROSPACE CORP.):** Well, I read German, no problem.



52301  
p-12

# Allan Deviation Computations of a Linear Frequency Synthesizer System Using Frequency Domain Techniques

Andy Wu  
The Aerospace Corporation  
El Segundo, California

## Abstract

*Allan Deviation computations of linear frequency synthesizer systems have been reported previously using real-time simulations. Even though it takes less time compared with the actual measurement, it is still very time consuming to compute the Allan Deviation for long sample times with the desired confidence level. Also noises, such as flicker phase noise and flicker frequency noise, can not be simulated precisely. The use of frequency domain techniques can overcome these drawbacks. In this paper the system error model of a fictitious linear frequency synthesizer is developed and its performance using a Cesium (Cs) atomic frequency standard (AFS) as a reference is evaluated using frequency domain techniques. For a linear timing system, the power spectral density at the system output can be computed with known system transfer functions and known power spectral densities from the input noise sources. The resulting power spectral density can then be used to compute the Allan Variance at the system output. Sensitivities of the Allan Variance at the system output to each of its independent input noises are obtained, and they are valuable for design trade-off and trouble-shooting.*

## 1. Introduction

A fictitious linear frequency synthesizer is used in this analysis. The system generates a system output frequency from a reference Cs Atomic Frequency Standard (AFS) operating at a different frequency. The system block diagram is shown in Figure 1. A reference epoch is generated every 1.5 s based on the AFS frequency and another 1.5 s interval system epoch is generated by the system clock, a voltage control crystal oscillator (VCXO). Both epochs are input to the Phase Meter (PM), and the PM computes the timing error between them. Based on the timing error value, the loop adjusts the phase of the VCXO-generated epoch, so that the VCXO is phase-locked to the reference AFS.

In this paper the system error model of the linear frequency synthesizer is developed and the performance at the system output is evaluated using frequency domain techniques. For a linear system, the power spectral density at the system output can be computed using known system transfer functions and known power spectral densities from the three independent noise sources: AFS, VCXO and PM. The resulting power spectral density can then be used to compute the

Allan Variance at the system output. Compared with time domain techniques, the use of frequency domain technique offers several benefits such as: (1) it provides another independent evaluation of the system performance, (2) flicker noise can be implemented precisely, (3) computation time for the Allan Variance of a given sample time ( $\tau$ ) is very short and is roughly the same for either short or long sample time ( $\tau$ ). The last two items are major drawbacks for the real-time/Monte Carlo simulations. Sensitivities of the output Allan Deviation to each of its input noises are provided, and they are valuable for design trade-off and trouble-shooting.

## 2. Noise Models

### 2.1 Phase Meter Noise

The PM noise with resolution of 100 ps is modeled as a white process with a constant power spectral density for all frequencies

$$\sigma_p(f) = \frac{(1 \times 10^{-10})^2}{6} . \quad (1)$$

And the Allan Variance of the PM noise is<sup>[1]</sup>:

$$\sigma_p^2(\tau) = \frac{(1 \times 10^{-10})^2}{6\tau^2} . \quad (2)$$

### 2.2 AFS Noise

The Allan Variances for the AFS is specified as:

$$\sigma_A^2(\tau) = \frac{9.0 \times 10^{-22}}{\tau} + 1.0 \times 10^{26} \quad (3)$$

This is consistent with that of the commercially available HP 5071 Cs AFS.

We assume that the two terms are independent of each other. Thus we can compute the associated noise power spectral densities using well known techniques<sup>[1]</sup>:

$$S_A(f) = 1.8 \times 10^{-21} + \frac{7.2134 \times 10^{-27}}{f} . \quad (4)$$

### 2.3 VCXO

The VCXO frequency noise is assumed to have the following Allan Variance:

$$\sigma_y^2(\tau) = 10^{-24} + 10^{-27}\tau . \quad (5)$$

Similarly, we assume that the two terms of equation (5) are independent of each other. As above, the power spectral density of the VCXO frequency noise can be expressed as<sup>[1]</sup>:

$$S_y(f) = \frac{7.2134 \times 10^{-25}}{|f|} + \frac{1.519 \times 10^{-28}}{f^2} . \quad (6)$$

### 3. System Transfer Functions

The system model as shown in Figure 1 results in the equivalent system error model indicated in Fig. 2 obtained using the Z-transform formalism.  $T_s$  is the sample period of the system, and is 1.5 s. Also two delays of one epoch each are introduced in Figure 2 to account for the fact that the effects of the computed VCXO frequency modification in the current epoch will not show on the Phase Meter until two epochs later. The transfer functions relating the system output frequency (T) to the input noises of the AFS(A), VCXO(V) and Phase Meter (P) are:

$$\frac{\text{SYSTEMOUTPUT}}{\text{PM}} = H_{TP}(Z) = \frac{T(Z)}{P(Z)} \quad (7)$$

$$\frac{\text{SYSTEMOUTPUT}}{\text{AFS}} = H_{TA}(Z) = \frac{T(Z)}{A(Z)} \quad (8)$$

$$\frac{\text{SYSTEMOUTPUT}}{\text{VCXO}} = H_{TV}(Z) = \frac{T(Z)}{V(Z)} \quad (9)$$

The Bode Plots (frequency responses) for these second order transfer functions with a time constant of 50 s are shown in Figure 3. It is seen that  $H_{TA}(Z)$  is a lowpass filter,  $H_{TV}(Z)$  is a highpass filter, and  $H_{TP}(Z)$  is a low gain highpass filter to reduce the PM quantization noise.

### 4. Power Spectral Density of the System Output Frequency

The power spectral density of the system output (ST(f)) can be computed as<sup>[2]</sup>:

$$S_T(f) = S_{TA}(f) + S_{TV}(f) + S_{TP}(f) \quad (10)$$

where:

$$S_{TA}(f) = |H_{TA}(e^{j2\pi fT_s})|^2 \times S_A(f), \text{ due to the AFS noise} \quad (11)$$

$$S_{TV}(f) = |H_{TV}(e^{j2\pi fT_s})|^2 \times S_V(f), \text{ due to the VCXO noise} \quad (12)$$

and

$$S_{TF}(f) = |H_{TF}(e^{2\pi fT_s})|^2 \times S_P(f), \text{ due to the PM noise.} \quad (13)$$

The power spectral densities for the noises ( $S_A(f)$ ,  $S_V(f)$  and  $S_P(f)$ ) and their contributions to the system frequency output ( $S_{TA}(f)$ ,  $S_{TV}(f)$  and  $S_{TP}(f)$ ) were calculated using equations (1), (4), (6), (11), (12) and (13), and are shown in Figure 4. As can be seen the system output power spectral densities are shaped by their corresponding transfer functions. Even though the power spectral densities of the PM ( $S_P(f)$ ) and the VCXO ( $S_V(f)$ ) are large when compared with that of the AFS, their contributions to the system output ( $S_{TP}(f)$  and  $S_{TV}(f)$ ) have been greatly reduced by their corresponding transfer functions ( $H_{TP}(j2\pi fT_s)$  and  $H_{TV}(j2\pi fT_s)$ ) especially at low frequency. Similarly, contributions from the AFS ( $S_{TA}$ ) is also suppressed considerably for high frequencies.

## 5. Allan Deviation of the System Output Frequency

The temporal behavior of the timing or frequency system is normally characterized by the Allan Deviation or square root of the Allan Variance,  $\sigma_y^2(\tau)$ , where  $\tau$  is the frequency sample time. The Allan Variance is related to the power spectral density by [1]

$$\sigma_y^2(\tau) = 2 \int_0^{f_n} S_y(f) A_D(f\tau) df \quad (14)$$

where:

$$A_D(f\tau) = \frac{\sin^4(\pi f\tau)}{(\pi f\tau)^2} \quad (15)$$

and  $f_n$  is the Nyquist frequency of the system and is equal to 1/3 Hz for a sampling period ( $T_s$ ) of 1.5 s.

### 5.1 Computation Consideration

In many cases integration of the equation (14) can not be carried out analytically, so it must be done by computer using numerical integration. It is important to choose a proper integration step size to achieve the desired accuracy in the computation.

The magnitude of the oscillatory window function ( $A_D(f)$ ) as given in equation (15) is inversely proportional to the square of  $f$  for a given  $\tau$ , and is plotted in Figure 5 for  $\tau=100$  s and  $\tau=1000$  s. As can be seen, its magnitude decreases rapidly after a few periods and its bandwidth decreases as  $\tau$  increases. Figure 5 shows that the bandwidth is roughly  $10^{-5}$  Hz for  $\tau=1000$  s. and  $10^{-2}$  Hz for  $\tau=100$  s. The portion of the power spectral density of the system noise outside the bandwidth of the window function has negligible effect of its Allan deviation computed by using equation (14).

Given the limitations in available computer memory it was found by trial and error that to provide adequate numerical accuracy, integration of the equation (14) can be carried out by using 20 integration steps, either for the first 50 periods of the window function or up to the Nyquist frequency, whichever is smaller. This technique is valid for sample times of up to 100,000 s provided that the power spectral density function,  $S_y(f)$ , does not contain any white phase modulation noise component, whose frequency power spectral density is proportional to  $f^2$ . Fortunately this condition is met by the frequency power spectral density at the system output. For white phase modulation noise such as the PM noise, the upper limit of the numerical integration has to be set at the Nyquist frequency. For larger sample times,  $\tau > 100,000$  s, a smaller integration step size is needed. The average time to compute the Allan Deviation for a given  $\tau$  is less than 15 s using a PC with Intel 486 DX2/50 CPU.

To show that this numerical integration technique is accurate enough the Allan Deviations of the two noise sources (AFS and VCXO) are computed from their corresponding power spectral densities using equation (14) and are shown in Figure 6. Figure 6 also shows the corresponding specified Allan Deviations, from which the power spectral densities were derived, as discussed in section 2. As can be expected, the computations are in very good agreement with the respective specifications. The Allan Deviation of the PM noise is also depicted. Figure 6 shows that the PM Allan Deviation is predominant for sample times up to 30 s and that of the VCXO noise predominates for longer time.

## 5.2 System Allan Deviation

The contribution to the Allan Deviations at the system output ( $\sigma_{TA}(\tau)$ ,  $\sigma_{TP}(\tau)$  and  $\sigma_{TV}(\tau)$ ) due to each of the independent input noises are computed using equation (14) with their power spectral densities at the system output ( $S_{TA}(f)$ ,  $S_{TP}(f)$ , and  $S_{TV}(f)$ ). The results are shown in Figure 7 and they can be considered as the sensitivities of the system output for each of the input noises. This technique can be used very effectively during the design, development and testing phase of the system to determine the loop time-constant, to define noise specifications and to provide data for trouble-shooting. It will be used below to identify the causes of some exceeding reference AFS specification conditions. It is apparent from Figure 8 that for short sample time the system performance is dominated by the PM, while for long sample time the system performance is governed by the AFS. The crossover sample time is around 20 s. The Allan Variance of the resulting system output can be obtained as:

$$\sigma_T^2(\tau) = \sigma_{TA}^2(\tau) + \sigma_{TV}^2(\tau) + \sigma_{TP}^2(\tau). \quad (16)$$

The Allan Deviations of the system output ( $\sigma_T(\tau)$ ) and the reference AFS specification are plotted in Figures 8. Figure 8 shows that the Allan Deviation of the system output barely exceeds the reference AFS specification for sample time from 70 s to 1000 s. By examining the system sensitivities as provided in Figure 7, it is found that this condition is caused by the AFS noise.

## 6. System Performance Using Other System Configurations

In the previous sections we only use  $T_c = 50$  s, Allan Deviation results using other time constants can be obtained easily. The result for a time constants of 15 s is shown in Figures 9. Figure 9 indicates that the system exceeds the reference AFS Allan Deviation specification for  $\tau > 1000$  s. The cause can be determined by examining the sensitivities as shown in Figure 10, and is identified to be the PM noise, which is the dominant noise contribution for short  $\tau$ ; its effect at the system output is not suppressed enough for the system with a short time constant. To reduce the effect due to the PM for short sample time, a better PM with resolution of 20 ps was used and the result is shown in Figure 11. As can be seen the Allan Deviation at the system output is less than that of the reference AFS for short sample time.

## 7. Conclusion

An efficient method of computing the Allan Deviation at the output of a linear system with known input power spectral densities is presented. Since the computation time is not a function of the sample time ( $\tau$ ), this technique is very attractive to compute Allan Deviations for long sample times. Sensitivities of the Allan Deviation at the system output for each of its independent input noises are also provided and they are valuable for design trade-off and trouble-shooting. Potential situations in which the system could exceed the reference AFS specification are pointed out, and causes are identified.

### References

- [1] J. Barnes, Andrew R. Chi, Leonard S. Cutler, Daniel B. Leeson, Thomas E. McGunigal, James A. Mullen, Jr., Warren L. Smith, Richard L. Sydnor, Robert F. C. Vesot, and Gernot M. R. Winkler, "Characterization of Frequency Stability," IEEE Trans. Instrumentation and Measurement, IM-20, May 1971.
- [2] A. Papoulis, "Probability, Random Variables, and Stochastic Processes," McGraw-Hill, New York, 1965.

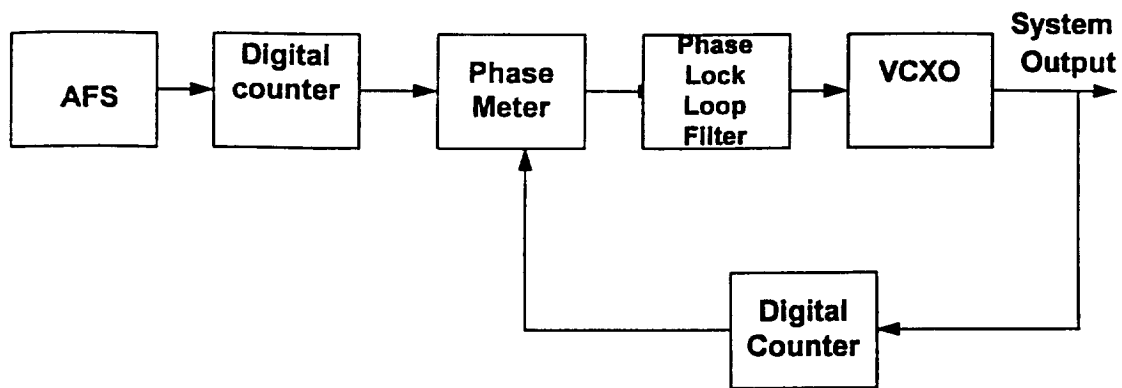


Figure 1. Linear Frequency Synthesizer

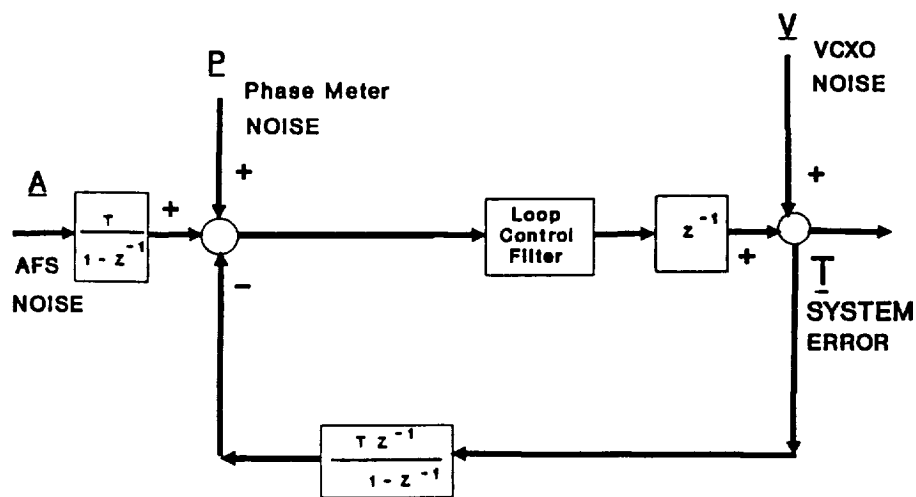


Figure 2. System Error Model

Fig. 3. Bode Plots of System Transfer Functions

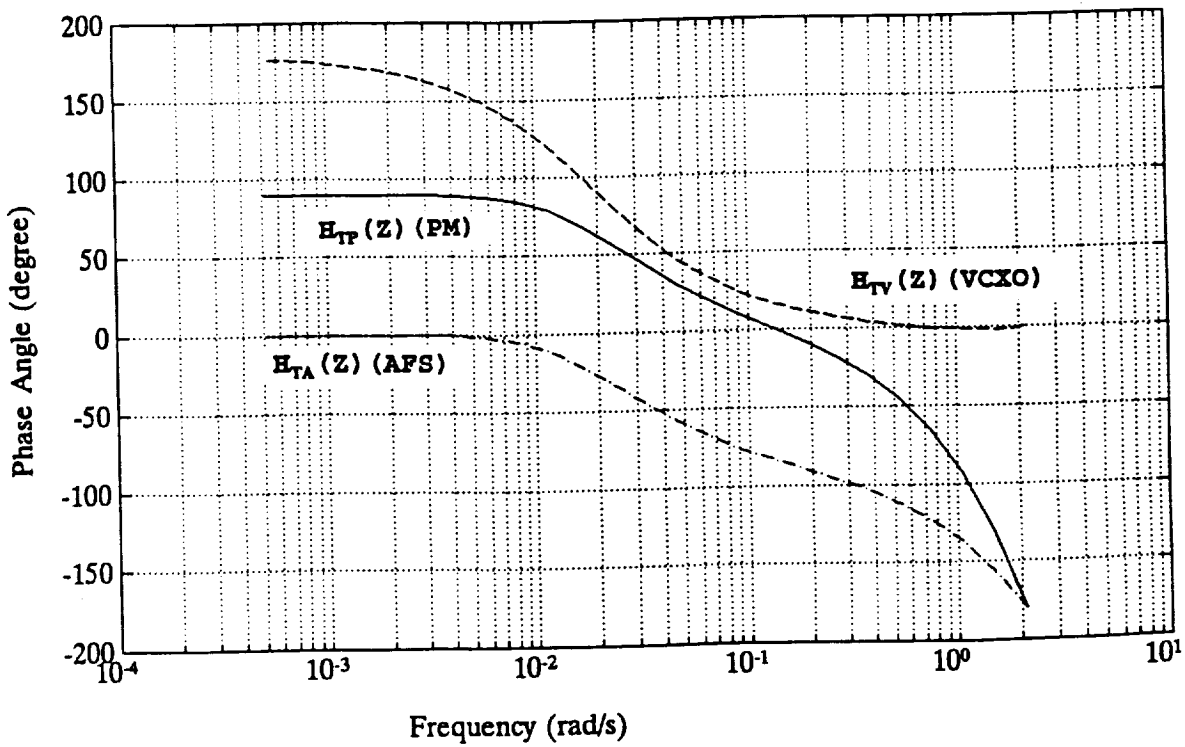
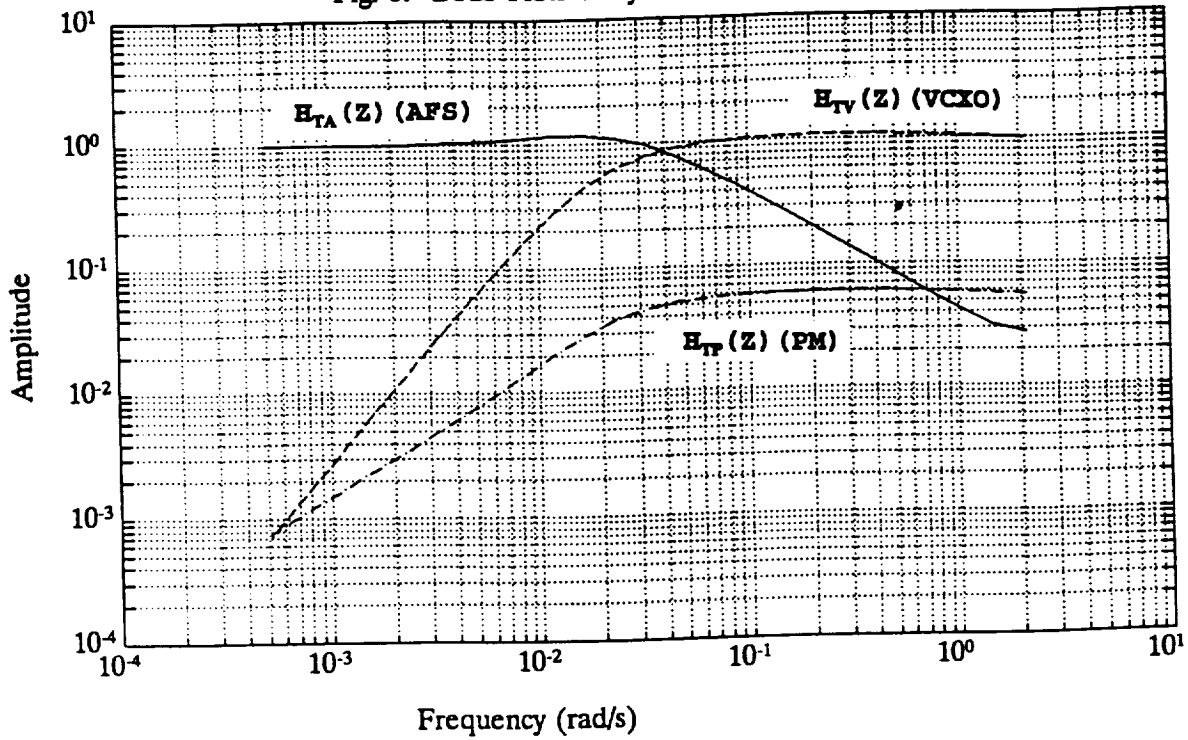


Figure 4. Power Spectral Densities of PM, VCXO and AFS

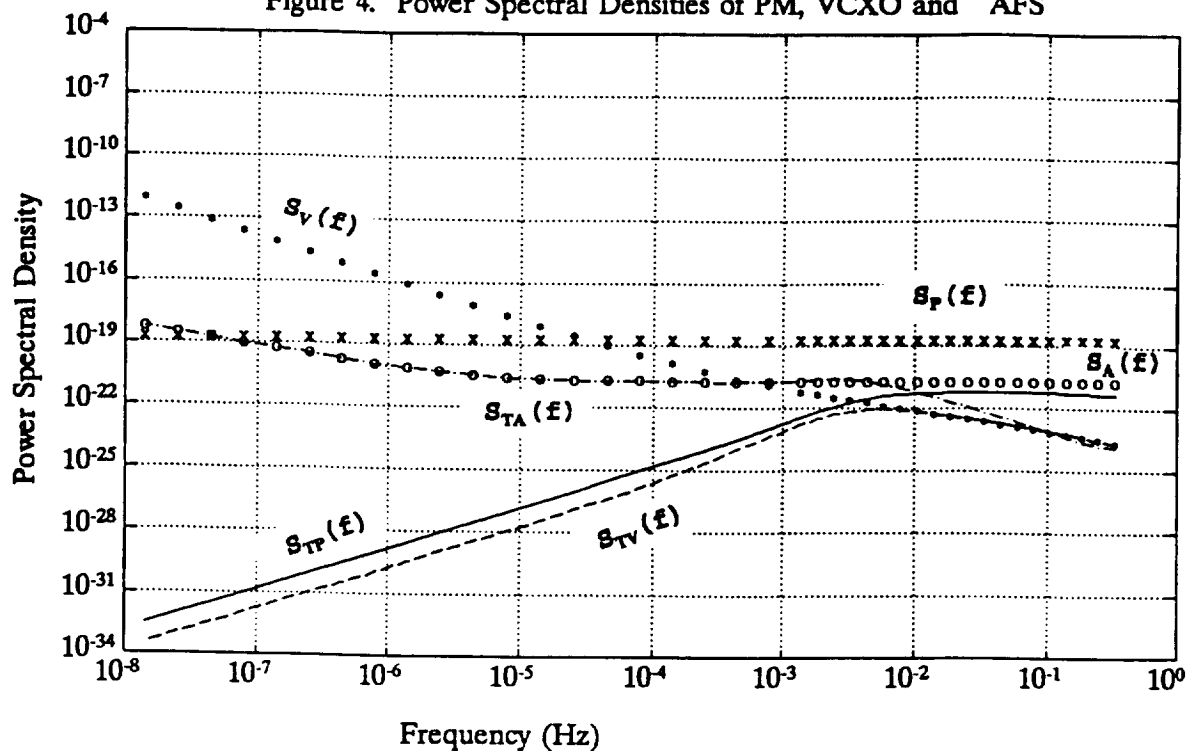


Figure 5. Plot of Window Function as functions of f and tau

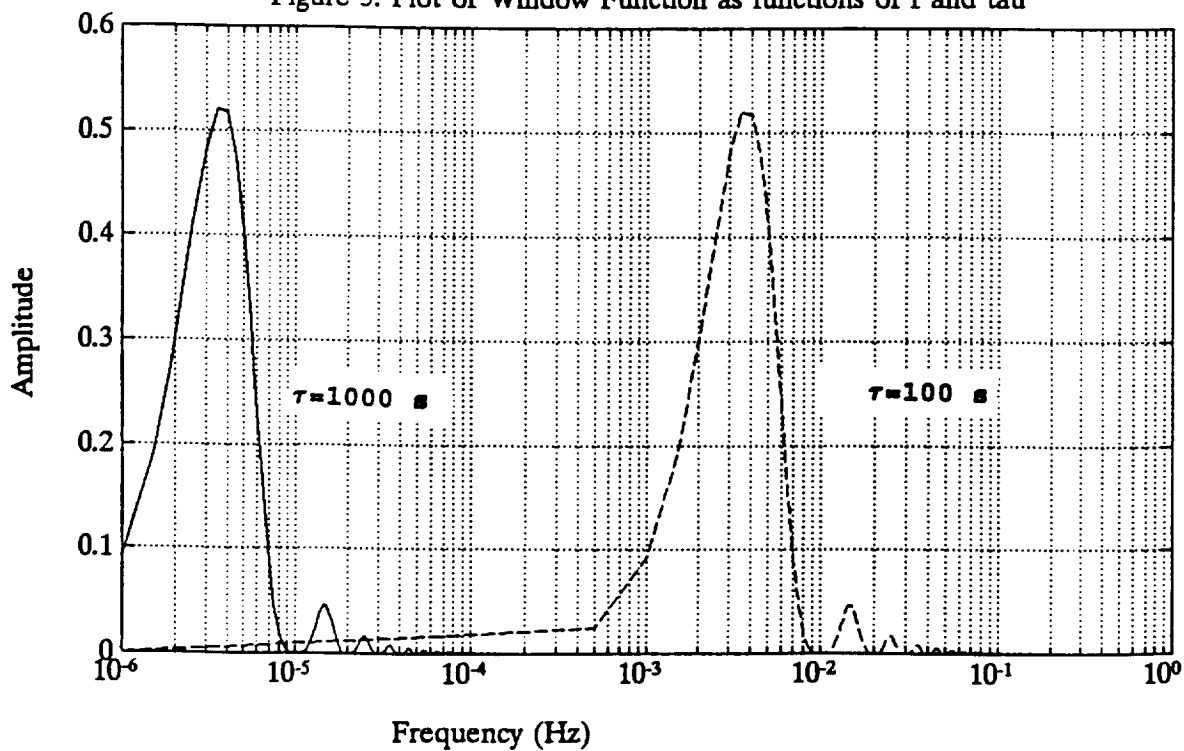


Figure 6. Allan Deviations of PM, VCXO and AFS

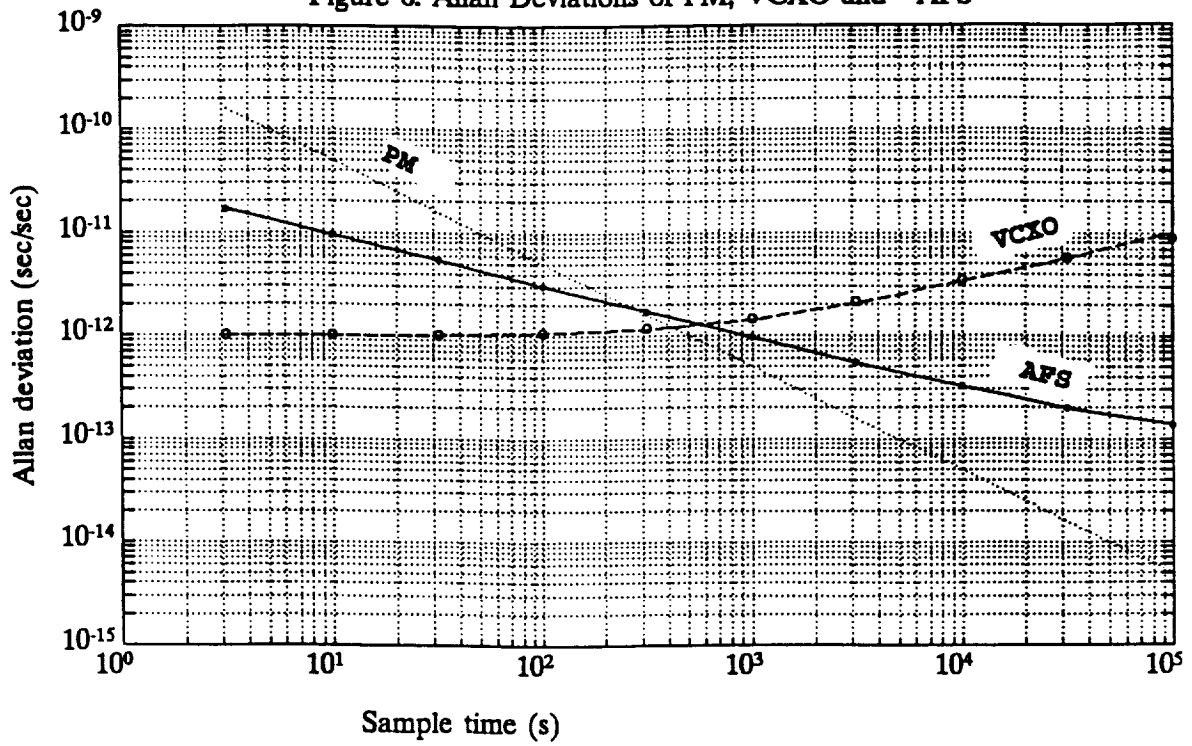


Figure 7. System Sensitivities

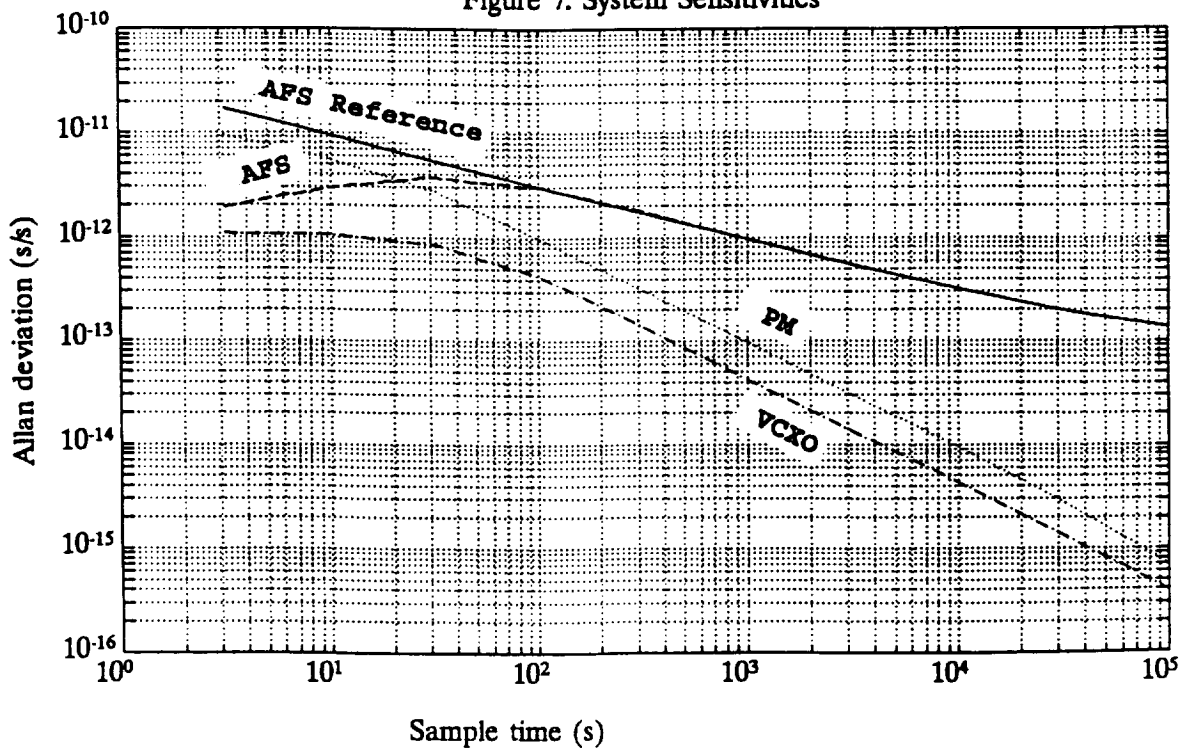


Figure 8. AFS Reference & System Output Allan Deviations

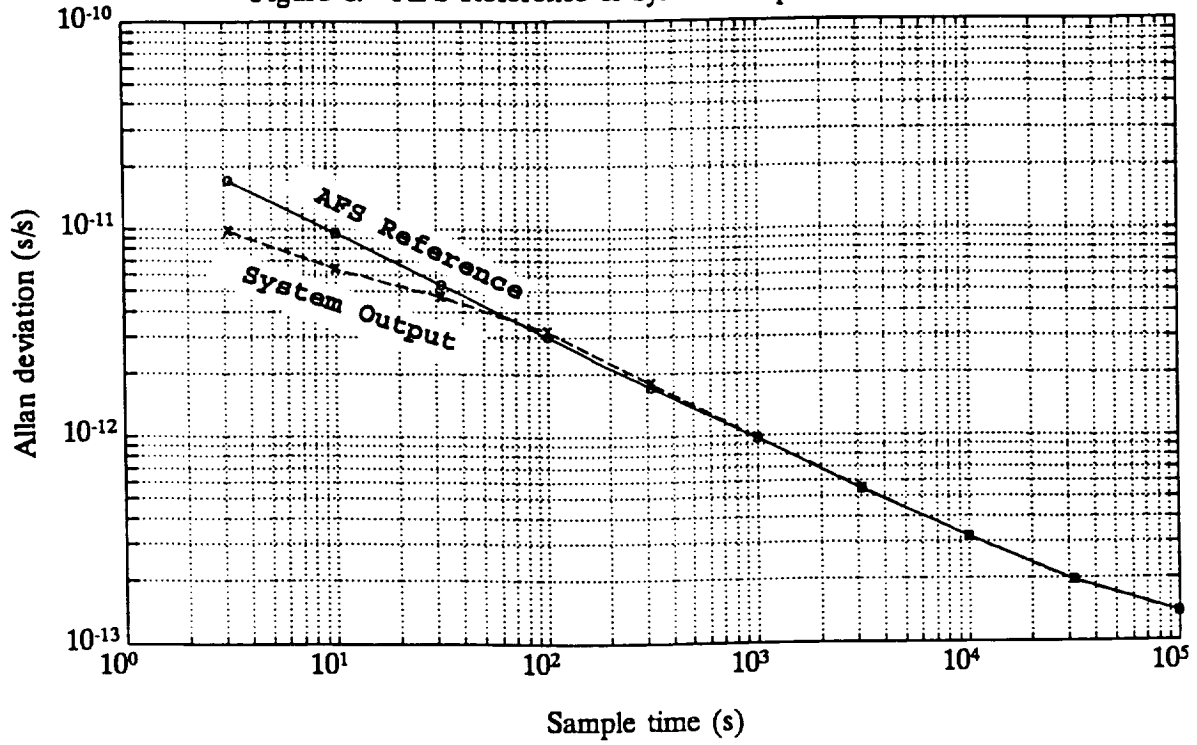


Figure 9. System Output Allan Deviation for  $T_c=15$  s

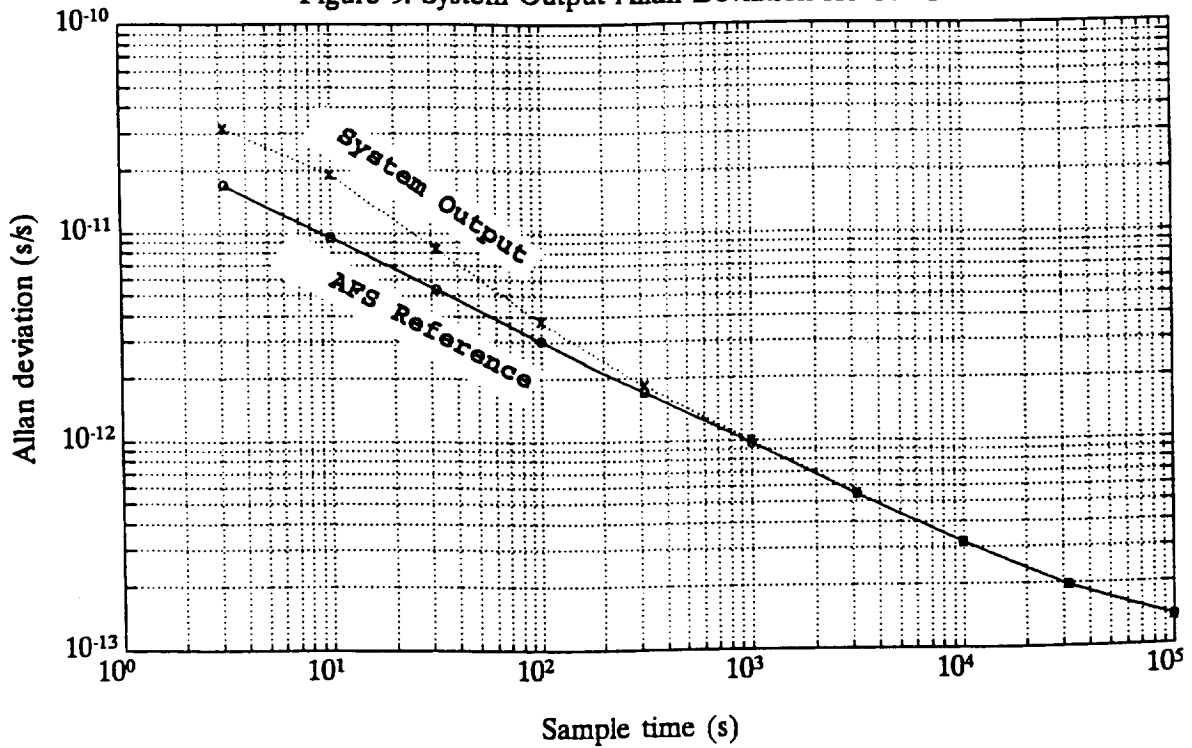


Figure 10. System Sensitivities for  $T_c=15$  s

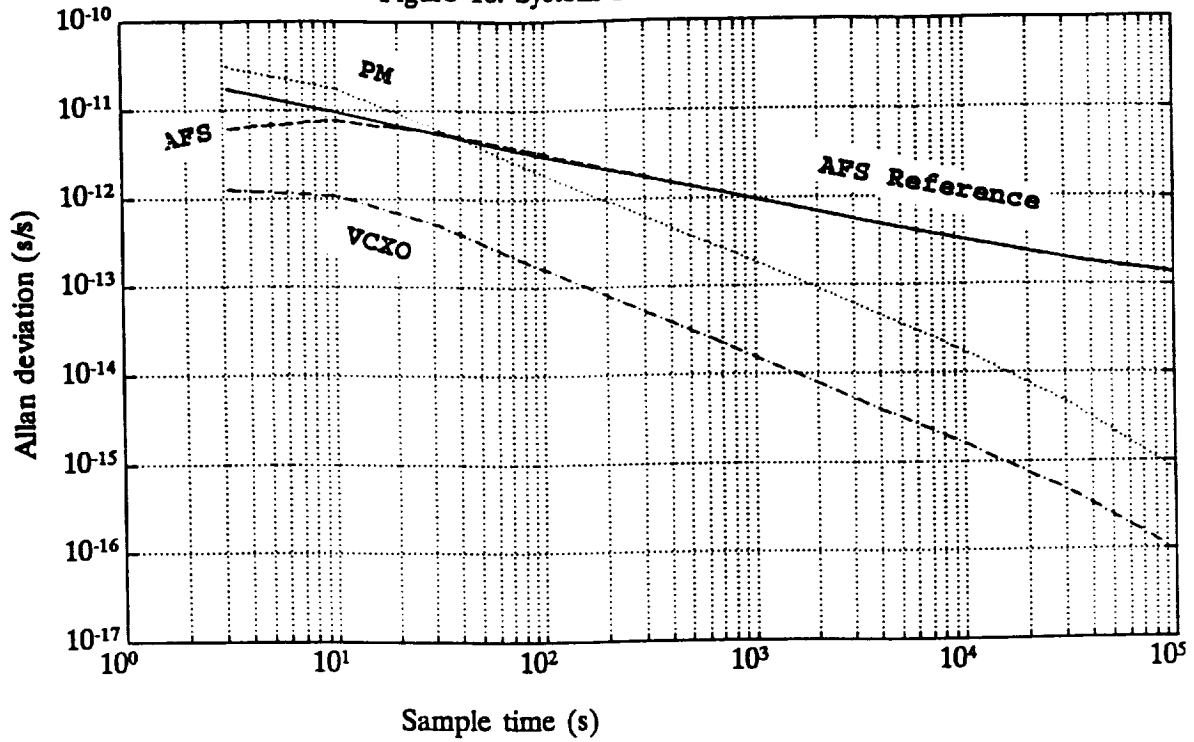
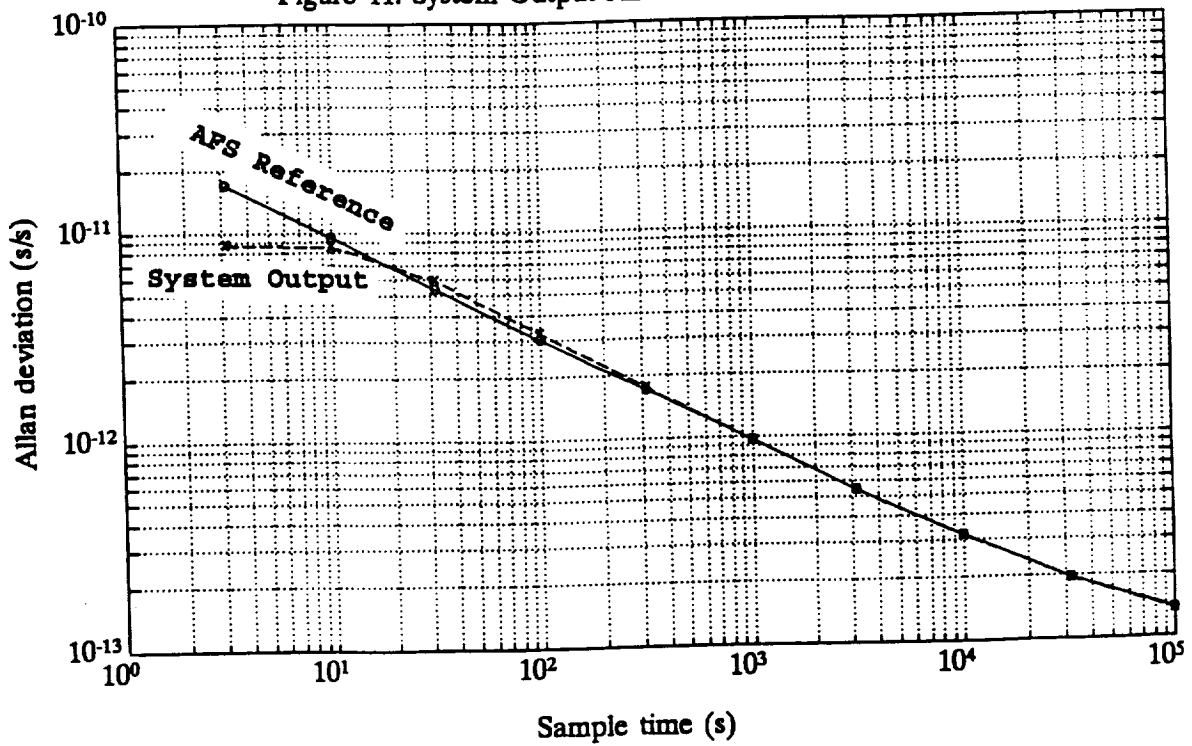


Figure 11. System Output Allan Deviation for Better PM



526-18

42302

p. 1

## SVN 9 END-OF-LIFE TESTING

1Lt Gregory E. Hatten  
2d Space Operations Squadron  
300 O'Malley Avenue Suite 41  
Falcon AFB CO 80912-3041

### Abstract

*SVN 9 was a GPS Block I research and development satellite. When it was launched in June of 1984, questions regarding the future performance of atomic frequency standards in orbit remained to be answered. In March of 1994, after performing for twice its designed life span, SVN 9 was deactivated as a member of the operational GPS satellite constellation. During the next two months, US Air Force and Rockwell personnel performed various tests to determine just how well the atomic frequency standards had withstood ten years in the space environment.*

*The results of these tests are encouraging. With a full constellation of Block II/IIA satellites on orbit, as well as the anticipated launch of the Block IIR satellites, results from the end of life testing will be helpful in assuring the continued success of the GPS program.*

## INTRODUCTION

When the opportunity to perform end of life testing on SVN 9's navigation payload arose, the limited amount of time available to perform these tests was a major constraint. Since the length of time devoted to navigation payload testing was limited by the amount of power available from the solar arrays, the onset of earth eclipse season presented an absolute boundary that could not be re-negotiated. Balancing the expected life span of the spacecraft with the amount of time required to test other, non-payload components meant that most navigation payload components would be excluded from the test.

Most of the navigation payload components aboard GPS satellites were extensively redesigned during the interim between experimental Block I production and the manufacture of the operational Block II/IIA design. The sole exception is the rubidium frequency standard manufactured by Rockwell. This made the decision to limit the testing to the rubidium frequency standards an easy one. The following tests were approved and carried out by personnel working from the GPS Master Control Station (MCS):

Test #1: Rubidium frequency standards are heavily temperature dependent. Program specifications limit their temperature dependence to frequency changes of 20 parts in  $10^{13}$  for every degree Celsius. By comparison, the FTS cesium frequency standards currently used on most operational GPS satellites must have a temperature coefficient less than 1 part in  $10^{13}$  per °C. By measuring the temperature coefficient of the current clock and comparing it to the

coefficient obtained during the pre-launch check-out process, we can estimate the effects of prolonged exposure to the space environment on the thermal properties of the GPS rubidium frequency standard.

Test #2: The nominal configuration of a GPS frequency standard involves locking the voltage controlled, quartz crystal oscillator (VCXO) to the stabilizing effects of the atomic physics package feedback loop. In the event that the atomic physics package becomes unusable, it may be necessary to use the VCXO in an open-loop configuration. The purpose of this test was to determine the operational feasibility of this plan.

Test #3: Due to the low reliability of atomic frequency standards, each GPS satellite carries four atomic clocks into orbit. When an operational clock fails, one of the standby clocks is powered up and brought on-line. SVN 9 was launched in June of 1984. The first clock (a cesium frequency standard manufactured by FTS) lasted an impressive nine years. In October 1993, the GPS control segment turned off the cesium clock and powered up the first of the three stand-by rubidium clocks. Test #3 was designed to initialize the two spare rubidium frequency standards after ten years of on-orbit cold storage. As part of this test, the two rubidium clocks were powered up separately and initialized according to standard Master Control Station procedures.

Test #4: The MCS can alter a rubidium frequency standard's output frequency by commanding the "C-field". This alters the magnitude of a uniform magnetic field surrounding the physics package. This ability to fine tune the frequency standard allows the MCS to adjust the 10.23 MHz output frequency as the clock ages and assumes new characteristics. When operating in the "open loop" mode, the current through the voltage controlled, quartz crystal oscillator (VCXO) can be commanded from MCS. Test #4 was designed to determine the extent to which the C-field and VCXO tuning ranges degraded with age.

## **NAVIGATION PAYLOAD TEST #1: Temperature Coefficient**

The Active Baseplate Temperature Control Unit (ABTCU) maintains a stable thermal environment for the rubidium frequency standard. The MCS has the capability of choosing from four separate settings: "A" (26.8 C), "B" (29.9 C), "C" (33.4 C), or "D" (37.5 C). At the operational setting of "D" the ABTCU should heat up to a temperature of  $37.5 \pm 1.5^\circ\text{C}$ . Once the ABTCU has stabilized, the temperature should not vary by more than  $\pm 0.1$  C.

For Test #1, the ABTCU was reset to setting "C" (33.4 C). Once the frequency standard had stabilized at this lower temperature, the Kalman Filter was able to estimate the new frequency. The magnitude of the resulting frequency change yielded the temperature coefficient.

After resetting the ABTCU to "C", the clock temperature changed from 37.6 to 34.6 over a course of 20 minutes. During the next 24 hours, the Kalman estimate of  $\Delta f/f$  changed from  $-20.57 \times 10^{-12}$  to  $-5.898 \times 10^{-12}$  s/s. After subtracting the change in frequency due to the aging coefficient ( $A_2$ ), we could assume the temperature change was responsible for the  $\Delta f/f$  of  $14.792 \times 10^{-12}$ . This increase in frequency yields a temperature coefficient of  $-4.93 \times 10^{-12} \Delta f/f$  per degree Celsius.

The original value of the temperature coefficient for this clock was taken from ground test data compiled in 1982. During the ground test the temperature was raised from 31 C to 35 C over a period of ten hours. After the test was complete, the accumulated phase error was used to derive the frequency offset. This 1982 data indicates that Rb #2 had a temperature coefficient of  $-1.54 \times 10^{-12} \Delta f/f$  per degree Celsius.

The results of this test indicate that the clock's temperature coefficient increased by a factor of three. There are several reasons other than prolonged exposure to the space environment that could explain the change in the coefficient. Since all ground tests on this frequency standard took place shortly after clock turn-on (a two to three week time span), the frequency standard may not have displayed normal operational behavior during this time. The clock used for this end of life test was powered up October 1, 1993. Since the clock had approximately six months to stabilize before the onset of end of life testing, the A2 term was more stable and was more accurately characterized in the Kalman Filter.

Other conditions existing during the end of life test and not present during the ground test should also be taken into account. The on-orbit satellite experiences large variations in the angle at which the sun falls on the satellite body. During the time span covered by this test, the incidence angle of the sun on the satellite body changed dramatically over the course of the day. This exposed the components aboard the vehicle to different temperatures depending on their on-board location. By comparison, during the ground test, the frequency standard was placed in a stabilized thermal vacuum chamber where these variations do not occur.

The elapsed time for the clock baseplate to stabilize at the new temperature was less than one hour. However, since there are no temperature telemetry sensors inside the clock, the actual time for the entire component to stabilize at a homogenous temperature may have been much longer. Even after available telemetry indicated that the frequency standard has stabilized, the internal temperature of the clock may still have been different from the baseplate temperature.

Conclusion: After almost ten years in space, the temperature coefficient for FS #2 changed less than one order of magnitude. This bodes well for future operations. The test indicates that ground test data for temperature related issues remains valid for several years and, if normal precautions are taken, can be trusted for operational use.

## NAVIGATION PAYLOAD TEST #2: VCXO Open-Loop Run

For this test, the feedback loop that ties the rubidium physics package to the VCXO was severed. At the same time, the MCS Kalman Filter was directed (via the SVCLKSEL directive and a modified KKS file) to increase the process noise ( $qs$ ) for the clock states. All  $q$  values were increased by three orders of magnitude. The  $qs$  for  $A_0$  (clock phase) increased from  $1.11 \times 10^{-22}$  to  $1.11 \times 10^{-19} s^2/s$ ; the  $qs$  for  $A_1$  (clock frequency) increased from  $3.33 \times 10^{-32}$  to  $3.33 \times 10^{-29} s^2/s^3$ ; the  $qs$  for  $A_2$  (clock frequency drift) increased from  $1.35 \times 10^{-43}$  to  $1.35 \times 10^{-40} s^2/s^5$ . These larger values compensated for the greater variation in measurement process noise brought on by the frequency instabilities of the VCXO.

Once the VCXO was tuned to an acceptable frequency, SVN 9 was treated as a normal member of the GPS constellation. Monitor stations tracked it; the Kalman Filter modeled

it; and routine navigation uploads were performed according to the daily contact schedule. Contingency uploads due to high ranging errors were not performed because of the excessive burden this would have placed on the MCS operations crew.

We performed the test twice. The first trial involved the VCXO from Frequency Standard #2; the next trial used Frequency Standard #1. The first run lasted 56 hours from 22 to 25 March. The second VCXO test lasted 73 hours from 8 to 11 April.

At the conclusion of the tests, each VCXO exhibited the following characteristics:

VCXO Clock State	VCXO Test #1	VCXO Test #2
VCXO Clock Bias ( $A_0$ )	$-8.77 \times 10^{-4}$ (s)	$-1.32 \times 10^{-3}$ (s)
VCXO Clock Drift ( $A_1$ )	$-2.55 \times 10^{-10}$ (s/s)	$-5.79 \times 10^{-10}$ (s/s)
VCXO Clock Drift Rate ( $A_2$ )	$1.20 \times 10^{-15}$ (s/s <sup>2</sup> )	$5.91 \times 10^{-15}$ (s/s <sup>2</sup> )
Maximum Drift Movement	$1.03 \times 10^{-10}$ (parts/day)	$5.49 \times 10^{-10}$ (parts/day)

These values are all too large in magnitude for sustained operational use. Through heavy Kalman Filter intervention and frequent adjusts of the payload timing (PRN) signal, it was possible to maintain a navigation signal for the duration of this test.

The rate at which the timing signal aboard the satellite diverged from GPS time would have required frequent PRN timing adjusts. The available space in the navigation message mandates that the SV-GPS time offset be less than 976,000 ns. If no adjustments to the timing signal had been performed, this absolute limit would have been exceeded every two to three days. In the case of SVN 9, this timing adjust was performed at the beginning of the test for each frequency standard. Each iteration of the test was concluded before this clock phase limit could have been exceeded.

The instabilities associated with the VCXO output signal necessitated intense control segment maintenance. Ranging errors associated with an incorrect navigation upload accumulated at a rate of 10–20 meters per hour. New, more accurate navigation uploads would have been required every 30 to 60 minutes in order to maintain ranging errors within the allowable operational limits. This is beyond the capability of the MCS in its current configuration.

Conclusions: The results of this test are mixed. The VCXO-specific process noise values ( $qs$ ) contained in the KKS file provided the Kalman Filter with the flexibility needed to model the very erratic VCXO clock states. This in turn allowed the MCS operations staff to build and transmit navigation uploads in order to monitor ERDs and other performance parameters. In this respect, Test #2 proved that the MCS is capable of handling a vehicle operating in the VCXO open-loop mode.

The discouraging result of the test was the accumulation of range error and the rapidly increasing SV-GPS timing discrepancy. Through sustained Kalman maintenance along with frequent navigation uploads and PRN timing adjusts, it is possible to maintain a healthy navigation signal. The ability to do this would impose an unacceptably large burden on the operations crew if the situation existed for an extended period of time.

## NAVIGATION PAYLOAD TEST #3: New Clock Initialization

Test #3 offered a chance to witness the start-up performance of the two standby rubidium clocks. The test followed standard MCS procedures for powering up and initializing a new rubidium clock. Although some procedures were customized to accommodate the specifics of each individual frequency standard, the following steps were common to all new rubidium clocks.

The new clocks were powered up and allowed to thermally stabilize for one to three days. A C-field tune was done soon afterwards to minimize any frequency residuals. As soon as the C-field tune was complete, the satellite was provided with a routine navigation upload. This entire process was completed within four days for both new frequency standards.

At this point, the satellite had to be monitored constantly to determine the rate of error accumulation in the ranging signal. Normally a rubidium frequency standard will settle down and exhibit acceptable operational characteristics after the passage of another week. Although a rubidium clock will continue to change its performance characteristics for the next few months, this luxury of time required to observe this phenomenon was not available. Each iteration of the test was concluded after two weeks.

To minimize the burden on the operations crew, the vehicle was only uploaded once per day regardless of the size of the ranging errors. The test ran for approximately two weeks on each of the two rubidium clocks. Two weeks is the normal initialization period for a new rubidium clock. After this time, we are usually prepared to set the SV healthy.

The test of Rubidium #1 ran 14 days from 25 March to 8 April. The test of Rubidium #3 ran 11 days from 11 April to 22 April. Both tests recorded Kalman Filter data as the clocks warmed up. The Kalman estimates of the clock states by the end of the respective tests are shown below. Also shown are the NIST estimates of the clock stability based on the Allan deviation.

Clock State	FS #1	FS #3
Clock Bias ( $A_0$ )	$-1.45 \times 10^{-4}$ (s)	$2.45 \times 10^{-4}$ (s)
Clock Drift ( $A_1$ )	$-6.74 \times 10^{-11}$ (s/s)	$3.03 \times 10^{-11}$ (s/s)
Clock Drift Rate ( $A_2$ )	$1.12 \times 10^{-17}$ (s/s <sup>2</sup> )	$1.66 \times 10^{-17}$ (s/s <sup>2</sup> )
Stability ( $\tau$ = one day)	$1.1 \times 10^{-12}$	$2.5 \times 10^{-13}$
Maximum Drift Movement	$1.27 \times 10^{-12}$ (parts/day)	$1.43 \times 10^{-12}$ (parts/day)

At the end of the test, the clocks exhibited characteristics similar to all new rubidium frequency standards. The phase offsets ( $A_0$ ) and frequency offsets ( $A_1$ ) are both slightly high but would be acceptable for normal operations. We would definitely need to adjust these parameters later in order to keep these clocks on-line. The one day stability for FS #1 is fairly high, but would be expected to come down with time. The one-day stability for FS #3 is better and meets program specifications ( $5.0 \times 10^{-13}$ ).

When a new clock is warming up, random variations in frequency should be expected. The maximum variations in frequency each day were 12 to 15 parts in  $10^{13}$ . Movements of this magnitude are higher than normal, but are partially attributed to the large  $A_2$  term. This large

frequency drift value will cause both the phase offset and frequency offset values to increase in magnitude over time.

The frequency drift value ( $A_2$ ) is often the biggest obstacle to overcome when setting a vehicle with a new rubidium clock healthy. Both of these clocks exhibit a value of  $A_2$  that is approximately one order of magnitude higher than normal. Experience has shown that the  $A_2$  term on most new rubidium clocks will slowly decrease in magnitude and become negative in sign. Since this process usually takes several months, the observation of this phenomenon was beyond the scope of this test.

Ranging errors for both clocks were slightly high but acceptable. By uploading SVN 9 once per day, ERDs (Estimated Range Deviations) exceeded ten meters daily. This exceeds the operational limits imposed on the MCS and indicates that the stability of the clocks and their estimate in the Kalman Filter were not yet at the optimal level.

Conclusions: After ten years in orbit, the two stand-by rubidium clocks powered up and began the initialization process as expected. After a two week warm-up period, the time allotted for the tests had expired. By this time, most of the characteristics measured by the GPS Kalman Filter identified these clocks as normal. The one-day stability measured by NIST also showed characteristics common to other, operational GPS clocks. The  $A_2$  term for both frequency standards was higher than those measured on any of the operational rubidium clocks, but this is not too unusual for a clock undergoing the initialization process. We would expect to see these values drop if the clocks remained on for an extended period of time.

## NAVIGATION PAYLOAD TEST #4: C-Field and VCXO Tuning

Method: A rubidium frequency standard normally operates with the atomic loop closed and a C-field tune of about 50%. This mid-field tune allows the MCS the potential to either increase or decrease the output frequency by an equal amount. For test #4, the C-field was tuned to the minimum possible frequency. Once the MCS Kalman Filter settled on a solution for the frequency, the command was sent to the clock ordering the maximum C-field tuning value. This procedure was repeated for the VCXO operating in the open-loop configuration.

The following chart details the C-field tuning values and their associated frequency residuals. This actual residual should be compared to the anticipated change in frequency based on ground test data collected in February 1982.

C-field tune	actual $\Delta f/f$	anticipated $\Delta f/f$
55.655%	$3.14727 \times 10^{-11}$ (s/s)	$2.9185482 \times 10^{-10}$ (s/s)
0.0%	$-2.650 \times 10^{-9}$ (s/s)	$-2.840 \times 10^{-9}$ (s/s)
100.0%	$2.398 \times 10^{-9}$ (s/s)	$2.404 \times 10^{-9}$ (s/s)

The analysis of these test results indicates that the overall range of the C-field decreased with age. The initial C-field range of  $5.244 \times 10^{-9}$  s/s decreased by 3.73% to  $5.048 \times 10^{-9}$  s/s. Because the range decreased asymmetrically, the mid-field frequency value shifted 1.75% ( $9.2 \times 10^{-11}$  s/s) towards the positive end of the scale. This is a well observed phenomenon

and must be accounted for during every new clock initialization.

After the atomic loop was disconnected from the VCXO, we tested the tuning characteristics of the VCXO. The following chart details the VCXO tuning values and their associated frequency residuals. This actual residual should be compared to the anticipated change in frequency based on ground test data from 1982.

VCXO tune	actual $\Delta f/f$	anticipated $\Delta f/f$
0.0%	$-2.51283 \times 10^{-7}$ (s/s)	$-2.52333 \times 10^{-7}$ (s/s)
100.0%	$1.91467 \times 10^{-7}$ (s/s)	$+2.20254 \times 10^{-7}$ (s/s)

The analysis of these test results indicates that the overall tuning range of the VCXO decreased with age. The initial VCXO tuning range of  $4.726 \times 10^{-7}$  s/s decreased by 6.32% to  $4.4275 \times 10^{-7}$  s/s. Based on the asymmetry in the decrease of the total range, it appears that the entire frequency range shifted 3.16% ( $1.4 \times 10^{-8}$  s/s) towards the negative end of the scale.

Conclusion: The C-field and VCXO tuning capabilities diminish during the accumulated time the satellite spends on-orbit. This loss of capability does not pose a problem to the normal operation of the frequency standard, because most C-field tunes differ from the mid-field tune by less than 10lost capacity observed in this test lies outside of the nominal tuning range.

This lost capacity, along with the shift in frequency of the center point (or "mid-field tune") requires the addition of a calibration factor to ensure accurate tuning performance. In practice, this may require transmitting more than a single tune command word to ensure the proper tune. Current operational practice allows for several (two or three) tunes to correct the satellite's frequency offset. This shift of the mid-field tune and change in tuning capacity does not hamper operational capabilities.

## CONCLUSION

The end of life testing conducted on SVN 9 provided valuable insight into the aging characteristics of rubidium frequency standards. Although none of the test results yielded dramatic, unexpected results; they served to strengthen the operational practices and conventional wisdom that rule the procedures found in the MCS.

We confirmed the reliability of the published thermal coefficients as well as the VCXO and C-field tuning values (Tests #1 and #4). Slight changes in the magnitude of these values did nothing to lessen the confidence we now maintain in the ground test results.

The abilities of the MCS to initialize new clocks and maintain an SV in the VCXO open loop mode (Tests #2 and #3) were observed with some relief. These seemingly routine sets of circumstances do not appear so routine in light of SVN 9's prolonged exposure to the space environment. The challenge to the operational crew to support the intense maintenance, while quite formidable, is something that could be overcome with increased manpower and ground segment support. Similarly, the somewhat poor performance of the two new initialized clocks should not be judged solely on 10 or 14 days worth of data. The fact that these clocks powered up and could be characterized in a normal manner, after twice the expected lifetime of the

satellite had passed, is a success.

Tests such as these enhance the ability of the MCS to perform GPS operations. With the expected demise of SVN 10 in spring of 1995, the last of the Block I vehicles will have expired. Their passing should not be seen as the disposal of a valuable resource; instead it is an opportunity to validate and improve the operational performance of the GPS Master Control Station.

## **ACKNOWLEDGEMENTS**

The author would like to thank the following individuals and their agencies for generous assistance to the SVN 9 End of Life Testing program and the creation of this paper:

Scott Boushell, 2d Space Operations Squadron  
Jeff Harvey, Rockwell Space Operations Company  
Steven Hutsell, 2d Space Operations Squadron  
Ted Moge, Rockwell Space Operations Company  
M. J. VanMelle, Rockwell Space Operations Company  
Marc Weiss, NIST  
The men and women of the 2d Space Operations Squadron

## **REFERENCES**

- 1 NIST Report on End of Life Testing, 25 Apr 94
- 2 Hutsell, Steven T., Capt, USAF, Recent MCS Improvements to GPS Timing, Proceedings of ION GPS-94, 20-23 Sep 94
- 3 GPS-OOH Vol 2 GPS-FSV-011

## QUESTIONS AND ANSWERS

**THOMAS CELANO (TASC):** I was wondering if you have any plans for the end-of-life testing for the last Block I.

**GREGORY HATTEN (USAF):** We should. PRN 9 is taking its slot in the A.1 position. So we have dual coverage with that satellite. So they will probably will give us a few months to do some tasks. I would anticipate that starting probably no earlier than March. So it's not expected to live past May or June, I don't think.

**SIGFRIDO M. LESCHIUTTA:** Two comments and one question. The first comment, I was really delighted to see the history of equipment working for 12 years.

The second comment, I think the figures shown is a tribute to the ingenuity of the designers of those clocks.

And third, the probability of a thing concerning the temperature coefficient. Do you have an idea of what could be the reason that there's more degradation in regard to efficient temperature? The physics of the cell?

**GREGORY HATTEN (USAF):** I really don't know. That would probably be more a question for the manufacturer. With my limited experience on that, I really couldn't answer that. Sorry.

**JAMES COMPARO (AEROSPACE CORP.):** I was going to ask you about Frequency Standard Number 3. You said the stability at one day was about a factor 10 worse than nominal for that rubidium clock. Was that clock on for nine days, and you took stability measurements everyday?

**GREGORY HATTEN (USAF):** No, it was on for -- we requested NIST to go ahead and give us some stability data after we thought it had settled out and we performed our last C-field tune. I believe it had been on -- pardon me, that was 11 days. And I believe it had been on eight days when we started taking tests. They took four, so the error bars at one day would be fairly large after a four- or five-day sample.

**JAMES COMPARO (AEROSPACE CORP.):** And were there any Allan Variance measurements taken at time scales shorter than one day?

**GREGORY HATTEN (USAF):** Yes, there were. And I don't think I have that data with me. But I do have it. NIST did provide it for us.

**PARTICIPANT:** What are the units of time on your frequency drift? Is that per second?

**GREGORY HATTEN (USAF):** Second per second squared.



207-74

52323

p. 12

# FIBER OPTIC REFERENCE FREQUENCY DISTRIBUTION TO REMOTE BEAM WAVEGUIDE ANTENNAS\*

MALCOLM CALHOUN, PAUL KUHNLE, and JULIUS LAW  
Jet Propulsion Laboratory  
California Institute of Technology  
Pasadena, California 91109

## Abstract

*In the NASA/JPL Deep Space Network (DSN), radio science experiments (probing outer planet atmospheres, rings, gravitational waves, etc.) and very long-base interferometry (VLBI) require ultra-stable, low phase noise reference frequency signals at the user locations. Typical locations for radio science/VLBI exciters and down-converters are the cone areas of the 34 m high efficiency antennas or the 70 m antennas, located several hundred meters from the reference frequency standards. Over the past three years, fiber optic distribution links have replaced coaxial cable distribution for reference frequencies to these antenna sites. Optical fibers are the preferred medium for distribution because of their low attenuation, immunity to EMI/RFI, and temperature stability. A new network of Beam Waveguide (BWG) antennas presently under construction in the DSN requires hydrogen maser stability at tens of kilometers distance from the frequency standards central location. The topic of this paper is the design and implementation of an optical fiber distribution link which provides ultra-stable reference frequencies to users at a remote BWG antenna.*

*The temperature profile from the earth's surface to a depth of six feet over a time period of six months was used to optimize the placement of the fiber optic cables. In-situ evaluation of the fiber optic link performance indicates Allan deviation on the order of parts in  $10^{-15}$  at 1000 and 10,000 seconds averaging time; thus, the link stability degradation due to environmental conditions still preserves hydrogen maser stability at the user locations. This paper reports on the implementation of optical fibers and electro-optic devices for distributing very stable, low phase noise reference signals to remote BWG antenna locations. Allan deviation and phase noise test results for a 16 km fiber optic distribution link are presented in the paper.*

## INTRODUCTION

The NASA/JPL Deep Space Network is expanding its spacecraft tracking capability with a network of 34 meter Beam Waveguide antennas. A cluster of three of these antennas at the Goldstone Tracking Station (GTS) is located a distance of 16 kilometers from the Signal

\*The research described in this paper was carried out at the Jet Propulsion Laboratory, California Institute of Technology, under a contract sponsored by the National Aeronautics and Space Administration.

Processing Center (SPC). Deep Space Station 24 (DSS 24), the first of the cluster to be completed is scheduled to go on-line in late 1994. In support of antenna tracking functions as well as radio science and VLBI experiments, precise time and stable reference frequency is required at this remote antenna site. The Frequency and Timing Systems Engineering Group at JPL is responsible for providing reference frequency and precise time to users at the antenna. Certain applications at the antenna require frequency stability and phase noise of the quality of a hydrogen maser. Since the hydrogen maser frequency standard is located at the SPC, the problem becomes one of distributing the signals to remote locations without signal degradation.

The distance between the SPC and the antennas is too great to consider coaxial cable for the reference frequency and time signals; also, microwave links do not provide the required stability. The method of choice for the distribution implementation is fiber optic links. Due to cost constraints, commercial off-the-shelf equipment was utilized as much as possible. The optical fibers in the link are standard, single mode SMF-28, 96 fibers contained in a direct burial cable. The burial depth is approximately 1.5 meters.

The hardware implementation for timing and reference frequency along with tests results measured after the installation was completed are presented in this paper. Also, stability considerations based on temperature effects on the optical fibers are discussed.

## DISTRIBUTION HARDWARE

The 5 MHz reference frequency signal and the modified IRIG-G time code signals are transmitted over separate fiber optic links to avoid corruption of the reference signal. The terminal equipment for the fiber links is the Wavelink model 3290 manufactured by the Grass Valley Group, a subsidiary of Tektronix, Inc. The transmitter consists of a 1300 nm laser diode along with the required bias and modulation circuits. The receiver contains a photodetector for converting the 1300 nm light to RF which is demodulated to recover the signal. In order to meet the phase noise requirements for radio science applications, the 5 MHz reference frequency recovered from the optical receiver is phase locked by a FTS 1050 Disciplined Frequency Standard (DFS) with a 1 Hz loop bandwidth. The signal from the DFS is then distributed to the antenna users. A block diagram of the frequency and timing distribution is shown in Figure 1.

The filtered 5 MHz from the disciplined frequency standard is applied to a distribution assembly where it is multiplied to 10 MHz and to 100 MHz for users who require these frequencies. The distribution assembly employs low noise, high isolation amplifiers. The entire assembly is temperature controlled for improved stability.

The modified IRIG-G time code signal utilizes a 100 KHz carrier frequency. The source signal is derived from the Time Insertion Distribution Assembly at the SPC, applied to the laser transmitter, and recovered at the fiber optic receiver in the antenna pedestal room. A travelling clock was used to set the time at the remote antenna; the time offset between DSS 24 and the SPC is less than 100 nanoseconds. Approximately 82 microseconds time delay was removed at the Time Code Translator because of the 16 km of optical fiber.

## TEMPERATURE EFFECTS ON STABILITY

The cables which distribute the reference signals to the remote antennas are buried at a depth of approximately 1.5 meters. This burial depth is sufficient to mitigate the effects of large diurnal temperature variations; however, seasonal changes and weather fronts can still be sensed even at a depth of 2 meters. Figure 2 is a plot of surface temperature variations at Goldstone Tracking Station, which is located in the California Mojave desert<sup>[1]</sup>. Temperatures were recorded at four hour intervals for the period 11 June 1992 to 14 June 1992. Observe the extremes from a low near 12°C to a high near 55°C, with an average  $T$  of 35°C per 12 hour interval.

The 1.5 meter burial depth was determined by observing the temperature profile of the earth in the Mojave desert for several months<sup>[1]</sup>. Thermocouples were buried at depths of 0.6, 0.9, 1.2, 1.5, and 1.8 meters, respectively. A data logger with a computer was used to record these data. The results of the measurements are shown in Figure 3. Measurements were begun on 14 January 1992 and terminated on 26 June 1992. Analysis of the data indicates that a burial depth of 1.5 meters is sufficient to attenuate the short term temperature variations. In Figure 3, the line with the larger variations is the daily average surface temperature.

The thermal coefficient of delay for the optical fiber is approximately 7 ppm/°C. The length of buried cable is 16 km. At a depth of 1.5 meters, a peak to peak temperature variation of 35°C is reduced to less than 0.1°C, peak to peak. The phase variations due to temperature effects may be calculated as follows:

$$\begin{aligned}\Delta\phi &= \Delta L \times 360^\circ/\lambda_o \\ \Delta L &= Lk\Delta T\end{aligned}$$

where  $\Delta\phi$  is the change in phase delay introduced by the temperature variation  $T$ ,  $k$  is the thermal coefficient of delay of the fiber in ppm/°C,  $L$  is the optical fiber length in meters, and  $\lambda_o$  is the wavelength of the reference signal in the medium. At a measurement frequency of 100 MHz, the wavelength in the fiber is 2.1 meters. Calculating the phase change for a 35°C surface excursion and a worst case 0.1°C peak to peak at the fiber yields 1.92° phase change at 100 MHz for the 16 km fiber link. This calculated value of  $\Delta\phi$  is compared with test results in the next section of this paper.

## STABILITY AND PHASE NOISE TEST RESULTS

Since there is no reference signal at the remote antenna site to compare the fiber optic distributed signal, the scheme shown in Figure 4 was used to measure the stability of the reference signal. The 5 MHz signal from the DFS was applied to the Reference Frequency Distribution Assembly where it is multiplied to 10 MHz and to 100 MHz. The 100 MHz output from this assembly was applied to the transmitter of a Fiber Optic Reference Frequency Distribution Assembly (FODA) which is known to have stability and phase noise performance an order of magnitude lower than a hydrogen maser<sup>[2]</sup>. The signal was then returned to the

SPC over a test fiber in the same cable bundle that was used to send the reference signal to DSS 24. Figure 5 shows the stability test results using the configuration shown in Figure 4. The Allan deviation shown in Figure 5 was taken with a temporary fiber optic cable to complete the cable run to DSS 24 before the installation was completed. Approximately 420 meters of fiber cable was exposed at the surface of the Mojave desert during these measurements. The temporary cable failed to meet system requirements. Figure 6 shows the change in phase delay as a function of time. The temporary fiber cable caused a change in time delay of approximately  $14^\circ$  per 12 hour period at 100 MHz. The corresponding Allan deviation at the half-day period is  $1.5 \times 10^{-14}$  which does not meet the system requirements.

Figure 7 shows the results of the stability test after the installation of the permanent fiber optic cable. The test results shown are for a fiber optic cable buried at approximately 1.5 meters, with a total length of 16 km. Note that the Allan deviation is well below the specification limits with the exception of  $\tau = 1$ . This stability anomaly is believed due to the DFS which has a loop bandwidth of less than 1 Hz and a slight overshoot at 1 Hz. The change in phase delay over the fiber optic link is shown in Figure 8. The results indicate a peak-to-peak time variation (at 100 MHz) of approximately 110 picoseconds, which equates to  $1.98^\circ$  (for 16 km) per 12 hour interval, almost an order of magnitude improvement over the temporary fiber installation. Using the

$\Delta\phi$  equation from the previous section yields a calculated value of  $1.92^\circ$  per 12 hour interval, which closely agrees with the measured phase delay. Observe in Figure 7 that the Allan deviation value at the half-day interval is approximately  $1.5 \times 10^{-15}$ , which is an order of magnitude better than the temporary fiber and also meets the system requirement for long term stability.

Phase noise tests at DSS 24 were run using the test configuration shown in Figure 9. The test system included a high quality test oscillator which was phase locked to the distributed reference signals. Test results are summarized in Table 1.

Table 1. SPC 10 to DSS 24 Phase Noise Test Results

PHASE NOISE TEST RESULTS AT DSS 24				
FREQUENCY OFFSET FROM CARRIER (Hz)	ESTIMATED PERFORMANCE AT X BAND: FROM D-LEVEL REVIEW 12-17-92 (dBc)	MEASURED AT 5 MHz (dBc)	MEASURED AT 100 MHz (dBc)	EQUIVALENT AT X-BAND ( $\mathcal{L}(f)$ 5 MHz -64 dB) (dBc)
1	-52	-121	-96	-57
10	-66	-140	-115	-76
100	-77	-148	-123	-84
1000	-77	-150	-125	-86
10000	-77	-151	-125	-87
100000	-77	-154	-126	-90

## TIMING DISTRIBUTION

The timing distribution signal for DSS 24 is obtained from the master clock at SPC 10. The signal is a modified IRIG-G time code which is derived from the Time Insertion Distribution Assembly (TIDS) at SPC 10. The signal flow from the source to the remote antenna is shown in Figure 1. In order to have the time offset at DSS 24 within the required 1 microsecond of the SPC 10 master clock, a travelling Cesium Clock was used to determine and remove the time delay over the 16 km fiber optic cable. Approximately 82 microseconds of time delay was removed by a special Time Code Translator (TCT) at the remote antenna. Consequently, the remote clock at DSS 24 is within 50 nanoseconds of the SPC 10 clock and the measured jitter at the antenna is less than 2 nanoseconds.

## CONCLUSIONS

The fiber optic reference frequency and timing distribution from SPC 10 to DSS 24 is complete. Testing was begun with a temporary fiber optic cable with 420 meters exposed to the desert extremes of hot and cold temperatures. Test results did not meet system requirements, and thus were delayed until a permanent, buried fiber cable was installed. Test results with the 16 km of buried cable indicate that the system phase noise performance meets requirements with some margin. The stability of the reference signals is within system requirements except at  $\tau = 1$ , where the commercial fiber optic terminal equipment and the DFS slightly degrade the Allan deviation. Commercial, off-the-shelf-equipment was used in order to stay within cost constraints of the project.

After removing 82 microseconds of cable delay, the remote clock at DSS 24 is within  $\pm 50$  nanoseconds time offset of the master clock with a jitter of less than 2 nanoseconds. The timing distribution meets all system requirements at the remote antenna site.

## REFERENCES

- [1.] M. Calhoun, P. Kuhnle, and J. Law, "*Environmental Effects on the Stability of Optical Fibers used for Reference Frequency Distribution*", Proceedings of the Institute of Environmental Sciences, Las Vegas, NV, May 1993.
- [2.] M. Calhoun and P. Kuhnle, "*Ultrastable Reference Frequency Distribution Utilizing a Fiber Optic Link*", Proceedings, 24th Precise Time and Time Interval Applications and Planning Meeting, Tysons Corner, VA, December, 1992.

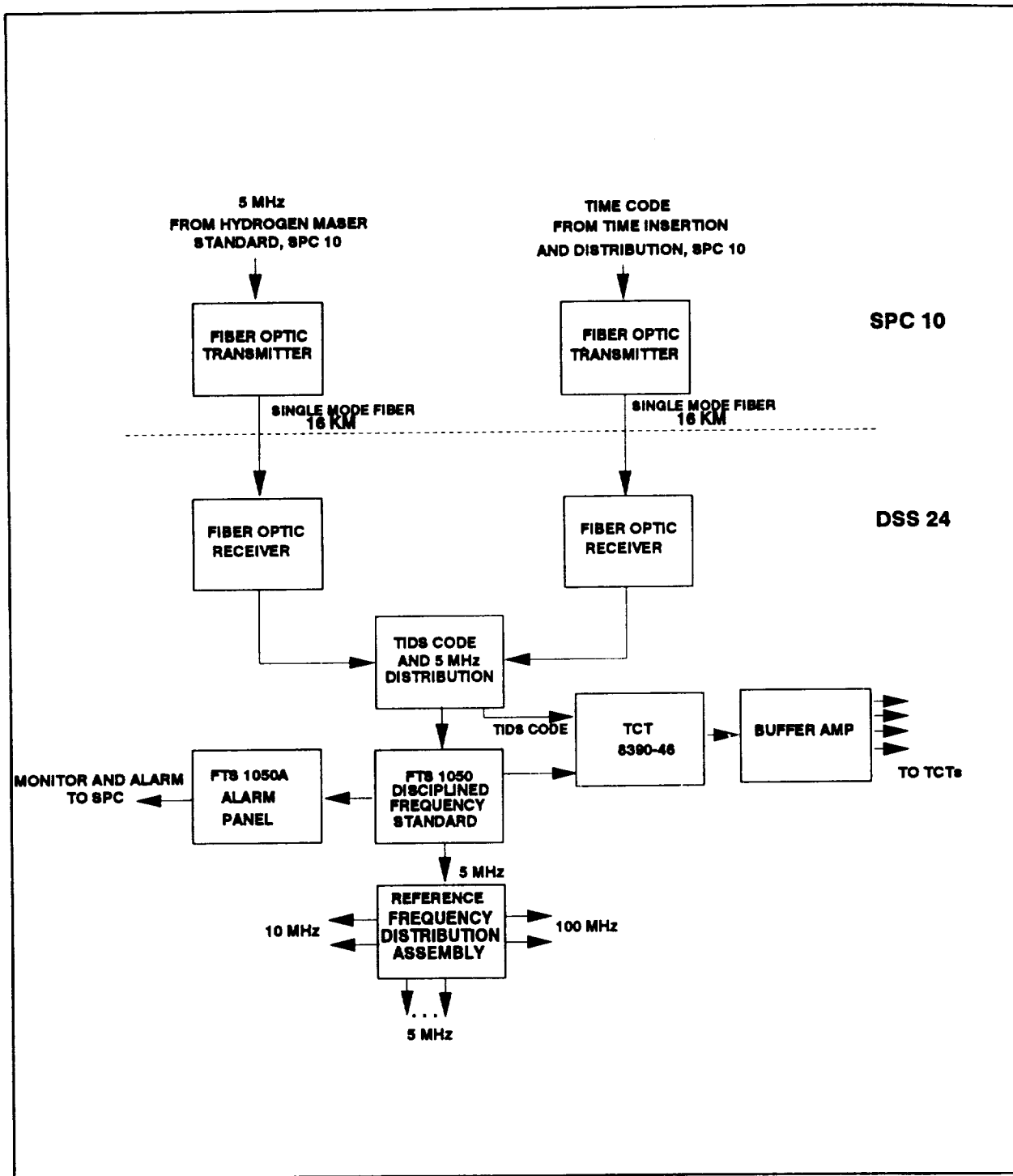
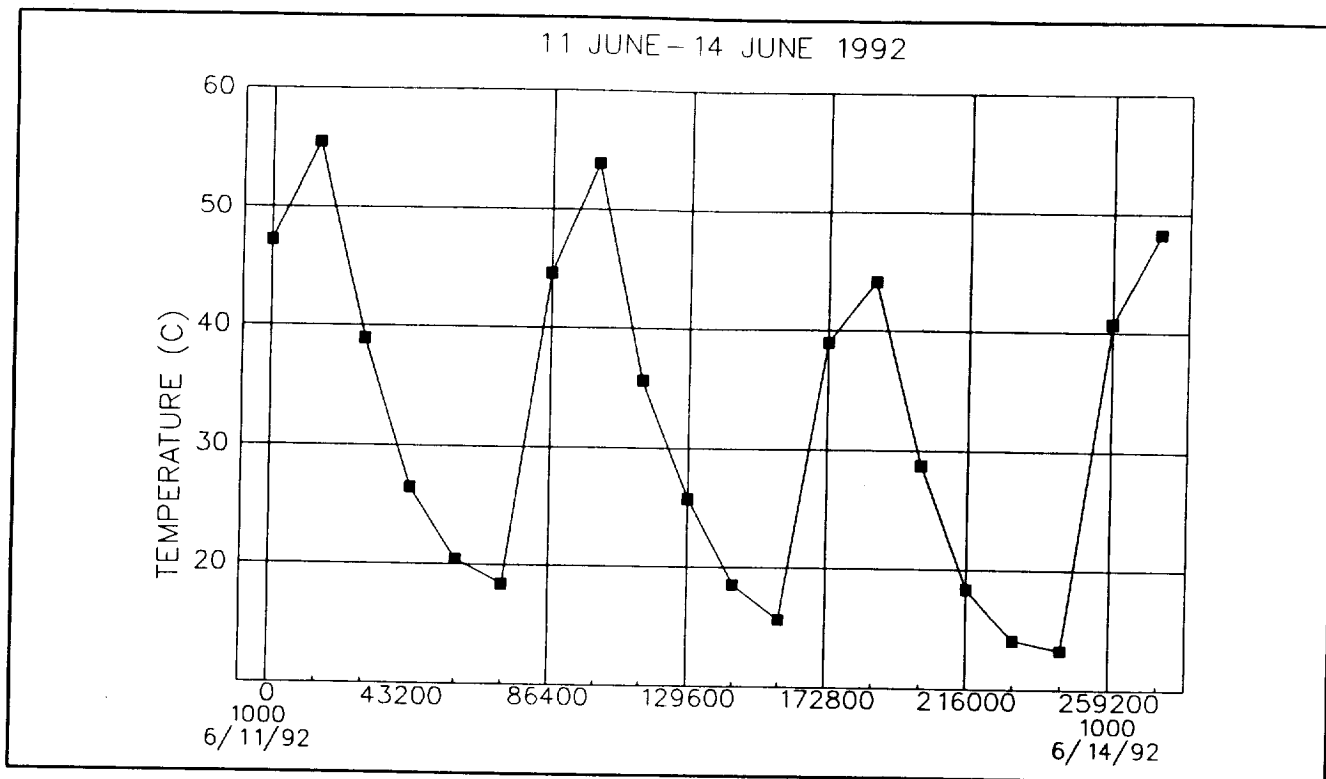
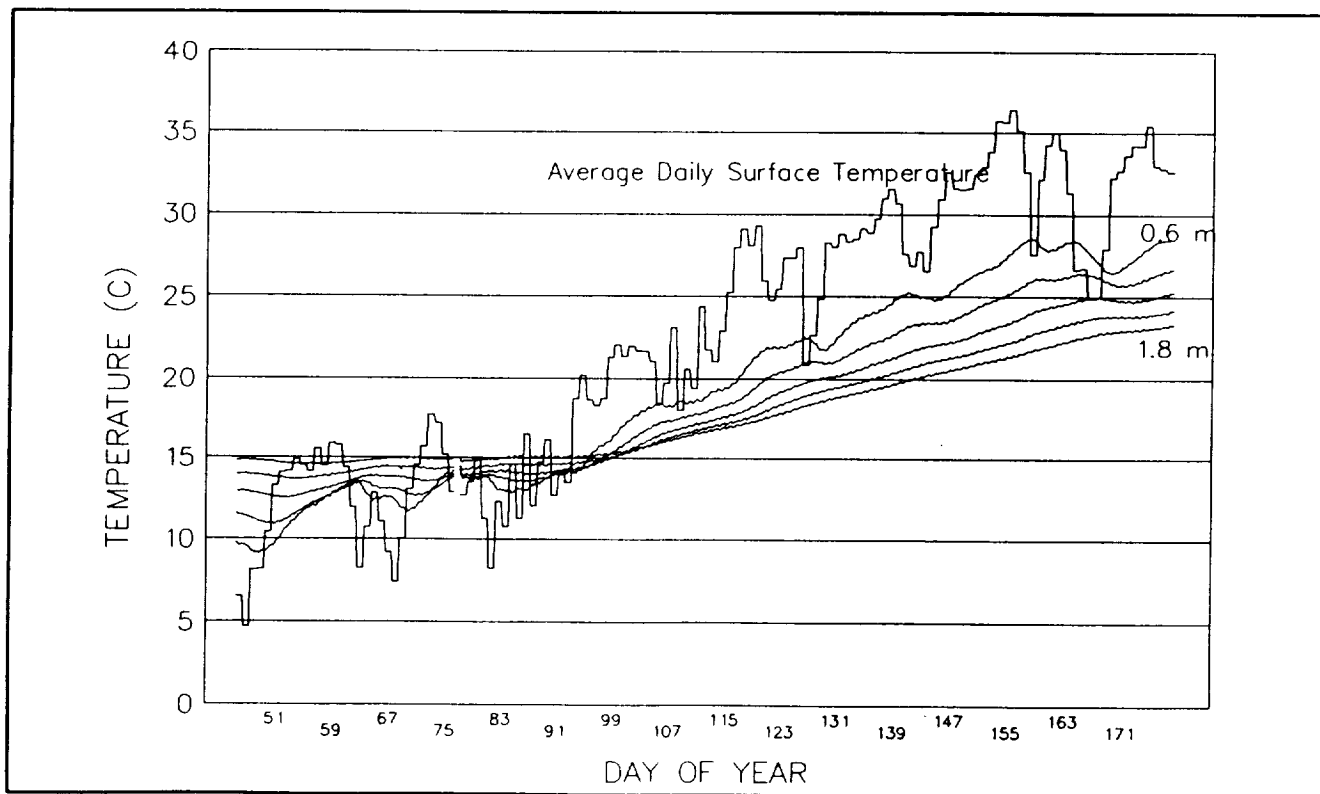


Figure 1. BLOCK DIAGRAM OF REFERENCE FREQUENCY AND TIMING DISTRIBUTION, SPC 10 TO DSS 24.



**Figure 2. SURFACE TEMPERATURE MEASURED AT GOLDSTONE TRACKING STATION**



**Figure 3. GROUND TEMPERATURE MEASURED AT GOLDSTONE TRACKING STATION**

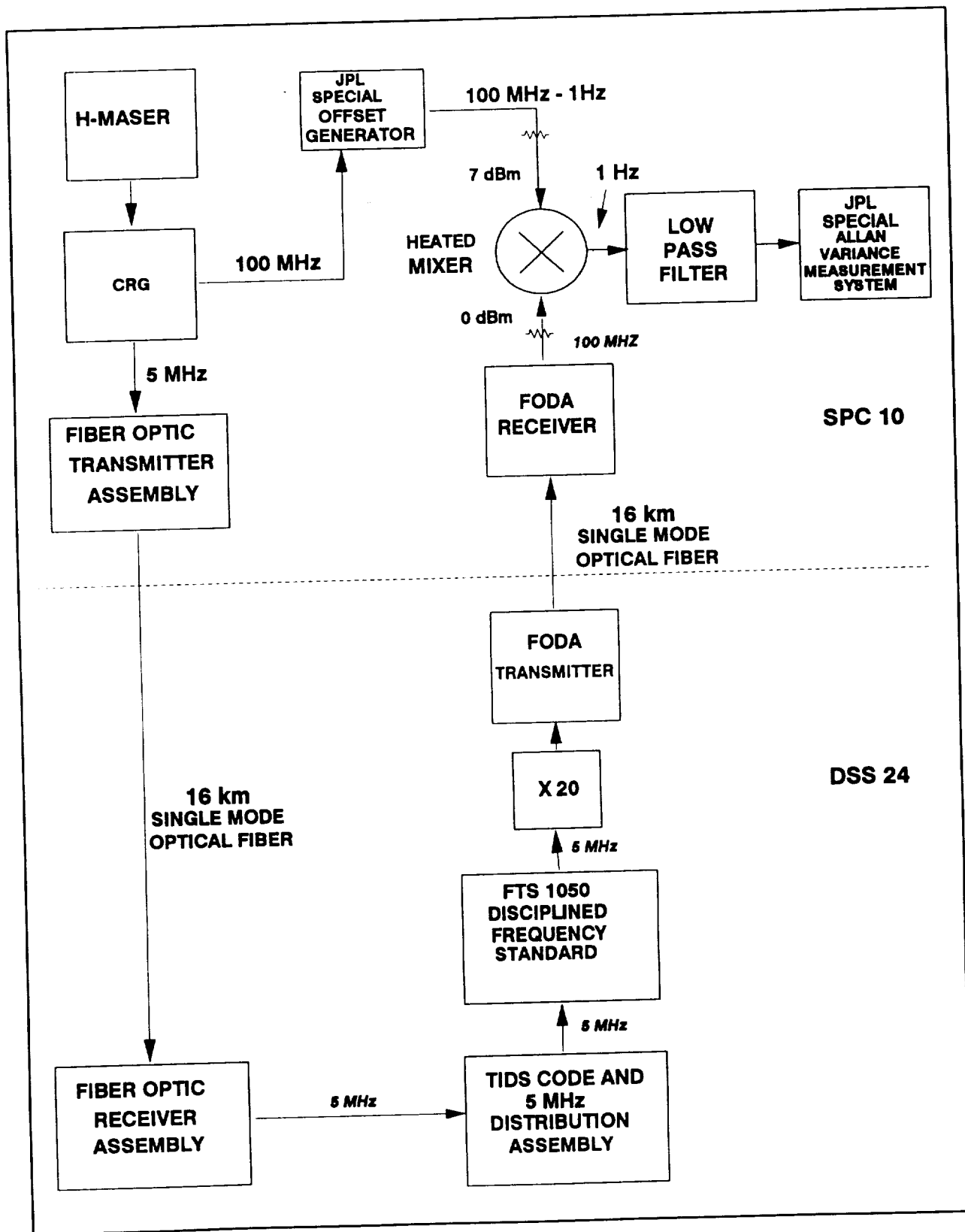


Figure 4. TEST CONFIGURATION FOR ALLAN DEVIATION MEASUREMENT, SPC 10 TO DSS 24.

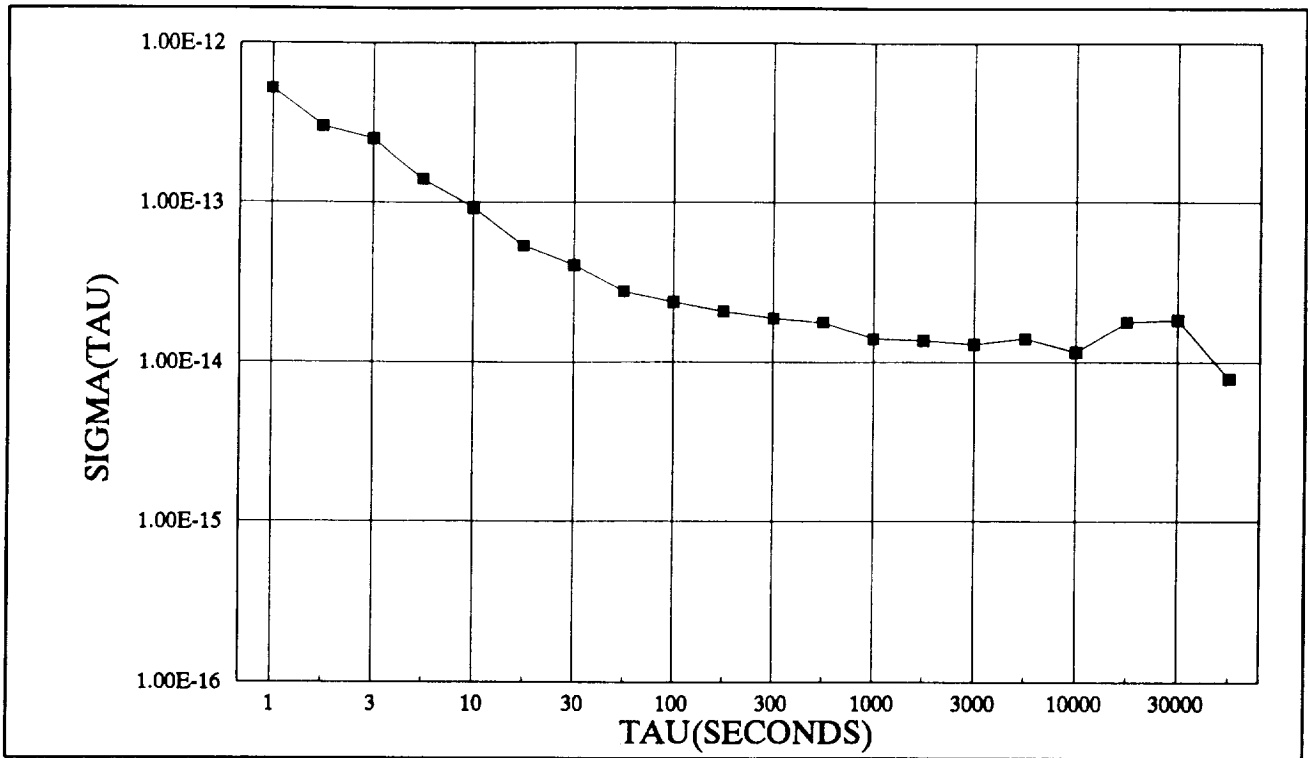


Figure 5. ALLAN DEVIATION AT DSS 24 WITH 420 METERS OF EXPOSED FIBER OPTIC CABLE

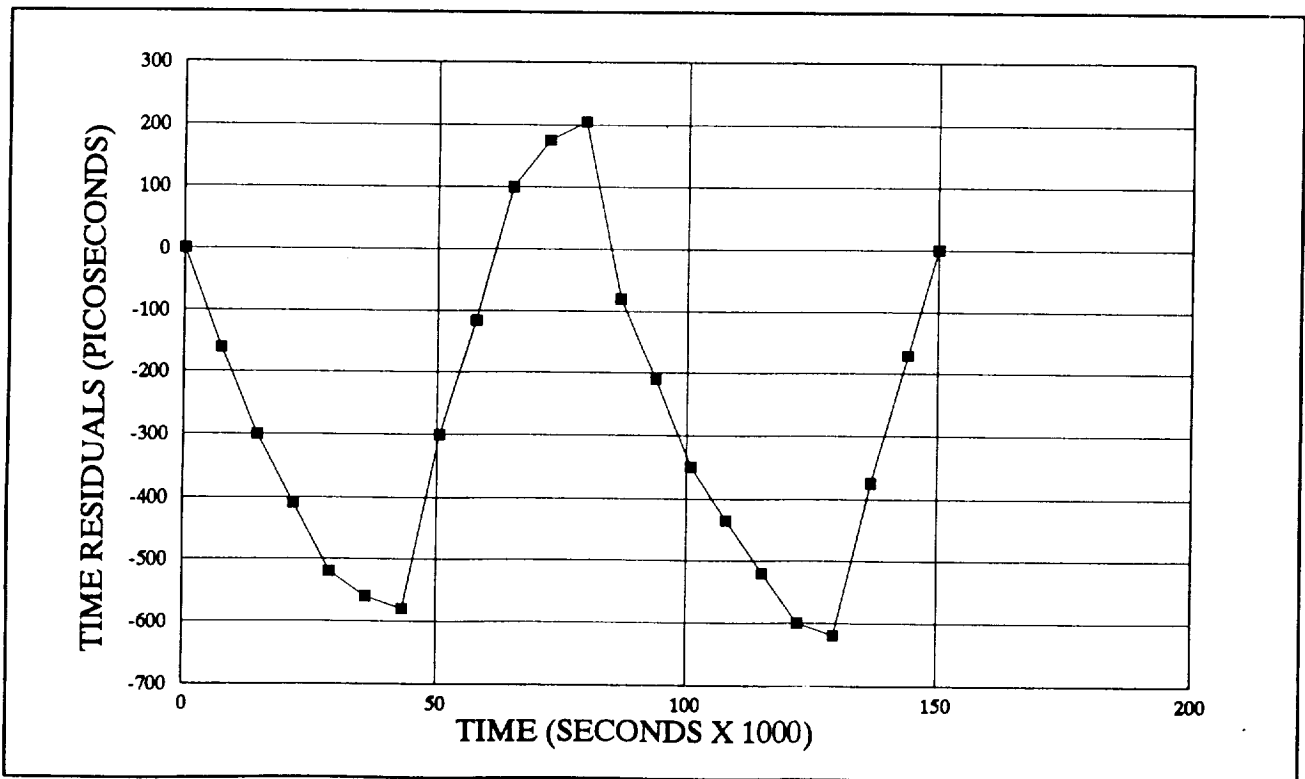


Figure 6. TIME RESIDUALS AT DSS 24 WITH 420 METERS OF EXPOSED FIBER OPTIC CABLE.

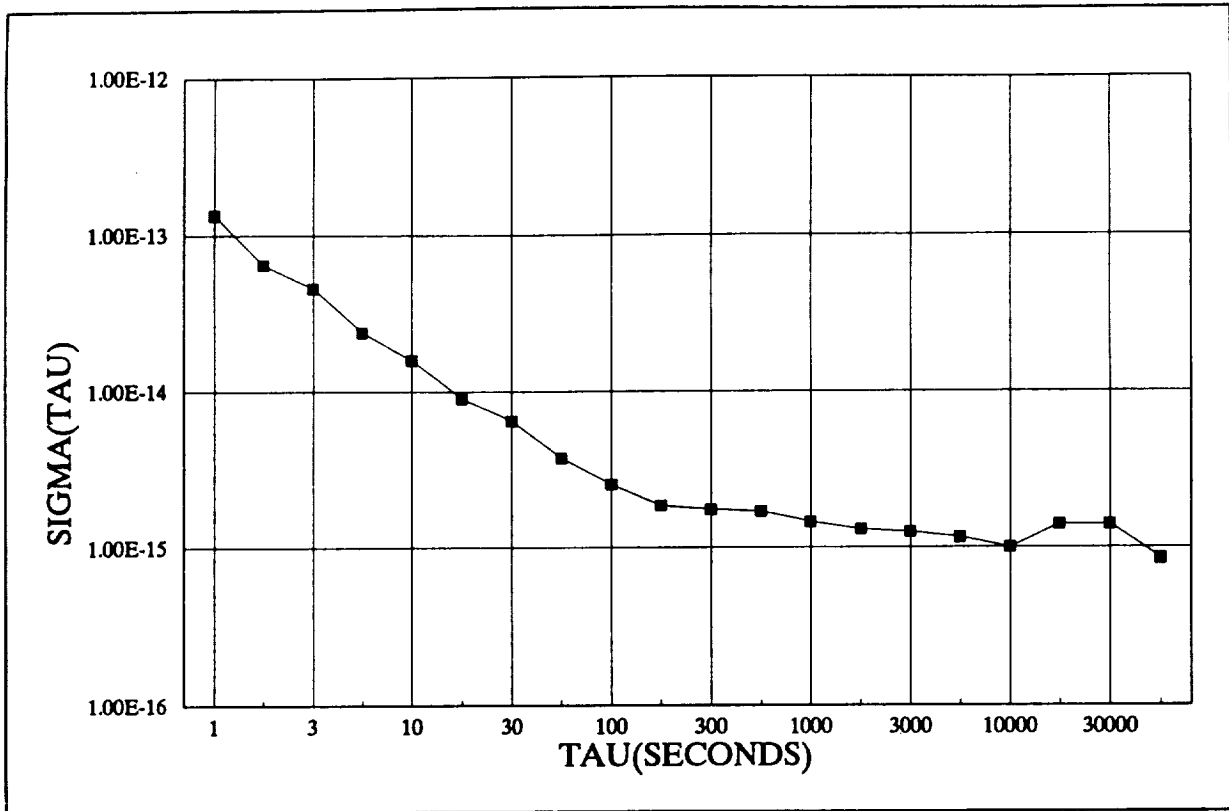


Figure 7. ALLAN DEVIATION AT DSS 24 WITH 16 km OF BURIED FIBER OPTIC CABLE

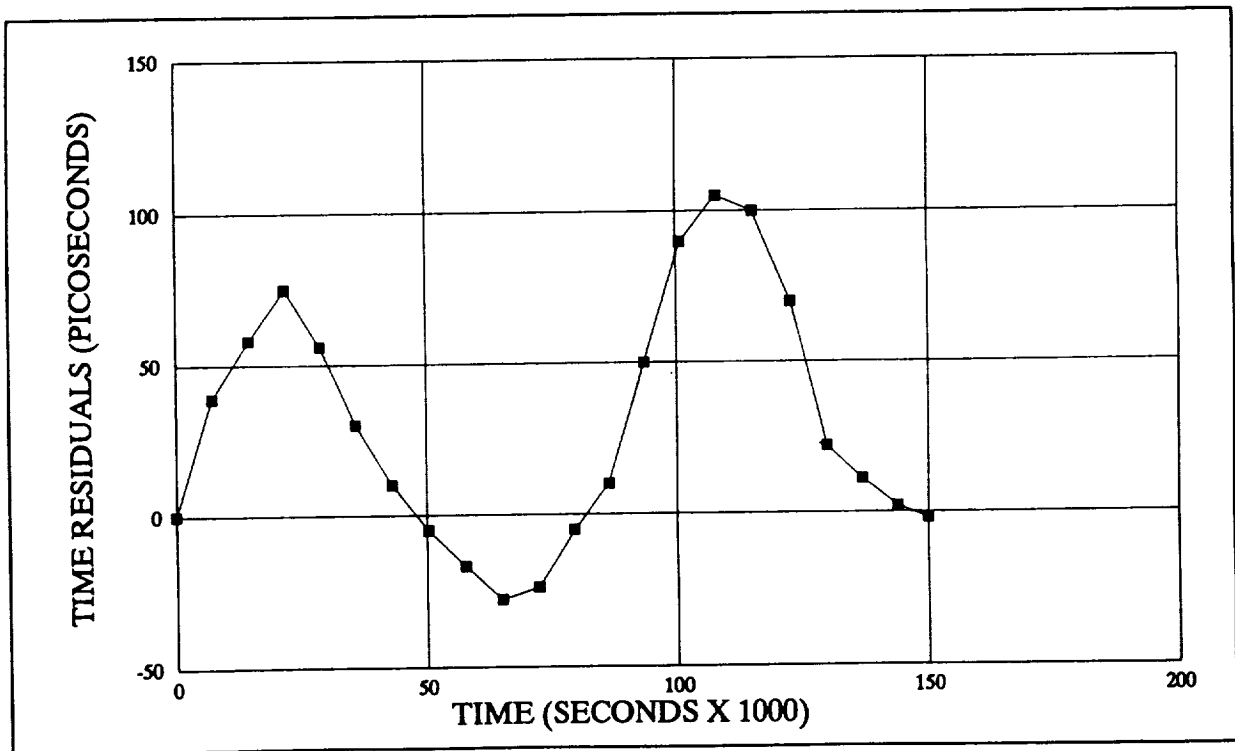


Figure 8. TIME RESIDUALS WITH 32 km OF BURIED FIBER OPTIC CABLE

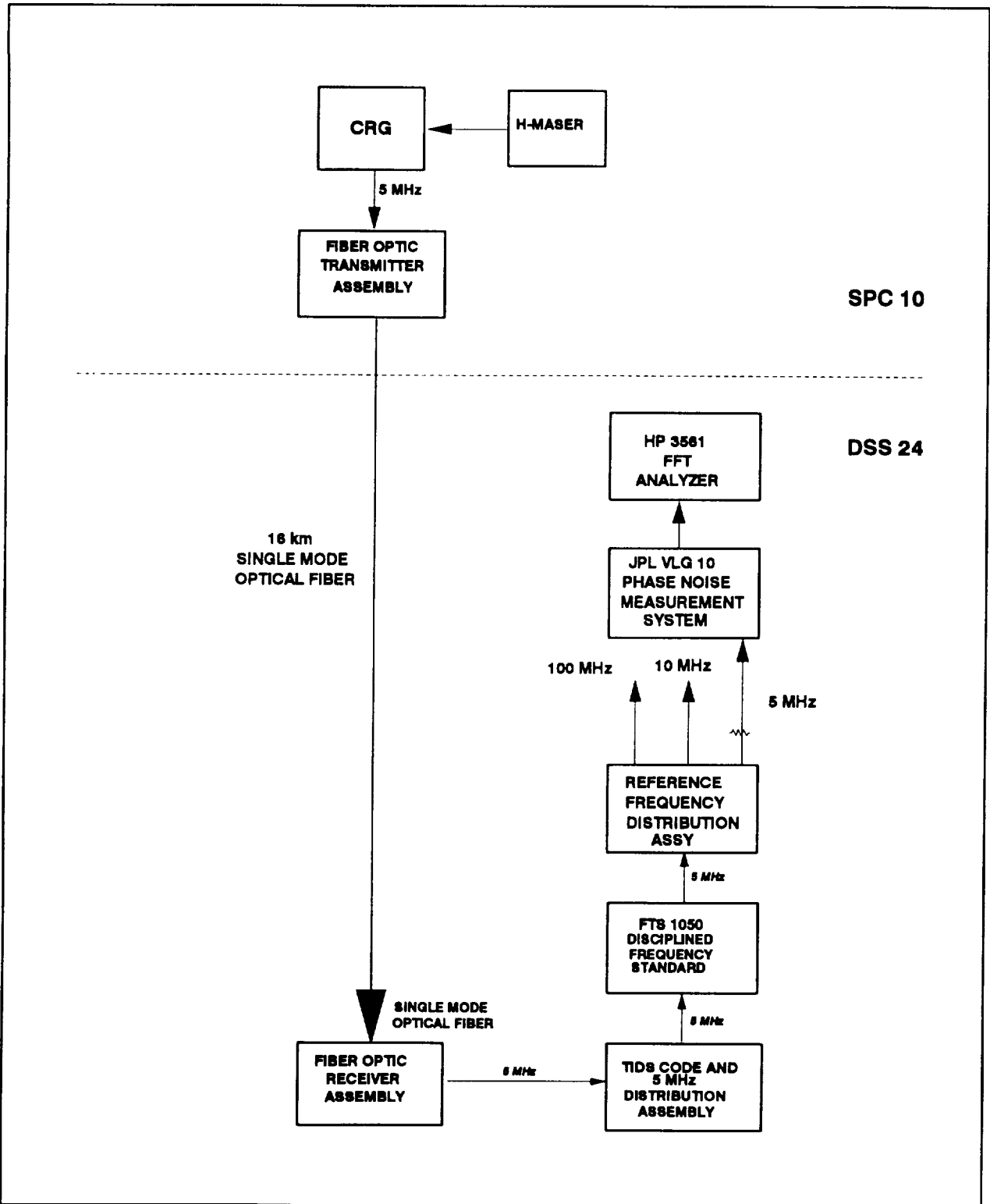


Figure 9. TEST CONFIGURATION FOR PHASE NOISE MEASUREMENT AT DSS 24

## QUESTIONS AND ANSWERS

**FREDERICK WALLS (NIST):** How much of the phase noise degradation was due to the optical transmit received and how much due to fiber noise?

**MALCOLM CALHOUN (JPL):** Anything within about three or four Hz was degraded by the optical fiber transmitted and received. The band width of this frequency standard brought the noise floor down very rapidly. At 10 Hz, we're minus 140 dB below the carrier. And the floor on this was limited by the oscillator in the disciplined frequency standard; it's about minus 155. So it's just a little bit -- very close into the carrier.

020 36  
2004  
1-15

# LASER RETROREFLECTOR EXPERIMENT ON NAVSTAR 35 AND 36

E. C. Pavlis

Dept. of Astronomy, University of Maryland, NASA/GSFC 926  
Space Geodesy Branch, Greenbelt, MD 20771

Ronald L. Beard

Space Applications Branch, Naval Center for Space Technology  
U.S. Naval Research Laboratory, Washington, D.C. 23075

## Abstract

*In GPS one of the primary errors contributing to positioning inaccuracy is the performance of the on-board atomic clock. To determine and predict the performance of this atomic clock has been a problem due to the ambiguity of the orbital position error and clock uncertainty in the Radio Frequency (RF) tracking of the navigation signals. The Laser Retroreflector Experiment (LRE) on-board NAVSTAR 35 and 36 provides a means of separating these ambiguous errors by enabling highly precise and accurate satellite positions to be determined independently of the RF signals. The results of examining onboard clock behavior after removing the orbital position signatures will be discussed. GPS RF tracking data from various DoD and other sites are used to reconstruct the onboard clock data and examine the clock behavior. From these data, the effects of clock performance on GPS positioning performance can be examined.*

## INTRODUCTION

The purpose of this project is to identify and investigate means of enhancing the Global Positioning System (GPS) system integrity and performance. This project involves installing laser retroreflector arrays on-board Global Positioning System (GPS) satellites, tracking the satellites involved in cooperation with the NASA Satellite Laser Ranging (SLR) network and collecting these data for analysis and comparison with GPS pseudorange data. The Laser Retroreflector Experiment (LRE), previously known as the Advanced Clock Ranging Experiment (ACRE)<sup>[1]</sup>, was submitted by the U. S. Naval Research Laboratory (NRL) to the TriDService Space Test Program for spacecraft integration funding as a TriDService space experiment. The objective of such an experiment is to provide an independent high precision measurement to compare or calibrate the GPS pseudorange signal. This project is a cooperative effort involving the NASA Goddard Spaceflight Center SLR group, the NRL and the University of Maryland. Installation of the LRE on the GPS satellite was performed in conjunction with the GPS Joint

Program Office and their contractor, Rockwell International, the Air Force Space Command and the Second Satellite Operations Squadron.

The GPS system is a predicted, real-time, passive ranging navigation system, made up of space, control and user segments. The space and control elements comprise the system proper, and the user segment operates passively utilizing the products of the system transmitted by the space segment. The user's information is computed from the control segment's tracking network's data and other data provided by external sources, such as the U.S. Naval Observatory (USNO) for Universal Coordinated Time (UTC) corrections. The tracking network data are similar in content to that used by the user segment and is relayed to the Master Control Station (MCS) for computation and prediction of the system states which are uploaded into the satellites for the users. Embedded in the space and control segments are atomic clocks to maintain all elements of the system in synchronization. These atomic clocks enable the precise time of propagation measurements (known as Pseudoranges) the users measure to determine range between themselves and the satellites, and the capability of determining the precise positions of the satellites needed as the users' position reference. Small, passive LRE on two GPS satellites, capable of supporting highly precise laser ranging to that satellite, tracked by a worldwide network of SLR stations are to produce highly precise and accurate orbital ephemerides. These data are being compared with GPS orbits generated by the MCS and the Defense Mapping Agency post-processed precise ephemerides to separate the satellite position and on-board atomic clock errors. This error separation should provide a foundation for better understanding the satellite clock on-orbit performance, error propagation within the MCS data computation process, and an independent calibration of GPS accuracy.

## **SATELLITE EQUIPMENT**

The LRE is a panel of a laser retroreflector cubes,  $24 \times 19.4$  cm ( $9.45 \times 7.64$  inches) as shown in Figure 1. This array consists of 32, 2.7 cm (1.06 inch) reflectors of the design used on-board Glonass satellites. These arrays were built and tested by the Russian Institute for Space Device Engineering in a cooperative arrangement with the University of Maryland. The placement on the selected satellites, NAVSTAR 35 and 36, is shown in Figures 2 and 3.

## **LASER TRACKING NETWORK**

The laser returns from the LRE is estimated to be a factor of 36 lower than that of Glonass, whose array size is about  $120 \times 120$  cm ( $47.2 \times 47.2$  inches), and a factor of 3 to 4 lower than Etalon (the Russian laser retroreflector satellite at Glonass/GPS altitudes). Good Glonass returns to the NASA mobile laser sites (MOBLAS) are roughly equal to that from LAGEOS. LAGEOS is routinely tracked by the NASA and cooperating laser sites. For Etalon tracking, a receiver threshold of 4 photoelectrons is used by MOBLAS for day/night operation. With the LRE and the same receiver threshold, the ranging returns are estimated to be 10 to 20 return, ranging returns could be increased to about the same level as Etalon if the receiver thresholds on the MOBLAS were reduced from four photoelectrons to one photoelectron (lunar mode) during night-time tracking. Daylight tracking from MOBLAS is more difficult due to the high

background noise rate and the single stop time interval units used rather than the multistop event timers used at the lunar ranging sites. Modifications to enable daytime tracking from MOBILAS has been prototyped and proven at the GSFC tracking site and the MOBILAS sites are being upgraded.

The results presented here are for NAVSTAR 35 only. NAVSTAR 36 was launched significantly later and has only been sporadically tracked. There are twelve sites which with varied frequency have successfully tracked NAVSTAR 35. The U.S. systems at Monument Pk., CA, Greenbelt, MD, Quincy, CA, McDonald Obs., TX, Haleakala, HI, Yarragadee, Australia and the international sites at Herstmonceux, U.K., Graz, Austria, Wettzell, Germany, Potsdam, Germany, Maidanak, Uzbekistan and Evpatoria, Ukraine. The distribution of the tracked "segments" by each of these stations indicate that some of the sites have only tracked over certain periods of time in a non-uniform way. This is due to the fact that tracking has been limited to daylight. Consequently, there are only short periods of a day or so when several sites were simultaneously successful in tracking the satellite. In particular, on November 18, 1993 ten passes of data were acquired. This is the reason why this day was chosen to do preliminary comparisons with the GPS-derived orbits for NAVSTAR 35.

## GPS TRACKING

For intercomparison with the GPS derived data, these data are being collected at NRL along with the laser tracking data. Tracking data from the GPS Control Segment stations, USNO, the broadcast position data and DMA precise ephemerides are being collected. These data are continuous over the inOrbit operation of the satellites. To utilize the GPS derived tracking data for intercomparison with the laser derived data, the local clocks at the GPS Monitor Station sites must be accounted for since they are the basis for the GPS tracking measurements. In GPS itself these clocks are accounted for by the use of GPS Time which is a common synchronization time computed at the MCS. However, the GPS ranging measurements are directly related to the local clocks whose performance must be removed if the satellite clock is to be isolated from the satellite orbital position and evaluated. The laser data is independent of this influence on ranging measurements since the local clock is used for timetagging.

To determine the performance of the station clocks, common view time comparisons with USNO were made to the Colorado Springs, Hawaii and Ascension stations. These comparisons provide local station clock compared to the Master clock at USNO. These data show that large jumps and discontinuities are present as shown in Figures 4, 5, and 6. These jumps are due to changes in the local clocks or switching necessary for the operation of the system. Navigation users would not be aware of these changes since they use GPS Time which is a computed time accounting for these changes. For this experiment, removal of the local clock and the satellite position error by laser derived positions from the GPS tracking data will leave the satellite clock as the principal error component.

## ORBITAL ANALYSIS AND RESULTS

The IERS Standards<sup>[4]</sup> with minor excursions (e.g. JGM-2 gravity field vs. GEM-T3) have been adopted to ensure as much compatibility with other analyses results as possible. The orbits are integrated in the mean system of J2000 and only the terrestrial effects due to relativity are used. Modeling of the perturbing forces on the satellite is tailored after the LAGEOS SLR analysis standards. The exception is the limited gravity field terms (18,18) required here due to the higher orbit of the target satellite. The time-varying part of the geopotential is accommodated by modeling the solid Earth and oceans tidal accelerations and the secular change in the terrestrial oblateness. Because the NAVSTAR satellites are not passive as LAGEOS, attitude variations must be accounted for and the implications these have on the solar and thermal forces acting on the satellite a various times. The model used to describe these forces is the abridged version of Rockwell International's "ROCK42" model by Fliegel-Gallini-Swift, the T20<sup>[5]</sup>. An additional acceleration along the satellite body-fixed Y-axis, the so-called Y-bias, is also adjusted. Due to the length of the arc used, once per revolution accelerations (with constraints) are also included and adjusted over the same intervals that the constant accelerations apply. The duration of these intervals is variable and they have been kept constant as long as the data allow in order to increase the robustness of the solution. The strategy followed has been to keep the same number of adjusted accelerations while lengthening the arc and to introduce a new set of accelerations once the data indicate a change in the orbit. These parameters along with the state vector at epoch are the only force model parameters that are adjusted.

Measurement modeling accounts for tropospheric refraction, tidal variations of the site including ocean loading (in all three directions), tectonic motions, and occasionally measurement biases. The tropospheric refraction model for SLR is the Marini-Murray model. Ocean loading effects at the SLR sites was computed using the Scherneck model for the eleven main tidal constituents of Schwiderskii's ocean tidal model. Tectonic motions for the sites are either from the LAGEOS-based solution SL8.3<sup>[6]</sup> or the NUVEL-1NNR<sup>[7]</sup>. Only simple measurement biases were adjusted on a few occasions for certain sites. Most of these biases are the result of "fine-tuning" of the ranging gates at the site in order to achieve the maximum number of returns possible. Once the sites are equipped with the better detection packages there should be no need to change these thresholds and therefore the chance of introducing biases to the data will be minimized.

The collected SLR data are analyzed and reduced based on the force and measurement models described in the previous section. A long arc of about 104 days was continuously extended as new data become available. This arc was used to check on the fidelity of the force model. The data fit the arc with an rms of 3 cm. The geographical distribution of the data set did not include southern hemisphere tracking and that can introduce significant biases in the orbits.

Table 1 shows the rms residual for each of the tracking sites. It is hard to assess the quality of the orbits without a uniform data distribution. November 18, 1993 being the best tracking day within our data set, it was used as a test day to verify orbit quality and gain some insight in the level of agreement with the "radiometric data"—determined orbits that the International GPS Service (IGS) for Geodynamics is routinely distributing<sup>[8]</sup>. Two fourteen day arcs were

fit to the data; one for November 5–18 inclusive and one beginning on November 18. These arcs have only 12 hours worth of data in common: 11:00 UT to 23:00 UT, on November 18. The data fit either arc with an rms residual of about 1.9 cm. In both cases, the state vector and one set of accelerations were estimated. The two orbits are based on just over 200 normal points each. For arcs of such length this can hardly be called a sufficient amount of data. The trajectories from the two adjustments were then compared in terms of radial, cross-track, and along-track differences over their common segment. The statistics from this comparison (mean and rms about the mean), are shown in Table 2.

Site	No. of Obs.	RMS [cm]
Monument Peak, CA	311	2.3
Haleakala, HI	215	3.1
McDonald Obs., TX	81	2.7
Quincy, CA	4	0.1
Greenbelt, MD	8	1.0
Graz, Austria	175	2.8
Herstmonceux, U.K.	101	3.4
Potsdam, FRG	47	2.1
Wetzell, FRG	121	3.1
Totals	1063	2.9

Component	Position [cm]			Velocity [cm/s]		
	Radial	Cross	Along	Radial	Cross	Along
Mean	5.1	21.8	-19.0	0.0028	0.0002	0.0012
RMS	3.2	37.0	10.9	0.0017	0.0015	0.0059

Despite the fact that the SLR data distribution is not as optimal as would be preferred for a precise orbit determination, it is still worthwhile comparing to the GPS-derived orbits distributed by IGS for geodetic work. The IGS orbit was rotated into the inertial frame and used as “observations” with the GEODYN data analysis software package to reconstitute a dynamic orbit fitting that data. The converged trajectory was then compared to the SLR-derived orbit in the radial, cross-track, and along-track directions (Figure 7). Statistics of these differences of the IGS orbit from both SLR 14-day arcs are shown in Tables 3 and 4. The common segment of course is only one day (November 18) in both cases.

Component	Position [cm]			Velocity [cm/s]		
	Radial	Cross	Along	Radial	Cross	Along
Mean	8.9	63.3	39.7	-0.0054	-0.0001	0.0004
RMS	7.7	56.5	75.1	0.0109	0.0102	0.0087

Table 4 Trajectory Differences SLR-2 vs. IGS GPS orbit						
Component	Position [cm]			Velocity [cm/s]		
Direction	Radial	Cross	Along	Radial	Cross	Along
Mean	3.6	41.5	58.7	-0.0082	-0.0003	-0.0008
RMS	9.8	90.9	72.9	0.0103	0.0093	0.0138

## CONCLUSIONS

The collection of the GPS tracking data is proceeding well and the SLR data is proceeding slowly. The complication of removing the local atomic clock offset and drift from the GPS data is being accomplished using the common view technique of simultaneous observations of the satellites at two sites. These comparisons should be of sufficient accuracy to remove these effects from the individual satellite tracking data. With SLR derived positions having sufficient confidence the resulting satellite atomic clock performance should be isolated for evaluation.

With limited SLR data, it is hard to come to firm conclusions. The two orbit comparisons show at least the level of compatibility of the SLR and IGS orbits at about 10 cm in the radial direction, whether it be in the mean or the rms sense. This is a very limited test, where neither technology has put forward its best accomplishments and capabilities. A much more uniform and extended SLR data set will be required before we can reliably determine an orbit at the few centimeter level of accuracy. On the other hand, reduction of GPS data directly within GEODYN will remove any inconsistencies in the standards and the reference frame used by the IGS analysis centers and the SLR group. Upcoming modifications to the SLR ground receivers will allow for a further increase in the tracking capabilities of several additional sites and add the needed southern hemisphere tracking. An initial effort to compare the SLR derived orbits with those distributed by IGS indicates that the two agree at the decimeter level radially and at the 0.5–1.0 meter level in the cross-track and along-track directions. The amount of collected data by site and geographical region is far from optimal for a reliable orbit determination, so these results should be interpreted with caution.

## REFERENCES

- [1] R.L. Beard, "The Advanced Clock/Ranging Experiment (ACRE)," CSTG Bulletin No. 11, New Satellite Missions for Solid Earth Studies, Status and Preparations, DGFI, June 1989
- [2] R.S. Nerem, B.H. Putney, J.A. Marshall, F.J. Lerch, E.C. Pavlis, S.M. Klosko, S.B. Luthcke, G.B. Patel, R.G. Williamson, and N.P. Zelensky, "Expected Orbit Determination Performance for the TOPEX/Poseidon Mission," IEEE Trans. Geosci. Remote Sensing, 31 (2), 333–354 (1993).
- [3] C. Boucher, Z. Altamimi, and L. Duhem, "ITRF 92 and its associated velocity field," IERS Technical Note 15, Observatoire de Paris, IERS (1993).

- [4] D.D. McCarthy (ed.), IERS Standards (1992), IERS Technical Note 13, Observatoire de Paris, IERS (1992).
- [5] H.F. Fliegel, T.E. Gallini, and E. Swift, "*Global Positioning System Radiation Force Models for Geodetic Applications*," J. Geophys. Res., 97 (B1), 559–568 (1992).
- [6] D.E. Smith, R. Kolenkiewicz, R.S. Nerem, P.J. Dunn, M.H. Torrence, J.W. Robbins, S.M. Klosko, R.G. Williamson, and E.C. Pavlis, "*Contemporary global horizontal crustal motion*," Geophys. J. Int., 119, 511–520 (1994).
- [7] C. DeMets, R.G. Gordon, D.F. Argus, and S. Stein, "*Current Plate Motions*," Geophys. J. Int., 101, 425–478 (1990).
- [8] G. Beutler, "*The 1992 IGS Test Campaign, Epoch '92, and the IGS PILOT Service: An Overview*," in: 1993 IGS Workshop, eds. G. Beutler and E. Brockmann, University of Berne, 1993, p. 3.

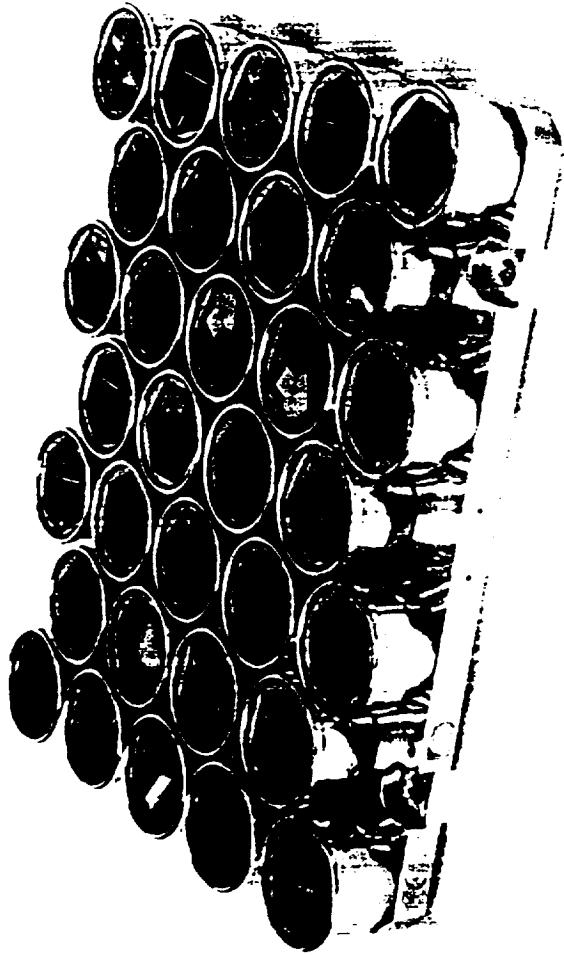


FIGURE 1

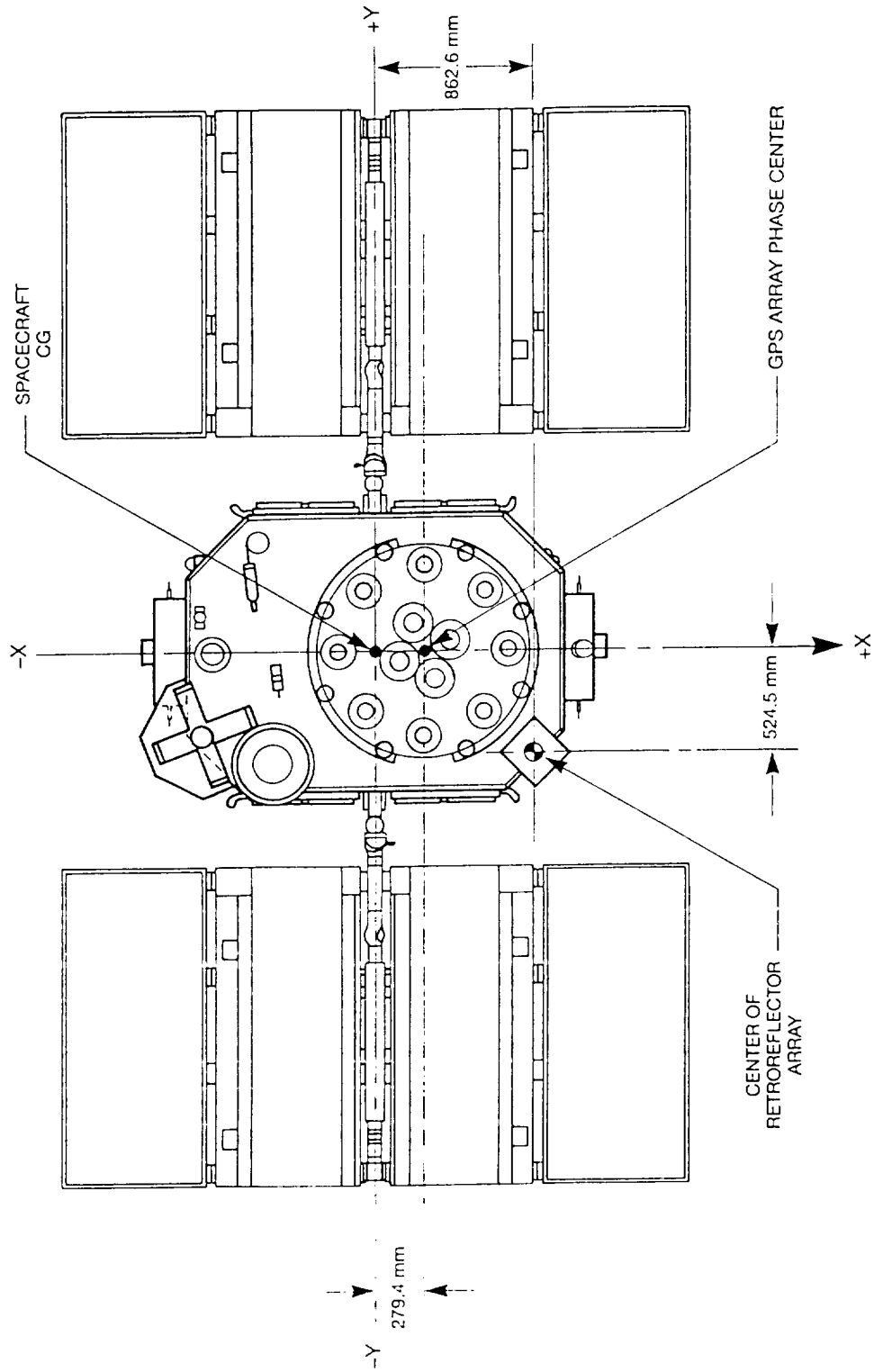


FIGURE 2

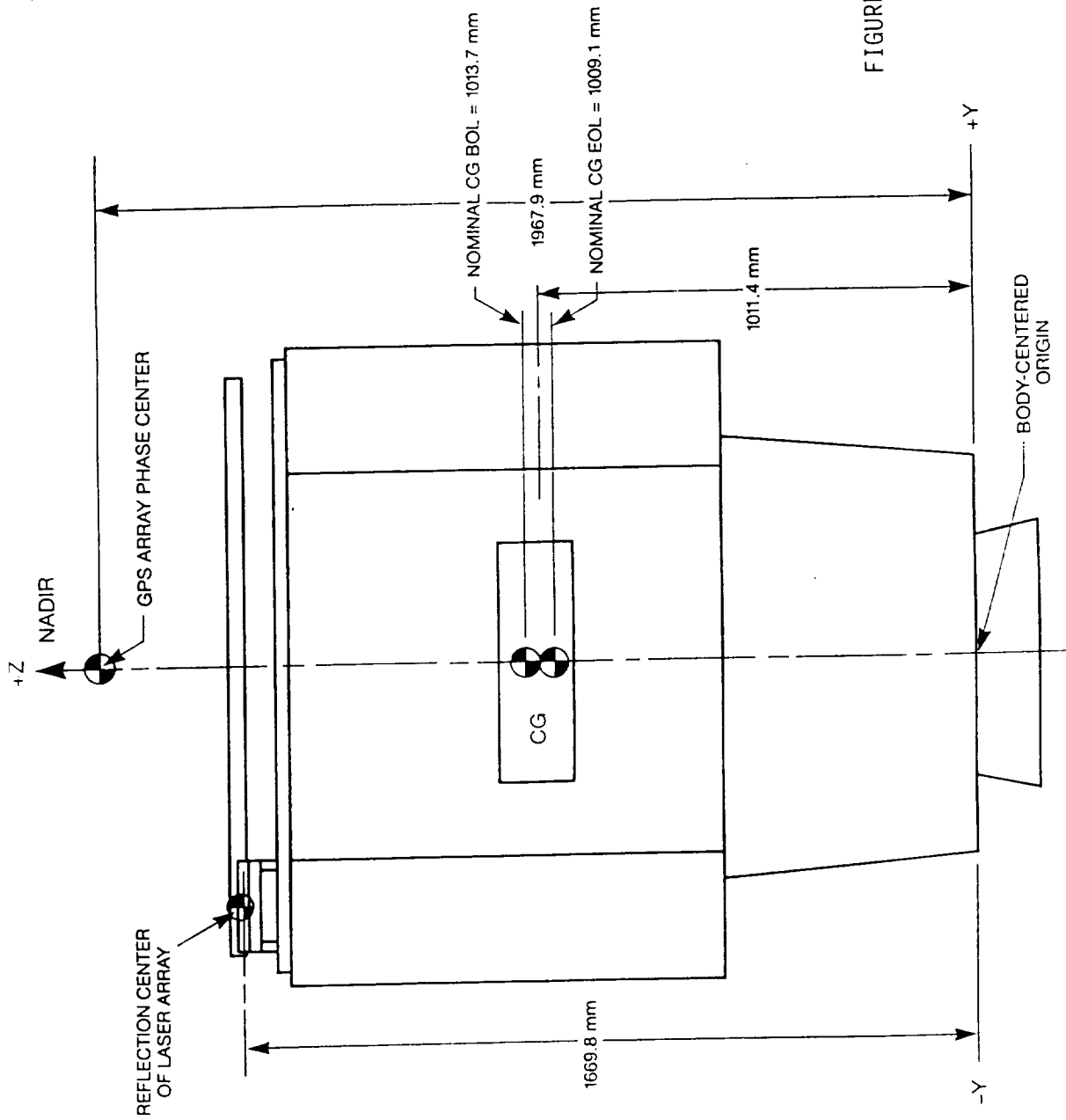


FIGURE 3

TIME TRANSFER VIA NAVSTAR 23  
 Colorado Springs Monitor Station  
 Naval Observatory, Washington, D.C.  
 PPS Receivers

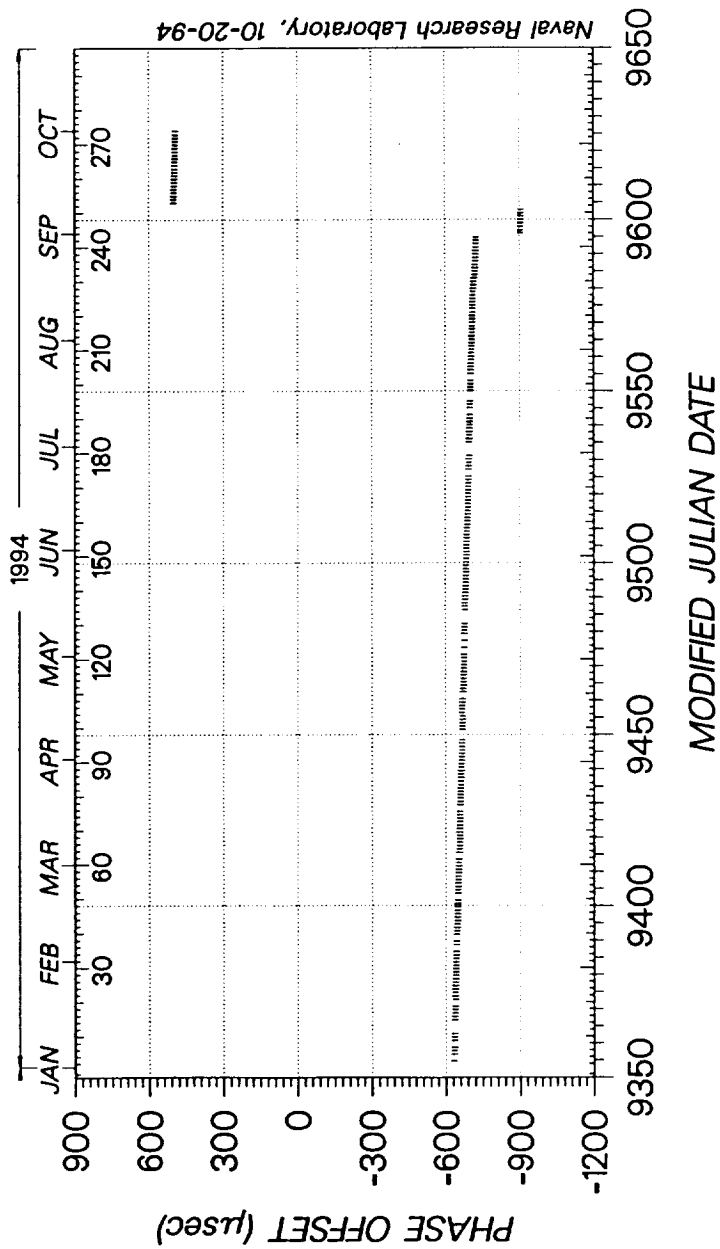


FIGURE 4

TIME TRANSFER VIA NAVSTAR 23 CORRECTED LINEAR RESIDUALS  
 Colorado Springs Monitor Station  
 Naval Observatory, Washington, D.C.  
 PPS Receivers

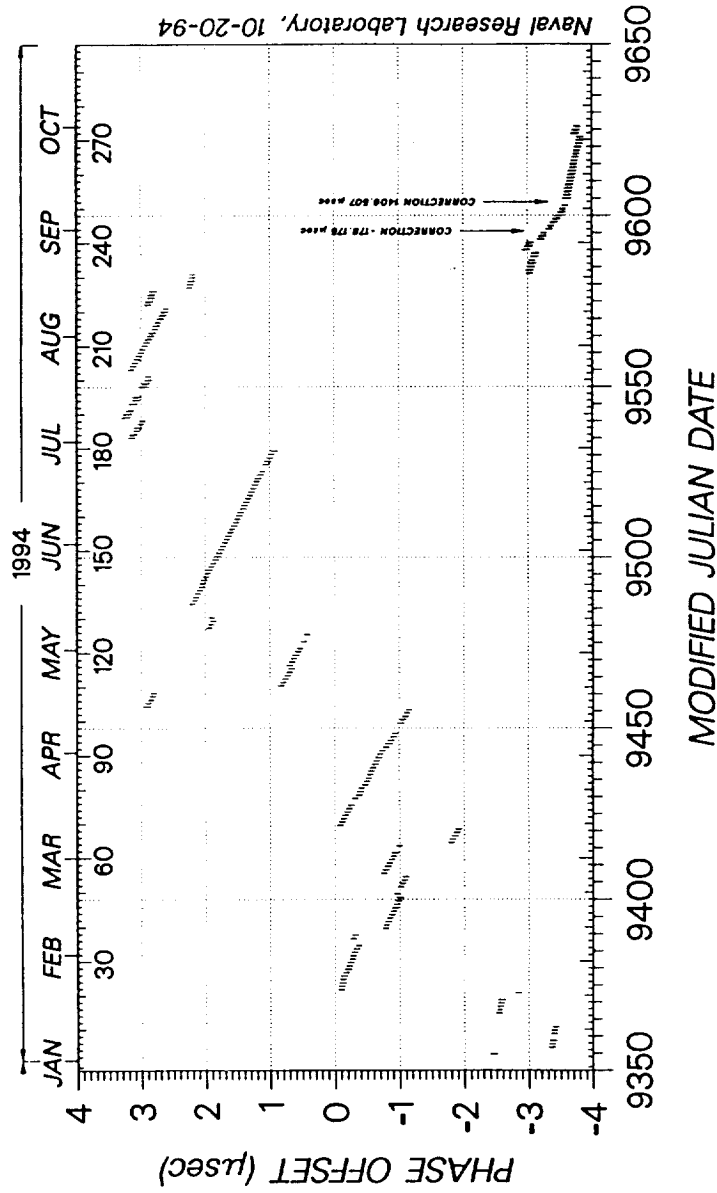


FIGURE 5

TIME TRANSFER VIA NAVSTAR 23 LINEAR RESIDUALS  
 Ascension Island Monitor Station  
 Naval Observatory, Washington, D.C.  
 PPS Receivers

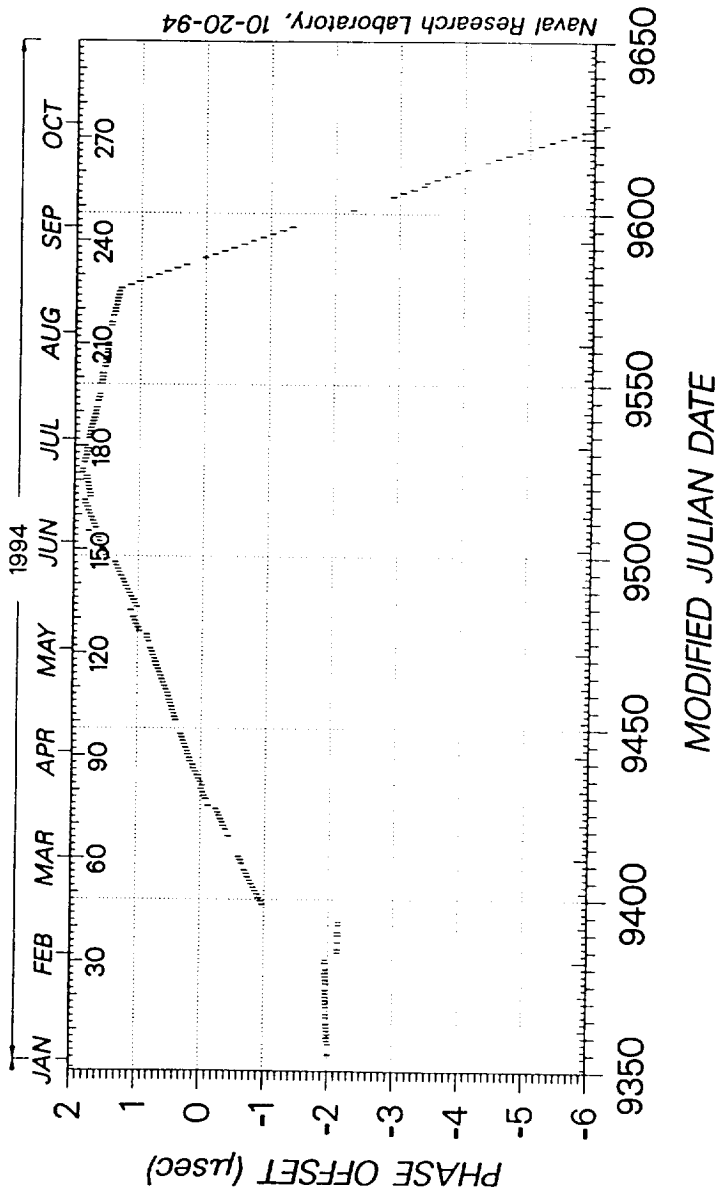


FIGURE 6

## QUESTIONS AND ANSWERS

**MARC WEISS (NIST):** On one of the plots of the residuals, I wasn't exactly sure what the data meant. There were normal plots for the laser ranging, and I thought they were open squares. Were those DMA or isiso-ephemeris ranging?

**RONALD BEARD (NRL):** The normal points from the satellite data you mean?

**MARC A. WEISS (NIST):** Yeah.

**RONALD BEARD (NRL):** I think, as John mentioned yesterday, they are doing a number of pulses, like 10 pulses per second, to get the returns. They have taken like five minutes of these returns, and they averaged those into one, what they call a "normal point."

**MARC A. WEISS (NIST):** And you were comparing those on the same plot?

**RONALD BEARD (NRL):** The normal points are made to the raw range measurements, if that is the one I think you mean.

**MARC A. WEISS (NIST):** It's the first one. And then there was an RMS of some two millimeters. The open squares are what?

**RONALD BEARD (NRL):** The open squares are the raw range measurements that they are making. They are getting like 10 a minute, or 10 a second.

**MARC A. WEISS (NIST):** So the RMS is really the self-consistency of the range measurements with the laser.

**RONALD BEARD (NRL):** That's correct.

**MARC A. WEISS (NIST):** Okay. I understand that you're trying to do orbit reconstruction based on laser measurements only. And it seems that you can get a simple measure of the consistency by just looking at range measurements for your laser and range estimates from, say, DMA orbits or broadcast orbits. Has that been done?

**RONALD BEARD (NRL):** Yes and no.

**MARC A. WEISS (NIST):** That seems a lot simpler. I would be very interested to know how they compare simply for range measurements.

**RONALD BEARD (NRL):** It's a lot more difficult than it appears on the surface. That's one of the reasons we want to try to do some simultaneous tracking, so we can do just that. Even the locations of the stations and the lasers, it's difficult to get enough correlation between the two to just simply do a comparison of those two. But we have been trying.

**JOHN LUCK (ORRORAL OBSERVATORY):** First remark: I think the comparison between the SLR-derived orbits and the IGS orbits for 35 and 36 are consistent at about 15 to 20 cm level. The graph that you were just looking at is the self-consistent residuals for the laser-derived orbit.

My question was: Seeing that this is a very powerful tool for geodetic investigation, such as height determinations, sea-level monitoring and things like that, are there any plans to include

retro-reflector arrays on future GPS spacecraft? And if so, could you please make them bigger?

**RONALD BEARD (NRL):** Well, no and yes. There are no plans to include them downstream that I'm aware of. There are no specific plans. There are recommendations for doing that, and various options have been discussed. If we do, we sure have the world as our incubator.



2001-06  
32348  
P 11

## T2L2

# Time Transfer by Laser Link

Christian Veillet and Patricia Fridelance  
Observatoire de la Côte d'Azur  
06130 Grasse, France

### Abstract

*T2L2 (Time Transfer by Laser Link) is a new generation time transfer experiment based on the principles of LASSO (Laser Synchronization from Synchronous Orbit) and used with an operational procedure developed at OCA (Observatoire de la Côte d'Azur) during the active intercontinental phase of LASSO. The hardware improvements could lead to a precision better than 10 ps for time transfer (flying clock monitoring or ground based clock comparison). Such a package could fly on any spacecraft with a stable clock. It is developed in France in the frame of the PHARAO project (cooled atom clock in orbit) involving CNES and different laboratories. But T2L2 could fly on any spacecraft carrying a stable oscillator. A GPS satellite would be a good candidate, as T2L2 could allow to link the flying clock directly to ground clocks using light, aiming to important accuracy checks, both for time and for geodesy. Radioastron (a flying VLBI antenna with a H-maser) is also envisioned, waiting for a PHARAO flight. The ultimate goal of T2L2 is to be part of more ambitious missions, as SORT (Solar Orbit Relativity Test), aiming to examine aspects of the gravitation in the vicinity of the Sun.*

## INTRODUCTION

The development of very stable clocks, and the increasing number of applications of their use in space (see for example [1]), urges to study the possibility of linking these clocks to the ground with better and better accuracies. The techniques used for transferring time between two remote clocks using satellites can be divided in two classes. The first uses electromagnetic signals in the radio domain, as two way time transfer through telecommunication satellites, or GPS. The second class deals also with electromagnetic signal, but at light frequencies, as LASSO or a laser link through the Ajisai satellite. It is not very easy to guess which precision and accuracy could reach these techniques within the next five to ten years. However, one can try to estimate what could be the more important limitations for each of them, starting with the radio domain.

## WHICH FUTURE FOR THE RADIO-FREQUENCY TIME TRANSFER ?

The current accuracy of GPS for time transfer is slightly better than 10 ns on long baselines (6000 km). It can be improved to around 3 ns on regional comparisons. Improvements in the receivers could bring to a sub-nanosecond accuracy, let say 500 ps, assuming that the receivers used in the time transfer experiment have been carefully calibrated, and that their environment will be well monitored in order to map properly the variation of their metrology characteristics. To do better seems very difficult, mainly due to the atmospheric correction, which will probably bring the ultimate limitation at around 500 ps.

Two-way time transfer is presently achieving a precision of around 200 ps, and an accuracy of 1 to 2 ns. One could think that the new methods of calibration to be used in order to reach a better accuracy could lead to a strong improvement. Nobody can tell now what could be the best calibration achievable. However, the atmosphere will be definitely a limitation at 50 ps, and, again, the accuracy will depend on how well the calibrations can be performed...

PRARETIME (the PRARE positioning system modified for precise time transfer) could reach an accuracy of 100 ps if comparing directly the clocks through their 5 MHz frequency, 200 to 300 ps being the overall accuracy when the time scales, as realized by the 1 pps, are compared<sup>[2]</sup>. Doing better seems very difficult if one wants to keep the original PRARE equipment with only slight modifications.

As a conclusion of this quick look to a mid-term evolution of the radio frequency time transfer techniques, 50 ps seems to be a reasonable limit, even assuming very careful calibrations and delay variation monitoring.

## TRANSFERRING TIME WITH LIGHT

The basic principle of time transfer using T2L2 is briefly described in [2], where can be found also a general uncertainty analysis of both PRARETIME and T2L2. A complete analysis of the T2L2 precursor, LASSO, can be found in [3]. We will detail here the uncertainty analysis of the T2L2 equipment.

### Short events

In contrast with the radio frequency techniques, optical time transfer is based on the timing of individual very short events with respect to a clock. We are now able to create such short events using lasers with pulse length of 20 ps or less, with enough energy to be sent in space, recorded by a flying detector, and still recorded on the ground after their reflection on a retroreflector array on the satellite. Even the geosynchronous orbit can be reached with such short pulses. The duration of the event to be timed will not be the limit of such techniques, as the uncertainty it brings will decrease by averaging measurements (typically, for 10 s, 100 events can be timed...). The problem now is to know how well we can time an event.

## **Rapid detectors**

The light event needs first to be transformed into an electric signal. This will be done through a detector. This detector has to be rapid, in order to benefit from the short event. Its transit time has to be very stable, and checked by a real time calibration. A photomultiplier is no longer a good candidate, as its transit time is varying depending on where the light is arriving on its photocathode. This transit time is also very long, and varying very quickly with the environment. Avalanche photodiodes are the kind of detectors widely used now in the laser ranging measurements. Some of them exhibit very short transit times, with small detector areas minimizing the jitter. Preliminary tests made at the LLR (Lunar Laser Ranging) station at OCA on various photodiodes allows to assign 50 ps to the detector uncertainty (single measurement).

## **The event timer**

Event-timers are rarely used in the laser ranging community, as the basic measurement is the flight time of a laser pulse to the target and back, which is a time interval. The start time itself has to be recorded with an accuracy not better than 0.1 ms. One can use a counter for an absolute timing if one measure for example the interval between the event to be timed and the next 5 MHz tick. Unfortunately, most of the counters, claiming precisions of 20 ps, are not accurate at that level, and there are no event-timers reaching a 2 ps resolution, or 10 ps accuracy... The extrapolation of the (more than 10 years old) LASSO event timer performances, using the up-to-date technology, should make possible timing with a 10 ps accuracy with respect to the reference frequency.

## **T2L2 uncertainty**

### **Atmosphere and modeling**

T2L2 will be made of a a detector and a timer flying on a satellite. The participating ground stations will be equipped with comparable detector and timer as the flying ones. The method is described in [2]. As we are working in a two-way mode, the only noise added by the atmosphere is the fluctuation between the way up and the way down of the troposphere. The more pessimistic value, with a very high satellite for which 250 ms will separate the start and the return of the light at the ground station, leads to a 20 ps uncertainty, with is purely random as there is no systematic in the very short term variations of the troposphere. As the stations and the satellite will be localized well enough, there is no influence of the modeling of the measurement in term of relativistic corrections which can be completed at the picosecond level.

### **Overall noise**

On a single measurement, the noise can be written as following:

$$\text{Satellite: } \sigma^2 = \underset{\text{detector}}{(50 \text{ ps})^2} + \underset{\text{timer}}{(10 \text{ ps})^2} + \underset{\text{laser}}{(20 \text{ ps})^2} = (55 \text{ ps})^2$$

Ground :  $\sigma^2 = (50 \text{ ps})^2 + (10 \text{ ps})^2 + (20 \text{ ps})^2 = (55 \text{ ps})^2$   
 with the same sources, as the equipment is basically the same

$$\text{Atmosphere : } \sigma^2 = (20 \text{ ps})^2$$

Overall single measurement noise :  $\sigma^2 < 80 \text{ ps}$

The uncertainty for a T2L2 clock offset determination, based on 100 measurements, is then smaller than 8 ps (one sigma).

**Overall accuracy ? It depends on the use of T2L2...**

How well will one be able to measure the variations of the equipment delays, i.e. to calibrate the flying equipment and the ground stations? The experience acquired for the LASSO experiment<sup>[4]</sup> clearly demonstrates how difficult it is to achieve such a calibration at the sub-nanosecond level. Depending on the goal of the mission using T2L2, we can approach the question on different manners.

### Flying clock monitoring

In that case, we have a very stable clock flying, and another one on the ground. We do not care really about the absolute offset between them, as the flying clock will be switched on some time after the launch, or behave during the launch in an unpredictable way. A consequence is that we will need only to keep constant all the delays at the station, or to monitor any change in its time characteristics, without the requirement of an absolute calibration. Concerning the flying package, careful laboratory tests will have to be made in the laboratory in order to parametrize the instrumental delays with respect to the environment, and to monitor the parameters all along the experiment. LASSO demonstrated that more problems arise from the ground, as the onboard equipment is free of any changes... Such a monitoring of the ground equipment and a good parametrization of T2L2 should lead to an uncertainty of 50 ps. We could perhaps do better, but need more investigations.

In one day, T2L2 could then reach a frequency transfer between the ground and the satellite with an accuracy of  $10^{-16}$ . Such an accuracy is promising if T2L2 is used for monitoring an ultra-stable clock (as cooled atom or trapped ion devices).

### Time transfer

Now, we need an absolute calibration, in order to allow a time scale comparison. Up to now, only relative calibrations<sup>[4]</sup> performed between the participating stations have been made. We clearly need to find another way to work, as we have to monitor all the variations which can arise after, or between, calibration campaigns. If the calibration itself could be achieved also at the 50 ps level, how to maintain it has to be explored. 100ps seems not too difficult, 10

ps is definitely a very difficult goal. It means that the time transfer accuracy will in fact be dominated by our capability to calibrate the ground equipments.

If we consider that we need to link the 1 pps of each station for a real time scale comparison, we have to add an uncertainty due to the link between the reference frequency used for timing and this 1pps. Estimated to be between 100 and 300 ps, it becomes the most important source of uncertainty. However, the meaning of the clock offset at a given time as provided by T2L2 without direct reference to a 1 pps signal has to be explored carefully.

### **The present status and near future of T2L2**

T2L2 is entering in a phase A study within CNES. It is part of the studies made in the PHARAO project. The clear goal of T2L2 will be to provide a link between the flying cooled atom clock and the ground. T2L2 will not be the main link as it is weather dependent. But it will provide the opportunity of a link based on a completely different technology, and able of a very high accuracy. T2L2 could then be used for calibrating the (main) microwave link, and, depending on the weather, provide continuous accurate monitoring on some extended periods, and accurate measurements from time to time.

In this one year T2L2 phase A, the flying package feasibility will be carefully studied. A ground version of the event-timer should be tested at the LLR station in the beginning of 1995, and the selection of a detector suitable for T2L2 should be made. In addition, a great attention will be paid to the following points :

- hardware requirements at the laser stations
- T2L2 clock offset determination meaning (with respect to time scale link)
- calibration procedures
- station delay real-time monitoring
- operational aspects (observation strategy, network organization,...)

Various scenarios for a first test flight of T2L2 will be envisioned, waiting for a (not decided yet) PHARAO mission. After the death of the ExTRAS / Space maser on Meteor 3-M project, other opportunities exist for T2L2. Radioastron could be one, as the timeframe of the launch is compatible with a possible schedule for the fabrication of T2L2. Another possible spacecraft, which would be very interesting for both time and geodesy, could be a GPS satellite equipped with retroreflectors. It would allow a direct link through light with the satellite clock, as well as a good satellite positioning through the laser ranging measurements which are a by product of T2L2. Other future missions are under consideration.

For the T2L2 observations, the SLR (Satellite Laser Ranging) network has been approached, and many positive answers have been received from many stations in more than 10 countries around the world. Time transfer is a new application of these ground equipments mainly used for geodesy and geophysics. At a time where SLR role in these applications is not as unique as it used to be in the past two decades, thanks to GPS, the laser stations find a new field of

application, pushing the technique at its limits. In countries where permanent SLR sites are operating, the national time laboratories should approach them in order to start a cooperation on these time transfer opportunities. In the same time, they could stress the importance of GPS ranging for both time and geodesy.

### Other scientific objectives of T2L2

T2L2, as well as a microwave link, and a very stable clock in orbit is rich of many applications. In an eccentric orbit around the Earth, it could provide an improvement by a factor 400 in the Vessot–Levine gravitational redshift measurement. It could give the opportunity of the still controversial East–West West–East independent measurement of the speed of light, as proposed by the first author for the TROLL project in 1991, which can be extended to a general check of the isotropy of light<sup>[5]</sup>. In orbit around the Sun, it could allow the measurement of the so-called Shapiro effect, the delay experienced by the light in a strong gravitational field. The PPN parameter  $g$  could be determined with an accuracy of  $10^{-7}$ . It is the SORT mission proposed to ESA<sup>[6]</sup>, where two similar satellites could also allow a simultaneous  $g$  measurement through interferometry. We are far from time transfer between ground clocks, but such dreams for a far future are driving the efforts of today...

## CONCLUSION

T2L2 could be able to monitor a flying clock or to transfer time with a 10 ps precision, and an accuracy depending on the capability of calibrating and monitoring the instrumental delays, 50 ps being a reasonable guess if the necessary efforts are made, and depending also on the necessity to work with a 1 pps for linking the time scales. If the phase A to be conducted in 1995 concludes on the feasibility of T2L2, and if the funding for its fabrication is obtained, a flight model could be available in mid 1997, ready to benefit from any spacecraft carrying a stable clock...

## REFERENCES

- [1] Leschiutta S., and Tavella P., These proceedings, 1994.
- [2] Thomas C., Wolf P., Uhrich P., Schaefer W., Nau H., and Veillet C., These proceedings, 1994.
- [3] Fridelance, "*The LASSO Experiment*", PhD dissertation, Observatoire de la Côte d'Azur, Oct.1994.
- [4] Gaignebet J. Hatat J.L., Klepczynski W.J, McCubbin L., Grudler P., Wiant J., Ricklefs R., Mangin J.F., and Torre J.M., These proceedings, 1994.
- [5] Wolf P., These proceedings, 1994.
- [6] Veillet C., "*SORT, a proposed mission for the ESA Horizon 2000+ programme*", Observatoire de la Côte d'Azur, 1993.

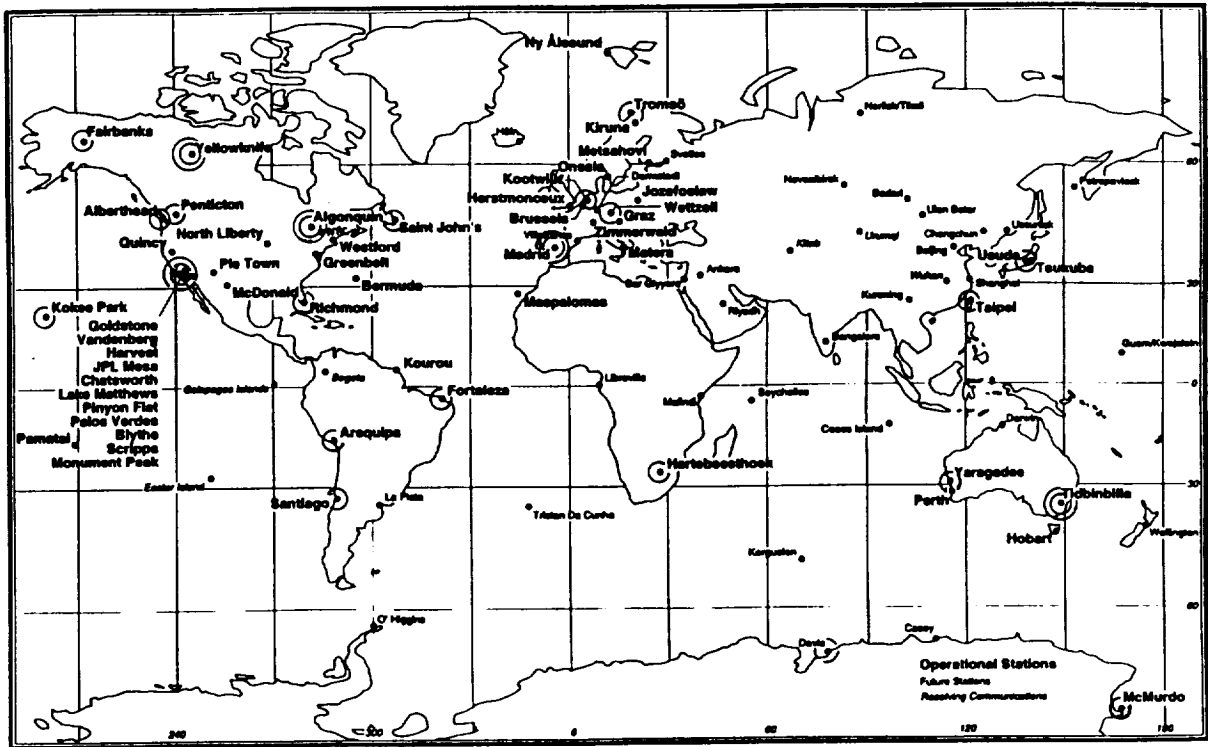


Figure 1. Map showing locations of GPS receiver stations of the International GPS Service for Geodynamics. Stations mentioned in the text have double circles. The global GPS solutions whose timing results are described in the text, use up to 24 stations - such as the set shown circled here.

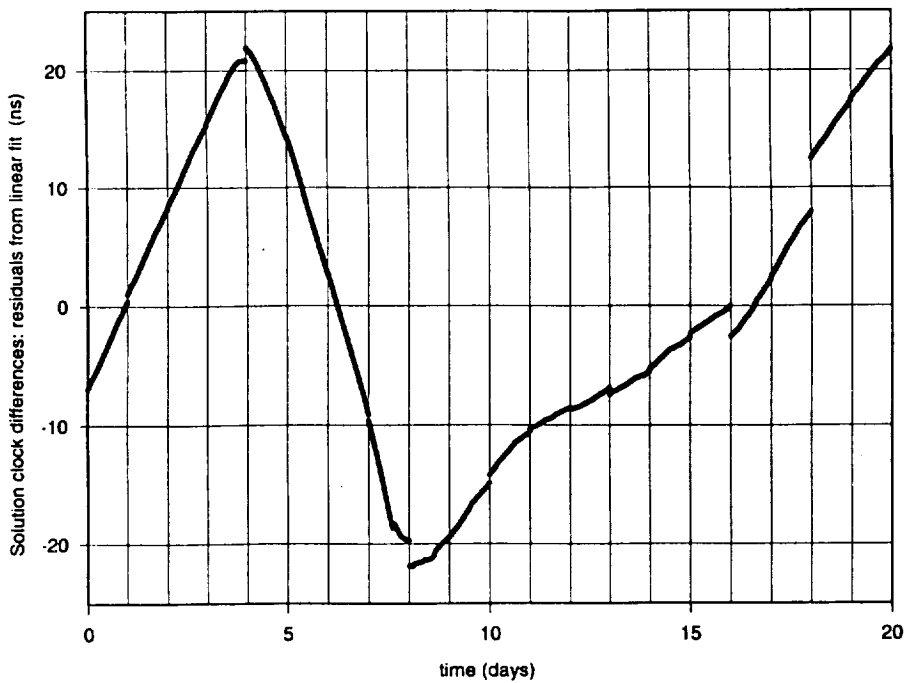
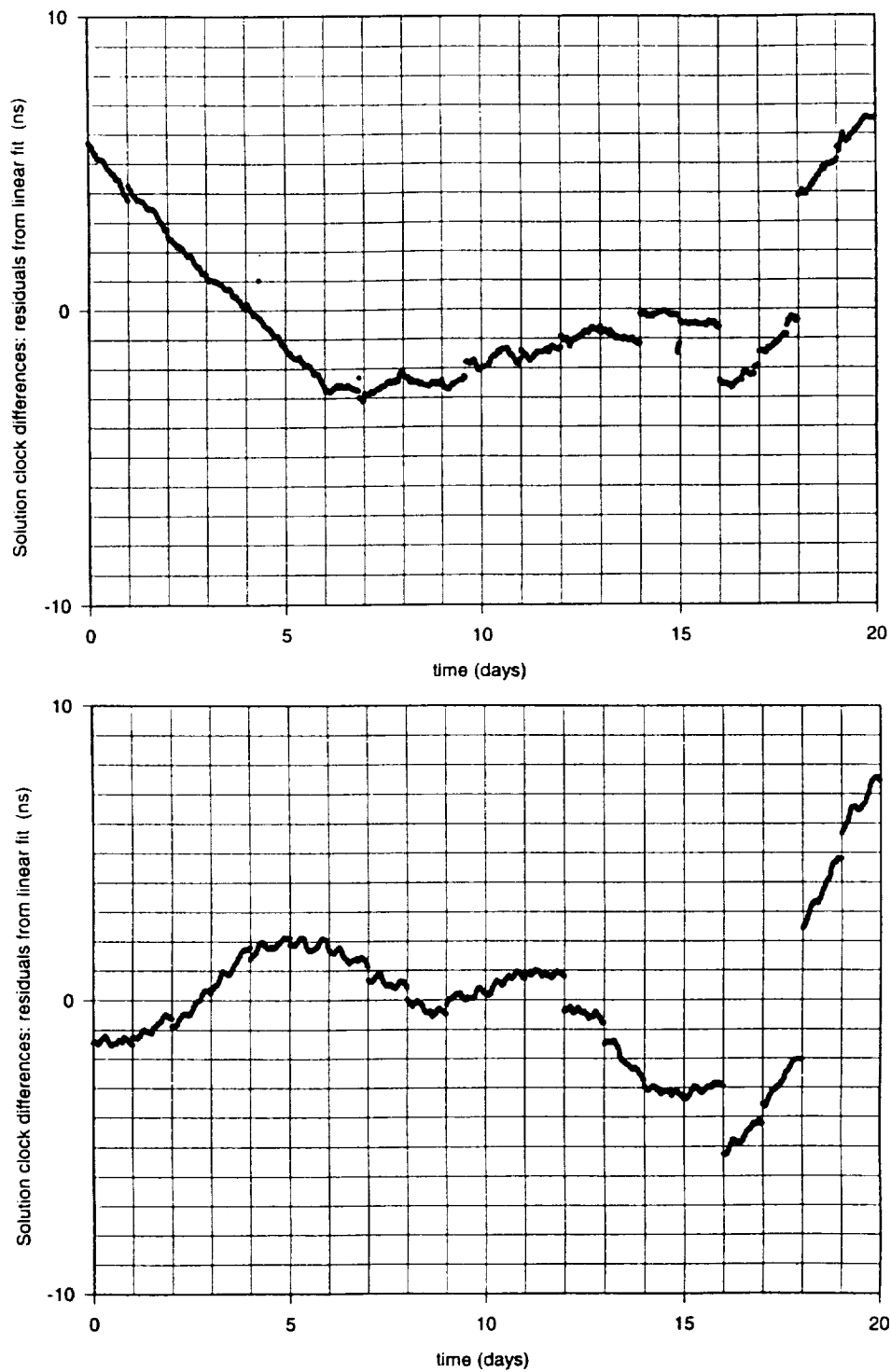
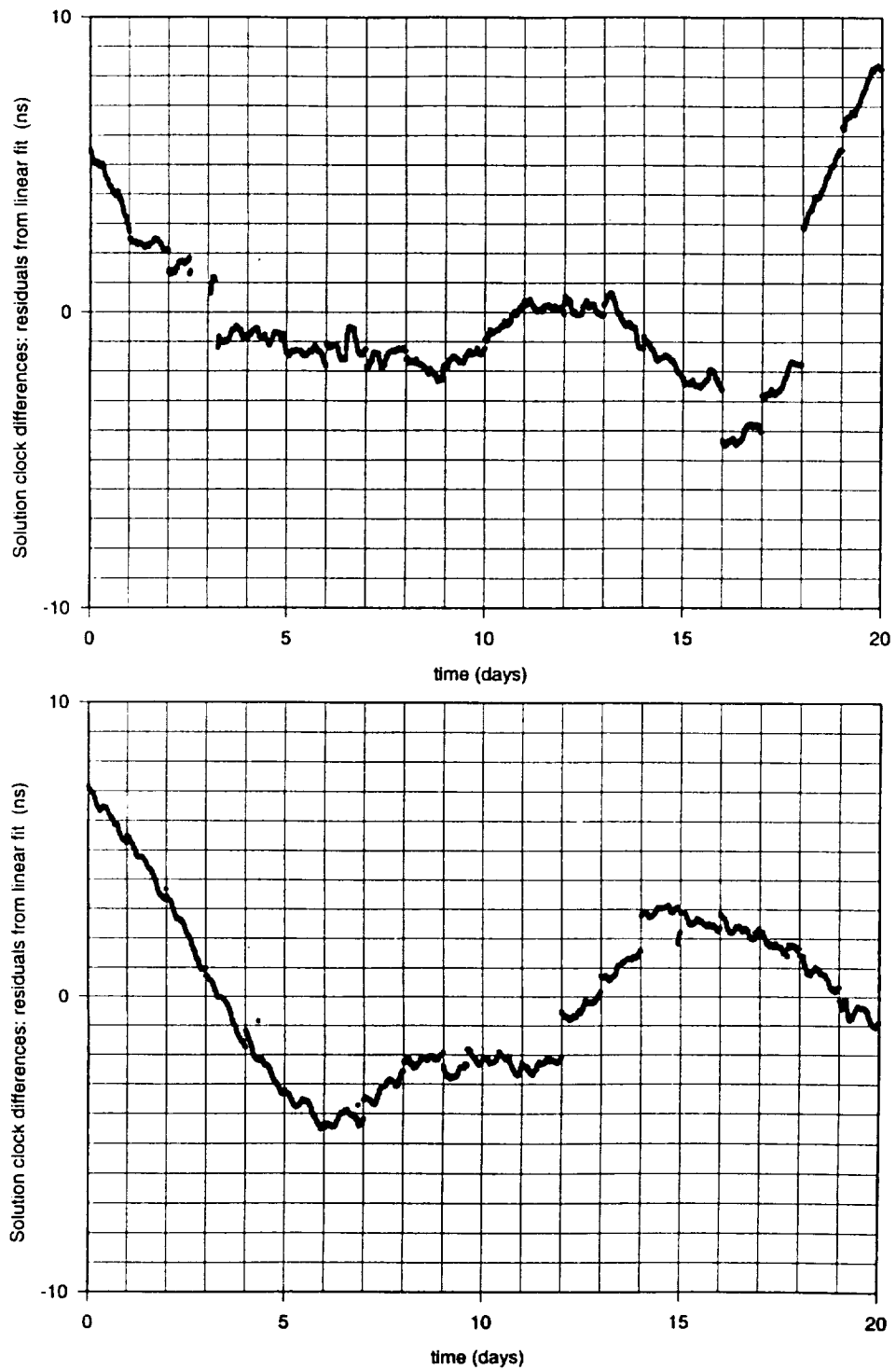


Figure 2. Maser clock differences between Algonquin and NRC, as calculated from the global solution. Each day is treated independently.



**Figure 3.** Maser clock differences between Goldstone and NRC, (top) and between Madrid and NRC (bottom), as calculated from the global solution. Some direct common view satellites exist for these pairs.



**Figure 4.** Maser clock differences between Tidbinbilla and NRC, (top) for which no direct common view satellites exist; and between Goldstone and Madrid (bottom), as calculated from the global solution via NRC only.

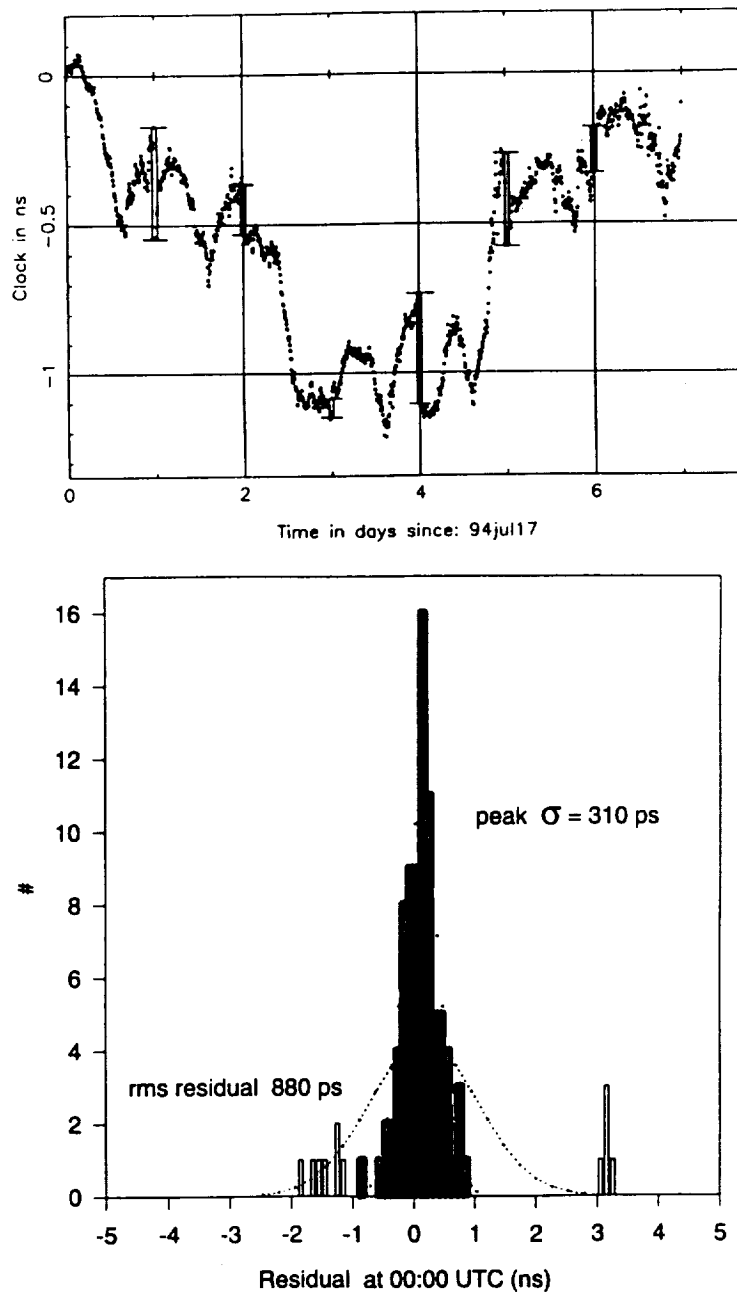


Figure 5. (Top) daily global solution discontinuities in Algonquin - NRC maser clock differences, emphasized by the “bars” at 00:00 each day. (Bottom) Histogram of daily solution discontinuities for the 19 days of Figs.2-4, between NRC and five IGS stations’ masers, scaled by  $1/\sqrt{2}$  to reflect the residual at the ends of the daily solutions. The open bars represent values included in the determination of the “rms” value, and excluded from the “peak  $\sigma$ ” value.

## QUESTIONS AND ANSWERS

**W. LEWANDOWSKI (BIPM):** I have a comment on that. There are some chances to put this equipment on GLONASS satellites. And that is interesting because GLONASS satellites are very often launched, so there is not this problem of metal, for example, on other satellites in which just one is launched. So I think that is something which should be –

**CHRISTIAN VEILLET (OBSERVATOIRE DE LA CÔTE D'AZUR):** You are right. Perhaps you could put this, too, on the back of GPS satellites and put the PRARE time on it. On GLONASS, yes.

I have just one more comment. It's concerning the fact that T2L2 has been announced with the satellite as a ranging network. And already at least 10 countries have expressed that they would be very happy to participate. And I think that you should approach your SLR stations in your country -- I'm not talking about the state, because you did that already. But now, SLR stations would be very happy to be used for something as geodesy and geophysics. As you know, SLR is not as important as it was in the last two decades for geodesy and geophysics, thanks to GPS. And so it means that they have nice devices, good satellites as running stations. And the need to use that -- and there is a very nice use of the stations which can be made for time.

I would so I would ask the your countries to approach these stations, because they could do a nice job for them. Thanks.



# Satellite Test of the Isotropy of the One-Way Speed of Light Using ExTRAS

Peter Wolf

Bureau International des Poids et Mesures,  
Pavillon de Breteuil, 92312 Sèvres CEDEX, France  
and  
Queen Mary and Westfield College, School of Mathematical Sciences,  
Mile End Road, London E1 4NS, Great Britain

*Abstract: A test of the second postulate of special relativity, the universality of the speed of light, using the ExTRAS (Experiment on Timing Ranging and Atmospheric Sounding) payload to be flown on board a Russian Meteor-3M satellite (launch date January 1997) is proposed. The propagation time of a light signal transmitted from one point to another without reflection would be measured directly by comparing the phases of two hydrogen maser clocks, one on board and one on the ground, using laser or microwave time transfer systems. An estimated uncertainty budget of the proposed measurements is given, resulting in an expected sensitivity of the experiment of  $\delta c/c < 8 \times 10^{-10}$  which would be an improvement by a factor of  $\sim 430$  over previous direct measurements and by a factor of  $\sim 4$  over the best indirect measurement. The proposed test would require no equipment additional to what is already planned and so is of inherently low-cost. It could be carried out by anyone having access to a laser or microwave ground station and a hydrogen maser.*

## 1. Introduction

Einstein's second postulate, affirming the universality of the speed of light for inertial frames, is fundamental to the theories of special and general relativity. It can be tested directly by comparing the propagation times of two light signals travelling from one point to another along the same path but in opposing directions (often referred to as a test of the isotropy of the one-way speed of light). The only such test, was carried out by Krisher

et al. [1], who compared the phases of two hydrogen masers separated by a distance of 21 km and linked via an ultrastable fibre optics link of the NASA deep space network. The sensitivity of this experiment, expressed as a limit on the anisotropy of the speed of light, was  $\delta c/c < 3,5 \times 10^{-7}$ , where  $c$  is the velocity of light in vacuum. Riis et al. [2] tested the isotropy of the first order Doppler shift of light emitted by an atomic beam (and indirectly thereby the second postulate) using fast-beam laser spectroscopy obtaining the currently best limit on the anisotropy,  $\delta c/c < 3 \times 10^{-9}$ . This presents a 10 fold improvement on previous values from experiments measuring the isotropy of the first order Doppler shift using the frequency links in the NASA GP-A rocket experiment [3] and so-called Mössbauer rotors [4, 5]. In the test theory of Mansouri and Sexl [6] the above results can be interpreted as limits on the parameter  $\alpha$  using the relation  $\delta c/c = (1+2\alpha)v/c$  [1, 2] where  $v$  is the velocity of the Earth with respect to the mean rest frame of the universe ( $v \sim 300$  km/s). This yields values of  $\alpha = -1/2 \pm 1,8 \times 10^{-4}$  and  $-1/2 \pm 1,4 \times 10^{-6}$  for the experiments by Krisher et al. [1] and Riis et al. [2] respectively.

The experiment proposed here would test the isotropy of the transmission time of light signals between two points directly and on a non-laboratory scale with an estimated accuracy of  $\delta c/c < 8 \times 10^{-10}$ , using the ExTRAS payload on board the Russian Meteor-3M satellite scheduled for launch in January 1997, T2L2 (Time Transfer by Laser Light) time transfer and a hydrogen maser at the ground station. This, if realized, would present a 430 fold improvement on previous direct measurements [1] and a slight improvement on the value obtained by Riis et al. [2]. In Section 2 the principle of the experiment is explained while Section 3 provides an evaluation of its sensitivity aimed at including all error sources that may exceed one picosecond and based on the uncertainty budget for the T2L2 method by Thomas & Uhrich [7].

## 2. Experimental principle

The ExTRAS payload consists of two active, auto-tuned hydrogen masers communicating with ground stations via a PRARE (Precise Range and Range-Rate Equipment) microwave link and a T2L2 laser link. Once operational, the system should reflect laser pulses, emit and receive microwave signals and date all such events on the on-board time scale provided by the hydrogen masers. The satellite will follow polar orbit, at an altitude of 1000 km with a period of order 100 min and a duration of one passage of  $\sim 17$  min.

In principle, the proposed experiment is similar to that performed by Krisher et al. [1]. A laser signal emitted from the station E is reflected at the satellite S and returned to E (see figure 1). The readings of the ground hydrogen maser at emission ( $\tau_0$ ) and reception ( $\tau_2$ ) and that of the space maser at the moment of reflection ( $\tau_1$ ) are recorded. The differences  $\tau_1 - \tau_0$  and  $\tau_2 - \tau_1$  represent the up and down transmission times  $T_1$  and  $T_2$  respectively plus some initial phase difference of the clocks. Note that no synchronization convention or

procedure is assumed. Einstein's second postulate would require that for a series of measurements, after accounting for the path asymmetries, the difference  $T_1 - T_2$  should be equal to a constant  $\Delta_0$  (due to the initial clock offset) independent of the spatial orientation of the individual links. More particularly one obtains for a single link (see [8] for more detail),

$$T_1 - T_2 = \Delta_0 + 2 \vec{R}(t_e) \cdot \vec{v}(t_e) / c^2 + (\Delta_{i(\text{up})} - \Delta_{i(\text{down})}) + O(c^{-3}) \quad (1)$$

where  $\vec{R}(t_e)$  is the vector from E to S at the coordinate time of emission of the signal  $t_e$  in a geocentric, inertial reference frame,  $\vec{v}(t_e)$  is the velocity of the ground station at signal emission in the same frame and  $\Delta_i$  are internal delays (cables etc.).

The initial clock offset  $\Delta_0$  is a constant, provided that the two clocks are syntonized. This can be achieved at the  $10^{-15}$  accuracy level (the best hydrogen maser stability) using time transfer data over a sufficiently long integration period and taking into account all known effects (gravitational redshift, second order Doppler, maser drift). One would expect the effect on the syntonization, of an eventual anisotropy of the propagation time of the light signals, to average out in a global treatment using time transfers in all spatial directions.

Terms of order  $c^{-2}$  amount to  $\sim 40$  ns and can be calculated to picosecond accuracy if  $\vec{R}(t_e)$  and  $\vec{v}(t_e)$  are known to within  $\sim 50$  m and  $\sim 0.01$  m/s respectively, which represents no difficulty for modern satellite orbitography. Of course, a possible anisotropy would also have an effect on the satellite orbit determination, but as the range  $R$  cancels to first order in (1) this effect would be negligible. Furthermore, the satellite orbit is obtained from round-trip ranging measurements, which should, again to first order, be insensitive to anisotropy of the propagation time of the light signals.

Terms of order  $c^{-3}$  can amount to several picoseconds but can be calculated to picosecond accuracy without difficulty [8]. The effect of asymmetry in the atmospheric delays for the up and down links is below one picosecond.

Hence, after accounting for path asymmetry, any variation of the difference  $T_1 - T_2$  with the spatial orientation of the laser link should be due to a violation of the second postulate.

### 3. Estimation of the experiment sensitivity

The sensitivity of the proposed test can be estimated by considering two individual laser links as shown in figure 2. The time intervals  $\tau_2 - \tau_0$ ,  $\tau_5 - \tau_3$  and  $\tau_3 - \tau_0$  are measured using the ground hydrogen maser with the interval  $\tau_4 - \tau_1$  obtained from the space hydrogen maser. Designating the individual transmission times by  $T_1$ ,  $T_2$ ,  $T_3$  and  $T_4$  as shown in figure 2 and

assuming that one of the links is colinear with the direction of the presumed anisotropy, the difference between the two links is given by,

$$(T_1 - T_2) - (T_3 - T_4) + \Delta_s = 2 \Delta_a(1-\cos\theta). \quad (2)$$

Here  $\Delta_s$  represents the correction due to the path asymmetries of the individual links;  $\Delta_a$  is the maximum delay for a single transmission due to the anisotropy, and  $\theta$  is the angle between the two links in the inertial geocentric frame.

If Einstein's second postulate is true the right hand side of equation (2) should be equal to zero within the measurement error.

The experiment should be capable of detecting an anisotropy under the condition

$$\epsilon < 2 \Delta_a(1-\cos\theta), \quad (3)$$

where  $\epsilon$  represents the total measurement uncertainty.

The sensitivity of the experiment is therefore given by,

$$\delta c/c = \Delta_a/T = \epsilon/[2T(1-\cos\theta)] \quad (4)$$

where  $T$  is a typical transmission time ( $T_{\max} \sim 12$  ms).

Maximal sensitivity is achieved when the measurements are taken at the beginning and the end of a single passage of the satellite directly above the station. In this case  $\theta \sim 180^\circ$ ,  $T \sim 12$  ms and the error accumulated due to the instability of the hydrogen masers is very small because of the short integration time of  $\sim 17$  min. Table 1 lists the individual sources of uncertainty that are estimated to exceed 1 ps. Four sources of uncertainty are listed in the table:

(i) The stability of the hydrogen masers for integration times of 1000 s is of the order 2,1 parts in  $10^{15}$  [7] which gives an accumulated uncertainty of  $\sim 2$  ps per maser over an integration time of 17 min.

(ii) As systematic errors in the on-board payload cancel when the two links are differenced, only its instability over 17 min contributes. Ten picoseconds [7] seems a conservative estimate for such a short integration time.

(iii) Only the instability of the Earth station during the experiment contributes. Degnan [9] states that the precision of satellite laser ranging stations is of order 1 to 3 mm, which corresponds to an uncertainty of less than ten picoseconds.

(iv) Information on the counter uncertainties is provided by the T2L2 proposing team.

In the calculation of  $(T_1 - T_2) - (T_3 - T_4)$  the differences  $\tau_4 - \tau_1$  and  $\tau_3 - \tau_0$  measured by the space and ground clock respectively appear with a factor of 2. Hence all uncertainty sources participating in the measurement of these intervals ((i),(ii),(iv)) have been multiplied by this factor.

For the measurement of anisotropy in a direction which is not in the plane of orbit, the two links are separated by the time necessary for the Earth station to change its position with the rotation of the Earth so as to see the satellite from opposing directions ( $\sim 14500$  s). The hydrogen maser stability for such integration times is of the order 1,5 parts in  $10^{15}$  [7], which gives an uncertainty of  $\sim 44\sqrt{2}$  ps in (i). Contributions from other error sources are those given in Table 1. Hence the value for the total measurement uncertainty is  $\epsilon \sim 72$  ps. Note also that in this case  $\theta$  cannot exceed  $120^\circ$ .

Substituting these values for  $\epsilon$  and  $\theta$  into (4) gives an experimental sensitivity of  $\delta c/c = 7,9 \times 10^{-10}$  when the direction of the anisotropy lies in the orbital plane of the satellite and  $\delta c/c = 2 \times 10^{-9}$  otherwise. Following Krisher et al. [1] the experiment can be interpreted in the framework of the test theory by Mansouri & Sexl [6] resulting in limits on the parameter  $\alpha$  of  $\alpha = -1/2 \pm 4 \times 10^{-7}$  and  $\alpha = -1/2 \pm 1 \times 10^{-6}$  for the two cases, assuming  $v = 300$  km/s.

## Conclusion

The proposed test of the special theory of relativity is expected to improve the upper limit on anisotropy of the propagation time of light signals obtained from the best previous direct measurement [1] by a factor of  $\sim 430$ . It should also provide an improvement (by a factor of  $\sim 4$ ) on the value inferred from the measurement of the first order Doppler shift by Riis et al. [2]. The extension of this type of experiment to space-time domains (separation of the clocks of  $\sim 3700$  km) which are not attainable in a laboratory may also be an advantage. And last but not least, the experiment does not call for the installation of additional equipment, hence it can be considered an essentially no-cost experiment which is generally a decisive factor for research in fundamental science.

The same experiment could be performed using the PRARE microwave transfer system in the two-way ranging mode [7] rather than the T2L2 links. This might be of advantage as the PRARE method is not weather dependent. However, uncertainties in the ionospheric propagation delays due to different up and down link frequencies introduce an additional uncertainty of  $\sim 20$  ps per link, which slightly decreases the overall sensitivity of the

experiment to  $\delta c/c = 9,8 \times 10^{-10}$  for the case where the direction of the anisotropy lies in the orbital plane of the satellite and to  $\delta c/c = 2,1 \times 10^{-9}$  otherwise.

It is likely that the sensitivity of the experiment can be improved if data taken continuously during the passage of the satellite is used to search for the sinusoidal variation with  $\theta$  of the signal due to anisotropy. Furthermore, if a likely orientation of the presumed anisotropy is identified, for example the direction of the observed dipole anisotropy of the cosmic microwave background [10], it should be possible to improve the experimental sensitivity by statistical treatment of data from different stations and from repeated measurements.

Finally, it should be mentioned that the same type of experiment would yield increased accuracy if performed on satellites at higher altitudes, as this would decrease the  $\epsilon/T$  ratio in (4). One possible candidate is the Radioastron 1 mission (apogee 85000 km, perigee 2000 km) scheduled for launch in late 1996.

**Acknowledgements:** Helpful discussions with Dr. Claudine Thomas and Gérard Petit are gratefully acknowledged.

## References

- [1] Krisher T.P. et al., Physical Review D (rapid communication) **42**, 731 (1990).
- [2] Riis E. et al., Physical Review Letters **60**, 81, (1988).
- [3] Vessot R.F.C. & Levine M.W., General Relativity & Gravitation **10**, 181, (1980).
- [4] Champeney D.C. et al., Physics Letters **7**, 241, (1963).
- [5] Turner K.C. & Hill H.A., Physical Review **134**, B252, (1964).
- [6] Mansouri R. & Sexl R.U., General Relativity and Gravitation **8**, 497, 515, 809, (1977).
- [7] Thomas C. & Uhrich P., *ExTRAS Impact in the Time Domain*, ESA report, (1994).
- [8] Petit G. & Wolf P., Astronomy & Astrophysics, **286**, 971, (1994).
- [9] Degnan J.J., *Millimeter Accuracy Satellite Ranging: A Review*, Contributions of Space Geodesy to Geodynamics: Technology, Geodynamics **25**, (1993).
- [10] Lubin P.M. et al., Physical Review Letters **50**, 616, (1983).

## Tables

Source of uncertainty	$\sigma$ /ps
Hydrogen masers(i)	$4\sqrt{2}$
On-board payload(ii)	20
Earth station(iii)	$10\sqrt{2}$
Counters(iv)	$20\sqrt{2}$
<hr/>	
Total(quadratic sum)	$\epsilon = 38$

*Table 1: Anticipated uncertainty budget for measurement of an anisotropy whose direction lies in the orbital plane. All uncertainties are in picoseconds and correspond to an estimated one standard uncertainty,  $\sigma$ .*

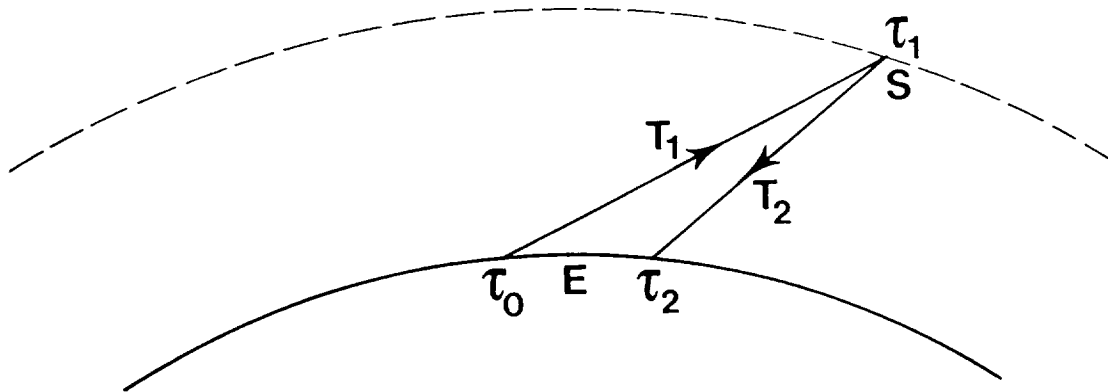


Figure 1: Two-way laser link between an Earth station and the satellite viewed in a geocentric, inertial frame.

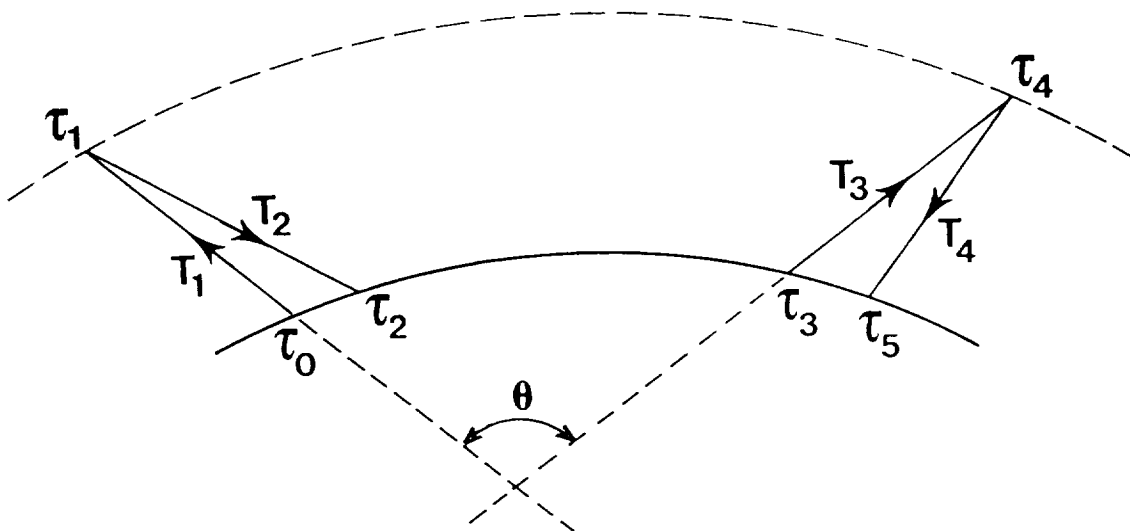


Figure 2: A pair of two-way laser links between an Earth station and the satellite, as viewed in a geocentric, inertial frame.

## QUESTIONS AND ANSWERS

**LUTE MALEKI (JPL):** The experiment that we did at JPL, as you know, was limited because of differential drift of the two H-masers which are not deterministic.

**PETER WOLF (BIPM):** Yeah, that was the first line of the error budget, which was – that is what I meant by “hydrogen maser,” their instability over the integration time, just to accumulate an error in time.

**LUTE MALEKI (JPL):** No, I’m not talking about the individual instability, I’m talking about the drift that is indeterministic; one maser moves on way, and the other maser moves the other way.

**PETER WOLF (BIPM):** I didn’t consider that. I will have to look into that. Thank you anyway.



**PTTI '94**  
**OFFICIAL ATTENDEES' LIST**

**Khalid S. Al-Dawood**

Saudi Arabian Standards Organization  
P.O. Box 3437  
11471 Riyadh  
SAUDI ARABIA

**Khalid K. Al-Dossary**

Saudi Arabian Standards Organization  
P.O. Box 3437  
11471 Riyadh  
SAUDI ARABIA

**David W. Allan**

Allan's Time  
P.O. Box 66  
Fountain Green, UT 84632 USA

**John C. Arnold**

AlliedSignal Technical Services Corporation  
One Bendix Road  
Columbia, MD 21245 USA  
410/964-7931

**Franklin G. Ascarrunz**

University of Colorado  
248 Pheasant Run  
Louisville, CO 80027 USA

**Thomas R. Bartholomew**

TASC  
1190 Winterson Road  
Linthicum, MD 21090 USA  
410/850-0070

**Perry C. Bates**

Techtrol Cyclonetics, Incorporated  
815 Market Street  
New Cumberland, PA 17070 USA

**Francoise S. Baumont**

Observatoire de la Cote d'Azur  
CERGA  
Avenue Nicolas Copernic  
06130 Grasse FRANCE  
33 93 405338

**Henry V. Bazak, Jr.**

Hughes Space and Communication  
P.O. Box 92919  
Los Angeles, CA 90274 USA  
310/416-4179

**Ronald L. Beard**

U.S. Naval Research Laboratory  
Code 8150  
4555 Overlook Avenue, Southwest  
Washington, DC 20375-5000 USA  
202/767-2595

**G. Thomas Becker**

Air System Technologies, Incorporated  
14232 Marsh Lane, Suite 339  
Dallas, TX 75234 USA  
214/402-9660

**Jacques Beser**

3S Navigation  
23141 Plaza Pte Drive  
Laguna Hills, CA 92653 USA

**Robert E. Blair**

U.S. Air Force  
Newark Air Force Base  
Newark, OH 43057 USA  
614-522-7377

**Scott S. Blake**

NASA/GSFC  
Code 5313  
Greenbelt, MD 20710 USA  
301/286-3224

**Richard E. Blunberg**

U.S. Naval Observatory  
3450 Massachusetts Avenue, Northwest  
Washington, DC 20392-5420 USA  
202/653-1538

**Jimmie Brad**

U.S. Naval Research Laboratory  
Code 8150  
4555 Overlook Avenue, Southwest  
Washington, DC 20375-5000 USA  
202/767-5039

**Keith L. Brandt**

Spectrum Geophysical Instruments  
1900 West Garvey Avenue South  
Suite 200  
West Covina, CA 91790 USA  
714/544-3000

**Lee A. Breakiron**

U.S. Naval Observatory  
3450 Massachusetts Avenue, Northwest  
Washington, DC 20392-5420 USA  
202/653-1888

**Gerhard Brenninger**  
ESG Elektroniksystem-und  
Logistik GmbH  
Einsteinstrasse 174  
D-81675 Munchen  
GERMANY  
49 89 9216 2681

**Ellis H. Bryant, Jr.**  
Weatherchron Company  
5400 New Peachtree Road  
Atlanta, Georgia 30341 USA

**James A. Buisson**  
Antoine Enterprises  
7714 Martel Place  
Springfield, VA 22152 USA

**Edward E. Burkhardt**  
Buckhardt Monitoring Service  
P.O. Box 1411  
Glen Allen, VA 23060 USA  
804/261-1800

**James A. Burton**  
CNO N63  
12739 Purdham Drive  
Woodbridge, VA 22192 USA  
703/695-8202

**Bob Bush**  
Leitch, Incorporated  
920 Corporate Lane  
Chesapeake, VA 23320 USA

**Edgar W. Butterline**  
AT&T  
900 Routes 202 and 206  
Bedminster, NJ 07921 USA  
908/234-4545

**Malcolm Calhoun**  
Jet Propulsion Laboratory  
4800 Oak Grove Drive  
Pasadena, CA 91109 USA  
818/354-9763

**James C. Camparo**  
The Aerospace Corporation  
P.O. Box 92957  
Los Angeles, CA 90009 USA  
310/336-6944

**Thomas P. Celano**  
TASC  
12100 Sunset Hills Road  
Reston, VA 22090 USA  
703/834-5000

**Harold Chadsey**  
U. S. Naval Observatory  
3450 Massachusetts Avenue, Northwest  
Washington, DC 20392-5420 USA  
202/653-1888

**Laura G. Charron**  
U.S. Naval Observatory  
3450 Massachusetts Avenue, Northwest  
Washington, DC 20392-5420 USA  
202/653-1529

**Raymond E. Claffin, III**  
Claffin Associates  
122 Morningside Drive  
Leominster, MA 01453 USA  
508/534-4777

**Randolph T. Clarke**  
U.S. Naval Observatory  
3450 Massachusetts Avenue, Northwest  
Washington, DC 20392-5420 USA  
202/653-1034

**Dwin Craig**  
U.S. Naval Research Laboratory  
Code 8150  
4555 Overlook Avenue, Southwest  
Washington, DC 20375-5000 USA  
202/404-7060

**Leonard S. Cutler**  
Hewlett-Packard Company  
3500 Deer Creek Road  
Palo Alto, CA 94303 USA  
415/857-5259

**William B. Dabney**  
U.S. Naval Observatory  
3450 Massachusetts Avenue, Northwest  
Washington, DC 20392-5420 USA  
202/653-1549

**Gerrit de Jong**  
NMi Van Swinden Laboratorium  
P. O. Box 654  
2600AR Delft  
THE NETHERLANDS  
31 15 691 623

**Steve D. Deines**  
Rockwell International  
350 Collins Road, Northeast  
MS 152-264  
Cedar Rapids, IA 52498 USA  
319/395-5038

**Edoardo V. Detoma**  
FIAT CIEI - SEPA  
Corso Giulio Cesare 300  
10154 Torino  
ITALY  
39 11 268 2523

**James A. DeYoung**  
U.S. Naval Observatory  
3450 Massachusetts Avenue, Northwest  
Washington, DC 20392-5420 USA  
202/653-1034

**Andrew R. Dickens**  
9812 Summerday Drive  
Burke, VA 22015 USA  
203/323-6299

**William A. Diener**  
Jet Propulsion Laboratory  
4800 Oak Grove Drive  
Pasadena, CA 91109 USA  
818/354-6670

**Rob Douglas**  
National Research Council of Canada  
M-36  
K1A 0R6 Ottawa  
CANADA  
613-993-5186

**James M. Eler**  
U.S. Naval Observatory  
3450 Massachusetts Avenue, Northwest  
Washington, DC 20392-5420 USA  
202/653-0350

**Donald A. Emmons**  
Frequency and Time Systems  
34 Tozer Road  
Beverly, MA 01519 USA  
508/927-8220

**John W. Evans**  
DISA  
10701 Parkridge Boulevard  
Reston, VA 22091 USA  
703/487-3173

**Sheila Faulkner**  
U. S. Naval Observatory  
3450 Massachusetts Avenue, Northwest  
Washington, DC 20392-5420 USA  
202/653-1460

**Raymond L. Filler**  
U.S. Army Research  
AMSRL EP ME  
Fort Monmouth, NJ 07703-5601 USA  
908/544-2467

**Richard H. Flamm**  
Lockheed Missiles and Space Company  
1992 Adams Avenue  
Melbourne, FL 32935 USA  
407/867-3145

**Henry F. Fliegel**  
Aerospace Corporation  
2350 El Segundo Boulevard  
El Segundo, CA USA  
310/336-1710

**Earl Fossler**  
TRAK Microwave Corporation  
Systems Division  
4726 Eisenhower Boulevard  
Tampa, FL 33634 USA  
813/884-1411

**Hugo Fruehauf**  
Ball Corporation  
3 Parker  
Irvine, CA 92718 USA  
714/770-5000

**Michael J. Full**  
NAPA-GPS  
955 L'Enfant Plaza North, Southwest  
Washington, DC 20024 USA  
202/651-8014

**Ivan J. Galysh**  
U.S. Naval Research Laboratory  
Code 8150  
4555 Overlook Avenue, Southwest  
Washington, DC 20375-5000 USA  
202/404-7060

**Joseph M. Gardner**  
Leitch, Incorporated  
920 Corporate Lane  
Chesapeake, VA 23302 USA

**Michael Garvey**  
Frequency and Time Systems  
34 Tozer Road  
Beverly, MA 01915 USA  
508/927-8220

**Richard Gast**  
TRAK Microwave Corporation  
Systems Division  
4726 Eisenhower Boulevard  
Tampa, FL 33634 USA  
813/884-1411

**Glen G. Gibbons**  
GPS World  
859 Willamette Street  
Eugene, OR 97401 USA  
503/984-5235

**Al Gifford**  
U.S. Naval Research Laboratory  
1101 Maryland Avenue, Northeast  
Washington, DC 20002 USA  
202/404-5039

**Asbjorn M. Gjelsvik**  
MITRE  
Burlington Road  
Bedford, MA 01730 USA  
617/271-3712

**Raymond L. Granata**  
NASA/Goddard Space Flight Center  
Greenbelt, Maryland 20771 USA  
301/286-3702

**Joe C. M. Green**  
AlliedSignal Technical Services Corporation  
129 North Hill Avenue  
Pasadena, CA USA  
818/584-4472

**Charles A. Greenhall**  
Jet Propulsion Laboratory  
4800 Oak Grove Drive  
MS 298-100  
Pasadena, CA 91109 USA  
818/393-6944

**Michael Grimm**  
Jet Propulsion Laboratory  
4800 Oak Grove Drive  
Pasadena, CA 91109 USA  
818/354-2245

**Fran Groat**  
Hewlett-Packard Company  
5301 Stevens Creek Boulevard  
Santa Clara, CA 95052-8059 USA  
408/553-2307

**Donald M. Haddox**  
U.S. Naval Observatory  
3450 Massachusetts Avenue, Northwest  
Washington, DC 20392-5420 USA

**Darrell R. Hale**  
AlliedSignal Technical Services Corporation  
One Bendix Road  
MS C-1300  
Columbia, MD 21045 USA  
410/964-7097

**Robert Hamell**  
Jet Propulsion Laboratory  
4800 Oak Grove Drive  
Pasadena, CA 91109 USA  
818/354-4944

**Wayne Hanson**  
National Institute of Standards and Technology  
325 Broadway  
Boulder, CO 80303 USA  
303/497-5233

**Michael D. Harkins**  
Applied Technology Associates, Incorporated  
6800 Backlick Road  
Suite 303  
Springfield, VA 22150 USA  
703/644-0301

**Bill Harron**  
Datum, Incorporated  
4545 Pilgrim Lane  
Boothwyn, PA 19061 USA  
610/485-9506

**Gregory E. Hatten**  
U.S. Air Force  
2nd Space Operations Squadron  
300 O'Malley Avenue  
Suite 41  
Falcon Air Force Base, CO 80912-3041 USA  
719/550-6377

**Helmut Hellwig**  
Air Force Office of Scientific Research  
110 Duncan Avenue, Suite B115  
Bolling Air Force Base  
Washington, DC 20332-0001 USA  
202/767-5017

**Thomas P. Holden**  
Stanford Telecommunications, Incorporated  
1221 Crossman Avenue  
Sunnyvale, CA 94089-1117 USA  
408/745-0818

**Terry A. Howell**  
U.S. Naval Observatory  
3450 Massachusetts Avenue, Northwest  
Washington, DC 20392-5420 USA  
202/653-1449

**Steven T. Hutsell**  
U.S. Air Force  
2nd Space Operations Squadron  
300 O'Malley Avenue  
Falcon Air Force Base, CO 80912-3041 USA  
719/550-6394

**Jeffrey S. Ingold**  
AlliedSignal Technical Services Corporation  
One Bendix Road  
Columbia, MD 21045 USA  
410/964-7188

**Andrew Johnson**  
U.S. Naval Observatory  
3450 Massachusetts Avenue, Northwest  
Washington, DC 20392-5420 USA  
202/653-1561

**Jeffrey A. Johnson**  
Overlook Systems Technologies, Incorporated  
1950 Old Gallows Road  
Suite 400  
Vienna, VA 22182 USA  
703/893-1411

**Edward C. Jones**  
U.S. Naval Research Laboratory  
Code 8150  
4555 Overlook Avenue, Southwest  
Washington, DC 20375-5000 USA  
202/767-0590

**Sarunas K. Karuza**  
The Aerospace Corporation  
P.O. Box 92957  
Los Angeles, CA 90009-2957 USA  
213/336-6837

**Shalom Kattan**  
Guide Technology, Incorporated  
920 Saratoga Avenue, Suite 205  
San Jose, CA 95129 USA  
408/246-9903

**Robert H. Kern**  
Kernco, Incorporated  
28 Harbor Street  
Danvers, MA 01923 USA  
508/777-1956

**Wendy L. King**  
U.S. Naval Observatory  
3450 Massachusetts Avenue, Northwest  
Washington, DC 20392-5420 USA  
202/653-0486

**William J. Klepczynski**  
U.S. Naval Observatory  
3450 Massachusetts Avenue, Northwest  
Washington, DC 20392-5420 USA  
202/653-1521

**Douglas E. Koch**  
Naval Space Command  
808 Pleasant Hill Lane  
Bowie, MD 20716 USA  
301/249-7494

**Paul A. Koppang**  
U.S. Naval Observatory  
3450 Massachusetts Avenue, Northwest  
Washington, DC 20392-5420 USA  
202/653-0350

**Guenter Kramer**  
Physikalisch-Technische Bundesanstalt  
P.O. Box 3345  
D-38023 Braunschweig, GERMANY  
49 431 592 4420

**Paul F. Kuhnle**  
Jet Propulsion Laboratory  
4800 Oak Grove Drive  
Pasadena, CA 91109 USA  
818/354-2715

**Eugen F. Kunzi**  
SIEMENS AG.  
Department SI E SY 4  
Landshuter Strabe 26  
D-85716 Unterschleissheim  
GERMANY  
49 89 3179 2297

**Jack Kusters**  
Hewlett-Packard Company  
5301 Stevens Creek Boulevard  
Santa Clara, CA 95052-8059 USA  
408/553-2041

**Graybill P. Landis**  
U.S. Naval Research Laboratory  
Code 8150  
4555 Overlook Avenue, Southwest  
Washington, DC 20375-5000 USA  
202/404-7061

**Marie M. Largay**  
U.S. Naval Research Laboratory  
Code 8153  
4555 Overlook Avenue, Southwest  
Washington, DC 20375-5000 USA  
202/767-9133

**Julius Law**  
Jet Propulsion Laboratory  
4800 Oak Grove Drive  
Pasadena, CA 91109 USA  
818/354-2988

**Ming C. Lee**  
Western Range U.S. Air Force  
826 13th Street  
Vandenberg Air Force Base, CA 93437 USA

**Albert Leong**  
The Aerospace Corporation  
P.O. Box 92957  
MS M1/135  
Los Angeles, CA 90009 USA  
310-336-6444

**Sigfrido M. Leschiutta**  
Politecnico di Torino  
24 Corso Abruzzi  
10125 Torino  
ITALY  
38 11 381 8715

**Judah Levine**  
National Institute of Standards and Technology  
Code 847  
325 Broadway  
Boulder, CO 80303 USA  
303/497-3903

**Wlodzimierz W. Lewandowski**  
Bureau International des Poids et Mesures  
Pavillon de Breteuil  
92310 Sevres  
FRANCE  
33 1 45 077063

**Chuck Little**  
Hewlett Packard Company  
5301 Stevens Creek Boulevard  
Santa Clara, CA 95052-8059 USA  
408/553-2506

**Michael A. Lombardi**  
National Institute of Standards and Technology  
325 Broadway  
Division 847  
Boulder, CO 80303 USA  
303/497-3212

**Gene E. Long**  
Odetics  
P.O. Box 2727  
LaPlata, MD 20646 USA  
301/870-3311

**Pete R. Lopez**  
TRAK Microwave Corporation  
Systems Division  
4726 Eisenhower Boulevard  
Tampa, FL 33634 USA  
813/884-1411

**John McK. Luck**  
Orroral Observatory, Auslis  
P.O. Box 2  
2611 Belconnen ACT  
AUSTRALIA  
61 6 288-3263

**Carl F. Lukac**  
U.S. Naval Observatory  
3450 Massachusetts Avenue, Northwest  
Washington, DC 20392-5420 USA  
202/653-1527

**Edward M. Lukacs**  
U.S. Naval Observatory  
11820 Southwest 166th Street  
Miami, FL 33177-2175 USA  
305/235-0515

**Collin C. MacMillan**  
Sigma Tau Corporation  
1711 Holt Road  
Tuscaloosa, AL 35404 USA  
205/553-0038

**Phu V. Mai**  
U.S. Naval Observatory  
3450 Massachusetts Avenue, Northwest  
Washington, DC 20392-5420 USA  
202/653-0350

**Lute Maleki**  
Jet Propulsion Laboratory  
4800 Oak Grove Drive  
Pasadena, CA 91109 USA  
818/354-3688

**David G. Markham**  
U.S. Navy  
COMSPAWARSYSCOM/PMW175  
2451 Crystal Drive  
Arlington, VA 22245 USA

**Demetrios N. Matsakis**  
U.S. Naval Observatory  
3450 Massachusetts Avenue, Northwest  
Washington, DC 20392-5420 USA  
202/653-0585

**Thomas B. McCaskill**  
U.S. Naval Research Laboratory  
Code 8153  
4555 Overlook Avenue, Southwest  
Washington, DC 20375-5000 USA  
202/404-7068

**Angela Davis McKinley**  
U.S. Naval Observatory  
3450 Massachusetts Avenue, Northwest  
Washington, DC 20392-5420 USA  
202/653-1528

**Norma G. Meyer**  
U.S. Naval Observatory  
3450 Massachusetts Avenue, Northwest  
Washington, DC 20392-5420 USA  
202/653-1525

**Mihran Miranian**  
U.S. Naval Observatory  
3450 Massachusetts Avenue, Northwest  
Washington, DC 20392-5420 USA  
202/653-1522

**Donald H. Mitchell**  
TrueTime, Incorporated  
2835 Duke Court  
Santa Rosa, CA 95407 USA  
707/528-1230

**Raymond W. Moskaluk**  
Hewlett-Packard Company  
5301 Stevens Creek Boulevard  
Santa Clara, CA 95128 USA  
408/553-3319

**David G. Munton**  
University of Texas  
Applied Research Laboratory  
10000 Burnet Road  
Austin, TX 78758 USA  
512/835-3831

**William J. Murphy**  
Computer Sciences Corporation  
P.O. Box 446  
Building 1440  
Edwards Air Force Base, CA 93523 USA  
805/277-2004

**James A. Murray**  
SEA, Incorporated  
6215 Houston Street  
Alexandria, VA 22310 USA  
202/404-7057

**Craig W. Nelson**  
SpectraDynamics, Incorporated  
445 South 43rd Street  
Boulder, CO 80303 USA

**Clyde C. Norris**  
Computer Sciences Corporation  
P. O. Box 217  
Clearfield, UT 84015 USA  
801/777-4845

**Jerry R. Norton**  
Johns Hopkins University  
Applied Physics Laboratory  
Johns Hopkins Road  
Laurel, MD 21104 USA

**Timothy W. Oakley**  
Sigma Tau Corporation  
1711 Holt Road  
Tuscaloosa, AL 35404 USA  
205/553-0038

**Jay Oaks**  
U.S. Naval Research Laboratory  
Code 8150  
4555 Overlook Avenue, Southwest  
Washington, DC 20375-5000 USA  
202/767-1434

**David B. Opie**  
Physical Sciences, Incorporated  
635 Slaters Lane  
Suite G101  
Alexandria, VA 22314 USA  
703/548-6410

**Jorge Osorio**  
Observatorio Naval Buenos Aires  
2099 Av. Espana  
1107 Buenos Aires  
ARGENTINA  
64 1 36 1162

**Terry N. Osterdock**  
Stellar GPS Corporation  
800 Charcot Avenue  
Suite 110  
San Jose, CA 95131 USA  
408/383-1520

**H. Bryan Owings**  
Sigma Tau Corporation  
1711 Holt Road  
Tuscaloosa, AL 35404 USA  
205/553-0038

**Thomas E. Parker**  
National Institute of Standards and Technology  
325 Broadway  
Boulder, CO 80303 USA  
303/497-7881

**Ralph E. Partridge**  
Los Alamos National Laboratory  
DX-12, MS-P947  
P.O. Box 1663  
Los Alamos, NM 87545 USA  
505/667-5255

**William H. Paul**  
Tecom NRO-DT-T  
White Sands Missile Range, NM 88002 USA  
505/674-9220

**Peter Z. Paulovich**  
NISE East Det Norfolk  
P. O. Box 1376  
Norfolk, VA 23501-1376 USA  
804/396-0287

**Bruce Penrod**  
TrueTime, Incorporated  
2835 Duke Court  
Santa Rosa, CA 95407 USA  
707/528-1230

**James C. Perry**  
NASA/Goddard Space Flight Center  
Greenbelt, MD 20771 USA  
301/286-3471

**Harry E. Peters**  
Sigma Tau Standards Corporation  
1711 Holt Road  
Tuscaloosa, AL 35404 USA  
205/553-0038

**Larry E. Peters**  
Sigma Tau Standards Corporation  
P.O. Box 1877  
Tuscaloosa, AL 35403 USA  
205/553-0038

**James S. Phelps**  
Scientific and Technical Analysis  
11300 Naples Mill Road  
Fairfax, VA 22043 USA  
703/934-0188

**William D. Phillips**  
National Institute of Standards and Technology  
PHY A167  
Gaithersburg, MD 20899 USA  
301/975-6554

**Eva F. Pikal**  
National Institute of Standards and Technology  
325 Broadway  
Boulder, CO 80303 USA  
303/497-5629

**William M. Powell**  
U. S. Naval Observatory  
3450 Massachusetts Avenue, Northwest  
Washington, DC 20392-5420 USA  
202/653-1528

**Edward D. Powers**  
U.S. Naval Research Laboratory  
Code 8150  
4555 Overlook Avenue, Southwest  
Washington, DC 20375-5000 USA  
202/767-5004

**Robert E. Price**  
AlliedSignal Technical Services Corporation  
One Bendix Road  
Columbia, MD 21045 USA  
410/964-7437

**David W. Rea**  
Spectrum Geophysical Instruments  
1900 West Garvey Avenue, South  
Suite 200  
West Covina, CA 91790 USA  
714/544-3000

**Elza K. Redman**  
DoD  
9800 Savage Road  
Fort Meade, MD 20577 USA  
301/688-7526

**Wilson G. Reid**  
Naval Research Laboratory  
Code 8150  
4555 Overlook Avenue, Southwest  
Washington, DC 20375-5000 USA  
202/404-7068

**Victor S. Reinhardt**  
Hughes Space and Communications  
P.O. Box 92919  
Los Angeles, CA 90009 USA

**William J. Riley**  
EG&G Rubidium  
35 Congress Street  
Salem, MA 01970 USA  
508/745-3200

**Eric B. Rodal**  
Trimble Navigation  
585 North Mary  
Sunnyvale, CA 94088 USA  
408/481-2039

**Ronald C. Roloff**  
Datum, FTS  
8005 McKenstry Drive  
Laurel, MD 20723 USA  
301/725-3636

**Harry W. Sadler III**  
AlliedSignal Technical Services Corporation  
One Bendix Road  
Columbia, MD 21045 USA  
410/964-7425

**Roberto O. Sartori**  
Observatorio Naval Buenos Aires  
2099 Av. Espana  
1107 Buenos Aires  
ARGENTINA  
54 1 361 1162

**Bernard R. Schlueter**  
Observatory of Neuchatel  
CH2000 Neuchatel  
SWITZERLAND  
41 38 241861

**Richard E. Schmidt**  
U.S. Naval Observatory  
3450 Massachusetts Avenue, Northwest  
Washington, DC 20392-5420 USA  
202/653-0487

**Steve Schumacher**  
Loral Space and Range Systems  
2900 Murrell Road  
Rockledge, FL 32955 USA  
407/635-7647

**Mike Shunfenthal**  
TASC  
12100 Sunset Hills Road  
Reston, VA 22090 USA  
703/834-5000

**Ralph E. Simons**  
Frequency and Time Systems  
34 Tozer Road  
Beverly, MA 01915 USA  
508/927-8220

**Hank T. Skalski**  
DOT/OST  
400 7th Street, Southwest  
Washington, DC 20590 USA  
202/366-4894

**Luke R. Smith**  
Sigma Tau Standards Corporation  
1711 Holt Road  
Tuscaloosa, AL 35403 USA  
205/553-0038

**Benjamin F. Smith**  
Stanford Telecommunications, Incorporated  
1221 Crossman Avenue  
Sunnyvale, CA 94089-1117 USA  
408/745-2640

**Andrew G. Snow**  
Frequency and Time Systems  
34 Tozer Road  
Beverly, MA 01915 USA  
508/927-8220

**Armin Soering**  
Deutsche Telekom AG  
3 AM Kavalleriesand  
64295 Darmstadt  
GERMANY  
49 6151 83 4549

**Samuel R. Stein**  
Timing Solutions Corporation  
1025 Rosewood Avenue, #200  
Boulder, CO 80304 USA  
303/939-8481

**Michael A. Street**  
Bonneville Power Administration  
905 Northeast 11th Avenue  
Portland, OR 97232 USA  
503/230-4363

**Richard L. Sydnor**  
Jet Propulsion Laboratory  
4800 Oak Grove Drive  
Pasadena, CA 91109 USA  
818/354-2763

**Philip E. Talley, Jr.**  
Retired  
1022 Eagle Crest  
Macon, GA 31211 USA  
913/745-4661

**Claudine Thomas**  
Bureau International des Poids et Mesures  
Pavillon de Breteuil  
92312 Sevres Cedex  
FRANCE  
33 1 45 07 7073

**Larry M. Thomas**  
Computer Sciences Corporation  
44609 North 86th Street East  
Lancaster, CA 93535 USA  
805/277-6130

**Roger Thornburn**  
Stellar GPS Corporation  
800 Charcot Avenue  
Suite 110  
San Jose, CA 95131 USA  
408/383-1522

**Terry L. Trisler**  
Ball Corporation  
Efratom Division  
3 Parker  
Irvine, CA 92718 USA  
714/770-5000

**Gregory B. Turetzky**  
Trimble Navigation  
645 North Mary Avenue  
Sunnyvale, CA 94086 USA  
408/252-9510

**David A. Turner**  
National Research Council  
2101 Constitution Avenue, Northwest  
HA-286  
Washington, DC USA  
202/334-2895

**Pierre J. M. Uhrich**  
LPTF Observatoire de Paris  
61 Avenue de L'Observatoire  
F-75014 Paris  
FRANCE  
33 1 40 512216

**M. J. VanMelle**  
Rockwell  
5505 Flintridge Drive  
Colorado Springs, CO 80918 USA  
719/550-2705

**Francine M. Vannicola**  
U.S. Naval Observatory  
3450 Massachusetts Avenue, Northwest  
Washington, DC 20392-5420 USA  
202/653-1525

**Vince Vannicola**  
U.S. Coast Guard  
7323 Telegraph Road  
Alexandria, VA 22015 USA  
703/313-5811

**Christian Veillet**  
Observatoire de La Côte d'Azur  
Avenue Nicolas Copernic  
06130 Grasse  
FRANCE

**John R. Vig**  
U.S. Army Research Laboratory  
AMSRL-EP-ME  
Fort Monmouth, NJ 07703-5601 USA

**Frank J. Voit**  
The Aerospace Corporation  
P.O. Box 92957  
Los Angeles, CA 90009-2957 USA  
310/336-6764

**Warren F. Walls**  
Femtosecond Systems  
P.O. Box 6005  
Columbia, MD 21045-8005 USA  
410/740-1427

**Heidi E. Walls**  
Femtosecond Systems  
P.O. Box 6005  
Columbia, MD 21045-8005 USA  
410/740-1427

**Fred L. Walls**  
National Institute of Standards and Technology  
325 Broadway  
Boulder, CO 80303 USA  
303/497-3207

**Harry T. M. Wang**  
Hughes Research Lab  
3011 Malibu Canyon Road  
Malibu, CA 90265 USA  
805/317-5431

**Fred L. Walls**  
National Institute of Standards and Technology  
325 Broadway  
Boulder, CO 80303 USA  
303/497-3207

**Harry T. M. Wang**  
Hughes Research Lab  
3011 Malibu Canyon Road  
Malibu, CA 90265 USA  
805/317-5431

**S. Clark Wardrip**  
AlliedSignal Technical Services Corporation  
726 Foxenwood Drive  
Santa Maria, CA 93455-4221 USA  
805/937-6448

**Marc A. Weiss**  
National Institute of Standards and Technology  
325 Broadway  
Boulder, CO 80303 USA  
303/497-3261

**Paul J. Wheeler**  
U.S. Naval Observatory  
3450 Massachusetts Avenue, Northwest  
Washington, DC 20392-5420 USA  
202/653-0516

**Joseph D. White**  
U.S. Naval Research Laboratory  
Code 8151  
4555 Overlook Avenue, Southwest  
Washington, DC 20375-5000 USA  
202/767-5111

**Carol A. Williams**  
Department of Mathematics  
University of South Florida  
4202 East Fowler Avenue  
PHY 114  
Tampa, FL 33620 USA  
813/974-3553

**Warren L. Wilson**  
Lockheed Missiles and Space Company  
701 East Thrift Avenue  
Kingsland, GA 31548-8213 USA  
912/673-1148

**Gernot M. R. Winkler**  
U. S. Naval Observatory  
3450 Massachusetts Avenue, Northwest  
Washington, DC 20392-5420 USA  
202/653-1520

**Peter Wolf**  
Bureau International des Poids et Mesures  
Pavillon de Breteuil  
92312 Sevres Cedex  
FRANCE  
33 14 507 7075

**William H. Wooden**  
Defense Mapping Agency  
8613 Lee Highway  
Stop A-13  
Fairfax, VA 22031-2137 USA  
703/285-9339

**David F. Wright**  
Radiocode Clocks Ltd.  
54 Watling Street South  
5467BQ Church Stretton Shropshire  
UNITED KINGDOM  
44 1694 723691

**James L. Wright**  
Computer Sciences Raytheon  
P.O. Box 4127  
Patrick Air Force Base, FL 32925 USA  
407/494-2014

**Andy Wu**  
The Aerospace Corporation  
2350 East El Segundo  
El Segundo, CA 90245-4691 USA  
310/336-0437

**Victor S. Zhang**  
National Institute of Standards and Technology  
325 Broadway  
Boulder, CO 80303 USA  
303/497-3977









# REPORT DOCUMENTATION PAGE

Form Approved  
OMB No. 0704-0188

Public reporting burden for this collection of information is estimated to average 1 hour per response, including the time for reviewing instructions, searching existing data sources, gathering and maintaining the data needed, and completing and reviewing the collection of information. Send comments regarding this burden estimate or any other aspect of this collection of information, including suggestions for reducing this burden, to Washington Headquarters Services, Directorate for Information Operations and Reports, 1215 Jefferson Davis Highway, Suite 1204, Arlington, VA 22202-4302, and to the Office of Management and Budget, Paperwork Reduction Project (0704-0188), Washington, DC 20503.

<b>1. AGENCY USE ONLY (Leave blank)</b>		<b>2. REPORT DATE</b> May 1995	<b>3. REPORT TYPE AND DATES COVERED</b> Conference Publication	
<b>4. TITLE AND SUBTITLE</b> 26th Annual Precise Time and Time Interval (PTTI) Applications and Planning Meeting			<b>5. FUNDING NUMBERS</b>  Code 502 C-NAS5-31000	
<b>6. AUTHOR(S)</b>  Dr. Richard Sydnor, Technical Editor				
<b>7. PERFORMING ORGANIZATION NAME(S) AND ADDRESS(ES)</b>  Goddard Space Flight Center Greenbelt, Maryland 20771			<b>8. PERFORMING ORGANIZATION REPORT NUMBER</b>  95B00083	
<b>9. SPONSORING/MONITORING AGENCY NAME(S) AND ADDRESS(ES)</b>  NASA Aeronautics and Space Administration Washington, D.C. 20546-0001			<b>10. SPONSORING/MONITORING AGENCY REPORT NUMBER</b>  CP-3302	
<b>11. SUPPLEMENTARY NOTES</b>  Richard Sydnor: Jet Propulsion Laboratory, Pasadena, CA. Other sponsors: U. S. Naval Observatory; Jet Propulsion Laboratory; Space and Naval Warfare Systems Command; Naval Research Laboratory; Army Electronics Technology and Devices Laboratory; Rome Laboratory; and Air Force Office of Scientific Research.				
<b>12a. DISTRIBUTION/AVAILABILITY STATEMENT</b>  Unclassified-Unlimited Subject Category: 70 Report available from the NASA Center for AeroSpace Information, 800 Elkridge Landing Road, Linthicum Heights, MD 21090; (301) 621-0390.			<b>12b. DISTRIBUTION CODE</b>	
<b>13. ABSTRACT (Maximum 200 words)</b>  This document is a compilation of technical papers presented at the 26th Annual PTTI Applications and Planning Meeting, held December 6 through December 8, 1994, at the Hyatt Regency Hotel, Reston, Virginia. Papers are in the following categories:  <ul style="list-style-type: none"> <li>• Recent developments in rubidium, cesium, and hydrogen-based frequency standards, and in cryogenic and trapped-ion technology.</li> <li>• International and transnational applications of Precise Time and Time Interval technology with emphasis on satellite laser tracking, GLONASS timing, intercomparison of national time scales and international telecommunications.</li> <li>• Applications of Precise Time and Time Interval technology to the telecommunications, power distribution, platform positioning, and geophysical survey industries.</li> <li>• Applications of PTTI technology to evolving military communications and navigation systems.</li> <li>• Dissemination of precise time and frequency by means of GPS, GLONASS, MILSTAR, LORAN, and synchronous communications satellites.</li> </ul>				
<b>14. SUBJECT TERMS</b>  Frequency Standards, Hydrogen Masers, Cesium, Rubidium, Trapped Ion, Crystals, Time Synchronization, Precise Time, Time Transfer, GPS, GLONASS, Satellite Clocks, Jitter, Phase Noise			<b>15. NUMBER OF PAGES</b>  505	
			<b>16. PRICE CODE</b>	
<b>17. SECURITY CLASSIFICATION OF REPORT</b>  Unclassified	<b>18. SECURITY CLASSIFICATION OF THIS PAGE</b>  Unclassified	<b>19. SECURITY CLASSIFICATION OF ABSTRACT</b>  Unclassified	<b>20. LIMITATION OF ABSTRACT</b>  Unlimited	